STRENGTH AND DUCTILITY OF WELDED JOINTS SUBJECTED TO OUT-OF-PLANE BENDING

by

Ivan Gomez
Amit Kanvinde

University of California, Davis

Yu Kay Kwan
Gilbert Grondin

University of Alberta

Final Report Presented to

American Institute of Steel Construction

July 2008

Executive Summary

The current AISC design specification for welded connections does not make a distinction between joints subjected to eccentric loads in the plane of the weld group, and those subjected to eccentric loads not in the plane of the weld group. The effect of loading perpendicular to the root notch and moment transfer by bearing of the connected plates in the compression zone of the welded joint are both factors that may affect significantly the load carrying capacity of these joints. To investigate the root notch effect and the load transfer mechanism, an experimental program was conducted consisting of 24 welded cruciform test specimens tested in direct tension and 60 cruciform weld specimens tested under combined shear and bending.

Results from twenty-four cruciform tests indicate that the strength of fillet welds is not affected significantly by the presence of the root notch. The E70T7-K2 welds show approximately twice the ductility of the E70T7 welds, whereas the E70T7 welds show a slightly reduced ductility as compared to previous published data for lap-welded joints. However, the ductility for all the welds is relatively insensitive to root notch length. Complementary fracture mechanics based finite element simulations are conducted to examine and generalize experimental findings. The simulations indicate that larger notch lengths do not further reduce the strength and ductility of the welds.

Earlier test results and the test results from this test program reveal that the current (13th Edition) AISC design tables for eccentrically loaded welds are highly conservative (i.e. test-to-predicted ratios are, on average, 1.75; with a coefficient of variation = 0.25) for joints with out-of-plane eccentricity. This conservatism is attributed to the disregard of plate bearing stresses that significantly alter the stress distribution in the joint. An alternate approach that explicitly incorporates this bearing effect is proposed, and the resulting strength predictions are determined to be significantly less conservative when compared to the current design standards. Limitations of the research and future work are outlined.

A total of 14 strength prediction models were evaluated. The model consisting of a modified version of the instantaneous center of rotation approach developed by Dawe and Kulak (1972) was found to provide the target safety index with a resistance factor of 0.75. A simple closed form model was developed and is proposed as a substitute for the more complex instantaneous center of rotation model. The proposed closed form model provides a safety index of 4.0 with a resistance factor of 0.75.

Acknowledgments

This project was conducted as a joint collaboration between the University of California Davis and the University of Alberta. The project was funded by the American Institute of Steel Construction (AISC) and the Natural Sciences and Engineering Research Council of Canada (NSERC). The authors gratefully acknowledge Mr. Tom Schlafly of AISC and Dr. Duane Miller of Lincoln Electric who provided valuable advice and reviewed the welding and shop procedures. Marshall Roberts, graduate student at UC Davis, assisted with the experimental setup, and Jorge Camacho, undergraduate researcher at UC Davis, assisted with the specimen measurements; the authors are thankful for their efforts. The assistance of Mr. David DeBlasio of Gayle Manufacturing Company in preparing the specimens is greatly appreciated. The authors also acknowledge Bill Sluis, laboratory technician at UC Davis for assistance with design of the test setup.

Table of Content

List of Tables

List of Figures

Chapter 1

Introduction

1.1 GENERAL

Fillet welded joints are widely used in civil engineering construction due to their relatively high strength and the ease of surface preparation required for such welds. In many joint configurations used in practice in-plane or out-of-plane eccentricity is unavoidable, creating more complex stress conditions in the joint than concentrically loaded joints where the welds are generally subjected to shear in only one direction. Design methods that account for load eccentricity on welded joints have been developed (Dawe and Kulak, 1974; Tide, 1980) for both in-plane and out-of-plane eccentricity.

In welded joints that are subjected to in-plane eccentricity (Figure 1.1a) the weld is free to deform over its entire length. In the case of welds subjected to out-of-plane eccentricity as shown in Figure 1.1b, the part of the weld in the compression zone is not free to deform because of direct bearing between the connected plates. This fundamental difference between the in-plane and out-of-plane eccentric loading has been recognized in the derivation of an ultimate limit state formulation for the strength of eccentric joints (Dawe and Kulak, 1974). The method of instantaneous centre, originally developed for bolted joints and welded joints with in-plane eccentricity, was modified for out-of-plane eccentricity to account for the bearing of the plate in the compression zone at ultimate load. The method proposed by Dawe and Kulak was adopted in the CISC Handbook of Steel Construction. However, a more conservative approach was adopted for the AISC Manual for Steel Construction. The approach treats the joint with out-of-plane eccentricity as a joint with in-plane eccentricity, thus ignoring load transfer by bearing on the compression side of the joint (Tide, 1980). The eccentrically loaded joint with out-of-plane eccentricity produces a root notch at the unused interface of the plates. Previous studies (e.g. Ng *et al.*, 2002; Pham, 1983 and Kanvinde *et al.*, 2008) indicate that such a root notch, perpendicular to the direction of the bending stresses in the connection may reduce both the strength and the ductility of the welds with respect to values implicitly assumed in the design table. Both the Canadian and American approaches ignore this effect. An investigation of this issue has been the primary motivation for the research program presented in this report.

1.2 BACKGROUND

Eccentrically loaded fillet-welded connections with out-of-plane eccentricity have received limited attention. An experimental investigation by Dawe and Kulak (1972) included eight specimens to investigate the behavior of weld groups subjected to out-of-plane eccentric loading. The test specimens consisted of a wide-flange section with its end welded to an end plate by fillet welds along the outer side of each flange. The test configuration involved loading the wide flange sections in minor axis bending to

determine the joint strength. The key variables investigated included the length of weld, the eccentricity of the load and the size of the wide flange section. Two nominal weld lengths (8" and 12") and four load eccentricities (ranging from 8" to 20") were considered. Since the specimens were loaded in the minor axis orientation, the effective bearing width was determined as twice the flange thickness of the wide-flange section. Using this interpretation, five nominal bearing widths (ranging from 0.86 inches to 1.52 inches) were investigated. All specimens were fabricated from ASTM A36 steel and used 1/4 in. welds deposited with AWS E60XX electrodes.

A larger experimental program was later conducted by Warren (1984) and Beaulieu and Picard (1985) and included a total of 24 fillet welded plate connections loaded eccentrically out-of-plane. The main variables investigated in this study included the weld size (nominally 1/4", 3/8", 5/16" and 1/2"), the load eccentricity (ranging between 3" and 14.75") and the bearing width (0.787" and 1.575"). All specimens were fabricated from ASTM A36 steel, and the welds (all approximately 10" long) were made with AWS E70XX electrodes. Weld failure, plate rupture and plate buckling were the various failure modes observed in the experimental program.

In addition to these two experimental programs, joint strength prediction methods were developed. Dawe and Kulak (1972) proposed a method based on the method of instantaneous center of rotation, accounting for moment transfer through plate bearing and weld tension. The model was later adopted by CISC for design, although a strength reduction factor was added to the model in addition to the resistance factor used for design of concentrically loaded welded joints. Although the model proposed by Dawe and Kulak is a rational and comprehensive approach, it involves an iterative procedure that makes it difficult to implement without the use of a computer program or special design tables. Simpler, closed form, solutions were proposed by Neis (1980), but these models never received broad acceptance. Beaulieu and Picard (1985) proposed a closed form design model similar to one of the models earlier proposed by Neis and expanded to account for joints with small eccentricity. This approach was recently adopted by the CISC in the ninth edition of the Handbook of Steel Construction.

The earlier work of Dawe and Kulak was based on load versus deformation behavior for fillet welds derived from small weld specimen tests conducted by Butler and Kulak (1971). Later, Lesik and Kennedy (1990) proposed a different set of equations to describe the fillet weld ultimate capacity, deformation and response under loading applied at various orientations.

The current design tables for the welded joints with out-of-plane eccentricity used in American Institute of Steel Construction (AISC) are generated using the instantaneous centre of rotation proposed by Butler *et al.* (1972) along with the load-deformation relationships given by Lesik and Kennedy (1990). Similar design tables are also produced by Canadian Institute of Steel Construction (CISC), and they are based on the closed-form solution derived by Picard and Beaulieu (1991).

Because of the limited amount of experimental research on welded joints subjected to combined shear and out-of-plane bending, the models used to predict the strength cannot

be evaluated for a wide range of parameters. The methods are based on several assumptions and weld load-deformation relationships derived from tests on lapped specimens. Therefore, none of the design methods consider the potentially detrimental effect of the root notch on the ductility of the welds. An examination of current AISC design tables indicates that significant aspects of physical response, such as bearing between the connected plates, are not considered in their development. To address these issues, the main objectives of the current study are to generate a larger database of test results to expand the range of parameters covered by earlier test programs and to evaluate the applicability of the current design standards to joints with out-of-plane eccentricity, and to suggest improved alternatives.

1.3 OBJECTIVES AND SCOPE

The main objectives of this part of the weld research program, conducted as a collaborative effort between the University of Californian Davis and the University of Alberta are to:

1. collect and document available test data from welded joints loaded under combined shear and out-of-plane bending
2. significantly expand the database of test results on welded joints subjected to combined shear and out-of-plane bending in order to create a statistically significant test population
3. investigate experimentally the effect of root notch size on the strength and ductility of fillet welds loaded perpendicular to the root notch
4. use the expanded database of test data to assess the existing strength prediction models, including the model implemented in the AISC Manual of Steel Construction
5. conduct a reliability analysis to assess the level of safety of the most promising design model and determine an appropriate resistance factor
6. make a recommendation for a design approach that is both easy to implement and offers the required level of safety

These objectives are met by conducting a series of tests on 84 fillet weld cruciform shape specimens. Twenty-four test specimens will be tested to investigate the behavior of transverse fillet welds loaded perpendicular to the weld root notch. An additional 60 cruciform specimens will be tested with out-of-plane eccentricity. The parameters to be examined experimentally are: length of the root notch (1.25 inches, 1.75 inches and 2.50 inches), weld metal with and without toughness classification, magnitude of eccentricity (3 in., 5.5 in. and 8.5 in.) and nominal weld size (5/16 in. and 1/2 in.). This experimental program will be supplemented by ancillary tests in the form of all-weld tension coupon tests, base metal tension coupon tests, Charpy V-Notch impact tests and spectro-chemical analyses.

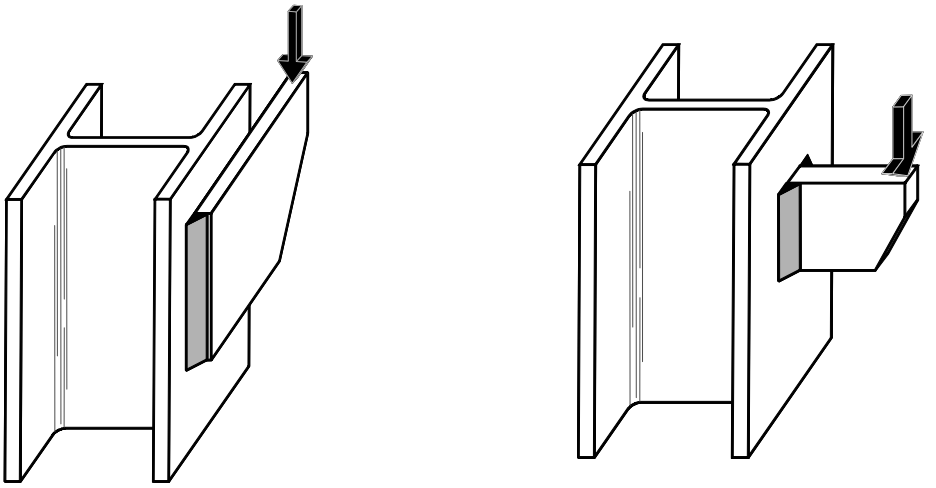

(a) In-plane eccentricity (b) Out-of-plane eccentricity

Figure 1.1 – Eccentrically loaded welded joints

Chapter 2

Literature Review

2.1 INTRODUCTION

Before Load and Resistance Factor Design (LRFD) was adopted, the design of eccentrically loaded welded joints loaded eccentrically was based on a simple elastic analysis where it was assumed that the weld element furthest from the centre of gravity of the weld group controlled the capacity of the welded joint. Although this elastic analysis approach was expedient, it was not appropriate for a LRFD design approach since it represented only the first yield of the weld group rather than its ultimate capacity. With the introduction of LRFD in the United States and Limit States Design in Canada, new design methods that attempted to predict the ultimate capacity of the weld group were introduced. This chapter presents a brief summary of various analytical models that have been proposed since the early 1970's for the prediction of the ultimate capacity of welded joints with out-of-plane eccentricity. A detailed development of these analytical models is presented in Chapter 6. First, a review of available test data on eccentrically loaded welded joints is presented.

2.2 BEHAVIOR OF FILLET WELDS UNDER LOAD

2.2.1 Butler and Kulak (1971)

Early investigations on transverse fillet welds (Ligtenburg, 1968) indicated that transverse fillet welds in tension (where the loading is applied perpendicular to the weld axis) were approximately 60% stronger than longitudinal fillet welds (welds where the line of axis of the applied load is parallel to the axis of the weld). Similar findings have been reported by others (Higgins and Preece, 1969; Clark, 1971).

Butler and Kulak (1971) conducted a series of 23 tests on specimens with 1/4 in. fillet welds loaded in tension at 0^o, 30^o, 60^o and 90^o to the weld axis. The purpose of their test was to establish the effect of load direction behavior to the load-deformation response of fillet welds. The test specimens were prepared using E60XX electrodes, CSA-G40.12 steel plate and the shielded metal arc welding (SMAW) process, with a specified yield stress of 44 ksi and a minimum tensile strength of 62 ksi. Based on the test results, Butler and Kulak concluded that the increase in loading angle improved the strength yet reduced the weld deformation capacity. Hence, an empirical equation was developed to predict the load capacity as a function of the direction of the applied load to the weld axis,

$$R_{ult} = \frac{10 + \theta}{0.92 + 0.0603\theta} \qquad [2.1]$$

where R_{ult} is the predicted capacity of a fillet weld of orientation θ (expressed in degrees) given in kips/inch. Another empirical equation was also proposed to predict the loads versus deformation response for various loading angles. This equation is described as the follows:

$$\Delta_{\max} = 0.225(\theta + 5)^{-0.47} \quad [2.2]$$

$$R = R_{ult}(1 - e^{-\mu\Delta})^{\lambda} \quad [2.3]$$

$$\mu = 75e^{0.0114\theta} \quad [2.4]$$

$$\lambda = 0.4e^{0.0146\theta} \quad [2.5]$$

Equation 2.2 defines the ultimate deformation of fillet welds (in inches) as a function of the angle θ between the line of action of the applied force and the axis of the weld. The relationship between the weld force R (kips/inch) and deformation Δ is given by Equation 2.3. The constants μ and λ are regression coefficients used to fit Equation 2.3 to test data.

2.2.2 Lesik and Kennedy (1990)

Lesik and Kennedy (1990) extended the work of Miazga and Kennedy (1989). They formulated a simplified version of the strength equation by using the method of instantaneous center (IC) of rotation to calculate the strength of fillet welds loaded eccentrically in-plane in various directions and proposed a load versus deformation relationship for welds loaded at an angle θ to the axis of the weld of the following form:

$$R_{\theta} = 0.60F_{EXX}A_w\left(1.0 + 0.5\sin^{1.5}\theta\right)f(\rho) \quad [2.6]$$

$$\frac{\Delta_u}{d} = 0.209(\theta + 2)^{-0.32} \quad [2.7]$$

$$\frac{\Delta_f}{d} = 1.087(\theta + 6)^{-0.65} \quad [2.8]$$

$$f(\rho) = 8.234\rho; \quad 0 < \rho \le 0.0325 \quad [2.9]$$

$$f(\rho) = -13.29\rho + 457.32\rho^{\frac{1}{2}} - 3385.9\rho^{\frac{1}{3}} + 9054.29\rho^{\frac{1}{4}} - 9952.13\rho^{\frac{1}{5}} + 3840.71\rho^{\frac{1}{6}}; \quad \rho > 0.0325 \qquad [2.10]$$

$$\rho = \frac{\Delta}{\Delta_u} \qquad [2.11]$$

where in Equation 2.6, R_θ is the load capacity of the fillet weld when loaded at an angle θ to the weld axis, 0.60 is the shear to tensile strength ratio for weld metal, A_w is the weld area calculated at the throat, F_{EXX} is the nominal tensile strength of the filler metal and ϕ is the resistance factor. The equation represents an empirical relationship between the angle of the load and the weld strength and it is shown to have a good agreement with the theoretical relationship developed by Miazga and Kennedy. It gives 50% higher prediction on weld strength when the specimen is subjected to a load in the longitudinal direction than in the transverse direction. Equation 2.7 and Equation 2.8 predict the deformations of the fillet weld at ultimate capacity and fracture, respectively. The deformations have been normalized by the weld size, *d*. Equation 2.9 and Equation 2.10 are used to predict the variation of load as a function of normalized deformation, ρ, taken as the ratio of weld deformation, Δ, to the ultimate deformation, Δ_u, obtained from Equation 2.7. The load versus deformation relationship described by equations 2.9 and 2.10 was obtained using a nonlinear regression analysis of test data. This work of Lesik and Kennedy was recently confirmed by Callele *et al*. (2005).

Figure 2.1 presents the comparison of load deformation curves of specimens loaded at varies angles predicted by Butler & Kulak (1971) and Lesik & Kennedy (1990). When comparing the weld strength of specimens loaded at each angle, the predictions by Butler and Kulak are about 50 percent higher than using the model proposed by Lesik and Kennedy. Figure 2.2 R_θ/R_o for the three different angles of loading predicted by Butler & Kulak and Lesik & Kennedy. By taking the ratio of the weld strength at an angle θ to the strength of a longitudinal weld ($\theta = 0^o$), similar predictions are observed from the two models. Note that both models show that the increase in strength results in a reduction of ductility as the loading direction changes from longitudinal ($\theta = 0^o$) to transverse ($\theta = 90^o$).

2.3 EXPERIMENTAL PROGRAMS ON JOINTS LOADED WITH OUT-OF-PLANE ECCENTRICITY

2.3.1 University of Alberta (Dawe and Kulak, 1972)

A series of eight tests consisting of full-size eccentricity loaded fillet weld connections were tested by Dawe and Kulak (1972) to investigate the behavior of weld groups subjected to shear and out-of-plane bending. The test results were used to validate an analysis procedure presented in section 2.2. Each test specimen was made of a wide

flange section with a 1/2 in. load plate welded to one end. The test end of the specimen was attached to a 3/4 in. reaction plate by one line of a fillet weld along the outer side of each flange. The reaction plate of the test specimen was bolted to the flange of a stub column. A vertical load was then applied to the test specimen through the load plate until failure of the welded joint.

The test variables were: length of weld, load eccentricity and thickness of the connected plate. The nominal weld length for the first six specimens was approximately 8.0 in. and the load eccentricity and the wide flange depth varied from 8 in. to 20 in. and 0.52 in. to 0.76 in., respectively. The weld length for the last two specimens was increased to 12 in. and the plate thickness remained constant at 0.62 in. The load eccentricity was varied from 15 in. and 20 in., resulting in eccentricity ratios (ratio of load eccentricity to weld length) from 1.03 to 2.56. The steel used in the connections was ASTM A36 and all test welds were made with 60 ksi shielded metal arc electrodes with nominal leg dimension of 1/4 in. To ensure weld uniformity throughout the test program, all welding on the specimens was performed by the same welder using electrodes from the same lot. The weld returns on the specimens were later removed to ensure uniform weld lengths. No filler metal material tests were conducted to determine the strength of the weld metal.

2.3.2 Université Laval (Beaulieu and Picard, 1985; Werren, 1984)

Werren (1984) and Beaulieu and Picard (1985) conducted a test program to expand the earlier work of Dawe and Kulak to include test specimens with smaller eccentricity ratios (0.3 to 1.5) than those investigated by Dawe and Kulak. Their experimental program included the testing of 24 specimens. The specimens tested were made up of assemblies consisting of a reaction column with a rectangular plate bracket at each end, representing a total of 24 eccentrically loaded plate connections. The specimens were fabricated using plates with thickness either 0.788 in. or 1.576 in. The weld length, L, used in each specimen was 10 in. and load eccentricities, e, were in the range of 3 in. to 15 in. corresponding to eccentricity ratios, a, of 0.3 and 1.5, respectively. Nominal fillet weld sizes of 1/4 in. and 7/16 in. were used for specimens with plate thickness of 0.788 in. (Type A specimens). Type B specimens consisted of plate thickness of 1.576 in. and nominal fillet weld sizes of 5/16 in. and 3/8 in. The grade of steel used for the plates was not identified, but the results of coupon tests were reported.

In addition to tests on joints with eccentric shear, double lapped splices where tested to determine the strength of welds loaded transverse to the weld axis and parallel to the weld axis. The test specimens made use of 1/4 in. welds of 70 ksi nominal strength and were used to confirm the load versus deformation relationships proposed by Butler and Kulak. No direct material tests were conducted on the weld metal.

2.4 THEORETICAL STUDIES ON ECCENTRICALLY LOADED WELDED JOINTS

A number of theoretical models have been proposed for the prediction of the strength of welded joints subjected to a combination of shear and out-of-plane eccentricity. These

models are briefly reviewed in the following. A detailed description of each model is presented in Chapter 6.

2.4.1 Butler, Pal and Kulak (1972)

A series of 13 tests were conducted by Butler, Pal and Kulak (1972) on eccentrically loaded fillet welded connections to study the behavior of weld groups subjected to a combination of direct shear and moment. Based on the test results, the researcher developed the method of instantaneous center of rotation. It is a theoretical method to predict the ultimate capacity of eccentrically loaded welded connections in which the weld is free to deform throughout its depth. This method contains the parameters of the direction of the applied load and the actual load-deformation response of elemental lengths of the fillet weld. The following assumptions had been made for predicting the ultimate capacities of a fillet welded connection that is eccentrically loaded:

1. All the segments in the weld group rotate about an instantaneous centre of rotation.
2. The deformation which occurs at any point in the weld group varies linearly with the distance from the instantaneous centre and acts in a direction perpendicular to a radius from that point.
3. The ultimate capacity of a connection is reached when the ultimate strength and deformation of any element of weld are reached.
4. The ultimate strength of a fillet weld subjected to a tension-induced shear is equivalent to an identical weld loaded in compression-induced shear.
5. The line of action of the load is parallel to the principal axis of the weld group.

2.4.2 Dawe and Kulak (1972)

Dawe and Kulak (1972) proposed an iterative procedure for determining the ultimate strength of welded joints with out-of-plane eccentricity based on the method of instantaneous centre of rotation earlier developed by Crawford and Kulak (1971) for bolted connections and adapted by Butler, Pal and Kulak (1972) for welded joints with in-plane eccentricity. The empirical relationships of the load versus deformation response of individual weld elements as proposed by Butler and Kulak (1971) were adopted. The approach proposed by Dawe and Kulak is based on the following assumptions:

1. The ultimate capacity of a connection is reached when a critical weld element reaches its ultimate deformation.
2. The load-induced resisting force of each weld element acts through the center gravity of that element.
3. The deformation of each weld element varies linearly with its distance from the instantaneous center and takes place in a direction perpendicular to its radius of rotation.
4. The connecting plates in the compression zone of the connection are in direct bearing at the time when the ultimate load is reached.

5. Although Dawe and Kulak investigated various bearing stress distributions in the compression zone, a linearly variable bearing stress distribution with a maximum stress equal to the yield strength of the plates in bearing was proposed. The proposed model was validated by comparison of predicted strength with the measured capacity of test specimens. A modified version of this model was later adopted by the Canadian Institute of Steel Construction for design of welded joints subjected to shear and out-of-plane bending.

2.4.3 Neis (1980)

Neis (1980) proposed simplified closed-form models in an attempt to find a suitable replacement for the more complex model proposed by Dawe and Kulak (1972). Seven models were developed; all with the maximum stress in the weld assumed to have reached the rupture stress at the extreme fiber on the tension side of the welded joint. The weld capacity was taken as the capacity of a transverse weld ($\theta = 90^o$) as predicted by the model proposed by Butler and Kulak (1971). Various stress distributions were investigated, both in the tension and in the compression zones of the connection.

2.4.4 Beaulieu and Picard (1985)

After a review of the simplified models proposed by Neis (1980), Beaulieu and Picard proposed a simple model that gave good correlation with the more complex model of Dawe and Kulak and the test data from Dawe and Kulak and new test data derived as part of their research program. Although the original prediction model proposed by Beaulieu and Picard was based on the weld metal strength predicted by Butler and Kulak (1971), the proposed model was later adapted to the weld strength predicted by Lesik and Kennedy (1990) (Picard and Beaulieu, 1991). This latter model was adopted by the Canadian Institute of Steel Construction for their current edition of the Steel Design Handbook (CISC, 2006).

2.5 CRUCIFORM JOINTS

The analytical methods presented in the previous section were all based on the assumption that the steel toughness (base metal and weld metal) is adequate to develop the same weld strength in joints with in-plane eccentricity as joints with out-of-plane eccentricity where the primary stress is applied perpendicular to the root notch. However, a study by Ng *et al*. (2002) featured a limited number of specimens with the root notch perpendicular to the direction of loading. A comparison of test results from cruciform specimens with test results from double lapped splice specimens with transverse welds indicated that the strength of fillet welds is affected slightly by the root notch, whereas the ductility is significantly reduced. With reference to welded joints with out-of-plane eccentricity, it is evident that the effect of the weld root notch on all aspects of the load versus deformation response is critical for the accurate characterization of the strength of joints, especially joints subjected to out-of-plane bending.

2.6 CONCLUSIONS

A limited number of test results for welded joints with shear and out-of-plane bending have been conducted by two different sources. Neither sources reported the filler metal material properties. The material properties in both cases were assumed to be similar to those reported by Butler and Kulak (1971) who reported the results of tests conducted on lapped joints to determine the effect of load direction on the strength of fillet welds. A comparison of the weld strength material model proposed by Butler and Kulak (1971) with later results from Lesik and Kennedy (1990) indicated that the model from Butler and Kulak predicts significantly higher strength for all load orientations. The ratio of weld strength at various angles of loading to the longitudinal weld strength is similar for the Butler and Kulak and the Lesik and Kennedy models.

An examination of several prediction models has indicated that although the model presented by Dawe and Kulak (1972) is the most rational since it accounts directly for the load versus deformation behavior of the welds, its complexity makes it difficult to implement in design practice. Several closed form models have been proposed as a replacement to the iterative procedure of Dawe and Kulak. These models present the distinct advantage of being simple to use.

In order to evaluate properly the various strength prediction models for welded joints subjected to combined shear and out-of-plane bending, a direct characterization of the weld metal used for the preparation of the welded joints is required. The effect of root notch size on strength and ductility should be further investigated. The work described in the following includes a detailed investigation of the root notch size effect on cruciform tension joints as well as several tests on joints loaded under combined shear and out-of-plane bending. The material properties of the weld metal used in these tests are established from all-weld metal coupon tests.

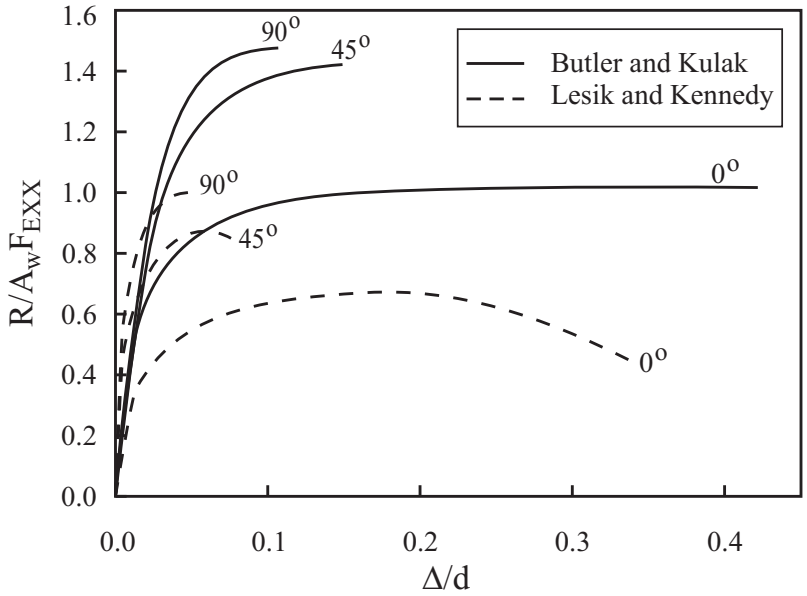

Figure 2.1 – Load versus deformation curves for fillet welds
(Modified from Butler and Kulak 1971 and Lesik and Kennedy 1990)

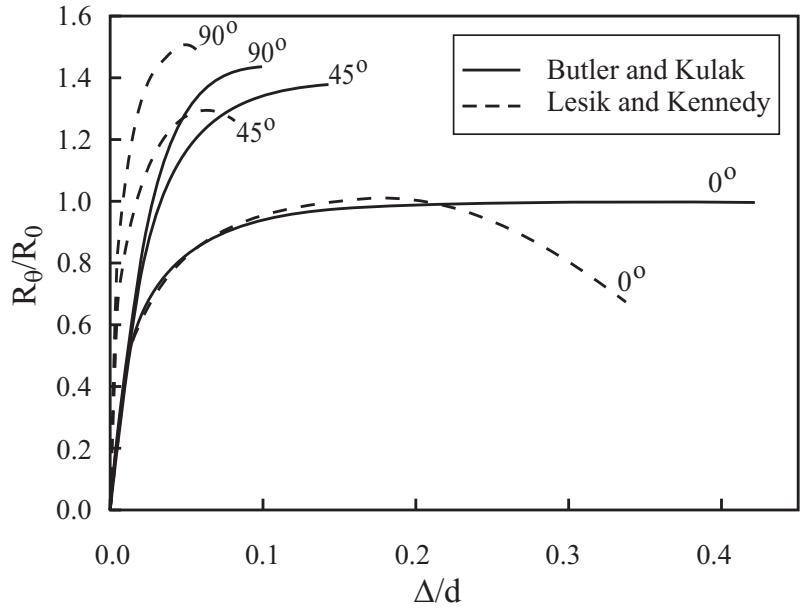

Figure 2.2 – Normalized load verse deformation curves for fillet welds
(Modified from Butler and Kulak 1971 and Lesik and Kennedy 1990)

Chapter 3

Cruciform Tension Experiments, Finite Element Simulations and Ancillary Tests

3.1 INTRODUCTION

As discussed previously, 24 cruciform tension tests were conducted to provide background and benchmark data for the bend tests. In addition to directly evaluating the effect of the weld root notch orientation on the strength of fillet welds, these experiments inform the development of the overall conclusions of this study that are focused on the bend tests that represent fillet weld joints loaded eccentrically out-of-plane. Recall that the development of design tables for eccentrically loaded joints (such as presented in the *Steel Construction Manual*, AISC, 2005) is based on the instantaneous center of rotation method, which relies on prescribed values of weld strength and ductility. In this context, the cruciform tension tests provide basic information about the effect of the root notch orientation on the strength as well as the ductility of welded connections loaded transversely. This Chapter describes the experimental program in detail by providing an overview of the test setup for the cruciform tension tests, testing procedures and fabrication details, while also describing how specimens were measured before and after testing. While key data associated with discussion of test results is presented in this Chapter, complete data for all experiments is provided in Appendices A (Welding Procedures and Specifications), B (Cruciform Specimen Measurements), C (Ancillary Test Data) and D (Tension Test Load Deformation Curves). The variables interrogated within the cruciform fillet weld tension specimens include two types of weld electrodes, two root notch lengths and two weld sizes, with three replicates of each parameter set. To compliment the cruciform tests as well as the bending tests (described later in Chapter 4), several sets of ancillary tests were conducted, including standard material tests on base metal and all-weld tension coupons. Charpy V-Notch (CVN) impact tests and spectrochemical analyses were also conducted for both electrodes and are outlined in this Chapter. The test procedures, results and a summary discussion of the tension experiments are also presented in this Chapter. In addition to the experiments, a series of fracture mechanics-based finite element simulations was conducted to examine the generality of the trends that were observed experimentally. This Chapter provides a brief summary of the simulation results as well.

3.2 FILLER METAL CLASSIFICATIONS

Two filler metals were selected for this study: E70T-7 (no toughness rating) and E70T7-K2 (toughness rated as defined by AWS A5.29 [AWS, 2005]). The electrodes used were Lincoln Electric NR-311 and toughness rated NR-311Ni. Data from the current research on cruciform specimens can be directly compared with data collected by Ng *et al.* (2002)

on lapped splice specimens since similar electrode classifications were tested in both studies. Material properties for the electrodes were determined via ancillary tests described in Section 3.4 and are presented in Tables 3.1, 3.2 and 3.3. Standard welding procedures and specifications were used for all tests; details of the electrodes and welding procedures are summarized in Appendix A.

3.3 BASE METAL TYPE

All connection plates used for the cruciform tests were ASTM A572 Grade 50 steel. Under nominal strength calculations, plates were sized to remain elastic during loading. Two plate thicknesses were used for the large outer plates, effectively changing the root notch length. The center plate dimensions were identical for all test specimens. Base metal material properties, determined via ancillary tests described in Section 3.4, are presented in Table 3.1.

3.4 ANCILLARY TESTS

To characterize material properties and support the cruciform tests (described in subsequent sections), three types of ancillary investigations were conducted: (1) Standard base metal and all-weld tension coupon tests, (2) Charpy V-Notch impact tests and (3) Spectrochemical analyses.

3.4.1 All-Weld and Base Metal Tension Coupons

To characterize material properties, four all-weld tension coupons (two for each electrode) were tested in accordance with AWS A5.20 (AWS, 2005). In addition, two base metal tension coupons were tested in accordance with ASTM E8 (ASTM, 2004). The coupon geometry for both types of tests is detailed in Figure 3.1. The all-weld coupons were extracted from a two-plate assembly as shown in Figure 3.2, fabricated in accordance with AWS A5.20 (AWS, 2005). Results from these tests are summarized in Table 3.1. Ductility is expressed in terms of the ratio of pre- to post-fracture cross section diameter d_0/d_f . The corresponding true fracture strains are also included. The mean ultimate strength $F_{u,weld}$ (from quasi-static tests) for both the E70T-7 and E70T7-K2 electrodes is approximately 97 ksi, 39% greater than the specified minimum (70 ksi). As expected, the average ductility d_0/d_f for the toughness rated (E70T7-K2) electrode is greater than the non-toughness rated (E70T-7) weld material (35% greater). Data from the base metal tension coupon tests are also summarized in Table 3.1. The average yield strength $F_{y,base}$ of the two coupons is approximately 55 ksi, 11% greater than the 50 ksi specified minimum for A572 steel. The average ultimate strength $F_{u,base}$ is approximately 72 ksi.

3.4.2 Charpy V-Notch Impact Tests

Two CVN impact tests were conducted for each electrode at three temperatures (-20°F, 70°F and 212°F) in accordance with ASTM E23 (ASTM, 2007) to establish the temperature transition behavior. Figure 3.2 details the extraction of CVN test specimens and Figure 3.3 illustrates the specimen geometry. Table 3.2 summarizes the results from

these tests. As expected, the toughness rated E70T7-K2 electrode exceeds the minimum toughness requirements (FEMA, 2000) of 20 lb-ft at -20°F and 40 lb-ft at 70°F. The non-toughness rated E70T-7 electrode does not meet these criteria.

3.4.3 Spectrochemical Analyses

Spectrochemical analyses were conducted on weld pads deposited in accordance with ANSI/AWS5.20 (AWS, 2005) to determine the chemical composition of the welds. Table 3.3 presents data from the spectrochemical analyses of weld pads. Both the electrodes meet ANSI/AWS5.20 (AWS, 2005) requirements, except for the 0.33% (by weight) carbon content in the E70T-7 electrode, which slightly exceeds the 0.30% maximum. The toughness rated E70T7-K2 electrode has a substantially higher nickel and manganese content and a lower carbon and aluminum content as compared to the non-toughness rated E70T-7 electrode.

3.5 CRUCIFORM SPECIMEN PREPARATION

Figure 3.4 schematically illustrates the typical cruciform specimen geometry. As shown, each configuration is comprised of three replicate specimens (nominally four inches wide) cut from an assembly of three steel plates welded together in a cruciform configuration. The length of the root notch was controlled by varying the thickness of the two outer plates. The plates themselves were sized to remain elastic under the nominal maximum calculated forces required to yield the welds. The overall width of the assembly was 13 inches allowing run-on and run-off regions at either end of the assembly to ensure relatively uniform weld dimensions and properties within each specimen. These regions were removed prior to testing.

As discussed earlier, two classifications of weld electrodes were tested, namely E70T-7 and E70T7-K2. One spool of wire was used for each filler metal type to minimize variability in weld properties. All welding was performed using the flux cored arc welding (FCAW) process. Each specimen, as shown in Figures 3.4 and 3.6, had test welds on one side (nominally 5/16” or 1/2”) and reinforced welds on the other to ensure failure on the predetermined test side, thereby minimizing instrumentation. Three weld passes were used for the 1/2” inch welds, while only one pass was used for the 5/16” inch welds. Based on detailed measurements outlined later, variations from nominal weld sizes were observed (see Figure 3.5).

3.6 CRUCIFORM TEST SETUP AND PROCEDURE

Twenty-four cruciform specimens were tested quasi-statically in monotonic tension with a 400-kip Tinius Olsen Universal Testing Machine at University of California, Davis. In addition to standard load measurements, deformation over the shear leg of the test welds was measured with four linear potentiometers photographed in Figure 3.6. The definition of “shear leg” is shown in Figure 3.5. The potentiometers were mounted onto specially developed carts, illustrated in Figure 3.7, to measure displacement in two locations for both test welds. Each potentiometer was mounted onto a unique cart which allowed for the detection of unsymmetrical deformations at the test welds. As indicated in Figure 3.7,

the carts ensure that the deformations were measured only over the shear leg of the weld and not the base metal.

Prior to testing, each specimen was photographed, and the outline of each specimen was traced to examine initial geometry (importantly the lack of alignment of the long outer plates). Detailed measurements were conducted to examine the weld geometry before fracture. These are described in the next section. All test specimens were loaded in displacement control, such that in the elastic range, the load was applied at an average rate of 0.16 kips/second (averaged with respect to all tests). Load rates for individual tests are summarized in Table 3.4. In this context, recall that since these are not standard tension tests, it is difficult to interpret standard specifications for testing rates, which are typically expressed in terms of strain rates (which may be expressed conveniently only for homogenously strained specimens such as cylindrical tension specimens). However, based on previous experiments conducted by Ng *et al.* (2002), these loading rates may be considered approximately quasi-static.

Qualitatively, each test exhibited a similar response including an initial elastic loading, a period of strain hardening, followed by fracture (representative load-deformation plot shown in Figure 3.8). Fracture typically initiated in one of the test welds, followed almost immediately by fracture in the other test weld. Some of the specimens suffered from an initial skewed angle (lack of straightness) introduced during specimen fabrication. For some tests, this led to slightly unsymmetrical behavior as the specimen straightened under tensile loading. Similar behavior was also observed by Ng *et al.* (2002). Measurements in Appendix B documents this initial skewed angle. The maximum initial skewed angle was measured to be 8° on test assembly #8, i.e. tests numbered 22, 23, and 24. Note that the response of Test #23 shows significant initial unsymmetrical response. After failure of the test welds, specimens were photographed again in detail, and post-fracture measurements (explained in Section 3.7.2) were conducted.

3.7 MEASUREMENTS

To enable a more effective interpretation of test data, and to eliminate bias in the evaluation of design formulas due to variations in weld geometry, detailed measurements were carried out on all the welds. Measurements for all test specimens are included in Appendix B. This section describes the measurement process, and serves as commentary for Appendix B.

3.7.1 Pre-Fracture Measurements

Prior to testing, dimensions of the base metal plates and test welds were measured on all of the twenty-four cruciform specimens. Pre-fracture measurements are archived in Appendix B. A fillet weld gage (photographed in Figure 3.9) was used to measure the throat thickness, shear leg length and tension leg length of all test welds (illustrated in Figure 3.10). For the 1/2" welds, two additional measurements were made along the profile, referred to as the "upper" and "lower" thicknesses (see Figure 3.10). All weld lengths and base metal thicknesses were measured using digital calipers, whereas the weld thicknesses and throats were measured using a weld gage with a tolerance of 0.015

inches (see Figure 3.9). All these measurements were made at nine locations along the length of each weld. "Upper" and "lower" measurements (see Figure 3.10) for four specimens, i.e. Test #1, Test #2, Test #3, and Test #7 were not measured prior to testing. These dimensions were obtained from the traced outline of the specimens.

3.7.2 Post-Fracture Measurements

Figure 3.11 shows a representative fractured surface of a test specimen. After testing, measurements were conducted on the fractured welds in nine locations along the length of the weld using digital calipers. These dimensions are illustrated in Figure 3.12 and archived in Appendix B. As indicated in the Figure, four measurements were acquired: (1) root notch length (outer plate thickness), (2) failure surface angle, (3) tension leg length and (4) width of the fracture surface. The failure angle was measured using a similar protractor as shown in Figure 3.13.

3.8 RESULTS OF CRUCIFORM TESTS

Results of the cruciform tests are summarized in Table 3.5. This Table includes various measured and experimental quantities: (1) theoretical throat area (A_{throat}), (2) maximum observed force ($P_{\max}$), (3) deformation at fracture ($\Delta_{fracture}$) and (4) maximum predicted force (P_u). For convenient interpretation of test data, Table 3.5 also includes the ratio between the experimental and predicted force for each specimen ($P_{\max}/P_u$). Since, for most tests, the maximum force was reached after both test welds were fully yielded, the total force and total weld area (test welds on both sides of the plate) are used to calculate $P_{\max}$. The predicted weld capacity P_u is calculated as per Equation 3.1 (adapted from AISC, 2005):

$$P_u = 2 \times 1.5 \times 0.6 \times F_{u,weld} \times A_{throat} \qquad [3.1]$$

where $F_{u,weld}$ is the measured ultimate strength of the weld material (given in Table 3.1) and A_{throat} is the theoretical area of the weld throat, calculated as follows:

$$A_{throat} = L_{weld} \times \frac{1}{\sqrt{(1/L_{shear})^2 + (1/L_{tension})^2}} \qquad [3.2]$$

where L_{shear} is the average measured shear leg (averaged from all the measurements along the length), $L_{tension}$ is the average measured tension leg and L_{weld} is the average measured length of the weld (typically within 0.1 inch of the nominal specimen width of 4 inches). The factor of 2 accounts for two welds contributing to the strength of the connection and the 1.5 factor reflects a 50% increase in strength for transverse welds, as predicted by Equation 3.3 (adapted from Lesik and Kennedy, 1990):

$$V_\theta / V_0 = 1 + 0.50 \sin^{1.5} \theta \qquad [3.3]$$

where θ is the angle of loading (relative to the axis of the weld) and V_θ, V_0 is the ultimate strength of a fillet weld loaded in shear at θ and $\theta = 0°$, respectively. For

transverse loading (i.e. for the tension tests), $\theta = 90^\circ$. The 0.6 factor relates tensile material strength to shear material strength. It is important to emphasize that the capacity P_u is determined based on measured (rather than specified) weld dimensions and properties. This offers a more meaningful interpretation of the data by eliminating bias due to either larger (or smaller) than specified weld sizes or material overstrength. While this estimate does not include the effects of weld root penetration or the shape of the weld profiles (see Figure 3.5), it is consistent with the way the welds are designed. Alternative estimators of capacity (e.g. based on post-fracture measurements of the fractured area) were considered as well. While these methods may more accurately represent the true fracture surface dimensions (for example, root penetration), they have disadvantages. In particular, they might not be conveniently applied to assess the effectiveness of design equations. For completeness, test-to-predicted ratios based on these post-fracture throat measurements are provided in Table 3.6. From the Table, it is apparent that on average, these ratios are smaller (0.86) as compared with ratios based on pre-fracture measurements (1.04) summarized in Table 3.5. These are not analyzed further in this report, since they are not directly relevant to the design process, but are provided for further analysis by other researchers.

Fracture deformation $\Delta_{fracture}$ is reported in Table 3.5 for the test weld that fractured first. An examination of the load-deformation curves for all the potentiometers reveals which weld fractured first. For some tests, due to unsymmetrical response (attributed to the straightening phenomenon as described above), one weld is observed to be initially loaded in compression until the specimen straightens. After this point, both welds are loaded in tension. Thus, for some tests, one weld accumulates significantly larger tensile deformations and fractures first. The mean of the two linear potentiometer measurements for this weld represents deformation for the weld. Figure 3.8 illustrates the measurement of $\Delta_{fracture}$ from one of the experimental load deformation curves. Figure 3.8 includes deformation data only from the weld that fractured first.

If $P_{\max} / P_u$ (shown in Table 3.5) has a value greater than 1.0, the design formula is conservative since it predicts a smaller weld strength than is observed experimentally. To maximize weld efficiency, the most desirable specimen set would have a predicted capacity very close to the test capacity (mean test-to-predicted ratio very close to 1.0 with a coefficient of variation very close to 0.0).

3.9 DISCUSSION OF CRUCIFORM RESULTS

In this section, results from the tension tests are compared to both previous research and current design codes used to predict the strength and ductility of welded connections.

3.9.1 Effects of Root Notch Length on Connection Strength

To compare the results of the cruciform tension tests of this study with other similar test programs, the ratio of the test-to-predicted capacity for specimens with various nominal root notch sizes are compared with the test results reported by Pham (1983) and Ng *et al*. (2002) in Table 3.7. For a description of these test programs, refer to the literature review in Chapter 2. An examination of Table 3.7 indicates that the ratio of experimental weld

strength to predicted weld strength decreases as the root notch length increases. The tension tests presented in this paper are representative of test specimens with a longer root notch compared to other test programs. The coefficients of variation (COV), listed in the last column of Table 3.7, seem to indicate a slightly lower COV as the root notch length increases. Figure 3.14 shows a plot of predicted capacity versus test capacity for all available cruciform tension test results. The solid line represents where the predicted and observed capacities are equal. The data points on Figure 3.14 indicate that most of the specimens tested have a capacity greater than the capacity predicted by Equation 3.1. Test results from the UC Davis experimental program are consistent with the results from other experimental programs.

Since a major focus of this paper is to investigate the effect of root notch length on weld strength, Figures 3.15a and 3.15b plot the ratio $P_{\max} / P_u$ for all the current tension tests against the specified root notch length (outer plate thickness). Figure 3.15a includes data for all the non-toughness rated welds (E70T-7), whereas Figure 3.15b includes data for all the toughness rated welds (E70T7-K2). Figure 3.15 also includes additional data points that are generated through finite element simulations of specimens with longer notch lengths. However, the discussion in this section is restricted to the experimental results only. The next section addresses the simulation results. Referring to the experimental data points on Figures 3.15a and 3.15b, and to Table 3.5, several key observations can be made:

- For most specimens, $P_{\max} / P_u$ values are slightly greater than 1 (average 1.04 for all tension tests), indicating that, on average, the design formulas predict weld strength with good accuracy.

- For the (E70T7-K2) toughness rated welds, $P_{\max} / P_u$ is typically greater than 1.0 (average = 1.1) for both the root notch lengths (i.e. the prediction is conservative).

- For the E70T-7 welds, the average $P_{\max} / P_u$ ratio is slightly less than 1.0 (average = 0.98). Given that the standard deviation of $P_{\max} / P_u$ is approximately 0.1, this does not indicate a significant unconservatism.

- For both weld classifications and sizes (within the range tested), no significant trend is observed with respect to the root notch length.

- Thus, experiments indicate that current weld strength design equations (AISC, 2005) can predict welded connection strength capacities with reasonable accuracy even in the presence of a crack-like root notch defect. The degree of conservatism of the equations is slightly reduced for the non-toughness rated welds.

3.9.2 Effects of Root Notch Length on Connection Ductility

Figures 3.16a and 3.16b show the normalized fracture deformations of the welds versus the root notch length. Similar to Fig. 3.15, the data points include experimental and simulated data points. The weld deformations are normalized by the average measured length of the shear legs (L_{shear}) which is representative of the "gage-length" of the weld

being loaded. Recall that these deformations are reported for the test weld that fractured first. If we restrict our discussion to the experimental data points in Figures 3.16a and 3.16b, it is obvious that the toughness rated E70T7-K2 electrode (Figure 3.16b) is more than twice as ductile (on average) as compared to the non-toughness rated E70T-7 electrode (Figure 3.16a). As root notch length is increased, the 1/2 inch welds (both weld classifications) exhibit a slight decrease in ductility. On the contrary, as root notch length is increased, the 5/16 inch welds (both weld classifications) exhibit a slight increase in ductility. Other than experimental randomness, there is no readily available explanation for this unexpected behavior. However, one may speculate that other factors including local heterogeneities in the welds, the shape of the weld profile or the bluntness (or sharpness) of the root notch (due to fabrication procedures) affect the ductility of the welds.

To determine the design strength for eccentrically loaded welded joints (using the instantaneous center of rotation method), the *Steel Construction Manual* (refer to Part 8 of AISC, 2005) provides a formula to estimate the ductility of fillet weld elements. This formula, adapted from the work of Lesik and Kennedy (1990) takes the following form:

$$\Delta_{fracture} / w = 1.087\left(\theta + 6\right)^{-0.65} \leq 0.17 \qquad [3.4]$$

where w is the weld size (comparable to the length of the shear leg (L_{shear}) in the context of this report) and θ is the angle between the loading direction and weld axis in degrees (90° for transverse welds). It is important to note that this equation was obtained from tests on lapped splice type specimens. As per this equation, the ductility of transverse fillet welds may be expressed as $\Delta_{fracture} / w = 0.056$. Referring to Figures 3.16a and 3.16b, it is apparent that the toughness rated E70T7-K2 specimens exhibit an average normalized fracture deformation (0.094) almost twice this value. On the other hand, the non-toughness rated E70T-7 specimens exhibit an average normalized fracture deformation (0.042) 25% less than the value predicted using Equation 3.4.

3.10 FINITE ELEMENT SIMULATIONS TO GENERALIZE TEST RESULTS

An important observation from the cruciform tests is that for the range of root notch lengths tested in this study, the weld strengths are not significantly affected. However, for smaller notch lengths, such a trend is observed by Pham (1983). In fact, for most of the cruciform weld tests, fracture occurs well after the welds are fully yielded and have reached their ultimate load (see Fig. 3.8). Thus, a small change in weld ductility will not affect the strength, since the failure point still lies on the "plateau" of the load versus deformation curve. However, one may speculate that for notch lengths significantly larger than those tested, the ductility may be reduced to the point that the strength is also affected. Moreover, the ductility itself features in the strength calculation of eccentrically loaded joints. In response to these questions, the main objective of the FEM simulations presented in this section is to generalize the test data investigating the effect of additional (larger) root notch lengths on weld strength and ductility.

The first step in the simulation process is to develop and validate a methodology that can be applied with confidence to extrapolate the test results. This is somewhat challenging, given the irregular shapes of the weld profiles (see Fig. 3.5) and the need to accurately calibrate the material constitutive response. The second step of the process involves comparing the models to experimental results to calibrate the fracture toughness of the various electrode classifications. The fracture toughness is expressed in terms of a critical J-integral, J_{IC}. In the final step, the validated methodology with calibrated estimates of the fracture toughness is applied to extrapolate the experimental findings to configurations with untested root notch lengths.

3.10.1 Development of FEM Models and Calibration of Fracture Toughness Values

Referring to the preceding discussion, the FEM models should represent the weld geometry with reasonable accuracy. As previously shown in Fig. 3.5, the weld profiles for all the tests are somewhat irregular and vary along the length of the welds. Recognizing the subjectivity in simulating other parameters (such as material properties and fracture toughness), it is difficult to justify simulating the full, irregular weld profile in three dimensions. Consequently, an approach that balances economy with accuracy was adopted. In this approach, for each test assembly (i.e. the three replicates for each test parameter set), a representative two-dimensional geometry was developed to reflect the mean weld profile of that test assembly. Figure 3.18 shows an example of a FEM mesh (developed in ABAQUS, 1998) based on the mean weld profile for Tests #1-3 (1/2 inch welds, 1.25 inch root notch). Figure 3.18 illustrates the dimpled shape of the multi-pass weld illustrated earlier in Fig. 3.5b. Similar profiles were developed for all simulations.

Referring to Fig. 3.18, the finite element simulations consist of a two-dimensional plane-strain model. Taking advantage of symmetry, only one quarter of each specimen was modeled. The FE meshes for the various welds consist of approximately 4000 8-node quadrilateral elements. As shown in Fig. 3.18, the mesh in the root notch region is suitably refined to accurately simulate the stress and strain gradients in the region, such that the elements are approximately 0.002 inches in size. The notch tip itself is modeled with a finite radius of 0.004 inches to facilitate numerical aspects of the simulation, recognizing that the root notch is not a perfectly sharp crack. Since this radius is much smaller than the anticipated crack tip blunting at fracture (about 0.01 inches), it does not affect the final results. All the finite element models incorporate large-deformations and isotropic von Mises plasticity. Hardening properties are based on uniaxial stress and strain data obtained from material tension coupons on the weld metal and base metal.

Eight finite element models were constructed, each based on the mean weld profile of the corresponding test assembly. Tensile loading in the form of displacement boundary conditions was applied to the FEM models and displacements were monitored at the toe of the welds (at the end of the shear leg) for consistent comparison with the experimental deformation data from the potentiometers. Since each test assembly corresponds to three replicate tests, the FEM simulation for every model was conducted thrice, each time

pulled in tension until the fracture displacement of the corresponding replicate test ($\Delta_{fracture}$ - see Table 3.5) was reached. At this point in the loading history, the contour J-integral was calculated by integrating stresses and strains over 20 contours around the crack tip. The J-integral calculated at the fracture displacement was retained as the fracture toughness capacity J_{IC} for the particular test. This process is repeated for all the tests to generate J_{IC} values for all the electrode classifications.

This method for determining the fracture toughness J_{IC} is not as precise as standard fracture mechanics test methods (e.g. ASTM E-1820, 2002). However, the standard methods rely on highly specific specimen geometries (such as compact tension or three-point bend specimens), often requiring large groove welds in the fracture region. Results from these tests may be difficult to generalize to fillet welds that may have different toughness properties. These issues, coupled with the expense of standard fracture tests justify the simplified method for determining fracture toughness, especially when the results are interpreted mainly in a qualitative sense.

Table 3.8 summarizes the average J_{IC} values for all the weld types and weld sizes. These J_{IC} values are comparable to values for welds reported by other researchers (Chi, 2000). Also included in Table 3.8 are the coefficients of variation (COV = $std\ dev / mean$) for all the J_{IC} values. The coefficients of variation for the every weld type and size are relatively low, indicating fairly consistent J_{IC} values. The J_{IC} values were determined for a given electrode classification (E70T-7 or E70T7-K2) and weld size, rather than simply the electrode classification, mainly because the larger 1/2 inch weld is a multi-pass weld where the tempering effect of the subsequent passes may toughen the material near the notch tip. However, this effect is observed only for the E70T-7, where the 1/2 inch weld shows a marginally greater toughness (J_{IC}) as compared to the smaller 5/16 inch weld. As expected, the J_{IC} values for E70T7-K2 are more than two times larger than those for the E70T-7. The final step in the FEM simulations involves applying the calibrated J_{IC} values to extrapolate the findings of the cruciform tests. This is the topic of the next section.

3.10.2 Generalization of Test Results using Validated Simulation Methodology and Calibrated Material Toughness

Based on the calibrated J_{IC} values and the modeling methodology, additional simulations were conducted to investigate the effect of the larger root notch length on the strength and ductility of the welds. For each weld size and electrode classification, two additional simulations were conducted with larger root notch lengths (3.5 inch and 5.0 inch). All these simulations were similar to the previously described simulations in terms of the meshes and material properties. For each simulation, the mean weld profile corresponding to the respective weld size and type is modeled.

Tensile loading is applied to all the simulation models. In addition to the force-displacement response, the J-integral is monitored at every loading increment. Similar to the calibration analyses, the J-integral is calculated based on 20 contour integrals evaluated around the crack tip. For each simulation, fracture is predicted to occur when the J-integral first exceeds the critical value J_{IC} for that particular weld size and type

(summarized in Table 3.8). The force and displacement corresponding to this instant in the loading history are recorded as the peak force and fracture displacement, respectively.

Based on these simulations, Figs. 3.15a and 3.15b (described previously) plot the normalized simulated strength along with the experimental values, while Figs. 3.16a and 3.16b plot the simulated fracture displacement (normalized with respect to the shear leg used in the simulation). Referring to the figures, including both the experimental and simulated data points, two key observations may be made:

- The larger simulated root notch lengths (3.5 inch and 5.0 inch) do not adversely affect the strength capacities as compared to the experimentally observed capacities. This trend is consistently observed for all weld types and weld sizes – see Figs 3.15a and 3.15b.

- A similar trend is observed for the weld fracture deformations as well, such that for both weld classifications the larger root notch sizes (3.5 inch and 5.0 inch) do not have a significant impact on the ductility – see Figs. 3.16a and 3.16b.

For the E70T7-K2 weld, even the larger notch lengths show ductilities well in excess of the 0.056 value typical of welds in lapped joints. However, for the E70T-7 weld, the simulated ductilities are somewhat lower (25%) than this value.

In summary, the simulation results corroborate the general experimental finding that neither fracture strength nor ductility are severely affected by increasing the length of crack-like root notch in the welded connections. Although this observation is reassuring from a design safety standpoint, it is worthy of some examination. Thus, it is informative to discuss the effect of the root notch length on fracture toughness demand (in this case, the J-integral) observed in these connections. An examination of the fracture mechanics simulation data indicates that for larger root notch lengths (approximately greater than one inch), the J-integral values (representative of the stress state at the notch tip) saturate, such that the incremental effect of notch length on toughness demand is smaller for the longer notches. In this context, the notch lengths for cruciform specimens investigated in this study are all relatively long, such that for a given deformation, an increase in notch length does not significantly increase the fracture toughness demand. For smaller notch lengths (approximately less than one inch), the J-integral reduces with respect to the notch length, suggesting a stronger dependence of ductility on the notch length in this range. Although the testing program presented in this paper does not encompass this range, Table 3.7 supports this observation when other testing programs (with smaller notch lengths) are included. Moreover, recent research by Woo *et al.* (2004) indicates that in relatively ductile weld details where significant yielding is present (similar to the cruciform specimens), the fracture toughness demand for a given imposed load or displacement is not significantly affected by the crack length. This is corroborated by Murakawa *et al.*'s (1998) study where the strength and fracture ductility of pre-cracked welded joints is reported to be insensitive to the crack length.

The preceding discussion provides an explanation of the experimental as well as the simulation data, and the apparent insensitivity of the weld strength and ductility to the

root notch length. The welds investigated experimentally in this study are ductile welds with relatively long notches, such that the stress-strain conditions at the notch tip (quantified by the J-integral) are already severe. Consequently, for a given displacement, increasing the notch length does not exacerbate conditions from a fracture perspective; i.e. the notch length does not diminish ductility any further. Even under this situation, fracture occurs significantly after the welds have been fully yielded, and so the strength is controlled by yielding of the welds rather than by fracture. Based on this rationale, this trend is expected to remain valid for larger notch lengths, such that neither the strength nor ductility will be affected. For smaller notch lengths (approximately less than one inch), the ductility will likely increase (given the reduced toughness demand in this range), but the strength, controlled by yielding itself, will likely not be affected.

3.11 FRACTOGRAPHIC STUDIES

A visual inspection of the fractured specimens (such as that shown in Figure 3.11) indicates that most specimens showed some initial crack growth (approximately 0.04-0.08 inches) in the direction of the root notch before the subsequent shear-type fracture led to complete failure. In addition to routine visual inspections, some fractured specimens were examined under a scanning electron microscope to determine the modes and mechanisms of fracture initiation and subsequent propagation. Figures 3.17a-c show photomicrographs from one such specimen (Test #16, 1.25 inch root notch, 5/16 inch toughness rated weld). Typically, fracture initiated in a ductile manner exhibiting classic microvoid growth and coalescence type fracture surfaces. Figure 3.17a shows a photomicrograph in this initiation region very close (< 0.02 inches) to the edge of the weld root notch. Figure 3.17b shows the transition region between the ductile initiation and brittle cleavage at about 0.02-0.04 inches from the edge of the root notch. Finally, after about 0.04-0.08 inches of crack extension in the direction of the root notch, the fracture transitions to a shear type rupture at an angle to the tension leg (between 20-80 degrees), thereby severing the weld. Figure 3.17c shows elongated microvoids in the shear rupture zone. A similar consistency in the initiation of the fracture in the direction of the root notch was observed during previous research (Ng *et al.*, 2002), wherein the fracture initiated and propagated at various angles between 0 and 90 degrees. The severe stress concentration produced by the notch in this study would favor Mode I (crack opening mode) type fracture initiation straight ahead of the crack-like defect. In fact, this validates the use of the Mode I J-integral for the fracture mechanics analyses.

3.12 SUMMARY OF OBSERVATIONS FROM CRUCIFORM TESTS

Current design equations of transverse fillet welds do not explicitly address the effect of the root notch orientation. The vast majority of the test data upon which the equations are based were obtained from tests on lapped splices where the root notch is parallel to the applied load. This Chapter presents data from 24 cruciform tests and ancillary tests to investigate the effect of the weld root notch on strength and ductility of the welded connections. The cruciform tension tests feature fillet welds with two different root notch lengths (1.25 inch and 2.5 inch), and two different electrode classifications (non-toughness rated E70T-7, and toughness rated E70T7-K2). Two weld sizes (single pass

5/16 inch and a multi-pass 1/2 inch) are considered. Three replicate tests are conducted for each parameter set.

The experimental results indicate that the strength of the welds is not significantly affected by the root notch length. However, an examination of test results from other sources with root notch lengths shorter than those investigated here indicates that root notch length may have an effect on the strength of welds. On average, the AISC (2005) design equation predicts the strength of the connection with good accuracy for all the weld sizes and electrode classifications investigated. The design equations are slightly more conservative for the toughness rated welds as compared to the non-toughness rated welds. The ductility of the welds does not show a strong dependence on the root notch length. However, for the E70T-7 electrode, the observed ductility is lower compared to the code-based estimate of ductility, which is used to develop design charts for eccentrically loaded joints.

A finite element based fracture mechanics study was conducted to generalize the experimental results for larger root notch lengths. The first phase of the analytical study involves running simulations corresponding to the tested specimens to calibrate the fracture toughness parameter (J_{IC}) for the different weld types and sizes. Based on the calibrated fracture toughness, additional simulations with longer root notch lengths (3.5 inch and 5.0 inch) were conducted to examine their response. The simulations indicate that even for the longer notch lengths, neither the strength nor the ductility is diminished further. This trend is explained based on a closer examination of the simulated fracture mechanics data, which suggests that the fracture toughness demand (J-integral) saturates with respect to the notch length, such that increasing the notch length beyond a certain limit ($\approx$ 1.0 inch) does not increase the toughness demand any further. Thus, for cruciform welded connections under tensile loading with large (approximately greater than one inch) root notch lengths, response is relatively insensitive to root notch length.

The findings of the testing and simulation program are encouraging, especially when assessing the applicability of current design approaches for the tensile strength of transverse fillet welds. The lower ductility (for the non-toughness rated welds) may affect design strength of eccentrically loaded joints subject to out of plane bending. However, an assessment of the applicability of design charts (AISC, 2005) for eccentrically loaded joints cannot be presented only on the basis of the cruciform tension test and simulation data. Subsequent Chapters 4 through 7 address this issue in detail. These Chapters consider a range of experimental data on welded connections eccentrically loaded out of plane. Sixty experiments are conducted as part of this study (described in Chapter 4). Based on a collection of all the experimental data (Chapter 5), and a reliability analysis (Chapter 6), conclusions are presented with respect to eccentrically loaded connections (in Chapter 7) and improved design charts are developed (Appendix I).

Table 3.1 – Basic Material Properties from Standard Tension Coupons

Material	Test	F_y[1] (ksi)	F_u[2] (ksi)	d_o/d_f	ε[3]
E70T-7 Weld	**1**	75.8	97.1	1.35	0.60
	2	76.8	97.2	1.15	0.28
	Mean	**76.3**	**97.1**	**1.25**	**0.44**
E70T7-K2 Weld	**1**	82.7	97.5	1.65	1.00
	2	83	97.4	1.74	1.11
	Mean	**82.8**	**97.4**	**1.69**	**1.05**
Base Metal (A572 Grade 50)	**1**	54.2	71.4	2.13	1.52
	2	57.1	71.8	2.08	1.46
	Mean	**55.7**	**71.6**	**2.11**	**1.49**

[1]Measured yield stress, based on 0.2% offset method; static value
[2]Measured ultimate strength; static value
[3] $\varepsilon = \ln\left(d_0 / d_f\right)^2$ = average true fracture strain across necked cross section of tension coupon

Table 3.2 – Results from Charpy V-Notch tests

Filler Metal	Test	CVN Energy (lb-ft)		
		-20°F	**70°F**	**212°F**
E70T-7	**1**	5.5	19.0	41.0
	2	6.0	18.0	41.0
	Mean	**5.75**	**18.5**	**41.0**
E70T7-K2	**1**	30.0	56.0	88.0
	2	23.0	62.0	88.0
	Mean	**26.5**	**59.0**	**88.0**

Table 3.3 – Chemical Composition of the Filler Metals (% by weight)

Filler Metal	Al	C	Cr	Cu	Mn	Mo	Ni	P	Si	S
E70T-7	1.74	0.33	0.02	0.02	0.37	0.01	0.01	0.006	0.08	0.005
E70T7-K2	1.16	0.08	0.03	0.03	1.27	0.02	1.68	0.009	0.24	0.005

Table 3.4 – Loading Rates for Cruciform Tension Tests

Test Number	Average Elastic Loading Rate (kips/second)
1	0.05
2	0.04
3	0.10
4	0.11
5	0.09
6	0.12
7	0.09
8	0.13
9	0.12
10	0.23
11	0.12
12	0.10
13	0.12
14	0.12
15	0.20
16	0.08
17	0.36
18	0.06
19	0.11
20	0.24
21	0.60
22	0.12
23	0.20
24	0.22

Table 3.5 – Test Matrix and Summary of Experimental Data from Cruciform Tension Tests

Test	Filler Metal	Weld Size[1] (inches)	Root Notch[2] (inches)	A_{throat}[3] (in^2)	P_u[4] (kips)	P_{max}[5] (kips)	P_{max}/P_u	$\Delta_{fracture}$ (inches)	$\Delta_{fracture}/L_{shear}$[6]
1	E70T-7	1/2	1.25	3.04	266.1	272.8	1.025	0.028	0.042
2				3.58	312.9	275.3	0.880	0.046	0.065
3				3.34	292.1	277.7	0.951	0.041	0.060
4		5/16	1.25	1.99	173.9	196.7	1.131	0.016	0.036
5				2.16	189.0	196.0	1.037	0.018	0.038
6				2.42	211.1	205.8	0.975	0.013	0.026
7		1/2	2.50	3.37	294.5	270.3	0.918	0.024	0.030
8				3.30	288.6	309.4	1.072	0.033	0.042
9				3.78	330.8	297.9	0.901	0.028	0.031
10		5/16	2.50	2.13	186.4	138.6	0.744	0.022	0.047
11				1.93	168.7	189.2	1.122	0.026	0.053
12				1.95	170.8	182.1	1.066	0.018	0.036
13	E70T7-K2	1/2	1.25	3.63	318.2	324.1	1.018	0.053	0.077
14				3.57	312.8	344.0	1.100	0.076	0.116
15				3.67	321.5	325.5	1.012	0.05	0.073
16		5/16	1.25	2.14	187.3	206.2	1.101	0.028	0.075
17				2.24	196.5	200.4	1.020	0.058	0.110
18				2.38	208.3	238.0	1.143	0.05	0.103
19		1/2	2.50	3.54	310.6	372.7	1.200	0.063	0.087
20				3.58	313.4	358.0	1.142	0.043	0.058
21				3.24	283.9	342.4	1.206	0.056	0.077
22		5/16	2.50	2.31	202.2	238.6	1.180	0.053	0.120
23				2.44	213.6	225.3	1.055	0.062	0.132
24				2.15	188.5	195.5	1.037	0.052	0.101

1) Specified weld size
2) Based on specified plate thickness (true notch length is slightly different due to root penetration)
3) Based on average *measured* tension and shear leg dimensions, i.e.

$$A_{throat} = L_{weld} \times \frac{1}{\sqrt{(1/L_{shear})^2 + (1/L_{tension})^2}}$$

4) $P_u = 1.5 \times 0.6 \times F_{u,measured} \times A_{throat}$
5) P_{max} = maximum force observed in experiments (including both test welds)
6) Fracture displacement normalized by dimension of weld that fractured first

Table 3.6 – Summary of Experimental Data from Cruciform Tests using Throat Area Based on Post-Fracture Measurements

Test	Filler Metal	Weld Size[1] (inches)	Root Notch[2] (inches)	$A_{throat,fract}$[3] (in^2)	$P_{u,fract}$[4] (kips)	P_{max}[5] (kips)	$P_{max}/P_{u,fract}$
1	E70T-7	1/2	1.25	3.52	341.3	272.8	0.799
2				3.67	356.3	275.3	0.773
3				3.66	355.4	277.7	0.781
4		5/16	1.25	2.19	212.9	196.7	0.924
5				2.70	262.1	196.0	0.748
6				2.27	220.7	205.8	0.933
7		1/2	2.50	3.61	351.0	270.3	0.770
8				3.40	330.6	309.4	0.936
9				3.37	327.7	297.9	0.909
10		5/16	2.50	2.19	212.9	138.6	0.651
11				2.38	230.8	189.2	0.820
12				2.27	220.7	182.1	0.825
13	E70T7-K2	1/2	1.25	3.44	334.6	324.1	0.969
14				3.72	361.9	344.0	0.950
15				3.90	380.3	325.5	0.856
16		5/16	1.25	2.32	225.7	206.2	0.914
17				2.48	241.8	200.4	0.829
18				2.86	278.8	238.0	0.854
19		1/2	2.50	3.52	342.4	372.7	1.088
20				4.33	421.5	358.0	0.849
21				4.16	405.7	342.4	0.844
22		5/16	2.50	2.61	253.9	238.6	0.940
23				2.74	267.0	225.3	0.844
24				2.38	232.1	195.5	0.842

1) Specified weld size
2) Based on specified plate thickness (true notch length is slightly different due to root penetration)
3) Based on average *measured* fracture throat size
4) $P_{u,fract} = 1.5 \times 0.6 \times F_{u,measured} \times A_{throat,fract}$
5) P_{max} = maximum force observed in experiments (including both test welds)

Table 3.7 – Summary of Data from Other Tension Test Programs on Cruciform Specimens

Source	Number of Tests	Root Notch Size (inches)	Test / Predicted	COV
Ng *et al*. (2002)	6	0.75	1.84	0.14
Pham (1983)	12	0.79	1.31	0.14
Pham (1983)	12	1.25	1.20	0.11
UC Davis (2007)	12	1.25	1.03	0.06
Pham (1983)	12	2.00	1.07	0.09
UC Davis (2007)	12	2.50	1.04	0.14

Table 3.8 – Calibrated J_{IC} values for different weld sizes and classifications

Weld classification	Nominal Weld Size (inches)	Average J_{IC} (ksi-in)	COV
E70T-7	1/2	1.17	0.21
	5/16	0.83	0.21
E70T7-K2	1/2	2.32	0.19
	5/16	2.38	0.24

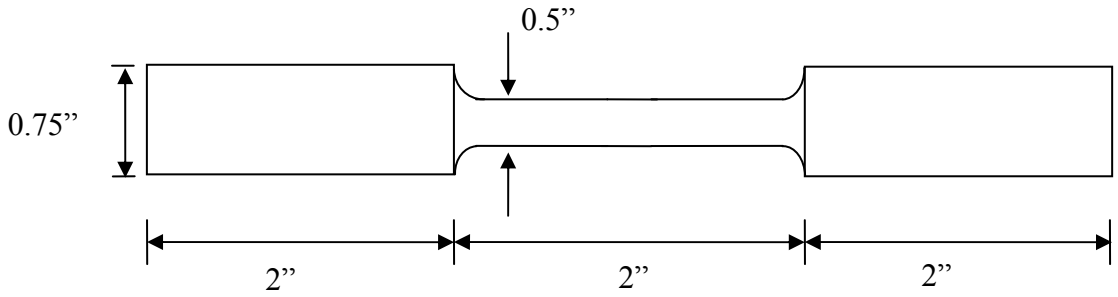

Figure 3.1 – Detail of standard tension all-weld and base metal test coupons

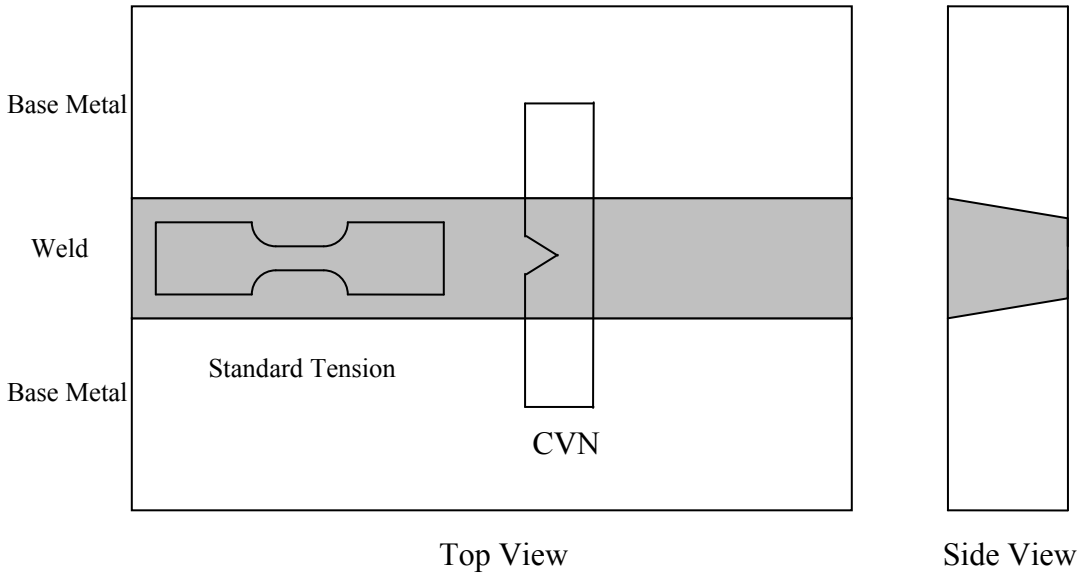

Figure 3.2 – Detail of plate assembly (in accordance with ANSI/AWS5.20) indicating the extraction of all-weld tension coupons and Charpy V-Notch specimens

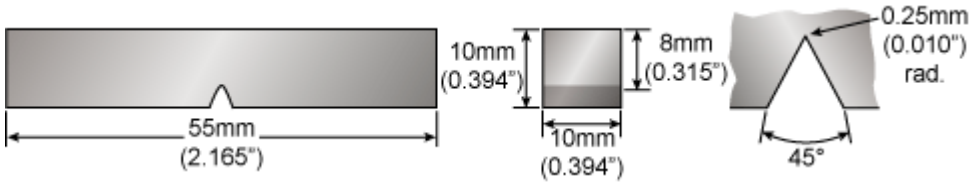

Figure 3.3 – Geometry of Charpy V-Notch impact test specimen

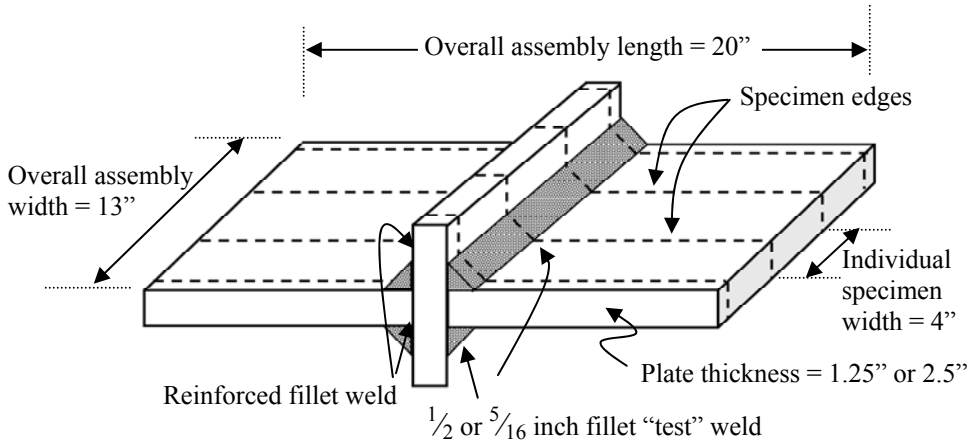

Figure 3.4 – Cruciform specimen assembly showing key dimensions and fabrication details

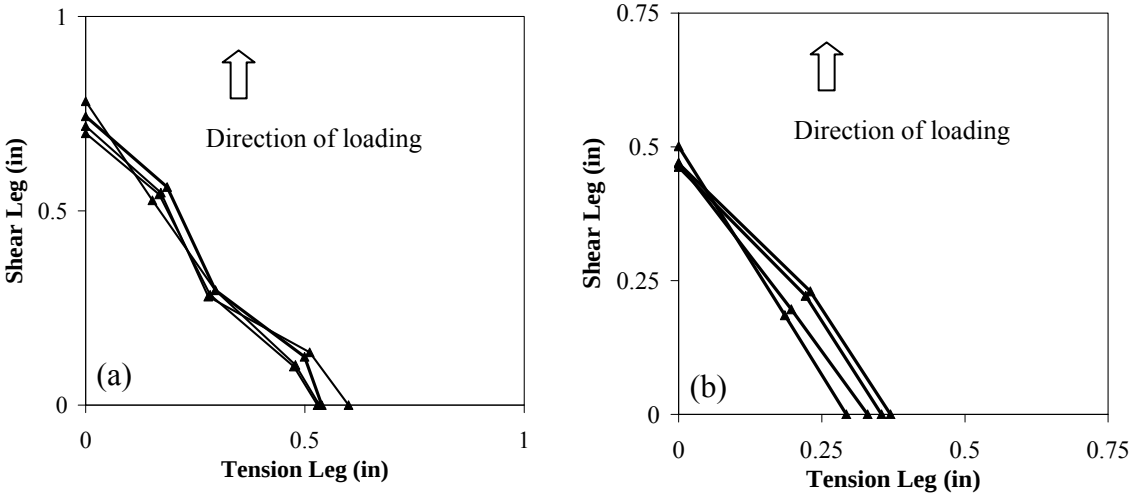

Figure 3.5 – Mean weld profiles for (a) all the 1/2 inch welds including the different filler metals and plate thicknesses (b) all the 5/16 inch welds including the different filler metals and plate thicknesses

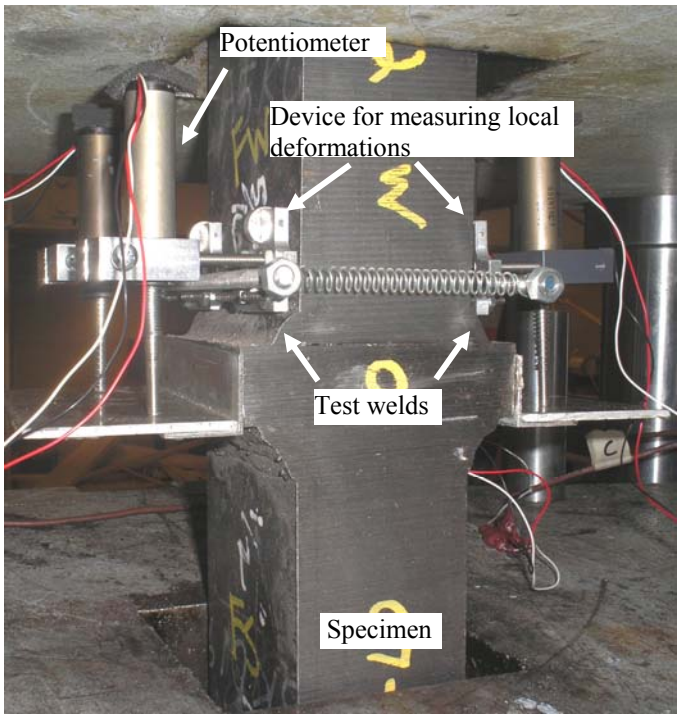

Figure 3.6 – Representative photograph showing specimen setup and instrumentation

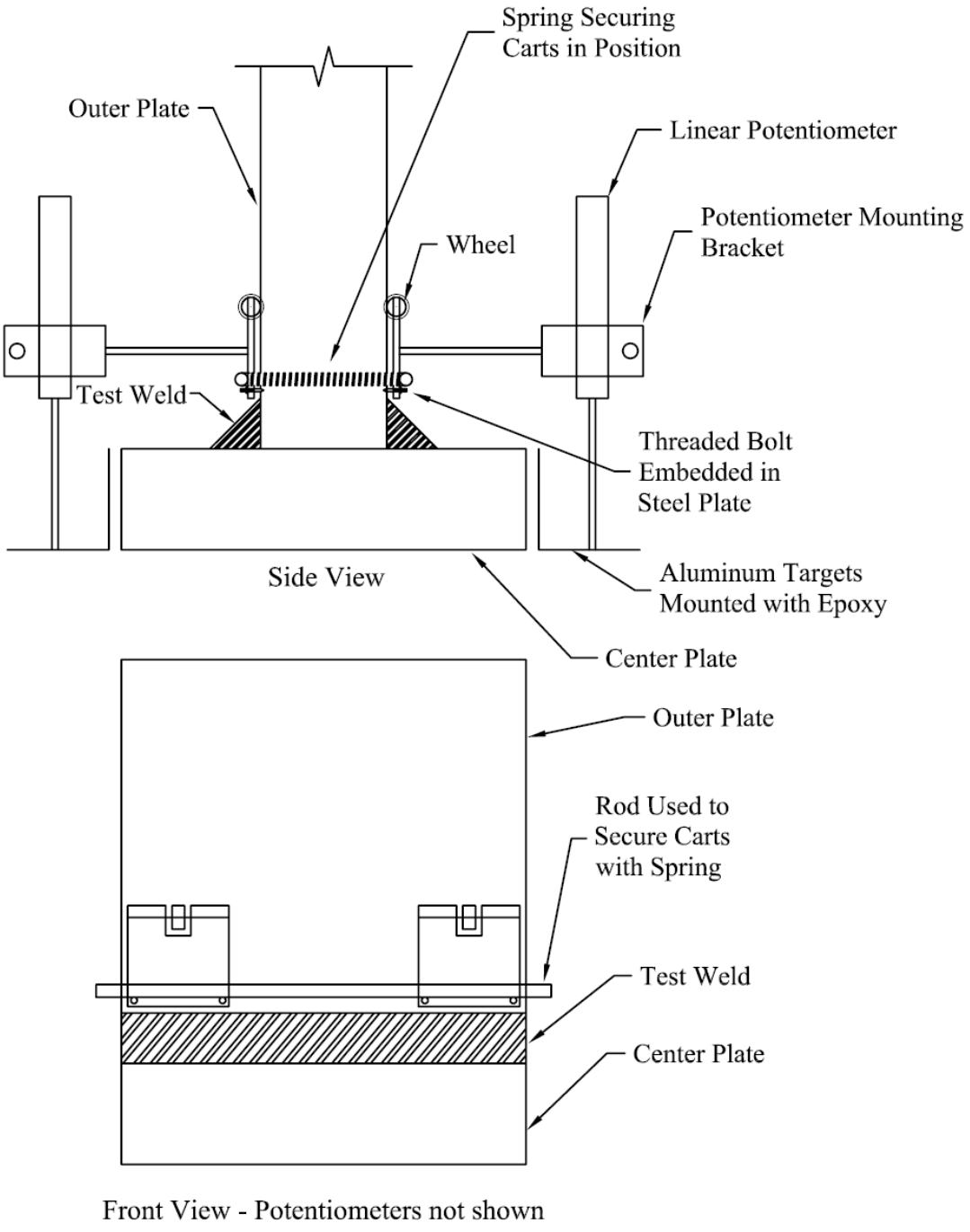

Figure 3.7 – Schematic of potentiometer mounting cart for measuring weld deformation

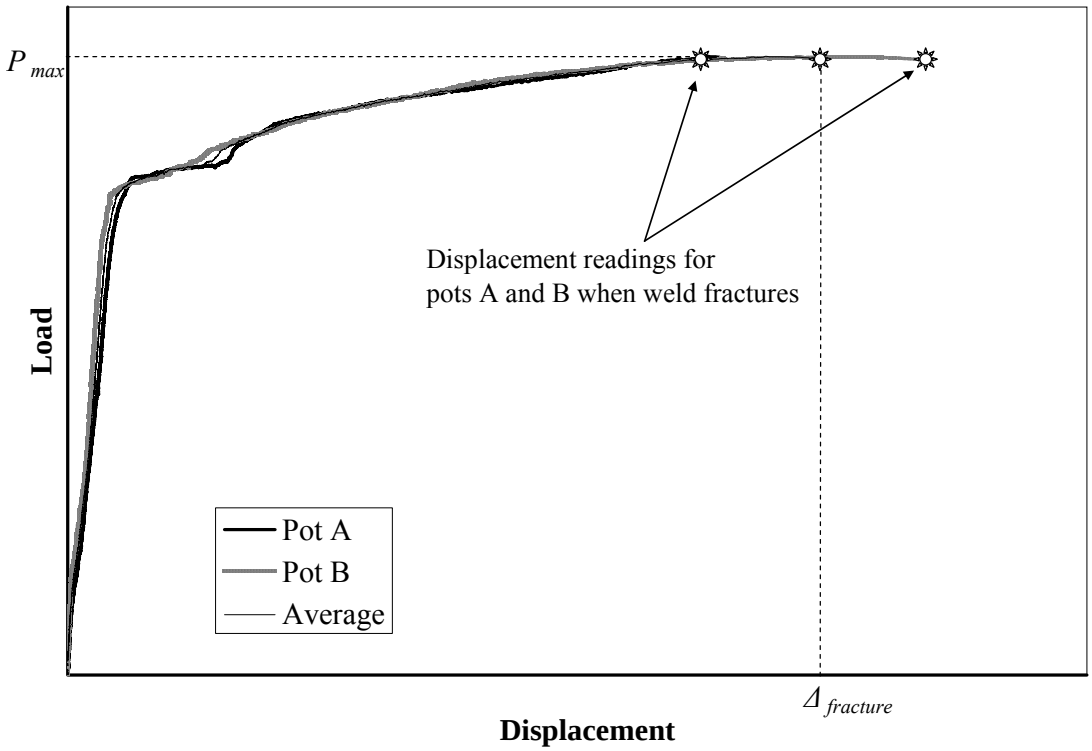

Figure 3.8 – Plot showing typical tension test experimental response

Figure 3.9 – Photograph of fillet weld gage

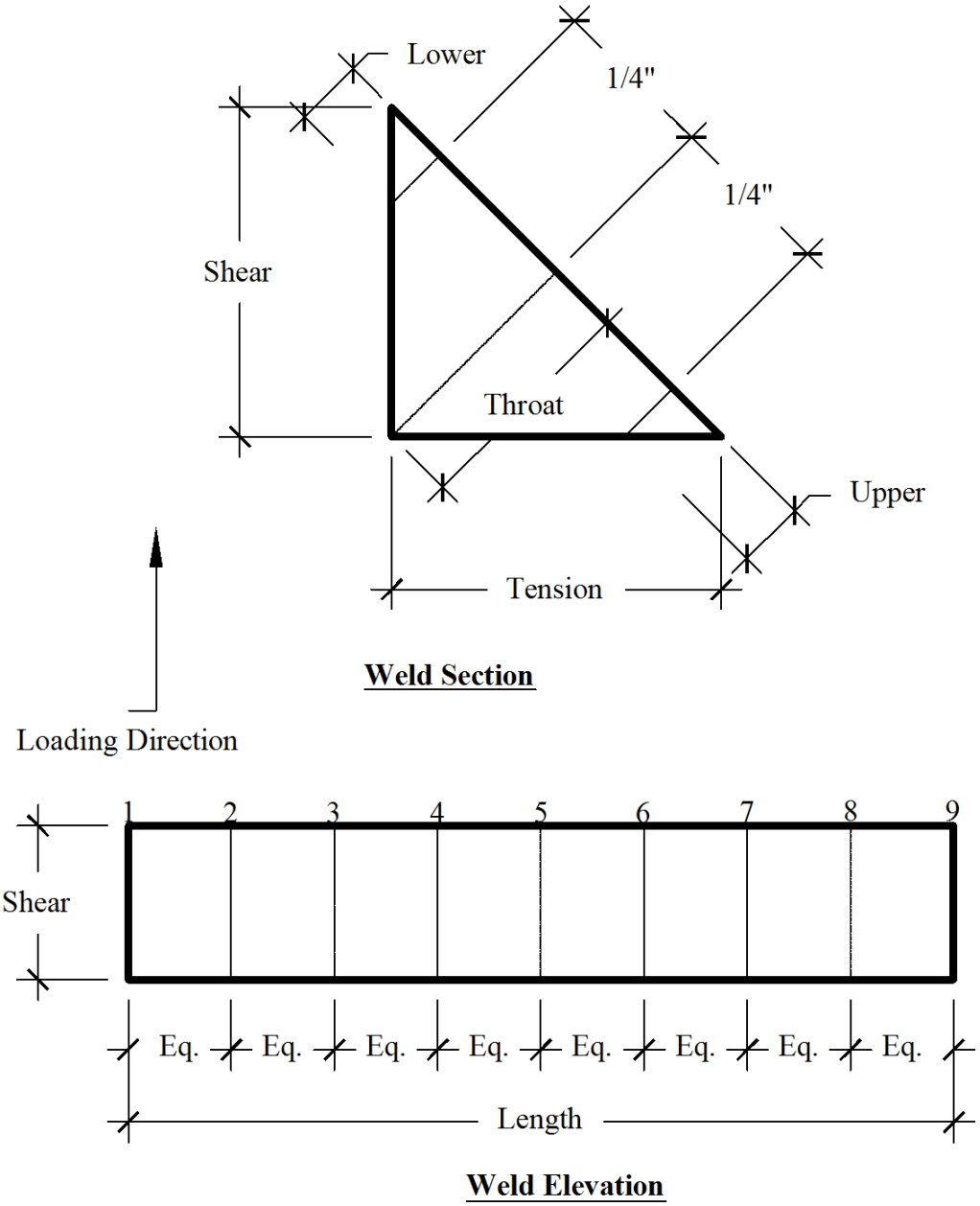

Figure 3.10 – Pre-fracture weld measurement locations

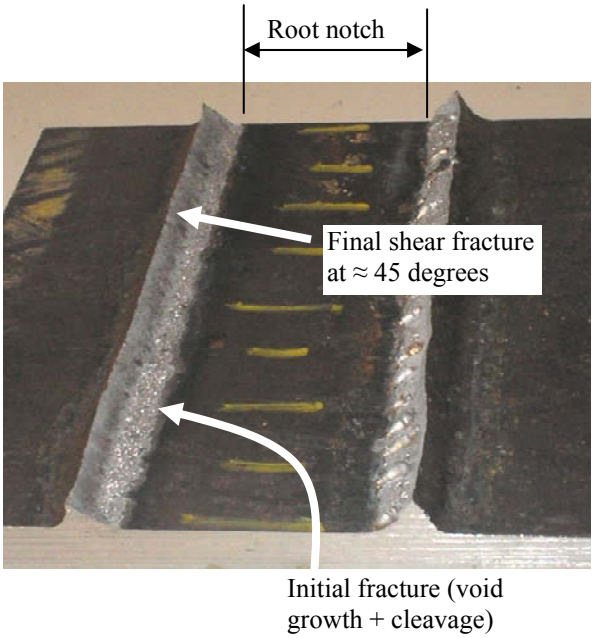

Figure 3.11 – Photograph of fractured surface showing initiation straight ahead of root notch followed by shear fracture (Test #16)

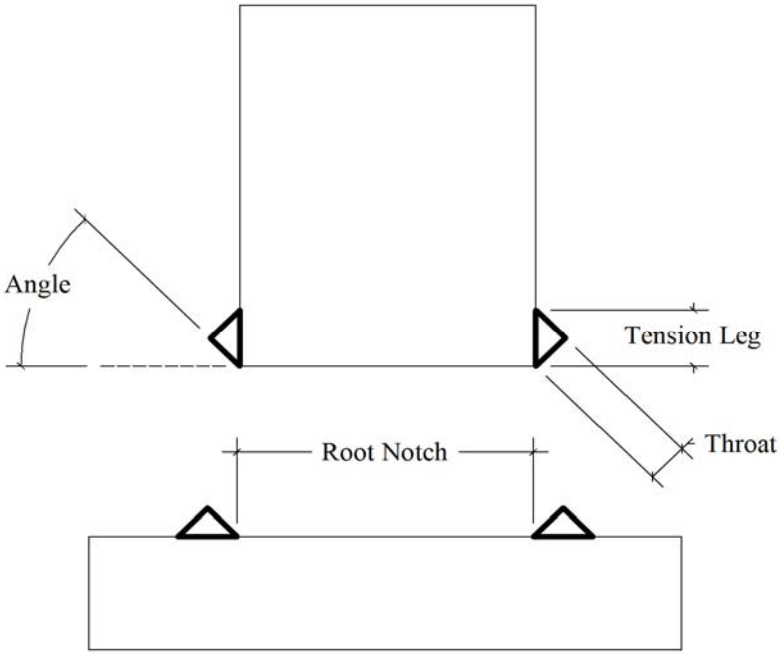

Figure 3.12 – Post-Fracture measurement diagram

Figure 3.13 – Protractor used for measuring fracture angle

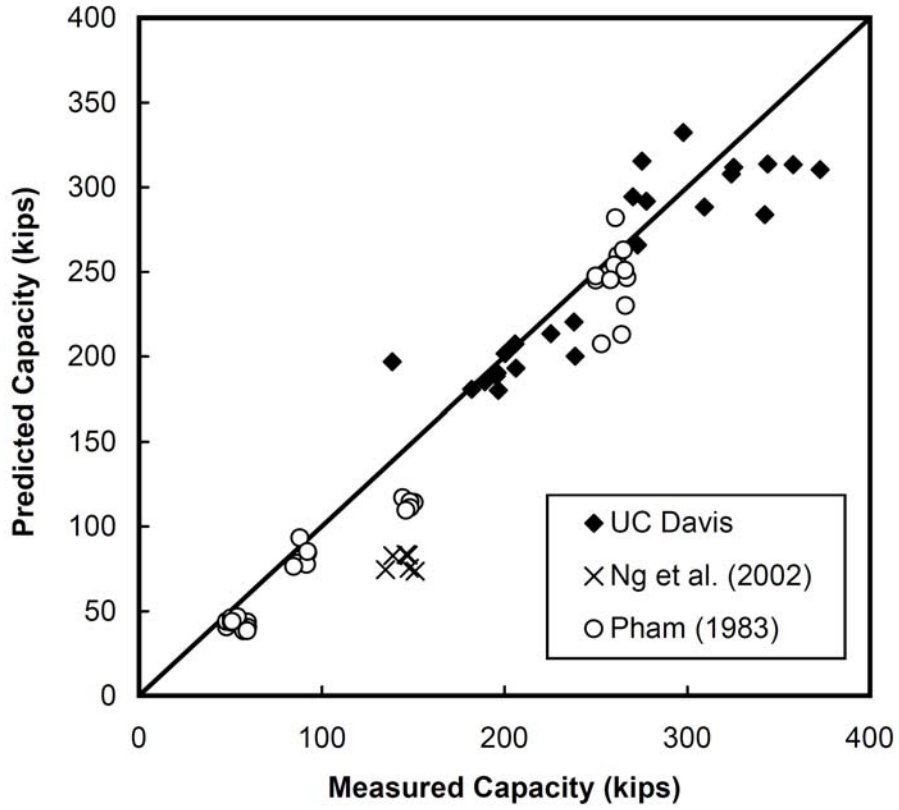

Figure 3.14 – Comparison of measured capacity from tests with capacity predicted using the AISC (2005) design equation ($\phi = 1.0$)

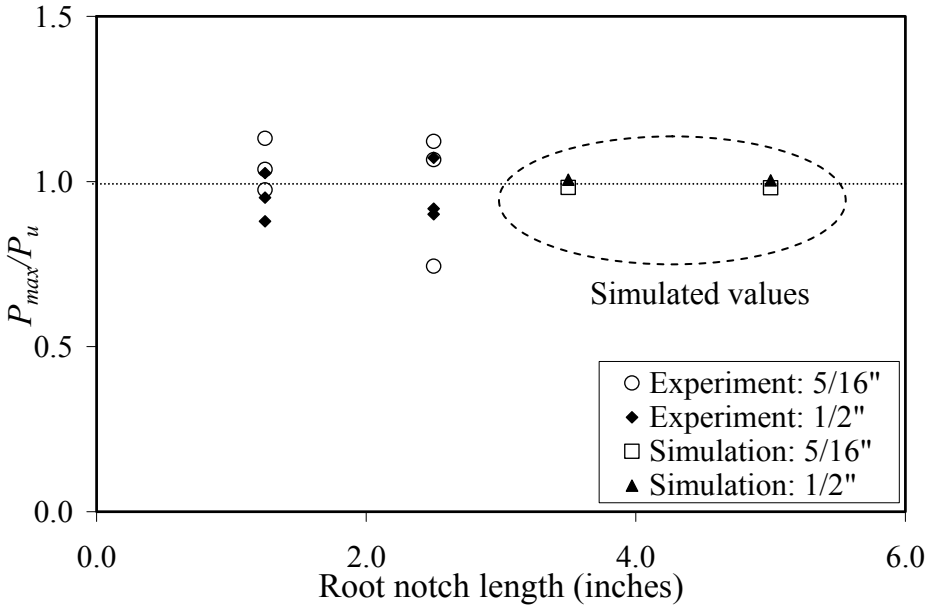

Figure 3.15 (a) Ratio of experimental and simulated capacities to predicted capacities for E70T-7 non-toughness rated filler material versus root notch length

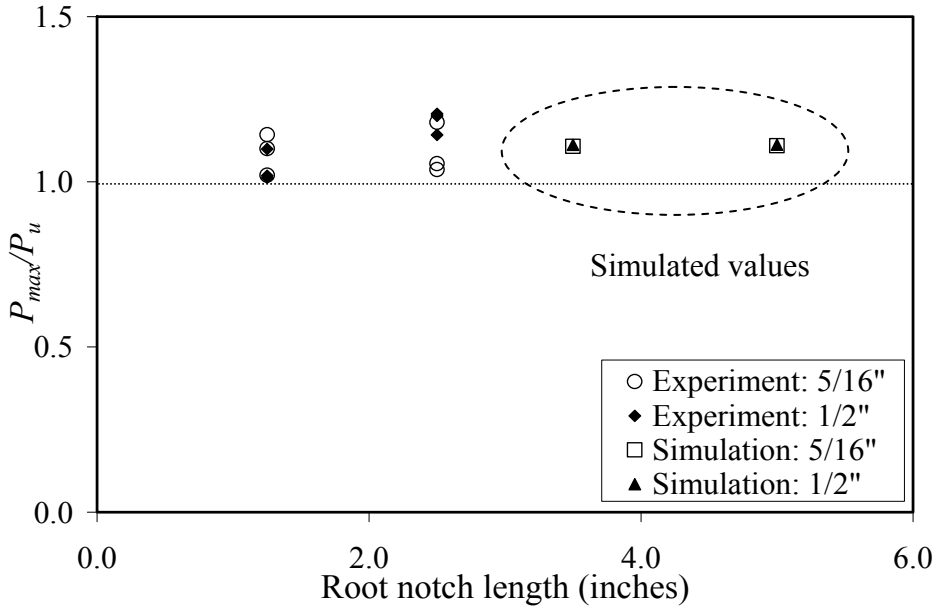

Figure 3.15 (b) Ratio of experimental and simulated capacities to predicted capacities for E70T7-K2 toughness rated filler material versus root notch length

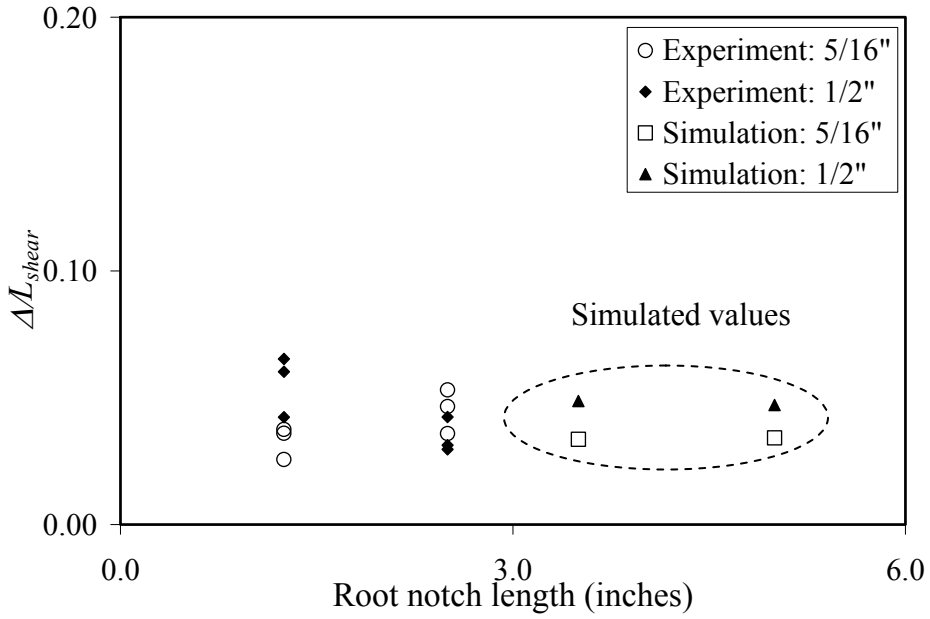

Figure 3.16 (a) Experimental and simulated normalized weld fracture deformations for E70T-7 non-toughness rated filler material versus root notch

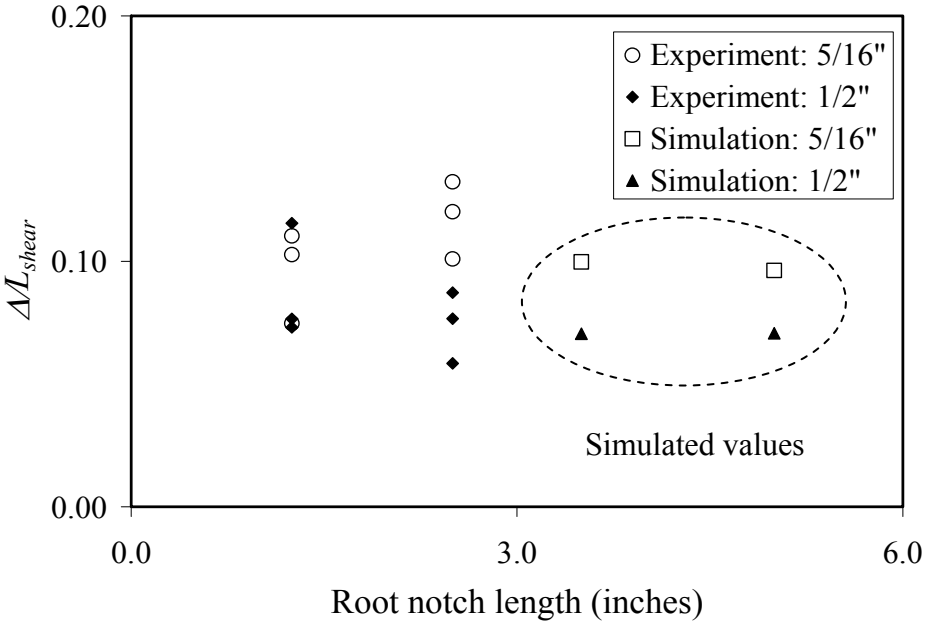

Figure 3.16 (b) Experimental and simulated normalized weld fracture deformations for E70T7-K2 toughness rated filler material versus root notch

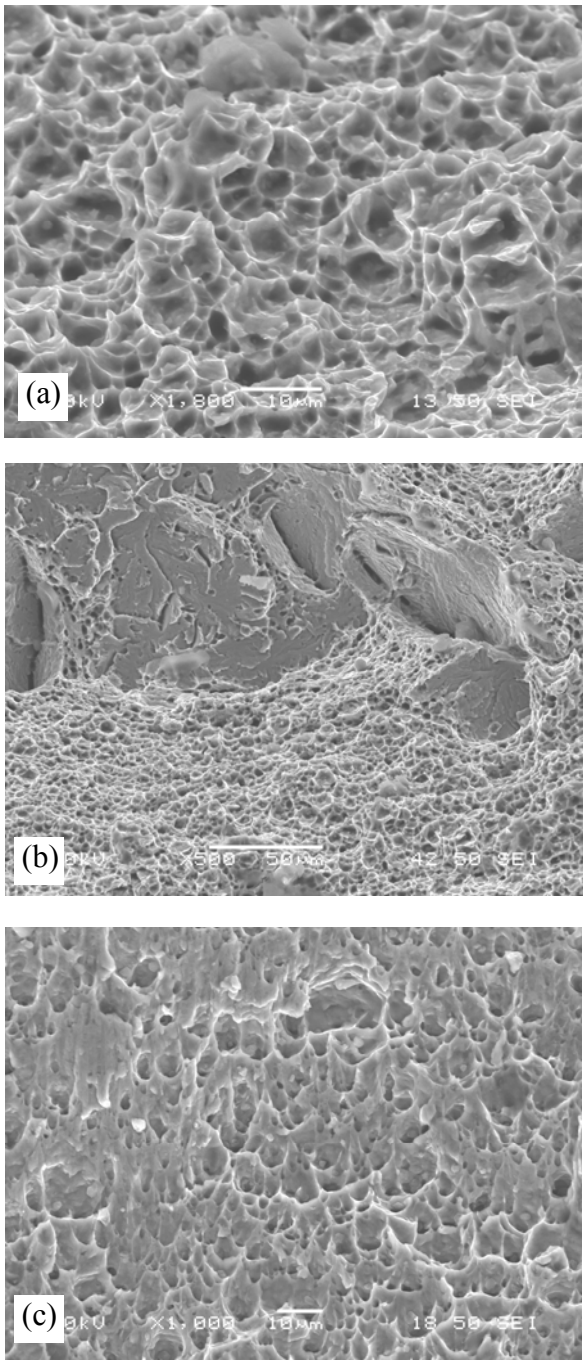

Figure 3.17 – Photomicrographs for Test #16 showing (a) fracture initiation due to microvoid growth within 0.02 inches of notch tip (b) transition to cleavage fracture 0.04 inches ahead of notch tip and (c) elongated microvoids indicative of final transition to shear rupture 0.08 inches ahead of notch tip

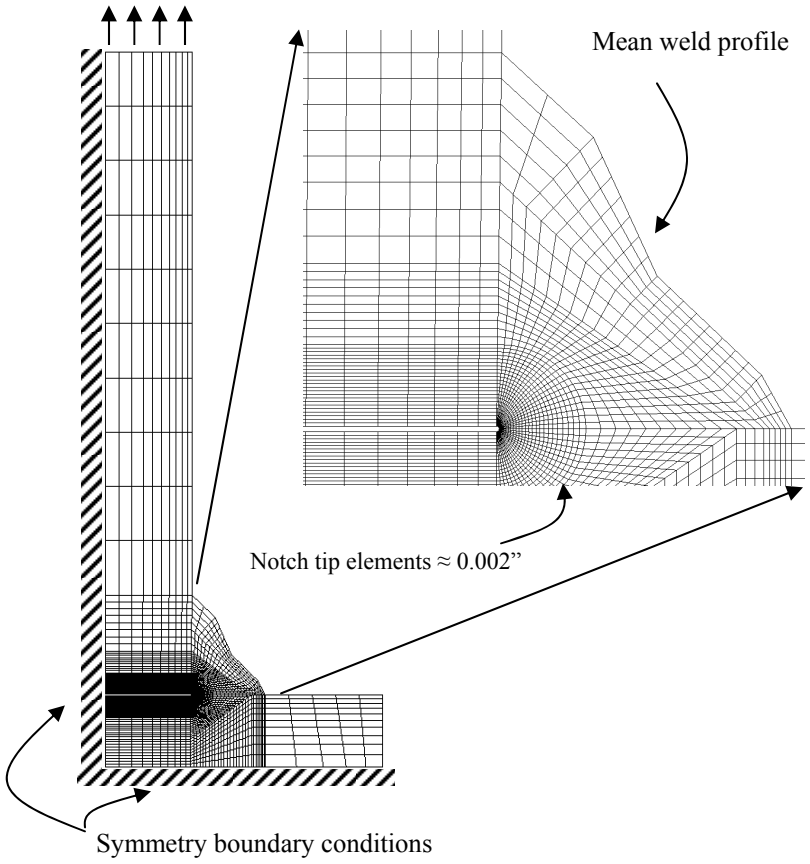

Figure 3.18 – Representative finite element simulation of 1/2 inch weld showing the weld geometry and mesh construction

Chapter 4

Cruciform Bend Experiments

4.1 INTRODUCTION

The previous Chapter discusses the effect of the root notch on the strength and ductility of cruciform specimens loaded in tension. As discussed towards the conclusion of the previous Chapter, the strength of fillet welded connections loaded eccentrically out-of-plane (such as shown in Fig. 4.1) depends on the effect of the root notch, and also on the bearing between the two connected plates. To address the effect of these various phenomena on the strength of eccentrically loaded welded connections, this Chapter describes a series of sixty three-point bend tests conducted at UC Davis on cruciform specimens similar to those described in Chapter 3. This Chapter provides a detailed outline of the experimental program by providing an overview of the test setup, testing procedures and key observations. Specimen fabrication details and measurements are similar to those as the tension tests (see Chapter 3). While key data associated with discussion of the bend test results is presented in this Chapter, complete data for all experiments is provided in Appendices A (Welding Procedures and Specifications), B (Cruciform Specimen Measurements), C (Ancillary Test Data) and E (Bend Test Experimental Response Results). The bend experimental program involves sixty cruciform fillet weld specimens featuring two electrodes, three root notch lengths, two weld sizes and three loading eccentricities. To obtain statistically significant data, and to support the reliability analysis outlined in Chapter 6, three replicate tests were performed for each parameter set. The specimens used for the bend tests are similar in many respects to those used for the tension tests, except that they are loaded in a different (i.e. bending) configuration. Thus, all aspects of specimen fabrication, including the weld processes and the selection of filler metals (non-toughness rated E70T-7 and toughness rated E70T7-K2) are identical to the tension tests already described in Chapter 3. Hence, the ancillary tests conducted for the tension tests (described in Chapter 3.4) are applicable to the bend tests as well. However, a difference in the test matrix is that in contrast to the tension tests that investigated only two root notch lengths, the bend tests interrogate three root notch lengths. A detailed test matrix is presented in Table 4.1. This Chapter summarizes the test setup, procedures and results for these tests. The next Chapter (i.e. Chapter 5) presents a detailed analysis of this data as well as similar data generated by other test programs.

4.2 BEND SPECIMEN PREPARATION, TEST SETUP, TEST PROCEDURE AND DESCRIPTION OF RECORDED DATA

This section describes the test setup and procedure used for the bend experiments as well as a brief description of the recorded data. Recall that the specimens used for the bend tests are similar to those used for the tension tests; thus the reader is referred to Chapter 3 and Appendices A and C for a detailed description of specimen preparation, materials

used and results from the ancillary tests that were conducted to determine material properties. Detailed measurements of the bend test specimens (as well as the tension test specimens) are provided in Appendix B.

4.2.1 Test Setup and Fixtures

This section focuses on the differences between the tension and bending tests, most importantly the test configuration itself. Figures 4.2 and 4.3 illustrate the basic test setup indicating part of the 400 kip Tinius Olsen universal testing machine (used previously for the tension tests) as well as a specimen being loaded in the three-point bend configuration. Also visible in the Figure is a three-point bend loading fixture developed specifically for the bend phase of testing. The fixture provides the facility to test the cruciform specimens in bending with different load eccentricities, while also providing approximately ideal pinned boundary conditions. The fixture consists of a steel base with smooth cut round grooves (at multiple pre-set locations) in which dowel pins may be seated as the supports. A similar dowel pin is connected to the central (upper) loading fixture. All dowel pins have a milled flat surface to prevent local indentation of the specimen at the points of support. The round dowels were lubricated to allow free rotation at the contact points. Horizontal forces created by friction between the dowels and specimen are negligible since the tests observed relatively small rotations at failure (on average less than 1.5 degrees). The fixture was designed to permit reuse for different eccentricities by simply reseating the dowels in different pre-set locations. The eccentricity for each test (refer Table 4.1) is defined as the horizontal distance between the centerline of the lower dowel and the surface of the specimen center plate (see Figure 4.2b). Special care was taken to center each specimen on the fixture for every test.

4.2.2 Test Matrix, Instrumentation and Test Procedure

Introduced earlier, Table 4.1 summarizes the test matrix. The numbering on the Table begins at 25, to reflect that these tests are conducted in addition to the 24 cruciform tension tests. Referring to the Table, two weld sizes (1/2 and 5/16 inch), three eccentricities (3.0 inch, 5.5 inch and 8.5 inch) and three root notch lengths (1.25 inch, 1.75 inch and 2.50 inch) were investigated for each of the two weld classifications. For budgetary reasons, the test matrix represents a fractional factorial matrix; i.e. not all possible parameter combinations are investigated explicitly. However, the matrix is designed to provide comparative evaluations of the effect of all parameters.

Using the load setup and fixture described in the preceding discussion, sixty cruciform specimens were tested quasi-statically to failure. All specimens were loaded in displacement control with an average loading rate for all tests of approximately 0.1 kip/second (Table 4.2 summarizes loading rates for individual specimens). Qualitatively, each test exhibited a similar response: initial elastic loading followed by a period of strain hardening concluding with a drop in force. Figure 4.4 shows load versus load-line deformation curves for two specimens. Failure for most tests with larger eccentricities (e.g. 5.5” and 8.5”) was gentle and weld rupture involved a gradual “un-zipping” of the specimen initiating at the bottom end of the weld (tension end) – see the curve labeled “Large Eccentricity” in Fig. 4.4. Other tests (especially tests with shorter eccentricities;

e.g. 3.0") exhibited sudden shearing failure that completely severed the test welds – see the curve labeled "Small Eccentricity" in Fig. 4.4. Similar load-line deformation plots for all sixty bend experiments are provided in Appendix E.

4.2.3 Description of Recorded Data

Similar to the tension tests described in the previous Chapter, various experimental response quantities were monitored and recorded throughout the tests. These include the load, cross-head displacement (approximately equal to the load-line deformation) and test weld deformation over the shear leg dimension. Figures 4.2 and 4.3 show the locations of the linear potentiometers that were installed to measure the weld deformations. Referring back to Chapter 3, the devices were installed in a manner similar to that used for the tension tests (recall Figure 3.7), i.e. the specially fabricated carts were designed to monitor local deformation over the weld shear leg dimension. For nine of the toughness rated weld experiments (discussed later), three uniaxial strain gages were installed to one face of the specimen in the vicinity of the test weld to record local strains in the connection member (see Fig. 4.5). The purpose of these detailed measurements is to develop insights into specimen response – primarily the stress/strain and deformation profiles at the connection interface region which may subsequently be used to inform refined strength models and design guidelines.

The most important recorded data is the peak load itself (indicated in Fig. 4.4) as this quantity is analyzed in detail in the subsequent Chapters. The peak observed loads corresponding to the welded connection capacity (expressed as half the observed peak load at the center of the three-point bend specimen) are summarized in Table 4.1. These are denoted as P_{max}. However, since Chapters 5 and 6 address the implications of the maximum force in detail, this Chapter provides a somewhat more detailed discussion of some deformation quantities are of interest in addition to the peak load. In this context, deformation measurements recorded by the potentiometers can be kinematically projected to the top and bottom edges of the specimens, under the assumption that the two long connecting plates remain rigid (see Figure 4.6). These deformation measurements are useful when interpreting the response of the individual welds, specifically the deformation demands imposed on them as they start to fracture. Based on these deformations and the corresponding kinematic projections, various types of response graphs may be generated (in addition previously outlined load versus load-line deformation graph). Figures 4.7a-c show examples of such graphs for one experiment (Test #58 – 1.25" root notch, toughness rated 1/2" weld, 5.5" eccentricity). Similar graphs for all bend tests are presented in Appendix E. Figure 4.7a plots the kinematically projected weld deformations (over the shear leg dimension) at the extreme top and bottom edges of the specimen test weld (see Fig. 4.6) versus load, while Figure 4.7b plots the average relative rotation (defined as the difference between the average extreme compression end weld deformation and the average extreme tension end weld deformation divided by the average weld length) versus load. Based on the kinematically projected weld deformations, Figure 4.7c plots the estimated location of the neutral axis (center of rotation) normalized by the beam depth. The normalized extreme tension end weld deformation (normalized by average shear leg length; to be explained later) at peak

load and the location of the neutral axis at peak load for all the experiments is summarized in Table 4.1. This type of information may be used to inform strength prediction models such as those described in the subsequent Chapters. It is relevant to mention here that the neutral axis location is based only on two measurements through the length of the weld disregarding deformation of the bearing surfaces. Moreover, it is also important to discuss that the projected deformations usually exhibit some unsymmetrical behavior (see the deformation response on compression side in Figure 4.7a), such that the deformations are slightly different on each weld face. This difference can be accounted for by the asymmetry in weld profiles and/or the slight crookedness of the specimens endured during fabrication.

For each test, the ultimate observed load P_{max} is reported in Table 4.1 along with other information. Note that the ultimate observed load listed in Table 4.1 is half the total load observed at the center of the three point load experiments (i.e. the eccentric load) in order to provide a consistent comparison with design predictions. In addition to this value, the average normalized projected tensile weld deformation at ultimate load and the normalized location of the neutral axis is summarized in Table 4.1 as well. Load response plots (where the load is plotted against various deformation quantities) for all experiments are presented in Appendix E. Strain gage data for all the tests are also presented in Appendix E.

4.3 MEASUREMENTS OF THE CRUCIFORM SPECIMENS

The bend test specimens were measured by similar means as the tension test specimens (recall section 3.7 from the previous Chapter). For the bend specimens, a few additional measurements were conducted and these are explained below. Measurements for all test specimens are archived in Appendix B. This section describes the measurement process and provides some observations.

4.3.1 Pre-Fracture Measurements

Prior to testing, dimensions of the steel connection plates and test weld profiles were measured for all the sixty bend specimens by similar means as the tension tests. All these pre-fracture measurements are archived in Appendix B. The same fillet weld gage (recall Figure 3.9 from Chapter 3) used for the tension test measurements was also used for the bend test measurements. The reader is referred to Figure 3.10 for a schematic illustration of the key measurements.

The dimensions of the test welds were also measured by similar means as the tension tests (recall Chapter 3.7.1 and Figure 3.10). Both test weld lengths (nominally 4 inches) were also measured. Figure 4.8a illustrates the average weld profiles (based on an average of all the measurements for a given assembly) for the 1/2 inch welds, while Figure 4.8b shows similar mean profiles for the 5/16 inch welds. In each Figure, average weld profiles from all the assemblies (corresponding to the given weld size) are overlaid on one another. Figure 4.9 indicates the definitions of “shear leg” and “tension leg” – terms that are used in various other parts of this report. In almost all cases, the shear leg was larger than the tension leg (on average 38% larger), although this difference was less

pronounced in the 1/2 inch welds (on average 34% larger). This might be explained by the position of the assembly during welding, where presumably, the shear leg would be horizontal, such that its size would be increased due to the effect of gravity. This effect is less pronounced in the multi-pass (1/2 inch) welds since the subsequent passes tend to rectify the unbalance created in the first pass. However, in most cases, the tension leg was at least as large as the specified weld size, whereas the shear leg was on average 44% larger then the specified minimum. Some welds (a total of ten specimens) did not meet the required minimum weld size although the difference was small (maximum 5% less than required). Also interesting to observe are the dimple shaped weld profiles for the ½ inch weld assemblies, which are produced by the multiple welding passes. In any case, it is important to emphasize that all the comparisons with the predicted values are made based on the measured weld profiles, rather than the nominal weld sizes. The position of the linear potentiometers on the specimen was also measured. These measurements enable accurate kinematic projections of deformation as described earlier. The position on the strain gages was also measured and is archived in Appendix B.

4.3.2 Post-Fracture Measurements

Figure 4.10 shows a representative photograph of a fractured specimen (shown here for Test #43 - 1.75 inch root notch, non-toughness 5/16 inch weld, 8.5 inch eccentricity). For most specimens, the fracture surface on the tension side consists of a region of initial crack propagation straight ahead of the root notch, before transitioning to shear type fracture at an angle. This type of failure surface was also observed from the tension test specimens. In many specimens, fracture did not occur on well-defined planes, and sometimes the fracture plane changed orientation along the length of a single weld. However, this change in orientation was less prevalent in the toughness rated specimens. Similar response was observed in prior test programs (Ng *et al.*, 2002). As with the tension tests, several measurements were conducted on the fractured specimens (refer Section 3.7.2 and Figure 3.12). Given the irregular shapes of the fracture surfaces, a majority of these post-fracture measurements are interesting only in a qualitative sense. Nevertheless, the fracture angle for all the specimens was, on average 50 degrees (measured with respect to the tension leg) for the non-toughness rated welds and 70 degrees for the toughness rated welds. Detailed documentation of all the fracture angles (measured at several equal lengths along each weld for all the specimens) is provided in Appendix B. Note that some entries for fracture angle in the measurement tables in Appendix B contain two values. These two values represent the two observed fracture angles at one measurement location, i.e. the fracture surface consists of two planes rather than the more commonly observed single fracture plane. Another observation from the fractured specimens is that the root notch length for the larger 1/2 inch weld is not exactly equal to the plate thickness but on average, slightly smaller, primarily due to the weld penetration into the base metal. A similar trend was not observed for the 5/16 inch weld.

4.4 EXPERIMENTAL RESULTS

As discussed in the previous section, key results from the bend tests are presented in Table 4.1. This Table lists the test matrix, the maximum eccentric force observed during

loading (P_{max}) and two deformation measures at this peak force: the average normalized extreme tension end weld deformation - Δ_u (determined from projected weld deformations) and the normalized location of the center of rotation (neutral axis) - R_u. The various data and trends recorded for the bend tests are presented in the discussion below which serves as a key for Appendix E. A more detailed analysis of the data (specifically the maximum loads) is presented in the subsequent Chapters. The following subsections address five key aspects of recorded data, i.e. the observed maximum force, the specimen rotation, the weld deformation, the location of the neutral axis, and finally the strain gage data. Each section provides a brief summary of the overall trends observed.

4.4.1 Ultimate Strength of Weld Group

As indicated earlier, the ultimate observed load listed in Table 4.1 is determined as half the maximum load recorded during testing. Recall that P_{max} (which corresponds to the strength of one weld group – i.e. the one on the "test" side) is, in fact, half the recorded load, given the symmetric three-point bending configuration. Two methods are currently used in design (i.e. AISC, 2005) to predict the connection capacity (P_u); namely the elastic method and the instantaneous center (IC) of rotation method. The elastic method typically gives conservative and variable margins of safety (Lesik and Kennedy, 1990). Thus, the preferred method of the connection strength calculation is the IC method, on which current design charts in the AISC Steel Construction Manual are based (AISC, 2005 – Table 8.4 of the Steel Construction Manual – reproduced as Table 4.3 in this Chapter). These charts (which are based on the IC method) rely on a series of coefficients to predict the weld group capacity P_u. The Equation 4.1 below uses these coefficients to predict the weld strength –

$$P_u = C\, C_1\, d\, L \qquad [4.1]$$

Where,

C = coefficient tabulated in AISC Table 8-4

C_1 = electrode strength coefficient tabulated in AISC Table 8-3 (1.0 for E70XX electrode)

d = number of sixteenths-of-an-inch of fillet weld size

L = characteristic length of the weld group, inches

As outlined in the previous discussion, this equation is used in conjunction with the design tables found in Table 8-4 in the 2005 AISC Manual (see Table 4.3). As with the tension tests, the capacity P_u is determined based on measured (rather than specified) weld dimensions and material properties to eliminate any bias from specified values. Descriptions and analysis of various ultimate load prediction models, including the instantaneous centre method used in the AISC manual, is presented in detail in the next Chapter.

Table 5.12 presented in the next Chapter lists P_{max}/P_u values for all the bend experiments. While a detailed discussion of these results is presented in Chapter 5, a brief discussion is presented here for completeness and continuity. Referring to Table 5.12, it is evident that current design equations do not accurately predict the strength of welded connections subjected to out-of-plane bending. Fortunately, the predictions are significantly conservative for all parameters tested (average P_{max}/P_u for all assemblies = 1.94, COV = 0.17).

The IC method, which is used to develop the current design tables in the AISC Manual, is based on a stress block pattern that neglects the bearing effect between the connected members in the zone of compression. Consequently, the tables assume that all the compressive forces are resisted by the welds themselves (which would be true in an in-plane bending situation in lapped connections). In reality, a large part of the compressive forces are transferred through bearing between the connected elements. Other models, such as those developed by Dawe & Kulak (1974) and Neis (1980) do consider the connection member bearing effect, but are not used in the current AISC design charts. A more detailed discussion of these issues is presented in Chapter 5, whereas Chapter 6 presents reliability analyses of the selected model and outlines design considerations.

4.4.2 Brief Discussion of Connection Rotation

Figure 4.7b plots the average relative rotation of the specimen (calculated from the kinematically projected weld deformations) versus load. As described previously, specimen rotation is defined as the difference between the average extreme compression end weld deformation and the average extreme tension end weld deformation divided by the average weld length. While this data is not explicitly analyzed in this report, the rotation data provides an approximate deformation measure of the entire connection, rather than a single location on the weld. Similar graphs for all the sixty bend specimens are provided in Appendix E.

4.4.3 Weld Deformation

The IC method implicitly assumes a predetermined weld deformation capacity at fracture (Lesik and Kennedy, 1990). In fact, the strength of the connection is associated with the rupture deformation of a critical weld element. In context of the weld groups discussed in this Chapter, this critical weld element is the extreme end region of the weld on the tension side of the connection. Thus, it is informative to examine the weld deformations sustained at this location when the peak load is reached; assuming that the peak load is controlled by fracture of the weld at this location.

Figure 4.7a plots the kinematically projected weld deformations at the extreme tension and compression ends versus load. As indicated schematically in Figure 4.6, the deformations (measured over the dimension of the shear leg) were projected in two-dimensions to the extreme ends of the weld lengths over the shear leg. Qualitatively, most weld deformation plots exhibit a similar response: initial elastic loading followed by a period of strain hardening concluding with a drop in force. This was observed for both compressive and tensile deformations. Notice in Figure 4.7a that four data streams are

plotted, one for each location of deformation measurement. This allows for the observation of any unsymmetrical behavior exhibited by the specimen. Similar graphs for all sixty bend experiments are provided in Appendix E.

Table 4.1 summarizes the normalized projected extreme tension end weld deformation values at ultimate load (Δ_u). Note that Δ_u is the average projected extreme tension end weld deformation (average deformation of both weld faces) normalized (or divided) by the average shear leg length of both welds in the connection (i.e. the average of all measured shear leg lengths). The shear leg is representative of the "gage-length" of the weld being loaded and provides a means of comparing deformation between all specimens.

Figure 4.11 plots the average normalized Δ_u values of the three replicate tests from each parameter set for both the toughness and non-toughness rated welds. Also provided in the Figure is a dashed line indicating the assumed value (in the IC method) of the normalized ultimate deformation of a weld element loaded in a direction transverse to its axis. This is calculated as 0.056 as per Equation 3.4 presented previously in context of the cruciform tension tests (based on the work of Lesik and Kennedy, 1990). Equation 3.4 is based on observations by several researchers (see Chapter 2) in which the transversely loaded welds have the minimum ductility, as compared to welds loaded at an angle. In general, the angle of loading at the critical weld element (i.e. the extreme tension end of the weld group) is approximately equal to (or slightly less than) 90 degrees such that the observed normalized displacement may be compared to 0.056 (a lower bound value) for a qualitative evaluation of the experimental trends.

Referring to Figure 4.11, and to Table 4.1, it is observed that the experimental normalized fracture deformation of the non-toughness rated welded connections is close to assumed values (on average 25% greater than the 0.056 value for a transversely loaded weld element). Recall that from the tension tests (Chapter 3) it was observed that the non-toughness rated E70T-7 tension specimens exhibited an average normalized fracture deformation (0.042) 25% less than the value predicted using Equation 3.4. As expected, the normalized fracture deformation for the toughness rated E70T7-K2 specimens is greater than the non-toughness rated specimens (on average 60% greater than the assumed value). These results are encouraging, in that the observed deformation capacity is close to (or slightly larger than) the values assumed in the application of IC method. The results are especially significant because they confirm that the presence of the transverse root notch does not have a strong detrimental effect on the ductility of the weld elements.

4.4.4 Location of the Center of Rotation/Neutral Axis

Approaches that incorporate the effect of bearing on the strength of eccentrically loaded weld groups loaded out of plane, such as those developed by Dawe & Kulak (1974) and Neis (1980) typically determine a location of the neutral axis, which separates the tension region of the connection (typically resisted only by the welds) and the compression region (typically resisted through bearing). The location of this neutral axis affects the assumed distribution of deformation and consequently the stress pattern. Since these

models are discussed in detail (and recommended for strength calculation) in the next Chapter, it is informative to comment on the measured location of the neutral axis from the experiments.

Figure 4.7c is a representative plot of the normalized location of the neutral axis (termed here as center of rotation; not to be confused with the instantaneous center of rotation) versus load. The normalized location of the neutral axis (location of zero weld deformation along the shear leg dimension) along the weld length is approximated from the average projected tension and compression weld deformations described above. This value is normalized such that positive unity indicates the location of the extreme end of the weld length on the compression side, negative unity indicates the location of the extreme end on the tension side and zero indicates the centerline (i.e. mid-depth) of the weld length. Qualitatively, most center of rotation plots exhibit a similar response as the one indicated in Fig. 4.7c: initially (at low loads) the location of the neutral axis is approximately near the centerline of the weld length, suggesting an elastic stress block without bearing. With increasing loads, the plates come into contact with one another, and the neutral axis migrates towards the compression side of the connection. Results from all bend tests provide a similar trend in that the neutral axis at ultimate load appears to be located at some distance (typically one-fifth of the connection height) beyond the centerline of the weld length on the compression side. Interestingly, for all tests other than with a large (i.e. 8.5") eccentricity, the location of the neutral axis at ultimate load appears to be closer to the compression end for the larger (1/2") weld size than for the smaller (5/16") weld size. Graphs of the normalized location of the center of rotation versus for all sixty bend tests are provided in Appendix E. The normalized location of the center of rotation at peak load (R_u) is listed in Table 4.1. In discussing these results, it is important to emphasize that the neutral axis location is determined based on the assumption that the bearing plates are rigid. Given the locations of the potentiometers and only two locations along the depth, this is the only assumption possible. In reality, the plates will deform as they come into contact. To examine this behavior more closely, the next section describes data from strain gages installed on some of the specimens.

4.4.5 Strain Gage Data

As discussed previously, strain gage data was collected for nine toughness-rated tests (from all but one parameter set; specifically test number 57, 60, 63, 66, 69, 72, 76, 81 and 82). Figure 4.12 shows a representative plot of strain versus load (shown here for Test #60 - 1.25 inch root notch, toughness rated 1/2 inch weld, 5.5 inch eccentricity) for three locations on the connecting member depth (i.e. along the weld length). Two gages were installed 0.75" from the compression and tension ends of the specimen while one gage was placed at the centerline of the depth (recall Figure 4.5). The gages were placed adjacent and perpendicular to the weld axis in an attempt to observe the strain profile at the connection interface region. Qualitatively, each individual gage exhibits a similar response when plotted against total load: an initial linear behavior followed by yielding.

It is interesting to observe the strain profiles recoded by the three gages at peak load. A consistent trend for the strain profile at peak load was observed for all recorded tests. Full

yielding (in compression) was observed on the compression side while tensile strain was observed on both the tension side as well as on the centerline of the specimen depth. For most tests yielding was observed for the tension side region as well as the centerline region. Given the onset of yielding and the availability of only three measurement locations, it is difficult to determine the location of the neutral axis from the strain data at peak load. However, it is evident from the strain recorded by the gage at the centerline region that the neutral axis at peak load lies in the compression side of the connection. This coincides with the observations the neutral axis deduced from the weld deformations.

Most importantly, strain recorded on the compression side may provide insight into the stress profile of the bearing region. Past researchers (Dawe and Kulak, 1974; Neis, 1980) developed models than assume a specific bearing region stress profile. For various approaches, linear, parabolic and uniform stress distributions have been proposed. Strain gage observations for the bend tests show that a region of connecting plate on the compression side (i.e. the bearing region) is fully yielded at peak load. While this behavior is measured at only one location, it lends credence to the assumption that the entire bearing region has yielded, given that the recorded strains at this one location are very large (on the order of 1%). This supports further analysis in the subsequent Chapters that evaluate and recommend approaches developed by past researchers that assume full compressive yielding of the bearing region. Furthermore, tests from Beaulieu and Picard (1985) also demonstrated a uniform strain distribution. Strain gage data recorded for the nine specimens is presented in Appendix E and measurements of the gage locations are presented in Appendix B.

4.5 SUMMARY OF OBSERVATIONS FROM CRUCIFORM BEND TESTS

Current design equations of transverse fillet welds subjected to out-of-plane bending do not explicitly address the effect of the root notch orientation. Furthermore, current design tables do not consider a bearing effect induced by the connecting members. This Chapter discusses an experimental program consisting of bend tests on sixty cruciform specimens. These experiments provide background for further analysis outlined in the subsequent Chapters. For completeness, this Chapter also briefly discusses key test results. The cruciform bend tests discussed in this Chapter feature fillet welds with three different root notch lengths (1.25 inch, 1.75 inch and 2.5 inch), and two different electrode classifications (non-toughness rated E70T-7, and toughness rated E70T7-K2). Two weld sizes (single pass 5/16 inch and a multi-pass 1/2 inch) are considered. Furthermore, three loading eccentricities (3.0 inch, 5.5 inch and 8.5 inch) are examined. Three replicate tests are conducted for each parameter set.

The experimental results indicate that, for the parameters tested, the strength of the connection is not accurately predicted by current design tables. The current design tables (AISC, 2005) are based on the IC method which does not consider bearing effects. Neglecting this effect leads to significantly conservative predictions in situations of out-of-plane bending when bearing has a dominant effect on the stress distribution. However, an analysis of the connection response at peak force indicates that, for the non-toughness

rated welds, the value of deformation at the extreme tension end of the weld compares well with expected values, and that the presence of the transverse root notch does not have a detrimental effect on weld ductility. For the toughness rated welds, the tension end weld deformation at peak load is greater, as expected. In addition, the location of the center of rotation (neutral axis) appears to lie in the compression half of the specimen. Results from strain gage data also indicate that the neutral axis (location of zero strain) for the connecting member is on the compression half of the specimen. More importantly, for the observed specimens, the bearing region of the connecting plate is yielded with large strains such that a uniform stress distribution may be assumed over the entire compression region with reasonable confidence. The data obtained from experiments described in this Chapter will be used in conjunction with data obtained from other similar testing programs to evaluate the validity of the current design tables and approaches (Chapter 5). Chapter 6 will present a reliability analysis that results in the selection and recommendation of suitable approaches, and the resulting improved design charts that are presented in Appendix I.

Table 4.1 – Test Matrix and Summary of Experimental Data from Bend Tests

Test	Assembly	Filler Metal	Eccentricity (inches)	Nominal Weld Size (inches)	Nominal Root Notch Length (inches)	Δ_u	R_u	P_{max} [1] (kips)
25	A	E70T-7 (non-toughness rated; F_u = 97.1 ksi)	5.5	5/16	1.25	0.039	0.32	44.0
26						0.053	0.41	53.5
27						0.074	0.25	52.0
28	B			1/2		0.067	0.57	73.0
29						0.077	0.36	72.0
30						0.068	0.46	71.0
31	C		3.0	5/16	1.75	0.075	0.37	119.0
32						0.051	0.26	118.0
33						0.087	0.18	123.0
34	D			1/2		0.089	0.53	153.0
35						0.101	0.49	174.5
36						0.093	0.35	152.0
37	E		5.5	5/16		0.061	0.20	61.0
38						0.050	0.26	59.5
39						0.066	0.13	62.5
40	F			1/2		0.065	0.26	89.5
41						0.079	0.39	76.0
42						0.085	0.41	79.0
43	G		8.5	5/16		0.095	0.30	38.5
44						0.053	0.36	30.0
45						0.066	0.35	33.5
46	H			1/2		0.069	0.34	52.0
47						0.072	0.40	50.5
48						0.073	0.33	53.0
49	I		5.5	5/16	2.50	0.065	0.27	61.5
50						0.061	0.19	58.5
51						0.066	0.15	57.5
52	J			1/2		0.063	0.28	86.5
53						0.067	0.31	101.0
54						0.061	0.38	94.5
55	K	E70T7-K2 (toughness rated; F_u = 97.4 ksi)	5.5	5/16	1.25	0.066	-0.02	50.0
56						0.099	0.49	57.0
57						0.113	0.43	60.0
58	L			1/2		0.093	0.35	81.5
59						0.133	0.33	84.5
60						0.189	0.38	98.5
61	M		3.0	5/16	1.75	0.184	0.28	165.0
62						0.128	0.29	160.0
63						0.141	0.64	155.0
64	N			1/2		0.145	0.58	192.5
65						0.119	0.60	202.5
66						0.109	0.55	184.5
67	O		5.5	5/16		0.097	0.30	86.5
68						0.044	0.22	69.5
69						0.084	0.44	77.5
70	P			1/2		0.113	0.55	99.0
71						0.077	0.49	90.0
72						0.060	0.35	86.0
73	Q		8.5	5/16		0.134	0.58	45.5
74						0.125	0.46	46.5
75						0.101	0.31	45.0
76	R			1/2		0.083	0.21	58.5
77						0.121	0.51	58.5
78						0.131	0.53	56.0
79	S		5.5	5/16	2.50	0.114	0.31	77.5
80						0.137	0.32	76.5
81						0.146	0.43	76.5
82	T			1/2		0.106	0.46	110.5
83						0.128	0.44	112.0
84						0.144	0.37	110.5

1) P_{max} = half maximum force observed in experiments, i.e. eccentric load

Table 4.2 – Bend Test Loading Rates

Non-Toughness Rated – E70T-7		
Test Number	**Specimen**	**Loading Rate (kip/sec)**
25	B125_A516_55_1	0.06
26	B125_A516_55_2	0.03
27	B125_A516_55_3	0.04
28	B125_A12_55_1	0.08
29	B125_A12_55_2	0.07
30	B125_A12_55_3	0.05
31	B175_A516_3_1	0.26
32	B175_A516_3_2	0.18
33	B175_A516_3_3	0.19
34	B175_A12_3_1	0.12
35	B175_A12_3_2	0.26
36	B175_A12_3_3	0.18
37	B175_A516_55_1	0.06
38	B175_A516_55_2	0.06
39	B175_A516_55_3	0.06
40	B175_A12_55_1	0.06
41	B175_A12_55_2	0.07
42	B175_A12_55_3	0.06
43	B175_A516_85_1	0.05
44	B175_A516_85_2	0.07
45	B175_A516_85_3	0.09
46	B175_A12_85_1	0.03
47	B175_A12_85_2	0.05
48	B175_A12_85_3	0.05
49	B250_A516_55_1	0.09
50	B250_A516_55_2	0.08
51	B250_A516_55_3	0.07
52	B250_A12_55_1	0.11
53	B250_A12_55_2	0.06
54	B250_A12_55_3	0.07

Toughness Rated – E70T7-K2		
Test Number	**Specimen**	**Loading Rate (kip/sec)**
55	B125_B516_55_1	0.04
56	B125_B516_55_2	0.06
57	B125_B516_55_3	0.13
58	B125_B12_55_1	0.07
59	B125_B12_55_2	0.09
60	B125_B12_55_3	0.13
61	B175_B516_3_1	0.13
62	B175_B516_3_2	0.25
63	B175_B516_3_3	0.28
64	B175_B12_3_1	0.17
65	B175_B12_3_2	0.45
66	B175_B12_3_3	0.40
67	B175_B516_55_1	0.05
68	B175_B516_55_2	0.13
69	B175_B516_55_3	0.13
70	B175_B12_55_1	0.07
71	B175_B12_55_2	0.10
72	B175_B12_55_3	0.09
73	B175_B516_85_1	0.03
74	B175_B516_85_2	0.06
75	B175_B516_85_3	0.04
76	B175_B12_85_1	0.08
77	B175_B12_85_2	0.07
78	B175_B12_85_3	0.07
79	B250_B516_55_1	0.05
80	B250_B516_55_2	0.07
81	B250_B516_55_3	0.14
82	B250_B12_55_1	0.12
83	B250_B12_55_2	0.09
84	B250_B12_55_3	0.11

Table 4.3 – Design Table from the Current (13th) Edition (2005) of the AISC Steel Construction Manual

Table 8–4
Coefficients *C*
for Eccentrically Loaded Weld Groups
Angle = 0°

Available Strength of a weld group, ϕR_n or R_n/Ω, is determined with
$R_n = CC_1Dl$ ($\phi = 0.75$, $\Omega = 2.00$)
or

LRFD	ASD
$C_{min} = \frac{P_u}{\phi C_1 Dl}$ $D_{min} = \frac{P_u}{\phi C C_1 l}$ $l_{min} = \frac{P_u}{\phi C C_1 D}$	$C_{min} = \frac{\Omega P_a}{C_1 Dl}$ $D_{min} = \frac{\Omega P_a}{C C_1 l}$ $l_{min} = \frac{\Omega P_a}{C C_1 D}$

where
P = required force, P_u or P_a, kips
D = number of sixteenths-of-an-inch in the fillet weld size
l = characteristic length of weld group, in.
$a = e_x / l$
e_x = horizontal component of eccentricity of P with respect to centroid of weld group, in.
C = coefficient tabulated below
C_1 = electrode strength coefficient from Table 8-3 (1.0 for E70XX electrodes)

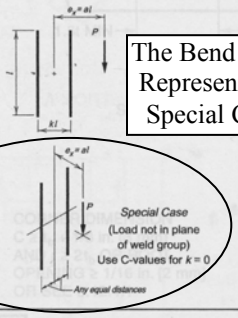

The Bend Tests Represent this Special Case

Bend Test Design Values

	k															
a	0	0.1	0.2	0.3	0.4	0.5	0.6	0.7	0.8	0.9	1.0	1.2	1.4	1.6	1.8	2.0
0.00	3.71	3.71	3.71	3.71	3.71	3.71	3.71	3.71	3.71	3.71	3.71	3.71	3.71	3.71	3.71	3.71
0.100	3.72	3.73	3.72	3.71	3.70	3.69	3.67	3.65	3.63	3.61	3.60	3.56	3.52	3.48	3.45	3.71
0.150	3.67	3.66	3.65	3.64	3.62	3.60	3.58	3.56	3.54	3.52	3.50	3.47	3.43	3.40	3.37	3.34
0.200	3.51	3.51	3.50	3.49	3.47	3.46	3.44	3.43	3.41	3.40	3.38	3.36	3.33	3.30	3.28	3.25
0.250	3.31	3.31	3.31	3.30	3.29	3.28	3.28	3.27	3.26	3.26	3.25	3.23	3.22	3.20	3.18	3.17
0.300	3.09	3.09	3.09	3.10	3.10	3.10	3.11	3.11	3.11	3.11	3.11	3.11	3.11	3.10	3.09	3.08
0.400	2.66	2.66	2.68	2.70	2.73	2.75	2.78	2.80	2.82	2.83	2.85	2.87	2.89	2.90	2.90	2.90
0.500	2.29	2.30	2.32	2.35	2.40	2.44	2.48	2.52	2.55	2.58	2.61	2.65	2.68	2.71	2.73	2.74
0.600	2.00	2.00	2.03	2.07	2.12	2.18	2.23	2.28	2.32	2.36	2.39	2.45	2.50	2.54	2.57	2.59
0.700	1.76	1.76	1.79	1.84	1.90	1.96	2.02	2.07	2.12	2.16	2.21	2.28	2.33	2.38	2.42	2.45
0.800	1.56	1.57	1.60	1.65	1.71	1.77	1.84	1.90	1.95	2.00	2.04	2.12	2.19	2.24	2.29	2.32
0.900	1.41	1.41	1.44	1.49	1.56	1.62	1.69	1.75	1.80	1.85	1.90	1.98	2.05	2.11	2.16	2.21
1.00	1.28	1.28	1.31	1.37	1.43	1.49	1.56	1.62	1.67	1.73	1.77	1.86	1.94	2.00	2.05	2.10
1.20	1.07	1.08	1.11	1.16	1.22	1.28	1.35	1.41	1.46	1.51	1.57	1.66	1.73	1.80	1.86	1.91
1.40	0.927	0.935	0.965	1.01	1.07	1.13	1.19	1.24	1.30	1.35	1.40	1.49	1.57	1.64	1.70	1.76
1.60	0.815	0.821	0.851	0.893	0.944	1.00	1.06	1.11	1.16	1.21	1.26	1.35	1.43	1.50	1.57	1.62
1.80	0.725	0.733	0.760	0.800	0.847	0.899	0.952	1.00	1.05	1.10	1.15	1.24	1.32	1.39	1.45	1.51
2.00	0.655	0.661	0.687	0.723	0.768	0.816	0.867	0.916	0.964	1.01	1.06	1.14	1.22	1.29	1.35	1.41
2.20	0.596	0.603	0.627	0.660	0.701	0.747	0.795	0.841	0.887	0.932	0.975	1.06	1.13	1.20	1.26	1.32
2.40	0.547	0.553	0.575	0.607	0.645	0.688	0.733	0.777	0.821	0.864	0.905	0.984	1.06	1.12	1.18	1.24
2.60	0.505	0.512	0.532	0.561	0.597	0.637	0.680	0.723	0.764	0.805	0.845	0.921	0.991	1.05	1.11	1.17
2.80	0.469	0.476	0.495	0.523	0.556	0.595	0.635	0.675	0.715	0.753	0.792	0.865	0.932	0.995	1.05	1.11
3.00	0.439	0.444	0.463	0.488	0.520	0.556	0.595	0.632	0.671	0.708	0.745	0.815	0.881	0.941	0.997	1.05

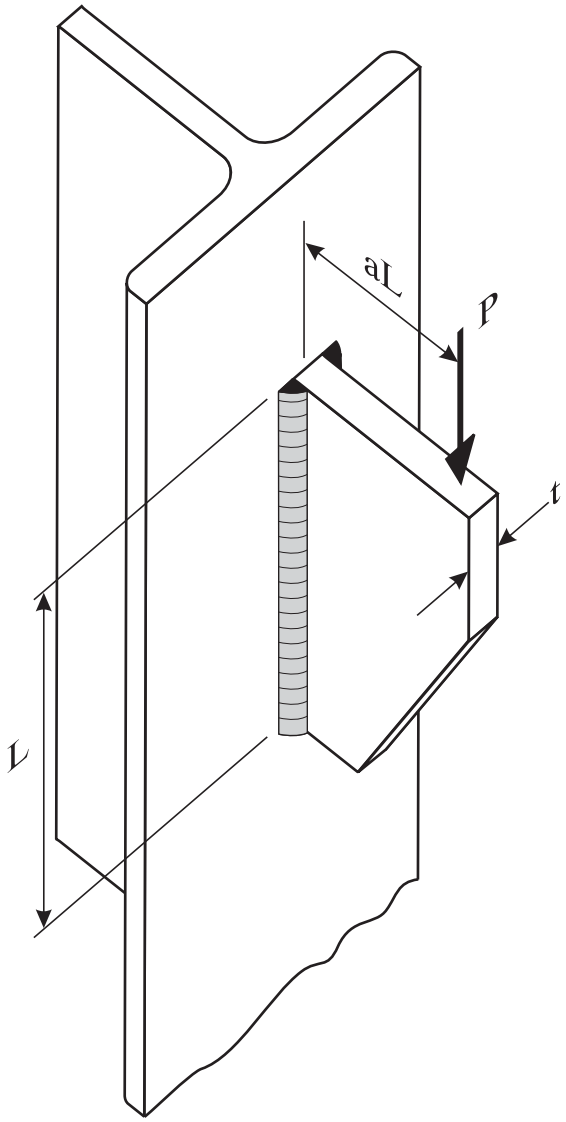

Figure 4.1 – Fillet weld connection loaded eccentrically out-of-plane
(Figure adapted from Neis, 1980)

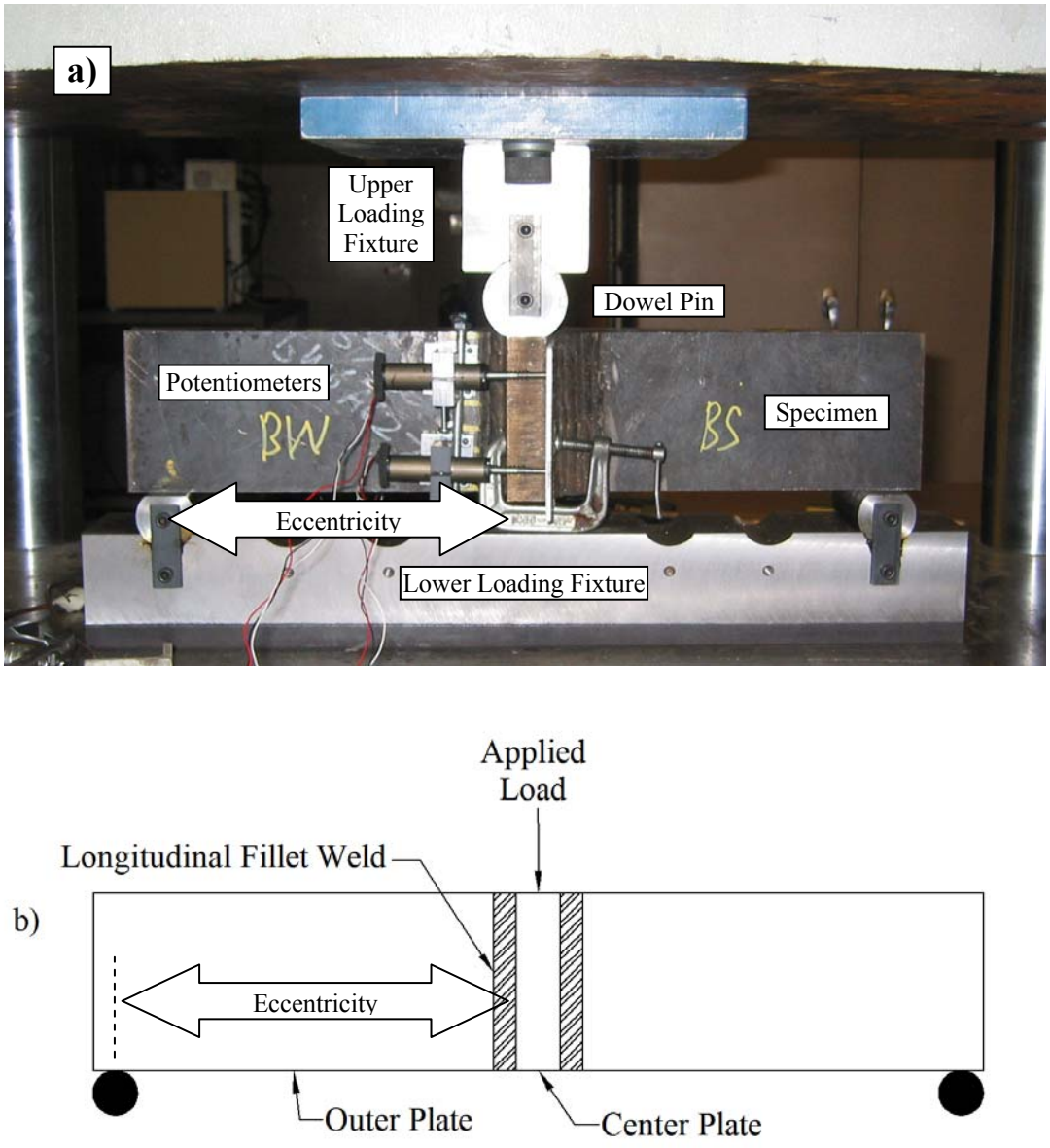

Figure 4.2 – Front view of bend test setup (a) Photograph (b) Schematic

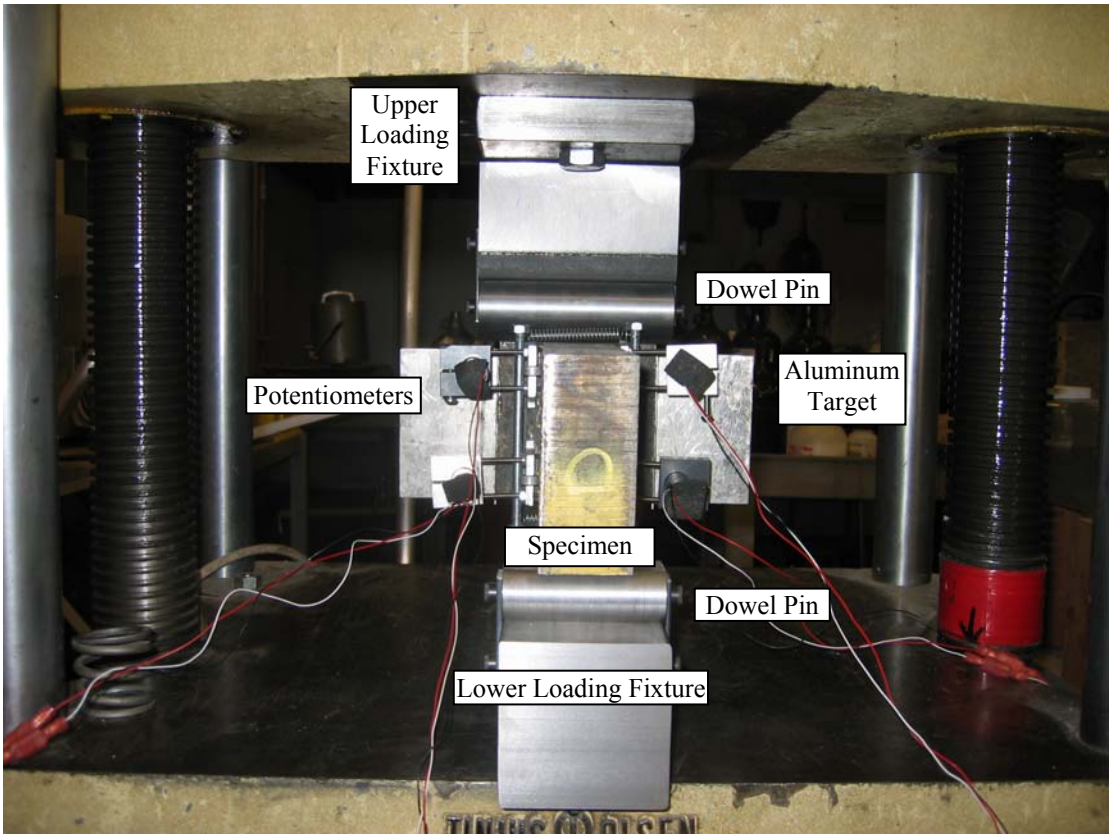

Figure 4.3– Side view of bend test setup showing the four linear potentiometers

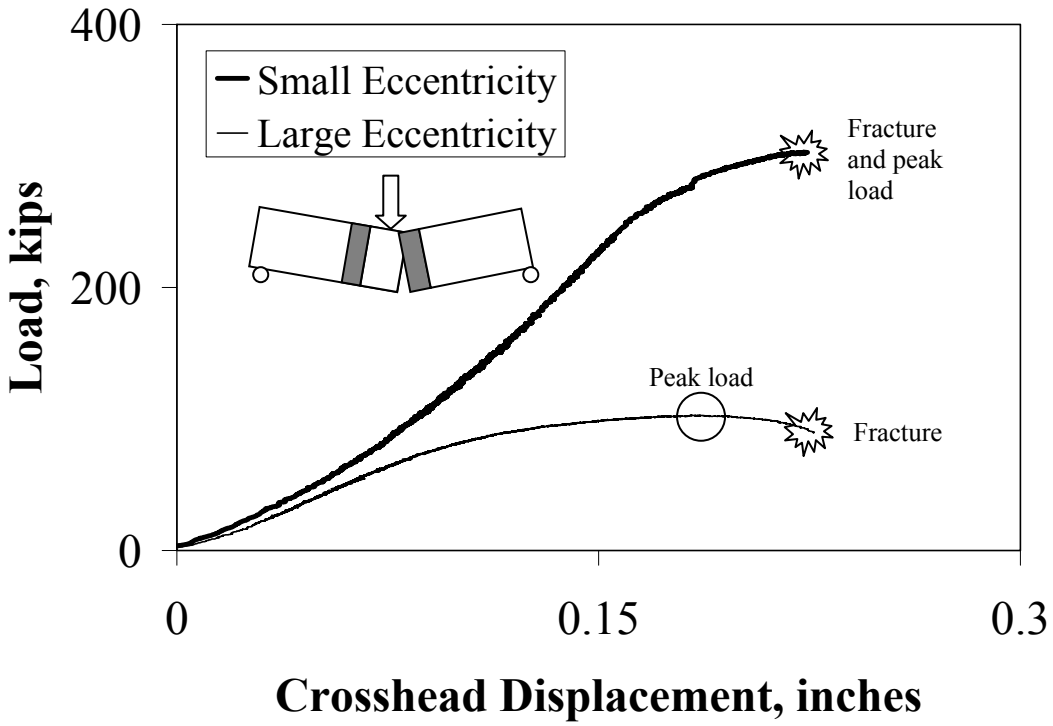

Figure 4.4 – Load-line displacement for representative small eccentricity (shown here for Test #36 – 1.75" root notch, 1/2" non-toughness weld, 3" eccentricity) and large eccentricity (shown here for Test #46 – 1.75" root notch, 1/2" non-toughness weld, 8.5" eccentricity)

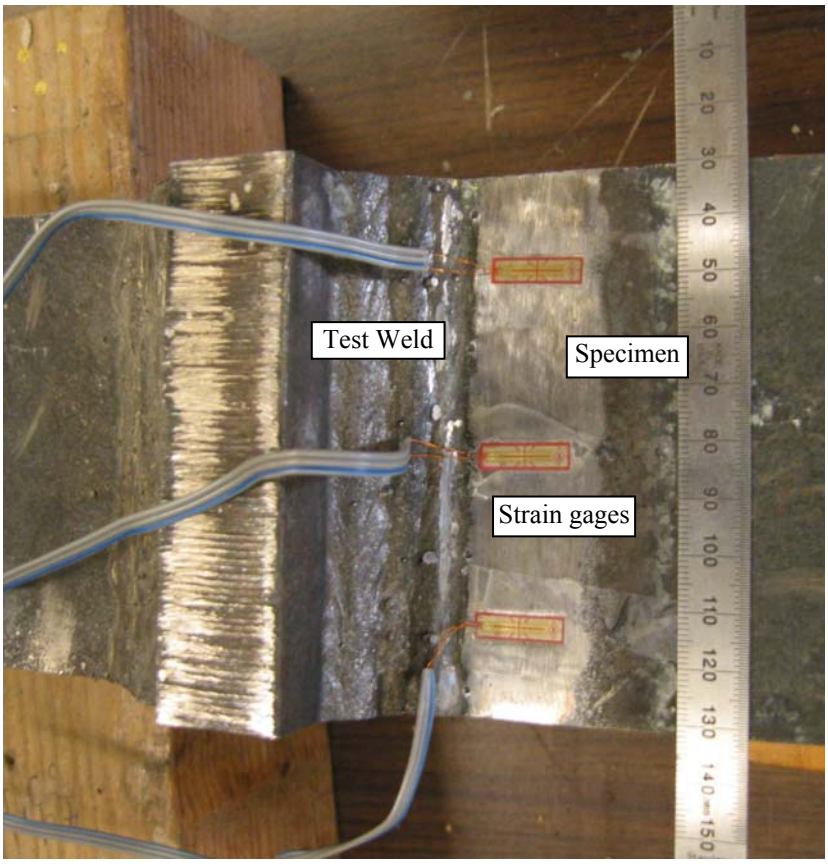

Figure 4.5 – Typical positioning of strain gages

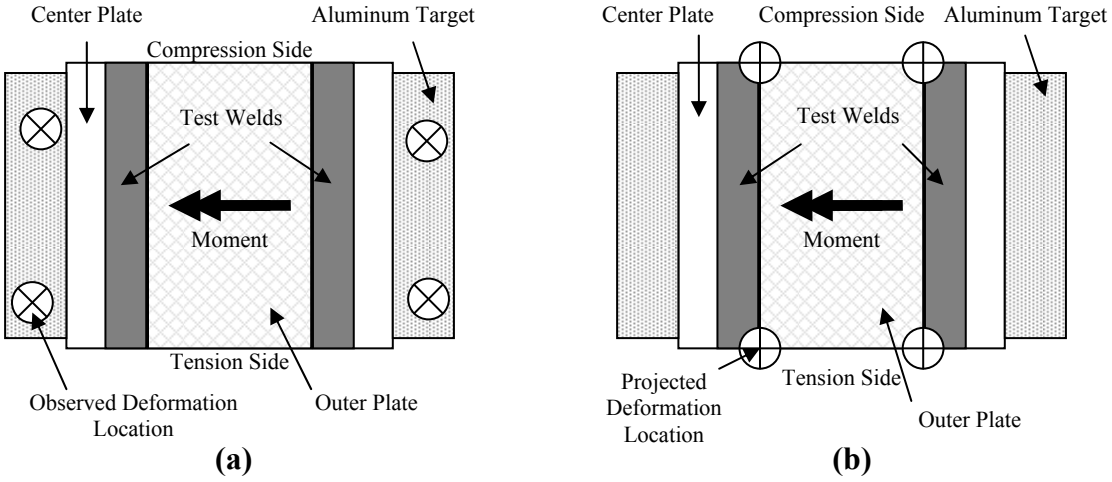

Figure 4.6 – A side view of the test setup (as photographed in Figure 4.3) indicating
(a) the observed weld deformation location and
(b) the kinematically projected weld deformation location

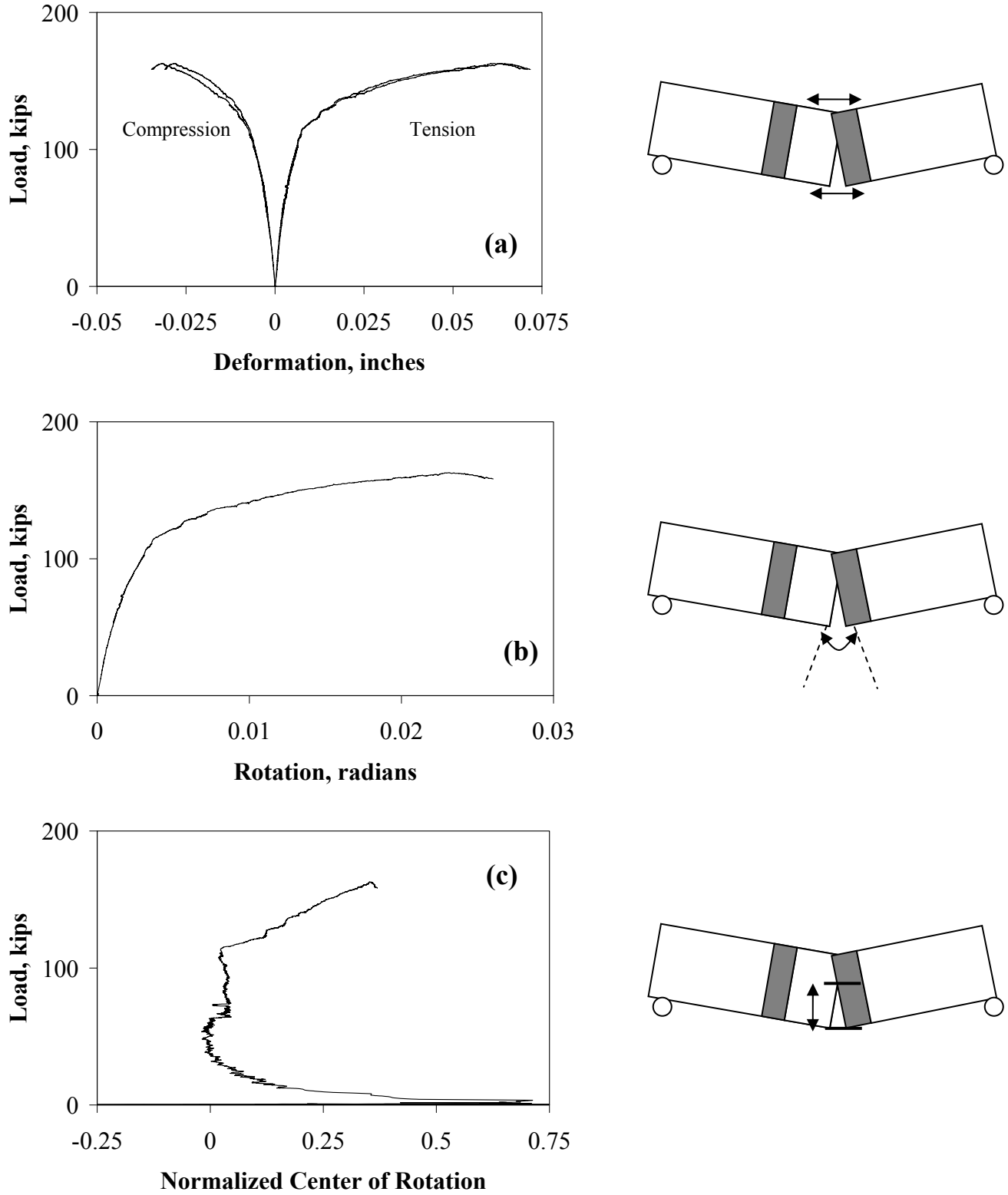

Figure 4.7 – Typical deformation response plots (shown here for Test #58 – 1.25" root notch, toughness rated 1/2" weld, 5.5" eccentricity)

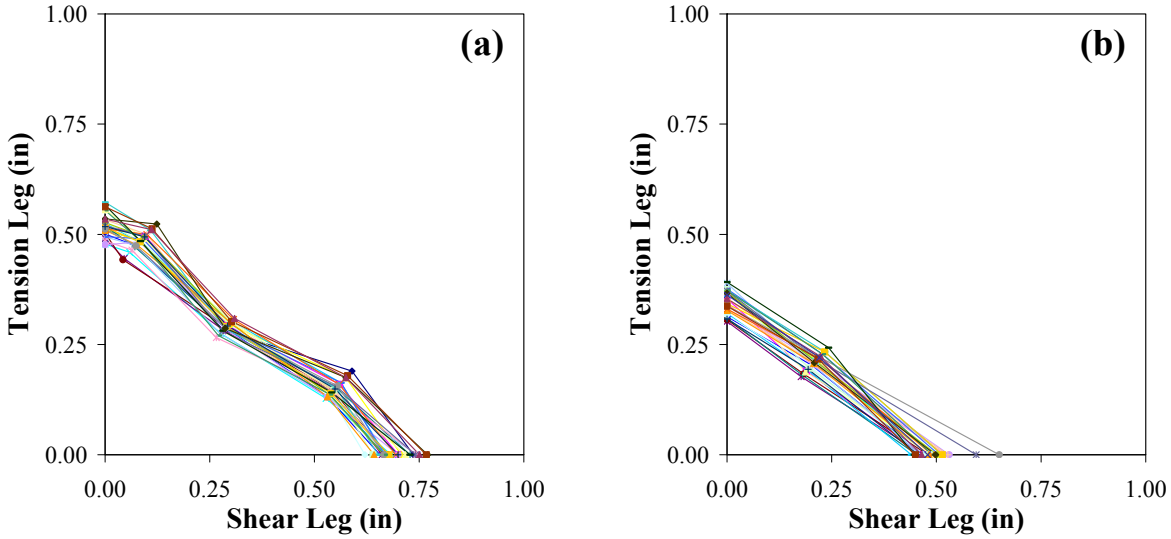

Figure 4.8 – Mean weld profiles for
(a) all the 1/2 inch welds including the different filler metals and plate thicknesses and
(b) all the 5/16 inch welds including the different filler metals and plate thicknesses

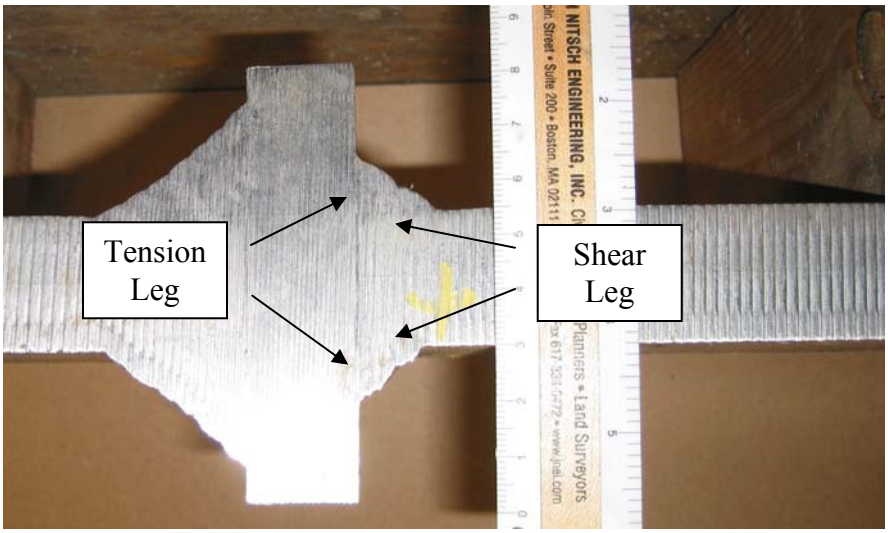

Figure 4.9 – Picture describing the tension leg and shear leg

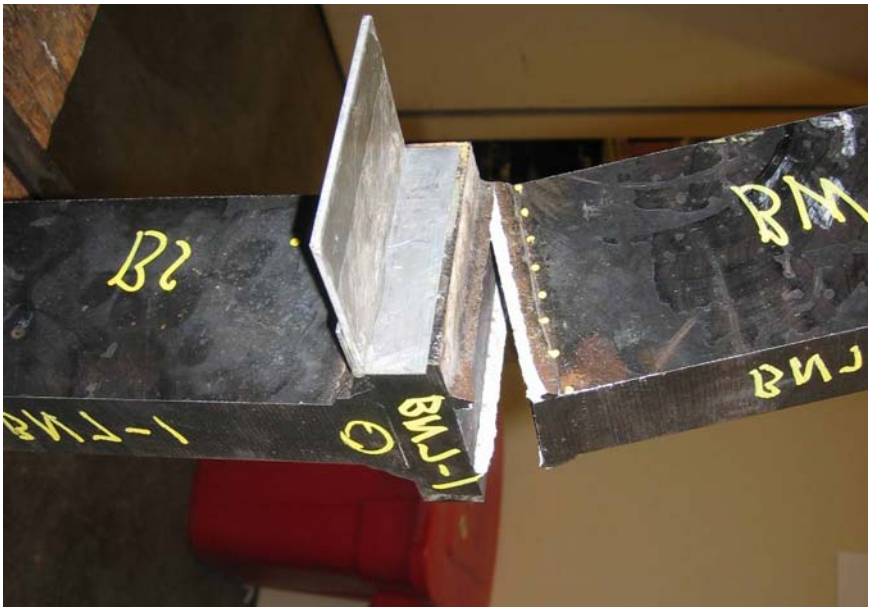

Figure 4.10 – A photograph of a fractured specimen (Test #43 - 1.75 inch root notch, non-toughness 5/16 inch weld, 8.5 inch eccentricity)

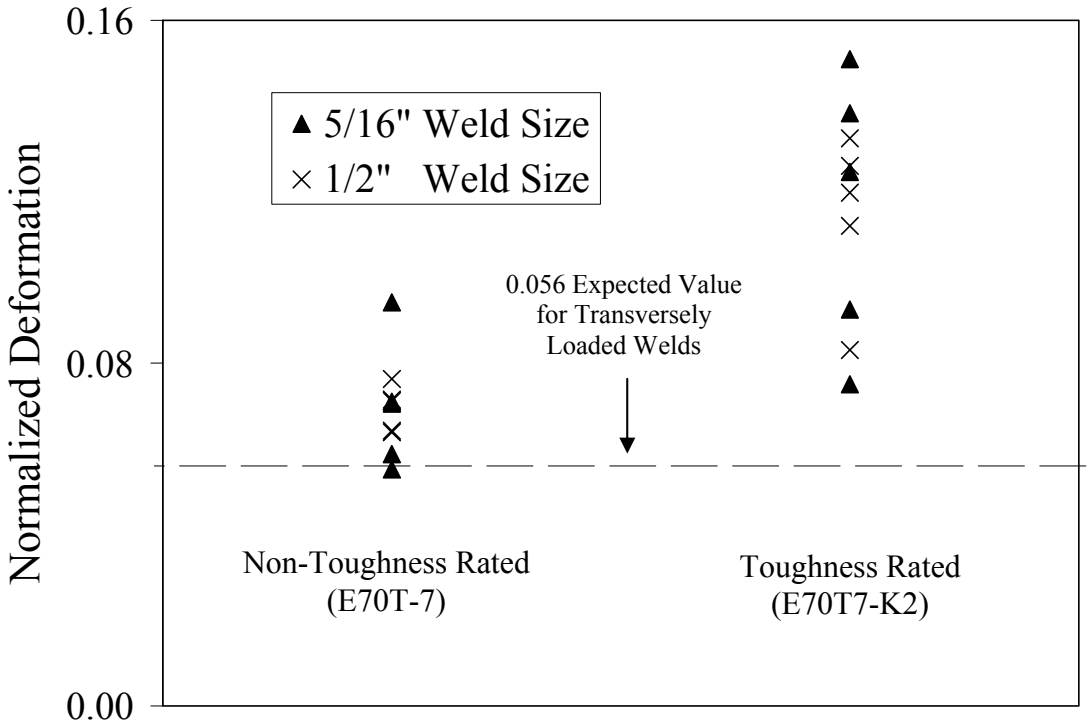

Figure 4.11 – Observed normalized extreme tension end weld deformations (weld deformation divided by shear leg length)

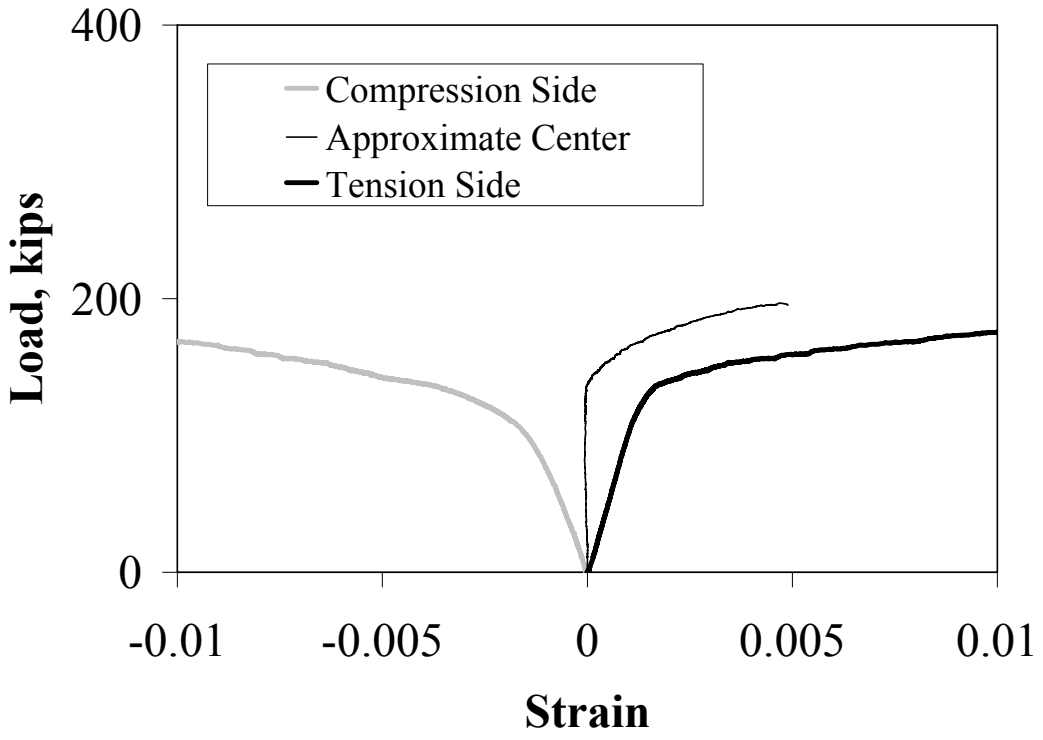

Figure 4.12 – A representative plot of strain versus load (shown here for Test #60 - 1.25 inch root notch, toughness rated 1/2 inch weld, 5.5 inch eccentricity)

Chapter 5

Collection of Test Data

5.1 INTRODUCTION

The primary objective of this chapter is to present test data on welded joints loaded with out-of-plane eccentricity. Researchers from some of the test programs have reported the welding electrode strength designation used for the preparation of the test specimens, but have not conducted ancillary tests to determine the actual weld metal strength. It is therefore important to conduct a review of the literature to collect information about the strength distribution for the grades of filler metal used in these test programs so that the strength of the weld metal for the tested specimens can be estimated more accurately. This chapter first presents a review of ancillary test results for various grades of welding electrodes. The second part of the chapter reports test results on welded joints loaded with out-of-plane eccentricity.

5.2 ANCILLARY TEST RESULTS

The actual tensile strength of the AWS E60 weld electrode used for the preparation of Dawe and Kulak's (1972) test specimens was not reported. Weld strength data for AWS E60 electrode were therefore collected from various sources and are presented in Table 5.1. Data were obtained from three sources, although the majority of the data (94 %) was obtained from a single source. The mean strength of the data collected is 67 ksi and the coefficient of variation, *COV*, is 0.063.

The 1985 test program by Beaulieu and Picard on welded joints with out-of-plane eccentricity made use of AWS E70 welding electrode. Although a series of lapped splice specimens with transverse and longitudinal welds was tested, no direct measurement of the weld metal strength was reported. Therefore, weld strength data for E70 electrode was collected and a summary of the data set is presented in Table 5.2. A comparison between Tables 5.1 and 5.2 indicates that the measured to nominal strength ratio for E60 electrode is slightly lower than for E70 electrode.

In order to correlate weld metal test data to the test data from Beaulieu and Picard (1985), only the weld electrodes that would have been available on the market during their research period was considered, namely, the tensile strength of welding electrodes tested in the period from 1978 to 1987 are taken into consideration. For this set of data the mean ratio of measured to nominal tensile strength is approximately 1.154 and the coefficient of variation is 0.090. The weld metal tensile strength used in the calculation of joint capacity was therefore taken as 80.1 ksi.

Alternatively, the tensile strength of the weld metal can be predicted by comparing the test results of tests on joints with transverse welds and joints with longitudinal welds

reported by Beaulieu and Picard (1985) with similar tests conducted at the University of Alberta by Ng *et al* (2002) and Callele *et al* (2005), for which all-welded metal coupon tests were conducted. The measured tensile strength of weld for Beaulieu and Picard can be predicted based on a relationship establish by the ratios of predicted tensile strength on transverse weld test specimens and the measured tensile strength on the all-welded coupon test specimens.

The tensile strength of filler metal can be predicted from the results of tests on joints with transverse weld, F_{EXX} ,

$$F_{EXX} = \frac{V_r}{(0.6)(1.5)A_w L} \quad [5.1]$$

Where V_r is the measured capacity of the transverse weld, A_w is the theoretical throat area calculated from the specified or measured leg size, and L is the length of weld. Based on equation 5.1, the predicted tensile strength of the filler metal used for the test joints with transverse weld tested by Beaulieu and Picard (1985) and by Ng *et al*. (2002) are 110 ksi (5/16 in. weld sizes) and 131 ksi (1/4 and 1/2 in. weld size), respectively. It should be noted that the predicted tensile strength from the latter is calculated respective to the average of two weld sizes. The mean measured tensile strength for 32 all-weld metal coupons tested at University of Alberta in the first four phases of this program is 80.1 ksi. Assuming that the same strength ratio exists for the all-weld metal coupons as for the transverse weld specimens the filler metal strength for the test program presented by Beaulieu and Picard (1985) is estimated to be 67.2 ksi.

Four all-weld metal coupons (two from E70T7-K2 filler metal and two from E70T-7 filler metal) and 12 standard Charpy V-notch coupons (six from E70T7-K2 filler metal and six from E70T-7 filler metal) were tested to determine the material tensile properties and fracture toughness of the UC Davis specimens. Each coupon was fabricated in accordance with Clause 8 of ANSI/AWS A5.20 (AWS, 2005). The results of the Charpy impact tests and the tension coupon tests are presented in Tables 5.3 and 5.4, respectively.

5.3 TESTS ON WELDED JOINTS WITH OUT-OF-PLANE ECCENTRICITY

5.3.1 Tests from University of Alberta (Dawe and Kulak, 1972, 1974)

The test program by Dawe and Kulak (1972) consisted of eight tests on specimens as described in Chapter 2. The test specimens consisted of a wide flange section with a 1/2 inch load plate welded to one end as shown in Figure 5.1. The other end of the specimen was connected to a 3/4 inch reaction plate by two lines of fillet weld on the exterior sides of each flange. ASTM A36 steel was used for the test specimens and AWS-E60 filler metal was used for the welds. In order to prevent load transfer through bearing of the web with the reaction plate, the web of each section was shortened by 1 inch from the end. The specimens were bolted to the flange of a reaction column and loaded quasi-statically to failure.

The test parameters and measured specimen strength are presented in Table 5.5. The types of section used are W10X39, W10X33, W10X66 and W12X65. The test parameters include load eccentricity, weld dimensions, flange thickness, the static yield strength and tensile strength of the plate, σ_y and σ_u, and measured weld capacity. The reported weld length and size are the average of both weld segments. Since the tensile strength of section was not reported by Dawe and Kulak (1972), there is a need to investigate the relationship of ultimate tensile strength and yield strength of the W-shape sections by considering the ratio between these two parameters. From Schmidt and Bartlett (2002), the bias coefficient of ultimate tensile strength for W-shape sections is 1.13 with nominal tensile strength of 65 ksi. The bias coefficient of yield strength is 1.11 with nominal yield strength of 50 ksi. By using these values, the ratio of ultimate tensile strength to yield strength is 1.323. As presented in Table 5.5, the ultimate tensile strength listed is 1.323 times the yield strength of the plate.

5.3.2 Tests from Université Laval (Beaulieu and Picard, 1985)

A total of 24 eccentrically loaded plate connections, as shown in Figure 5.2, were tested. According to the test records, five failure modes were observed. The specimens were failed by one of the following modes: weld rupture in tension, shear failure of weld, plate rupture in tension, plate shear failure or failure by excessive twisting. In reality, it is not easy to identify the distinctions between tension and shear failure. Therefore, both weld rupture in tension and shear failure of weld are considered to be weld failure for simplicity. Similarly, plate rupture in tension and plate shear failure are considered as plate failure. For the purpose of this research, the specimens failed by excessive twisting are ignored. This reduces the specimen quantity to 22. The load eccentricities, E, considered in the tests were in the range of 2.955 to 14.775 in., corresponding to eccentricity ratios, a, from 0.3 to 1.5 for a weld length, L, of 9.85 in. The plate thicknesses, t, were 0.788 and 1.576 in. Nominal fillet weld sizes of 1/4 and 1/2 in. were selected for specimens of type A (t = 0.788 in.) and weld sizes of 5/16 and 3/8 in. were selected for type B (t = 1.576 in.). The measured dimensions of the test specimens and test results are presented in Table 5.6. The test specimens are designated by type (A or B), weld size (1/4, 5/16, 3/8, or 1/2 in.), eccentricity and test specimen number two of each test specimens were tested. The weld length reported in the table is an average of both welds in a test specimen.

5.3.3 Tests from University of California Davis

The data obtained from UC Davis are presented in detail in Chapter 4 and summarized in Table 5.7. Twenty cruciform type specimens were fabricated in assemblies sufficiently large to contain three test specimens. Three test specimens were cut from each assembly. The test specimens were tested eccentricity was varied by varying the length, L, of the test specimen. Triplicate tests were conducted to obtain a good estimate of variation within each set of variables. The specimens were tested under three-point bending. The test variables were the plate thickness (1.25, 1.75 and 2.5 in.), load eccentricity (3, 5.5 and 8.5 in.), weld size (5/16 and 1/2 in.), and weld electrode classification (toughness and non-toughness rated E70XX electrode).

5.4 COMPARISONS BETWEEN THE TEST PROGRAMS

5.4.1 Loading Protocols and Test Setups

As described in the previous section, the test setups used by Dawe and Kulak (1972) and Beaulieu and Picard (1985) were similar. The test setup used in the test program described in Chapter 4 achieved a similar loading condition as the two other test programs, but with a substantially simpler test setup. The loading condition achieved in all three test programs is similar, namely, a combination of shear and bending moment on the welded joint.

The eccentricity ratio (ratio of load eccentricity to weld length) used by Dawe and Kulak, Beaulieu and Picard and UC Davis are listed in Table 5.8. An examination of Tables 5.5 to 5.8 and Figure 5.3 indicates that a higher ultimate joint capacity was observed for the specimens with higher eccentricity ratio. The eccentricity ratios for all specimens from the three data sets varied within different ranges. Dawe and Kulak (1972) used an eccentricity ratio varying from 1.03 to 2.56. Beaulieu and Picard (1985) used a range of eccentricity ratio between 0.30 and 1.51, whereas UC Davis used values varying from 0.73 to 2.23. A comparison between the test specimens from Dawe and Kulak with those from Beaulieu and Picard indicates that the latter tend to have lower eccentricity ratios than those of Dawe and Kulak. The specimens from UC Davis cover a broader range of eccentricity ratio, although they do not go as high as those tested by Dawe and Kulak or as low as those tested by Beaulieu and Picard. The loading protocol used in the three test programs was not identical. Dawe and Kulak used quasi-static loading and UC Davis applied a slow and continuous monotonic load. The loading protocol used in the Beaulieu and Picard tests is not described (Warren, 1984).

5.4.2 Results of Bend Tests

The results of bend tests from three sources and their predicted capacities using the current AISC approach (AISC, 2005) are presented in Tables 5.9, 5.10, 5.11 and 5.12. The capacity predicted using the AISC approach for the Dawe and Kulak specimens are presented in Table 5.9. It is observed that this approach predicts the test results conservatively, with a mean test-to-predicted value of 1.173. Tables 5.10 and 5.11 show that the AISC approach also provides conservative predictions for the test specimens from Beaulieu and Picard (1985) based on an estimated weld metal tensile strength of 80.1 ksi and 67.2 ksi, respectively. The weld metal strength of 80.1 ksi yields a mean test-to-predicted value of 1.321 and the weld metal strength of 67.2 ksi yields a mean test-to-predicted value of 1.575. Table 5.12 presents the test and predicted capacities for the UC Davis test specimens. The AISC approach gives a mean test-to-predicted value of 1.946, with individual values ranging from 1.5 to 2.8. On average, the specimens tested at UC Davis show higher joint strengths than the specimens from the earlier test programs. This discrepancy between the UC Davis test results and the earlier test result prompted a comparison between the earlier phases of this research program conducted at the University of Alberta (Ng *et al.* 2002) to ensure that the test specimens fabricated for the UC Davis test program were consistent with earlier test results.

The test specimens from Dawe and Kulak result a COV of about 12% whereas those from Beaulieu and Picard and UC Davis give a COV of 20% and 17%, respectively. Due to the high values of COV, the test-to-predicted values are plotted as a function of various parameters in Figures 5.4 to 5.8 to investigate the possible problems in order to improve the model. The parameters considered are plate thickness, eccentricity, weld length, weld size and eccentricity ratio. In Figure 5.4, it shows that the plate thickness has no effect on the test-to-predicted values. It may be caused by the independence of plate thickness in the AISC approach.

In Figure 5.5, the data points from all the sources scatter apart and the test-to-predicted values are not affected by the weld size. In Figure 5.6, the trend is not found because the variation of weld length in each data set is limited, therefore the comparison within the data sets is not made. In Figure 5.7 and 5.8, it shows that test-to-predicted values reduce as eccentricity and eccentricity ratio increase. From all the plots that are discussed above, the reason to explain the large fluctuation of COVs is not determined by examining these parameters. In Figure 5.9, the comparison between test-to-predicted ratios of the filler metal classification is presented. It shows that the weld toughness might have an effect on the strength of eccentrically loaded welded joints. However, such effect is not considered in this model.

5.5 COMPARISON OF MATERIAL PROPERTIES

An examination of test data on eccentrically loaded welded joints from three sources seems to indicate that the joints used in the UC Davis test program have a significantly higher capacity than those tested by Dawe and Kulak (1972) and Beaulieu and Picard (1985). In order to determine whether the UC Davis test specimens had unusually high weld strength, the test results from the cruciform specimens were compared with recent test results obtained from the first phase of this research program on welded joints (Ng *et al.* 2002). Both series of tests made use of welding electrodes of the same classification and were accompanied by tension tests on all-weld metal coupons and Charpy V-notch tests at -20^{o}F, 70^{o}F and 212^{o}F to characterize the weld metal properties.

5.5.1 Cruciform Specimen Tests at U of Alberta (2002)

Five different electrode classifications were investigated, namely, E7014, E70T-4, E70T-7, E70T7-K2, and E71T8-K6. Only the test specimens fabricated with E70T-4, E70T-7 and E70T7-K2 electrodes are considered here since these filler metal designations, or equivalent, were also used in the UC Davis test program. E70T-4 and E70T-7 electrodes have no specified toughness requirement whereas E70T7-K2 electrodes have a specified toughness requirement of 20 ft-lb at -20^{o}F. The weld metal tension coupons and Charpy V-notch impact specimens were machined from a standard groove welded assembly fabricated in accordance to Clause 8 of ANSI/AWS A5.20 (AWS 2005) for flux cored arc welded specimens. A total of nine specimens were fabricated for all-weld-metal tension coupon tests: one set of five specimens from E70T-4 and two sets of two specimens were from E70T-7 and E70T7-K2. Total of 42 Charpy impact V notch specimens were prepared for testing at different temperatures: two sets each of 18

specimens from E70T-4 and E70T-7 electrodes and one set of six specimens from E70T7-K2 electrode. Cruciform specimens with a single pass 1/4 in. welds were welded using an automated welding track. In every case, three nominally identical specimens were cut from a single assembly and milled to a width of 3 in. Six specimens were fabricated in a cruciform configuration and two welds from each specimen were reinforced to ensure failure would occur at two test welds to measure the weld joint capacity. The specimens were loaded to fail by applied quasi-static and static readings were taken at multiple points during the tests.

5.5.2 Cruciform Specimen Tests at UC Davis

Two filler metal classifications (E70T7-K2 and E70T-7) and two weld sizes (1/2 in. and 5/16 in.) were tested. A total of 24 cruciform specimens were tested in direct tension. Two all-weld-metal tension coupons were tested for each classification. Six specimens for each classification were prepared for Charpy V-Notch tests at three different temperatures as per the ANSI/AWS A5.20 and A5.29 (2005) standards. Three test specimens, approximately 4 in. wide, were cut from each assembly of three plates (A572 Grade 50) welded in a cruciform configuration. Three weld passes were performed for the specimens with 1/2 in. welds and only one pass was performed for the specimens with 5/16 in. welds. As for the test configuration used for the test specimens at U of Alberta, one side of the cruciform joint had been reinforced to ensure failure on the side of the test welds. The test specimens were loaded monotonically and continuously until failure of the test specimens.

5.5.3 Comparison of Test Results

Although the test program conducted by Ng *et al*. (2002) included five different welding electrodes, only the E70T-4 and E70T7-K2 electrode were used for the fabrication of cruciform specimens. However, E70T-7 and E70T7-K2 were tested at UC Davis. E70T-4 and E70T-7 welding electrodes do not have toughness requirement. In addition, based on the Charpy V-Notch impact test results presented in Table 5.13, both electrodes show similar CVN energy. Therefore, it is considered appropriate to compare E70T-4 to E70T-7 directly.

5.5.3.1 Charpy V-notch Impact Test

Table 5.13 presents the results from the Charpy V-notch impact tests from the U of Alberta and from UC Davis. As expected, the toughness rated E70T7-K2 filler metal generally demonstrated much higher impact energy than those non-toughness rated filler metals at all three temperatures. The electrodes with no toughness requirement, E70T-4 and E70T-7, have similar toughness values at -20^{o}F and 212^{o}F, but the E70T-7 electrode showed a higher toughness than the E70T-4 electrode at 70^{o}F. In sort, all the test results on toughness rated filler metal E70T7-K2 from UC Davis met the entire toughness requirements.

5.5.3.2 All-Weld-Metal Tension Coupon Test

A total of 13 all-weld-metal tension coupon tests were conducted in two test programs and a summary of the measured and average static yield strength and static tensile strength is presented in Table 5.14. Both coupons made with non-toughness rated filler metal E70T-4 at U of Alberta and E70T-7 at UC Davis met the tensile strength of the required range of 70 ksi to 95 ksi. A comparison of the E70T-7 electrodes from the U of Alberta and the UC Davis test programs indicates that the latter has yield strength and a tensile strength from 10 to 15 percent higher than the strength values from the U of Alberta filler metal. The static tensile strength of the E70T-7 electrode from UC Davis is approximately 20% greater than the tensile strength of the E70T-4 electrode from U of Alberta. The coupons made with the toughness rated E70T7-K2 electrode used at U of Alberta exhibited a static tensile strength in the required range of 70 ksi to 90 ksi. However, the same classification of filler metal used in the UC Davis test program exceeded the upper limit of 90 ksi. In addition, all coupons met the required minimum static yield strength of 58 ksi, except the E70T-4 coupons used in U of Alberta with static yield strength of 51.3 ksi. Two filler coupons, E70T-4 and E70T7-K2, from U of Alberta have the mean elongations of 22.3% and 24.6% respectively. They both met the AWS elongation specifications as 22% for E70T-4 and 20% for E70T7-K2.

5.5.3.3 Tension Test for Cruciform Specimen

The tests on cruciform specimens conducted by Ng *et al.* (2002) were conducted under quasi-static loading (i.e. static values of loading were obtained at regular intervals during the tests) whereas the UC Davis tests were conducted under "dynamic" loading (i.e. the test specimens were loaded continuously, although very slowly, until failure). Observations from the U of A showed "dynamic" tension gave higher load readings; however, the difference between the two loading procedures is very small.

The measured ultimate joint capacity and the test/predicted ratio using AISC approach for welds loaded transverse to their axis are presented in Table 5.15. The predicted capacity using the AISC (2005) strength equation is given as:

$$V_r = 0.60\,\phi\,A_W\,F_{EXX}\left(1.0+0.5\sin^{1.5}\theta\right) \qquad [5.2]$$

where ϕ is the resistance factor, A_w is the theoretical throat area as a function of leg size, F_{EXX} is the minimum specified tensile strength of filler metal and θ is the angle of loading with respect to the weld axis.

For all the cases, the predicted capacity is determined by using the measured tensile strength of the weld metal and the resistance factor is taken as 1.0. A_w is the effective throat area of the weld (calculated from the measured leg dimensions, but neglecting the root penetration and weld reinforcement), F_{EXX} was determined using the measured strength for the all-weld-metal tension coupon tests for the given electrode classification, and θ is 90^o.

The AISC design equation which is used on the E70T-4 and E70T7-K2 data sets from Ng *et al.* provides significantly conservative prediction of the weld capacity. However, the equation gives predictions closer to the tested weld capacities for UC Davis E70T-7 and E70T7-K2 data sets. The mean test-to-predicted values for the Ng *et al.* (2002) data vary from 1.735 to 1.947 as shown in Table 5.15. On the other hand, the mean test-to-predicted values for the UC Davis test data are reduced to 0.97 to 1.10. It is apparent that the UC Davis test specimens provide lower capacity than the earlier U of Alberta test specimens.

Figure 5.10 presents a plot of capacity predicted using the AISC equation versus the measured test capacity for the cruciform test specimens discussed above. The solid line represents a test-to-predicted value of unity. The data points that appear below the solid line are considered to be conservative while the data points that appear above the line are considered as non-conservative predictions. In Figure 5.11, it shows that the root notch distances have no affect to the test to predicted ratio from the test data from UC Davis (when root notches equal to 1.25 in. and 2.5 in.). However, the test-to-predict value is slightly affected when comparing with the test data from U of Alberta (when root notch used is 0.75 in.). It indicates that the test-to-predicted value for U of Alberta is higher than UC Davis and also shows it is in the conservative region as observed in Figure 5.10. An overview of the weld stress, calculated on the throat dimension calculated from the measured leg size, as a function of electrode classification and the test program is presented in Figure 5.12. The mean test result is represented by a solid diamond and the range of test results is represented by a vertical bar. The lower variation in test results observed in the U of Alberta test results compared to the UC Davis results is attributed to the much smaller sample size used in the U of Alberta test program. It is observed that the weld stresses for the electrodes used by Ng *et al.* (2002) are significantly higher than those used in the UC Davis test program.

5.6 CONCLUSIONS

Test results from welded joints loaded under out-of-plane eccentricity obtained from the test programs of Dawe and Kulak (1972), Beaulieu and Picard (1985) and UC Davis were presented and compared. Based on the current AISC approach, the predicted weld capacities are close to the test results by Dawe & Kulak and Beaulieu & Picard. However, the AISC method provides very conservative predictions of the UC Davis data set. Therefore, an investigation of the test data from the UC Davis program was conducted by comparing test results from this program with a limited number of test results from cruciform test specimens and material tests from Ng *et al.* (2002). Also, the COV of the AISC approach are found to be around 11% to 20%; unfortunately, the explanation to the problem is not determined by considering the test parameters. A comparison of the all-weld-metal tension coupons and Charpy V-notch impact test results obtained from U of Alberta and UC Davis indicated that the material properties from the two test programs are similar. The filler metals used in the UC Davis test program were found to meet the strength and toughness requirements of AWS A5.20 and A5.29 standards. Also, the tested fillet weld capacities from UC Davis are well predicted by using design equation in AISC approach. By comparing the root notch distance with test-

to-predicated ratios from UC Davis and U of Alberta, the data shows that the root notch has no significant affect to the test-to-predicted ratio. The effect of loading rate was found to be negligible when test results from U of Alberta were compared with those from UC Davis. In conclusion, the over-predicted weld capacity by AISC approach on UC Davis combined shear and moment test results is not caused by the dissimilarity in material properties of the specimens and the method of loading.

Table 5.1 - Material Factor Specific for E60

Source of Data	Sample size, N	Nominal tensile strength, (ksi) F_{EXX}	Mean tensile strength, (ksi) σ_u	Ratio of Measured to Nominal strength $\rho_{(60)}$	Coefficient of Variation V
Swannell and Skewes (1979)	2	60	78	1.302	0.020
Fisher at al. (1978)	127	60	66	1.099	0.039
Mansell and Yadav (1982)	6	60	81	1.349	0.027
All Sources	**135**	**60**	**67**	**1.113**	**0.063**

Table 5.2 - Material Factor Specific for E70

Source of Data	Sample size, N	Nominal tensile strength, (ksi) F_{exx}	Mean tensile strength, (ksi) σ_u	Ratio of Measured to Nominal $\rho_{(70)}$	Coefficient of Variation V
Bowman and Quinn (1994)	3	70	69.0	0.986	0.029
Callele *et al* (2005)†	32	70	80.1	1.151	0.084
Miazga and Kennedy (1986)	3	70	78.0	1.120	0.014
Pham (1981)	3	70	72.5	1.042	0.044
UC Davis (2008)	4	70	97.3	1.398	0.002
Fisher *et al* (1978)	40	70	86.8	1.239	0.114
	128	70	85.4	1.219	0.056
	138	70	74.9	1.069	0.036
Gagnon and Kennedy (1987)	10	70	84.1	1.208	0.036
All Sources	**361**	**70**	**80.9**	**1.155**	**0.092**

† Including all weld metal tension coupon tests from Phases 1 through 4.

Table 5.3 - Charpy V-Notch Impact Test Results (UC Davis)

Source of Data	Filler Metal	Test	CVN Energy (ft lb)		
			-20°F	70°F	212°F
UC Davis	E70T-7	1	5.5	19.0	41.0
		2	6.0	18.0	41.0
		Mean	**5.8**	**18.5**	**41.0**
	E70T7-K2	1	30.0	56.0	88.0
		2	23.0	62.0	88.0
		Mean	**26.5**	**59.0**	**88.0**

Table 5.4 - Weld Metal Tension Coupon Test Results (UC Davis)

Source of Data	Filler Metal	Test	Static Yield Strength, F_y (ksi)	Static Tensile Strength, F_{exx} (ksi)
UC Davis	E70T-7	1	75.8	97.1
		2	76.8	97.2
		Mean	**76.3**	**97.2**
	E70T7-K2	1	82.7	97.5
		2	83.0	97.4
		Mean	**82.9**	**97.5**

Table 5.5 – Specimen Data from Dawe and Kulak (1972)

Specimen number	Type of Section	Load eccentricity, e, (in)	Average weld dimensions, (in)		Flange thickness, t (in)	Static yield of base metal, σ_y, (ksi)	Tensile strength of base plate, σ_u, (ksi)	Test capacity, (kips)
			Length, L	Effective leg size, D_e				
A-1	W10X39	8	7.77	0.31	1.04	43.3	65.4	62.5
A-2	W10X39	12	7.86	0.31	1.04	43.3	65.4	39.0
A-3	W10X39	16	7.87	0.30	1.04	41.9	63.3	23.1
A-4	W10X39	20	7.81	0.30	1.06	41.9	63.3	19.5
A-5	W10X33	16	7.84	0.30	0.86	38.1	57.5	23.6
A-6	W10X66	16	7.92	0.32	1.52	38.4	58.0	32.6
A-7	W12X65	15	11.86	0.29	1.24	39.3	59.3	59.7
A-8	W12X65	20	11.8	0.31	1.24	39.3	59.3	49.6

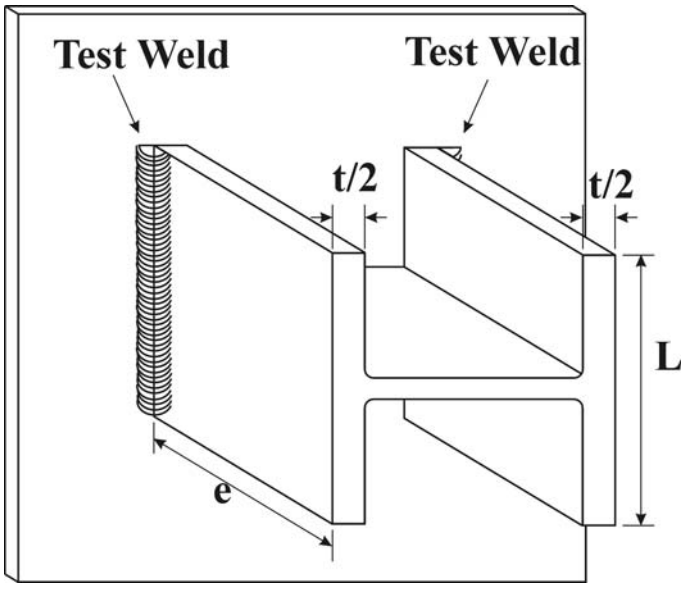

Table 5.6 – Specimen Data from Picard and Beaulieu (1985)

Specimen number	Load eccentricity (in)	Weld dimensions (in)			Plate thickness, t (in)	σ_y (ksi)	σ_u (ksi)	Test Capacity (kips)	Actual Failure Mode
		Length	Leg size, D_{e1}	Leg size, D_{e2}					
A-6-375-1	14.775	9.842	0.315	0.291	0.776	41.6	70.9	50.9	Weld
A-6-375-2[1]	14.775	9.724	0.489	0.494	0.776	41.6	70.9	82.3	Twist
A-12-375-1[2]	14.775	9.882	0.524	0.552	0.776	41.6	70.9	61.9	Weld
A-12-375-2	14.775	9.882	0.563	0.510	0.776	41.6	70.9	68.4	Plate
A-6-125-1	4.925	9.921	0.327	0.305	0.776	41.6	70.9	157.9	Weld
A-6-125-2	4.925	9.925	0.296	0.322	0.776	41.6	70.9	141.7	Weld
A-12-125-1	4.925	9.834	0.556	0.549	0.776	41.6	70.9	164.8	Plate
A-12-125-2[1]	4.925	9.941	0.536	0.504	0.776	41.6	70.9	211.3	Twist
A-6-75-1	2.955	9.925	0.424	0.390	0.776	41.6	70.9	267.7	Plate
A-6-75-2	2.955	9.901	0.319	0.312	0.776	41.6	70.9	245.9	Weld
A-12-75-1	2.955	9.807	0.467	0.534	0.776	41.6	70.9	240.9	Plate
A-12-75-2	2.955	9.905	0.538	0.498	0.776	41.6	70.9	254.4	Plate
B-8-375-1	14.775	9.811	0.506	0.445	1.602	46.0	71.5	93.5	Weld
B-8-375-2	14.775	9.909	0.431	0.496	1.602	46.0	71.5	96.1	Weld
B-10-375-1	14.775	9.807	0.462	0.476	1.602	46.0	71.5	61.3	Weld
B-10-375-2	14.775	9.803	0.509	0.436	1.602	46.0	71.5	109.1	Weld
B-8-125-1	4.925	9.885	0.410	0.433	1.602	46.0	71.5	235.7	Weld
B-8-125-2	4.925	9.885	0.390	0.442	1.602	46.0	71.5	286.6	Weld
B-10-125-1	4.925	9.878	0.410	0.413	1.602	46.0	71.5	266.2	Weld
B-10-125-2	4.925	9.779	0.448	0.433	1.602	46.0	71.5	249.5	Weld
B-8-75-1	2.955	9.803	0.361	0.360	1.602	46.0	71.5	334.6	Weld
B-8-75-2	2.955	9.787	0.337	0.347	1.602	46.0	71.5	313.4	Weld
B-10-75-1[2]	2.955	9.692	0.487	0.502	1.602	46.0	71.5	381.5	Weld
B-10-75-2[2]	2.955	9.803	0.506	0.463	1.602	46.0	71.5	358.7	Weld

[1]Test stopped due to torsion of plate

[2]Weld returns removed

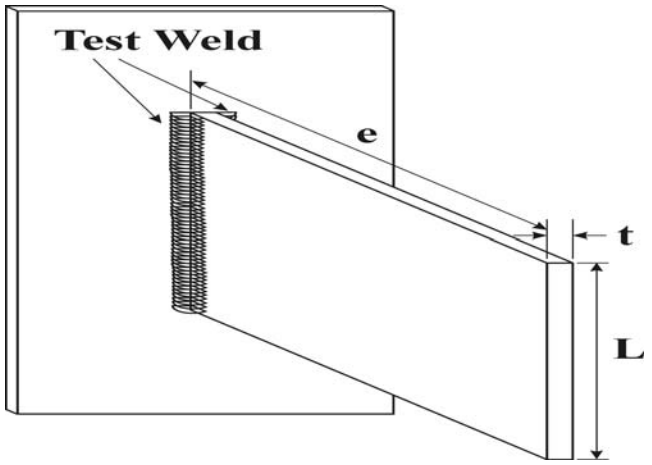

Table 5.7 – Summary of Test Results from Chapter 4

Test number	Specimen tag	Load eccentricity, (in)	Weld Dimensions, (in)				Plate thickness, t (in)	σ_y (ksi)	σ_u (ksi)	Test Capacity (kips)
			Length, L_1	Leg size, D_{e1}	Length, L_2	Leg size, D_{e2}				
25	B_125_A516_55_1	5.5	3.877	0.428	3.875	0.371	1.259	53.4	71.6	44.4
26	B_125_A516_55_2	5.5	3.906	0.410	3.914	0.387	1.256	53.4	71.6	53.7
27	B_125_A516_55_3	5.5	3.818	0.410	3.925	0.412	1.256	53.4	71.6	52.5
28	B_125_A12_55_1	5.5	3.814	0.595	3.999	0.590	1.265	53.4	71.6	73.4
29	B_125_A12_55_2	5.5	3.960	0.616	3.912	0.565	1.288	53.4	71.6	72.2
30	B_125_A12_55_3	5.5	3.970	0.593	4.000	0.581	1.269	53.4	71.6	71.1
31	B_175_A516_3_1	3.0	3.930	0.362	3.959	0.356	1.750	53.4	71.6	120.0
32	B_175_A516_3_2	3.0	3.982	0.373	3.985	0.357	1.753	53.4	71.6	119.0
33	B_175_A516_3_3	3.0	4.077	0.355	4.067	0.367	1.750	53.4	71.6	123.9
34	B_175_A12_3_1	3.0	3.868	0.570	3.872	0.532	1.767	53.4	71.6	153.4
35	B_175_A12_3_2	3.0	4.001	0.551	3.998	0.558	1.765	53.4	71.6	175.0
36	B_175_A12_3_3	3.0	3.816	0.560	3.910	0.580	1.764	53.4	71.6	152.1
37	B_175_A516_55_1	5.5	4.067	0.391	4.058	0.343	1.759	53.4	71.6	61.7
38	B_175_A516_55_2	5.5	4.050	0.389	4.055	0.343	1.752	53.4	71.6	59.7
39	B_175_A516_55_3	5.5	3.927	0.378	3.977	0.364	1.759	53.4	71.6	63.0
40	B_175_A12_55_1	5.5	4.085	0.610	4.079	0.585	1.796	53.4	71.6	90.0
41	B_175_A12_55_2	5.5	3.797	0.568	3.825	0.558	1.801	53.4	71.6	76.6
42	B_175_A12_55_3	5.5	3.919	0.575	3.885	0.592	1.778	53.4	71.6	79.6
43	B_175_A516_85_1	8.5	3.870	0.446	3.890	0.390	1.750	53.4	71.6	39.0
44	B_175_A516_85_2	8.5	3.806	0.418	3.819	0.425	1.750	53.4	71.6	30.1
45	B_175_A516_85_3	8.5	3.919	0.376	3.900	0.458	1.758	53.4	71.6	33.4
46	B_175_A12_85_1	8.5	4.056	0.592	4.070	0.578	1.771	53.4	71.6	51.9
47	B_175_A12_85_2	8.5	4.070	0.567	4.062	0.584	1.774	53.4	71.6	51.3
48	B_175_A12_85_3	8.5	4.011	0.618	4.062	0.625	1.769	53.4	71.6	53.0
49	B_250_A516_55_1	5.5	4.081	0.448	4.162	0.361	2.522	53.4	71.6	62.0
50	B_250_A516_55_2	5.5	3.977	0.439	3.985	0.366	2.518	53.4	71.6	58.7
51	B_250_A516_55_3	5.5	4.111	0.406	4.116	0.386	2.534	53.4	71.6	58.3
52	B_250_A12_55_1	5.5	3.947	0.582	4.004	0.581	2.533	53.4	71.6	86.9
53	B_250_A12_55_2	5.5	4.138	0.590	4.174	0.559	2.528	53.4	71.6	101.6
54	B_250_A12_55_3	5.5	4.118	0.547	4.101	0.562	2.521	53.4	71.6	94.5

Table 5.7 – Cont'd

Test number	Specimen tag	Load eccentricity (in)	Weld Dimensions, (in)				Plate thickness, t (in)	σ_y (ksi)	σ_u (ksi)	Test Capacity (kips)
			Length, L_1	Leg size, D_{e1}	Length, L_2	Leg size, D_{e2}				
55	B_125_B516_55_1	5.5	3.779	0.419	3.779	0.434	1.272	53.4	71.6	50.5
56	B_125_B516_55_2	5.5	3.848	0.420	3.828	0.431	1.275	53.4	71.6	57.4
57	B_125_B516_55_3	5.5	3.750	0.388	3.760	0.454	1.273	53.4	71.6	60.8
58	B_125_B12_55_1	5.5	4.027	0.604	3.973	0.574	1.273	53.4	71.6	82.0
59	B_125_B12_55_2	5.5	3.943	0.583	3.950	0.541	1.291	53.4	71.6	84.5
60	B_125_B12_55_3	5.5	4.104	0.597	4.101	0.619	1.274	53.4	71.6	98.8
61	B_175_B516_3_1	3.0	3.977	0.371	4.013	0.435	1.774	53.4	71.6	165.2
62	B_175_B516_3_2	3.0	4.132	0.376	4.096	0.388	1.768	53.4	71.6	160.4
63	B_175_B516_3_3	3.0	4.081	0.398	4.061	0.375	1.774	53.4	71.6	155.3
64	B_175_B12_3_1	3.0	4.072	0.578	4.085	0.587	1.771	53.4	71.6	193.2
65	B_175_B12_3_2	3.0	4.036	0.578	4.045	0.582	1.780	53.4	71.6	200.0
66	B_175_B12_3_3	3.0	4.056	0.561	4.083	0.564	1.782	53.4	71.6	185.4
67	B_175_B516_55_1	5.5	3.993	0.514	4.058	0.375	1.761	53.4	71.6	86.7
68	B_175_B516_55_2	5.5	4.015	0.517	4.040	0.331	1.755	53.4	71.6	69.8
69	B_175_B516_55_3	5.5	4.034	0.382	4.051	0.337	1.764	53.4	71.6	78.0
70	B_175_B12_55_1	5.5	4.002	0.573	4.026	0.593	1.794	53.4	71.6	99.3
71	B_175_B12_55_2	5.5	3.914	0.647	3.816	0.556	1.787	53.4	71.6	90.0
72	B_175_B12_55_3	5.5	3.947	0.532	3.816	0.616	1.787	53.4	71.6	86.6
73	B_175_B516_85_1	8.5	4.070	0.428	4.090	0.410	1.786	53.4	71.6	45.9
74	B_175_B516_85_2	8.5	3.977	0.422	3.977	0.410	1.750	53.4	71.6	46.8
75	B_175_B516_85_3	8.5	3.960	0.435	3.990	0.400	1.760	53.4	71.6	46.0
76	B_175_B12_85_1	8.5	4.076	0.615	4.073	0.560	1.780	53.4	71.6	59.3
77	B_175_B12_85_2	8.5	4.000	0.593	3.990	0.609	1.810	53.4	71.6	59.9
78	B_175_B12_85_3	8.5	3.790	0.625	3.830	0.636	1.779	53.4	71.6	57.1
79	B_250_B516_55_1	5.5	3.940	0.386	4.096	0.376	2.540	53.4	71.6	77.9
80	B_250_B516_55_2	5.5	3.965	0.396	3.985	0.400	2.534	53.4	71.6	77.0
81	B_250_B516_55_3	5.5	3.965	0.424	3.883	0.389	2.523	53.4	71.6	76.4
82	B_250_B12_55_1	5.5	4.004	0.582	3.995	0.659	2.540	53.4	71.6	110.5
83	B_250_B12_55_2	5.5	3.900	0.608	3.950	0.675	2.550	53.4	71.6	112.0
84	B_250_B12_55_3	5.5	3.850	0.593	3.920	0.637	2.540	53.4	71.6	110.7

Table 5.7 – Cont'd

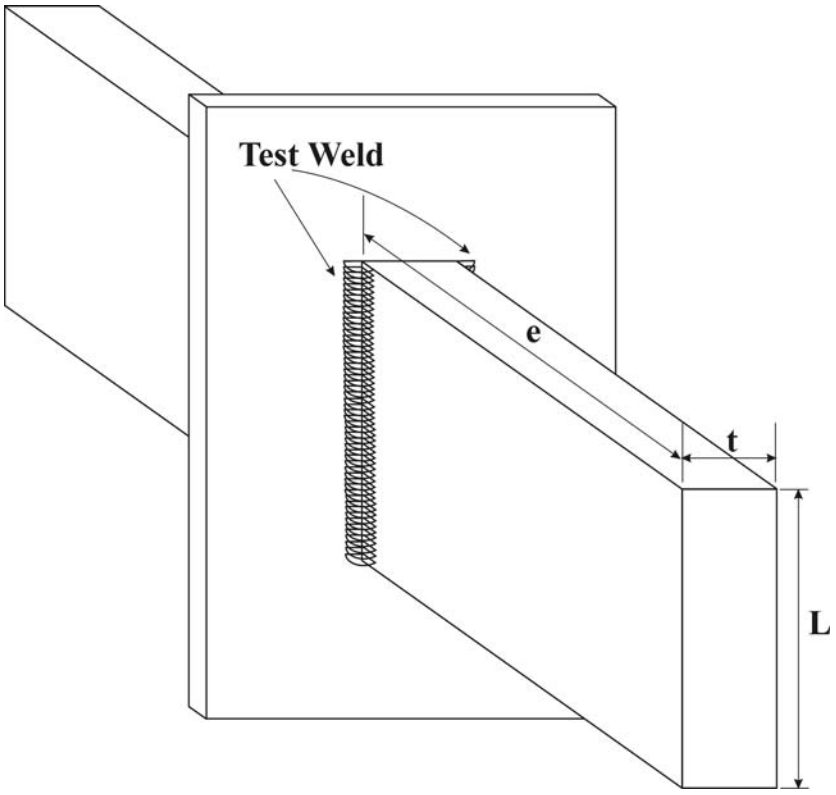

Table 5.8 – Specimen Eccentricity Ratio used by Dawe and Kulak, Picard and Beaulieu and UC Davis

Dawe and Kulak (1972)		Picard and Beaulieu (1985)		UC Davis	
Specimen number	Eccentricity ratio, a	Specimen number	Eccentricity ratio, a	Specimen tag	Eccentricity ratio, a
A-1	1.03	A-6-375-1	1.50	B_125_A516_55_1	1.42
A-2	1.53	A-6-125-1	0.50	B_125_A516_55_2	1.41
A-3	2.03	A-6-125-2	0.50	B_125_A516_55_3	1.42
A-4	2.56	B-8-375-1	1.51	B_125_A12_55_1	1.41
A-5	2.04	B-8-375-2	1.49	B_125_A12_55_2	1.40
A-6	2.02	B-10-375-1	1.51	B_125_A12_55_3	1.38
A-7	1.26	B-10-375-2	1.51	B_175_A516_3_1	0.76
A-8	1.69	B-8-125-1	0.50	B_175_A516_3_2	0.75
		B-8-125-2	0.50	B_175_A516_3_3	0.74
		B-10-125-2	0.50	B_175_A12_3_1	0.78
		B-10-125-1	0.50	B_175_A12_3_2	0.75
		A-6-75-2	0.30	B_175_A12_3_3	0.78
		B-8-75-1	0.30	B_175_A516_55_1	1.35
		B-8-75-2	0.30	B_175_A516_55_2	1.36
		B-10-75-1	0.30	B_175_A516_55_3	1.39
		B-10-75-2	0.30	B_175_A12_55_1	1.35
		A-6-75-1	0.30	B_175_A12_55_2	1.44
		A-12-75-1	0.30	B_175_A12_55_3	1.41
		A-12-75-2	0.30	B_175_A516_85_1	2.19
		A-12-375-1	1.50	B_175_A516_85_2	2.23
		A-12-375-2	1.50	B_175_A516_85_3	2.17
		A-12-125-1	0.50	B_175_A12_85_1	2.09
				B_175_A12_85_2	2.09
				B_175_A12_85_3	2.11
				B_250_A516_55_1	1.33
				B_250_A516_55_2	1.38
				B_250_A516_55_3	1.34
				B_250_A12_55_1	1.38
				B_250_A12_55_2	1.32
				B_250_A12_55_3	1.34
				B_125_B516_55_1	1.46
				B_125_B516_55_2	1.43
				B_125_B516_55_3	1.46
				B_125_B12_55_1	1.38
				B_125_B12_55_2	1.39
				B_125_B12_55_3	1.34
				B_175_B516_3_1	0.75
				B_175_B516_3_2	0.73
				B_175_B516_3_3	0.74
				B_175_B12_3_1	0.74
				B_175_B12_3_2	0.74
				B_175_B12_3_3	0.74

Table 5.8 – Cont'd

UC Davis	
Specimen number	Eccentricity ratio, A
B_175_B516_55_1	1.37
B_175_B516_55_2	1.37
B_175_B516_55_3	1.36
B_175_B12_55_1	1.37
B_175_B12_55_2	1.42
B_175_B12_55_3	1.42
B_175_B516_85_1	2.08
B_175_B516_85_2	2.14
B_175_B516_85_3	2.14
B_175_B12_85_1	2.09
B_175_B12_85_2	2.13
B_175_B12_85_3	2.23
B_250_B516_55_1	1.37
B_250_B516_55_2	1.38
B_250_B516_55_3	1.40
B_250_B12_55_1	1.38
B_250_B12_55_2	1.40
B_250_B12_55_3	1.42

Table 5.9 –Predicted Welded Joint Capacity on Test Results from University of Alberta (Dawe and Kulak, 1972)

Specimen number	Measured ultimate load, (kips)	Predicted capacity (kips)	
		AISC approach	Test-to-predicted ratio
A-1	62.5	45.0	1.388
A-2	39.0	31.3	1.248
A-3	23.1	22.9	1.009
A-4	19.5	18.1	1.078
A-5	23.6	22.7	1.039
A-6	32.6	24.7	1.319
A-7	59.7	52.9	1.128
A-8	49.6	42.4	1.170
Mean of ratios			**1.173**
Coefficient of variation, V			**0.116**

Table 5.10 – Predicted Welded Joint Capacity on Test Results from Université Laval (Beaulieu and Picard , 1985) using F_{EXX} = 80.1 ksi

Specimen number	Measured ultimate load (kips)	Predicted capacity (kips)	
		AISC approach	Test-to-predicted ratio
A-12-375-1	61.9	84.5	0.732
A-6-125-1	157.9	132.2	1.194
A-6-125-2	141.7	129.3	1.096
A-6-375-1	50.9	47.2	1.077
A-6-75-2	245.9	176.9	1.390
B-10-125-1	266.2	170.7	1.560
B-10-125-2	249.5	179.5	1.390
B-10-375-1	61.3	72.5	0.845
B-10-375-2	109.1	73.1	1.493
B-10-75-1	381.5	268.9	1.419
B-10-75-2	358.7	267.8	1.339
B-8-125-1	235.7	175.2	1.345
B-8-125-2	286.6	172.9	1.658
B-8-375-1	93.5	73.7	1.269
B-8-375-2	96.1	73.1	1.314
B-8-75-1	334.6	199.3	1.679
B-8-75-2	313.4	188.5	1.663
Mean of ratios			**1.321**
Coefficient of variation, V			**0.204**

Table 5.11 –Predicted Welded Joint Capacity on Test Results from Université Laval (Beaulieu and Picard , 1985) using F_{EXX} = 67.2 ksi

Specimen number	Measured ultimate load (kips)	Predicted capacity (kips)	
		AISC approach	Test/predicted ratio
A-12-375-1	61.9	70.9	0.872
A-6-125-1	157.9	110.9	1.423
A-6-125-2	141.7	108.5	1.306
A-6-375-1	50.9	39.6	1.284
A-6-75-2	245.9	148.4	1.656
B-10-125-1	266.2	143.2	1.859
B-10-125-2	249.5	150.6	1.656
B-10-375-1	61.3	60.8	1.008
B-10-375-2	109.1	61.3	1.779
B-10-75-1	381.5	225.6	1.691
B-10-75-2	358.7	224.7	1.597
B-8-125-1	235.7	146.9	1.604
B-8-125-2	286.6	145.0	1.976
B-8-375-1	93.5	61.8	1.513
B-8-375-2	96.1	61.3	1.566
B-8-75-1	334.6	167.2	2.001
B-8-75-2	313.4	158.1	1.982
Mean of ratios			**1.575**
Coefficient of variation, V			**0.204**

Table 5.12 –Predicted Welded Joint Capacity on Test results from University of California, Davis

Specimen tag	Measured ultimate load (kips)	Predicted capacity (kips)	
		AISC approach	Test/predicted ratio
B_125_A516_55_1	44.4	31.5	1.41
B_125_A516_55_2	53.7	31.9	1.682
B_125_A516_55_3	52.5	32.3	1.626
B_125_A12_55_1	73.4	47.4	1.55
B_125_A12_55_2	72.2	48	1.504
B_125_A12_55_3	71.1	48.8	1.458
B_175_A516_3_1	120	51.3	2.337
B_175_A516_3_2	119	53.3	2.234
B_175_A516_3_3	123.9	54.8	2.259
B_175_A12_3_1	153.4	76.1	2.016
B_175_A12_3_2	175	81.6	2.146
B_175_A12_3_3	152.1	78.5	1.938
B_175_A516_55_1	61.7	31.7	1.946
B_175_A516_55_2	59.7	31.4	1.898
B_175_A516_55_3	63	30.3	2.077
B_175_A12_55_1	90	52	1.729
B_175_A12_55_2	76.6	42.9	1.788
B_175_A12_55_3	79.6	46.5	1.711
B_175_A516_85_1	39	21.5	1.813
B_175_A516_85_2	30.1	21	1.434
B_175_A516_85_3	33.4	21.8	1.536
B_175_A12_85_1	51.9	33	1.571
B_175_A12_85_2	51.3	32.6	1.576
B_175_A12_85_3	53	34.7	1.527
B_250_A516_55_1	62	35.9	1.727
B_250_A516_55_2	58.7	33.4	1.758
B_250_A516_55_3	58.3	35.1	1.66
B_250_A12_55_1	86.9	48.1	1.805
B_250_A12_55_2	101.6	51.9	1.959
B_250_A12_55_3	94.5	49	1.929

Table 5.12 – Cont'd

Specimen number	Measured ultimate load (kips)	Predicted capacity (kips)	
		AISC approach	Test/predicted ratio
B_125_B516_55_1	50.5	31.9	1.582
B_125_B516_55_2	57.4	32.8	1.75
B_125_B516_55_3	60.8	31.1	1.954
B_125_B12_55_1	82	49.3	1.661
B_125_B12_55_2	84.5	45.8	1.843
B_125_B12_55_3	98.8	53.6	1.844
B_175_B516_3_1	165.2	59.2	2.792
B_175_B516_3_2	160.4	59.2	2.708
B_175_B516_3_3	155.3	58.8	2.639
B_175_B12_3_1	193.2	88.9	2.173
B_175_B12_3_2	200	86.9	2.301
B_175_B12_3_3	185.4	85.5	2.169
B_175_B516_55_1	86.7	37.6	2.306
B_175_B516_55_2	69.8	36	1.941
B_175_B516_55_3	78	30.8	2.533
B_175_B12_55_1	99.3	49.2	2.018
B_175_B12_55_2	90	47.2	1.907
B_175_B12_55_3	86.6	45.2	1.917
B_175_B516_85_1	45.9	23.9	1.923
B_175_B516_85_2	46.8	22.5	2.082
B_175_B516_85_3	46	22.6	2.042
B_175_B12_85_1	59.3	33.4	1.777
B_175_B12_85_2	59.9	32.8	1.825
B_175_B12_85_3	57.1	31.4	1.822
B_250_B516_55_1	77.9	32.2	2.42
B_250_B516_55_2	77	32.9	2.337
B_250_B516_55_3	76.4	32.9	2.325
B_250_B12_55_1	110.5	52	2.125
B_250_B12_55_2	112	51.8	2.164
B_250_B12_55_3	110.7	48.7	2.274
Mean of ratios			**1.946**
Coefficient of variation, V			**0.167**

Table 5.13 – Charpy V-Notch Impact Test Results

Source of Data	Filler Metal	Test	CVN Energy (ft lb)		
			-20°F	70°F	212°F
Ng *et al.* (2002)	E70T-4	1	5.2	5.9	22.9
		2	5.2	5.9	19.9
		3	6.6	11.1	42.0
		4	5.9	13.3	34.7
		5	3.7	14.0	53.1
		6	3.7	11.1	56.1
		Mean	**5.0**	**10.2**	**38.1**
	E70T-7	1	5.2	11.8	36.1
		2	3.7	11.1	41.3
		3	8.1	17.7	45.7
		4	3.7	22.1	55.3
		5	5.2	14.0	31.7
		6	5.2	14.8	36.1
		Mean	**5.2**	**15.2**	**41.1**
	E70T7-K2	1	25.1	55.3	121.7
		2	10.3	65.6	132.8
		Mean	**17.7**	**60.5**	**127.2**
UC Davis	E70T-7	1	5.5	19.0	41.0
		2	6.0	18.0	41.0
		Mean	**5.8**	**18.5**	**41.0**
	E70T7-K2	1	30.0	56.0	88.0
		2	23.0	62.0	88.0
		Mean	**26.5**	**59.0**	**88.0**

Table 5.14 – Weld Metal Tension Coupon Test Results

Source of Data	Filler Metal	Test	Static Yield Strength, F_y (ksi)	Static Tensile Strength, F_{exx} (ksi)
Ng *et al.* (2002)	E70T-4	1	45.7	74.4
		2	45.2	74.4
		3	54.5	80.8
		4	55.5	80.8
		Mean	**51.3**	**77.6**
	E70T-7	1	67.4	88.3
		2	68.3	87.0
		Mean	**67.9**	**87.7**
	E70T7-K2	1	76.9	85.8
		2	75.8	85.7
		Mean	**76.3**	**85.8**
UC Davis	E70T7	1	75.8	97.1
		2	76.8	97.2
		Mean	**76.3**	**97.2**
	E70T7-K2	1	82.7	97.5
		2	83.0	97.4
		Mean	**82.9**	**97.5**

Table 5.15 – Comparison of Cruciform Tension Test Results with Prediction by Current AISC Method

Source of data	Filler metal	Nominal leg size (in)	Root notch (in)	Total A_w (in^2)	Measured capacity P_{max} (kips)	AISC			
						Predicted capacity, P_u (kips)	Test / predicted	Mean ratio	COV
Ng *et la* (2002)	E70T-4	1/4	3/4	1.05	151.2	73.4	2.061	1.947	0.065
				1.08	148.1	75.1	1.972		
				1.07	135.0	74.6	1.809		
	E70T7-K2	1/4	3/4	1.08	146.3	83.7	1.747	1.735	0.031
				1.07	147.4	82.7	1.782		
				1.07	139.1	82.9	1.676		
UC Davis	E70T-7	1/2	1.25	3.04	272.8	265.8	1.026	0.966	0.109
				3.57	275.3	312.0	0.882		
				3.34	277.7	291.8	0.952		
			2.5	3.37	270.3	294.3	0.918		
				3.30	309.4	288.3	1.073		
				3.78	297.9	330.7	0.901		
		5/16	1.25	2.06	196.7	180.0	1.093		
				2.19	196.0	191.8	1.022		
				2.37	205.8	207.4	0.992		
			2.5	2.25	138.7	196.9	0.704		
				2.12	189.2	184.9	1.023		
				2.07	182.1	180.7	1.008		
	E70T7-K2	1/2	1.25	3.51	324.1	307.7	1.054	1.097	0.065
				3.58	344.0	313.7	1.097		
				3.56	325.5	311.7	1.044		
			2.5	3.54	372.7	310.3	1.201		
				3.58	358.0	313.4	1.142		
				3.24	342.4	283.7	1.207		
		5/16	1.25	2.20	206.2	193.1	1.068		
				2.30	200.4	201.8	0.993		
				2.51	238.0	220.4	1.080		
			2.5	2.28	238.6	200.1	1.192		
				2.44	225.3	213.6	1.055		
				2.15	195.5	188.5	1.037		

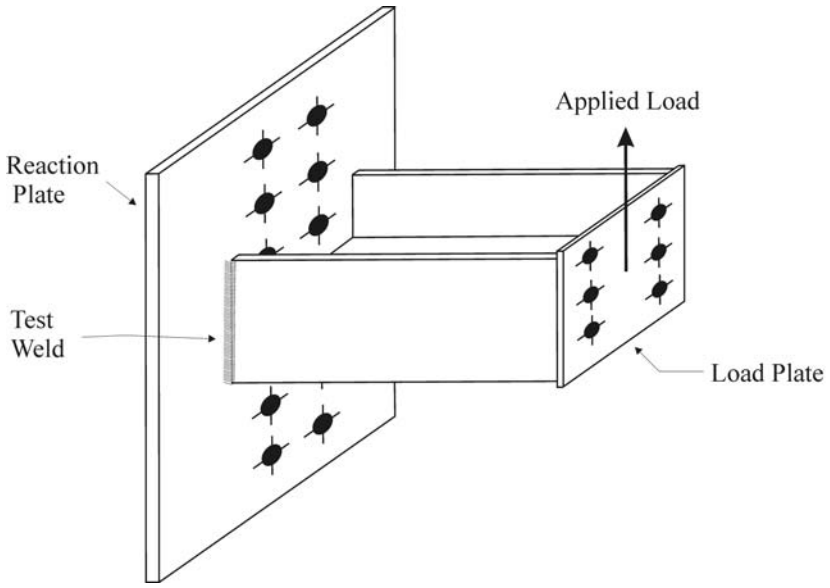

Figure 5.1 – Typical test specimen used in Dawe and Kulak (1972) test program

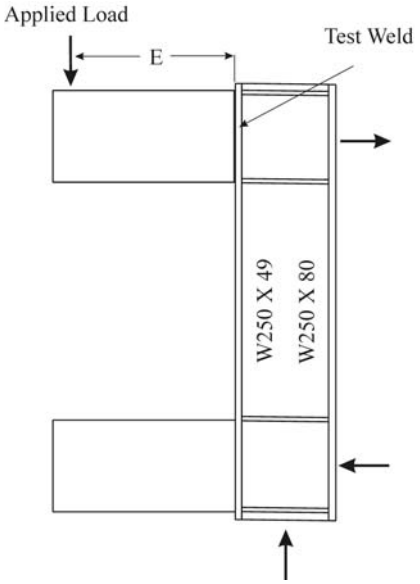

Figure 5.2 – Typical test specimen used in Beaulieu and Picard (1985) test program

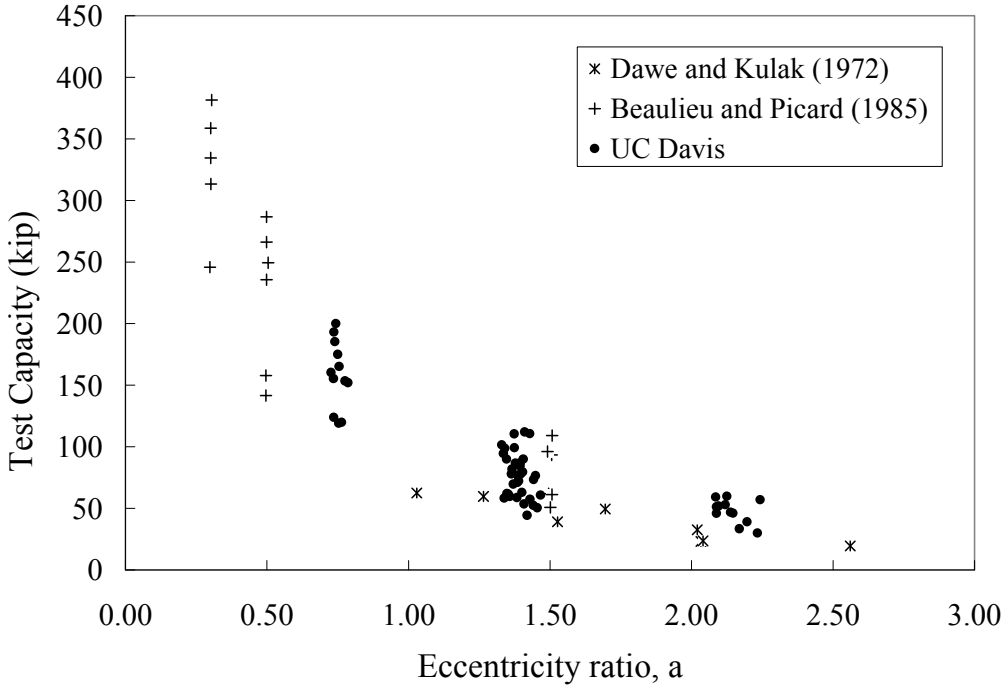

Figure 5.3 – Test capacity versus eccentricity ratio

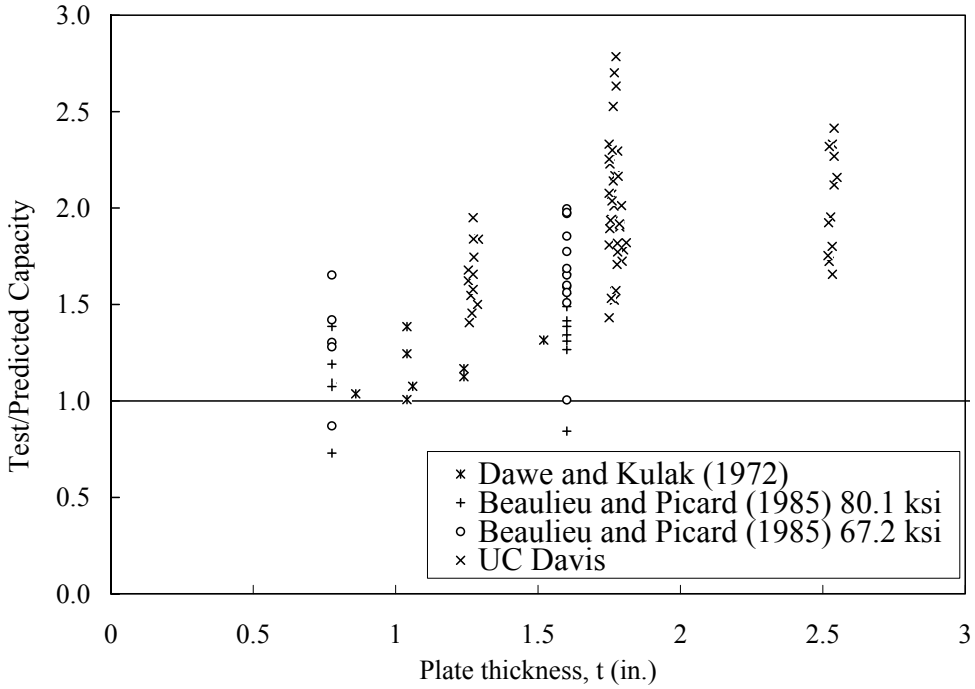

Figure 5.4 – Test-to-predicted ratio versus plate thickness

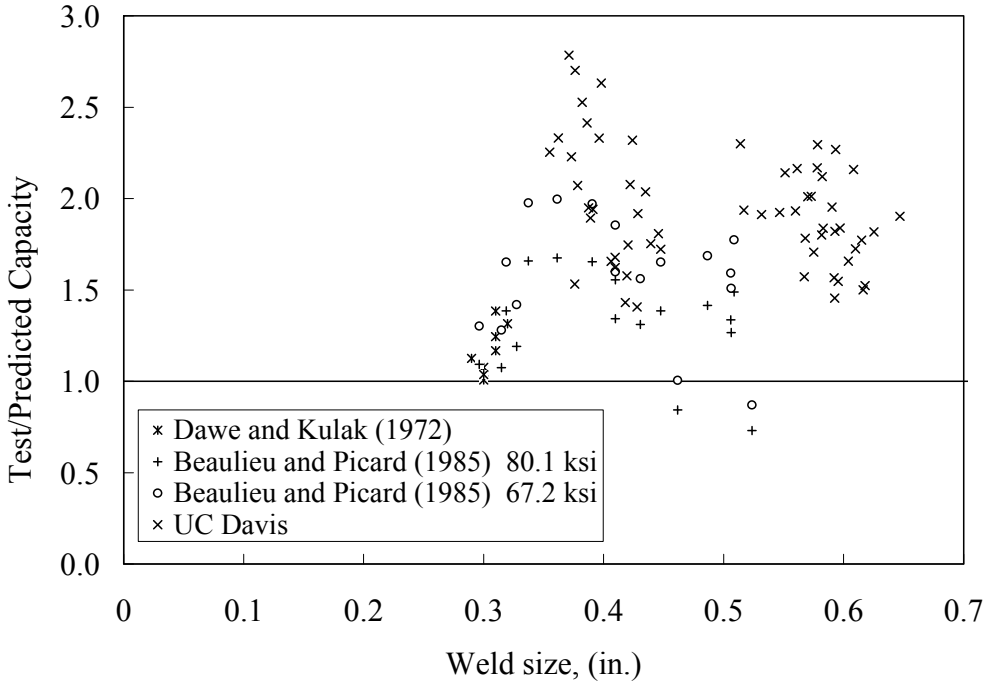

Figure 5.5 – Test-to-predicted ratio versus weld size

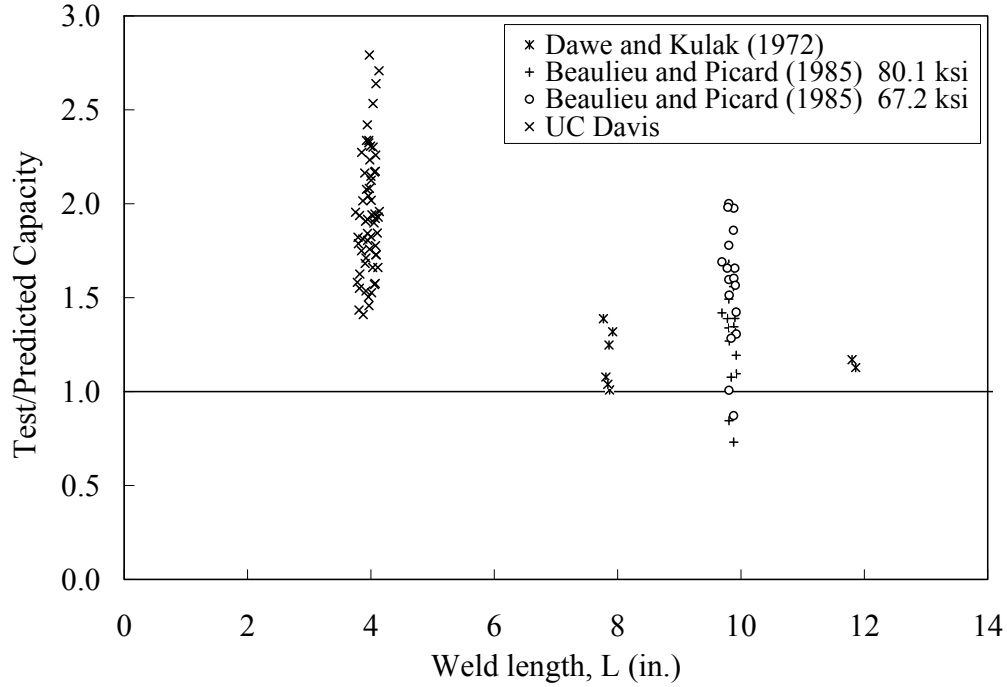

Figure 5.6 – Test-to-predicted ratio versus weld length

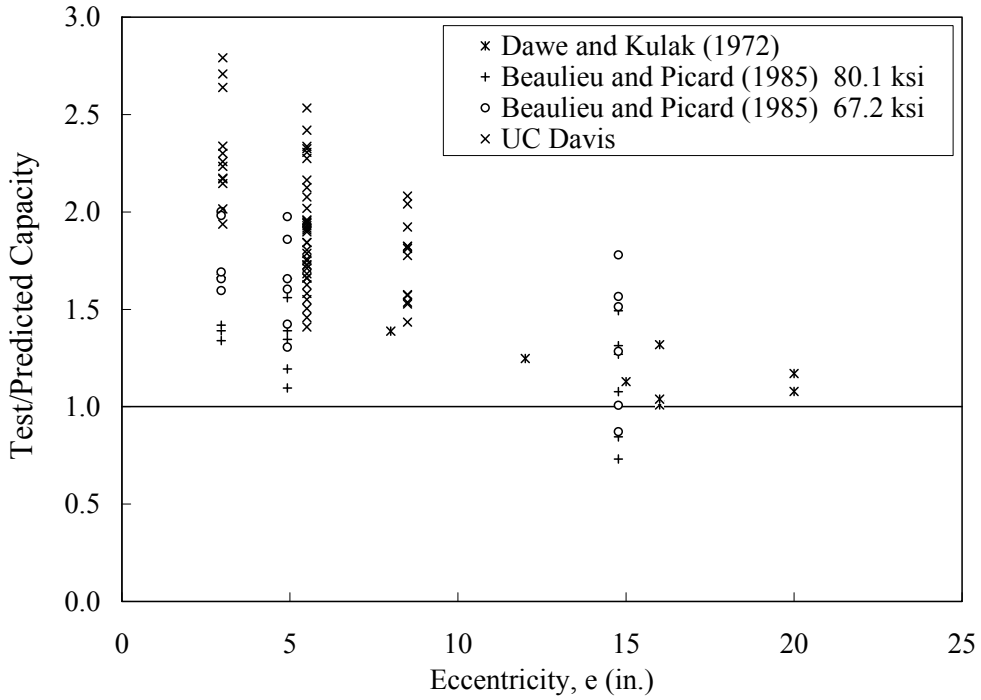

Figure 5.7 – Test-to-predicted ratio versus eccentricity

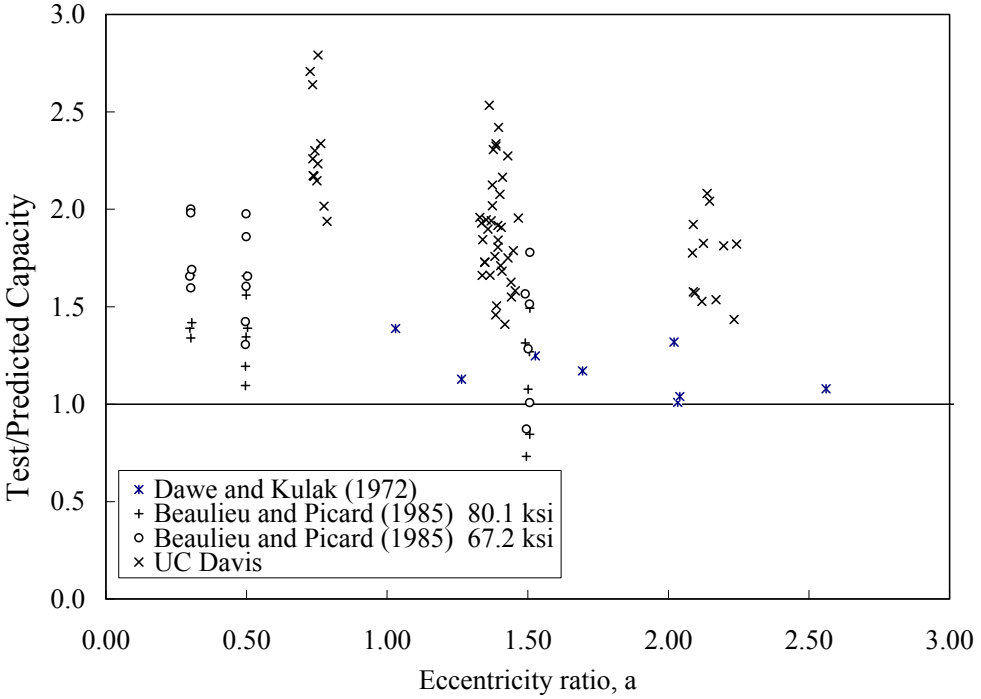

Figure 5.8 – Test-to-predicted ratio versus eccentricity ratio

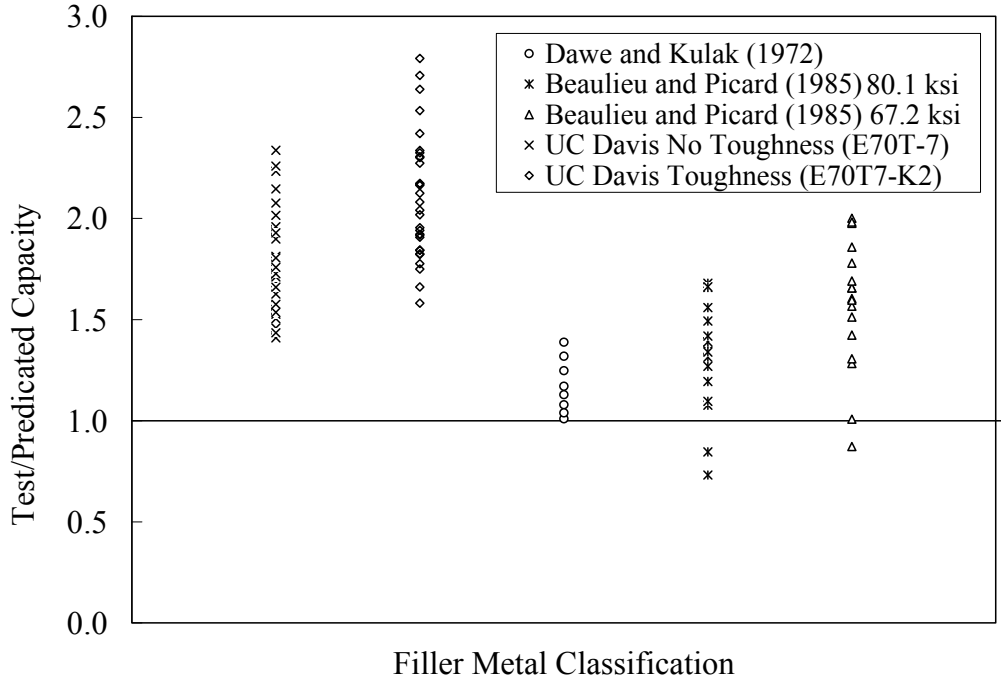

Figure 5.9 – Test-to-predicted ratio versus filler metal classification

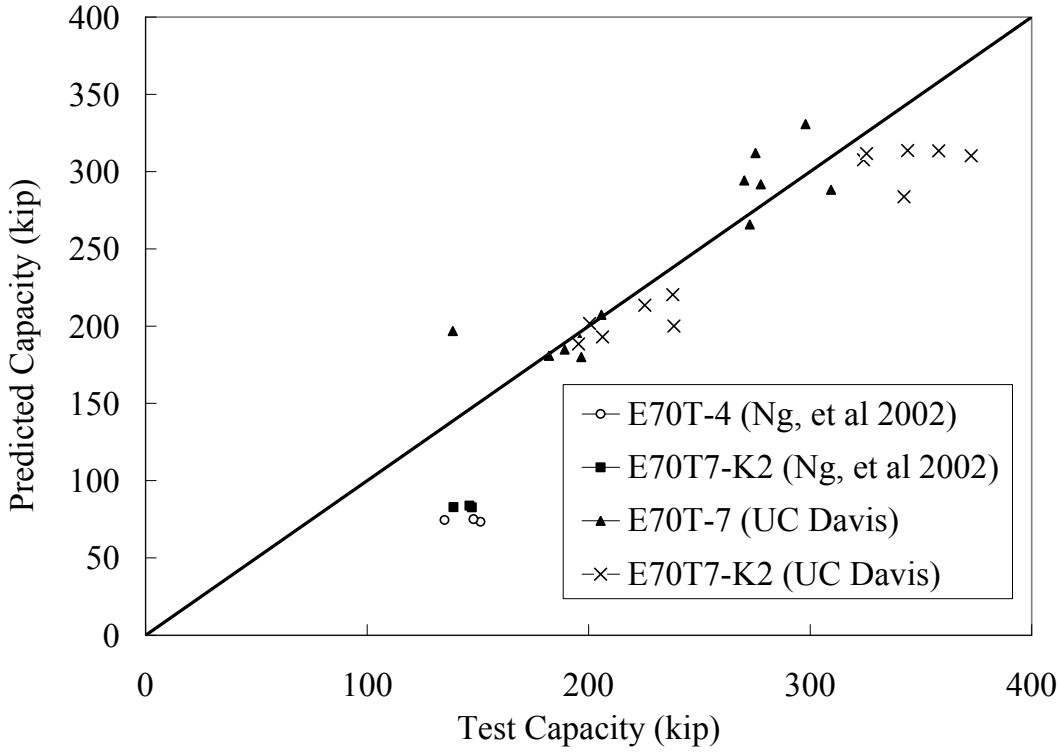

Figure 5.10 – Predicted capacity of cruciform specimens using AISC

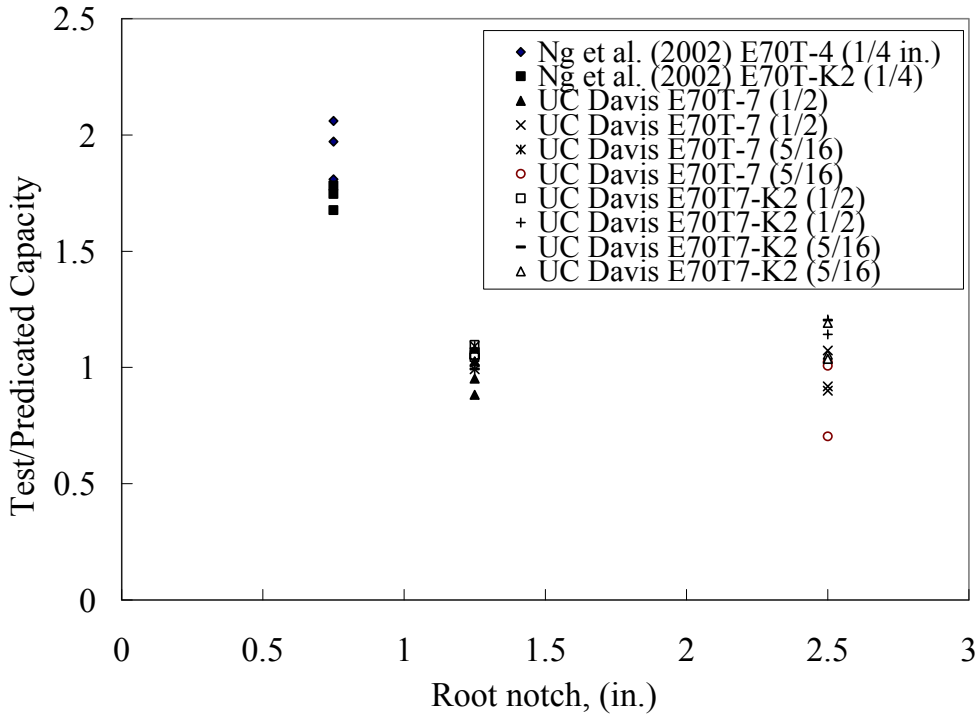

Figure 5.11 – Test-to-predicted ratio versus root notch of cruciform specimens

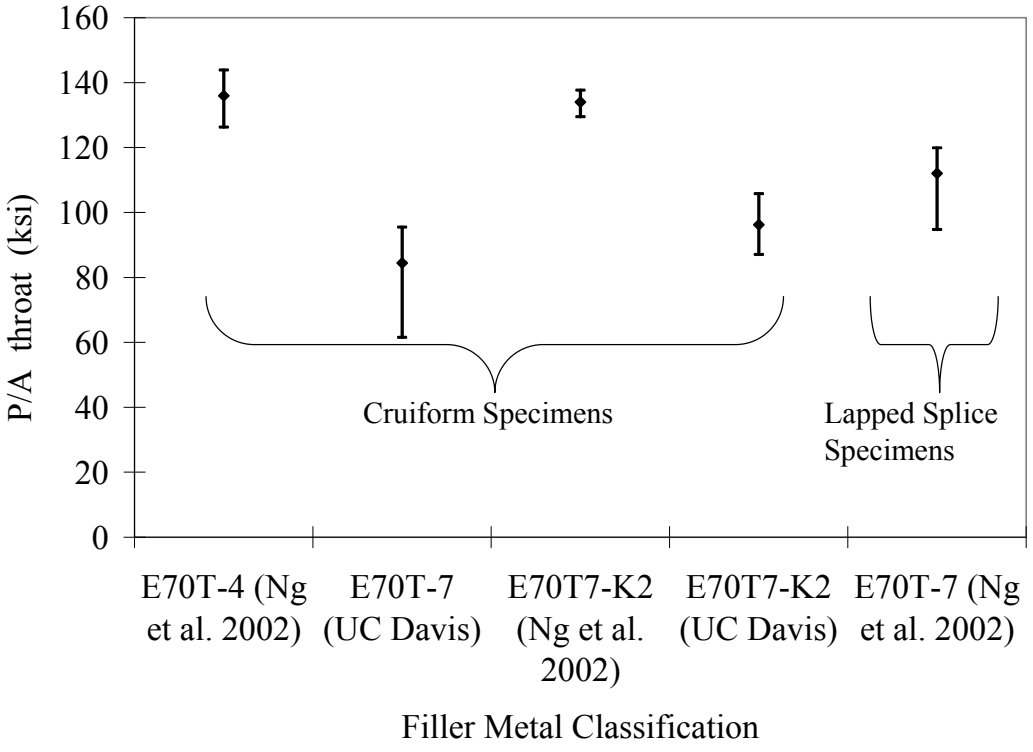

Figure 5.12 – Effect of filler metal classification on fillet weld behavior

Chapter 6

Analysis and Discussion

6.1 INTRODUCTION

Several strength calculation models have been presented for welded joints with combined out-of-plane bending and shear (Dawe and Kulak, 1972; Neis, 1980; Beaulieu and Picard, 1985). These models, modified versions of these models, and the models used in current North American design codes (AISC, 2005; CISC, 2006) are presented in detail in this chapter. This represents a total of 14 different prediction models, which are evaluated by comparing the capacities predicted by these models with test results from three different sources. The most promising models are then evaluated using a reliability analysis to assess the level of safety provided by each one of them.

6.2 DESCRIPTION OF EXISTING ANALYTICAL MODELS

Several strength prediction models have been proposed by various researchers to predict the capacity of welded joints under combined shear and out-of-plane bending. The majority of the models investigated are models proposed to replace the procedure proposed by Dawe and Kulak (1972), which requires an iterative procedure to determine the welded joint capacity. A review of the various prediction models is first presented. These models will then be assessed by comparing the predicted capacity with test results obtained from three different sources, namely, the test program by Dawe and Kulak (1972), by Beaulieu and Picard (1985), and the recent tests conducted at UC Davis as reported in Chapter 4.

6.2.1 Model 1 – Instantaneous Centre of Rotation Approach Proposed by Dawe and Kulak (1972) with the Load versus Deformation Model of Butler and Kulak (1969)

Dawe and Kulak (1972) proposed an iterative procedure based on the method of instantaneous centre of rotation to predict the ultimate strength of welded joints with out-of-plane eccentricity. The method, illustrated in Figure 6.1, makes use of the instantaneous centre of rotation in the tension zone of the connection and assumes load transfer in the compression zone by bearing of the connected plates. A triangular stress distribution was assumed in the compression zone, with the maximum stress taken as the yield strength of the steel plates. Since the normal force in the compression zone (H_B in Figure 6.1) is carried by bearing of the two plates, the weld in that zone is assumed to carry a vertical force V_B corresponding to the strength of the weld loaded at an angle $\theta = 0°$.

In the original work of Dawe and Kulak, the load versus deformation behavior of the weld segments in the tension zone followed the model proposed by Butler and Kulak (1969) as presented in Chapter 2.

6.2.2 Model 2 – Modified Dawe and Kulak's Instantaneous Centre of Rotation Approach with the Load versus Deformation Model of Butler and Kulak

Although Dawe and Kulak suggested that a triangular stress block is the most appropriate stress distribution in the compression zone, a rectangular stress block will be investigated since the rectangular stress block is a better representation of the ultimate limit state (full capacity of the connection). The rectangular stress block can develop only if sufficient ductility is available in the tension zone to allow stress redistribution after yielding. The iterative procedure of Dawe and Kulak is therefore investigated with the database of test results presented later in this chapter. The load versus deformation behavior for the weld still remains that proposed by Butler and Kulak (1969).

6.2.3 Model 3 – Dawe and Kulak's Instantaneous Centre of Rotation Approach with the Load versus Deformation Model of Lesik and Kennedy

The third model consists of the instantaneous centre of rotation approach presented by Dawe and Kulak (1972), with the exception that the load versus deformation behavior for the welds is the one proposed by Lesik and Kennedy (1990) as presented in Chapter 2. The triangular stress block proposed by Dawe and Kulak for the compression zone is adopted for Model 3.

6.2.4 Model 4 – Modified Dawe and Kulak's Instantaneous Centre of Rotation Approach with the Load versus Deformation Model of Lesik and Kennedy

This model is similar to Model 3 except that it uses a rectangular stress block in the compression zone of the welded joint.

6.2.5 Model 5 – Current AISC Approach

The current method used in the 13th edition of the AISC steel design handbook is based on the instantaneous centre of rotation method and assumes that the compression side of the welded joint transfers forces through the weld only, with no transfer of force in bearing. The method therefore reverts to the instantaneous centre of rotation method originally proposed for joints with in-plane load eccentricity (refer to Figure 6.2). Therefore, this method is identical to the case illustrated in Figure 6.3 where two parallel lines of weld are loaded with in-plane eccentricity.

The load versus deformation relationship for the weld segments proposed by Lesik and Kennedy and presented in Chapter 2 (Equations 2.6 to 2.11) was adopted for the derivation of the design tables in the AISC steel design handbook.

The value of k shown in Figure 6.3 defines the distance between two vertical weld segments as a fraction of the weld length, L. When an eccentric load is applied to a weld

group, each element is subjected to strains proportional to their distance from the instantaneous centre, which is determined iteratively. Since the AISC approach assumes that no load transfer takes place by bearing in the compression zone, the value of k is effectively taken as 0 (Figure 6.4).

6.2.6 Model 6 – Modified AISC Approach with Load versus Deformation Model of Butler and Kulak

This method adopts the load versus deformation model for the welds proposed by Butler and Kulak (1969) as presented in the previous section (Equation 2.1 to Equation 2.5). All other aspects of the model are identical to model 5.

6.2.7 Model 7 – Models proposed by Neis (1980)

Neis (1980) presented several models to predict the ultimate capacity of welded joints loaded in combined shear and out-of-plane bending. His models offered considerable simplification compared to the iterative procedure proposed by Dawe and Kulak. This simplification resulted in a closed form solution for welded joints with an eccentricity ratio, a, greater than or equal to 0.4. The stress distribution in the weld at rupture is based on the load versus deformation behavior proposed by Butler and Kulak (1969) for a weld loaded perpendicular to its axis ($\theta = 90^o$). A total of seven different stress distributions, consisting of various combinations of stress block geometries and bearing stress intensities in the compression zone, were investigated. The investigated stress distributions are illustrated in Figure 6.5 and the details of each model are discussed in the following.

6.2.7.1 Case 1

Neis' first case considers a parabolic stress distribution in the tension zone with the maximum stress at the extreme fiber equal to $1.476\,F_{EXX}$, where the constant 1.476 reflects the increase in strength of a weld segment loaded perpendicular to the axis of the weld as proposed by Butler and Kulak. A triangular bearing stress distribution was assumed in the compression zone. The limiting bearing stress at the extreme fiber of the plate is equal to the yield strength of the plate, F_y. The capacity of the welded joint, P_u, loaded with an eccentricity e, is given as a function of a non-dimensional factor, Q, as follows:

$$P_u = \frac{F_y t L(1+0.2739Q)}{3\,a\,(1+0.3093Q)^2} \qquad [6.1]$$

$$Q = \frac{F_y t}{F_{EXX} D} \qquad [6.2]$$

$$a = \frac{e}{L} \qquad [6.3]$$

where t is the thickness of the plate, F_{EXX} is the tensile strength of the filler metal, L is the length of the weld and D is the weld size.

6.2.7.2 Case 2

The model proposed for Case 2 assumes the same stress distributions as Case 1 except the limiting bearing stress in the compression zone is set to the tensile strength, F_u. The capacity of the eccentrically loaded joint is given as:

$$P_u = \frac{F_u\, t\, L\,(1 + 0.2739 Q_u)}{3\, a\,(1 + 0.3093 Q_u)^2} \qquad [6.4]$$

$$Q_u = \frac{F_u\, t}{F_{EXX}\, D} \qquad [6.5]$$

where Q_u is a non-dimensional factor equal to the ratio of the base metal strength to the weld metal strength.

6.2.7.3 Case 3

In this model a triangular stress distribution is adopted in the tension and the compression zones. The maximum stress in the tension zone is taken as $1.476\, F_{EXX}$ and F_u in the compression zone. The resulting predicted capacity is given as:

$$P_u = \frac{F_u\, t\, L}{3\, a\,(1 + 0.4791 Q_u)} \qquad [6.6]$$

6.2.7.4 Case 4

As for Case 1, Neis suggested a parabolic stress distribution in the tension zone with a maximum stress of $1.476\, F_{EXX}$ at the extreme fiber. The stress in the compression zone is represented by a rectangular stress block with a magnitude equal to the yield strength of the plate, F_y. The joint capacity is given as:

$$P_u = \frac{F_y\, t\, L\,(1 + 0.7304 Q)}{2\, a\,(1 + 0.6186 Q)^2} \qquad [6.7]$$

where Q is as defined by Equation 6.2.

6.2.7.5 Case 5

This case represents the upper bound of all the cases investigated by Neis. The stresses are assumed to be constant along the weld length in both tension and compression zones.

Neis suggested using $1.414\,F_{EXX}$ as the tensile stress and the yield strength of the plate, F_y, as the compressive stress. The joint capacity predicted from this model is given as:

$$P_u = \frac{F_y\,t\,L}{a\,(2+Q)} \qquad [6.8]$$

where Q is as defined by Equation 6.2.

6.2.7.6 Case 6

This case was proposed for thick plates ($2.09 < Q \leq 3.5$) where the ultimate strength of welded joint is reached as the rupture of the weld may occur before yielding of the plate. Neis proposed linear stress distributions in the tension and compression zones. The maximum stresses in the extreme fiber in tension and compression zones are taken as $1.476\,F_{EXX}$ and F_y, respectively. The capacity of the welded joint is given as:

$$P_u = \frac{F_y\,t\,L}{3\,a\,(1+0.479Q)} \qquad [6.9]$$

6.2.7.7 Case 7

Case 7 was proposed for the thin plates ($0.6 \leq Q \leq 2.09$) where the plate material yields before the weld deforms sufficiently to rupture. The central portion of the cross-section is assumed to carry the shear load and is taken as $0.577\,F_y$ based on the Hencky-von Mises yield condition. Constant stress distribution is assumed along the weld length. In the tension and compression zone, the stress is taken as F_y. The resulting connection capacity is expressed as:

$$P_u = 0.577 F_y\,t\,L\left(\sqrt{1+1.332\,a^2} - 1.154\,a\right) \qquad [6.10]$$

6.2.8 Model 8 – Model Proposed by Beaulieu and Picard (1991)

Beaulieu and Picard (1991) presented the results of an experimental investigation of welded joints with out-of-plane eccentricity and an evaluation of the model proposed by Dawe and Kulak and the models presented by Neis. Using an approach similar to that proposed by Neis (1980) a new model that agreed well with the more complex procedure of Dawe and Kulak was proposed. The new model is based on the stress distribution shown in Figure 6.6 where the stress in the tension zone is based on the load versus deformation behavior proposed by Lesik and Kennedy (1990) for a weld loaded perpendicular to its axis ($\theta = 90^o$) and the stress in the compression zone, resulting from bearing of the steel plates, is equal to the yield strength of the connected plates. The model proposed by Beaulieu and Picard also assumes that the weld area on the tension side of the joint is equal to the leg area rather than the throat area. This closed form solution is based on the assumption that the moment on the welded joint is sufficiently large to make the shear contribution negligible. Therefore, the use of this model was

limited to values of eccentricity factor, a, greater than 0.4. For smaller values of a, it was recommended that a parabolic interpolation between P_0 (the resistance of the joint with no eccentricity) and $P_{0.4}$ (the resistance of the joint with $a = 0.40$) be used. This model was adopted by CISC in the latest edition of the CISC Handbook of Steel Construction (CISC, 2006). The predicted welded joint capacity is therefore given as:

$$P_u = \frac{0.5F_y tL}{a(Q+2)} \qquad a \geq 0.40 \text{ and } t \leq 40\text{mm} \qquad [6.11]$$

where

$$Q = \frac{F_y t}{F_{EXX} D}$$

$$P_u = P_0 + \frac{a^2(P_{0.4} - P_0)}{0.16} \qquad a < 0.40 \text{ and } t \leq 40\text{mm} \qquad [6.12]$$

where $P_0 = 2(0.60)0.7071F_{EXX}DL$ and $P_{0.4} = P_u$ calculated using Equation 6.11 for $a = 0.4$

The reduction factor of 0.5 in the Equation 6.11 was proposed to give results in very close agreement with the design table provided in the previous edition of the CISC Handbook.

6.3 EVALUATION OF THE EXISTING MODELS

A total of 14 analytical models are available for the prediction of the weld capacities of test specimens from three different sources: Dawe and Kulak (1972), Beaulieu and Picard (1985) and UC Davis (details presented in Chapter 4). A comparison of the test results with the joint capacities predicted using the models presented above are summarized in Table 6.1.

As detailed in Appendix F, the models that are based on the instantaneous centre of rotation method, Models 1 to 6, are applicable to all ranges of load eccentricity. However, the cases considered in Model 7 are limited to joints loaded with a large eccentricity ($a > 0.4$). Model 8, which was proposed by Beaulieu and Picard, contains two equations to cover the full range of load eccentricity. All the test specimens from Dawe and Kulak had a large eccentricity and hence all eight specimens are considered in the models. Out of the 22 welded joints tested by Beaulieu and Picard (1985), 17 failed in the weld. These 17 test results are used to assess models 1 to 6 and 8. Only 11 test results from the Beaulieu and Picard test program are used to assess all cases of Model 7 since only these specimens satisfied the eccentricity requirement for Model 7 ($a > 0.4$). All the 60 test results from UC Davis were loaded with a load eccentricity ratio greater than 0.4 and

none failed in the plate. Therefore, all the test results from the UC Davis test program were compared with the 14 different models.

6.3.1 Prediction of test results

The test results from various test programs were compared with the current prediction method used in AISC and the results of this comparison are found in Chapter 5. In this comparison the weld shear strength was taken as 0.6 times the tensile strength of the weld metal (see Equation 2.6). In order to conduct a reliability analysis for the various prediction models, all the sources of variation must be accounted for. One of these sources of variation is the shear strength of the weld metal, explicitly used in all the models based on the Lesik and Kennedy weld strength model. The shear strength is expressed as a constant (shear factor), taken as 0.6 in the AISC specification (AISC, 2005), times the tensile strength, F_{EXX} . Therefore, the bias coefficient and coefficient of variation (COV) for the shear strength can be evaluated by assessing these two statistical parameters for the tensile strength and the shear factor (0.6 for the AISC approach). When evaluating the professional factor (ratio of test capacity to the predicted capacity using measured dimensions and material properties) required for the reliability analysis, the actual shear strength of the weld metal must be used. A shear factor representative of the actual shear strength of the weld metal is therefore required. As explained in detail in section 6.5, the ratio of shear strength to tensile strength for weld metal was evaluated from tests conducted by Deng *et al.* (2003). The shear factor is found to be 0.78. This shear factor is used in the calculation of the predicted test capacity rather than the nominal value of 0.6 currently used in AISC (2005). The discrepancy between the actual shear factor (0.78) and the design shear factor (0.6 for the AISC design approach) will be accounted for in the reliability analysis through the introduction of a second material factor.

6.3.2 Comparison of test results with predicted capacity

The mean test-to-predicted ratio and the COV are used as a measure of the ability of each model to predict the test capacities. Because Beaulieu and Picard did not measure the weld metal tensile strength directly, the predicted values for their test specimens were calculated using two values of tensile strength for the weld metal, namely, 67.2 ksi, which was deduced from the results of their tests on lapped joints with transverse or longitudinal welds, and 80.1 ksi, obtained from material test results published by Fisher *et al*. (1978), Pham (1981), Miazga and Kennedy (1986) and Gagnon and Kennedy (1987). As indicated in Chapter 5, the tensile strength for the weld metal used in the test program by Dawe and Kulak was taken as 67 ksi based on weld metal tests on similar electrode designation reported by other researchers. For all the 14 models investigated, the professional factor ranges from 1.044 to 1.934 and the coefficient of variation varies from 0.225 to 0.259.

Table 6.1 indicates that the UC Davis test data lead to a higher professional factor than those of Dawe and Kulak and Beaulieu and Picard. However, an investigation of the various test programs presented in Chapter 5 indicated that the difference in capacities observed in the UC Davis test specimens is neither caused by the dissimilarity in material

properties of the specimens nor the method of loading. The difference is believed to be caused by changes in the filler metal properties over time.

The COV for the pooled data is relatively large at values of 0.225 to 0.259 for all models investigated. However, Table 6.1 indicates that the COV within individual test programs is significantly lower. In an attempt to identify the source of variation of the test-to-predicted ratio, its value was plotted against various geometric parameters such as plate thickness, eccentricity, weld length, weld size, eccentricity ratio and filler metal classification. The plots were used to determine whether a trend exists between the test-to-predicted ratio and any of these parameters.

6.3.2.1 Model 1 – Dawe and Kulak's Instantaneous Center of Rotation Approach with the Load versus Deformation Model of Butler and Kulak

Model 1 provides conservative predictions. However, the predicted capacities of Dawe and Kulak's data set are higher than the measured capacities. The mean test-to-predicted ratio for this test program is 0.851. The COV for the data sets from Dawe and Kulak, Beaulieu and Picard and UC Davis vary from 11 to 17%, with a COV of about 26% for the pooled data.

The effect of various geometric parameters and filler metal classification are examined independently in Figure 6.7. Although the variability in the test-to-predicted ratio is large there is a visibly noticeable tendency of the test-to-predicted value to decrease as the weld length increases, and to be larger for filler metals with toughness requirement. No trend is apparent between the test-to-predicted ratio and the other parameters presented in Figure 6.7. However, because of the large scatter in the test-to-predicted values, the observed trend is statistically insignificant. The fact that weld size, plate thickness and load eccentricity and eccentricity ratio do not show any correlation with the test-to-predicted ratio indicates that these parameters are accounted for suitably in the prediction model. Although there seems to be a weld length effect, this effect disappears when plotted as the ratio of eccentricity to weld length, thus indicating that the weld length parameter is also accounted for suitably in the model. The model, however, does not account for weld toughness. It seems from this analysis that weld toughness might have an effect on the strength of eccentrically loaded welded joints. None of the models investigated here account for the weld metal toughness.

6.3.2.2 Model 2 – Modified Dawe and Kulak's Instantaneous Center of Rotation Approach with the Load versus Deformation Model of Butler and Kulak

Because this model assumes a rectangular stress block in the compression zone of the joint rather than the triangular stress block assumed in Model 1, this model predicts a higher capacity than Model 1. It generally overestimates the capacity of the specimens tested by Dawe and Kulak and Beaulieu and Picard, but provides a generally conservative estimate of the test results from UC Davis. The test-to-predicted ratio for the three test programs varies from 0.671 to 1.175 with an overall average of 1.065. The COV varies from 0.10 to 0.14, with an overall value of 24%.

The plots of test-to-predicted ratio versus geometric parameters and filler metal toughness requirement are shown in Figures 6.8a to 6.8f. The plots have similar appearance to the plots for Model 1, showing similar trend with a change in weld length and filler metal toughness requirement. It should be noted that scatter in the test-to-predicted values for Model 2 is smaller than the scatter observed for Model 1. Nevertheless, the observed trend between the test-to-predicted ratio and the weld length is still statistically insignificant at a level of significance of 5%.

6.3.2.3 Model 3 – Dawe and Kulak's Instantaneous Center of Rotation Approach with the Load versus Deformation Model of Lesik and Kennedy

Compared to Model 1, the Lesik and Kennedy load versus deformation curves implemented in Model 3 gives a more conservative prediction of joint capacity and leads to slightly less scatter.

From Figures 6.9a to 6.9c similar trends to those observed for the earlier two models are also observed for Model 3. Both the weld length and the toughness requirement show up as influential, although this influence is statistically insignificant.

6.3.2.4 Model 4 – Modified Dawe and Kulak's Instantaneous Center of Rotation Approach with the Load versus Deformation Model of Lesik and Kennedy

As expected, since the model is based on Model 3, but modified with a rectangular stress block, it is less conservative for all three sources of data as shown in Table 6.1. Model 4 overestimates the joint capacity for the specimens tested by Dawe and Kulak, with a mean professional factor of 0.760 and a COV of 0.10. The model provides generally conservative predictions of the test results from the UC Davis test program, but over predicts the capacity of the test specimens from Dawe and Kulak considerably.

Once again, the same trends observed in the previous models are observed for Model 4. Figures 6.10a to 6.10f show that the weld length and toughness requirement seem to have an effect on the joint strength, however, this effect is statistically insignificant.

6.3.2.5 Model 5 – Current AISC Approach

A discussion of the current AISC approach was presented in Chapter 5. Table 6.1 and Figures 5.4 to 5.8 present the test-to-predicted ratios for this model and the effect of various geometric parameters on the test-to-predicted ratio. The mean test-to-predicted ratio for all the test specimens examined is 1.38.

Figure 5.4 indicates that, in contrast to the previously examined models, the test-to-predicted ratio for the AISC model increases with an increase in plate thickness, indicating that the plate thickness should be incorporated into the prediction model. Figure 5.6 indicates that there is also an influence of the weld length. As for the other models, the effect of weld size and load eccentricity on the test-to-predicted ratio is negligible.

6.3.2.6 Model 6 – Modified AISC Approach with Load–Deformation Model of Butler and Kulak

This model is a modified version of the AISC approach where the load versus weld deformation relationship of Lesik and Kennedy is replaced by the load versus deformation relationship proposed by Butler and Kulak. As for the AISC model, load transfer in the compression side of the connection is assumed to be through the weld only.

Table 6.1 shows that the predicted capacities are conservative for the test specimens from the UC Davis test program only. The model over-estimates the joint capacity of the specimens from Dawe and Kulak and Beaulieu and Picard, giving professional factors of 0.735 and 0.938, respectively. The COV for the tests from Dawe and Kulak is 0.11 and 0.19 for the test program by Beaulieu and Picard, The model gives conservative prediction for the joints tested at UC Davis, with a mean professional factor of 1.215 and COV of 16%. The overall professional factor is 1.114 and COV is 22%.

Plots of test-to-predicted ratio versus geometric parameters are presented in Figures 6.11a to 6.11f. The plots have comparable behaviors as observed for Model 5, however, the data points show less dispersion than in Model 5.

6.3.2.7 Model 7 – Models proposed by Neis (1980)

Neis (1980) proposed seven different models with varying stress magnitudes and stress distributions. Test-to-predicted ratios for all seven models, designated as Case 1 to Case 7, were calculated and the results are presented below.

(a) Case 1

The overall test-to-predicted ratio for all the combined test programs predicted by Neis Model Case 1 is 1.337 and the COV is 0.23. The test-to-predicted ratio and COV for each individual data set are presented in Table 6.1 where they are ranging from 0.827 to 1.459 and 0.10 to 0.16, respectively. A comparison with Models 1 and 2 indicates that the results from Case 1 model lie between the two models.

In Figures 6.12a to 6.12f, the test-to-predicted ratios are plotted against the plate thickness, weld size, weld length, eccentricity, eccentricity ratio and filler metal classification. It is observed that the parameters of plate thickness, weld size and load eccentricity and eccentricity ratio do not have any direct relationships to the test-to-predicted ratio as the data points are dispersed randomly in the plots. However, as for Models 1 to 6 there seems to be a weak correlation with weld length and weld metal classification.

(b) Case 2

The mean test-to-predicted value and its COV for the all the test data collected are 1.117 and 25%, respectively. As for Case 1, this model over-predicts the weld capacities for the

specimens tested by Dawe and Kulak and Beaulieu and Picard, with mean test-to-predicted values of 0.63 and 0.81, respectively.

Since Case 2 the tensile strength of the steel plate rather than the yield strength in the compression zone, the model is expected to yield a higher predicted capacity than the model in Case 1. This is demonstrated by the lower test-to-predicted values, which are significantly below 1.0 for the test specimens from the early test programs. Plots of test-to-predicted ratios versus various parameters presented in Figures 6.13a to 6.13f show similar trends as were observed for the model of Case 1.

(c) Case 3

The test-to-predicted ratios tabulated in Table 6.1 for the specimens of all three test programs range from 0.808 to 1.467. The COV ranges from 0.10 to 0.14 and it increases to 0.23 when all the test results are pooled together. This case is basically a modification of Case 2 as a triangular stress block is assumed in the tension zone instead of the parabolic stress block used in Case 2.

The test-to-predicted ratios are plotted against the geometric parameters such as plate thickness, weld size, weld length, eccentricity, eccentricity ratio and filler metal classification in Figures 6.14a to 6.14f. The scatter in the test data is similar to that observed in the previous models proposed by Neis. It is concluded that the plate thickness, weld size and weld length are not factors that directly influence test-to-predicted ratios.

(d) Case 4

For this case, the triangular stress block used for Case 1 is replaced by a rectangular stress block, resulting in a higher predicted capacity. The overall test-to-predicted ratio is 1.071 and it is on the lower range as comparing with other models and cases. The test-to-predicted ratios for three data sets are 0.670 for Dawe and Kulak and 0.833 for Beaulieu and Picard and 1.168 for UC Davis. The respective COVs are 10%, 13% and 14% and the overall COV is 22%.

Comparisons between test-to-predicted ratio on the weld capacities and the geometric parameters of specimen have been made and reported in Figures 6.15a to 6.15f. The data points appear in narrow bands in all plots as contrast to the plots for Case 1 in Neis' Model (Figures 6.12a to 6.12f).

(e) Case 5

The parabolic stress blocks adopted in the tension and compression zone is replaced by the parabola stress block in the tension zone. The predicted weld capacity would further increase as the extra resistance is provided in the tension zone. The test-to-predicted ratio values and the COVs for all data sets are presented in Table 6.1 and they are ranging from 0.658 to 1.148 and 10% to 14%, respectively. The lowest test-to-predicted ratio is also found in this case, it is reported as 1.053 and its COV is 22%.

Figures 6.16a to 6.16f show the plots that compare the test-to-predicted ratio to the geometric parameters. The data points are further condensed as comparing with the plots for Case 4 (Figures 6.15a to 6.15f). As similar to Case 4, the plate thickness, weld size and weld size have made no effects on the test-to-predicted ratios.

(f) Combined Case 6 and Case 7

The Q parameters for the specimens being tested are ranging from 0.73 to 3.66. Case 6 is formulated for thick connecting plates with large values of Q, between 2.09 and 3.5. Case 7 is formulated for thin connecting plates with small values of Q, between 0.6 and 2.09. By using the combined Case 6 and Case 7, it accounts entire specimens in the test program. The test-to-predicted weld capacity ratios and COVs by using Model 7 Case 6 and Case 7 are presented in Table 6.1. The test-to-predicted ratios for 3 data sets are ranging from 0.937 to 1.556 where the overall is 1.446. The COVs are ranging from 12% to 17% with an overall COV of 22%. These combined cases give higher predicted capacity than the other cases.

The test-to-predicted ratio is made comparison to the geometric parameters, and the plots are presented in Figures 6.17a to 6.17f. The effects occur in all plots and the overall appearances of plots remain unchanged.

6.3.2.8 Model 8 – Model Proposed by Beaulieu and Picard (1991)

This model was adopted in the ninth edition of the CISC Handbook of Steel Construction (CISC 2006). The original model proposed by Beaulieu and Picard provides the most promising predictions on the weld capacity from all the models using Lesik and Kennedy load deformation relationship. In the later stage of their derivation of a simplified closed form model, Beaulieu and Picard applied a reduction factor of 0.5 to their original model to get good agreement with the previous CISC design table, which was based on Model 1 by Dawe and Kulak. As mentioned above, this model contains two equations to account for specimens subject to small eccentricity ratio ($a < 0.4$) and large eccentricity ratio ($a \geq 0.4$). Only five test specimens fall in the category of small eccentricity and they are all from the test program presented by Beaulieu and Picard. As shown in Table 6.1, the test-to-predicted ratio is 1.403 and COV is 0.064. A total of 80 test specimens from all three test programs satisfy the requirement for large eccentricity. The test-to-predicted ratio for these test specimens from Dawe and Kulak, Beaulieu and Picard and UC Davis are 1.215, 1.524 and 2.134, respectively. The COVs are 10%, 13% and 15%, respectively. The overall test-to-predicted ratio and COV for all the test specimens with large eccentricity are 1.951 and 22%, respectively.

The comparisons between the geometric parameters and test-to-predicted ratio of weld capacity are presented in Figures 6.18a to 6.18f. Figure 6.18a shows that Model 8 gives a slightly higher test-to-predicted ratio for the UC Davis specimens with plate thickness of 1.25 in. compared to the values predicted using the model currently used in the ASIC Steel Construction Manual (Model 5) (see Figure 5.4). The other data points are similar in both plots. However, the trends observed for the two models are reversed: the AISC

model shows an upward trend as plate thickness increases whereas model 8 shows a downward trend. In Figure 6.18b, the data points predicted by Model 8 for weld size less than 0.5 in. are similar to the data points in Figure 5.5 for Model 5. For the specimens with weld size larger than 0.5 in., Model 8 gives higher test-to-predicted ratio and is found to be more conservative than Model 5. The data points shown in Figure 6.18c for test-to-predicted ratio versus weld length are dispersed as randomly as in Figure 5.5 for Model 5. Once again, the test-to-predicted value seems to be influenced by the weld metal classification as shown in Figure 6.18f.

6.4 SEGREGATION OF TEST SPECIMENS IN ACCORDANCE TO TOUGHNESS REQUIREMENT

The welded joint specimens tested at UC Davis and prepared with the toughness rated filler metal E70T7-K2 showed higher weld strengths than those with non toughness rated filler metal. Because the higher strength of these test specimens tend to increase the overall test-to-predicted value. When the test specimens with toughness rated filler metal are combined with the other test specimens the COV for the overall data set also increases. It was necessary to consider the specimens with toughness and non toughness requirements separately in the reliability analysis. The data set that gives the lower resistance factor should be adopted for design. Only the test program conducted at UC Davis reported the filler metal classification for the specimens. Although the classification of the filler metals used in the Dawe and Kulak (1972) and Beaulieu and Picard (1985) test programs were not reported, they were all considered as filler metals with no toughness requirement.

Although 14 different strength prediction models are evaluated, the models that are based on the load versus deformation behavior proposed by Lesik and Kennedy (1990), namely, Models 4, 5 and 8, will be receiving more attention for the following three reasons: 1) the load versus deformation model for fillet welds proposed by Lesik and Kennedy has received general acceptance in North American design codes; 2) the equation proposed by Lesik and Kennedy was developed based on various weld sizes whereas Butler and Kulak's model was developed based on tests conducted on 1/4 inch welds only (Ng *et al.* (2002) found that smaller fillet welds tend to provide significantly higher unit strength than larger welds); 3) Models 4, 5 and 8 all show promising predictions when considering all available test results.

The test-to-predicted ratios for the specimens prepared with weld with no toughness requirement and those prepared with toughness requirement are presented in Tables 6.2 and 6.3, respectively. Thus, the effect of filler metal classification is eliminated. The resulting test-to-predicted ratios for the specimens with no toughness requirement show a mean value closer to 1.0 and a lower COV.

6.5 RELIABILITY ANALYSIS

The level of safety is assessed for each of the proposed strength prediction models. The traditional target safety index, β, is usually taken as 3.0 for ductile structures but can be

as high as 4.0 to 4.5 for parts of structures that require a reduced probability of failure, such as connections. The safety index for each model is unique as the procedure to obtain the joint capacity varies between models. It can be determined by using the equation for the resistance factor, ϕ, which was originally proposed by Galambos and Ravindra (1978):

$$\phi = C\rho_R \exp(-\beta\alpha_R V_R) \qquad [6.13]$$

The separation variable, α_R, is set to 0.55 as proposed by Galambos and Ravindra. C is an adjustment factor for modifying the resistance factor for cases where β adopts a value other than 3.0. An equation for C, derived using a procedure proposed by Fisher *et al*. (1978) for welded and bolted connections, is adopted to calculate the adjustment factor for a live to dead load ratio of 3.0:

$$C = 0.0078\beta^2 - 0.156\beta + 1.400 \qquad [6.14]$$

It should be noted that the above equation is applicable for a range of safety index from 1.5 to 6.0. For values of β greater than 6.0, the probability of failure is so low that any refinement in the resistance factor is unwarranted.

The bias coefficient for the resistance, ρ_R, represents the ratio of the expected mean resistance to the nominal resistance and V_R is a function of the variability in the parameters that define the strength. These statistical parameters can be obtained as:

$$\rho_R = \rho_G \rho_M \rho_P \qquad [6.15]$$

and the associated coefficient of variation, V_R, is given as:

$$V_R^2 = V_G^2 + V_M^2 + V_P^2 \qquad [6.16]$$

where the geometric parameter, ρ_G, is the ratio of mean-to-nominal relevant geometric properties such as the throat area, and V_G is the associated coefficient of variation. It can be calculated as the mean value of the ratio of the measured throat dimension (*MTD*) to 0.707 times the nominal weld leg size, namely,

$$\rho_G = Mean\left(\frac{MTD}{0.707 \times (\text{nominal weld leg size})}\right) \qquad [6.17]$$

Due to the difference in reported test data, *MTD* was calculated differently for the Dawe and Kulak, the Beaulieu and Picard and the UC Davis test programs. Dawe and Kulak reported only the average of the tension and shear leg sizes. Beaulieu and Picard also reported only the average of the shear and tension leg sizes although both legs were reportedly measured at several locations (Werren, 1984). Therefore, *MTD* for this test data is calculated as:

$$MTD = 0.707 \times \left(\text{average of two leg sizes}\right) = 0.707 \times \frac{s_1 + s_2}{2} \quad [6.18]$$

where s_1 and s_2 are the two weld leg sizes. For the data from UC Davis, the two leg sizes were measured and reported. In here, MTD is taken as the minimum throat dimension, obtained from the measured size of the two weld leg:

$$MTD = \frac{s_1 \times s_2}{\sqrt{s_1^2 + s_2^2}} \quad [6.19]$$

It should also be noted that, both Equations 6.18 and 6.19 neglect the reinforcement at the weld face and the variability of weld root penetration.

The material ratio, ρ_M, is the mean-to-nominal ratio of the relevant material property. As explained in section 6.3.1, the relevant material property is the shear strength of the weld metal. However, in design practice the shear strength is taken as the tensile strength times a shear factor. Therefore, ρ_M is a function of two parameters, ρ_{M1} and ρ_{M2}. The factor ρ_{M1} addresses the variation in the weld metal tensile strength, yielding strength or tensile strength of the plate, while ρ_{M2} addresses the variation in the conversion from the tensile strength to shear strength. Thus, the material ratio and its coefficient of variation are represented by the following equations:

$$\rho_M = \rho_{M1}\rho_{M2} \quad [6.20]$$

$$V_M^2 = V_{M1}^2 + V_{M2}^2 \quad [6.21]$$

The various strength prediction models examined in this study involve either weld material strength or plate material strength or the combination of both. Therefore, the first material bias coefficient, ρ_{M1}, can be approximately taken as the mean value of the measured to nominal weld metal tensile strength and the measured to nominal static yield strength of the plate.

The mean value of the measured to nominal weld metal tensile strength is expressed as:

$$\rho_{M1} = \text{Mean}\left(\frac{\text{Measured Tensile Strength, } \sigma_u}{\text{Specified Tensile Strength, } F_{exx}}\right) \quad [6.22]$$

where σ_u is determined from all-weld-metal tension coupons.

The mean value of the measured to nominal static yield strength of the plate is expresses as:

$$\rho_{M1} = \text{Mean}\left(\frac{\text{Measured Static Yield Strength, } \sigma_y}{\text{Specified Static Yield Strength, } F_y}\right) \quad [6.23]$$

The mean value of the measured to nominal ultimate tensile strength of the plate:

$$\rho_{M1} = \text{Mean}\left(\frac{\text{Mean Ultimate Tensile Strength, } \sigma_u}{\text{Specified Ultimate Tensile Strength, } F_u}\right) \quad [6.24]$$

The second material bias coefficient, ρ_{M2}, accounts for the relationship between the tensile strength and the shear strength. For the shear factor used in the AISC Specification (AISC, 2005), it is expressed as:

$$\rho_{M2} = \text{Mean}\left(\frac{\text{Measured Shear Strength, } \tau_u / \text{Measured Tensile Strength, } \sigma_u}{0.60}\right) \quad [6.25]$$

The second material bias coefficient is only incorporated in the models that adopted the Lesik and Kennedy (1988) load versus deformation relationship (Models 4 and 5) and the Beaulieu and Picard approach (Model 8). The measured shear strength to tensile strength ratio is obtained from longitudinal weld test specimens. The shear strength, τ_u, based on the fracture surface area, $A_{fracture}$ which accounts for the additional area due to root penetration and weld face reinforcement. These specimens are only presented by Deng *et al.* (2003). V_{M1} and V_{M2} are the associated coefficients of variation of ρ_{M1} and ρ_{M2}, respectively.

The professional factor, ρ_P, accounts for variation between the test and predicted capacities by taking the ratio of observed test capacity to the predicted capacity:

$$\rho_P = \text{Mean}\left(\frac{\text{Test Capacity}}{\text{Predicted Capacity}}\right) \quad [6.26]$$

V_P is the associated coefficient of variation for the test-to-predicted ratios. The predicted capacity is calculated using any of the prediction models with the measured values of the relevant material and geometric properties and the resistance factor, ϕ, equal to 1.0.

6.5.1 Summary of Test Data from Different Sources

6.5.1.1 Geometric Factor, ρ_G

The bias coefficient, ρ_G, and the coefficient of variation, V_G, for the mean-to-nominal throat dimension based on the work collected by Li *et al*. (2007) are summarized in Table 6.4. Additional data from the Beaulieu and Picard and the UC Davis test programs were also added to the values reported by Li *et al*. The table includes the results based on two methods to measure the weld dimensions: measured throat dimension and measured leg size. The mean ratios of the geometric factor (ρ_G) and associated coefficient of variation (V_G) are obtained by pooling the respective factor from each data group. The mean value of ρ_G was found to be 1.07 and the coefficient of variation, V_G, 0.154.

Tables 6.5 to 6.8 provide the leg size measurements at the shear face, the tensile face and the throat dimension measured at 45° from any shear or tensile face. It also presents the calculated measured throat dimension (*MTD*) and the bias coefficient (ρ_G) for the specimens tested at UC Davis. The same parameters for the specimens tested by Beaulieu and Picard are also presented in Tables 6.9 to 6.12. It should be noted that the *MTD* for the Beaulieu and Picard specimens and the UC Davis specimens are calculated using Equations 6.18 and 6.19, respectively.

6.5.1.2 Material Factor, ρ_{M1}

The material factor (ρ_{M1}) and its corresponding coefficient of variation (V_{M1}) collected from the several sources are summarized in Tables 6.13 to 6.15. For the model that assumes no transfer of load by plate bearing in the compression zone (Model 5), the material factor (ρ_{M1}) is simply taken as a function tensile strength of the electrode only. Table 6.13 presents the values of ρ_{M1} compiled from various sources by Li *et al*. (2007) and augmented here by the values measured for the test program presented in Chapters 3 and 4. However, a modification has been made to the material factor for the models that assume load transfer by bearing in the compression zone. In to simplify the statistical analysis, for models 4 and 8, ρ_{M1} is taken as either a function of the nominal tensile strength of the weld or the nominal static yield strength of the plates, whichever provides the most conservative result. The correct value should lie between the two values of bias coefficient. Two independent bias coefficients for the resistance (ρ_R) and associated COV were calculated; one based on the value of ρ_{M1} for the tensile strength of the filler metal and one based on the yield strength of the plate steel.

6.5.1.3 Material Factor, ρ_{M2}

Table 6.16 presents a summary of the material factor (ρ_{M2}) and its associated coefficient of variation (V_{M2}) as collected from Deng *et al.* (2003). This parameter is a function of the shear strength (τ_u) of the filler metal as calculated according to Equation 6.25 and the shear coefficient used in the design equation to relate the shear resistance to the tensile strength. This material factor is only applicable to the models based on the load-deformation relationship proposed by Lesik and Kennedy (Models 4 and 5) and the approach proposed by Beaulieu and Picard (Model 8).

6.5.1.4 Professional Factor, ρ_P

The professional factor, ρ_P , and the associated coefficient of variation, V_P , for the welded joint with out-of-plane eccentricity for the various strength prediction models presented earlier are summarized in Tables 6.2 and 6.3 for specimens with filler metals with no toughness requirement and with toughness requirement, respectively. The actual weld shear strength (τ_u) , which is used to replace $0.60 \times F_{EXX}$ in Equation 2.6 when evaluating the professional factor was not evaluated for the weld metal used in the reported test programs. Therefore, the ratio of shear strength to tensile strength of 0.78, calculated from the test results of Deng *et al.* (2003) and reported in Table 6.16, was used to calculate the shear strength of the weld metal from the reported (or assessed in the case

of the test programs from Dawe and Kulak and Beaulieu and Picard) tensile strength of the weld metal. The detailed calculations of the professional factor for the various prediction models are presented in Appendix G. It should be noted that the predicted strength for the test specimens from Beaulieu and Picard was calculated for two different values of weld metal strength (62.7 ksi and 80.1 ksi), as explained in Chapter 5.

6.6 LEVEL OF SAFETY PROVIDED BY EXISTING MODELS

Test results from three independent test programs are used to conduct a reliability analysis to determine the level of safety provided by three selected models for design of welded joints with out-of-plane eccentricity. These models are Model 4, which makes use of the method proposed by Dawe and Kulak (modified with a rectangular stress block in the compression zone) with the weld metal behavior proposed by Lesik and Kennedy, Model 5 currently implemented in the AISC Steel Construction Manual, and Model 8 proposed by Beaulieu and Picard as a substitute for the more complex instantaneous center approach. The results of the analysis and the resistance factors for different values of safety index are presented in Tables 6.17 and 6.18 for filler metal with no toughness requirement and filler metal with toughness requirement, respectively.

Table 6.17 shows that the difference in the calculated value of safety index less than 2% when ρ_{M1} is based on the tensile strength of the weld metal versus the base metal. This difference is considered negligible. For a resistance factor, ϕ, of 0.75, the safety index for Models 4, 5 and 8 varies from 4.26 to 6.76. All three models are found to be conservative, although the method of instantaneous centre of rotation provides a value close to the target value of 4.0. A safety index of 4.0 is obtained with a resistance factor of 0.80 for Model 4 and 0.87 for Model 5.

A comparison of Table 6.17 with Table 6.18 indicates that the level of safety provided by filler metals with toughness requirement provide a higher level of safety than the filler metals with no toughness requirement. This reflects the earlier observation that the strength of filler metals with toughness requirement seem to be higher than filler metals of the same nominal tensile strength with no toughness requirement. The safety index varies from 6.47 to 6.58 for Model 4, 6.60 for Model 5 and from 9.28 to 9.54 for Model 8. Once again, whether the reliability analysis is based on the material factor for the tensile strength of the weld metal or the yield strength of the base metal does not make a significant difference. Since only UC Davis test program included test specimens with weld metal with toughness requirement, there are no data for joints with small eccentricity ratio.

6.7 PROPOSED NEW MODEL

Based on the reliability analysis presented in the previous section, it is found that Model 8 provides the most conservative weld strength predictions. The method of instantaneous center of rotation with a rectangular stress block and weld metal deformation characteristics proposed by Lesik and Kennedy provide the desired level of safety with a

resistance factor of 0.80. The method currently used by AISC lies between the other two models.

Although Model 4 is presents a rational approach and produces the desired level of safety, it is a model that is relatively difficult to implement since it requires an iterative approach and the use of a computer program to calculate the strength of welded joints. A simple closed form solution, similar to that proposed by Beaulieu and Picard is more desirable. However, close examination of Model 8 reveals a few problems with the model. The first one is an inconsistency with the calculation of the weld strength on the tension side of the connection since it is based on the leg size rather than the throat size of the weld. Earlier work in welded joint research program (Ng *et al*., 2002) indicated that fillet weld strengths should be calculated based on the throat area for any angle of loading. Therefore, it is necessary to modify the model that accounts for the throat area on the tension side. The second problem is the inclusion of an arbitrary reduction factor of 0.5 in Equation 6.11. This was done to obtain values similar to earlier CISC Handbook (eighth and earlier editions) values. The earlier CISC Handbook used Model 1, which is based on the load versus weld deformation behavior proposed by Butler and Kulak, and a triangular stress block in the compression zone. In addition, the method as implemented in the earlier editions of the CISC Handbook incorporated a reduction factor of 0.67 on the strength of the weld metal. The reason for this reduction factor is not clear, although it was referred to as a shear factor by Lesik and Kennedy (1990). Therefore, it is not surprising that Model 8, which was developed to produce values in good agreement with the CISC Handbook of Steel Construction, provides a high level of safety. A modified version of Model 8 is therefore proposed as a substitute to the more complex Model 4.

The proposed new model (Model 9) is represented by three equations to cover the typical range of welded joints loaded eccentrically (joints with large and small eccentricity and joint with thick and thin plates). The derivation of the equations is detailed in Appendix H.

6.7.1 Thick Plate Connection (Weld Failure)

6.7.1.1 For a/Q > 0.59

For values of eccentricity ratio, a, to strength ratio Q (defined by equation 6.2) greater than 0.59, Appendix H demonstrates that failure of the joint will be governed by bending rather than shear. Figure 6.19 illustrates the assumed stress distribution in the joint at weld failure. From this stress distribution, the welded joint capacity for connections with thick plate can be expressed as:

$$P_r = \frac{0.637\, F_y\, t\, L}{a(Q + 1.273)} \qquad [6.27]$$

where all the parameters are as defined earlier.

6.7.1.2 For a/Q ≤ 0.59

As eccentricity is reduced, shear failure becomes the dominant failure mode of the welded joint. For this situation, the stress distribution shown in Figure 6.20 is used to predict the combine shear and moment capacities. The derived expression for the capacity of the joint for the assumed stress distribution is quite complex, as shown in Appendix H. A simpler approach using a simplified equation obtained by using a linear interpolation between P_{ro} and P_{r45} is proposed:

$$P_r = P_{ro}\left(1-1.69\left(a/Q\right)\right)+1.69\left(a/Q\right)P_{r59} \qquad [6.28]$$

where

$$P_{ro} = 2\left(0.60\times 0.707\right)D\,F_{EXX}\,L \qquad [6.29]$$

and P_{r59} is obtained using equation 6.27 for an eccentricity ratio *a* that yields a value of *a/Q* of 0.59 for the applicable value of *Q*.

The proposed equations 6.27 and 6.28 are based on a shear factor of 0.60 and the derivations are presented in Appendix H. However, the professional factor presented in Table 6.19 is based on the actual shear strength of the weld metal rather than the nominal value of 0.6 times the tensile strength. Therefore, equations 6.27 and 6.28 should be expressed in terms of the weld shear strength, τ_u, which is equal to the empirical value of the shear factor, 0.78, times the measured tensile strength of the weld metal. Equations 6.27 and 6.28 can be re-written in terms of the measured shear strength τ_u as follows:

$$P_r = \frac{1.061F_y\,t\,\tau_u\,D\,L}{a\left(F_y\,t+2.121\tau_u\,D\right)} \qquad \frac{a}{Q}>0.59 \qquad [6.30]$$

$$P_r = P_{ro}\left(1-1.69\left(a/Q\right)\right)+1.69\left(a/Q\right)P_{r59} \qquad \frac{a}{Q}\le 0.59 \qquad [6.31]$$

where

$$P_{ro} = 2\left(0.707\right)\tau_u\,D\;L \qquad [6.32]$$

$$P_{r59} = \frac{1.061F_y\,t\,\tau_u\,D\,L}{0.59Q\left(F_y\,t+2.121\tau_u\,D\right)} \qquad [6.33]$$

where Q was defined in equation 6.11. Equation 6.33 was obtained by substituting equation 6.32 into equation 6.30.

6.7.2 Thin Plate Connections (Plate Failure)

For failure in the plate (thin plate behavior), a simple interaction equation presented by Chen and Han (1988), based on a lower bound approach, is proposed. The equation considers strictly material strength failure. Failure by possible plate instability is beyond the scope of this research project. Appendix H shows that the interaction equation can be solved for the capacity P_r of the joint. The following equation for the plate capacity is obtained:

$$P_r = \frac{2V_p\left(\sqrt{a^2L^2V_p{}^2 + 3M_p{}^2} - aLV_p\right)}{3M_p} \qquad [6.34]$$

where,

$$M_p = \frac{1}{4}tL^2F_u \qquad [6.35]$$

$$V_p = \frac{1}{2}tLF_u \qquad [6.36]$$

Although the interaction equation presented by Chen and Han (1988) is based on the plastic moment, the yield strength was substituted by the tensile strength in the plastic moment and plastic shear calculations. This was found to yield more accurate prediction of the test results since plate rupture rather than plate yielding was observed as the failure mode in the limited number of test specimens that failed in this mode. The test-to-predicted values for the proposed model (Model 9) are presented in Table 6.19. The specimens are grouped according to the filler metal toughness requirement. For filler metals with no toughness requirement the values of the test-to-predicted ratio are further divided according the failure mode (weld failure and plate failure). A total of 27 specimens from three data sets fall into the group that represents weld failure with large eccentricity ($a/Q > 0.59$). The mean test-to-predicted value is 1.00 and its coefficient of variation is 22%. A total of 28 test specimens meet the requirement for small eccentricity ratio ($a/Q \leq 0.59$). The mean test-to-predicted value and coefficient of variation for this group are 1.07 and 22%, respectively. Lastly, only five test specimens from the Beaulieu and Picard test program failed by plate rupture. The mean test-to-predicted ratio and the coefficient of variation for these five test specimens are 1.03 and 16%, respectively.

The same categories are used for specimens used weld metal with toughness requirement. Only the specimens from UC Davis are considered since only the UC Davis test program incorporated test specimens with filler metal of this grade. The test program included 20 specimens with a high eccentricity ratio. The mean test-to-predicted ratio for this set of data is 1.35 and its COV is 8%. Ten specimens fall into the low eccentricity ratio group. The mean test-to-predicted value and COV are 1.26 and 19%, respectively.

A comparison of the data presented in Table 6.19 for Model 9 with the data presented in Tables 6.2 and 6.3 for Models 4, 5 and 8, shows that the proposed model gives the best predictions of the test results with the professional factor closest to 1.0 of all the models investigated. However, the coefficient of variation is still relatively high.

A summary of reliability analysis conducted for Model 9 is presented in Tables 6.20 and 6.21. The current resistance factor of 0.75 provides a minimum safety index of 3.9 for the weld failure mode and 4.2 for the mode of plate failure for joints welded with filler metal with no toughness requirement. It is noted that the minimum value of safety index is obtained when the weld metal tensile strength for the Beaulieu and Picard test program is assumed to be 80.1 ksi. The reader is reminded that this value is based weld metal tensile strengths reported by other researchers for welding electrodes of that era. The tests on concentric lap splices conducted by Beaulieu and Picard indicated that the weld metal strength was substantially lower than 80.1 ksi (67.2 ksi). Using the lower strength filler metal as a basis for predicting the test capacities, the resulting safety index is 4.0 for failure in the weld.

As expected, the safety index for filler metal with toughness requirement is higher than the value for weld metal with no toughness requirement. The minimum value of β observed in Table 6.21 is 5.1 for joints with small eccentricity and 6.3 for joints with large eccentricity.

6.8 CONCLUSIONS

A total of 92 specimens tested in three independent test programs were examined and analyzed using 14 existing models. A detailed assessment of three of these models was presented in this chapter. It was observed that filler metals with toughness requirement have higher test-to-predicted ratio than the specimens with filler metal with no toughness requirement. The test specimens were therefore separated into two groups according to the toughness requirement and analyzed using Models 4, 5 and 8. Unlike other current models, these three models are developed using the most recent load deformation relationship proposed by Lesik and Kennedy (1990). Based on a reliability analysis, the safety index provided by Models 5 and 8 are significantly higher than target value of 4.0. Although Model 4 provides an acceptable level of safety, the computation procedure is complicated and time consuming. Moreover, none of the existing models with Lesik and Kennedy load versus deformation relationship consider plate fracture, which could become critical as the plate thickness is reduced. Therefore, a simpler, closed form, model that is applicable to both weld and plate failure modes is proposed. This model provides reliable prediction and satisfactory safety index ($\beta = 4.0$) with a resistance factor of 0.75.

Table 6.1 – Summary of Professional Factor, ρ_P, for Existing Models

	Source of Data	Sample Size	Professional factor	Coefficient of Variation
		n	ρ_p	V_p
Model 1	Dawe and Kulak (1972)	8	0.851	0.109
	Beaulieu and Picard (1985) **67.2 ksi** / 80.1ksi	17	**1.061** / 0.992	**0.133** / 0.146
	UC Davis	60	1.520	0.167
	All Sources	85	**1.365** / 1.351	**0.244** / 0.256
Model 2	Dawe and Kulak (1972)	8	0.671	0.101
	Beaulieu and Picard (1985) **67.2 ksi** / 80.1ksi	17	**0.863** / 0.779	**0.114** / 0.114
	UC Davis	60	1.175	0.144
	All Sources	85	**1.065** / 1.048	**0.218** / 0.237
Model 3	Dawe and Kulak (1972)	8	0.909	0.104
	Beaulieu and Picard (1985) **67.2 ksi** / 80.1ksi	17	**1.213** / 1.094	**0.120** / 0.114
	UC Davis	60	1.603	0.150
	All Sources	85	**1.460** / 1.436	**0.218** / 0.236
Model 4	Dawe and Kulak (1972)	8	0.760	0.103
	Beaulieu and Picard (1985) **67.2 ksi** / 80.1ksi	17	**1.065** / 0.938	**0.157** / 0.137
	UC Davis	60	1.326	0.142
	All Sources	85	**1.221** / 1.195	**0.207** / 0.225
Model 5	Dawe and Kulak (1972)	8	0.900	0.116
	Beaulieu and Picard (1985) **67.2 ksi** / 80.1ksi	17	**1.208** / 1.014	**0.204** / 0.204
	UC Davis	60	1.493	0.167
	All Sources	85	**1.380** / 1.341	**0.221** / 0.246
Model 6	Dawe and Kulak (1972)	8	0.735	0.114
	Beaulieu and Picard (1985) **67.2 ksi** / 80.1ksi	17	**0.938** / 0.787	**0.187** / 0.187
	UC Davis	60	1.215	0.162
	All Sources	85	**1.114** / 1.084	**0.222** / 0.251
Model 8 (a<0.4)	Beaulieu and Picard (1985) **67.2 ksi** / 80.1ksi	5	**1.403** / 1.226	**0.064** / 0.062
	All Sources	5	**1.403** / 1.226	**0.064** / 0.062
Model 8 (a≥0.4)	Dawe and Kulak (1972)	8	1.215	0.101
	Beaulieu and Picard (1985) **67.2 ksi** / 80.1ksi	12	**1.524** / 1.411	**0.129** / 0.131
	UC Davis	60	2.134	0.147
	All Sources	80	**1.951** / 1.934	**0.222** / 0.234

Table 6.1 – Cont'd

	Source of Data	Sample Size	Professional factor	Coefficient of Variation
		n	ρ_p	V_p
Model 7 Case 1	Dawe and Kulak (1972)	8	0.827	0.104
	Beaulieu and Picard (1985) **67.2 ksi** / 80.1ksi	11	**1.042** / 0.974	**0.138** / 0.142
	UC Davis	60	1.459	0.155
	All Sources	79	**1.337** / 1.327	**0.227** / 0.236
Model 7 Case 2	Dawe and Kulak (1972)	8	0.627	0.108
	Beaulieu and Picard (1985) **67.2 ksi** / 80.1ksi	11	**0.806** / 0.738	**0.137** / 0.135
	UC Davis	60	1.240	0.144
	All Sources	79	**1.117** / 1.108	**0.247** / 0.259
Model 7 Case 3	Dawe and Kulak (1972)	8	0.808	0.098
	Beaulieu and Picard (1985) **67.2 ksi** / 80.1ksi	11	**0.967** / 0.873	**0.143** / 0.139
	UC Davis	60	1.467	0.135
	All Sources	79	**1.330** / 1.317	**0.230** / 0.245
Model 7 Case 4	Dawe and Kulak (1972)	8	0.670	0.099
	Beaulieu and Picard (1985) **67.2 ksi** / 80.1ksi	11	**0.833** / 0.765	**0.134** / 0.135
	UC Davis	60	1.168	0.140
	All Sources	79	**1.071** / 1.061	**0.217** / 0.229
Model 7 Case 5	Dawe and Kulak (1972)	8	0.658	0.100
	Beaulieu and Picard (1985) **67.2 ksi** / 80.1ksi	11	**0.819** / 0.754	**0.134** / 0.135
	UC Davis	60	1.148	0.142
	All Sources	79	**1.053** / 1.044	**0.218** / 0.229
Model 7 Case 6 and Case 7	Dawe and Kulak (1972)	8	0.937	0.122
	Beaulieu and Picard (1985) **67.2 ksi** / 80.1ksi	11	**1.218** / 1.049	**0.157** / 0.246
	UC Davis	60	1.556	0.169
	All Sources	79	**1.446** / 1.422	**0.220** / 0.243

Table 6.2 – Summary of Professional Factor, ρ_P, for Specimens with Filler Metals with No Toughness Requirement

	Source of Data	Sample Size	Test/Predicted	Coefficient of Variation
		n	ρ_p	V_p
Model 4	Dawe and Kulak (1972)	8	0.760	0.103
	Beaulieu and Picard (1985) **67.2 ksi** / 80.1ksi	17	**1.065** / 0.938	**0.157** / 0.137
	UC Davis	30	1.213	0.128
	All Sources	55	**1.101** / 1.062	**0.196** / 0.210
Model 5	Dawe and Kulak (1972)	8	0.900	0.116
	Beaulieu and Picard (1985) **67.2 ksi** / 80.1ksi	17	**1.208** / 1.014	**0.204** / 0.204
	UC Davis	30	1.371	0.143
	All Sources	55	**1.252** / 1.192	**0.207** / 0.230
Model 8 (a<0.4)	Beaulieu and Picard (1985) **67.2 ksi** / 80.1ksi	5	**1.403** / 1.226	**0.064** / 0.062
	All Sources	5	**1.403** / 1.226	**0.064** / 0.062
Model 8 (a≥0.4)	Dawe and Kulak (1972)	8	1.215	0.101
	Beaulieu and Picard (1985) **67.2 ksi** / 80.1ksi	12	**1.524** / 1.411	**0.129** / 0.131
	UC Davis	30	1.952	0.139
	All Sources	50	**1.731** / 1.704	**0.215** / 0.228

Table 6.3 – Summary of Professional Factor, ρ_P, for Specimens with Filler Metal with Toughness Requirement

	Source of Data	Sample Size	Test/Predicted	Coefficient of Variation
		n	ρ_p	V_p
Model 4	UC Davis	30	1.440	0.102
Model 5	UC Davis	30	1.615	0.147
Model 8 (a>0.4)	UC Davis	30	2.317	0.103

Table 6.4 – Summary of Geometric Factor ρ_G from Various Sources (Li *et al.*, 2007)

Weld Dimension Measurement Method	Source of Data	Nominal leg size	Sample Size	Ratio of Measured to Nominal	Coefficient of Variation
		(in)	n	ρ_G	V_G
Measured Throat Dimension	Bornscheuer and Feder (1966)	0.225	18	0.957	0.090
		0.445	6	0.938	0.048
		0.670	5	0.921	0.020
	Ligtenberg (1968)	0.165	97	1.230	0.168
		0.197	67	1.121	0.163
		0.225	91	1.109	0.171
		0.252	13	1.071	0.096
		0.280	302	1.056	0.155
		0.335	145	1.039	0.147
		0.418	41	0.986	0.098
		0.445	87	0.997	0.100
		0.556	31	0.996	0.124
	Kato and Morita (1969)	0.197	8	1.057	0.065
		0.276	1	1.041	0.000
		0.394	3	1.009	0.021
		0.473	1	0.953	0.000
		0.591	6	1.014	0.005
		0.788	3	0.960	0.079
		0.867	1	0.929	0.000
		1.182	1	1.000	0.000
		1.576	2	0.940	0.090
	Clark (1971)	0.311	18	0.985	0.065
	Pham (1981)	0.197	17	1.072	0.102
		0.394	6	1.058	0.051
		0.630	3	1.030	0.054
	All Specimens with Measured Throat Dimension	N.A.	973	1.065	0.159

Table 6.4 – Cont'd

Weld Dimension Measurement Method	Source of Data	Nominal leg size	Sample Size	Ratio of Measured to Nominal	Coefficient of Variation
		(in)	n	ρ_G	V_G
Measured Leg Size	Butler and Kulak (1969)	0.252	31	1.138	0.069
	Dawe and Kulak (1972)	0.252	43	1.158	0.075
	Swannell (1979b)	0.252	21	1.070	0.031
	Pham (1983a,b)	0.236	22	1.346	0.060
		0.394	23	1.118	0.106
		0.630	23	1.072	0.081
	Beaulieu and Picard (1985)	0.236	12	1.510	0.206
		0.315	12	1.311	0.135
		0.394	12	1.172	0.076
		0.473	12	1.116	0.053
	Miazga and Kennedy (1986)	0.197	21	1.040	0.026
		0.355	21	1.030	0.027
	Bowman and Quinn (1994)	0.252	8	1.182	0.082
		0.374	4	1.128	0.040
		0.500	6	1.087	0.030
	Ng *et al*. (2002)	0.252	126	1.026	0.102
		0.500	78	0.954	0.073
	Deng *et al*. (2003)	0.500	54	0.836	0.053
	Callele *et al*. (2005)	0.311	48	1.118	0.061
		0.500	180	0.981	0.082
	Li *et al.* (2007)	0.500	24	0.914	0.055
	UC Davis (tensile data)	0.311	24	1.266	0.075
		0.500	24	1.234	0.081
	UC Davis (bending data)	0.311	60	1.175	0.050
		0.500	60	1.277	0.094
	All Specimens with Measured Throat Dimension	N.A.	949	1.076	0.149
All Sources		N.A.	1922	1.070	0.154

Table 6.5 – Geometric Factor ρ_G for Tensile Specimens from UC Davis (Leg size = 0.5 in)

Specimen	Nominal Leg Size (in)	Weld	Tension Leg Size (in)	Shear Leg Size (in)	45° Meas. (in)	MTD (in)	Ratio ρ_G
T_125_A12_1	**0.5**	Front	0.462	0.710	0.391	0.387	1.096
		Back	0.457	0.623	0.415	0.368	1.042
T_125_A12_2	**0.5**	Front	0.691	0.736	0.361	0.504	1.425
		Back	0.521	0.667	0.413	0.410	1.161
T_125_A12_3	**0.5**	Front	0.514	0.681	0.373	0.410	1.160
		Back	0.528	0.781	0.455	0.437	1.237
T_125_B12_1	**0.5**	Front	0.594	0.802	0.277	0.477	1.350
		Back	0.531	0.688	0.431	0.420	1.189
T_125_B12_2	**0.5**	Front	0.594	0.757	0.361	0.467	1.322
		Back	0.604	0.656	0.427	0.444	1.257
T_125_B12_3	**0.5**	Front	0.611	0.684	0.313	0.456	1.289
		Back	0.552	0.722	0.417	0.439	1.241
T_250_A12_1	**0.5**	Front	0.538	0.872	0.438	0.458	1.295
		Back	0.503	0.733	0.469	0.415	1.174
T_250_A12_2	**0.5**	Front	0.490	0.774	0.408	0.414	1.172
		Back	0.486	0.681	0.373	0.396	1.119
T_250_A12_3	**0.5**	Front	0.649	0.885	0.424	0.524	1.481
		Back	0.531	0.747	0.396	0.433	1.224
T_250_B12_1	**0.5**	Front	0.528	0.806	0.361	0.441	1.249
		Back	0.531	0.719	0.441	0.427	1.209
T_250_B12_2	**0.5**	Front	0.563	0.729	0.406	0.445	1.260
		Back	0.594	0.740	0.479	0.463	1.310
T_250_B12_3	**0.5**	Front	0.486	0.736	0.375	0.406	1.148
		Back	0.531	0.729	0.448	0.429	1.215
All Specimens			Mean Ratio				1.234
			Coefficient of Variation, V				0.081

Table 6.6 – Geometric Factor ρ_G for Tensile Specimens from UC Davis (Leg size = 0.313 in)

Specimen	Nominal Leg Size (in)	Weld	Tension Leg Size (in)	Shear Leg Size (in)	45° Meas. (in)	MTD (in)	Ratio ρ_G
T_125_A516_1	0.313	Front	0.302	0.453	0.281	0.251	1.138
		Back	0.333	0.464	0.278	0.271	1.225
T_125_A516_2	0.313	Front	0.323	0.469	0.250	0.266	1.204
		Back	0.337	0.472	0.302	0.274	1.241
T_125_A516_3	0.313	Front	0.365	0.451	0.264	0.284	1.284
		Back	0.347	0.514	0.292	0.288	1.302
T_125_B516_1	0.313	Front	0.344	0.524	0.288	0.287	1.301
		Back	0.406	0.375	0.319	0.276	1.247
T_125_B516_2	0.313	Front	0.351	0.524	0.313	0.291	1.319
		Back	0.413	0.368	0.309	0.275	1.244
T_125_B516_3	0.313	Front	0.368	0.500	0.309	0.296	1.342
		Back	0.444	0.483	0.344	0.327	1.480
T_250_A516_1	0.313	Front	0.313	0.479	0.347	0.262	1.185
		Back	0.344	0.503	0.219	0.284	1.285
T_250_A516_2	0.313	Front	0.278	0.486	0.219	0.241	1.092
		Back	0.344	0.500	0.260	0.283	1.282
T_250_A516_3	0.313	Front	0.288	0.531	0.229	0.253	1.147
		Back	0.319	0.507	0.299	0.270	1.223
T_250_B516_1	0.313	Front	0.406	0.441	0.344	0.299	1.352
		Back	0.313	0.476	0.313	0.261	1.182
T_250_B516_2	0.313	Front	0.406	0.469	0.319	0.307	1.390
		Back	0.410	0.476	0.319	0.310	1.405
T_250_B516_3	0.313	Front	0.372	0.514	0.344	0.301	1.363
		Back	0.313	0.438	0.313	0.254	1.151
All Specimens			Mean Ratio				1.266
			Coefficient of Variation, V				0.075

Table 6.7 – Geometric Factor ρ_G for Bending Specimens from UC Davis (Leg size = 0.5 in)

Specimen	Nominal Leg Size (in)	Weld	Tension Leg Size (in)	Shear Leg Size (in)	45° Meas. (in)	MTD (in)	Ratio ρ_G
B_125_A12_55_1	0.5	Front	0.520	0.717	0.378	0.421	1.191
		Back	0.500	0.756	0.420	0.417	1.180
B_125_A12_55_2	0.5	Front	0.534	0.755	0.433	0.436	1.233
		Back	0.508	0.646	0.396	0.400	1.131
B_125_A12_55_3	0.5	Front	0.516	0.719	0.424	0.419	1.185
		Back	0.509	0.697	0.414	0.411	1.163
B_125_B12_55_1	0.5	Front	0.538	0.702	0.391	0.427	1.208
		Back	0.529	0.633	0.401	0.406	1.148
B_125_B12_55_2	0.5	Front	0.509	0.702	0.434	0.412	1.166
		Back	0.480	0.632	0.385	0.382	1.081
B_125_B12_55_3	0.5	Front	0.576	0.621	0.366	0.422	1.194
		Back	0.570	0.683	0.443	0.437	1.237
B_175_A12_3_1	0.5	Front	0.474	0.765	0.408	0.403	1.140
		Back	0.482	0.601	0.371	0.376	1.064
B_175_A12_3_2	0.5	Front	0.467	0.707	0.399	0.390	1.102
		Back	0.514	0.616	0.400	0.395	1.117
B_175_A12_3_3	0.5	Front	0.484	0.689	0.382	0.396	1.120
		Back	0.522	0.663	0.437	0.410	1.160
B_175_A12_55_1	0.5	Front	0.534	0.732	0.429	0.431	1.220
		Back	0.504	0.725	0.383	0.414	1.170
B_175_A12_55_2	0.5	Front	0.511	0.650	0.430	0.402	1.136
		Back	0.491	0.663	0.383	0.395	1.116
B_175_A12_55_3	0.5	Front	0.529	0.635	0.428	0.407	1.150
		Back	0.520	0.704	0.427	0.418	1.183
B_175_A12_85_1	0.5	Front	0.554	0.639	0.437	0.419	1.184
		Back	0.556	0.602	0.403	0.409	1.156
B_175_A12_85_2	0.5	Front	0.529	0.615	0.434	0.401	1.135
		Back	0.527	0.665	0.426	0.413	1.168
B_175_A12_85_3	0.5	Front	0.559	0.701	0.414	0.437	1.236
		Back	0.553	0.734	0.437	0.442	1.250
B_175_B12_3_1	0.5	Front	0.538	0.629	0.409	0.409	1.156
		Back	0.516	0.701	0.436	0.415	1.175
B_175_B12_3_2	0.5	Front	0.508	0.688	0.434	0.409	1.157
		Back	0.523	0.668	0.389	0.412	1.165
B_175_B12_3_3	0.5	Front	0.525	0.607	0.414	0.397	1.123
		Back	0.493	0.678	0.434	0.399	1.129
B_175_B12_55_1	0.5	Front	0.505	0.678	0.435	0.405	1.146
		Back	0.520	0.710	0.434	0.419	1.186
B_175_B12_55_2	0.5	Front	0.558	0.799	0.426	0.457	1.294
		Back	0.480	0.684	0.369	0.393	1.112

Table 6.7 – Cont'd

Specimen	Nominal Leg Size (in)	Weld	Tension Leg Size (in)	Shear Leg Size (in)	45° Meas. (in)	MTD (in)	Ratio ρ_G
B_175_B12_85_1	0.5	Front	0.529	0.765	0.441	0.435	1.230
		Back	0.507	0.634	0.386	0.396	1.120
B_175_B12_85_2	0.5	Front	0.568	0.621	0.379	0.419	1.185
		Back	0.541	0.714	0.386	0.431	1.219
B_175_B12_85_3	0.5	Front	0.577	0.688	0.391	0.442	1.251
		Back	0.556	0.768	0.404	0.450	1.273
B_250_A12_55_1	0.5	Front	0.482	0.790	0.380	0.411	1.163
		Back	0.507	0.703	0.397	0.411	1.163
B_250_A12_55_2	0.5	Front	0.497	0.768	0.372	0.417	1.181
		Back	0.473	0.721	0.379	0.396	1.119
B_250_A12_55_3	0.5	Front	0.452	0.743	0.381	0.387	1.093
		Back	0.500	0.656	0.430	0.398	1.125
B_250_B12_55_1	0.5	Front	0.490	0.758	0.394	0.412	1.164
		Back	0.580	0.783	0.417	0.466	1.319
B_250_B12_55_2	0.5	Front	0.529	0.738	0.420	0.430	1.217
		Back	0.596	0.796	0.435	0.477	1.349
B_250_B12_55_3	0.5	Front	0.525	0.697	0.421	0.420	1.187
		Back	0.544	0.804	0.454	0.451	1.275
All Specimens			Mean Ratio				1.176
			Coefficient of Variation, V				0.049

Table 6.8 – Geometry Factor ρ_G for Bending Specimens from UC Davis (Leg size = 0.313 in)

Specimen	Nominal Leg Size (in)	Weld	Tension Leg Size (in)	Shear Leg Size (in)	45° Meas. (in)	MTD (in)	Ratio ρ_G
B_125_A516_55_1	0.313	Front	0.374	0.516	0.286	0.303	1.370
		Back	0.335	0.423	0.249	0.263	1.189
B_125_A516_55_2	0.313	Front	0.354	0.505	0.304	0.290	1.311
		Back	0.356	0.428	0.302	0.274	1.239
B_125_A516_55_3	0.313	Front	0.361	0.484	0.282	0.290	1.311
		Back	0.368	0.476	0.318	0.291	1.318
B_125_B516_55_1	0.313	Front	0.370	0.495	0.318	0.297	1.342
		Back	0.382	0.518	0.326	0.307	1.390
B_125_B516_55_2	0.313	Front	0.364	0.515	0.354	0.297	1.345
		Back	0.380	0.511	0.306	0.305	1.379
B_125_B516_55_3	0.313	Front	0.337	0.470	0.300	0.274	1.240
		Back	0.402	0.534	0.299	0.321	1.453
B_175_A516_3_1	0.313	Front	0.306	0.467	0.262	0.256	1.160
		Back	0.299	0.468	0.239	0.252	1.139
B_175_A516_3_2	0.313	Front	0.312	0.495	0.280	0.264	1.195
		Back	0.300	0.465	0.238	0.252	1.142
B_175_A516_3_3	0.313	Front	0.313	0.421	0.250	0.251	1.136
		Back	0.307	0.487	0.261	0.260	1.175
B_175_A516_55_1	0.313	Front	0.342	0.471	0.316	0.277	1.252
		Back	0.284	0.467	0.258	0.243	1.099
B_175_A516_55_2	0.313	Front	0.348	0.449	0.298	0.275	1.245
		Back	0.293	0.431	0.246	0.242	1.097
B_175_A516_55_3	0.313	Front	0.320	0.487	0.287	0.267	1.211
		Back	0.313	0.451	0.275	0.257	1.165
B_175_A516_85_1	0.313	Front	0.407	0.498	0.281	0.315	1.426
		Back	0.341	0.469	0.274	0.276	1.248
B_175_A516_85_2	0.313	Front	0.371	0.489	0.268	0.296	1.338
		Back	0.370	0.516	0.263	0.301	1.360
B_175_A516_85_3	0.313	Front	0.379	0.373	0.266	0.266	1.203
		Back	0.400	0.551	0.312	0.324	1.464
B_175_B516_3_1	0.313	Front	0.319	0.461	0.305	0.262	1.188
		Back	0.366	0.567	0.355	0.308	1.393
B_175_B516_3_2	0.313	Front	0.329	0.451	0.282	0.266	1.204
		Back	0.325	0.514	0.304	0.275	1.243
B_175_B516_3_3	0.313	Front	0.348	0.478	0.316	0.281	1.274
		Back	0.313	0.501	0.304	0.265	1.200
B_175_B516_55_1	0.313	Front	0.419	0.730	0.331	0.363	1.645
		Back	0.324	0.460	0.281	0.265	1.200
B_175_B516_55_2	0.313	Front	0.415	0.770	0.343	0.365	1.654
		Back	0.261	0.530	0.283	0.234	1.060

Table 6.8 – Cont'd

Specimen	Nominal Leg Size (in)	Weld	Tension Leg Size (in)	Shear Leg Size (in)	45° Meas. (in)	MTD (in)	Ratio ρ_G
B_175_B516_85_1	0.313	Front	0.386	0.489	0.309	0.303	1.371
		Back	0.359	0.492	0.336	0.290	1.313
B_175_B516_85_2	0.313	Front	0.386	0.471	0.365	0.299	1.351
		Back	0.397	0.424	0.322	0.290	1.312
B_175_B516_85_3	0.313	Front	0.382	0.518	0.234	0.308	1.392
		Back	0.350	0.479	0.356	0.283	1.279
B_250_A516_55_1	0.313	Front	0.385	0.558	0.324	0.317	1.433
		Back	0.299	0.487	0.254	0.255	1.154
B_250_A516_55_2	0.313	Front	0.368	0.579	0.318	0.311	1.406
		Back	0.307	0.482	0.281	0.259	1.171
B_250_A516_55_3	0.313	Front	0.338	0.543	0.305	0.287	1.300
		Back	0.323	0.511	0.286	0.273	1.235
B_250_B516_55_1	0.313	Front	0.349	0.439	0.330	0.273	1.236
		Back	0.325	0.461	0.285	0.266	1.203
B_250_B516_55_2	0.313	Front	0.358	0.449	0.329	0.280	1.268
		Back	0.349	0.481	0.302	0.283	1.279
B_250_B516_55_3	0.313	Front	0.394	0.462	0.337	0.300	1.357
		Back	0.331	0.496	0.288	0.275	1.246
All Specimens			Mean Ratio				1.281
			Coefficient of Variation, V				0.093

Table 6.9 – Geometric Factor ρ_G for Specimens from Beaulieu and Picard (Leg size = 0.236 in)

Specimen	Nominal Leg Size (in)	Weld	De (in)	MTD (in)	Ratio ρ_G
A-6-375-1	0.236	Front	0.315	0.223	1.332
		Back	0.291	0.206	1.230
A-6-375-2	0.236	Front	0.489	0.345	2.067
		Back	0.494	0.349	2.088
A-6-125-1	0.236	Front	0.327	0.231	1.385
		Back	0.305	0.216	1.290
A-6-125-2	0.236	Front	0.296	0.209	1.253
		Back	0.322	0.228	1.363
A-6-75-1	0.236	Front	0.424	0.299	1.792
		Back	0.390	0.276	1.652
A-6-75-2	0.236	Front	0.319	0.225	1.348
		Back	0.312	0.221	1.320
All Specimens			Mean Ratio		1.510
			Coefficient of Variation, V		0.206

Table 6.10 – Geometric Factor ρ_G for Specimens from Beaulieu and Picard (Leg size = 0.473 in)

Specimen	Nominal Leg Size (in)	Weld	De (in)	MTD (in)	Ratio ρ_G
A-12-375-1	0.473	Front	0.524	0.370	1.108
		Back	0.552	0.390	1.167
A-12-375-2	0.473	Front	0.563	0.398	1.190
		Back	0.510	0.360	1.078
A-12-125-1	0.473	Front	0.556	0.393	1.176
		Back	0.549	0.388	1.161
A-12-125-2	0.473	Front	0.536	0.379	1.134
		Back	0.504	0.356	1.065
A-12-75-1	0.473	Front	0.467	0.330	0.988
		Back	0.534	0.378	1.130
A-12-75-2	0.473	Front	0.538	0.380	1.138
		Back	0.498	0.352	1.053
All Specimens			Mean Ratio		1.116
			Coefficient of Variation, V		0.053

Table 6.11 – Geometric Factor ρ_G for Specimens from Beaulieu and Picard (Leg size = 0.315 in)

Specimen	Nominal Leg Size (in)	Weld	De (in)	MTD (in)	Ratio ρ_G
B-8-375-1	0.315	Front	0.501	0.358	1.606
		Back	0.441	0.315	1.413
B-8-375-2	0.315	Front	0.426	0.304	1.366
		Back	0.491	0.351	1.574
B-8-125-1	0.315	Front	0.406	0.290	1.300
		Back	0.428	0.306	1.373
B-8-125-2	0.315	Front	0.386	0.276	1.239
		Back	0.438	0.313	1.403
B-8-75-1	0.315	Front	0.358	0.255	1.146
		Back	0.356	0.255	1.143
B-8-75-2	0.315	Front	0.334	0.238	1.070
		Back	0.343	0.245	1.100
All Specimens			Mean Ratio		1.311
			Coefficient of Variation, V		0.135

Table 6.12 – Geometric Factor ρ_G for Specimens from Beaulieu and Picard (Leg size = 0.394 in)

Specimen	Nominal Leg Size (in)	Weld	De (in)	MTD (in)	Ratio ρ_G
B-10-375-1	0.394	Front	0.462	0.326	1.172
		Back	0.476	0.337	1.209
B-10-375-2	0.394	Front	0.509	0.360	1.291
		Back	0.436	0.308	1.107
B-10-125-1	0.394	Front	0.410	0.290	1.040
		Back	0.413	0.292	1.047
B-10-125-2	0.394	Front	0.448	0.316	1.136
		Back	0.433	0.306	1.100
B-10-75-1	0.394	Front	0.487	0.344	1.235
		Back	0.502	0.355	1.274
B-10-75-2	0.394	Front	0.506	0.358	1.284
		Back	0.463	0.327	1.174
All Specimens			Mean Ratio		1.172
			Coefficient of Variation, V		0.076

Table 6.13 – Summary of Material Factor ρ_{M1} for tensile strength of the weld

Source of Data	Sample size,	Nominal tensile strength, (ksi)	Mean tensile strength, (ksi)	Ratio of Measured to Nominal	Coefficient of Variation
	n	F_{EXX}	σ_u	ρ_{M1}	V_{M1}
Miazga and Kennedy (1986)	3	69.6	78.0	1.12	0.014
Gagnon and Kennedy (1987)	10	69.6	84.1	1.21	0.036
Swannell and Skewes (1979)	2	59.4	78.1	1.31	0.020
Fisher et al. (1978)	127	60.0	66.0	1.10	0.039
	138	70.0	74.9	1.07	0.036
	136	80.0	87.9	1.10	0.049
	16	90.0	100.2	1.11	0.043
	72	109.9	116.9	1.06	0.040
	128	70.0	85.4	1.22	0.056
	40	70.0	86.8	1.24	0.114
Pham (1981)	3	69.6	72.5	1.04	0.044
Mansell and Yadav (1982)	6	59.4	80.9	1.36	0.027
Bowman and Quinn (1994)	3	70.0	69.0	0.98	0.029
Callele et al. (2005)†	32	69.6	80.1	1.15	0.084
UC Davis	4	69.6	97.3	1.40	0.002
All Sources	720	N.A.	N.A.	1.13	0.082

† Including all weld metal tension coupon tests from phases 1 through 4.

Table 6.14 – Summary of Material Factor ρ_{M1} for static yield strength of the plate

Source of Data	Thickness (in)	Sample size,	Nominal static yield strength, (ksi)	Mean static yield strength, (ksi)	Ratio of Measured to Nominal	Coefficient of Variation
	t	n	F_y	σ_y	ρ_{M1}	V_{M1}
Schmidt and Bartlett (2002)	0.394-0.784	1231	50.8	56.3	1.11	0.054
	0.788-1.178	239	50.8	56.3	1.11	0.053
	1.182-1.572	157	50.8	58.9	1.16	0.063
	1.576-1.966	186	50.8	60.9	1.20	0.055
All Sources		1813	N.A.	N.A.	1.12	0.061

Table 6.15 – Summary of Material Factor ρ_{M1} for ultimate tensile strength of the plate

Source of Data	Thickness (in)	Sample size,	Nominal ultimate tensile strength, (ksi)	Mean ultimate tensile strength, (ksi)	Ratio of Measured to Nominal	Coefficient of Variation
	t	n	F_u	σ_u	ρ_{M1}	V_{M1}
Schmidt and Bartlett (2002)	0.394-0.784	1231	65.2	77.6	1.19	0.034
	0.788-1.178	239	65.2	79.0	1.21	0.029
	1.182-1.572	157	65.2	81.6	1.25	0.040
	1.576-1.966	186	65.2	86.1	1.32	0.037
All Sources		1813	N.A.	N.A.	1.21	0.048

Table 6.16 – Summary of Material Factor ρ_{M2} (Deng *et al.*, 2003)

Weld Dimension Measurement Method	Specimen Designation	AWS Classification	$P/A_{fracture}$, τ_u (ksi)	Tensile Strength, σ_u (ksi)	τ_u / σ_u	$0.60\,\sigma_u$ (ksi)	ρ_{M2}
Fracture Surface Area	L1-1	E70T-4	—	91.5	—	54.9	—
			—	91.5	—	54.9	—
			73.0	91.5	0.798	54.9	1.330
			73.4	91.5	0.802	54.9	1.337
	L1-2	E70T-4	71.6	91.5	0.782	54.9	1.304
			61.1	91.5	0.668	54.9	1.113
			—	91.5	—	54.9	—
			—	91.5	—	54.9	—
	L1-3	E70T-4	67.9	91.5	0.742	54.9	1.237
			67.2	91.5	0.735	54.9	1.225
			—	91.5	—	54.9	—
			—	91.5	—	54.9	—
	L2-1	E70T-7	—	87.7	—	52.6	—
			63.3	87.7	0.722	52.6	1.203
			—	87.7	—	52.6	—
			—	87.7	—	52.6	—
	L2-2	E70T-7	—	87.7	—	52.6	—
			—	87.7	—	52.6	—
			—	87.7	—	52.6	—
			74.6	87.7	0.851	52.6	1.418
	L2-3	E70T-7	—	87.7	—	52.6	—
			—	87.7	—	52.6	—
			68.9	87.7	0.785	52.6	1.309
			—	87.7	—	52.6	—
	L3-1	E71T8-K6	59.9	71.5	0.837	42.9	1.395
			54.2	71.5	0.758	42.9	1.263
			56.9	71.5	0.797	42.9	1.328
			51.5	71.5	0.720	42.9	1.201
	L3-2	E71T8-K6	—	71.5	—	42.9	—
			54.9	71.5	0.768	42.9	1.281
			—	71.5	—	42.9	—
			—	71.5	—	42.9	—
	L3-3	E71T8-K6	64.3	71.5	0.899	42.9	1.499
			—	71.5	—	42.9	—
			—	71.5	—	42.9	—
			—	71.5	—	42.9	—
All Specimens			Mean Ratio				1.296
			Coefficient of Variation, V				0.075

Table 6.17 – Reliability Analysis for Models 4, 5 and 8 and Filler Metal with No Toughness Requirement

Model		Model 4 (Modified Dawe & Kulak I.C. Approach w/ Lesik & Kennedy)	Model 5 (AISC Approach w/ Lesik & Kennedy)	Model 8 (Beaulieu and Picard Approach) (a < 0.4)	Model 8 (Beaulieu and Picard Approach) (a ≥ 0.4)
ρ_G		1.070	1.070	1.070	1.070
V_G		0.154	0.154	0.154	0.154
ρ_{M1} (F_{EXX})		1.127	1.127	1.127	1.127
V_{M1} (F_{EXX})		0.082	0.082	0.082	0.082
ρ_{M1} (F_y)		1.124	—	1.124	1.124
V_{M1} (F_y)		0.061	—	0.061	0.061
ρ_{M2}		1.296	1.296	1.296	1.296
V_{M2}		0.075	0.075	0.075	0.075
$\rho_{p\ (67.2\ ksi)}$		1.101	1.252	1.403	1.731
$V_{p\ (67.2\ ksi)}$		0.196	0.207	0.064	0.215
$\rho_{p\ (80.1\ ksi)}$		1.062	1.192	1.226	1.704
$V_{p\ (80.1\ ksi)}$		0.210	0.230	0.062	0.228
ρ_R (F_{EXX}) 67.2ksi		1.721	1.957	2.193	2.705
V_R (F_{EXX}) 67.2 ksi		0.273	0.281	0.200	0.287
ρ_R (F_y) 67.2 ksi		1.716	—	2.187	2.698
V_R (F_y) 67.2 ksi		0.267	—	0.193	0.282
ρ_R (F_{EXX}) 80.1ksi		1.660	1.863	1.916	2.663
V_R (F_{EXX}) 80.1 ksi		0.283	0.298	0.200	0.297
ρ_R (F_y) 80.1 ksi		1.655	—	1.911	2.656
V_R (F_y) 80.1 ksi		0.278	—	0.192	0.292
β (F_{EXX}) 67.2 ksi	$\Phi = 0.75$	4.50	4.93	6.62	6.17
Φ	β = 4.5	0.75	0.84	1.14	1.14
Φ	β = 4.0	0.85	0.95	1.27	1.30
β (F_y) 67.2 ksi	$\Phi = 0.75$	4.54	—	6.76	6.24
Φ	β = 4.5	0.76	—	1.16	1.15
Φ	β = 4.0	0.86	—	1.29	1.31
β (X_u) 80.1 ksi	$\Phi = 0.75$	4.26	4.56	5.92	5.97
Φ	β = 4.5	0.70	0.76	1.00	1.09
Φ	β = 4.0	0.80	0.87	1.11	1.25
β (F_y) 80.1 ksi	$\Phi = 0.75$	4.30	—	6.04	6.03
Φ	β = 4.5	0.71	—	1.02	1.10
Φ	β = 4.0	0.81	—	1.13	1.26

Table 6.18 – Summary of Safety Indices for Models 4, 5 and 8 on the Specimens with Toughness Requirement

Model		Model 4 (Modified Dawe & Kulak I.C. Approach w/ Lesik & Kennedy)	Model 5 (AISC Approach w/ Lesik & Kennedy)	Model 8 (Beaulieu and Picard Approach) (a ≥ 0.4)
ρ_G		1.07	1.07	1.07
V_G		0.154	0.154	0.154
ρ_{M1} (F_{EXX})		1.127	1.127	1.127
V_{M1} (F_{EXX})		0.082	0.082	0.082
ρ_{M1} (Fy)		1.124	—	1.124
V_{M1} (Fy)		0.061	—	0.061
ρ_{M2}		1.296	1.296	1.296
V_{M2}		0.075	0.075	0.075
ρ_p		1.44	1.615	2.317
V_p		0.102	0.147	0.103
ρ_R (F_{EXX})		2.250	2.524	3.621
V_R (F_{EXX})		0.216	0.240	0.216
ρ_R (F_y)		2.244	—	3.611
V_R (F_y)		0.208	—	0.209
β (F_{EXX})	$\Phi = 0.75$	6.47	6.60	9.28
Φ	β = 4.5	1.13	1.19	1.82
Φ	β = 4.0	1.26	1.34	2.03
β (F_y)	$\Phi = 0.75$	6.58	—	9.54
Φ	β = 4.5	1.15	—	1.84
Φ	β = 4.0	1.28	—	2.05

Table 6.19 – Summary of Professional Factor, ρ_P, for Model 9

			Source of Data	Sample Size	Mean Test/Predicted	Coefficient of Variation
				n	ρ_p	V_p
Model 9 No toughness requirement	Weld Failure	*a/Q* > 0.59	Dawe and Kulak (1972)	6	0.721	0.076
			Beaulieu and Picard (1985) **67.2 ksi** / 80.1ksi	**6** / 6	**0.906** / 0.829	**0.174** / 0.173
			UC Davis	15	1.152	0.108
			All Sources	**27** / 27	**1.001** / 0.984	**0.216** / 0.229
		a/Q ≤ 0.59	Dawe and Kulak (1972)	2	0.667	0.194
			Beaulieu and Picard (1985) **67.2 ksi** / 80.1ksi	**11** / 11	**1.181** / 1.026	**0.153** / 0.140
			UC Davis	15	1.043	0.206
			All Sources	**28** / 28	**1.070** / 1.010	**0.217** / 0.202
	Plate Failure	all *a* values	Dawe and Kulak (1972)	—	—	—
			Beaulieu and Picard (1985) **67.2 ksi** / 80.1ksi	**5**./ 5	**1.027** / 1.027	**0.155** / 0.155
			UC Davis	—	—	—
			All Sources	**5**./ 5	**1.027** / 1.027	**0.155** / 0.155
Model 9 With toughness requirement	Weld Failure	*a/Q* > 0.59	Dawe and Kulak (1972)	—	—	—
			Beaulieu and Picard (1985) **67.2 ksi** / 80.1ksi	—	—	—
			UC Davis	20	1.350	0.084
			All Sources	20	1.350	0.084
		a/Q ≤ 0.59	Dawe and Kulak (1972)	—	—	—
			Beaulieu and Picard (1985) **67.2 ksi** / 80.1ksi	—	—	—
			UC Davis	10	1.260	0.193
			All Sources	10	1.260	0.193
	Plate Failure	all *a* values	Dawe and Kulak (1972)	—	—	—
			Beaulieu and Picard (1985) **67.2 ksi** / 80.1ksi	—	—	—
			UC Davis	—	—	—
			All Sources	—	—	—

Table 6.20 – Safety Index for Model 9 and Filler Metal with No Toughness Requirement

Thick Plate (Weld Failure)				Thin Plate (Plate Failure)	
Parameter		Model 9 (a/Q > 0.59)	Model 9 (a/Q ≤ 0.59)	Parameter	Model 9 (all a values)
ρ_G		1.07	1.07	—	—
V_G		0.154	0.154	—	—
ρ_{M1} (F_{EXX})		1.127	1.127	—	—
V_{M1} (F_{EXX})		0.082	0.082	—	—
ρ_{M1} (F_y)		1.124	1.124	ρ_{M1} (F_u)	1.21
V_{M1} (F_y)		0.061	0.061	V_{M1} (F_u)	0.048
ρ_{M2}		1.296	1.296	—	—
V_{M2}		0.075	0.075	—	—
$\rho_{p\ (67.2\ ksi)}$		1.001	1.07	$\rho_{p\ (67.2\ ksi)}$	1.027
$V_{p\ (67.2\ ksi)}$		0.216	0.217	$V_{p\ (67.2\ ksi)}$	0.155
$\rho_{p\ (80.1\ ksi)}$		0.984	1.01	$\rho_{p\ (80.1\ ksi)}$	1.027
$V_{p\ (80.1\ ksi)}$		0.229	0.202	$V_{p\ (80.1\ ksi)}$	0.155
ρ_R (F_{EXX}) 67.2 ksi		1.564	1.672	—	—
V_R (F_{EXX}) 67.2 ksi		0.288	0.288	—	—
ρ_R (F_y) 67.2 ksi		1.560	1.668	ρ_R (F_u) 67.2 ksi	1.243
V_R (F_y) 67.2 ksi		0.282	0.283	V_R (F_u) 67.2 ksi	0.162
ρ_R (F_{EXX}) 80.1ksi		1.538	1.578	—	—
V_R (F_{EXX}) 80.1 ksi		0.297	0.277	—	—
ρ_R (F_y) 80.1 ksi		1.534	1.574	ρ_R (F_u) 80.1 ksi	1.243
V_R (F_y) 80.1 ksi		0.292	0.272	V_R (F_u) 80.1 ksi	0.162
β (F_{EXX}) 67.2 ksi	$\Phi = 0.75$	3.99	4.24	—	—
Φ	β = 4.5	0.66	0.70	—	—
Φ	β = 4.0	0.75	0.80	—	—
β (F_y) 67.2 ksi	$\Phi = 0.75$	4.03	4.28	β (F_u) 67.2 ksi	4.23
Φ	β = 4.5	0.66	0.71	Φ	0.71
Φ	β = 4.0	0.76	0.81	Φ	0.78
β (F_{EXX}) 80.1 ksi	$\Phi = 0.75$	3.85	4.12	—	—
Φ	β = 4.5	0.63	0.68	—	—
Φ	β = 4.0	0.72	0.77	—	—
β (F_y) 80.1 ksi	$\Phi = 0.75$	3.88	4.15	β (F_u) 80.1 ksi	4.23
Φ	β = 4.5	0.64	0.69	Φ	0.71
Φ	β = 4.0	0.73	0.78	Φ	0.78

Table 6.21 – Safety Index for Model 9 and Filler Metal with Toughness Requirement

Parameter		Thick Plate (Weld Failure)	
		Model 9 (a/Q > 0.59)	Model 9 (a/Q ≤ 0.59)
ρ_G		1.070	1.070
V_G		0.154	0.154
ρ_{M1} (F_{EXX})		1.127	1.127
V_{M1} (F_{EXX})		0.082	0.082
ρ_{M1} (F_y)		1.124	1.124
V_{M1} (F_y)		0.061	0.061
ρ_{M2}		1.296	1.296
V_{M2}		0.075	0.075
ρ_p		1.350	1.260
V_p		0.084	0.193
ρ_R (F_{EXX})		2.110	1.969
V_R (F_{EXX})		0.208	0.271
ρ_R (F_y)		2.104	1.964
V_R (F_y)		0.200	0.265
β (F_{EXX})	Φ = 0.75	6.28	5.07
Φ	β = 4.5	1.08	0.86
Φ	β = 4.0	1.20	0.98
β (F_y)	Φ = 0.75	6.40	5.12
Φ	β = 4.5	1.10	0.87
Φ	β = 4.0	1.22	0.99

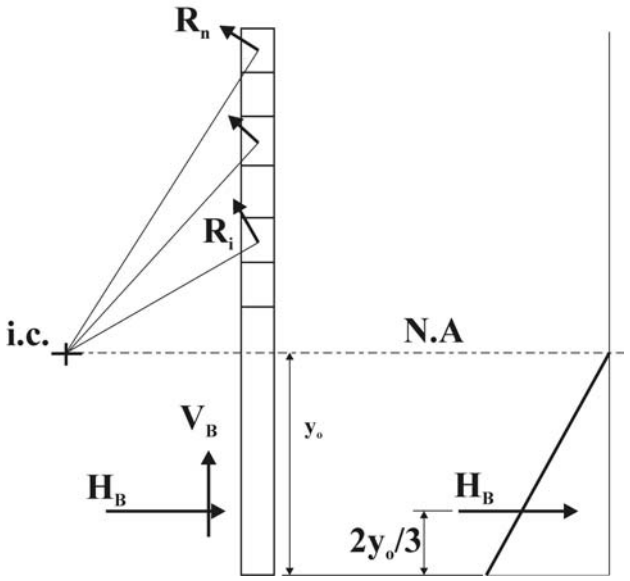

Figure 6.1 – Force distribution in weld loaded in shear and bending

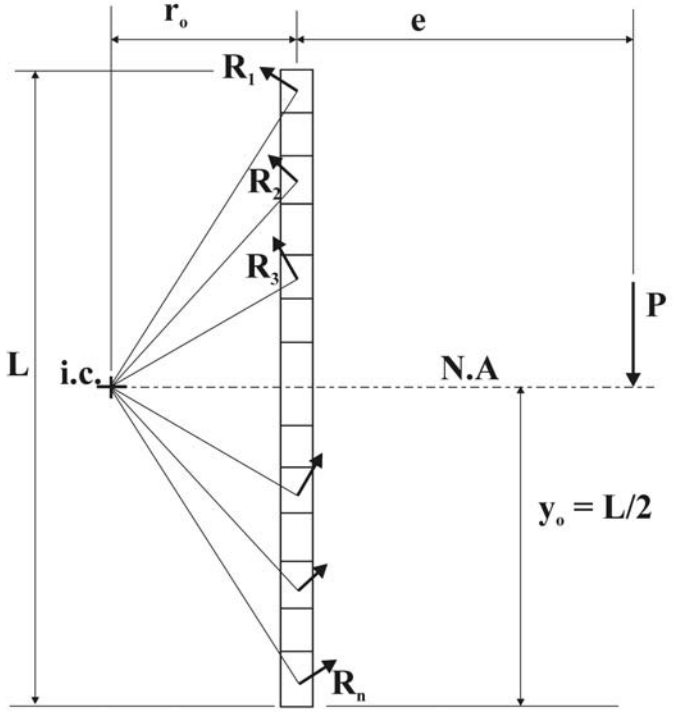

Figure 6.2 – Eccentrically loaded fillet weld (AISC Approach)

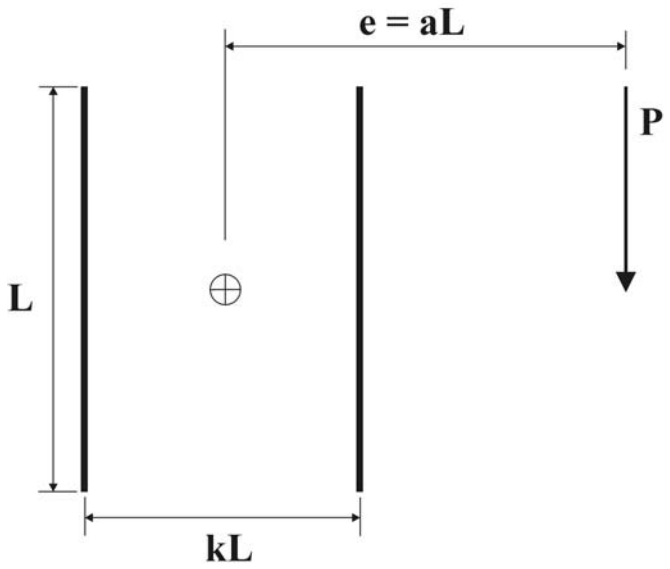

Figure 6.3 – In-plane eccentricity

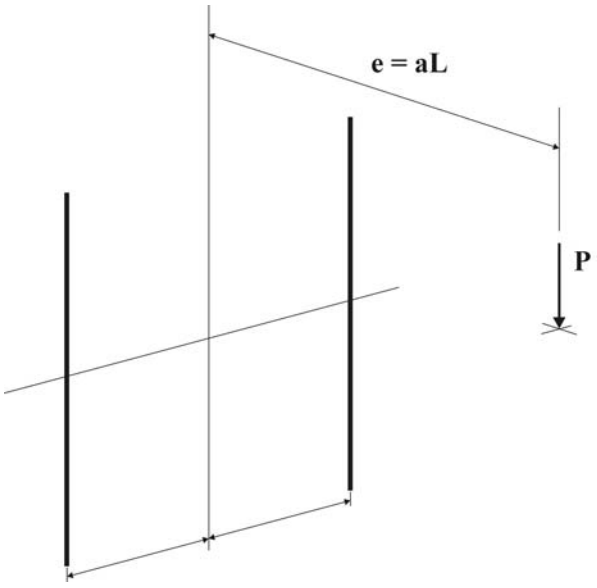

Figure 6.4 – Out-of-plane eccentricity

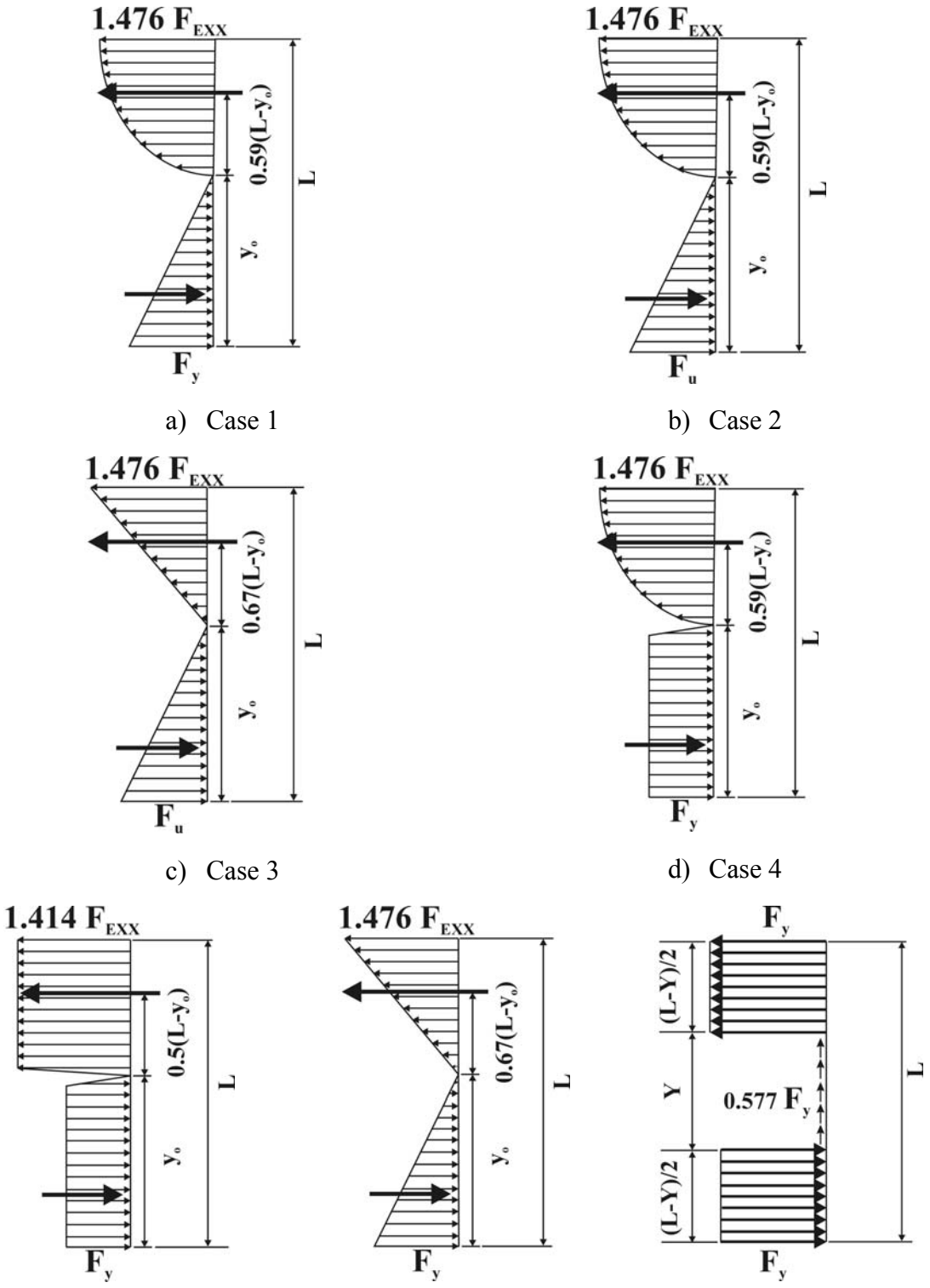

Figure 6.5 – Stress distributions proposed by Neis (1980)

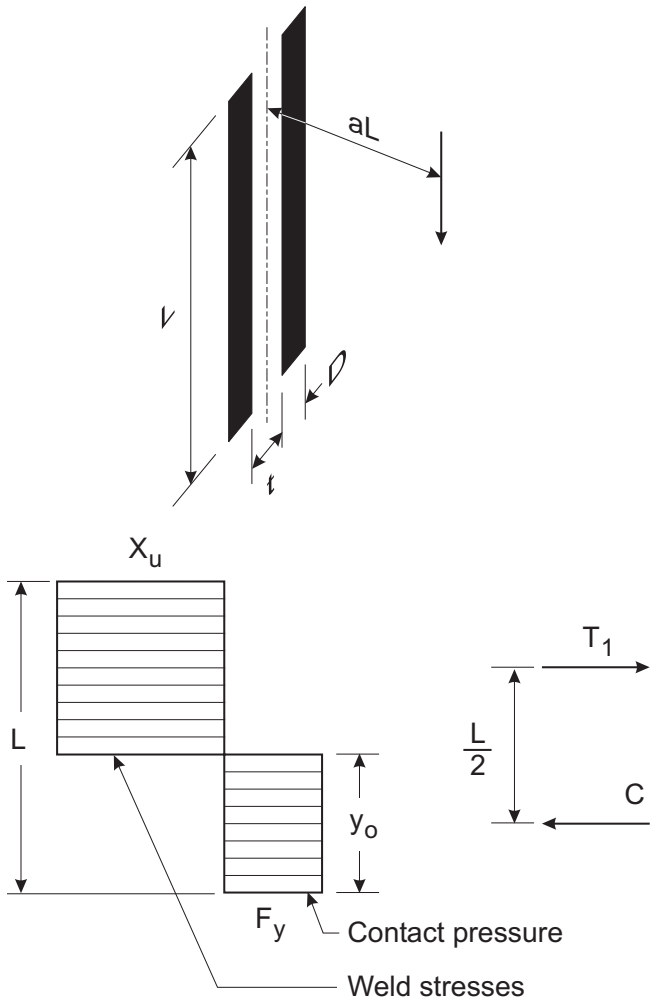

Figure 6.6 – Stress distribution assumed by Beaulieu and Picard (1991)

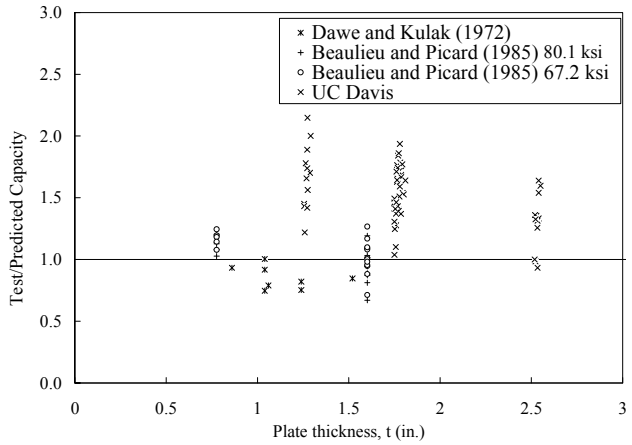

a) Test-to-predicted ratio versus plate thickness

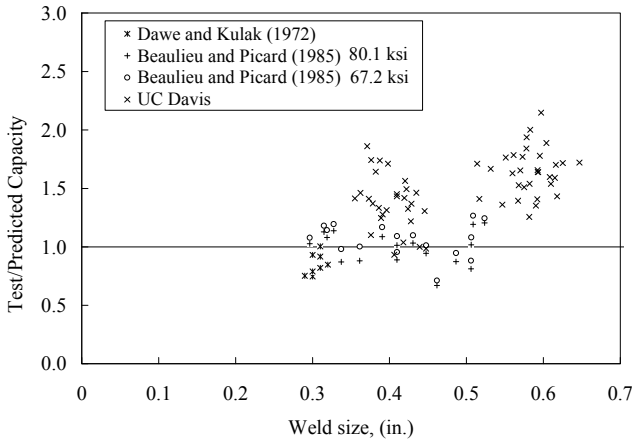

b) Test-to-predicted ratio versus weld size

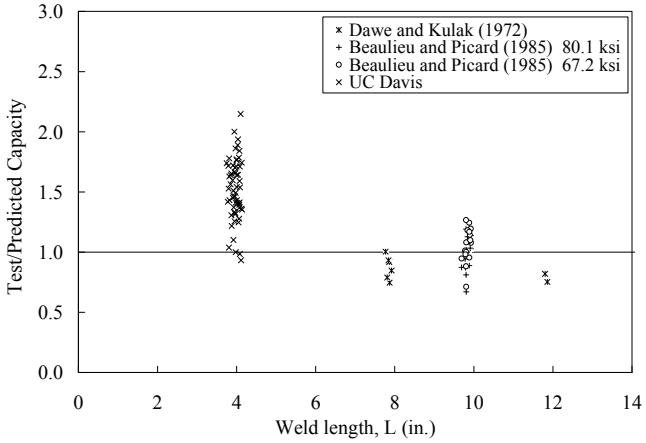

c) Test-to-predicted ratio versus weld length

Figure 6.7 – Model 1 - Test Parameters vs. Test-to-Predicted Ratios

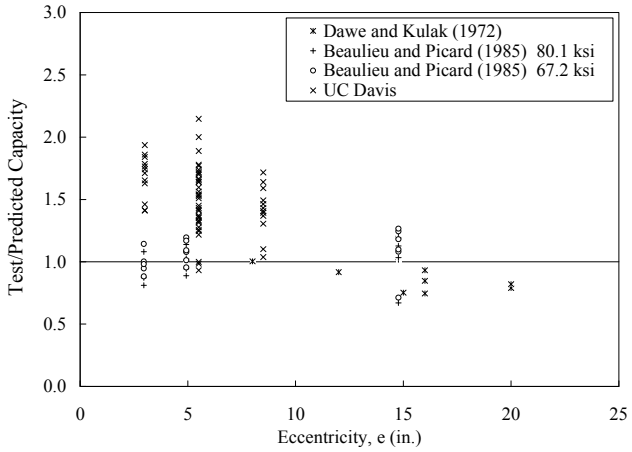

d) Test-to-predicted ratio versus eccentricity

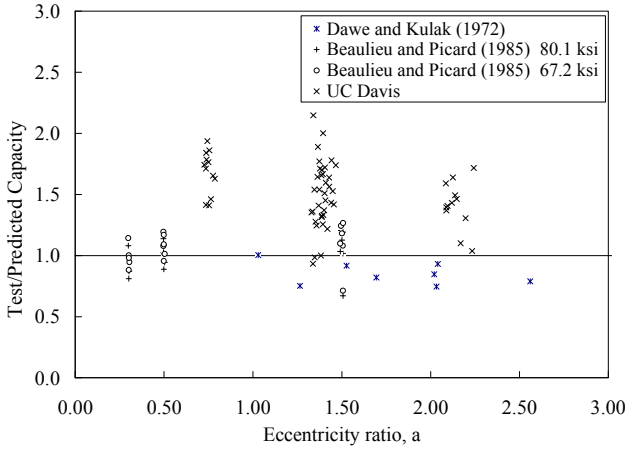

e) Test-to-predicted ratio versus eccentricity ratio

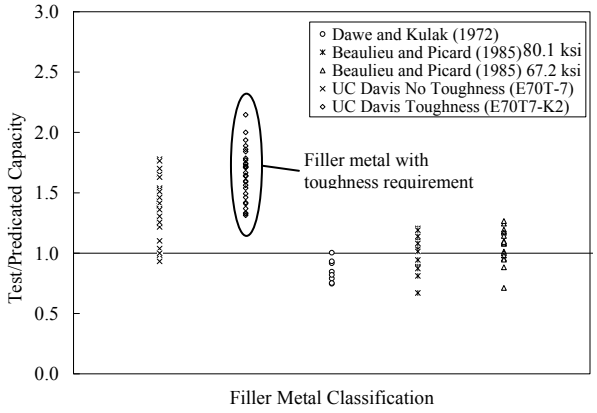

f) Test-to-predicted ratio versus filler metal classification

Figure 6.7 – (cont'd)

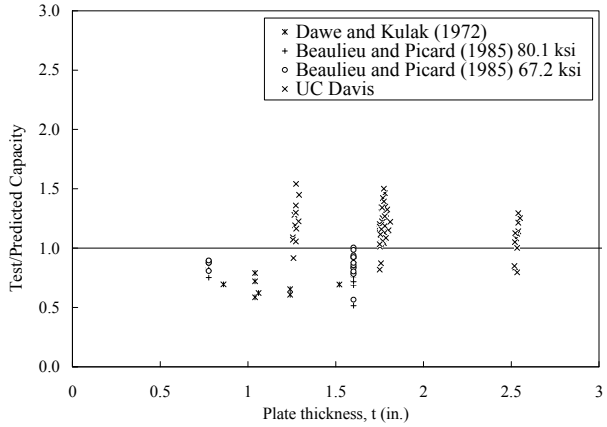

a) Test-to-predicted ratio versus plate thickness

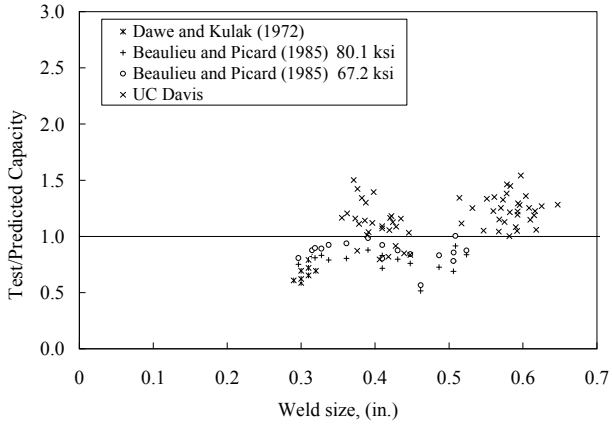

b) Test-to-predicted ratio versus weld size

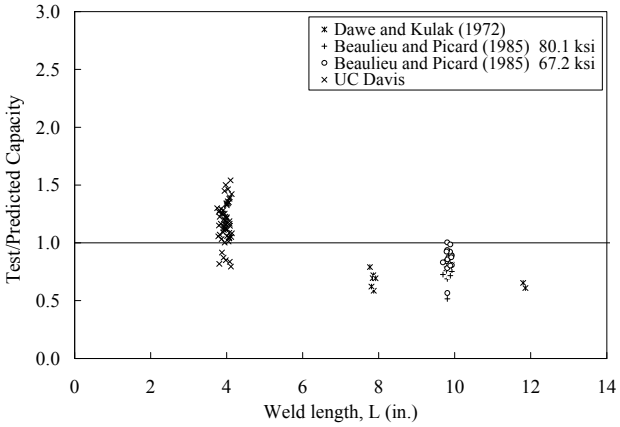

c) Test-to-predicted ratio versus weld length

Figure 6.8 – Model 2 - Test Parameters vs. Test-to-Predicted Ratios

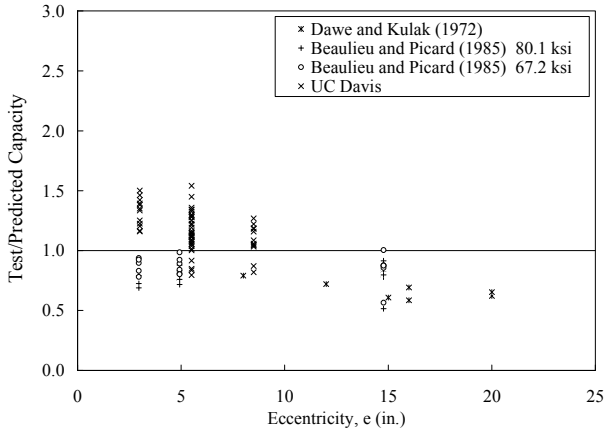

d) Test-to-predicted ratio versus eccentricity

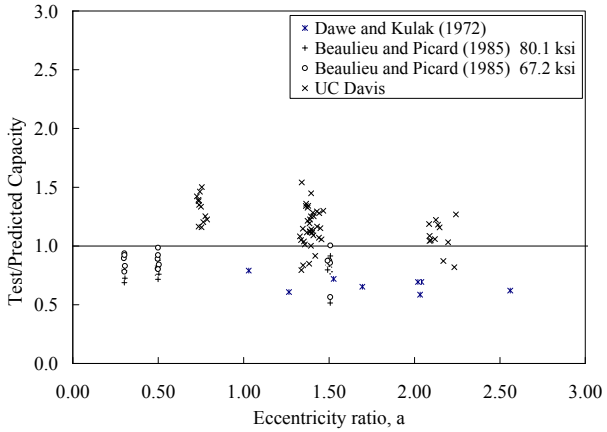

e) Test-to-predicted ratio versus eccentricity ratio

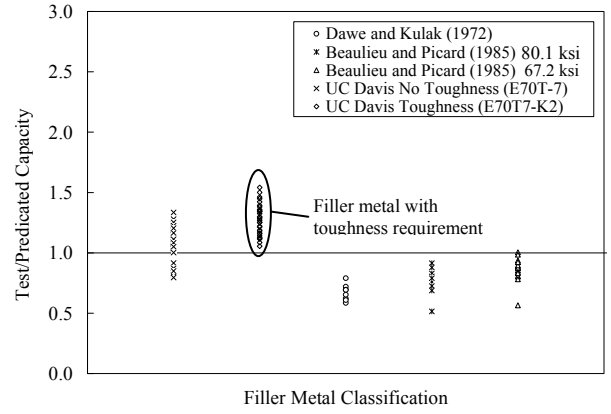

f) Test-to-predicted ratio versus filler metal classification

Figure 6.8 – (cont'd)

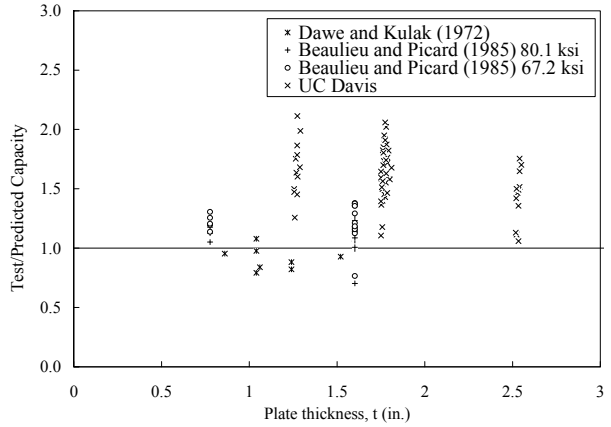

a) Test-to-predicted ratio versus plate thickness

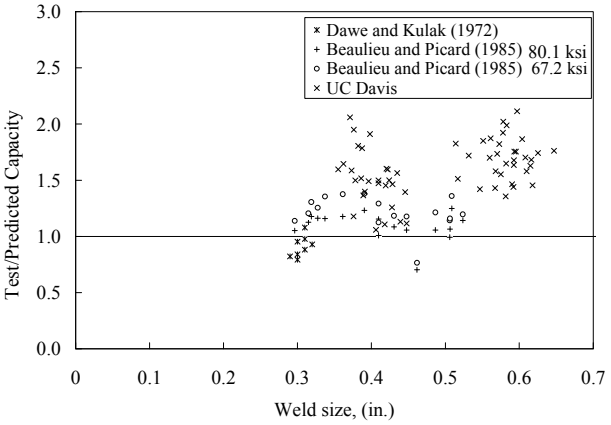

b) Test-to-predicted ratio versus weld size

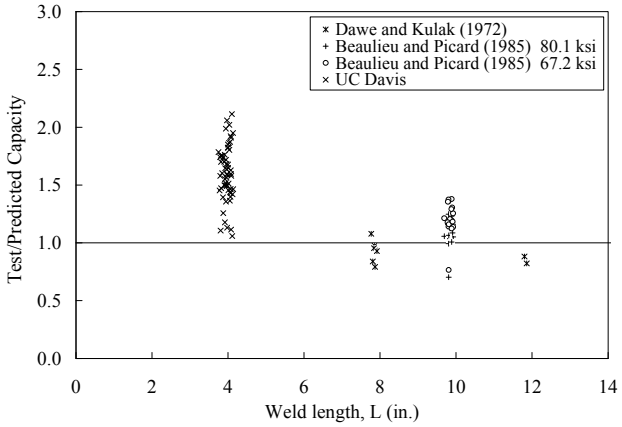

c) Test-to-predicted ratio versus weld length

Figure 6.9 – Model 3 - Test Parameters vs. Test-to-Predicted Ratios

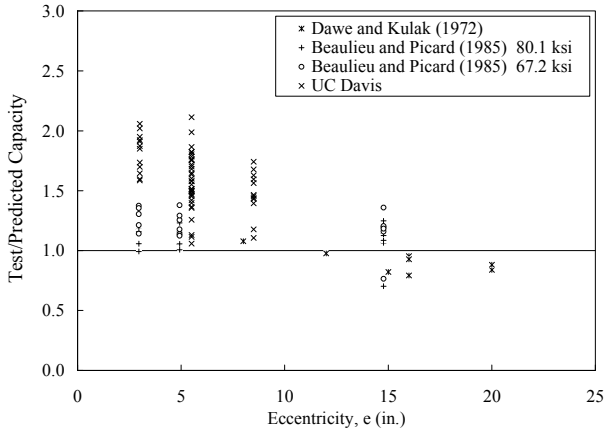

d) Test-to-predicted ratio versus eccentricity

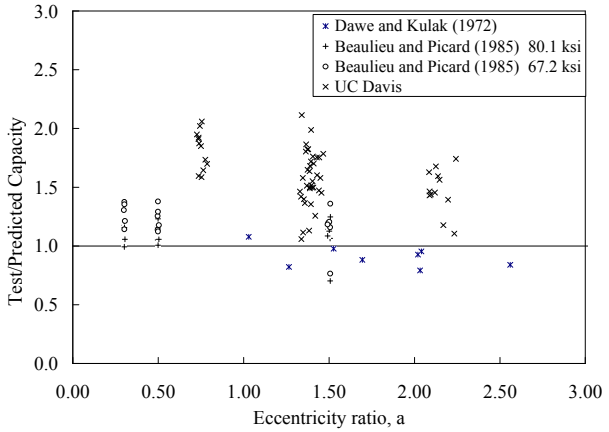

e) Test-to-predicted ratio versus eccentricity ratio

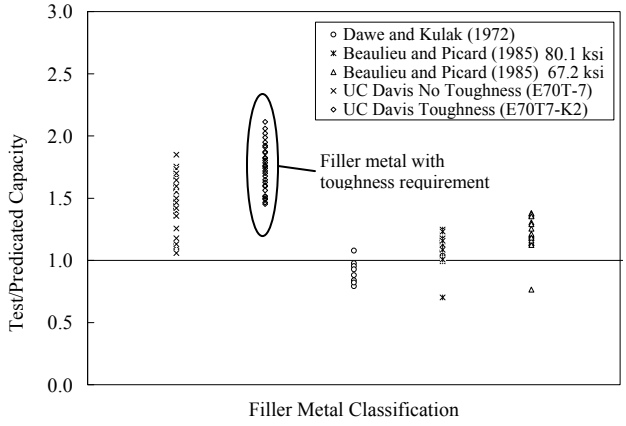

f) Test-to-predicted ratio versus filler metal classification

Figure 6.9 – (cont'd)

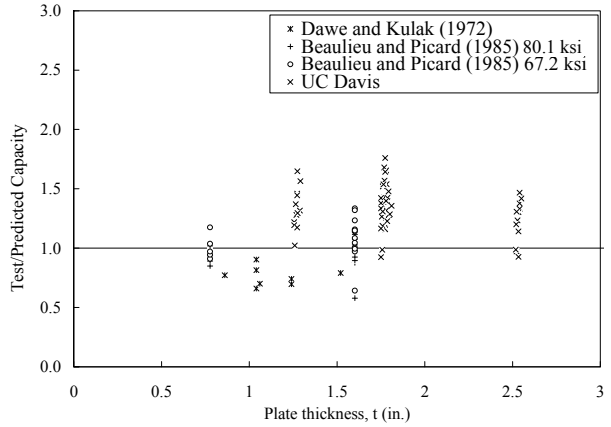

a) Test-to-predicted ratio versus plate thickness

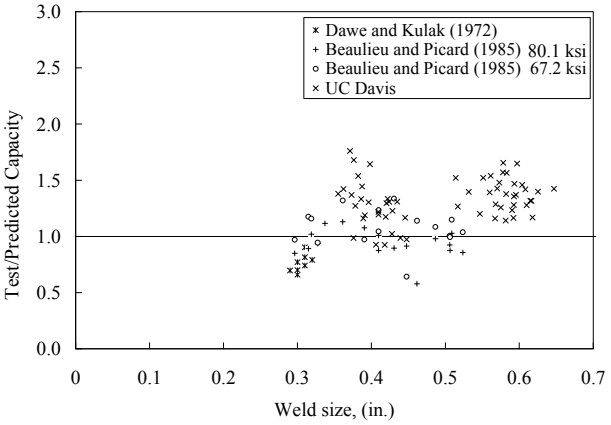

b) Test-to-predicted ratio versus weld size

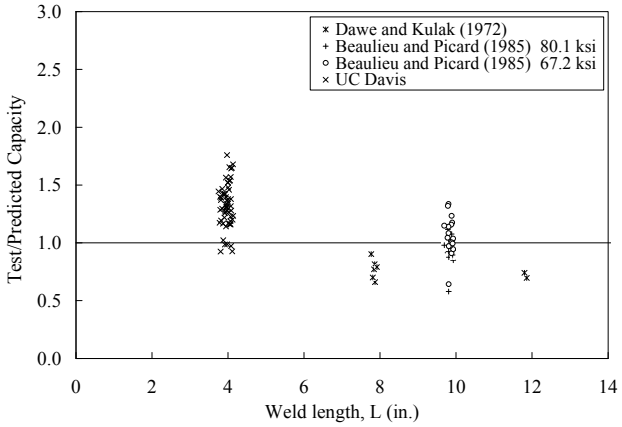

c) Test-to-predicted ratio versus weld length

Figure 6.10 – Model 4 - Test Parameters vs. Test-to-Predicted Ratios

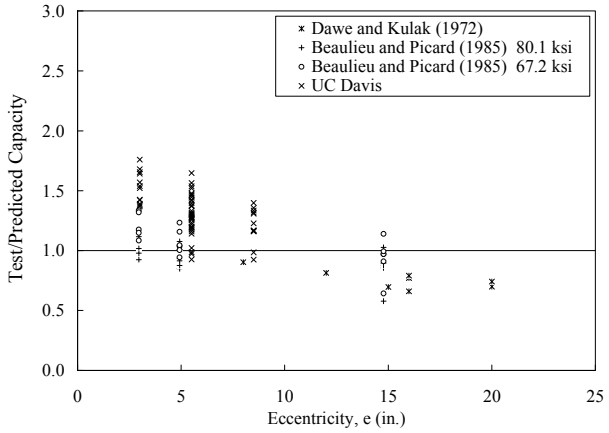

d) Test-to-predicted ratio versus eccentricity

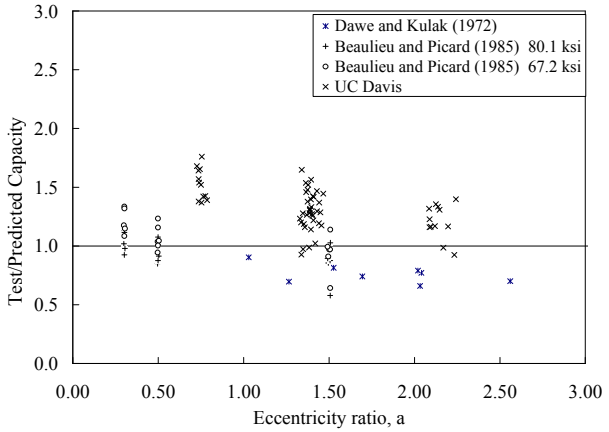

e) Test-to-predicted ratio versus eccentricity ratio

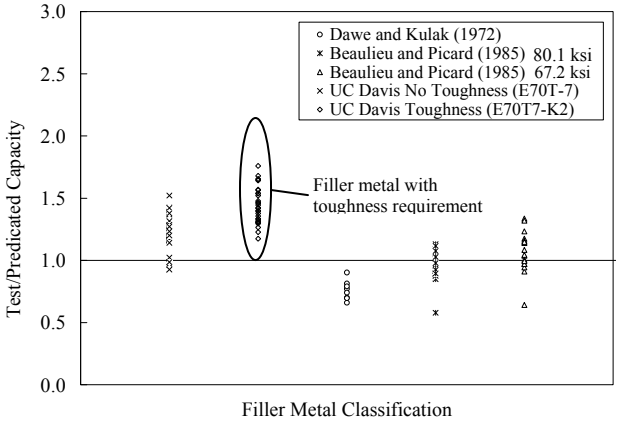

f) Test-to-predicted ratio versus filler metal classification

Figure 6.10 – (cont'd)

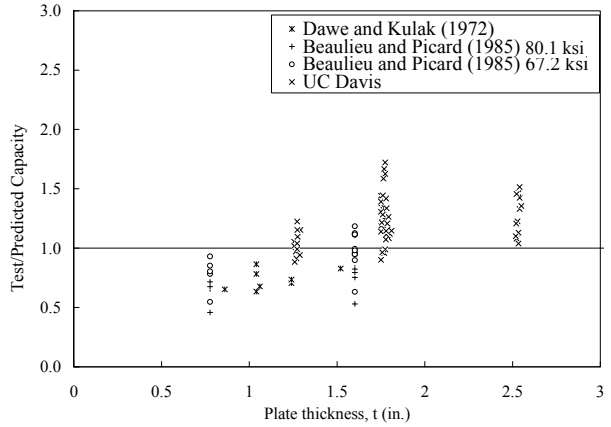

a) Test-to-predicted ratio versus plate thickness

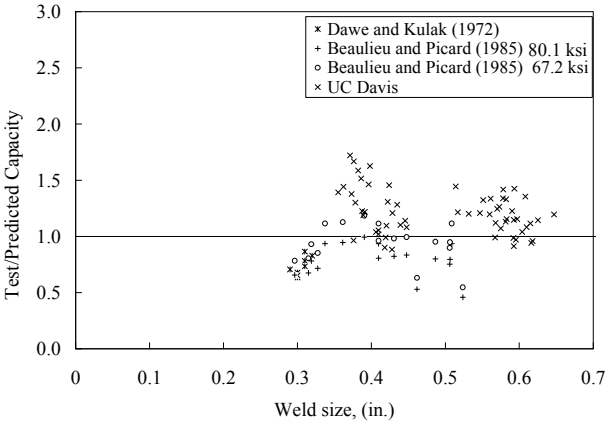

b) Test-to-predicted ratio versus weld size

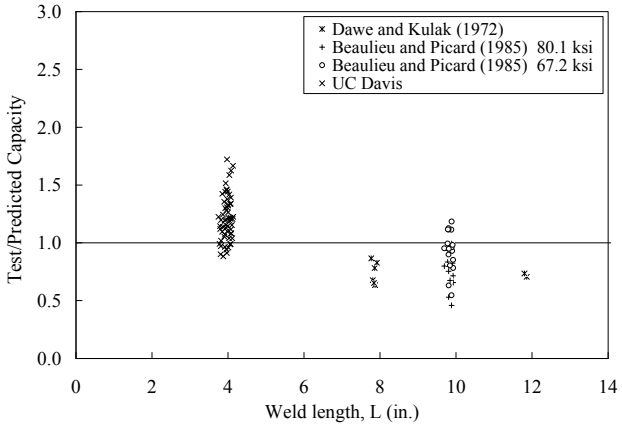

c) Test-to-predicted ratio versus weld length

Figure 6.11 – Model 6 - Test Parameters vs. Test-to-Predicted Ratios

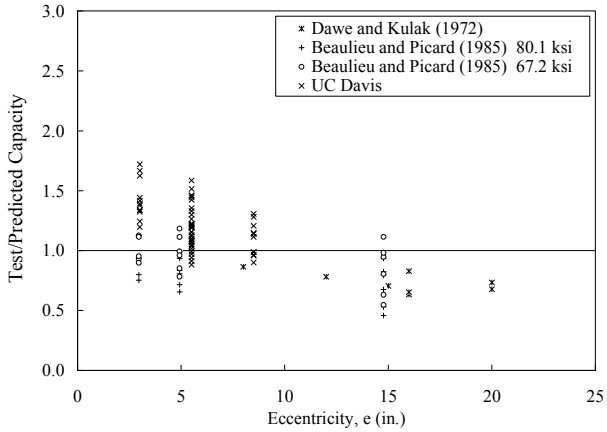

d) Test-to-predicted ratio versus eccentricity

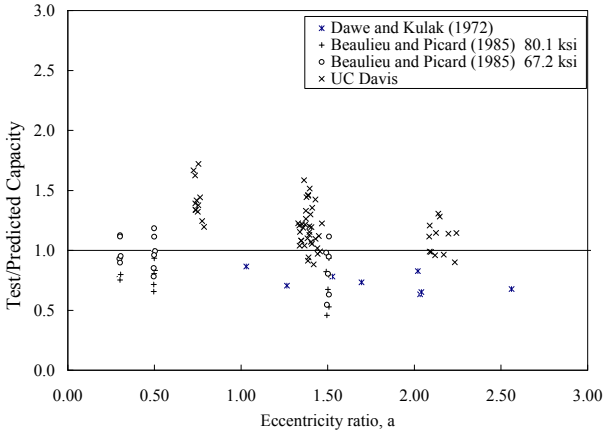

e) Test-to-predicted ratio versus eccentricity ratio

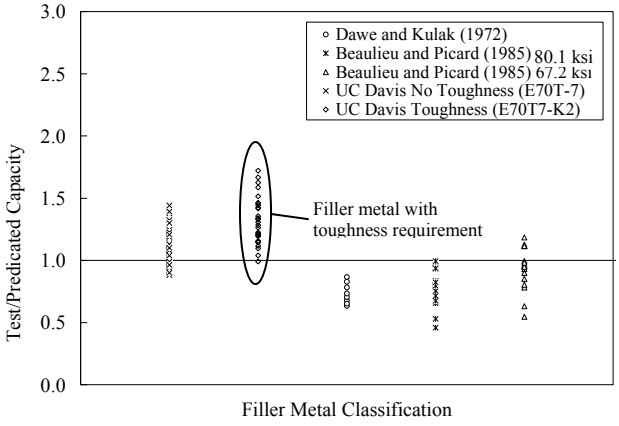

f) Test-to-predicted ratio versus filler metal classification

Figure 6.11 – (cont'd)

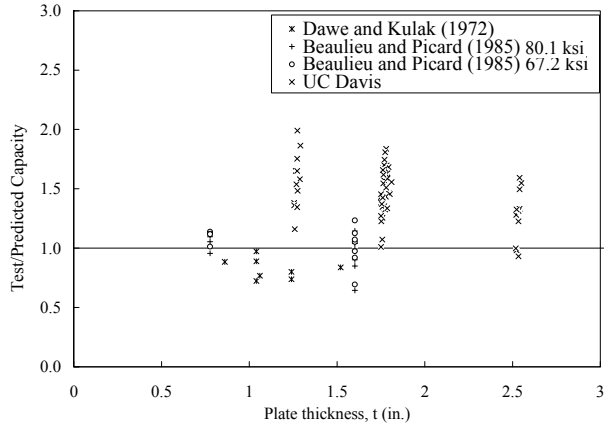

a) Test-to-predicted ratio versus plate thickness

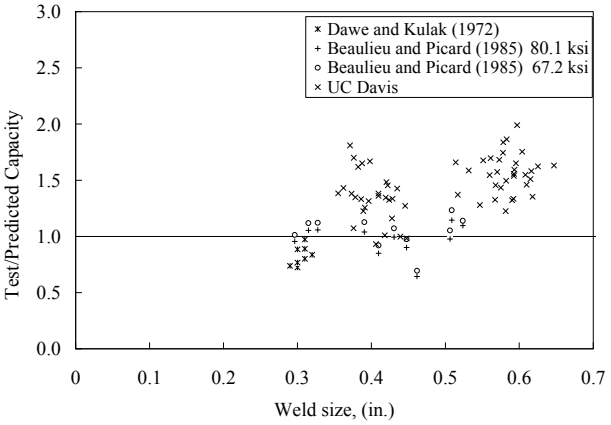

b) Test-to-predicted ratio versus weld size

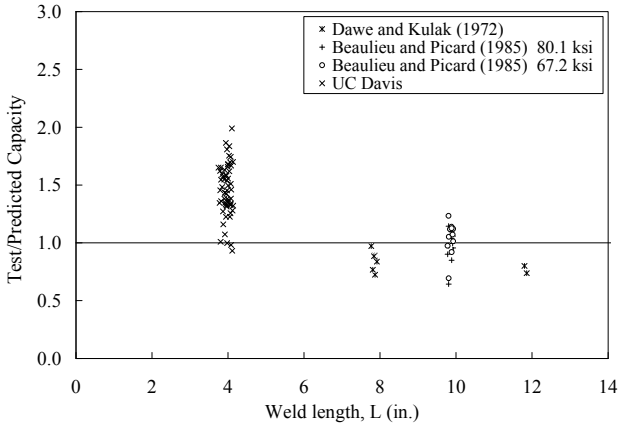

c) Test-to-predicted ratio versus weld length

Figure 6.12 – Model 7 Case 1 - Test Parameters vs. Test-to-Predicted Ratios

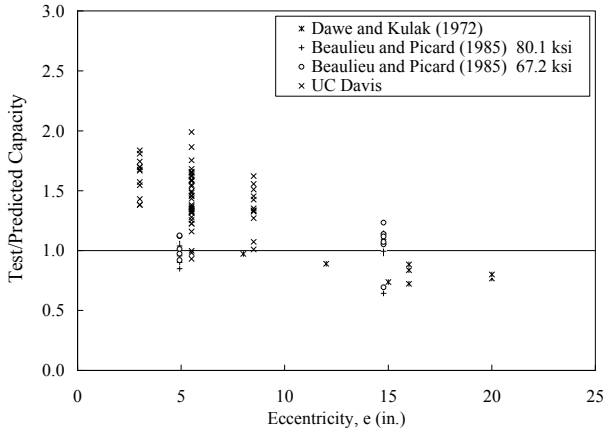

d) Test-to-predicted ratio versus eccentricity

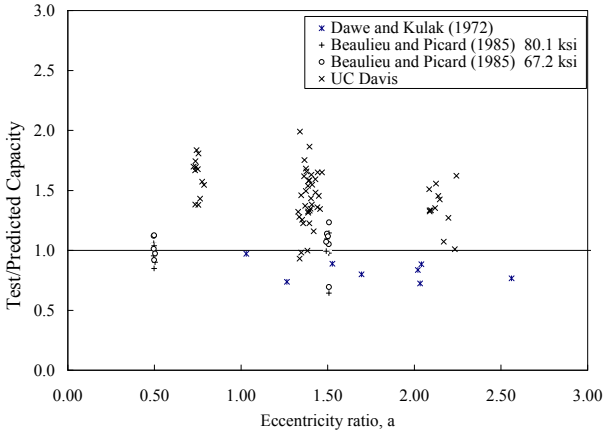

e) Test-to-predicted ratio versus eccentricity ratio

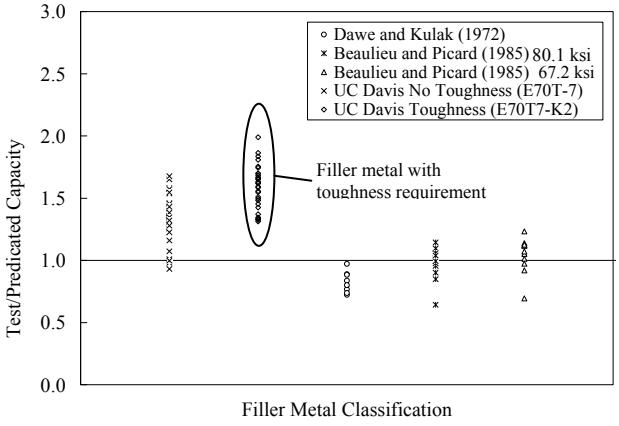

f) Test-to-predicted ratio versus filler metal classification

Figure 6.12 – (cont'd)

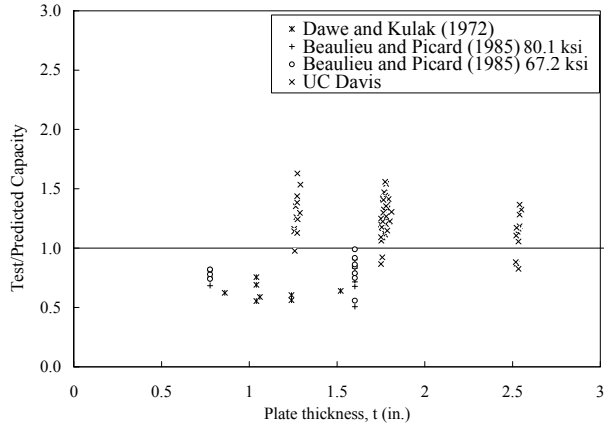

a) Test-to-predicted ratio versus plate thickness

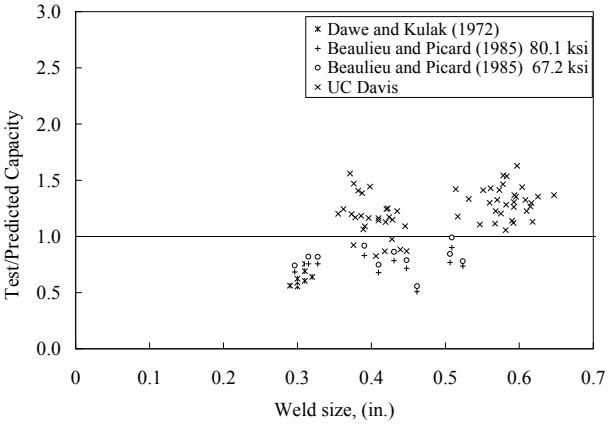

b) Test-to-predicted ratio versus weld size

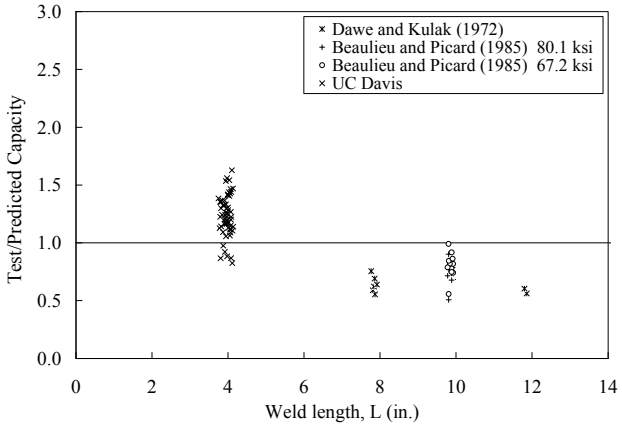

c) Test-to-predicted ratio versus weld length

Figure 6.13 – Model 7 Case 2 - Test Parameters vs. Test-to-Predicted Ratios

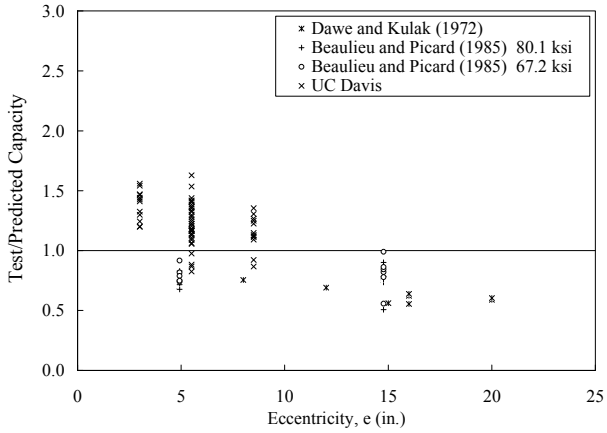

d) Test-to-predicted ratio versus eccentricity

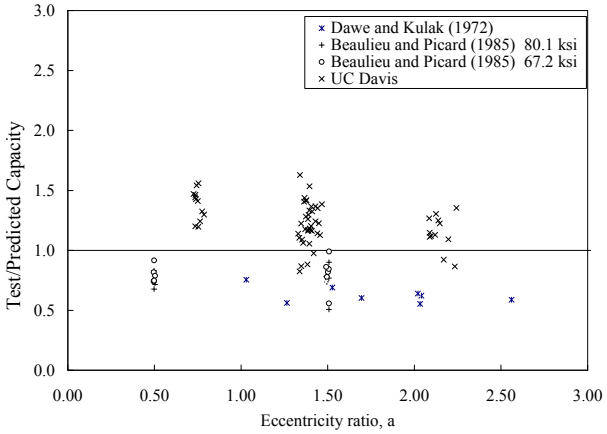

e) Test-to-predicted ratio versus eccentricity ratio

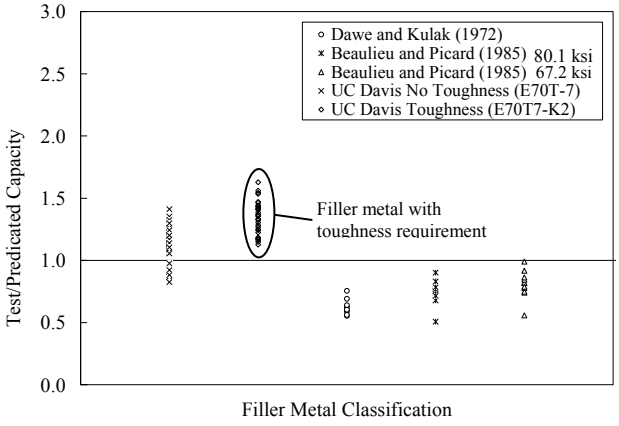

f) Test-to-predicted ratio versus filler metal classification

Figure 6.13 – (cont'd)

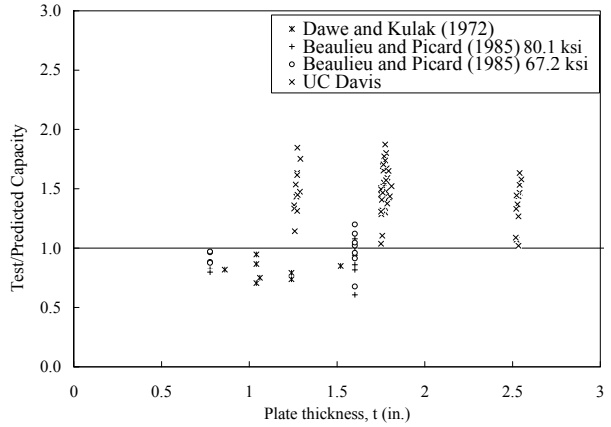

a) Test-to-predicted ratio versus plate thickness

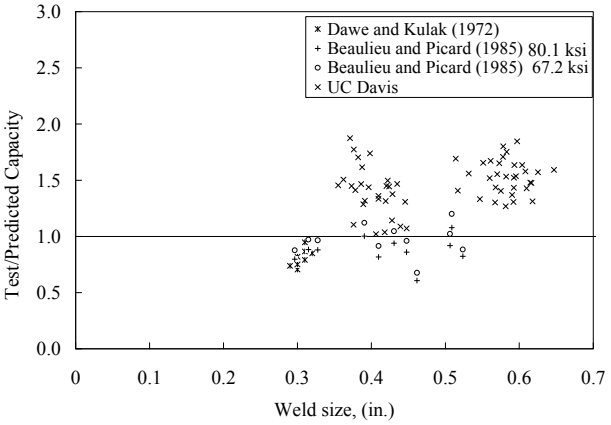

b) Test-to-predicted ratio versus weld size

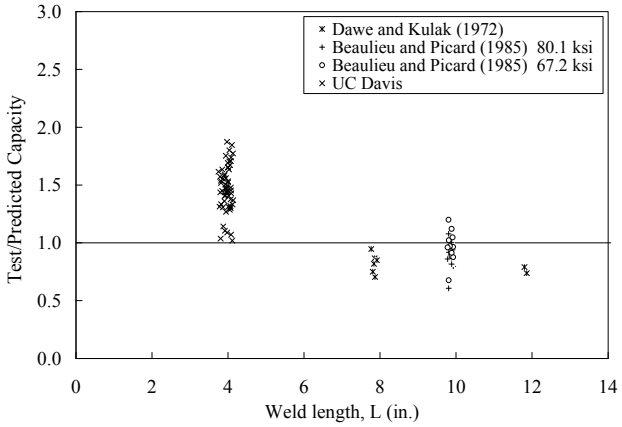

c) Test-to-predicted ratio versus weld length

Figure 6.14 – Model 7 Case 3 - Test Parameters vs. Test-to-Predicted Ratios

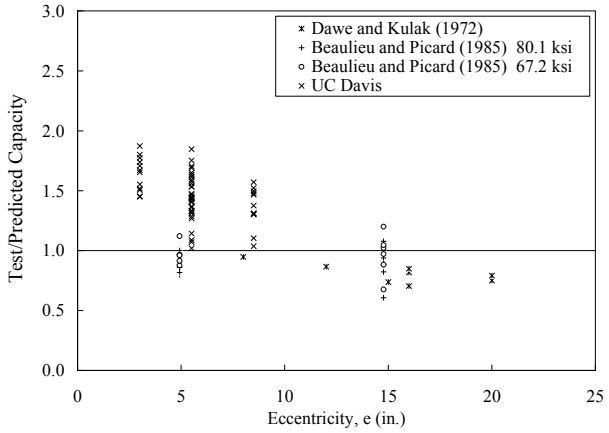

d) Test-to-predicted ratio versus eccentricity

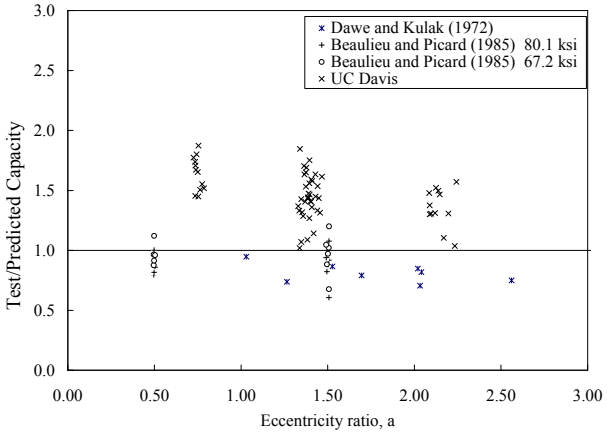

e) Test-to-predicted ratio versus eccentricity ratio

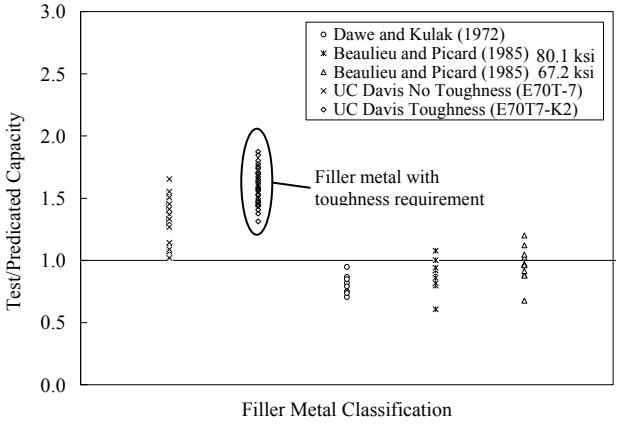

f) Test-to-predicted ratio versus filler metal classification

Figure 6.14 – (cont'd)

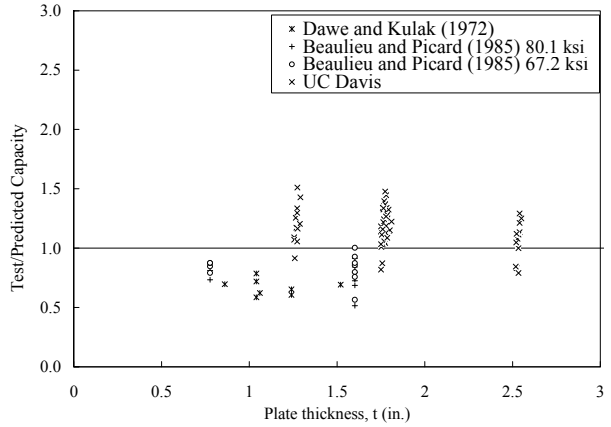

a) Test-to-predicted ratio versus plate thickness

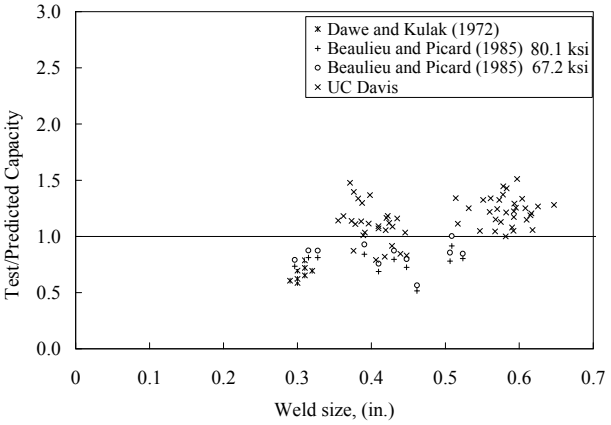

b) Test-to-predicted ratio versus weld size

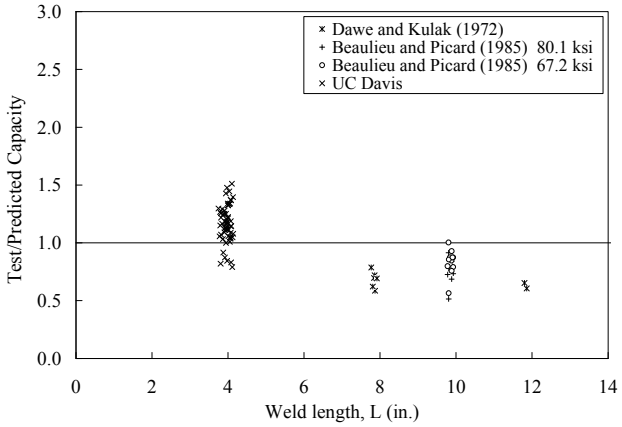

c) Test-to-predicted ratio versus weld length

Figure 6.15 – Model 7 Case 4 - Test Parameters vs. Test-to-Predicted Ratios

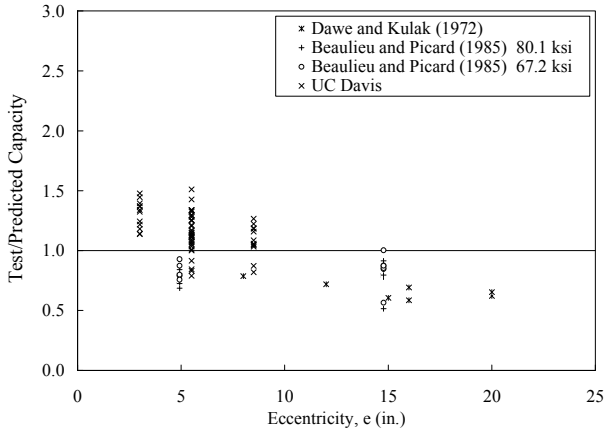

d) Test-to-predicted ratio versus eccentricity

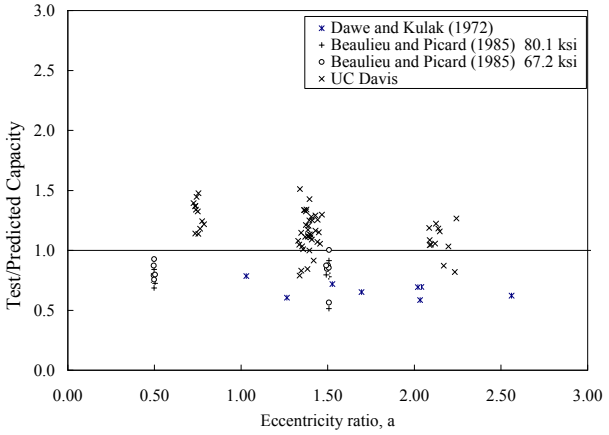

e) Test-to-predicted ratio versus eccentricity ratio

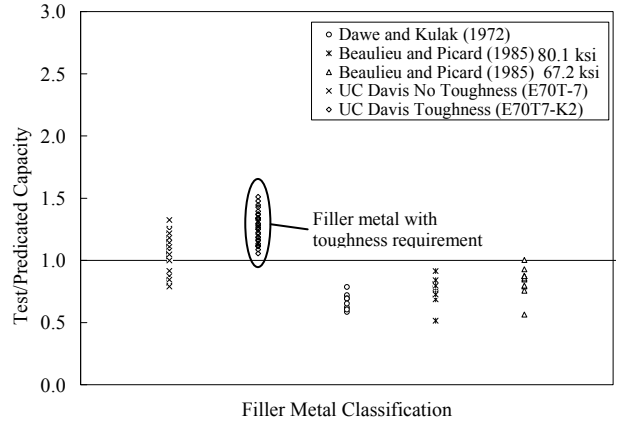

f) Test-to-predicted ratio versus filler metal classification

Figure 6.15 – (cont'd)

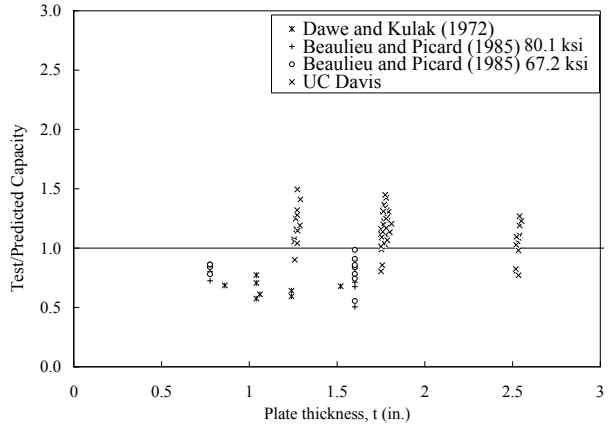

a) Test-to-predicted ratio versus plate thickness

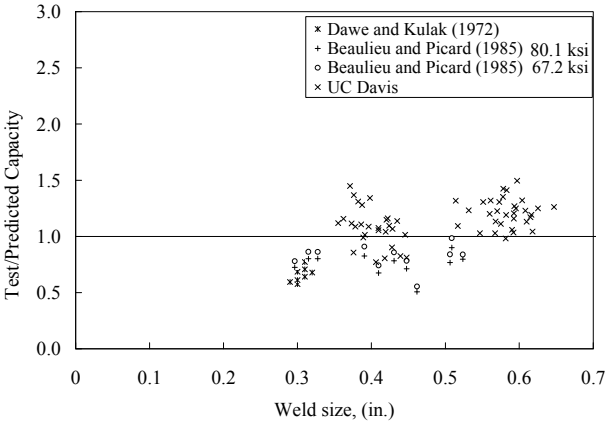

b) Test-to-predicted ratio versus weld size

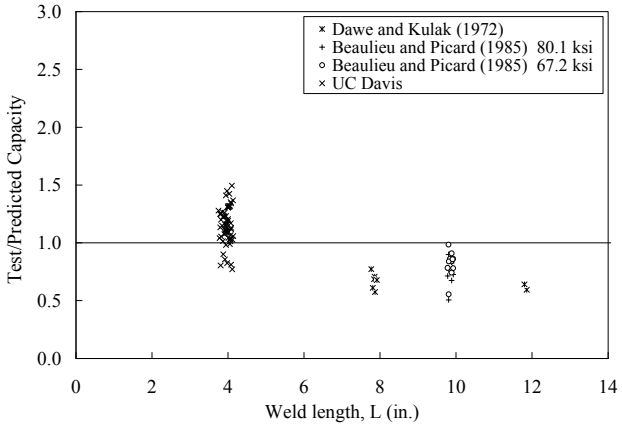

c) Test-to-predicted ratio versus weld length

Figure 6.16 – Model 7 Case 5 - Test Parameters vs. Test-to-Predicted Ratios

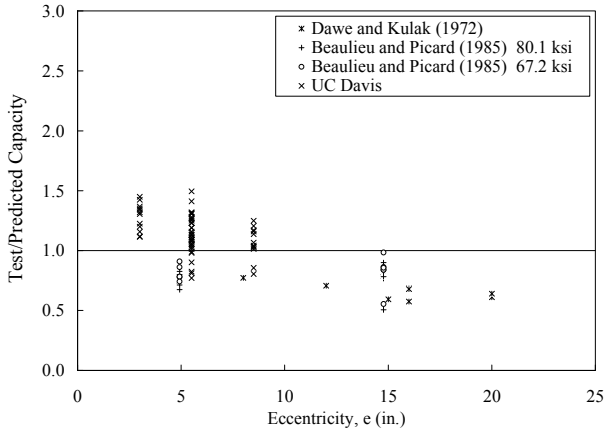

d) Test-to-predicted ratio versus eccentricity

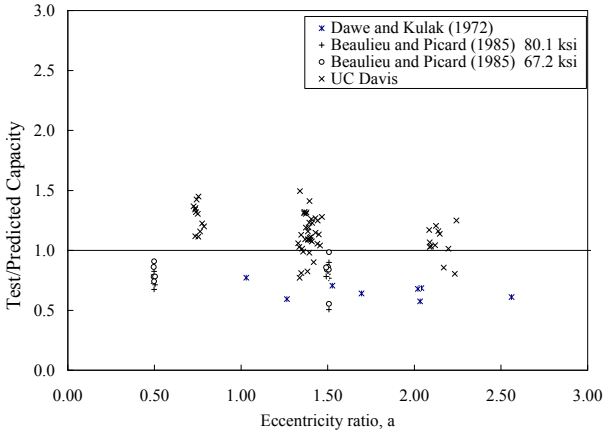

e) Test-to-predicted ratio versus eccentricity ratio

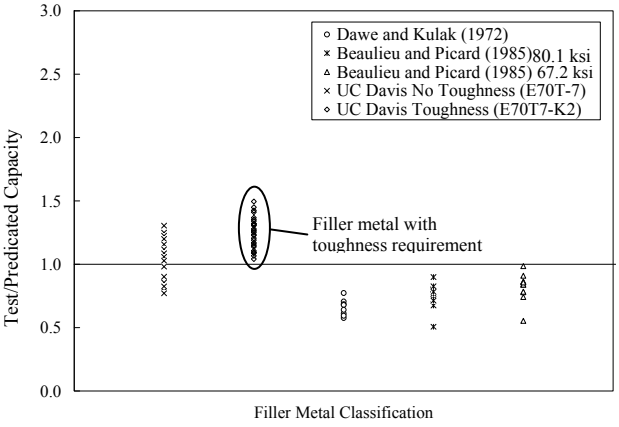

f) Test-to-predicted ratio versus filler metal classification

Figure 6.16 – (cont'd)

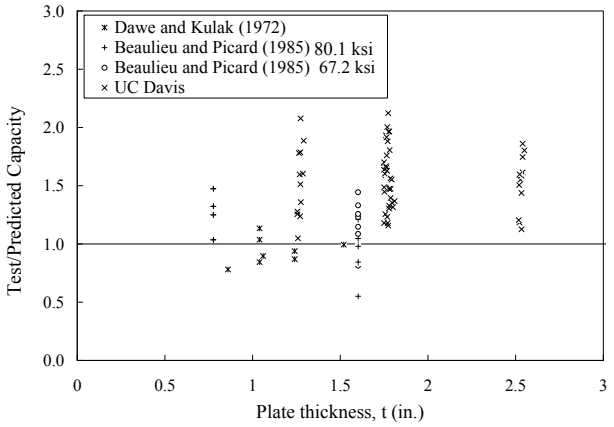

a) Test-to-predicted ratio versus plate thickness

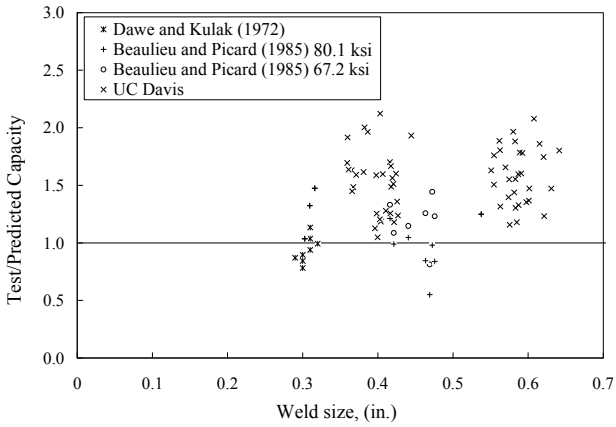

b) Test-to-predicted ratio versus weld size

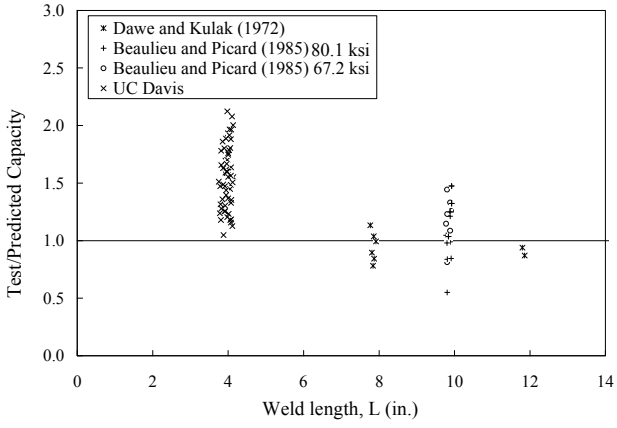

c) Test-to-predicted ratio versus weld length

Figure 6.17 – Model 7 Case 6/7 - Test Parameters vs. Test-to-Predicted Ratios

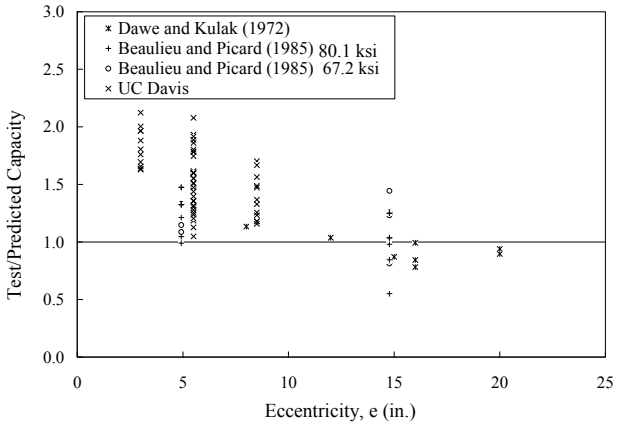

d) Test-to-predicted ratio versus eccentricity

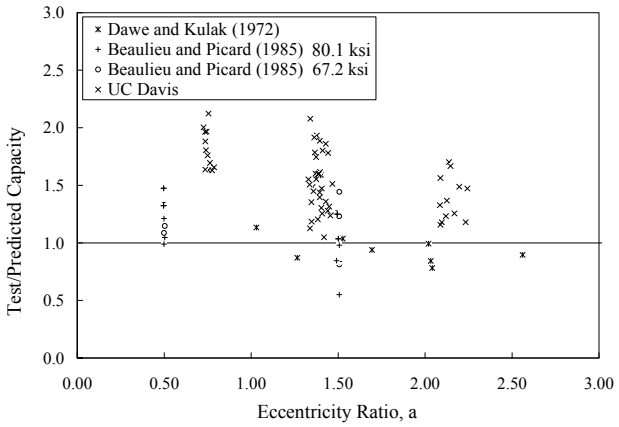

e) Test-to-predicted ratio versus eccentricity ratio

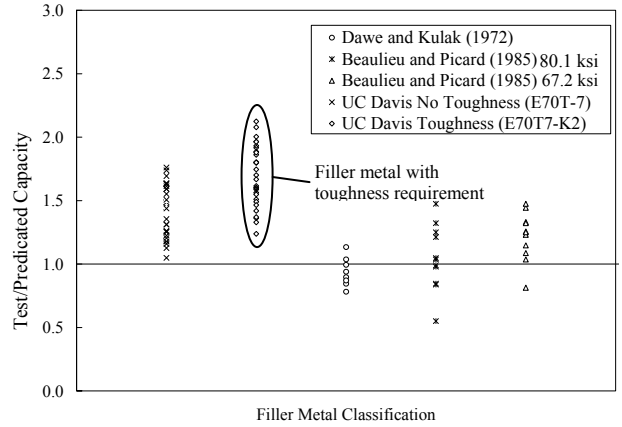

f) Test-to-predicted ratio versus filler metal classification

Figure 6.17 – (cont'd)

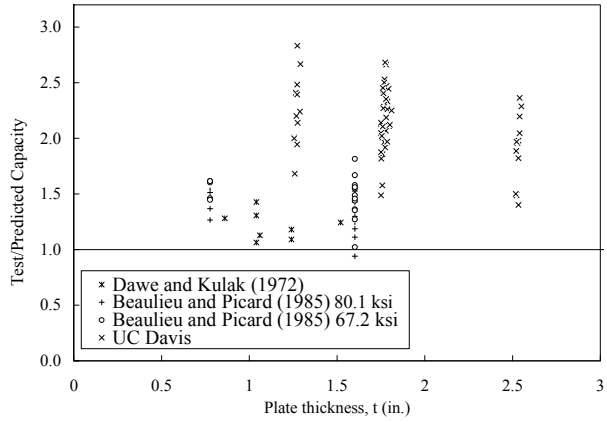

a) Test-to-predicted ratio versus plate thickness

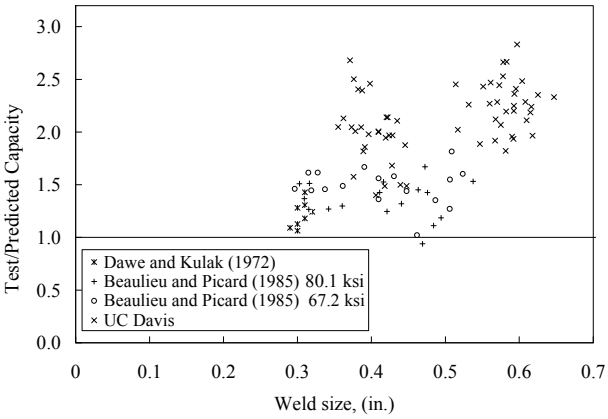

b) Test-to-predicted ratio versus weld size

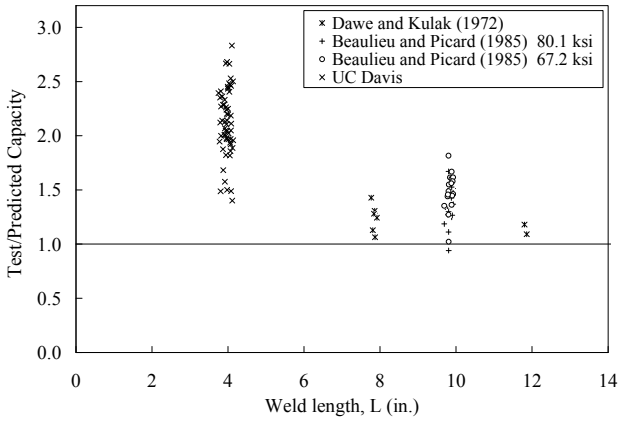

c) Test-to-predicted ratio versus weld length

Figure 6.18 – Model 8 - Test Parameters vs. Test-to-Predicted Ratios

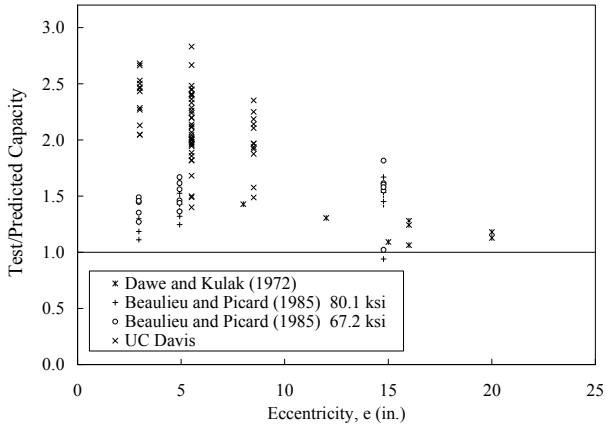

d) Test-to-predicted ratio versus eccentricity

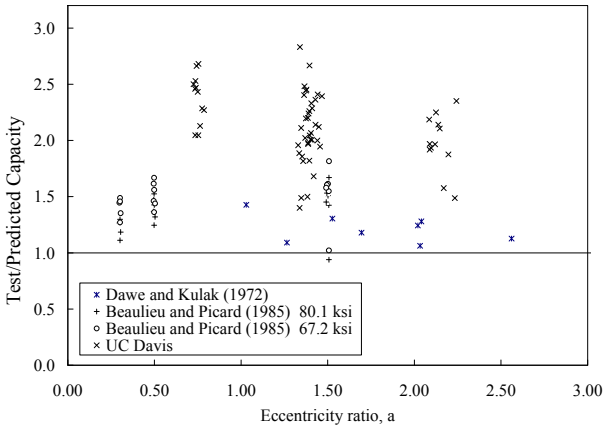

e) Test-to-predicted ratio versus eccentricity ratio

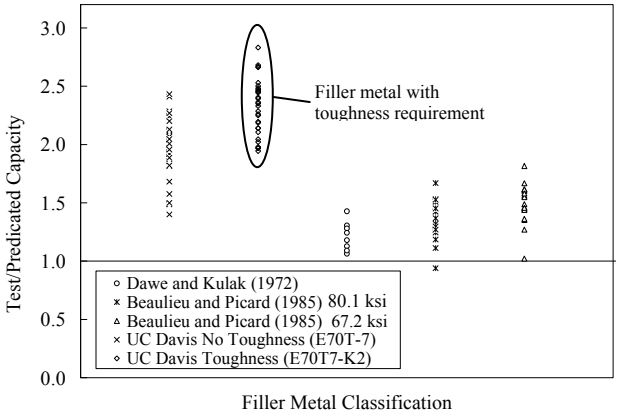

f) Test-to-predicted ratio versus filler metal classification

Figure 6.18 – (cont'd)

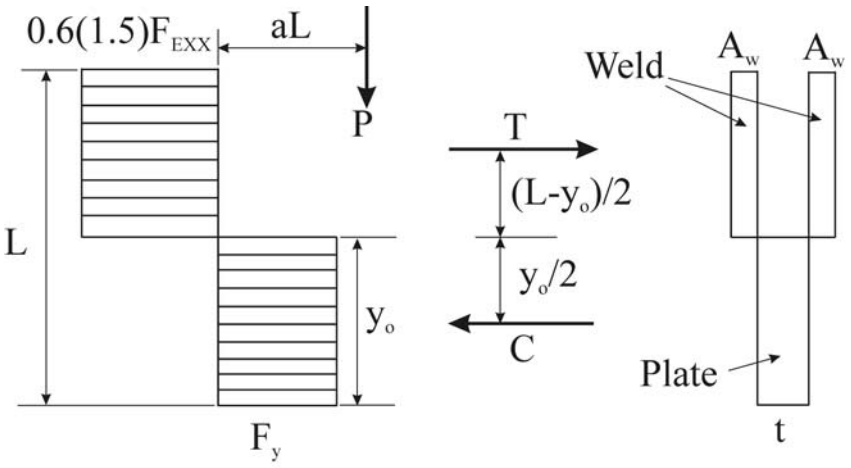

Figure 6.19 – Proposed Model for Large Load Eccentricity

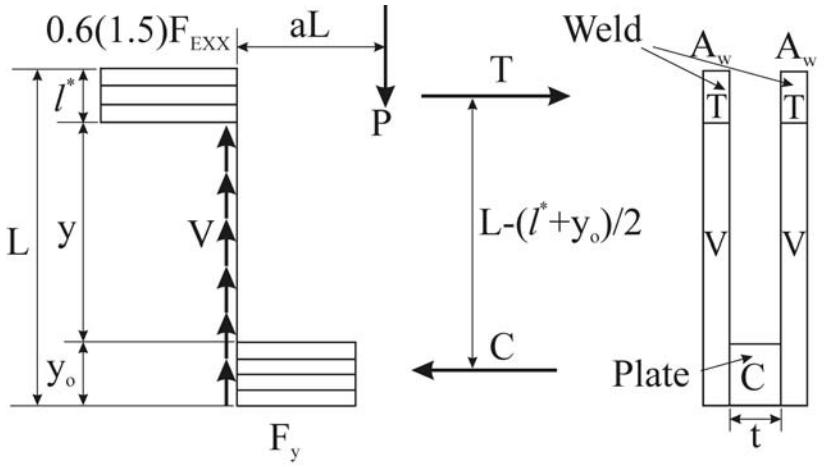

Figure 6.20 – Proposed Model for Small Load Eccentricity

Chapter 7

Summary and Conclusions

7.1 SUMMARY

Current design tables (AISC, 2005) for the strength of fillet welded joints under combined shear and out-of-plane bending do not consider two effects that may potentially impact their accuracy. First, they do not incorporate the possible effect of root notch on weld ductility and strength and they ignore the contribution of moment transfer through bearing between the two connected plates. The vast majority of the test data upon which the equations are based were obtained from tests on lapped splices where the root notch is parallel to the applied load. This research report presents an investigation of these two effects on the strength of welded joints loaded under combined shear and out-of-plane bending.

Test results from earlier test programs on joints under combined shear and bending were collected. Only two such test programs were conducted, providing a total of 32 test results have been conducted. From these test programs, strength prediction models were proposed; one using an extension of the instantaneous center of rotation previously used for bolted connections, and the other a closed form solution proposed as an alternative to the more complex instantaneous center method.

A test program consisting of 24 direct tension tests on cruciform specimens, 60 bending tests on cruciform specimens and ancillary tests to investigate the strength of welded connections with an out-of-plane load eccentricity was performed. These specimens feature connections with three different plate bearing thicknesses (1.25, 1.75 and 2.50 inches), two nominal weld sizes (1/2 inch and 5/16 inch), three load eccentricities (3.0, 5.5 and 8.5 inches) and two weld classifications ("non-toughness" rated E70T-7 and "toughness" rated E70T7-K2). Three replicate tests were conducted for each parameter set.

The database of available test results, now consisting of a total of 92 test results, was used to evaluate 14 different prediction models. Four of these models consisted of the instantaneous centre of rotation proposed by Dawe and Kulak, but modified to consider both triangular and rectangular stress distribution in the compression zone of the connection where stresses are developed by bearing of the connected plates and incorporating load versus deformation models for fillet welds proposed by Butler and Kulak (1972) and by Lesik and Kennedy (1990). Two other models based on the method of instantaneous center, without moment transfer by bearing of the connected plates in the compression zone, were also investigated. One of these models corresponds to the model used to derive the AISC (2005) design table and the other model made use of the load versus deformation model for fillet welds proposed by Butler and Kulak (1972).

Finally, seven closed form models proposed by Neis (1980) and one closed form model proposed by Beaulieu and Picard (1985) were also evaluated.

A reliability analysis was conducted on the three most promising models to determine the level of safety offered by each of the four models.

7.2 CONCLUSIONS

7.2.1 Cruciform joints in direct tension

The experimental results on cruciform specimens tested in direct tension indicate that the strength of the welds is not significantly affected by the root notch length. However, an examination of test results from other sources with root notch lengths shorter than those investigated here indicates that root notch length may have an effect on the strength of welds. On average, the AISC (2005) design equation predicts the strength with good accuracy for all the weld sizes and electrode classifications investigated. The design equations are more conservative for the toughness rated welds as compared to the non-toughness rated welds. The ductility of the welds does not show a strong dependence on the root notch length. However, for the E70T7 electrode, the observed ductility is lower compared to the code-based estimate of ductility, which is used to develop design charts for eccentrically loaded joints.

A finite element based fracture mechanics study was conducted to generalize the experimental results to larger root notch lengths. The first phase of the analytical study involves running simulations corresponding to the tested specimens to calibrate the fracture toughness parameter (J_{IC}) for the different weld types and sizes. Based on the calibrated fracture toughness, additional simulations with longer root notch lengths (3.0 in. and 5.0 in.) were conducted to examine their response. The simulations indicated that even for the longer notch lengths, neither the strength nor the ductility was significantly decreased. This trend was explained based on a closer examination of the simulated fracture mechanics data, which suggests that the fracture toughness demand (J-integral), saturates with respect to the notch length, such that increasing the notch length beyond a certain limit (≈ 1.0 inch) does not increase the toughness demand any further. Thus, specimen response is relatively insensitive to root notch length.

7.2.2 Joints under combined shear and out-of-plane bending

An analysis of the connection response at peak force indicated that, for the non-toughness rated welds, the value of deformation at the extreme tension end of the weld compares well with expected values, and that the presence of the transverse root notch does not have a detrimental effect on weld ductility. For the toughness rated welds, the tension end weld deformation at peak load was found to be greater than for non-toughness rate welds. In addition, the location of the center of rotation (neutral axis) was found to lie in the compression half of the specimen. Results from strain gage data also indicated that the neutral axis for the connecting member is on the compression half of the specimen. More importantly, the gauge test specimens indicated that the bearing region of the connecting

plate reached strains large enough to justify a uniform stress distribution over the entire compression region.

The experimental results of all documented tests on fillet welded joints with out-of-plane eccentricity indicate that the current design approach used in the Manual of Steel Construction (AISC, 2005) is conservative, yielding a safety index of 4.9. A closer analysis of the data indicated that this conservatism may be attributed to a bearing mechanism between the connected plates, which is not incorporated in the approach used for the development of the AISC design table. In the presence of this beneficial effect, the accompanying influence of the root notch (whose length is equal to the bearing plate thickness) is minor.

The toughness of the filler metal was also determined to affect the conservatism of the design approach: filler metals with toughness requirement provided a higher test-to-predicted value.

Although 14 strength prediction models were evaluated by comparison of predicted strength with the test results, a detailed assessment of the models was conducted on only three of these models. The remaining models did not yield particularly good prediction of the test results and were based on a load versus deformation curve for fillet welds that is no longer in use. Since the test specimens prepared with toughness rated filler metal showed higher strength than those with filler metals with no toughness requirement, the test specimens were separated into two groups according to the toughness requirement and analyzed using Model 4 (modified Dawe and Kulak approach to incorporate a rectangular stress block in the compression zone and the load versus deformation relationship for welds suggested by Lesik and Kennedy (1990)), Model 5 (the current AISC approach) and Model 8 (a closed form model proposed by Beaulieu and Picard). Based on a reliability analysis, the safety index provided by Models 5 and 8 are significantly higher than the target value of 4.0. Although Model 4 provides an acceptable level of safety, the computation procedure is complicated and time consuming. Moreover, none of the existing models with the Lesik and Kennedy load versus deformation relationship consider plate fracture, which could become critical as the plate thickness is reduced. Therefore, a simpler, closed form, model that is applicable to both weld and plate failure modes was proposed. This model provides reliable prediction and satisfactory safety index ($\beta = 4.0$) for a resistance factor of 0.75. The new proposed model consists of three equations, namely, Equation 6.27 for weld failure with large eccentricity ($a/Q > 0.59$), Equation 6.28 for weld failure under small load eccentricity, and Equation 6.34 for plate failure.

References

AISC (2005), "Steel Construction Manual," 13th Edition, American Institute of Steel Construction, Chicago, IL.

ASTM E-1820 (2002), "Standard Test Methods for the Measurement of Fracture Toughness", ASTM International, West Conshohocken, PA.

AWS (2005), "Specification for Carbon Steel Electrodes for Flux Cored Arc Welding," ANSI/AWS A5.20-05, American Welding Society, Miami, FL.

AWS (2005), "Specification for Low Alloy Steel Electrodes for Flux Cored Arc Welding," ANSI/AWS A5.29-2005. American Welding Society, Miami, FL.

Beaulieu, D., and Picard, A. (1985). "Résultats d'essais sur des assemblages soudés excentriques en flexion," Canadian Journal of Civil Engineering, Vol. 12, pp. 494-506.

Bornscheuer, F. W., and Feder, D. (1996). "Tests on Welded Connections with Long or Thick Fillet Welds, IIW Doc. XV-214-66," International Institute of Welding, pp. 1-10.

Bowman, M. D., and Quinn, B. P. (1994). "Examination of Fillet Weld Strength," Engineering Journal, AISC, Vol. 31, No. 3, pp. 98-108.

Butler, L. J., and Kulak, G. L. (1969). "Behaviour of Eccentrically Loaded Welded Connection," Studies in Structural Engineering No. 7, Nova Scotia Technical College, Halifax, Canada.

Butler, L. J., and Kulak, G. L. (1971). "Strength of Fillet Welds as a Function of Direction of Load," Welding Journal, Welding Research Supplement, Vol. 36, No. 5, pp. 231s-234s.

Butler, L. J., Pal, S., and Kulak, G. L. (1972). "Eccentrically Loaded Welded Connections," Journal of the Structural Division, ASCE, Vol. 98, ST5, May, pp. 989-1005.

Callele, L. J., Grondin, G. Y., and Driver, R. G. (2005). "Strength and Behaviour of Multi-Orentation Fillet Weld Connections," Structural Engineering Report 225, Department of Civil and Environmental Engineering, University of Alberta, Edmonton, AB.

Canadian Institute of Steel Construction (2006): Handbook of Steel Construction. Ninth Edition., Toronto, Ontario.

Chen, W. F., and Han, D. J. (1988). "Plasticity for Structural Engineers," Springer-Verlag, N.Y.

Chi. W-M. (2000), "Prediction of steel connection failure using computational fracture mechanics," Ph.D. Thesis submitted to Stanford University, Stanford, CA

Clark, P. J. (1971). "Basis of Design for Fillet-Welded Joints under Static Loading," Proceedings of Conference on Improving Welded Product Design," The Welding Institute, Cambridge, England, Vol. 1, pp. 85-96.

Crawford, S.F., and G.L. Kulak (1971) "Eccentrically Loaded Bolted Connections," Journal of the Structural Division, ASCE, Vol. 97, No. ST3, pp. 765-783.

CSA, (2001). "Limit States Design of Steel Structures," CSA S16-01, Canadian Standards Association, Toronto, ON.

Dawe, J. L., and Kulak, G. L. (1972). "Welded Connections under Combined Shear and Moment," Journal of the Structural Division, ASCE, Vol. 100, No. ST4, May, pp. 727-741.

Dawe, J.L., and Kulak, G.L., (1974), "Welded connections under combined shear and moment," Journal of the Structural Division, Proceedings of the ASCE, Vol. 100, No. ST4, pp. 727-741

Deng, K., Driver, R. G., and Grondin, G. Y. (2003). "Effect of Loading Angle on the Behaviour of Fillet Welds," Structural Engineering Report 251, Department of Civil and Environmental Engineering, University of Alberta, Edmonton, AB.

FEMA (2000), "Recommended Design Criteria for New Steel Moment-Frame Buildings FEMA–350," Federal Emergency Management Agency, July 2000.

Fisher, J. W., Galambos, T. V., Kulak, G. L., and Ravindra, M. K. (1978). "Load and Resistance Factor Design Criteria for Connectors," Journal of the Structural Division, ASCE, Vol. 104, No. ST9, Sept., pp. 1427-1441.

Gagnon, D. P., and Kennedy, D. J. L. (1987). "Behaviour and Ultimate Strength of Partial Joint Penetration Groove Welds," Structural Engineering Report 151, Department of Civil and Environmental Engineering, University of Alberta, Edmonton, AB.

Galambos, T. V., and M. K. Ravindra, (1978). "Load and Resistance Factor Design for Steel," Journal of the Structural Division, ASCE, Vol. 104, No. ST9, Sept., pp. 1337-1353.

Higgins, T.R., and Preece, F. R. (1969). "Proposed Working Stresses for Fillet Welds in Building Construction," Engineering Journal, AISC, Vol. 6, No. 1, pp. 16-20.

Iwankiw, N. R., (1997), “Rational Basis for Increased Fillet Weld Strength,” Engineering Journal, AISC, 34(2), 68-71.

Kanvinde, A., Deierlein, G.G., (2004), “Micromechanical Simulation of Earthquake Induced Fractures in Steel Structures,” Blume Center TR145, Stanford University, Stanford, CA.

Kanvinde A.M., Gomez I.R., Roberts M., Fell B.V. and Grondin, G.Y, (2008 - accepted), "Strength and ductility of fillet welds with transverse root notch," Journal of Constructional Steel Research, Elsevier.

Kanvinde A.M., G.Y. Grondin , I.R. Gomez and Y.K. Kwan (2008 - in review), “Experimental Investigation of Fillet Welded Joints Subjected to Out-of-Plane Eccentric Loads” Engineering Journal, AISC

Kato, B., and Morita, K. (1969). “The Strength of Fillet Welded Joints, IIW Doc. XV-267-69,” International Institute of Welding.

Kennedy, D. J. L., and Gad-Aly, M. (1980). “Limit states design of steel structures-performance factors,” Canadian Journal of Civil Engineering, Vol. 7, pp. 45-77.

Lesik, D. F., and D. J. L. Kennedy, (1988). “Ultimate Strength of Eccentrically Loaded Fillet Welded Connections,” Structural Engineering Report 159, Department of Civil Engineering, University of Alberta, Edmonton, AB.

Lesik, D. F., and D. J. L. Kennedy, (1990). “Ultimate Strength of Fillet Welded Connections Loaded in Plane,” Canadian Journal of Civil Engineering, Vol. 17, No. 1, pp. 55-67.

Li, C., (2007), “Reliability Analysis of Concentrically Loaded Fillet Welds,” MSc thesis, Department of Civil and Environmental Engineering, University of Alberta, Edmonton, Alberta, October.

Li, C., Grondin, G. Y., and Driver, R. G. (2007). “Reliability Analysis of Concentrically Loaded Fillet Welds,” Structural Engineering Report 271, Department of Civil and Environmental Engineering, University of Alberta, Edmonton, AB.

Ligtenberg, F. K. (1968). “International Test Series Final Report, IIW Doc. XV-242-68,” International Institute of Welding.

Mansell, D. S., and Yadav, A. R. (1982). “Failure Mechanisms in Fillet Welds,” ACMSM 8: Proceedings of Eighth Australasian Conference on Mechanics of Structures and Materials, University of Newcastle, Newcastle, Australia, pp. 25.1-25.6.

McMeeking, R.M. and Parks, D.M. (1979), “On Criteria for J-Dominance of Crack-Tip Fields in Large Scale Yielding,” Elastic-Plastic Fracture, ASTM STP 668, 175-194.

Miazga, G.S., and Kennedy, D. J. L. (1986). "Behaviour of Fillet Welds as a Function of the Angle of Loading," Structural Engineering Report 133, Department of Civil Engineering, University of Alberta, Edmonton, AB.

Miazga, G. S., and Kennedy, D. J. L. (1989). "Behaviour of Fillet Welds as a Function of the Angle of Loading," Canadian Journal of Civil Engineering, Vol. 16, No. 4, pp. 583-599.

Murakawa, H., Lei, Y., Shi, Y., Ueda, Y., (1998), "Dependence of J-integral and failure assessment diagram on strength mismatching and crack length for welded joint specimen," Welding Research Abroad, 44(1), 13-22.

Neis, V.V. (1980). "Factored Resistance of Welded Connections Subject to Shear and Moment," Canadian Journal of Civil Engineering, Vol. 7, No. 1, pp. 84-92.

Ng, A. K. F., Driver, R. G., and Grondin, G. Y. (2002). "Behaviour of Transverse Fillet Welds," Structural Engineering Report 245, Department of Civil and Environmental Engineering, University of Alberta, Edmonton, AB.

Pham, L. (1981). "Effect of Size on the Static Strength of Fillet Welds," CSIRO Division of Building Research Technical Publication, Melbourne, Victoria, Australia.

Pham, L. (1983a). "Co-ordinated Testing of Fillet Welds Part 1-Cruciform Specimens-AWRA Contract 94, AWRA Document P6-35-82," Australian Welding Research, Vol. 12, pp. 16-25.

Pham, L. (1983b). "Co-ordinated Testing of Fillet Welds Part 2-Werner Specimens-AWRA Report P6-35-82," Australian Welding Research, Vol. 12, pp. 54-60.

Picard, A., and D.Beaulieu, (1991). "Calcul des charpentes d'acier," Canadian Institute of Steel Construction, Toronto, Ont.

Picard, A., and Werren, A. (1984). "Comportement expérimental et Calcul des assemblages soudés excentriques en flexion," Rapport GCI-84-01, Département de Génie civil, Université Laval, Ste-Foy, Québec, 140 p.

Rice, J.R. (1968), "Path independent Integral and the Approximate Analysis of Strain Concentration for Notches and Cracks." Journal of Applied Mechanics, 35, 379-386.

Roberts, M. (2008), "Experimental and analytical investigations of the strength and ductility of fillet welds with transverse root notch," Masters Thesis, Department of Civil and Environmental Engineering, University of California, Davis, CA.

Salmon, C. G. and Johnson, J. E. (1996), "Steel Structures, Design and Behavior", Fourth Edition, Chapter 16. New York: Harper Collins College Publishers

Schmidt, B.J., and Bartlett, F.M. (2002). “Review of resistance factor for steel: Data Collection,” Canadian Journal of Civil Engineering, Vol. 29, pp. 98-108.

Sanaei, E. and Kamtekar, A.G. (1988), “Experiments on Some Arbitrarily Loaded Fillet Welds.” Welding Journal, Welding Research Supplement, Vol. 67, No. 5, pp. 103-109

Swannell, P. (1981a). “Rational Design of Fillet Weld Groups,” Journal of the Structural Division, ASCE, Vol. 107, No. ST5, May, pp. 789-802.

Swannell, P. (1981b). “Weld Group Behavior,” Journal of the Structural Division, ASCE, Vol. 107, No. ST5, May, pp. 803-815.

Swannell, P., and Skewes, I. C. (1979a). “The Design of Welded Brackets Loaded In-Plane: Elastic and Ultimate Load Techniques-AWRA Report P6-8-77,” Australian Welding Research, Vol. 7, Jan., pp. 28-59.

Swannell, P., and Skewes, I. C. (1979b). “The Design of Welded Brackets Loaded In-Plane: General Theoretical Ultimate Load Techniques and Experimental Programme,” Australian Welding Research, Vol. 7, Apr., pp. 55-70.

Tide, R.H.R, (1980), “Eccentrically loaded weld groups – AISC Design Tables,” Engineering Journal, AISC, 17(4), 90-95.

Werren, A. (1984), "Comportement Expérimental et Calcul des Assemblages Soudés Excentriques en Flexion" (*Experimental behavior and design of welded joints with out-of-plane bending*), MSc Thesis, University Laval, Quebec.

Woo, K.S., Hong, C.H., Basu, P.K., (2004), “J-integral and fatigue life computations in the incremental plasticity analysis of large scale yielding by p-version of F.E.M.,” Structural Engineering and Mechanics, 17(1), 51-68

Appendix A

Welding Procedures and Specifications

Pass #	Class	Diam. (inches)	Polarity	Wire Feed Speed (inch/min)	Amperage	Volts	Travel Speed (inch/min)
1	E70T-7	3/32	DC-	146	315	28.0	16
2	E70T-7	3/32	DC-	146	315	28.0	13
3	E70T-7	3/32	DC-	146	315	28.0	14
1	E70T7-K2	5/64	DC-	196	280	26.5	11

Figure A.1 – Welding Specimens and Procedures

INNERSHIELD NR-311 AWS A5.20-95: E70T-7

Very high deposition rates and fast travel speeds. Welds thicker mild steels and some low alloy steels. Good bead shape and easy slag removal.

ADVANTAGE LINCOLN

- High deposition rates and fast travel speeds.
- Smooth operation. Good bead shape.
- Deep penetration.
- Easy slag removal in deep grooves.
- Resists weld cracking on high sulfur steels.
- Self-shielded, flux-cored. No need for external gas or flux.
- Produces quality welds in moderate wind conditions with no tenting.
- Our quality driven manufacturing system – certified to ISO 9002 – and our exceptionally high grade raw materials mean every coil of Innershield delivers great arc characteristics and superior feedability.

TYPICAL APPLICATIONS

- Fillet, lap and butt welds on 1/8" (3.2mm) and thicker steels.
- Horizontal butt welds such as column-to-column structural connections not subject to seismic requirements.
- General fabrication and assembly welding.

WELDING POSITIONS

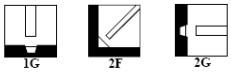

CONFORMANCE

AWS A5.20-95: E70T-7
ASME SFA-5.20: E70T-7
ABS: E70T-7 per AWS A5.20-95

MECHANICAL PROPERTIES(1) - *As Welded per AWS A5.20*

Condition	Yield Strength psi (MPa)	Tensile Strength psi (MPa)	Elongation (%)	Hardness Rockwell B
Requirements AWS E70T-7	58,000 (400) min.	70,000 (480) min.	22 min.	—
Test Results	60,000 - 66,000 (414 - 455)	82,000 - 90,000 (565 - 620)	22 - 26	87 - 92

(1) The strength and elongation properties reported were obtained from a .505" tensile specimen artificially aged at 220°F (104°C) for 48 hours, as permitted by AWS A5.20-95. A naturally aged tensile specimen may take months to achieve the specified properties. See AWS A5.20-95, paragraph A8.3. The time required for the natural aging of weld deposits is dependent upon ambient conditions, weldment geometry, the metallurgical structure of the weld deposit and other factors.

DIAMETERS / PACKAGING

Diameter Inches (mm)	14 Lb. Coil	22 Lb. Readi-Reel	50 Lb. Coil	600 Lb. Speed-Feed Reel	600 Lb. Speed-Feed Drum
5/64 (2.0)	ED014464	ED014515	ED014459		
3/32 (2.4)			ED012629		ED012628
7/64 (2.8)			ED012632	ED012633	ED012631

Figure A.2 – Page one of Lincoln Electric Data Sheet for electrode E70T-7

INNERSHIELD NR-311 AWS A5.20-95: E70T-7

TYPICAL OPERATING PROCEDURES

Wire, Polarity Electrical Stickout Wire Weight	Wire Feed Speed in/min (m/min)	Arc Voltage (volts)	Approx. Current (amps)	Melt-Off Rate lbs/hr (kg/hr)	Deposition Rate lbs/hr (kg/hr)	Efficiency (%)
5/64" DC- 1-1/4" (32mm) 1.07 lbs/1000"	100 (2.5)	21	190	6.4 (2.9)	5.0 (2.3)	78
	160 (4.1)	25	275	10.3 (4.7)	8.0 (3.6)	78
	240 (6.1)	26	355	15.4 (7.0)	12.4 (5.6)	80
	300 (7.6)	28	410	19.3 (8.8)	15.8 (7.2)	82
3/32" DC- 1-1/2" (38mm) 1.62 lbs/1000"	75 (1.9)	21	200	7.0 (3.2)	5.4 (2.5)	77
	135 (3.4)	24	300	13.1 (5.9)	10.2 (4.6)	78
	150 (3.8)	25	325	14.6 (6.6)	11.4 (5.2)	78
	210 (5.3)	27	400	20.4 (9.3)	16.5 (7.5)	81
	270 (6.9)	30	450	26.2 (11.9)	22.0 (10.0)	84
7/64" DC- 1-1/2" (38mm) 2.05 lbs/1000"	100 (2.5)	23.5	325	12.0 (5.4)	10.0 (4.5)	83
	145 (3.7)	25.5	400	17.8 (8.1)	14.5 (6.6)	82
	175 (4.4)	27	450	21.5 (9.8)	18.0 (8.2)	83
	240 (6.1)	30.5	550	29.5 (13.4)	25.5 (11.6)	86
	300 (7.6)	33	625	36.9 (16.7)	33.0 (15.0)	89

NOTE: Above typical operating procedures are starting points and may be adjusted as required.

DEPOSIT COMPOSITION

	%C	%Mn	%P	%S	%Si	%Al
Requirements AWS E70T-7	Report Only	1.75 max.	.03 max.	.03 max.	.60 max.	1.8 max.
Test Results	.25	.50	.008	<.003	.10	1.46

This electrode, and others of the same AWS classification, are not required to deposit weld metal capable of delivering any minimum specified Charpy V-Notch (CVN) properties. It should not be used in applications where minimum specified CVN properties are required. Typical applications where minimum specified CVN properties are required include, but are not restricted to, bridges, pressure vessels, and buildings in seismic zones. The user of this product is responsible for determining whether minimum CVN properties are required for the specific application.

Figure A.3 – Page two of Lincoln Electric Data Sheet for electrode E70T-7

INNERSHIELD NR-311 Ni AWS A5.29-98: E70T7-K2

Similar to NR-311, but with good Charpy V-Notch properties. High deposition rates. Fast travel speeds. For single and multiple pass welding.

ADVANTAGE LINCOLN

- High deposition rates and fast travel speeds.
- Produces a nominal 1.5% Nickel deposit for notch toughness.
- Color match on weathering steel applications.
- Produces quality welds in moderate wind conditions with no tenting.
- Self-shielded, flux-cored. No need for external gas or flux.
- Our quality driven manufacturing system – certified to ISO 9002 – and our exceptionally high grade raw materials mean every coil of Innershield delivers great arc characteristics and superior feedability.

TYPICAL APPLICATIONS

- Fillet and lap welds.
- Horizontal butt welds such as column-to-column structural connections.
- Deep groove welds.
- Square edge butt welds.
- Structural fabrication, including applications involving seismic requirements.

WELDING POSITIONS

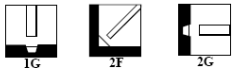

CONFORMANCE

AWS A5.29-98: E70T7-K2
ASME SFA5.29: E70T7-K2
Lloyd's: 2S-2YS
DNV: IIYMS
GL: 2YS
BV: SA2YM
NKK: KSW 52 NH10

MECHANICAL PROPERTIES[1] - *As Welded per AWS A5.29*

Condition	Yield Strength psi (MPa)	Tensile Strength psi (MPa)	Elongation (%)	Charpy V-Notch ft-lbs (Joules) @ -20°F	(-29°C)	Hardness Rockwell B
Requirements AWS E70T7-K2	58,000 (400) min.	70,000 (482) min.	20 min.	20 min.	(27) min.	—
Test Results	64,000 - 75,000 (441 - 517)	80,000 - 89,000 (551 - 613)	22 - 31	20 - 50	(27 - 68)	87 - 92

(1) The strength and elongation properties reported were obtained from a .505" tensile specimen artificially aged at 220°F (104°C) for 48 hours, as permitted by AWS A5.29-98. A naturally aged tensile specimen may take months to achieve the specified properties. The time required for the natural aging of weld deposits is dependent upon ambient conditions, weldment geometry, the metallurgical structure of the weld deposit and other factors.

DIAMETERS / PACKAGING

Diameter Inches (mm)	22 Lb. Readi-Reel	50 Lb. Coil
5/64 (2.0)	ED017819	
3/32 (2.4)		ED017822
7/64 (2.8)		ED017824

Figure A.4 – Page one of Lincoln Electric Data Sheet for electrode E70T7-K2

INNERSHIELD NR-311 Ni AWS A5.29-98: E70T7-K2

TYPICAL OPERATING PROCEDURES

Wire, Polarity Electrical Stickout Wire Weight	Wire Feed Speed in/min (m/min)	Arc Voltage (volts)	Approx. Current (amps)	Melt-Off Rate lbs/hr (kg/hr)	Deposition Rate lbs/hr (kg/hr)	Efficiency (%)
5/64" DC- 1" (25mm) 0.930 lbs/1000"	100 (2.5)	22	170	5.5 (2.5)	3.9 (1.8)	70
	130 (3.3)	25	205	7.2 (3.3)	5.2 (2.4)	72
	160 (4.0)	26	235	8.8 (4.0)	6.5 (2.9)	73
	200 (5.0)	27	270	11.0 (5.0)	8.3 (3.8)	75
	240 (6.1)	28	295	13.3 (6.1)	10.0 (4.5)	75
3/32" DC- 1-1/4" (32mm) 1.39 lbs/1000"	75 (1.9)	21	200	6.2 (2.8)	4.2 (1.9)	67
	100 (2.5)	22	245	8.3 (3.8)	5.9 (2.7)	71
	125 (3.1)	24	285	10.4 (4.7)	7.5 (3.4)	72
	150 (3.8)	26	330	12.5 (5.7)	9.1 (4.1)	72
	175 (4.4)	27	365	14.5 (6.6)	10.8 (4.9)	74
	200 (5.0)	28	390	16.6 (7.6)	12.3 (5.6)	74
7/64" DC- 1-1/2" (38mm) 1.89 lbs/1000"	100 (2.5)	23	310	11.4 (5.2)	8.4 (3.8)	73
	140 (3.5)	25	370	15.8 (7.2)	11.8 (5.4)	74
	170 (4.3)	27	430	19.5 (8.9)	14.5 (6.6)	74
	200 (5.0)	29	470	22.8 (10.4)	17.0 (7.7)	74
	240 (6.1)	30	520	27.2 (12.4)	20.4 (9.2)	75

NOTE: Above typical operating procedures are starting points and may be adjusted as required.

DEPOSIT COMPOSITION

	%C	%Mn	%P	%S	%Si	%Al	%Ni	%Mo	%Cr	%V
Requirements AWS E70T7-K2	.15 max.	.50 - 1.75	.03 max.	.03 max.	.80 max.	1.80 max.	1.00 - 2.00	.35 max.	.15 max.	.05 max.
Test Results	.06	1.23	.005	<.003	.20	1.24	1.28	<.01	.03	<.01

This electrode has been tested in accordance with FEMA 353 - *Recommended Specifications and Quality Assurance Guidelines for Steel Moment-Frame Construction for Seismic Applications* and is capable of depositing weld metal that delivers minimum CVN properties of 40 ft-lbs. at 70°F (95 Joules at 21°C)at low and high heat input levels. As required by the AWS classification, it meets a minimum CVN of 20 ft-lbs. at -20°F (27 Joules at -29°C), when tested in accordance with AWS A5.20. This electrode will also deposit weld metal that will meet the requirements for H16 as tested according to AWS A4.3

FEMA 353 test certificates are available upon request.

Figure A.5 – Page two of Lincoln Electric Data Sheet for electrode E70T7-K2

Appendix B

Cruciform Specimen Measurements

Nomenclature Guide of Experimental Specimens

Naming of tension specimens (Tests #1-#24); e.g. T125_A12_1

- "T" refers to a tension test specimen.
- "125" refers to a root notch length of 1.25 inches. "250" refers to a root notch length of 2.50 inches.
- "A" refers to the non-toughness rated electrode E70T-7. "B" refers to the toughness rated electrode E70T7-K2.
- "12" refers to a nominal 1/2" weld (leg) size. "516" refers to a nominal 5⁄16" weld (leg) size.
- The suffix "1", "2" or "3" represents the three replicate specimens for each assembly.

Naming of bend specimens (Tests #25-#84); e.g. B125_A516_55_1

- "B" refers to a bend test specimen.
- "125" refers to a root notch length of 1.25 inches. "175" refers to a root notch length of 1.75 inches. "250" refers to a root notch length of 2.50 inches.
- "A" refers to the non-toughness rated electrode E70T-7. "B" refers to the toughness rated electrode E70T7-K2.
- "12" refers to a nominal 1/2" weld (leg) size. "516" refers to a nominal 5⁄16" weld (leg) size.
- "3" refers to a 3.0 inch load eccentricity. "55" refers to a 5.5 inch load eccentricity. "85" refers to an 8.5 inch load eccentricity.
- The suffix "1", "2" or "3" represents the three replicate specimens for each assembly.

B.1 PRE-FRACTURE MEASUREMENTS

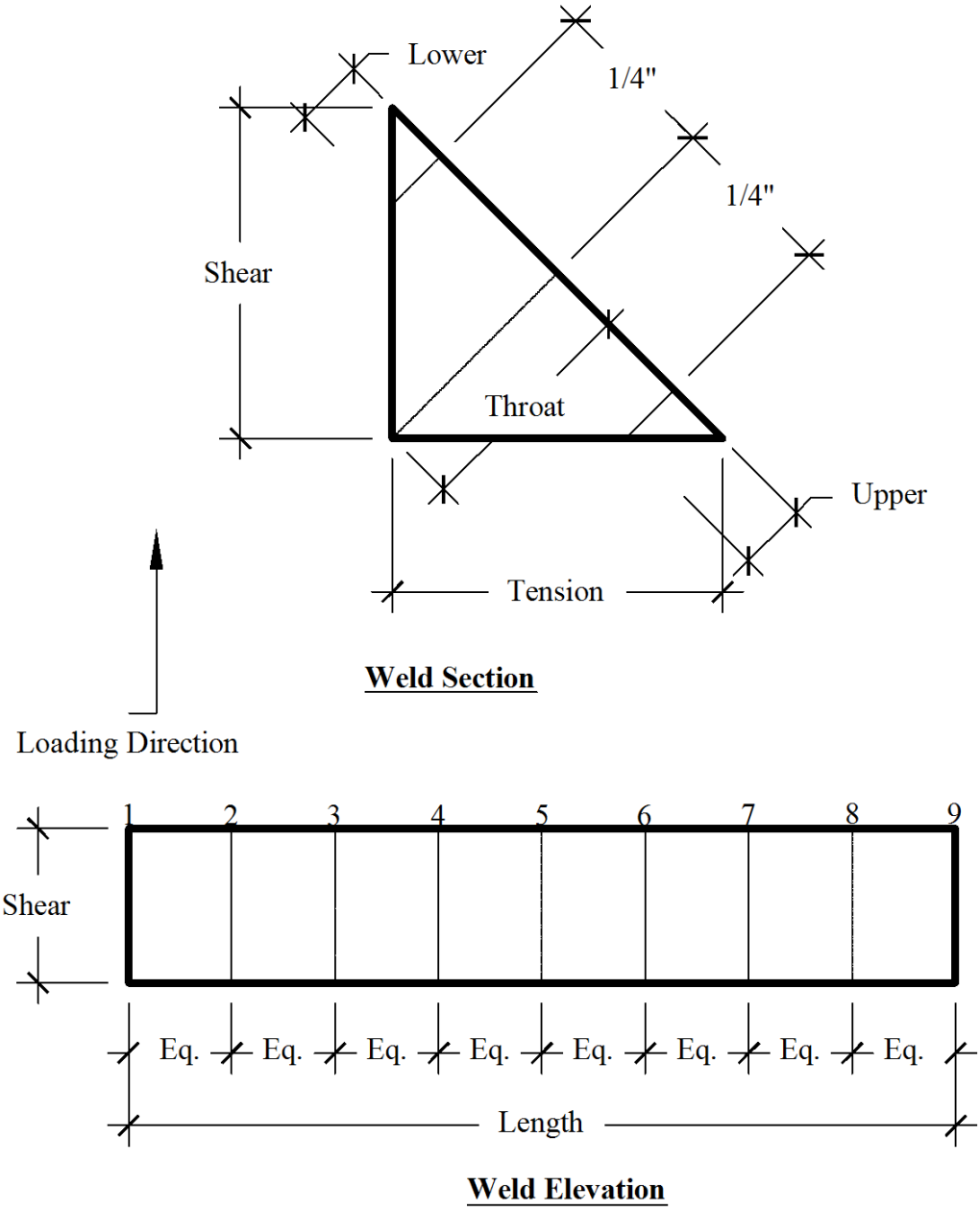

Figure B.1.1 – (a) Weld Section Schematic Showing Shear Leg, Tension Leg, Upper, Lower, and Throat Measurements (b) Weld Elevation Schematic Showing Location of Nine or Eight Pre- and Post-Fracture Measurements[1]

[1] For the bend tests, an "X" next to measurement "1" indicates the side of the weld where the load was applied; i.e. the compression side

Table B.1.1 – Test #1, T125_A12_1

	Pre-Fracture Measurements									
	Front Side, inches					Back Side, inches				
Meas. Num.	**Shear Leg**	**Lower**	**Throat**	**Upper**	**Tension Leg**	**Shear Leg**	**Lower**	**Throat**	**Upper**	**Tension Leg**
1	0.703	0.220	0.422	0.110	0.453	0.625	0.250	0.425	0.150	0.453
2	0.688		0.406		0.500	0.625		0.425		0.406
3	0.672		0.391		0.484	0.609		0.406		0.469
4	0.703		0.406		0.469	0.641		0.394		0.469
5	0.719		0.391		0.469	0.625		0.406		0.500
6	0.766		0.375		0.469	0.604		0.419		0.469
7	0.703		0.375		0.438	0.625		0.425		0.469
8	0.719		0.375		0.438	0.625		0.419		0.438
9	0.719	0.250	0.375	0.130	0.438	0.625	0.250	0.419	0.170	0.438
Mean	**0.710**	**0.235**	**0.391**	**0.120**	**0.462**	**0.623**	**0.250**	**0.415**	**0.160**	**0.457**
Initial Skewed Angle (°)		**0**								

Table B.1.2 – Test #2, T125_A12_2

	Pre-Fracture Measurements									
	Front Side, inches					Back Side, inches				
Meas. Num.	**Shear Leg**	**Lower**	**Throat**	**Upper**	**Tension Leg**	**Shear Leg**	**Lower**	**Throat**	**Upper**	**Tension Leg**
1	0.750	0.220	0.375	0.150	0.500	0.688	0.210	0.422	0.140	0.500
2	0.750		0.375		0.500	0.656		0.422		0.531
3	0.750		0.375		0.469	0.656		0.406		0.531
4	0.750		0.375		0.500	0.656		0.406		0.531
5	0.688		0.350		0.469	0.656		0.406		0.531
6	0.750		0.350		0.469	0.688		0.438		0.531
7	0.781		0.350		0.469	0.688		0.406		0.531
8	0.750		0.350		0.469	0.688		0.406		0.500
9	0.656	0.230	0.350	0.080	0.500	0.625	0.260	0.406	0.160	0.500
Average	**0.736**	**0.225**	**0.361**	**0.115**	**0.483**	**0.667**	**0.235**	**0.413**	**0.150**	**0.521**
Initial Skewed Angle (°)		**0**								

Table B.1.3 – Test #3, T125_A12_3

	Pre-Fracture Measurements									
	Front Side, inches					Back Side, inches				
Meas. Num.	**Shear Leg**	**Lower**	**Throat**	**Upper**	**Tension Leg**	**Shear Leg**	**Lower**	**Throat**	**Upper**	**Tension Leg**
1	0.688	0.230	0.375	0.150	0.531	0.875	0.260	0.453	0.170	0.531
2	0.656		0.375		0.531	0.813		0.469		0.531
3	0.688		0.375		0.531	0.781		0.469		0.531
4	0.656		0.375		0.500	0.781		0.453		0.531
5	0.656		0.375		0.500	0.781		0.453		0.531
6	0.656		0.359		0.500	0.781		0.469		0.531
7	0.688		0.359		0.531	0.750		0.453		0.531
8	0.688		0.375		0.500	0.750		0.438		0.500
9	0.750	0.250	0.391	0.130	0.500	0.719	0.210	0.438	0.150	0.531
Average	**0.681**	**0.240**	**0.373**	**0.140**	**0.514**	**0.781**	**0.235**	**0.455**	**0.160**	**0.528**
Initial Skewed Angle (°)		**0**								

Table B.1.4 – Test #4, T125_A516_1

	Pre-Fracture Measurements					
	Front Side, inches			Back Side, inches		
Meas. Num.	**Shear Leg**	**Throat**	**Tension Leg**	**Shear Leg**	**Throat**	**Tension Leg**
1	0.469	0.281	0.313	0.469	0.313	0.281
2	0.469	0.281	0.281	0.469	0.281	0.344
3	0.406	0.281	0.313	0.438	0.250	0.344
4	0.469	0.266	0.313	0.469	0.281	0.313
5	0.469	0.281	0.313	0.453	0.250	0.344
6	0.469	0.281	0.281	0.500	0.281	0.344
7	0.453	0.297	0.297	0.469	0.281	0.344
8	0.438	0.281	0.313	0.469	0.281	0.344
9	0.438	0.281	0.297	0.438	0.281	0.344
Mean	**0.453**	**0.281**	**0.302**	**0.464**	**0.278**	**0.333**
Initial Skewed Angle (°)		**0**				

Table B.1.5 – Test #5, T125_A516_2

	Pre-Fracture Measurements					
	Front Side, inches			Back Side, inches		
Meas. Num.	**Shear Leg**	**Throat**	**Tension Leg**	**Shear Leg**	**Throat**	**Tension Leg**
1	0.500	0.250	0.344	0.469	0.313	0.313
2	0.469	0.250	0.375	0.500	0.313	0.344
3	0.469	0.250	0.313	0.500	0.313	0.344
4	0.469	0.250	0.313	0.500	0.313	0.344
5	0.500	0.250	0.313	0.500	0.313	0.344
6	0.469	0.250	0.313	0.438	0.313	0.344
7	0.453	0.250	0.313	0.438	0.281	0.344
8	0.453	0.250	0.313	0.406	0.281	0.313
9	0.438	0.250	0.313	0.500	0.281	0.344
Average	**0.469**	**0.250**	**0.323**	**0.472**	**0.302**	**0.337**
Initial Skewed Angle (°)		**0**				

Table B.1.6 – Test #6, T125_A516_3

	Pre-Fracture Measurements					
	Front Side, inches			Back Side, inches		
Meas. Num.	**Shear Leg**	**Throat**	**Tension Leg**	**Shear Leg**	**Throat**	**Tension Leg**
1	0.438	0.313	0.406	0.500	0.313	0.344
2	0.422	0.250	0.406	0.500	0.281	0.344
3	0.484	0.281	0.375	0.500	0.281	0.344
4	0.438	0.281	0.344	0.500	0.281	0.344
5	0.438	0.250	0.375	0.500	0.281	0.344
6	0.469	0.250	0.375	0.500	0.281	0.344
7	0.500	0.250	0.375	0.500	0.281	0.344
8	0.438	0.250	0.313	0.563	0.313	0.344
9	0.438	0.250	0.313	0.563	0.313	0.375
Average	**0.451**	**0.264**	**0.365**	**0.514**	**0.292**	**0.347**
Initial Skewed Angle (°)		**0**				

Table B.1.7 – Test #7, T250_A12_1

	Pre-Fracture Measurements									
	Front Side, inches					Back Side, inches				
Meas. Num.	**Shear Leg**	**Lower**	**Throat**	**Upper**	**Tension Leg**	**Shear Leg**	**Lower**	**Throat**	**Upper**	**Tension Leg**
1	0.906	0.250	0.438	0.120	0.563	0.813	0.230	0.531	0.100	0.500
2	0.906		0.438		0.563	0.781		0.500		0.469
3	0.875		0.469		0.563	0.750		0.469		0.469
4	0.875		0.438		0.563	0.719		0.469		0.531
5	0.875		0.438		0.531	0.750		0.438		0.531
6	0.844		0.406		0.531	0.719		0.469		0.500
7	0.875		0.438		0.531	0.688		0.469		0.563
8	0.844		0.438		0.531	0.688		0.438		0.531
9	0.844	0.230	0.438	0.110	0.469	0.688	0.210	0.438	0.110	0.438
Average	**0.872**	**0.240**	**0.438**	**0.115**	**0.538**	**0.733**	**0.220**	**0.469**	**0.105**	**0.503**
Initial Skewed Angle (°)		**7.0**								

Table B.1.8 – Test #8, T250_A12_2

	Pre-Fracture Measurements									
	Front Side, inches					Back Side, inches				
Meas. Num.	**Shear Leg**	**Lower**	**Throat**	**Upper**	**Tension Leg**	**Shear Leg**	**Lower**	**Throat**	**Upper**	**Tension Leg**
1	0.719	0.208	0.406	0.145	0.484	0.656	0.145	0.344	0.192	0.500
2	0.750	0.223	0.406	0.137	0.484	0.656	0.145	0.375	0.192	0.438
3	0.781	0.192	0.406	0.145	0.477	0.688	0.145	0.375	0.192	0.469
4	0.813	0.208	0.406	0.145	0.500	0.688	0.145	0.375	0.192	0.500
5	0.781	0.208	0.406	0.151	0.500	0.719	0.145	0.375	0.201	0.469
6	0.781	0.208	0.406	0.148	0.500	0.688	0.114	0.375	0.176	0.500
7	0.781	0.208	0.391	0.129	0.500	0.719	0.145	0.391	0.214	0.500
8	0.781	0.215	0.422	0.129	0.469	0.656	0.145	0.375	0.208	0.500
9	0.781	0.220	0.425	0.145	0.500	0.656	0.145	0.375	0.208	0.500
Average	**0.774**	**0.210**	**0.408**	**0.142**	**0.490**	**0.681**	**0.142**	**0.373**	**0.197**	**0.486**
Initial Skewed Angle (°)		**7.0**								

Table B.1.9 – Test #9, T250_A12_3

	Pre-Fracture Measurements									
	Front Side, inches					Back Side, inches				
Meas. Num.	**Shear Leg**	**Lower**	**Throat**	**Upper**	**Tension Leg**	**Shear Leg**	**Lower**	**Throat**	**Upper**	**Tension Leg**
1	0.906	0.301	0.438	0.145	0.656	0.781	0.208	0.406	0.176	0.531
2	0.906	0.270	0.438	0.145	0.656	0.688	0.208	0.406	0.176	0.500
3	0.906	0.270	0.406	0.145	0.656	0.688	0.208	0.406	0.176	0.531
4	0.906	0.270	0.438	0.114	0.656	0.813	0.208	0.406	0.176	0.531
5	0.875	0.270	0.406	0.145	0.625	0.750	0.208	0.406	0.176	0.531
6	0.875	0.270	0.438	0.145	0.656	0.750	0.208	0.375	0.176	0.563
7	0.875	0.270	0.438	0.145	0.656	0.750	0.208	0.406	0.176	0.531
8	0.875	0.270	0.406	0.145	0.656	0.750	0.208	0.375	0.176	0.531
9	0.844	0.270	0.406	0.145	0.625	0.750	0.208	0.375	0.176	0.531
Average	**0.885**	**0.273**	**0.424**	**0.142**	**0.649**	**0.747**	**0.208**	**0.396**	**0.176**	**0.531**
Initial Skewed Angle (°)		**7.0**								

Table B.1.10 – Test #10, T250_A516_1

	Pre-Fracture Measurements					
	Front Side, inches			Back Side, inches		
Meas. Num.	**Shear Leg**	**Throat**	**Tension Leg**	**Shear Leg**	**Throat**	**Tension Leg**
1	0.469	0.344	0.344	0.500	0.219	0.344
2	0.469	0.344	0.313	0.500	0.219	0.344
3	0.469	0.344	0.313	0.500	0.219	0.344
4	0.469	0.344	0.313	0.500	0.219	0.344
5	0.469	0.344	0.313	0.500	0.219	0.344
6	0.469	0.344	0.313	0.500	0.219	0.344
7	0.469	0.344	0.313	0.500	0.219	0.344
8	0.469	0.344	0.313	0.531	0.219	0.344
9	0.563	0.375	0.281	0.500	0.219	0.344
Average	**0.479**	**0.347**	**0.313**	**0.503**	**0.219**	**0.344**
Initial Skewed Angle (°)		**5.0**				

Table B.1.11 – Test #11, T250_A516_2

	Pre-Fracture Measurements					
	Front Side, inches			Back Side, inches		
Meas. Num.	**Shear Leg**	**Throat**	**Tension Leg**	**Shear Leg**	**Throat**	**Tension Leg**
1	0.531	0.250	0.250	0.500	0.281	0.344
2	0.500	0.250	0.313	0.500	0.281	0.344
3	0.500	0.219	0.281	0.500	0.281	0.344
4	0.500	0.250	0.250	0.500	0.250	0.344
5	0.469	0.219	0.281	0.500	0.250	0.344
6	0.469	0.219	0.281	0.500	0.250	0.344
7	0.469	0.188	0.281	0.500	0.250	0.344
8	0.469	0.188	0.281	0.500	0.250	0.344
9	0.469	0.188	0.281	0.500	0.250	0.344
Average	**0.486**	**0.219**	**0.278**	**0.500**	**0.260**	**0.344**
Initial Skewed Angle (°)		**5.0**				

Table B.1.12 – Test #12, T250_A516_3

	Pre-Fracture Measurements					
	Front Side, inches			Back Side, inches		
Meas. Num.	**Shear Leg**	**Throat**	**Tension Leg**	**Shear Leg**	**Throat**	**Tension Leg**
1	0.531	0.219	0.313	0.563	0.313	0.313
2	0.531	0.219	0.313	0.563	0.313	0.313
3	0.531	0.219	0.313	0.531	0.313	0.313
4	0.531	0.219	0.281	0.531	0.281	0.313
5	0.531	0.219	0.281	0.500	0.313	0.344
6	0.531	0.219	0.281	0.469	0.313	0.344
7	0.531	0.250	0.250	0.469	0.281	0.313
8	0.531	0.250	0.281	0.469	0.281	0.313
9	0.531	0.250	0.281	0.469	0.281	0.313
Average	**0.531**	**0.229**	**0.288**	**0.507**	**0.299**	**0.319**
Initial Skewed Angle (°)		**5.0**				

Table B.1.13 – Test #13, T125_B12_1

	Pre-Fracture Measurements									
	Front Side, inches					Back Side, inches				
Meas. Num.	**Shear Leg**	**Lower**	**Throat**	**Upper**	**Tension Leg**	**Shear Leg**	**Lower**	**Throat**	**Upper**	**Tension Leg**
1	0.813	0.239	0.406	0.176	0.594	0.688	0.239	0.438	0.145	0.531
2	0.781	0.239	0.406	0.176	0.594	0.688	0.239	0.438	0.145	0.531
3	0.750	0.239	0.406	0.176	0.594	0.688	0.239	0.438	0.145	0.531
4	0.750	0.270	0.406	0.176	0.594	0.688	0.239	0.438	0.145	0.531
5	0.844	0.239	0.438	0.176	0.594	0.688	0.239	0.438	0.145	0.531
6	0.813	0.239	0.438	0.176	0.563	0.688	0.239	0.406	0.145	0.531
7	0.813	0.270	0.406	0.176	0.563	0.688	0.239	0.438	0.145	0.531
8	0.813	0.239	0.438	0.176	0.625	0.688	0.239	0.438	0.145	0.531
9	0.844	0.239	0.469	0.176	0.625	0.688	0.239	0.406	0.145	0.531
Average	**0.802**	**0.246**	**0.424**	**0.176**	**0.594**	**0.688**	**0.239**	**0.431**	**0.145**	**0.531**
Initial Skewed Angle (°)		**0**								

Table B.1.14 – Test #14, T125_B12_2

	Pre-Fracture Measurements									
	Front Side, inches					Back Side, inches				
Meas. Num.	**Shear Leg**	**Lower**	**Throat**	**Upper**	**Tension Leg**	**Shear Leg**	**Lower**	**Throat**	**Upper**	**Tension Leg**
1	0.781	0.208	0.375	0.239	0.594	0.719	0.270	0.438	0.208	0.594
2	0.781	0.208	0.375	0.239	0.594	0.625	0.270	0.438	0.208	0.594
3	0.750	0.145	0.375	0.239	0.594	0.688	0.270	0.406	0.208	0.594
4	0.750	0.145	0.344	0.239	0.594	0.656	0.270	0.438	0.208	0.594
5	0.750	0.145	0.313	0.239	0.594	0.656	0.270	0.406	0.208	0.594
6	0.750	0.176	0.344	0.239	0.594	0.656	0.270	0.438	0.208	0.594
7	0.750	0.239	0.375	0.239	0.594	0.625	0.270	0.438	0.208	0.625
8	0.750	0.239	0.375	0.239	0.594	0.625	0.270	0.406	0.208	0.625
9	0.750	0.239	0.375	0.239	0.594	0.656	0.270	0.438	0.208	0.625
Average	**0.757**	**0.194**	**0.361**	**0.239**	**0.594**	**0.656**	**0.270**	**0.427**	**0.208**	**0.604**
Initial Skewed Angle (°)		**0**								

Table B.1.15 – Test #15, T125_B12_3

	Pre-Fracture Measurements									
	Front Side, inches					Back Side, inches				
Meas. Num.	**Shear Leg**	**Lower**	**Throat**	**Upper**	**Tension Leg**	**Shear Leg**	**Lower**	**Throat**	**Upper**	**Tension Leg**
1	0.750	0.208	0.313	0.208	0.625	0.813	0.270	0.406	0.176	0.563
2	0.688	0.208	0.344	0.208	0.625	0.781	0.270	0.406	0.176	0.531
3	0.688	0.208	0.344	0.208	0.594	0.750	0.270	0.438	0.176	0.563
4	0.688	0.208	0.281	0.208	0.594	0.688	0.270	0.406	0.176	0.531
5	0.688	0.208	0.281	0.208	0.625	0.688	0.270	0.406	0.176	0.563
6	0.688	0.208	0.313	0.208	0.625	0.688	0.270	0.406	0.176	0.563
7	0.625	0.208	0.313	0.208	0.625	0.688	0.270	0.406	0.176	0.563
8	0.625	0.208	0.313	0.208	0.594	0.719	0.270	0.438	0.176	0.563
9	0.719	0.208	0.313	0.208	0.594	0.688	0.270	0.438	0.176	0.531
Average	**0.684**	**0.208**	**0.313**	**0.208**	**0.611**	**0.722**	**0.270**	**0.417**	**0.176**	**0.552**
Initial Skewed Angle (°)		**0**								

Table B.1.16 – Test #16, T125_B516_1

	Pre-Fracture Measurements					
	Front Side, inches			Back Side, inches		
Meas. Num.	**Shear Leg**	**Throat**	**Tension Leg**	**Shear Leg**	**Throat**	**Tension Leg**
1	0.563	0.313	0.313	0.375	0.344	0.406
2	0.531	0.313	0.406	0.375	0.313	0.406
3	0.500	0.281	0.406	0.375	0.344	0.406
4	0.531	0.281	0.313	0.375	0.313	0.406
5	0.594	0.313	0.313	0.375	0.313	0.406
6	0.469	0.250	0.344	0.375	0.313	0.406
7	0.531	0.313	0.344	0.375	0.313	0.406
8	0.500	0.250	0.344	0.375	0.313	0.406
9	0.500	0.281	0.313	0.375	0.313	0.406
Average	**0.524**	**0.288**	**0.344**	**0.375**	**0.319**	**0.406**
Initial Skewed Angle (°)		**4.0**				

Table B.1.17 – Test #17, T125_B516_2

	Pre-Fracture Measurements					
	Front Side, inches			Back Side, inches		
Meas. Num.	**Shear Leg**	**Throat**	**Tension Leg**	**Shear Leg**	**Throat**	**Tension Leg**
1	0.531	0.25	0.344	0.375	0.313	0.406
2	0.531	0.3125	0.344	0.375	0.281	0.406
3	0.563	0.3125	0.344	0.344	0.313	0.406
4	0.531	0.28125	0.344	0.344	0.313	0.406
5	0.500	0.3125	0.344	0.344	0.313	0.406
6	0.500	0.375	0.375	0.344	0.313	0.375
7	0.500	0.34375	0.375	0.375	0.313	0.469
8	0.563	0.3125	0.344	0.406	0.313	0.438
9	0.500	0.3125	0.344	0.406	0.313	0.406
Average	**0.524**	**0.313**	**0.351**	**0.368**	**0.309**	**0.413**
Initial Skewed Angle (°)		**4.0**				

Table B.1.18 – Test #18, T125_B516_3

	Pre-Fracture Measurements					
	Front Side, inches			Back Side, inches		
Meas. Num.	**Shear Leg**	**Throat**	**Tension Leg**	**Shear Leg**	**Throat**	**Tension Leg**
1	0.500	0.313	0.375	0.500	0.344	0.469
2	0.500	0.313	0.375	0.500	0.375	0.438
3	0.500	0.313	0.375	0.469	0.375	0.469
4	0.500	0.313	0.375	0.469	0.375	0.469
5	0.500	0.313	0.375	0.469	0.313	0.438
6	0.500	0.313	0.344	0.469	0.313	0.438
7	0.500	0.313	0.344	0.469	0.313	0.438
8	0.500	0.281	0.375	0.500	0.344	0.406
9	0.500	0.313	0.375	0.500	0.344	0.438
Average	**0.500**	**0.309**	**0.368**	**0.483**	**0.344**	**0.444**
Initial Skewed Angle (°)		**4.0**				

Table B.1.19 – Test #19, T250_B12_1

	Pre-Fracture Measurements									
	Front Side, inches					Back Side, inches				
Meas. Num.	**Shear Leg**	**Lower**	**Throat**	**Upper**	**Tension Leg**	**Shear Leg**	**Lower**	**Throat**	**Upper**	**Tension Leg**
1	0.906	0.301	0.344	0.176	0.531	0.750	0.270	0.438	0.208	0.531
2	0.844	0.301	0.344	0.176	0.531	0.719	0.270	0.438	0.208	0.531
3	0.813	0.301	0.344	0.176	0.531	0.719	0.270	0.438	0.208	0.531
4	0.813	0.301	0.375	0.176	0.531	0.719	0.270	0.469	0.208	0.531
5	0.781	0.301	0.375	0.176	0.531	0.719	0.270	0.438	0.208	0.531
6	0.750	0.301	0.375	0.176	0.531	0.719	0.270	0.438	0.208	0.531
7	0.781	0.301	0.406	0.176	0.531	0.719	0.270	0.438	0.208	0.531
8	0.781	0.301	0.344	0.145	0.500	0.688	0.270	0.438	0.208	0.531
9	0.781	0.270	0.344	0.145	0.531	0.719	0.270	0.438	0.208	0.531
Average	**0.806**	**0.298**	**0.361**	**0.169**	**0.528**	**0.719**	**0.270**	**0.441**	**0.208**	**0.531**
Initial Skewed Angle (°)		**3.0**								

Table B.1.20 – Test #20, T250_B12_2

	Pre-Fracture Measurements									
	Front Side, inches					Back Side, inches				
Meas. Num.	**Shear Leg**	**Lower**	**Throat**	**Upper**	**Tension Leg**	**Shear Leg**	**Lower**	**Throat**	**Upper**	**Tension Leg**
1	0.719	0.208	0.438	0.176	0.594	0.688	0.270	0.469	0.208	0.594
2	0.719	0.208	0.438	0.176	0.594	0.688	0.270	0.469	0.208	0.594
3	0.750	0.208	0.438	0.176	0.594	0.688	0.270	0.469	0.208	0.594
4	0.750	0.208	0.406	0.176	0.563	0.781	0.270	0.469	0.208	0.594
5	0.750	0.208	0.406	0.176	0.563	0.781	0.270	0.469	0.208	0.594
6	0.719	0.208	0.406	0.176	0.563	0.750	0.270	0.469	0.208	0.594
7	0.719	0.208	0.375	0.176	0.531	0.750	0.270	0.469	0.208	0.594
8	0.719	0.208	0.375	0.176	0.531	0.750	0.270	0.500	0.208	0.594
9	0.719	0.208	0.375	0.176	0.531	0.781	0.333	0.531	0.208	0.594
Average	**0.729**	**0.208**	**0.406**	**0.176**	**0.563**	**0.740**	**0.277**	**0.479**	**0.208**	**0.594**
Initial Skewed Angle (°)		**3.0**								

Table B.1.21 – Test #21, T250_B12_3

	Pre-Fracture Measurements									
	Front Side, inches					Back Side, inches				
Meas. Num.	**Shear Leg**	**Lower**	**Throat**	**Upper**	**Tension Leg**	**Shear Leg**	**Lower**	**Throat**	**Upper**	**Tension Leg**
1	0.750	0.270	0.375	0.176	0.531	0.688	0.270	0.438	0.145	0.531
2	0.750	0.270	0.375	0.145	0.438	0.688	0.208	0.438	0.145	0.531
3	0.750	0.270	0.375	0.145	0.438	0.688	0.208	0.438	0.145	0.531
4	0.781	0.270	0.375	0.145	0.469	0.750	0.270	0.438	0.145	0.531
5	0.719	0.270	0.375	0.145	0.500	0.750	0.270	0.438	0.145	0.531
6	0.719	0.270	0.375	0.145	0.500	0.750	0.270	0.438	0.145	0.531
7	0.719	0.270	0.375	0.145	0.500	0.750	0.270	0.438	0.145	0.531
8	0.719	0.270	0.375	0.145	0.500	0.750	0.270	0.469	0.145	0.531
9	0.719	0.270	0.375	0.145	0.500	0.750	0.270	0.500	0.145	0.531
Average	**0.736**	**0.270**	**0.375**	**0.148**	**0.486**	**0.729**	**0.256**	**0.448**	**0.145**	**0.531**
Initial Skewed Angle (°)		**3.0**								

Table B.1.22 – Test #22, T250_B516_1

	Pre-Fracture Measurements					
	Front Side, inches			Back Side, inches		
Meas. Num.	**Shear Leg**	**Throat**	**Tension Leg**	**Shear Leg**	**Throat**	**Tension Leg**
1	0.438	0.344	0.406	0.469	0.313	0.313
2	0.438	0.344	0.406	0.469	0.313	0.313
3	0.438	0.344	0.406	0.469	0.313	0.313
4	0.438	0.344	0.406	0.500	0.313	0.313
5	0.438	0.344	0.406	0.500	0.313	0.313
6	0.469	0.344	0.406	0.469	0.313	0.313
7	0.438	0.344	0.406	0.469	0.313	0.313
8	0.438	0.344	0.406	0.469	0.313	0.313
9	0.438	0.344	0.406	0.469	0.313	0.313
Average	**0.441**	**0.344**	**0.406**	**0.476**	**0.313**	**0.313**
Initial Skewed Angle (°)		**8.0**				

Table B.1.23 – Test #23, T250_B516_2

	Pre-Fracture Measurements					
	Front Side, inches			Back Side, inches		
Meas. Num.	**Shear Leg**	**Throat**	**Tension Leg**	**Shear Leg**	**Throat**	**Tension Leg**
1	0.500	0.313	0.406	0.469	0.313	0.406
2	0.500	0.313	0.406	0.469	0.313	0.406
3	0.469	0.313	0.406	0.469	0.344	0.406
4	0.469	0.313	0.406	0.531	0.344	0.438
5	0.469	0.313	0.406	0.469	0.313	0.406
6	0.438	0.313	0.406	0.469	0.313	0.406
7	0.500	0.313	0.406	0.469	0.313	0.406
8	0.438	0.344	0.406	0.469	0.313	0.406
9	0.438	0.344	0.406	0.469	0.313	0.406
Mean	**0.469**	**0.319**	**0.406**	**0.476**	**0.319**	**0.410**
Initial Skewed Angle (°)		**8.0**				

Table B.1.24 – Test #24, T250_B516_3

	Pre-Fracture Measurements					
	Front Side, inches			Back Side, inches		
Meas. Num.	**Shear Leg**	**Throat**	**Tension Leg**	**Shear Leg**	**Throat**	**Tension Leg**
1	0.531	0.375	0.375	0.438	0.313	0.313
2	0.531	0.375	0.375	0.438	0.313	0.313
3	0.531	0.375	0.375	0.438	0.313	0.313
4	0.531	0.313	0.344	0.438	0.313	0.313
5	0.531	0.313	0.375	0.438	0.313	0.313
6	0.500	0.313	0.375	0.438	0.313	0.313
7	0.500	0.344	0.375	0.438	0.313	0.313
8	0.500	0.344	0.375	0.406	0.313	0.313
9	0.469	0.344	0.375	0.469	0.313	0.313
Average	**0.514**	**0.344**	**0.372**	**0.438**	**0.313**	**0.313**
Initial Skewed Angle (°)		**8.0**				

Table B.1.25 – Test #25, B125_A516_55_1

	Pre-Fracture Measurements					
	Front Side, inches			Back Side, inches		
Meas. Num.	**Shear Leg**	**Throat**	**Tension Leg**	**Shear Leg**	**Throat**	**Tension Leg**
1 - X	0.531	0.300	0.406	0.438	0.250	0.313
2	0.563	0.306	0.391	0.406	0.256	0.344
3	0.469	0.300	0.375	0.422	0.238	0.344
4	0.531	0.281	0.375	0.438	0.238	0.313
5	0.563	0.294	0.375	0.406	0.250	0.328
6	0.469	0.269	0.359	0.453	0.256	0.344
7	0.500	0.263	0.359	0.422	0.256	0.344
8	0.500	0.288	0.359	0.391	0.256	0.344
Average	**0.516**	**0.286**	**0.374**	**0.423**	**0.249**	**0.335**

Table B.1.26 – Test #26, B125_A516_55_2

	Pre-Fracture Measurements					
	Front Side, inches			Back Side, inches		
Meas. Num.	**Shear Leg**	**Throat**	**Tension Leg**	**Shear Leg**	**Throat**	**Tension Leg**
1 - X	0.516	0.319	0.375	0.438	0.294	0.359
2	0.531	0.313	0.359	0.406	0.294	0.344
3	0.500	0.319	0.375	0.406	0.300	0.375
4	0.484	0.294	0.344	0.453	0.306	0.359
5	0.484	0.300	0.344	0.391	0.300	0.359
6	0.500	0.300	0.328	0.438	0.306	0.344
7	0.516	0.294	0.359	0.469	0.306	0.344
8	0.531	0.306	0.359	0.438	0.313	0.375
Average	**0.505**	**0.304**	**0.354**	**0.428**	**0.302**	**0.356**

Table B.1.27 – Test #27, B125_A516_55_3

	Pre-Fracture Measurements					
	Front Side, inches			Back Side, inches		
Meas. Num.	**Shear Leg**	**Throat**	**Tension Leg**	**Shear Leg**	**Throat**	**Tension Leg**
1 - X	0.500	0.300	0.359	0.438	0.331	0.375
2	0.500	0.294	0.375	0.406	0.313	0.375
3	0.500	0.288	0.375	0.531	0.313	0.375
4	0.500	0.288	0.359	0.469	0.319	0.375
5	0.484	0.256	0.328	0.484	0.313	0.344
6	0.484	0.263	0.344	0.484	0.319	0.375
7	0.438	0.288	0.375	0.500	0.325	0.359
8	0.469	0.306	0.391	0.469	0.319	0.375
Average	**0.484**	**0.282**	**0.361**	**0.476**	**0.318**	**0.368**

Table B.1.28 – Test #28, B125_A12_55_1

	Pre-Fracture Measurements									
	Front Side, inches					Back Side, inches				
Meas. Num.	**Shear Leg**	**Lower**	**Throat**	**Upper**	**Tension Leg**	**Shear Leg**	**Lower**	**Throat**	**Upper**	**Tension Leg**
1 -X	0.750	0.238	0.381	0.119	0.500	0.750	0.281	0.406	0.156	0.500
2	0.719	0.231	0.369	0.125	0.500	0.750	0.281	0.381	0.131	0.469
3	0.750	0.244	0.369	0.125	0.500	0.719	0.281	0.406	0.119	0.500
4	0.688	0.231	0.381	0.119	0.531	0.750	0.300	0.431	0.119	0.469
5	0.750	0.250	0.381	0.125	0.469	0.688	0.306	0.425	0.125	0.531
6	0.688	0.231	0.375	0.125	0.563	0.750	0.313	0.431	0.094	0.531
7	0.719	0.244	0.388	0.156	0.563	0.844	0.306	0.444	0.081	0.500
8	0.656	0.250	0.394	0.131	0.531	0.844	0.306	0.444	0.094	0.500
Average	**0.717**	**0.239**	**0.378**	**0.129**	**0.520**	**0.756**	**0.297**	**0.420**	**0.113**	**0.500**

Table B.1.29 – Test #29, B125_A12_55_2

	Pre-Fracture Measurements									
	Front Side, inches					Back Side, inches				
Meas. Num.	**Shear Leg**	**Lower**	**Throat**	**Upper**	**Tension Leg**	**Shear Leg**	**Lower**	**Throat**	**Upper**	**Tension Leg**
1 -X	0.781	0.250	0.406	0.131	0.531	0.688	0.219	0.481	0.138	0.563
2	0.813	0.250	0.431	0.125	0.531	0.625	0.219	0.406	0.138	0.531
3	0.719	0.250	0.438	0.131	0.563	0.656	0.206	0.425	0.131	0.531
4	0.688	0.250	0.438	0.169	0.563	0.625	0.206	0.381	0.125	0.500
5	0.813	0.244	0.431	0.156	0.531	0.625	0.194	0.381	0.131	0.500
6	0.750	0.250	0.431	0.131	0.500	0.656	0.194	0.375	0.119	0.500
7	0.750	0.238	0.438	0.144	0.531	0.656	0.200	0.375	0.125	0.469
8	0.719	0.231	0.438	0.138	0.500	0.688	0.231	0.381	0.131	0.500
Average	**0.755**	**0.246**	**0.433**	**0.142**	**0.534**	**0.646**	**0.206**	**0.396**	**0.129**	**0.508**

Table B.1.30 – Test #30, B125_A12_55_3

	Pre-Fracture Measurements									
	Front Side, inches					Back Side, inches				
Meas. Num.	**Shear Leg**	**Lower**	**Throat**	**Upper**	**Tension Leg**	**Shear Leg**	**Lower**	**Throat**	**Upper**	**Tension Leg**
1 -X	0.688	0.194	0.406	0.119	0.531	0.625	0.250	0.375	0.081	0.500
2	0.688	0.219	0.406	0.125	0.531	0.656	0.250	0.394	0.106	0.500
3	0.719	0.219	0.438	0.131	0.500	0.656	0.250	0.406	0.094	0.469
4	0.719	0.250	0.431	0.119	0.500	0.688	0.263	0.425	0.119	0.500
5	0.750	0.244	0.431	0.113	0.531	0.719	0.281	0.419	0.106	0.500
6	0.688	0.244	0.444	0.156	0.531	0.719	0.256	0.431	0.119	0.531
7	0.750	0.244	0.406	0.125	0.500	0.750	0.269	0.419	0.113	0.563
8	0.750	0.231	0.406	0.113	0.500	0.750	0.256	0.431	0.119	0.500
Average	**0.719**	**0.233**	**0.424**	**0.127**	**0.516**	**0.697**	**0.260**	**0.414**	**0.108**	**0.509**

Table B.1.31 – Test #31, B175_A516_3_1

	Pre-Fracture Measurements					
	Front Side, inches			Back Side, inches		
Meas. Num.	**Shear Leg**	**Throat**	**Tension Leg**	**Shear Leg**	**Throat**	**Tension Leg**
1 - X	0.500	0.281	0.281	0.422	0.244	0.250
2	0.469	0.263	0.250	0.469	0.256	0.297
3	0.500	0.263	0.313	0.469	0.244	0.344
4	0.453	0.263	0.328	0.469	0.244	0.313
5	0.469	0.263	0.344	0.438	0.219	0.281
6	0.438	0.263	0.313	0.500	0.219	0.281
7	0.469	0.256	0.313	0.500	0.250	0.297
8	0.453	0.244	0.281	0.438	0.244	0.297
Average	**0.467**	**0.262**	**0.306**	**0.468**	**0.239**	**0.299**

Table B.1.32 – Test #32, B125_A516_3_2

	Pre-Fracture Measurements					
	Front Side, inches			Back Side, inches		
Meas. Num.	**Shear Leg**	**Throat**	**Tension Leg**	**Shear Leg**	**Throat**	**Tension Leg**
1 - X	0.531	0.313	0.313	0.438	0.244	0.297
2	0.500	0.300	0.313	0.438	0.250	0.313
3	0.531	0.263	0.313	0.438	0.244	0.297
4	0.484	0.281	0.328	0.469	0.244	0.313
5	0.500	0.288	0.313	0.484	0.231	0.297
6	0.484	0.269	0.313	0.500	0.244	0.313
7	0.469	0.269	0.313	0.469	0.219	0.281
8	0.469	0.269	0.266	0.469	0.231	0.281
Average	**0.495**	**0.280**	**0.312**	**0.465**	**0.238**	**0.300**

Table B.1.33 – Test #33, B125_A516_3_3

	Pre-Fracture Measurements					
	Front Side, inches			Back Side, inches		
Meas. Num.	**Shear Leg**	**Throat**	**Tension Leg**	**Shear Leg**	**Throat**	**Tension Leg**
1 - X	0.391	0.219	0.281	0.453	0.244	0.297
2	0.438	0.225	0.313	0.484	0.269	0.297
3	0.406	0.250	0.313	0.484	0.269	0.313
4	0.406	0.263	0.313	0.469	0.263	0.297
5	0.438	0.263	0.328	0.500	0.263	0.313
6	0.422	0.256	0.313	0.484	0.256	0.344
7	0.422	0.256	0.313	0.500	0.256	0.281
8	0.438	0.250	0.313	0.516	0.250	0.313
Average	**0.421**	**0.250**	**0.313**	**0.487**	**0.261**	**0.307**

Table B.1.34 – Test #34, B175_A12_3_1

	Pre-Fracture Measurements									
	Front Side, inches					Back Side, inches				
Meas. Num.	**Shear Leg**	**Lower**	**Throat**	**Upper**	**Tension Leg**	**Shear Leg**	**Lower**	**Throat**	**Upper**	**Tension Leg**
1 -X	0.776	0.200	0.419	0.069	0.431	0.553	0.163	0.381	0.106	0.500
2	0.800	0.200	0.419	0.069	0.468	0.556	0.144	0.375	0.113	0.469
3	0.779	0.200	0.388	0.069	0.463	0.559	0.138	0.369	0.081	0.469
4	0.765	0.200	0.425	0.106	0.460	0.603	0.163	0.363	0.081	0.484
5	0.728	0.200	0.419	0.094	0.516	0.568	0.144	0.356	0.075	0.469
6	0.709	0.200	0.388	0.069	0.453	0.630	0.169	0.375	0.081	0.484
7	0.773	0.206	0.406	0.081	0.500	0.677	0.175	0.381	0.081	0.500
8	0.837	0.250	0.406	0.075	0.484	0.684	0.181	0.381	0.088	0.500
Average	**0.765**	**0.204**	**0.408**	**0.080**	**0.474**	**0.601**	**0.157**	**0.371**	**0.087**	**0.482**

Table B.1.35 – Test #35, B175_A12_3_2

	Pre-Fracture Measurements									
	Front Side, inches					Back Side, inches				
Meas. Num.	**Shear Leg**	**Lower**	**Throat**	**Upper**	**Tension Leg**	**Shear Leg**	**Lower**	**Throat**	**Upper**	**Tension Leg**
1 -X	0.672	0.206	0.400	0.000	0.469	0.563	0.175	0.375	0.106	0.469
2	0.719	0.200	0.394	0.000	0.484	0.594	0.188	0.381	0.125	0.469
3	0.781	0.219	0.375	0.000	0.500	0.563	0.188	0.394	0.138	0.531
4	0.656	0.213	0.406	0.000	0.438	0.594	0.200	0.413	0.144	0.547
5	0.719	0.206	0.388	0.000	0.469	0.625	0.200	0.394	0.131	0.531
6	0.688	0.200	0.406	0.000	0.438	0.641	0.188	0.413	0.113	0.531
7	0.688	0.200	0.431	0.000	0.500	0.688	0.219	0.406	0.131	0.500
8	0.719	0.219	0.381	0.000	0.406	0.656	0.206	0.425	0.125	0.500
Average	**0.707**	**0.207**	**0.399**	**0.000**	**0.467**	**0.616**	**0.196**	**0.400**	**0.128**	**0.514**

Table B.1.36 – Test #36, B175_A12_3_3

	Pre-Fracture Measurements									
	Front Side, inches					Back Side, inches				
Meas. Num.	**Shear Leg**	**Lower**	**Throat**	**Upper**	**Tension Leg**	**Shear Leg**	**Lower**	**Throat**	**Upper**	**Tension Leg**
1 -X	0.750	0.256	0.400	0.000	0.531	0.688	0.200	0.456	0.113	0.531
2	0.719	0.256	0.400	0.000	0.469	0.688	0.206	0.444	0.125	0.531
3	0.625	0.194	0.369	0.000	0.484	0.656	0.200	0.425	0.106	0.484
4	0.688	0.194	0.381	0.000	0.438	0.641	0.181	0.438	0.125	0.531
5	0.688	0.200	0.381	0.000	0.469	0.656	0.194	0.431	0.125	0.516
6	0.688	0.200	0.388	0.000	0.500	0.656	0.213	0.438	0.125	0.531
7	0.688	0.194	0.363	0.000	0.516	0.688	0.206	0.438	0.113	0.531
8	0.719	0.194	0.381	0.000	0.500	0.625	0.194	0.438	0.131	0.531
Average	**0.689**	**0.209**	**0.382**	**0.000**	**0.484**	**0.663**	**0.200**	**0.437**	**0.120**	**0.522**

Table B.1.37 – Test #37, B175_A516_55_1

	Pre-Fracture Measurements					
	Front Side, inches			Back Side, inches		
Meas. Num.	**Shear Leg**	**Throat**	**Tension Leg**	**Shear Leg**	**Throat**	**Tension Leg**
1 - X	0.462	0.375	0.374	0.503	0.250	0.229
2	0.455	0.328	0.339	0.477	0.250	0.316
3	0.455	0.313	0.327	0.498	0.250	0.287
4	0.478	0.313	0.317	0.472	0.250	0.296
5	0.482	0.313	0.339	0.426	0.250	0.285
6	0.481	0.313	0.328	0.430	0.250	0.270
7	0.470	0.313	0.336	0.486	0.280	0.278
8	0.486	0.313	0.373	0.476	0.280	0.280
9	0.450	0.281	0.387	0.438	0.250	0.289
Average	**0.471**	**0.316**	**0.342**	**0.467**	**0.258**	**0.284**

Table B.1.38 – Test #38, B175_A516_55_2

	Pre-Fracture Measurements					
	Front Side, inches			Back Side, inches		
Meas. Num.	**Shear Leg**	**Throat**	**Tension Leg**	**Shear Leg**	**Throat**	**Tension Leg**
1 - X	0.422	0.297	0.356	0.425	0.234	0.300
2	0.446	0.297	0.355	0.460	0.250	0.294
3	0.442	0.281	0.336	0.423	0.250	0.294
4	0.438	0.281	0.335	0.441	0.250	0.277
5	0.445	0.313	0.352	0.422	0.250	0.299
6	0.451	0.313	0.352	0.443	0.250	0.294
7	0.433	0.297	0.350	0.412	0.234	0.273
8	0.487	0.297	0.349	0.439	0.250	0.310
9	0.484	0.313	0.355	0.390	0.234	0.307
Average	**0.449**	**0.298**	**0.348**	**0.431**	**0.246**	**0.293**

Table B.1.39 – Test #39, B175_A516_55_3

	Pre-Fracture Measurements					
	Front Side, inches			Back Side, inches		
Meas. Num.	**Shear Leg**	**Throat**	**Tension Leg**	**Shear Leg**	**Throat**	**Tension Leg**
1 - X	0.493	0.313	0.395	0.499	0.281	0.324
2	0.508	0.297	0.325	0.455	0.297	0.324
3	0.465	0.266	0.339	0.462	0.297	0.314
4	0.477	0.281	0.320	0.444	0.297	0.311
5	0.515	0.281	0.281	0.442	0.250	0.312
6	0.454	0.281	0.281	0.438	0.281	0.312
7	0.508	0.281	0.339	0.440	0.250	0.303
8	0.474	0.297	0.304	0.468	0.250	0.310
9	0.494	0.313	0.365	0.428	0.281	0.322
Average	**0.487**	**0.287**	**0.320**	**0.451**	**0.275**	**0.313**

Table B.1.40 – Test #40, B175_A12_55_1

	Pre-Fracture Measurements									
	Front Side, inches					Back Side, inches				
Meas. Num.	**Shear Leg**	**Lower**	**Throat**	**Upper**	**Tension Leg**	**Shear Leg**	**Lower**	**Throat**	**Upper**	**Tension Leg**
1 -X	0.781	0.250	0.438	0.125	0.531	0.813	0.213	0.406	0.075	0.531
2	0.750	0.250	0.444	0.125	0.563	0.719	0.206	0.406	0.063	0.500
3	0.781	0.256	0.425	0.131	0.500	0.719	0.188	0.381	0.069	0.500
4	0.719	0.238	0.425	0.131	0.531	0.750	0.188	0.375	0.069	0.469
5	0.719	0.244	0.425	0.131	0.531	0.719	0.188	0.369	0.069	0.500
6	0.719	0.238	0.431	0.131	0.563	0.719	0.188	0.375	0.075	0.500
7	0.688	0.206	0.431	0.131	0.531	0.688	0.188	0.375	0.075	0.531
8	0.719	0.213	0.406	0.131	0.500	0.719	0.188	0.394	0.094	0.531
Average	**0.732**	**0.238**	**0.429**	**0.130**	**0.534**	**0.725**	**0.192**	**0.383**	**0.072**	**0.504**

Table B.1.41 – Test #41, B175_A12_55_2

	Pre-Fracture Measurements									
	Front Side, inches					Back Side, inches				
Meas. Num.	**Shear Leg**	**Lower**	**Throat**	**Upper**	**Tension Leg**	**Shear Leg**	**Lower**	**Throat**	**Upper**	**Tension Leg**
1 -X	0.719	0.194	0.425	0.119	0.531	0.656	0.181	0.394	0.094	0.531
2	0.656	0.188	0.431	0.131	0.531	0.688	0.188	0.388	0.081	0.500
3	0.688	0.175	0.431	0.131	0.531	0.656	0.188	0.381	0.081	0.500
4	0.688	0.181	0.431	0.119	0.500	0.719	0.188	0.381	0.075	0.500
5	0.625	0.181	0.431	0.119	0.500	0.688	0.188	0.381	0.088	0.500
6	0.688	0.181	0.431	0.119	0.500	0.625	0.200	0.381	0.088	0.438
7	0.563	0.181	0.425	0.125	0.500	0.625	0.188	0.381	0.088	0.500
8	0.563	0.181	0.425	0.119	0.500	0.625	0.194	0.381	0.094	0.469
Average	**0.650**	**0.182**	**0.430**	**0.123**	**0.511**	**0.663**	**0.189**	**0.383**	**0.085**	**0.491**

Table B.1.42 – Test #42, B175_A12_55_3

	Pre-Fracture Measurements									
	Front Side, inches					Back Side, inches				
Meas. Num.	**Shear Leg**	**Lower**	**Throat**	**Upper**	**Tension Leg**	**Shear Leg**	**Lower**	**Throat**	**Upper**	**Tension Leg**
1 -X	0.625	0.181	0.406	0.131	0.500	0.625	0.250	0.444	0.119	0.531
2	0.594	0.181	0.425	0.131	0.531	0.656	0.250	0.431	0.119	0.500
3	0.594	0.188	0.419	0.125	0.531	0.625	0.219	0.406	0.069	0.500
4	0.625	0.181	0.419	0.125	0.531	0.719	0.263	0.438	0.113	0.531
5	0.625	0.219	0.425	0.131	0.531	0.813	0.281	0.406	0.075	0.531
6	0.656	0.219	0.431	0.131	0.531	0.719	0.250	0.431	0.119	0.531
7	0.688	0.238	0.438	0.131	0.531	0.719	0.263	0.438	0.119	0.531
8	0.719	0.256	0.475	0.125	0.531	0.719	0.281	0.438	0.119	0.500
Average	**0.635**	**0.206**	**0.428**	**0.129**	**0.529**	**0.704**	**0.256**	**0.427**	**0.104**	**0.520**

Table B.1.43 – Test #43, B175_A516_85_1

	Pre-Fracture Measurements					
	Front Side, inches			Back Side, inches		
Meas. Num.	**Shear Leg**	**Throat**	**Tension Leg**	**Shear Leg**	**Throat**	**Tension Leg**
1 - X	0.469	0.281	0.344	0.500	0.281	0.344
2	0.469	0.281	0.344	0.500	0.313	0.344
3	0.469	0.250	0.406	0.500	0.281	0.344
4	0.500	0.313	0.438	0.469	0.281	0.344
5	0.531	0.281	0.438	0.438	0.250	0.313
6	0.531	0.281	0.438	0.438	0.250	0.344
7	0.500	0.281	0.406	0.469	0.250	0.344
8	0.500	0.281	0.406	0.438	0.313	0.375
Average	**0.498**	**0.281**	**0.407**	**0.469**	**0.274**	**0.341**

Table B.1.44 – Test #44, B175_A516_85_2

	Pre-Fracture Measurements					
	Front Side, inches			Back Side, inches		
Meas. Num.	**Shear Leg**	**Throat**	**Tension Leg**	**Shear Leg**	**Throat**	**Tension Leg**
1 - X	0.469	0.250	0.375	0.531	0.281	0.375
2	0.469	0.250	0.375	0.531	0.281	0.375
3	0.469	0.250	0.375	0.531	0.250	0.344
4	0.500	0.281	0.406	0.500	0.250	0.344
5	0.500	0.281	0.375	0.531	0.250	0.375
6	0.500	0.281	0.375	0.531	0.281	0.344
7	0.500	0.281	0.344	0.469	0.250	0.406
8	0.500	0.250	0.313	0.500	0.281	0.438
Average	**0.489**	**0.268**	**0.371**	**0.516**	**0.263**	**0.370**

Table B.1.45 – Test #45, B175_A516_85_3

	Pre-Fracture Measurements					
	Front Side, inches			Back Side, inches		
Meas. Num.	**Shear Leg**	**Throat**	**Tension Leg**	**Shear Leg**	**Throat**	**Tension Leg**
1 - X	0.469	0.271	0.438	0.590	0.351	0.406
2	0.438	0.271	0.438	0.560	0.326	0.375
3	0.438	0.271	0.406	0.590	0.311	0.406
4	0.438	0.265	0.344	0.560	0.318	0.406
5	0.406	0.263	0.344	0.530	0.283	0.406
6	0.188	0.264	0.344	0.530	0.305	0.406
7	0.219	0.261	0.375	0.530	0.312	0.406
8	0.531	0.261	0.375	0.530	0.312	0.375
Average	**0.373**	**0.266**	**0.379**	**0.551**	**0.312**	**0.400**

Table B.1.46 – Test #46, B175_A12_85_1

	Pre-Fracture Measurements									
	Front Side, inches					Back Side, inches				
Meas. Num.	**Shear Leg**	**Lower**	**Throat**	**Upper**	**Tension Leg**	**Shear Leg**	**Lower**	**Throat**	**Upper**	**Tension Leg**
1 -X	0.563	0.156	0.431	0.125	0.531	0.625	0.188	0.381	0.000	0.594
2	0.625	0.188	0.431	0.119	0.531	0.563	0.181	0.406	0.131	0.563
3	0.656	0.238	0.438	0.125	0.563	0.594	0.188	0.381	0.131	0.594
4	0.688	0.194	0.438	0.125	0.563	0.625	0.194	0.381	0.125	0.531
5	0.625	0.188	0.438	0.125	0.531	0.594	0.188	0.406	0.125	0.531
6	0.625	0.194	0.438	0.125	0.563	0.625	0.194	0.425	0.125	0.563
7	0.656	0.188	0.444	0.125	0.594	0.594	0.194	0.431	0.125	0.563
8	0.625	0.188	0.431	0.125	0.531	0.625	0.194	0.394	0.131	0.500
Average	**0.639**	**0.195**	**0.437**	**0.124**	**0.554**	**0.602**	**0.190**	**0.403**	**0.119**	**0.556**

Table B.1.47 – Test #47, B175_A12_85_2

	Pre-Fracture Measurements									
	Front Side, inches					Back Side, inches				
Meas. Num.	**Shear Leg**	**Lower**	**Throat**	**Upper**	**Tension Leg**	**Shear Leg**	**Lower**	**Throat**	**Upper**	**Tension Leg**
1 -X	0.625	0.194	0.438	0.119	0.531	0.719	0.219	0.425	0.094	0.531
2	0.625	0.188	0.431	0.113	0.500	0.688	0.244	0.438	0.125	0.531
3	0.656	0.194	0.438	0.069	0.500	0.656	0.231	0.419	0.131	0.500
4	0.625	0.188	0.438	0.119	0.531	0.625	0.200	0.419	0.125	0.500
5	0.625	0.194	0.431	0.125	0.563	0.656	0.219	0.438	0.125	0.531
6	0.625	0.188	0.431	0.125	0.563	0.656	0.206	0.431	0.119	0.563
7	0.563	0.194	0.431	0.119	0.531	0.688	0.244	0.419	0.125	0.531
8	0.531	0.156	0.438	0.125	0.500	0.656	0.244	0.406	0.125	0.531
Average	**0.615**	**0.189**	**0.434**	**0.113**	**0.529**	**0.665**	**0.225**	**0.426**	**0.123**	**0.527**

Table B.1.48 – Test #48, B175_A12_85_3

	Pre-Fracture Measurements									
	Front Side, inches					Back Side, inches				
Meas. Num.	**Shear Leg**	**Lower**	**Throat**	**Upper**	**Tension Leg**	**Shear Leg**	**Lower**	**Throat**	**Upper**	**Tension Leg**
1 -X	0.750	0.194	0.431	0.131	0.531	0.750	0.188	0.419	0.125	0.563
2	0.656	0.188	0.431	0.138	0.563	0.719	0.188	0.406	0.094	0.531
3	0.594	0.188	0.438	0.138	0.563	0.688	0.188	0.431	0.125	0.500
4	0.656	0.188	0.406	0.125	0.594	0.719	0.194	0.494	0.125	0.531
5	0.656	0.194	0.406	0.125	0.563	0.750	0.194	0.438	0.119	0.563
6	0.750	0.194	0.381	0.119	0.531	0.750	0.244	0.438	0.156	0.594
7	0.813	0.244	0.406	0.138	0.563	0.750	0.219	0.425	0.131	0.594
8	0.844	0.256	0.438	0.156	0.531	0.781	0.219	0.438	0.125	0.563
Average	**0.701**	**0.202**	**0.414**	**0.132**	**0.559**	**0.734**	**0.204**	**0.437**	**0.125**	**0.553**

Table B.1.49 – Test #49, B250_A516_55_1

	Pre-Fracture Measurements					
	Front Side, inches			Back Side, inches		
Meas. Num.	**Shear Leg**	**Throat**	**Tension Leg**	**Shear Leg**	**Throat**	**Tension Leg**
1 - X	0.509	0.328	0.402	0.478	0.250	0.272
2	0.523	0.313	0.403	0.517	0.250	0.318
3	0.521	0.313	0.406	0.473	0.266	0.309
4	0.571	0.344	0.388	0.502	0.250	0.316
5	0.606	0.328	0.379	0.467	0.250	0.278
6	0.562	0.344	0.365	0.501	0.250	0.305
7	0.556	0.313	0.394	0.490	0.250	0.287
8	0.574	0.328	0.355	0.479	0.266	0.306
9	0.582	0.297	0.371	0.452	0.250	0.270
Average	**0.558**	**0.324**	**0.385**	**0.487**	**0.254**	**0.299**

Table B.1.50 – Test #50, B250_A516_55_2

	Pre-Fracture Measurements					
	Front Side, inches			Back Side, inches		
Meas. Num.	**Shear Leg**	**Throat**	**Tension Leg**	**Shear Leg**	**Throat**	**Tension Leg**
1 - X	0.561	0.328	0.357	0.448	0.281	0.309
2	0.548	0.297	0.330	0.457	0.297	0.314
3	0.542	0.297	0.366	0.476	0.297	0.320
4	0.534	0.313	0.382	0.489	0.281	0.313
5	0.608	0.313	0.392	0.519	0.281	0.324
6	0.594	0.344	0.406	0.483	0.281	0.279
7	0.603	0.328	0.349	0.474	0.266	0.304
8	0.614	0.328	0.360	0.496	0.281	0.296
9	0.614	0.328	0.359	0.479	0.250	0.296
Average	**0.579**	**0.318**	**0.368**	**0.482**	**0.281**	**0.307**

Table B.1.51 – Test #51, B250_A516_55_3

	Pre-Fracture Measurements					
	Front Side, inches			Back Side, inches		
Meas. Num.	**Shear Leg**	**Throat**	**Tension Leg**	**Shear Leg**	**Throat**	**Tension Leg**
1 - X	0.549	0.281	0.384	0.478	0.250	0.275
2	0.560	0.313	0.355	0.459	0.281	0.312
3	0.537	0.313	0.332	0.492	0.313	0.326
4	0.551	0.281	0.312	0.507	0.297	0.335
5	0.526	0.297	0.350	0.510	0.313	0.335
6	0.520	0.313	0.323	0.551	0.281	0.351
7	0.529	0.313	0.336	0.547	0.266	0.310
8	0.553	0.328	0.346	0.504	0.281	0.321
9	0.603	0.281	0.327	0.565	0.250	0.299
Average	**0.543**	**0.305**	**0.338**	**0.511**	**0.286**	**0.323**

Table B.1.52 – Test #52, B250_A12_55_1

	Pre-Fracture Measurements									
	Front Side, inches					Back Side, inches				
Meas. Num.	**Shear Leg**	**Lower**	**Throat**	**Upper**	**Tension Leg**	**Shear Leg**	**Lower**	**Throat**	**Upper**	**Tension Leg**
1 -X	0.875	0.206	0.394	0.119	0.500	0.750	0.219	0.381	0.069	0.500
2	0.844	0.181	0.388	0.106	0.469	0.750	0.238	0.419	0.106	0.500
3	0.813	0.181	0.388	0.106	0.500	0.719	0.219	0.419	0.119	0.531
4	0.750	0.150	0.388	0.100	0.469	0.719	0.194	0.394	0.119	0.500
5	0.750	0.150	0.369	0.088	0.469	0.688	0.188	0.375	0.119	0.500
6	0.781	0.169	0.381	0.081	0.500	0.688	0.181	0.375	0.125	0.500
7	0.781	0.175	0.369	0.081	0.469	0.656	0.181	0.406	0.125	0.500
8	0.750	0.175	0.369	0.081	0.500	0.656	0.175	0.400	0.125	0.531
Average	**0.790**	**0.171**	**0.380**	**0.095**	**0.482**	**0.703**	**0.200**	**0.397**	**0.116**	**0.507**

Table B.1.53 – Test #53, B250_A12_55_2

	Pre-Fracture Measurements									
	Front Side, inches					Back Side, inches				
Meas. Num.	**Shear Leg**	**Lower**	**Throat**	**Upper**	**Tension Leg**	**Shear Leg**	**Lower**	**Throat**	**Upper**	**Tension Leg**
1 -X	0.719	0.175	0.363	0.119	0.500	0.688	0.194	0.369	0.063	0.406
2	0.750	0.175	0.369	0.081	0.500	0.688	0.188	0.369	0.056	0.500
3	0.688	0.188	0.356	0.063	0.438	0.688	0.188	0.369	0.094	0.500
4	0.750	0.188	0.369	0.088	0.469	0.719	0.219	0.375	0.113	0.469
5	0.781	0.188	0.375	0.094	0.500	0.750	0.219	0.375	0.113	0.469
6	0.813	0.188	0.381	0.119	0.531	0.781	0.238	0.375	0.106	0.438
7	0.813	0.188	0.381	0.119	0.531	0.688	0.250	0.406	0.056	0.469
8	0.844	0.200	0.381	0.106	0.531	0.781	0.250	0.406	0.056	0.531
Average	**0.768**	**0.186**	**0.372**	**0.096**	**0.497**	**0.721**	**0.217**	**0.379**	**0.086**	**0.473**

Table B.1.54 – Test #54, B250_A12_55_3

	Pre-Fracture Measurements									
	Front Side, inches					Back Side, inches				
Meas. Num.	**Shear Leg**	**Lower**	**Throat**	**Upper**	**Tension Leg**	**Shear Leg**	**Lower**	**Throat**	**Upper**	**Tension Leg**
1 -X	0.750	0.181	0.425	0.094	0.469	0.656	0.181	0.444	0.131	0.500
2	0.750	0.181	0.381	0.094	0.438	0.656	0.181	0.444	0.131	0.531
3	0.813	0.175	0.381	0.094	0.438	0.656	0.188	0.444	0.131	0.500
4	0.750	0.175	0.381	0.075	0.438	0.656	0.188	0.438	0.131	0.500
5	0.719	0.181	0.381	0.081	0.438	0.656	0.194	0.438	0.131	0.500
6	0.719	0.181	0.381	0.125	0.469	0.625	0.194	0.406	0.138	0.500
7	0.719	0.181	0.369	0.138	0.469	0.688	0.194	0.413	0.138	0.469
8	0.719	0.181	0.356	0.125	0.500	0.656	0.194	0.406	0.131	0.500
Average	**0.743**	**0.179**	**0.381**	**0.102**	**0.452**	**0.656**	**0.189**	**0.430**	**0.133**	**0.500**

Table B.1.55 – Test #55, B125_B516_55_1

	Pre-Fracture Measurements					
	Front Side, inches			Back Side, inches		
Meas. Num.	**Shear Leg**	**Throat**	**Tension Leg**	**Shear Leg**	**Throat**	**Tension Leg**
1 - X	0.563	0.306	0.375	0.531	0.319	0.375
2	0.531	0.319	0.375	0.500	0.344	0.406
3	0.531	0.356	0.406	0.500	0.325	0.375
4	0.469	0.319	0.375	0.531	0.331	0.406
5	0.500	0.313	0.344	0.500	0.319	0.375
6	0.469	0.319	0.344	0.531	0.313	0.375
7	0.438	0.294	0.375	0.531	0.313	0.344
8	0.500	0.313	0.375	0.531	0.369	0.406
Average	**0.495**	**0.318**	**0.370**	**0.518**	**0.326**	**0.382**

Table B.1.56 – Test #56, B125_B516_55_2

	Pre-Fracture Measurements					
	Front Side, inches			Back Side, inches		
Meas. Num.	**Shear Leg**	**Throat**	**Tension Leg**	**Shear Leg**	**Throat**	**Tension Leg**
1 - X	0.563	0.350	0.344	0.500	0.294	0.344
2	0.531	0.375	0.344	0.500	0.306	0.344
3	0.500	0.356	0.344	0.531	0.313	0.406
4	0.500	0.325	0.344	0.500	0.281	0.375
5	0.500	0.356	0.406	0.500	0.313	0.375
6	0.500	0.369	0.375	0.500	0.313	0.375
7	0.531	0.344	0.375	0.531	0.313	0.406
8	0.531	0.363	0.375	0.531	0.319	0.406
Average	**0.515**	**0.354**	**0.364**	**0.511**	**0.306**	**0.380**

Table B.1.57 – Test #57, B125_B516_55_3

	Pre-Fracture Measurements					
	Front Side, inches			Back Side, inches		
Meas. Num.	**Shear Leg**	**Throat**	**Tension Leg**	**Shear Leg**	**Throat**	**Tension Leg**
1 - X	0.531	0.306	0.313	0.500	0.294	0.406
2	0.500	0.313	0.375	0.531	0.369	0.375
3	0.469	0.306	0.344	0.531	0.344	0.406
4	0.469	0.300	0.313	0.563	0.313	0.438
5	0.438	0.294	0.313	0.531	0.250	0.406
6	0.469	0.294	0.344	0.531	0.294	0.375
7	0.438	0.288	0.344	0.531	0.250	0.406
8	0.500	0.306	0.344	0.531	0.250	0.406
Average	**0.470**	**0.300**	**0.337**	**0.534**	**0.299**	**0.402**

Table B.1.58 – Test #58, B125_B12_55_1

	Pre-Fracture Measurements									
	Front Side, inches					Back Side, inches				
Meas. Num.	**Shear Leg**	**Lower**	**Throat**	**Upper**	**Tension Leg**	**Shear Leg**	**Lower**	**Throat**	**Upper**	**Tension Leg**
1 -X	0.750	0.238	0.425	0.131	0.531	0.625	0.188	0.375	0.125	0.563
2	0.750	0.219	0.406	0.119	0.531	0.625	0.194	0.419	0.094	0.531
3	0.719	0.219	0.394	0.119	0.531	0.625	0.206	0.381	0.125	0.531
4	0.719	0.206	0.388	0.131	0.531	0.594	0.200	0.400	0.138	0.531
5	0.656	0.194	0.381	0.144	0.531	0.594	0.200	0.388	0.169	0.500
6	0.688	0.194	0.381	0.156	0.563	0.625	0.219	0.406	0.169	0.531
7	0.656	0.188	0.381	0.131	0.531	0.688	0.250	0.419	0.169	0.531
8	0.719	0.194	0.394	0.156	0.563	0.750	0.250	0.419	0.219	0.531
Average	**0.702**	**0.205**	**0.391**	**0.135**	**0.538**	**0.633**	**0.212**	**0.401**	**0.147**	**0.529**

Table B.1.59 – Test #59, B125_B12_55_2

	Pre-Fracture Measurements									
	Front Side, inches					Back Side, inches				
Meas. Num.	**Shear Leg**	**Lower**	**Throat**	**Upper**	**Tension Leg**	**Shear Leg**	**Lower**	**Throat**	**Upper**	**Tension Leg**
1 -X	0.750	0.281	0.456	0.125	0.500	0.625	0.175	0.431	0.069	0.469
2	0.688	0.256	0.444	0.119	0.500	0.656	0.188	0.394	0.081	0.438
3	0.750	0.306	0.450	0.131	0.500	0.688	0.194	0.381	0.119	0.500
4	0.719	0.281	0.431	0.131	0.500	0.625	0.194	0.388	0.131	0.531
5	0.688	0.250	0.438	0.156	0.500	0.625	0.200	0.369	0.144	0.469
6	0.625	0.244	0.400	0.144	0.531	0.656	0.200	0.381	0.131	0.469
7	0.719	0.281	0.438	0.094	0.531	0.563	0.188	0.381	0.144	0.469
8	0.719	0.250	0.419	0.181	0.500	0.594	0.188	0.381	0.131	0.500
Average	**0.702**	**0.269**	**0.434**	**0.132**	**0.509**	**0.632**	**0.192**	**0.385**	**0.122**	**0.480**

Table B.1.60 – Test #60, B125_B12_55_3

	Pre-Fracture Measurements									
	Front Side, inches					Back Side, inches				
Meas. Num.	**Shear Leg**	**Lower**	**Throat**	**Upper**	**Tension Leg**	**Shear Leg**	**Lower**	**Throat**	**Upper**	**Tension Leg**
1 -X	0.781	0.206	0.381	0.169	0.594	0.625	0.156	0.425	0.169	0.563
2	0.625	0.194	0.381	0.169	0.594	0.656	0.194	0.438	0.125	0.563
3	0.625	0.194	0.344	0.156	0.563	0.688	0.219	0.438	0.181	0.563
4	0.625	0.194	0.356	0.119	0.531	0.656	0.238	0.438	0.138	0.594
5	0.594	0.188	0.375	0.119	0.563	0.750	0.250	0.450	0.188	0.594
6	0.594	0.188	0.356	0.131	0.594	0.688	0.250	0.444	0.181	0.563
7	0.594	0.219	0.369	0.131	0.594	0.656	0.250	0.456	0.194	0.563
8	0.625	0.244	0.381	0.156	0.594	0.750	0.256	0.456	0.169	0.531
Average	**0.621**	**0.199**	**0.366**	**0.141**	**0.576**	**0.683**	**0.230**	**0.443**	**0.168**	**0.570**

Table B.1.61 – Test #61, B175_B516_3_1

	Pre-Fracture Measurements					
	Front Side, inches			Back Side, inches		
Meas. Num.	**Shear Leg**	**Throat**	**Tension Leg**	**Shear Leg**	**Throat**	**Tension Leg**
1 - X	0.516	0.319	0.375	0.531	0.375	0.406
2	0.453	0.319	0.359	0.531	0.363	0.406
3	0.406	0.306	0.359	0.516	0.344	0.375
4	0.453	0.306	0.313	0.578	0.331	0.359
5	0.469	0.325	0.281	0.563	0.356	0.391
6	0.484	0.306	0.313	0.625	0.369	0.359
7	0.469	0.281	0.281	0.609	0.363	0.313
8	0.484	0.256	0.281	0.563	0.344	0.313
Average	**0.461**	**0.305**	**0.319**	**0.567**	**0.355**	**0.366**

Table B.1.62 – Test #62, B175_B516_3_2

	Pre-Fracture Measurements					
	Front Side, inches			Back Side, inches		
Meas. Num.	**Shear Leg**	**Throat**	**Tension Leg**	**Shear Leg**	**Throat**	**Tension Leg**
1 - X	0.469	0.263	0.281	0.500	0.294	0.250
2	0.500	0.269	0.313	0.563	0.294	0.281
3	0.453	0.263	0.313	0.563	0.319	0.344
4	0.453	0.288	0.328	0.469	0.300	0.344
5	0.422	0.294	0.328	0.500	0.319	0.359
6	0.438	0.275	0.344	0.500	0.294	0.344
7	0.438	0.300	0.359	0.500	0.300	0.328
8	0.438	0.313	0.359	0.500	0.306	0.281
Average	**0.451**	**0.282**	**0.329**	**0.514**	**0.304**	**0.325**

Table B.1.63 – Test #63, B175_B516_3_3

	Pre-Fracture Measurements					
	Front Side, inches			Back Side, inches		
Meas. Num.	**Shear Leg**	**Throat**	**Tension Leg**	**Shear Leg**	**Throat**	**Tension Leg**
1 - X	0.438	0.319	0.344	0.406	0.306	0.344
2	0.500	0.313	0.344	0.438	0.300	0.313
3	0.469	0.319	0.344	0.469	0.306	0.313
4	0.469	0.319	0.344	0.531	0.313	0.313
5	0.500	0.313	0.344	0.531	0.306	0.313
6	0.469	0.313	0.344	0.563	0.300	0.313
7	0.469	0.319	0.375	0.500	0.300	0.313
8	0.500	0.313	0.344	0.531	0.306	0.281
Average	**0.478**	**0.316**	**0.348**	**0.501**	**0.304**	**0.313**

Table B.1.64 – Test #64, B175_B12_3_1

	Pre-Fracture Measurements									
	Front Side, inches					Back Side, inches				
Meas. Num.	**Shear Leg**	**Lower**	**Throat**	**Upper**	**Tension Leg**	**Shear Leg**	**Lower**	**Throat**	**Upper**	**Tension Leg**
1 -X	0.625	0.175	0.406	0.125	0.563	0.750	0.238	0.444	0.144	0.531
2	0.625	0.188	0.413	0.131	0.500	0.719	0.231	0.431	0.163	0.500
3	0.656	0.144	0.406	0.131	0.500	0.719	0.244	0.431	0.144	0.531
4	0.594	0.175	0.419	0.144	0.563	0.688	0.194	0.419	0.138	0.500
5	0.656	0.156	0.406	0.138	0.563	0.688	0.213	0.450	0.138	0.531
6	0.594	0.169	0.394	0.119	0.563	0.688	0.206	0.444	0.119	0.531
7	0.625	0.175	0.406	0.113	0.531	0.719	0.206	0.438	0.125	0.500
8	0.688	0.181	0.438	0.119	0.531	0.625	0.194	0.438	0.125	0.500
Average	**0.629**	**0.169**	**0.409**	**0.128**	**0.538**	**0.701**	**0.216**	**0.436**	**0.137**	**0.516**

Table B.1.65 – Test #65, B175_B12_3_2

	Pre-Fracture Measurements									
	Front Side, inches					Back Side, inches				
Meas. Num.	**Shear Leg**	**Lower**	**Throat**	**Upper**	**Tension Leg**	**Shear Leg**	**Lower**	**Throat**	**Upper**	**Tension Leg**
1 -X	0.656	0.213	0.444	0.131	0.531	0.750	0.194	0.388	0.119	0.500
2	0.688	0.231	0.488	0.131	0.563	0.625	0.188	0.388	0.119	0.531
3	0.688	0.188	0.419	0.131	0.531	0.688	0.188	0.394	0.119	0.531
4	0.719	0.219	0.431	0.131	0.531	0.625	0.188	0.375	0.119	0.500
5	0.719	0.200	0.431	0.131	0.469	0.688	0.181	0.381	0.106	0.500
6	0.688	0.206	0.431	0.106	0.438	0.688	0.181	0.388	0.106	0.563
7	0.656	0.206	0.406	0.094	0.500	0.625	0.181	0.406	0.119	0.531
8	0.656	0.194	0.425	0.119	0.531	0.750	0.206	0.394	0.113	0.500
Average	**0.688**	**0.208**	**0.434**	**0.121**	**0.508**	**0.668**	**0.186**	**0.389**	**0.115**	**0.523**

Table B.1.66 – Test #66, B175_B12_3_3

	Pre-Fracture Measurements									
	Front Side, inches					Back Side, inches				
Meas. Num.	**Shear Leg**	**Lower**	**Throat**	**Upper**	**Tension Leg**	**Shear Leg**	**Lower**	**Throat**	**Upper**	**Tension Leg**
1 -X	0.656	0.194	0.406	0.106	0.500	0.719	0.194	0.425	0.094	0.469
2	0.594	0.181	0.406	0.094	0.531	0.656	0.194	0.438	0.094	0.469
3	0.594	0.169	0.406	0.094	0.531	0.719	0.194	0.438	0.094	0.500
4	0.656	0.169	0.406	0.081	0.531	0.656	0.188	0.438	0.094	0.500
5	0.594	0.169	0.425	0.125	0.531	0.625	0.188	0.431	0.119	0.500
6	0.594	0.175	0.425	0.125	0.531	0.656	0.188	0.431	0.119	0.500
7	0.594	0.181	0.406	0.113	0.500	0.719	0.219	0.431	0.138	0.500
8	0.594	0.188	0.438	0.113	0.531	0.719	0.200	0.431	0.131	0.500
Average	**0.607**	**0.176**	**0.414**	**0.106**	**0.525**	**0.678**	**0.195**	**0.434**	**0.110**	**0.493**

Table B.1.67 – Test #67, B175_B516_55_1

	Pre-Fracture Measurements					
	Front Side, inches			Back Side, inches		
Meas. Num.	**Shear Leg**	**Throat**	**Tension Leg**	**Shear Leg**	**Throat**	**Tension Leg**
1 - X	0.740	0.281	0.402	0.540	0.281	0.296
2	0.749	0.328	0.377	0.504	0.281	0.306
3	0.666	0.281	0.406	0.469	0.297	0.326
4	0.705	0.344	0.462	0.480	0.281	0.338
5	0.706	0.344	0.470	0.424	0.266	0.299
6	0.836	0.344	0.405	0.441	0.266	0.329
7	0.706	0.344	0.400	0.446	0.281	0.361
8	0.742	0.359	0.405	0.444	0.297	0.326
9	0.720	0.313	0.456	0.404	0.281	0.322
Average	**0.730**	**0.331**	**0.419**	**0.460**	**0.281**	**0.324**

Table B.1.68 – Test #68, B175_B516_55_2

	Pre-Fracture Measurements					
	Front Side, inches			Back Side, inches		
Meas. Num.	**Shear Leg**	**Throat**	**Tension Leg**	**Shear Leg**	**Throat**	**Tension Leg**
1 - X	0.727	0.281	0.393	0.500	0.281	0.304
2	0.755	0.344	0.451	0.482	0.281	0.281
3	0.762	0.375	0.467	0.514	0.281	0.303
4	0.742	0.328	0.406	0.553	0.281	0.259
5	0.794	0.375	0.401	0.554	0.281	0.246
6	0.736	0.328	0.377	0.539	0.297	0.248
7	0.836	0.328	0.408	0.521	0.281	0.217
8	0.752	0.375	0.406	0.573	0.281	0.242
9	0.839	0.281	0.416	0.509	0.281	0.290
Average	**0.770**	**0.343**	**0.415**	**0.530**	**0.283**	**0.261**

Table B.1.69 – Test #69, B175_B516_55_3

	Pre-Fracture Measurements					
	Front Side, inches			Back Side, inches		
Meas. Num.	**Shear Leg**	**Throat**	**Tension Leg**	**Shear Leg**	**Throat**	**Tension Leg**
1 - X	0.459	0.281	0.337	0.516	0.281	0.299
2	0.459	0.297	0.357	0.453	0.281	0.322
3	0.463	0.297	0.349	0.510	0.266	0.293
4	0.439	0.281	0.332	0.484	0.266	0.256
5	0.447	0.297	0.333	0.481	0.234	0.258
6	0.452	0.297	0.342	0.407	0.234	0.257
7	0.452	0.297	0.322	0.437	0.234	0.275
8	0.434	0.297	0.314	0.418	0.250	0.275
Average	**0.451**	**0.294**	**0.337**	**0.463**	**0.254**	**0.278**

Table B.1.70 – Test #70, B175_B12_55_1

	Pre-Fracture Measurements									
	Front Side, inches					Back Side, inches				
Meas. Num.	**Shear Leg**	**Lower**	**Throat**	**Upper**	**Tension Leg**	**Shear Leg**	**Lower**	**Throat**	**Upper**	**Tension Leg**
1 -X	0.719	0.194	0.444	0.144	0.438	0.656	0.238	0.431	0.131	0.563
2	0.719	0.263	0.444	0.138	0.469	0.688	0.244	0.425	0.131	0.531
3	0.688	0.206	0.431	0.156	0.531	0.719	0.244	0.431	0.138	0.531
4	0.656	0.188	0.438	0.156	0.531	0.688	0.244	0.431	0.113	0.469
5	0.656	0.194	0.438	0.156	0.469	0.781	0.250	0.438	0.138	0.531
6	0.719	0.181	0.425	0.131	0.563	0.719	0.263	0.438	0.144	0.500
7	0.625	0.194	0.431	0.131	0.500	0.688	0.244	0.444	0.156	0.531
8	0.656	0.194	0.431	0.125	0.500	0.719	0.250	0.425	0.175	0.531
Average	**0.678**	**0.203**	**0.435**	**0.143**	**0.505**	**0.710**	**0.247**	**0.434**	**0.139**	**0.520**

Table B.1.71 – Test #71, B175_B12_55_2

	Pre-Fracture Measurements									
	Front Side, inches					Back Side, inches				
Meas. Num.	**Shear Leg**	**Lower**	**Throat**	**Upper**	**Tension Leg**	**Shear Leg**	**Lower**	**Throat**	**Upper**	**Tension Leg**
1 -X	0.844	0.288	0.450	0.194	0.594	0.750	0.200	0.375	0.125	0.438
2	0.781	0.294	0.456	0.200	0.594	0.719	0.206	0.381	0.125	0.438
3	0.781	0.256	0.431	0.188	0.594	0.719	0.181	0.363	0.113	0.469
4	0.781	0.250	0.431	0.138	0.594	0.656	0.181	0.369	0.113	0.469
5	0.781	0.250	0.406	0.138	0.531	0.656	0.156	0.344	0.119	0.469
6	0.875	0.238	0.406	0.119	0.500	0.656	0.175	0.375	0.119	0.500
7	0.781	0.231	0.406	0.125	0.531	0.656	0.175	0.375	0.119	0.563
8	0.781	0.244	0.438	0.125	0.531	0.719	0.175	0.375	0.119	0.469
Average	**0.799**	**0.255**	**0.426**	**0.152**	**0.558**	**0.684**	**0.180**	**0.369**	**0.118**	**0.480**

Table B.1.72 – Test #72, B175_B12_55_3

	Pre-Fracture Measurements									
	Front Side, inches					Back Side, inches				
Meas. Num.	**Shear Leg**	**Lower**	**Throat**	**Upper**	**Tension Leg**	**Shear Leg**	**Lower**	**Throat**	**Upper**	**Tension Leg**
1 -X	0.656	0.206	0.375	0.088	0.469	0.719	0.250	0.444	0.131	0.594
2	0.625	0.194	0.381	0.094	0.469	0.750	0.250	0.431	0.131	0.594
3	0.594	0.188	0.375	0.063	0.438	0.719	0.256	0.438	0.131	0.563
4	0.594	0.188	0.369	0.081	0.469	0.750	0.263	0.438	0.125	0.531
5	0.594	0.194	0.381	0.094	0.500	0.688	0.238	0.431	0.113	0.500
6	0.594	0.188	0.381	0.081	0.500	0.719	0.250	0.431	0.119	0.531
7	0.625	0.188	0.381	0.075	0.500	0.719	0.244	0.438	0.131	0.531
8	0.563	0.194	0.375	0.094	0.500	0.781	0.244	0.469	0.138	0.531
Average	**0.605**	**0.191**	**0.378**	**0.082**	**0.480**	**0.727**	**0.250**	**0.437**	**0.126**	**0.544**

Table B.1.73 – Test #73, B175_B516_85_1

	Pre-Fracture Measurements					
	Front Side, inches			Back Side, inches		
Meas. Num.	**Shear Leg**	**Throat**	**Tension Leg**	**Shear Leg**	**Throat**	**Tension Leg**
1 - X	0.530	0.300	0.375	0.440	0.340	0.344
2	0.470	0.300	0.406	0.530	0.290	0.344
3	0.470	0.310	0.375	0.470	0.370	0.344
4	0.530	0.320	0.375	0.470	0.360	0.375
5	0.470	0.320	0.375	0.500	0.330	0.375
6	0.470	0.320	0.375	0.530	0.330	0.344
7	0.500	0.310	0.406	0.470	0.320	0.375
8	0.500	0.260	0.406	0.500	0.370	0.375
Average	**0.489**	**0.309**	**0.386**	**0.492**	**0.336**	**0.359**

Table B.1.74 – Test #74, B175_B516_85_2

	Pre-Fracture Measurements					
	Front Side, inches			Back Side, inches		
Meas. Num.	**Shear Leg**	**Throat**	**Tension Leg**	**Shear Leg**	**Throat**	**Tension Leg**
1 - X	0.500	0.377	0.375	0.438	0.330	0.406
2	0.469	0.326	0.375	0.438	0.310	0.406
3	0.406	0.406	0.344	0.406	0.320	0.375
4	0.500	0.406	0.375	0.438	0.260	0.375
5	0.469	0.406	0.406	0.375	0.320	0.406
6	0.500	0.328	0.406	0.406	0.350	0.406
7	0.469	0.328	0.406	0.469	0.350	0.406
8	0.469	0.328	0.406	0.438	0.360	0.406
Average	**0.471**	**0.365**	**0.386**	**0.424**	**0.322**	**0.397**

Table B.1.75 – Test #75, B175_B516_85_3

	Pre-Fracture Measurements					
	Front Side, inches			Back Side, inches		
Meas. Num.	**Shear Leg**	**Throat**	**Tension Leg**	**Shear Leg**	**Throat**	**Tension Leg**
1 - X	0.470	0.220	0.344	0.470	0.390	0.344
2	0.500	0.240	0.406	0.470	0.330	0.375
3	0.500	0.240	0.375	0.500	0.380	0.344
4	0.530	0.240	0.375	0.530	0.330	0.344
5	0.530	0.210	0.375	0.470	0.340	0.344
6	0.560	0.230	0.375	0.470	0.360	0.344
7	0.530	0.240	0.406	0.440	0.370	0.344
8	0.470	0.250	0.375	0.470	0.390	0.375
Average	**0.518**	**0.234**	**0.382**	**0.479**	**0.356**	**0.350**

Table B.1.76 – Test #76, B175_B12_85_1

	Pre-Fracture Measurements									
	Front Side, inches					Back Side, inches				
Meas. Num.	**Shear Leg**	**Lower**	**Throat**	**Upper**	**Tension Leg**	**Shear Leg**	**Lower**	**Throat**	**Upper**	**Tension Leg**
1 -X	0.875	0.256	0.438	0.156	0.563	0.844	0.219	0.419	0.131	0.500
2	0.875	0.244	0.438	0.188	0.563	0.594	0.194	0.394	0.119	0.469
3	0.813	0.250	0.469	0.131	0.531	0.594	0.175	0.375	0.094	0.469
4	0.719	0.219	0.444	0.156	0.531	0.625	0.181	0.381	0.125	0.500
5	0.719	0.238	0.444	0.138	0.531	0.656	0.181	0.381	0.106	0.500
6	0.688	0.219	0.481	0.156	0.500	0.625	0.181	0.375	0.125	0.531
7	0.750	0.244	0.375	0.119	0.500	0.625	0.188	0.394	0.119	0.563
8	0.719	0.231	0.431	0.131	0.531	0.625	0.181	0.388	0.169	0.531
Average	**0.765**	**0.236**	**0.441**	**0.147**	**0.529**	**0.634**	**0.185**	**0.386**	**0.119**	**0.507**

Table B.1.77 – Test #77, B175_B12_85_2

	Pre-Fracture Measurements									
	Front Side, inches					Back Side, inches				
Meas. Num.	**Shear Leg**	**Lower**	**Throat**	**Upper**	**Tension Leg**	**Shear Leg**	**Lower**	**Throat**	**Upper**	**Tension Leg**
1 -X	0.660	0.220	0.390	0.130	0.590	0.720	0.190	0.420	0.160	0.560
2	0.590	0.210	0.410	0.140	0.590	0.660	0.200	0.400	0.120	0.560
3	0.660	0.200	0.360	0.100	0.560	0.720	0.190	0.390	0.110	0.530
4	0.560	0.200	0.390	0.120	0.560	0.720	0.180	0.390	0.110	0.530
5	0.630	0.220	0.390	0.130	0.560	0.750	0.160	0.370	0.110	0.560
6	0.590	0.170	0.370	0.120	0.560	0.720	0.170	0.370	0.110	0.530
7	0.660	0.220	0.360	0.140	0.560	0.720	0.190	0.390	0.110	0.530
8	0.660	0.200	0.360	0.130	0.590	0.690	0.180	0.360	0.110	0.530
Average	**0.621**	**0.204**	**0.379**	**0.126**	**0.568**	**0.714**	**0.182**	**0.386**	**0.115**	**0.541**

Table B.1.78 – Test #78, B175_B12_85_3

	Pre-Fracture Measurements									
	Front Side, inches					Back Side, inches				
Meas. Num.	**Shear Leg**	**Lower**	**Throat**	**Upper**	**Tension Leg**	**Shear Leg**	**Lower**	**Throat**	**Upper**	**Tension Leg**
1 -X	0.660	0.180	0.400	0.130	0.560	0.720	0.190	0.380	0.120	0.560
2	0.690	0.180	0.400	0.130	0.590	0.720	0.210	0.400	0.130	0.530
3	0.720	0.190	0.390	0.110	0.590	0.780	0.200	0.380	0.120	0.530
4	0.690	0.200	0.400	0.120	0.590	0.750	0.230	0.390	0.090	0.560
5	0.660	0.190	0.370	0.120	0.630	0.780	0.220	0.420	0.140	0.590
6	0.720	0.140	0.390	0.100	0.560	0.750	0.240	0.430	0.160	0.590
7	0.660	0.180	0.400	0.110	0.530	0.840	0.230	0.410	0.120	0.530
8	0.690	0.160	0.380	0.080	0.530	0.780	0.240	0.410	0.120	0.560
Average	**0.688**	**0.179**	**0.391**	**0.114**	**0.577**	**0.768**	**0.221**	**0.404**	**0.126**	**0.556**

Table B.1.79 – Test #79, B250_B516_55_1

	Pre-Fracture Measurements					
	Front Side, inches			Back Side, inches		
Meas. Num.	**Shear Leg**	**Throat**	**Tension Leg**	**Shear Leg**	**Throat**	**Tension Leg**
1 - X	0.490	0.344	0.327	0.447	0.250	0.289
2	0.417	0.313	0.369	0.469	0.281	0.320
3	0.447	0.313	0.334	0.453	0.281	0.336
4	0.400	0.328	0.338	0.491	0.313	0.340
5	0.472	0.313	0.354	0.480	0.313	0.318
6	0.408	0.344	0.360	0.430	0.266	0.336
7	0.435	0.344	0.361	0.438	0.297	0.328
8	0.436	0.344	0.341	0.473	0.281	0.311
9	0.514	0.344	0.338	0.463	0.234	0.331
Average	**0.439**	**0.330**	**0.349**	**0.461**	**0.285**	**0.325**

Table B.1.80 – Test #80, B250_B516_55_2

	Pre-Fracture Measurements					
	Front Side, inches			Back Side, inches		
Meas. Num.	**Shear Leg**	**Throat**	**Tension Leg**	**Shear Leg**	**Throat**	**Tension Leg**
1 - X	0.442	0.313	0.337	0.515	0.250	0.300
2	0.435	0.313	0.364	0.461	0.281	0.322
3	0.410	0.328	0.333	0.540	0.313	0.376
4	0.459	0.344	0.372	0.496	0.297	0.337
5	0.503	0.375	0.348	0.434	0.313	0.352
6	0.436	0.313	0.359	0.461	0.313	0.348
7	0.469	0.313	0.354	0.442	0.313	0.376
8	0.446	0.313	0.376	0.505	0.313	0.350
9	0.427	0.359	0.385	0.505	0.297	0.365
Average	**0.449**	**0.329**	**0.358**	**0.481**	**0.302**	**0.349**

Table B.1.81 – Test #81, B250_B516_55_3

	Pre-Fracture Measurements					
	Front Side, inches			Back Side, inches		
Meas. Num.	**Shear Leg**	**Throat**	**Tension Leg**	**Shear Leg**	**Throat**	**Tension Leg**
1 - X	0.431	0.375	0.406	0.533	0.281	0.349
2	0.429	0.359	0.405	0.463	0.281	0.376
3	0.451	0.375	0.385	0.526	0.281	0.327
4	0.489	0.344	0.387	0.493	0.281	0.304
5	0.443	0.281	0.393	0.516	0.281	0.350
6	0.488	0.313	0.385	0.476	0.297	0.338
7	0.458	0.328	0.394	0.474	0.297	0.300
8	0.522	0.344	0.420	0.529	0.313	0.287
Average	**0.462**	**0.337**	**0.394**	**0.496**	**0.288**	**0.331**

Table B.1.82 – Test #82, B250_B12_55_1

	Pre-Fracture Measurements									
	Front Side, inches					Back Side, inches				
Meas. Num.	**Shear Leg**	**Lower**	**Throat**	**Upper**	**Tension Leg**	**Shear Leg**	**Lower**	**Throat**	**Upper**	**Tension Leg**
1 -X	0.781	0.244	0.438	0.138	0.469	0.750	0.250	0.431	0.250	0.563
2	0.750	0.238	0.406	0.138	0.438	0.781	0.250	0.431	0.194	0.594
3	0.750	0.281	0.381	0.144	0.500	0.781	0.244	0.438	0.194	0.563
4	0.750	0.238	0.381	0.138	0.500	0.781	0.244	0.438	0.194	0.563
5	0.750	0.250	0.388	0.138	0.469	0.813	0.244	0.419	0.188	0.563
6	0.750	0.250	0.394	0.144	0.469	0.781	0.269	0.381	0.188	0.563
7	0.750	0.250	0.394	0.194	0.531	0.750	0.225	0.381	0.206	0.625
8	0.844	0.250	0.400	0.194	0.594	0.844	0.219	0.431	0.200	0.625
Average	**0.758**	**0.251**	**0.394**	**0.151**	**0.490**	**0.783**	**0.244**	**0.417**	**0.198**	**0.580**

Table B.1.83 – Test #83, B250_B12_55_2

	Pre-Fracture Measurements									
	Front Side, inches					Back Side, inches				
Meas. Num.	**Shear Leg**	**Lower**	**Throat**	**Upper**	**Tension Leg**	**Shear Leg**	**Lower**	**Throat**	**Upper**	**Tension Leg**
1 -X	0.750	0.240	0.380	0.130	0.510	0.750	0.220	0.420	0.190	0.590
2	0.670	0.210	0.370	0.140	0.470	0.830	0.220	0.390	0.180	0.590
3	0.710	0.210	0.440	0.160	0.510	0.790	0.280	0.390	0.160	0.630
4	0.670	0.250	0.440	0.150	0.550	0.750	0.250	0.440	0.190	0.550
5	0.750	0.250	0.440	0.130	0.510	0.830	0.240	0.470	0.160	0.590
6	0.790	0.310	0.430	0.160	0.550	0.750	0.280	0.470	0.170	0.590
7	0.830	0.270	0.420	0.140	0.550	0.830	0.280	0.450	0.170	0.630
8	0.750	0.290	0.410	0.150	0.630	0.830	0.250	0.450	0.160	0.590
Average	**0.738**	**0.252**	**0.420**	**0.146**	**0.529**	**0.796**	**0.255**	**0.435**	**0.172**	**0.596**

Table B.1.84 – Test #84, B250_B12_55_3

	Pre-Fracture Measurements									
	Front Side, inches					Back Side, inches				
Meas. Num.	**Shear Leg**	**Lower**	**Throat**	**Upper**	**Tension Leg**	**Shear Leg**	**Lower**	**Throat**	**Upper**	**Tension Leg**
1 -X	0.720	0.230	0.410	0.130	0.510	0.790	0.280	0.460	0.160	0.500
2	0.710	0.230	0.430	0.130	0.510	0.910	0.240	0.470	0.190	0.500
3	0.710	0.270	0.420	0.140	0.530	0.830	0.250	0.430	0.190	0.500
4	0.670	0.240	0.400	0.130	0.520	0.790	0.220	0.460	0.170	0.550
5	0.700	0.260	0.420	0.140	0.500	0.750	0.250	0.470	0.180	0.550
6	0.690	0.240	0.420	0.150	0.560	0.790	0.280	0.460	0.180	0.550
7	0.697	0.260	0.440	0.140	0.550	0.750	0.230	0.440	0.150	0.630
8	0.690	0.260	0.420	0.130	0.500	0.830	0.220	0.430	0.180	0.550
Average	**0.697**	**0.249**	**0.421**	**0.137**	**0.525**	**0.804**	**0.246**	**0.454**	**0.176**	**0.544**

B.2 POST-FRACTURE MEASUREMENTS

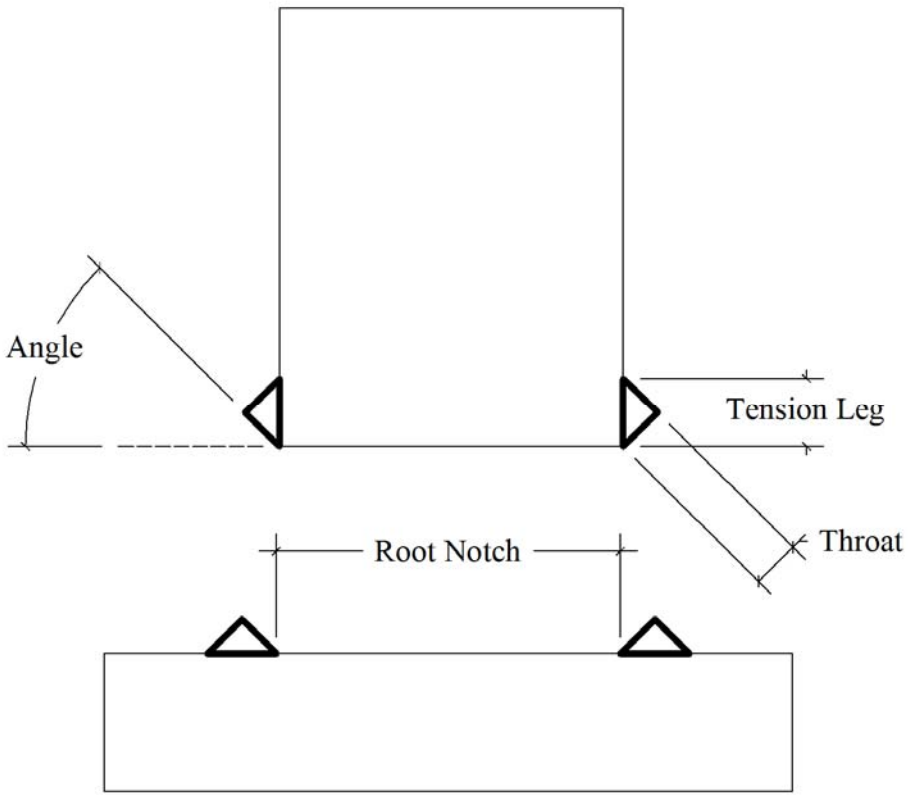

Figure B.2.1 – Cruciform Section Schematic Showing Post-Fracture Measurements (Refer to Figure B.1.1 for Locations of Measurements Along Length of Weld)

Table B.2.1 – Test #1, T125_A12_1

	Post-Fracture Measurements						
		Front Side, inches			Back Side, inches		
Meas. Num.	**Root Notch, inches**	**Throat, inches**	**Angle, degrees**	**Tension Leg**	**Throat, inches**	**Angle, degrees**	**Tension Leg**
1	1.2500	0.4685	71	0.5480	0.4870	70	0.5195
2	1.2600	0.4320	71	0.5870	0.4350	72	0.5115
3	1.2520	0.4575	74	0.5465	0.4355	70	0.5155
4	1.2370	0.4465	69	0.5435	0.4345	73	0.5225
5	1.2135	0.4115	59	0.5170	0.3970	67	0.5320
6	1.1990	0.4140	55	0.5335	0.4510	71	0.5390
7	1.1955	0.4345	57	0.5580	0.4110	60	0.5500
8	1.1840	0.4505	56	0.5390	0.4005	58	0.5750
9	1.1970		52	0.5390	0.3790	63	0.5555
Mean	**1.2209**	**0.4394**	**62.7**	**0.5457**	**0.4256**	**67.1**	**0.5356**

Table B.2.2 – Test #2, T125_A12_2

	Post-Fracture Measurements						
		Front Side, inches			Back Side, inches		
Meas. Num.	**Root Notch, inches**	**Throat, inches**	**Angle, degrees**	**Tension Leg**	**Throat, inches**	**Angle, degrees**	**Tension Leg**
1	1.1910	0.4600	62	0.5525	0.4810	10	0.5595
2	1.1995	0.4715	70	0.5450	0.4700	12	0.5595
3	1.2100	0.4355	70	0.5275	0.4550	15	0.5685
4	1.2070	0.4550	69	0.5405	0.4580	19	0.5490
5	1.1870	0.4620	62	0.5510	0.4600	16	0.5505
6	1.1825	0.4415	65	0.4845	0.4575	21	0.5395
7	1.1815	0.4525	67	0.4835	0.4835	18	0.5585
8	1.2160	0.4785	69	0.4860	0.4600	14	0.5590
9	1.1905	0.4715	68	0.5170	0.4590	17	0.5680
Average	**1.1961**	**0.4587**	**66.9**	**0.5208**	**0.4649**	**15.8**	**0.5569**

Table B.2.3 – Test #3, T125_A12_3

	Post-Fracture Measurements						
		Front Side, inches			Back Side, inches		
Meas. Num.	**Root Notch, inches**	**Throat, inches**	**Angle, degrees**	**Tension Leg**	**Throat, inches**	**Angle, degrees**	**Tension Leg**
1	1.2370	0.4420	29	0.5335	0.4495	74	0.6125
2	1.2250	0.4880	22	0.5360	0.4395	70	0.5730
3	1.2330	0.4450	22	0.5145	0.4280	75	0.5465
4	1.1915	0.4715	18	0.5230	0.4250	66	0.5935
5	1.1930	0.4585	20	0.5180	0.4245	75	0.5655
6	1.9600	0.4660	22	0.5110	0.4185	65	0.5805
7	1.1940	0.4520	24	0.5550	0.4110	69	0.5620
8	1.1985	0.4730	23	0.5215	0.4400	65	0.5325
9	1.2295	0.4220	32	0.5405	0.4405	65	0.5430
Average	**1.2957**	**0.4576**	**23.6**	**0.5281**	**0.4307**	**69.3**	**0.5677**

Table B.2.4 – Test #4, T125_A516_1

	Post-Fracture Measurements						
		Front Side, inches			Back Side, inches		
Meas. Num.	**Root Notch, inches**	**Throat, inches**	**Angle, degrees**	**Tension Leg, inches**	**Throat, inches**	**Angle, degrees**	**Tension Leg, inches**
1	1.2320	0.2725	48	0.3650	0.2965	50	0.3675
2	1.2685	0.2670	43	0.3335	0.2630	51	0.2730
3	1.2390	0.2685	46	0.3620	0.2640	40	0.3970
4	1.2195	0.2700	46	0.3870	0.2650	40	0.3950
5	1.2585	0.2715	47	0.3630	0.2720	50	0.3620
6	1.2400	0.2600	52	0.3595	0.2880	42	0.3570
7	1.2120	0.2950	47	0.3830	0.2815	50	0.3710
8	1.2390	0.2795	47	0.3825	0.2775	49	0.3725
9	1.2430	0.2825	48	0.3565	0.2795	56	0.3650
Mean	**1.2391**	**0.2741**	**47.1**	**0.3658**	**0.2763**	**47.6**	**0.3622**

Table B.2.5 – Test #5, T125_A516_2

	Post-Fracture Measurements						
		Front Side, inches			Back Side, inches		
Meas. Num.	**Root Notch, inches**	**Throat, inches**	**Angle, degrees**	**Tension Leg, inches**	**Throat, inches**	**Angle, degrees**	**Tension Leg, inches**
1	1.2480	0.2875	47	0.3415	0.3200	36	0.3595
2	1.2220	0.3315	46	0.4240	0.3370	36	0.3820
3	1.2285	0.3370	46	0.4130	0.3385	39	0.3845
4	1.2410	0.2880	44	0.3630	0.3085	41	0.3715
5	1.2580	0.2700	48	0.3710	0.3125	32	0.3995
6	1.2585	0.2865	52	0.3870	0.3960	30	0.3655
7	1.2335	0.2825	50	0.3545	0.3700	44	0.3890
8	1.2775	0.2945	47	0.3465	0.3695	30	0.3340
9	1.2665	0.2965	48	0.3815	0.2850	43	0.3575
Average	**1.2482**	**0.2971**	**47.6**	**0.3758**	**0.3374**	**36.8**	**0.3714**

Table B.2.6 – Test #6, T125_A516_3

	Post-Fracture Measurements						
		Front Side, inches			Back Side, inches		
Meas. Num.	**Root Notch, inches**	**Throat, inches**	**Angle, degrees**	**Tension Leg, inches**	**Throat, inches**	**Angle, degrees**	**Tension Leg, inches**
1	1.2435	0.3180	65	0.3620	0.2925	59	0.3995
2	1.2760	0.3100	62	0.3620	0.3145	45	0.3970
3	1.2505	0.3730	58	0.3555	0.2795	51	0.3490
4	1.3670	0.3085	45	0.3090	0.2320	50	0.3465
5	1.2775	0.2815	53	0.3255	0.3205	61	0.3400
6	1.2825	0.3155	56	0.3200	0.2665	50	0.3665
7	1.3940	0.2415	50	0.3895	0.2550	52	0.3355
8	1.3115	0.2470	48	0.3145	0.2510	59	0.3550
9	1.3030	0.2295	60	0.2720	0.3450	54	0.4735
Average	**1.3006**	**0.2916**	**55.2**	**0.3344**	**0.2841**	**53.4**	**0.3736**

Table B.2.7 – Test #7, T250_A12_1

	Post-Fracture Measurements						
		Front Side, inches			Back Side, inches		
Meas. Num.	**Root Notch, inches**	**Throat, inches**	**Angle, degrees**	**Tension Leg**	**Throat, inches**	**Angle, degrees**	**Tension Leg**
1	2.4740	0.4365	9	0.3950	0.4175	68	0.5055
2	2.4735	0.4300	6	0.5285	0.4720	73	0.5505
3	2.4870	0.4240	6	0.5310	0.4150	70	0.5530
4	2.4235	0.4340	10	0.5410	0.4460	66	0.5805
5	2.4550	0.4320	5	0.5155	0.3820	52	0.5335
6	2.4535	0.4570	5	0.5315	0.3730	46	0.5880
7	2.4490	0.4925	0	0.5030	0.3765	64	0.5620
8	2.4845	0.4930	0	0.5340	0.4005	59	0.6015
9	2.4915	0.4675	0	0.5570	0.4750	62	0.5630
Average	**2.4657**	**0.4518**	**4.6**	**0.5152**	**0.4175**	**62.2**	**0.5597**

Table B.2.8 – Test #8, T250_A12_2

	Post-Fracture Measurements						
		Front Side, inches			Back Side, inches		
Meas. Num.	**Root Notch, inches**	**Throat, inches**	**Angle, degrees**	**Tension Leg**	**Throat, inches**	**Angle, degrees**	**Tension Leg**
1	2.4490	0.4475	24	0.5500	0.4860	0	0.5460
2	2.4405	0.4390	26	0.5585	0.4720	0	0.5730
3	2.4405	0.4230	30	0.5880	0.4055	0	0.5285
4	2.4510	0.3940	32	0.5470	0.4150	10	0.5600
5	2.4545	0.4150	34	0.5435	0.4155	21	0.5390
6	2.5850	0.4365	38	0.5095	0.4150	14	0.5835
7	2.4590	0.4200	34	0.5530	0.4215	6	0.5610
8	2.4585	0.4010	29	0.5275	0.4600	0	0.5610
9	2.4630	0.4540	25	0.5685	0.4325	0	0.5525
Average	**2.4668**	**0.4256**	**30.2**	**0.5495**	**0.4359**	**5.7**	**0.5561**

Table B.2.9 – Test #9, T250_A12_3

	Post-Fracture Measurements						
		Front Side, inches			Back Side, inches		
Meas. Num.	**Root Notch, inches**	**Throat, inches**	**Angle, degrees**	**Tension Leg**	**Throat, inches**	**Angle, degrees**	**Tension Leg**
1	2.5325	0.4460	321	0.4960	0.4470	0	0.6665
2	2.4625	0.4220	25	0.5180	0.4810	0	0.5695
3	2.5035	0.3620	29	0.5475	0.4720	8	0.5225
4	2.5275	0.4240	28	0.5595	0.4730	0	0.5030
5	2.4535	0.4235	25	0.5140	0.4660	0	0.4980
6	2.4565	0.4390	25	0.4955	0.4590	0	0.5360
7	2.4050	0.4350	25	0.5575	0.4965	0	0.5785
8	2.4095	0.4185	26	0.5420	0.4710	0	0.5265
9	2.4865	0.4265	29	0.5540	0.4635	0	0.4805
Average	**2.4708**	**0.4218**	**59.2**	**0.5316**	**0.4699**	**0.9**	**0.5423**

Table B.2.10 – Test #10, T250_A516_1

	Post-Fracture Measurements						
		Front Side, inches			Back Side, inches		
Meas. Num.	**Root Notch, inches**	**Throat, inches**	**Angle, degrees**	**Tension Leg, inches**	**Throat, inches**	**Angle, degrees**	**Tension Leg, inches**
1	2.5075	0.2035	41	0.3560	0.2645	22	0.3300
2	2.5295	0.1990	46	0.3250	0.2100	31	0.4905
3	2.5165	0.2160	52	0.3140	0.2110	45	0.2990
4	2.5270	0.2190	49	0.3485	0.2260	46	0.2950
5	2.5510	0.2360	49	0.3200	0.2260	43	0.3270
6	2.5710	0.2360	48	0.3055	0.2405	47	0.2720
7	2.5425	0.2305	45	0.3090	0.2215	59	0.1900
8	2.5735	0.2305	47	0.3305	0.1880	0	0.2990
9	2.6130	0.2260	45	0.2470	0.1760	44	0.2220
Average	**2.5479**	**0.2218**	**46.9**	**0.3173**	**0.2182**	**37.4**	**0.3027**

Table B.2.11 – Test #11, T250_A516_2

	Post-Fracture Measurements						
		Front Side, inches			Back Side, inches		
Meas. Num.	**Root Notch, inches**	**Throat, inches**	**Angle, degrees**	**Tension Leg, inches**	**Throat, inches**	**Angle, degrees**	**Tension Leg, inches**
1	2.5285	0.2050	48	0.2530	0.2000	45	0.3240
2	2.5530	0.2320	52	0.3445	0.2175	47	0.2955
3	2.5275	0.2135	49	0.3205	0.2355	45	0.3300
4	2.4620	0.1890	47	0.3475	0.2230	45	0.3470
5	2.5350	0.2420	52	0.3050	0.2320	38	0.3630
6	2.5075	0.2480	50	0.3175	0.2210	37	0.3075
7	2.5135	0.2110	48	0.3140	0.2390	41	0.2990
8	2.5275	0.2180	49	0.2805	0.2215	36	0.3180
9	2.5380	0.1990	35	0.3020	0.2030	46	0.2980
Average	**2.5214**	**0.2175**	**47.8**	**0.3094**	**0.2214**	**42.2**	**0.3202**

Table B.2.12 – Test #12, T250_A516_3

	Post-Fracture Measurements						
		Front Side, inches			Back Side, inches		
Meas. Num.	**Root Notch, inches**	**Throat, inches**	**Angle, degrees**	**Tension Leg, inches**	**Throat, inches**	**Angle, degrees**	**Tension Leg, inches**
1	2.5870	0.1835	0	0.2515	0.2475	45	0.3095
2	2.5475	0.2455	0	0.2750	0.2290	45	0.3415
3	2.5345	0.1670	0	0.2050	0.2525	49	0.3005
4	2.5610	0.2100	37	0.2900	0.2320	49	0.3510
5	2.4735	0.2005	39	0.3195	0.2640	57	0.3540
6	2.5145	0.2150	30	0.3195	0.2815	57	0.3435
7	2.5570	0.1775	36	0.2810	0.2555	52	0.3300
8	2.5420	0.2255	46	0.2715	0.2200	55	0.3225
9	2.5025	0.2000	35	0.3435	0.2370	52	0.3275
Average	**2.5355**	**0.2027**	**24.8**	**0.2841**	**0.2466**	**51.2**	**0.3311**

Table B.2.13 – Test #13, T125_B12_1

	Post-Fracture Measurements						
		Front Side, inches			Back Side, inches		
Meas. Num.	**Root Notch, inches**	**Throat, inches**	**Angle, degrees**	**Tension Leg**	**Throat, inches**	**Angle, degrees**	**Tension Leg**
1	1.1300	0.4475	35	0.6430	0.3455	73	0.5980
2	1.1480	0.4465	32	0.6905	0.4630	70	0.5435
3	1.1660	0.4445	24	0.6035	0.4840	74	0.5690
4	1.1815	0.4330	30	0.6310	0.5195	73	0.5925
5	1.1805	0.4885	28	0.6350	0.4365	62	0.5450
6	1.1860	0.3965	24	0.6350	0.4055	56	0.5390
7	1.1455	0.4535	23	0.6420	0.4130	57	0.5345
8	1.1510	0.4490	12	0.6545	0.3985	55	0.5870
9	1.1645	0.4425	10	0.6890	0.3995	50	0.5380
Average	**1.1614**	**0.4446**	**24.2**	**0.6471**	**0.4294**	**63.3**	**0.5607**

Table B.2.14 – Test #14, T125_B12_2

	Post-Fracture Measurements						
		Front Side, inches			Back Side, inches		
Meas. Num.	**Root Notch, inches**	**Throat, inches**	**Angle, degrees**	**Tension Leg**	**Throat, inches**	**Angle, degrees**	**Tension Leg**
1	1.1545	0.5120	54	0.6670	0.5190	11	0.5955
2	1.1400	0.4730	60	0.6650	0.5065	13	0.5910
3	1.1785	0.4695	60	0.6520	0.5235	12	0.6100
4	1.1145	0.4515	64	0.6185	0.4500	12	0.6315
5	1.1355	0.4415	64	0.6335	0.4520	15	0.8525
6	1.1750	0.4635	66	0.6255	0.4095	14	0.5985
7	1.1925	0.5480	72	0.6360	0.4400	18	0.5980
8	1.1285	0.4990	62	0.6370	0.4375	21	0.6395
9	1.1725	0.4545	58	0.6420	0.4425	25	0.6185
Average	**1.1546**	**0.4792**	**62.2**	**0.6418**	**0.4645**	**15.7**	**0.6372**

Table B.2.15 – Test #15, T125_B12_3

	Post-Fracture Measurements						
		Front Side, inches			Back Side, inches		
Meas. Num.	**Root Notch, inches**	**Throat, inches**	**Angle, degrees**	**Tension Leg**	**Throat, inches**	**Angle, degrees**	**Tension Leg**
1	1.3000	0.3935	70	0.4990	0.4370	0	0.4935
2	1.1370	0.4200	60	0.6400	0.4760	10	0.5200
3	1.1355	0.3560	40	0.6280	0.4610	14	0.5800
4	1.1375	0.3595	39	0.6405	0.4985	19	0.5675
5	1.1440	0.4230	49	0.6440	0.4875	31	0.5600
6	1.1215	0.5000	64	0.6805	0.4910	39	0.5120
7	1.1060	0.4675	64	0.6900	0.5085	42	0.5630
8	1.1350	0.5285	67	0.6280	0.5175	70	0.6030
9	1.1055	0.6005	73	0.6660	0.5155	65	0.5720
Average	**1.1469**	**0.4498**	**58.4**	**0.6351**	**0.4881**	**32.2**	**0.5523**

Table B.2.16 – Test #16, T125_B516_1

	Post-Fracture Measurements						
		Front Side, inches			Back Side, inches		
Meas. Num.	**Root Notch, inches**	**Throat, inches**	**Angle, degrees**	**Tension Leg, inches**	**Throat, inches**	**Angle, degrees**	**Tension Leg, inches**
1	1.1900	0.3255	19	0.4875	0.3280	72	0.3330
2	1.2090	0.2650	32	0.4850	0.3110	80	0.3075
3	1.2005	0.3210	34	0.4780	0.3225	75	0.3565
4	1.1755	0.3130	25	0.5080	0.3345	84	0.3520
5	1.2470	0.3125	24	0.4405	0.2880	77	0.2845
6	1.1795	0.2305	29	0.4585	0.2880	80	0.3225
7	1.2045	0.2650	29	0.4710	0.3445	77	0.3350
8	1.1600	0.2510	34	0.4455	0.3435	75	0.3555
9	1.1475	0.3230	28	0.5005	0.3345	81	0.3655
Average	**1.1904**	**0.2896**	**28.2**	**0.4749**	**0.3216**	**77.9**	**0.3347**

Table B.2.17 – Test #17, T125_B516_2

	Post-Fracture Measurements						
		Front Side, inches			Back Side, inches		
Meas. Num.	**Root Notch, inches**	**Throat, inches**	**Angle, degrees**	**Tension Leg, inches**	**Throat, inches**	**Angle, degrees**	**Tension Leg, inches**
1	1.2080	0.3475	60	0.3175	0.4575	84	0.4765
2	1.1505	0.2975	56	0.3280	0.3770	80	0.5250
3	1.1860	0.2990	56	0.3210	0.3705	82	0.4720
4	1.1545	0.2800	56	0.3240	0.3935	81	0.5125
5	1.1795	0.2805	58	0.3150	0.3980	79	0.4880
6	1.2075	0.3095	60	0.3205	0.4120	77	0.4480
7	1.1235	..325	61	0.3185	0.4825	79	0.5480
8	1.2315	0.3500	61	0.3055	0.4700	86	0.4950
9	1.2030	0.3185	63	0.3480	0.4995	87	0.4795
Average	**1.1827**	**0.3103**	**59.0**	**0.3220**	**0.4289**	**81.7**	**0.4938**

Table B.2.18 – Test #18, T125_B516_3

	Post-Fracture Measurements						
		Front Side, inches			Back Side, inches		
Meas. Num.	**Root Notch, inches**	**Throat, inches**	**Angle, degrees**	**Tension Leg, inches**	**Throat, inches**	**Angle, degrees**	**Tension Leg, inches**
1	1.2150	0.4150	75	0.4720	0.3760	65	0.3290
2	1.2515	0.3300	74	0.4000	0.3305	67	0.3300
3	1.3055	0.3050	74	0.4100	0.3910	76	0.3360
4	1.2430	0.3380	71	0.4730	0.3380	68	0.3390
5	1.2265	0.3520	71	0.4560	0.3100	60	0.3340
6	1.1770	0.3440	68	0.4895	0.3130	61	0.3430
7	1.2250	0.6140	71	0.5065	0.3700	60	0.3355
8	1.2380	0.3195	68	0.4530	0.3840	69	0.3535
9	1.2080	0.3785	67	0.5730	0.4075	65	0.4065
Average	**1.2322**	**0.3773**	**71.0**	**0.4703**	**0.3578**	**65.7**	**0.3452**

Table B.2.19 – Test #19, T250_B12_1

	Post-Fracture Measurements						
		Front Side, inches			Back Side, inches		
Meas. Num.	**Root Notch, inches**	**Throat, inches**	**Angle, degrees**	**Tension Leg**	**Throat, inches**	**Angle, degrees**	**Tension Leg**
1	2.4560	0.5475	61	0.5525	0.4785	42	0.5505
2	2.3690	0.4045	52	0.5745	0.4815	47	0.6085
3	2.3990	0.4325	56	0.5885	0.4655	55	0.5625
4	2.4020	0.4555	56	0.5845	0.4425	59	0.6400
5	2.3980	0.5035	65	0.6065	0.4430	59	0.6240
6	2.3756	0.5920	66	0.5915	0.4000	62	0.5755
7	2.4175	0.5840	61	0.5705	0.4035	56	0.5495
8	2.3655	0.4895	58	0.6250	0.4010	59	0.5365
9	2.4540	0.4745	61	0.5400	0.4395	53	0.5845
Average	**2.4041**	**0.4982**	**59.6**	**0.5815**	**0.4394**	**54.7**	**0.5813**

Table B.2.20 – Test #20, T250_B12_2

	Post-Fracture Measurements						
		Front Side, inches			Back Side, inches		
Meas. Num.	**Root Notch, inches**	**Throat, inches**	**Angle, degrees**	**Tension Leg**	**Throat, inches**	**Angle, degrees**	**Tension Leg**
1	2.3260	0.5665	62	0.7445	0.4610	38	0.6270
2	2.3545	0.5770	63	0.7320	0.4125	42	0.6370
3	2.3735	0.5955	64	0.6420	0.4415	67	0.6020
4	2.3477	0.5295	57	0.6360	0.4170	66	0.5700
5	2.3955	0.5375	63	0.5670	0.4715	62	0.5675
6	2.3620	0.5400	56	0.6645	0.4780	67	0.5700
7	2.3705	0.5010	59	0.5980	0.4650	67	0.6160
8	2.4030	0.4915	57	0.6105	0.4465	30	0.5750
9	2.3695	0.5300	57	0.6375	0.4860	28	0.6060
Average	**2.3669**	**0.5409**	**59.8**	**0.6480**	**0.4532**	**51.9**	**0.5967**

Table B.2.21 – Test #21, T250_B12_3

	Post-Fracture Measurements						
		Front Side, inches			Back Side, inches		
Meas. Num.	**Root Notch, inches**	**Throat, inches**	**Angle, degrees**	**Tension Leg**	**Throat, inches**	**Angle, degrees**	**Tension Leg**
1	2.4185	0.4220	56	0.6305	0.4175	35	0.5650
2	2.4285	0.4425	55	0.5435	0.4130	36	0.5760
3	2.4275	0.4615	57	0.5740	0.4460	55	0.5860
4	2.3605	0.5490	59	0.6270	0.4570	64	0.5645
5	2.4050	0.5350	61	0.6510	0.4805	59	0.5420
6	2.3240	0.5915	59	0.7110	0.4835	63	0.6015
7	2.3750	0.5755	65	0.6460	0.4490	34	0.6025
8	2.3555	0.5575	61	0.6160	0.4870	35	0.5585
9	2.3570	0.5510	59	0.6830		36	0.5880
Average	**2.3835**	**0.5206**	**59.1**	**0.6313**	**0.4542**	**46.3**	**0.5760**

Table B.2.22 – Test #22, T250_B516_1

	Post-Fracture Measurements						
		Front Side, inches			Back Side, inches		
Meas. Num.	**Root Notch, inches**	**Throat, inches**	**Angle, degrees**	**Tension Leg, inches**	**Throat, inches**	**Angle, degrees**	**Tension Leg, inches**
1	2.4785	0.3695	73	0.4275	0.2625	0	0.3580
2	2.4935	0.3010	58	0.3945	0.3060	59	0.3330
3	2.4580	0.3325	56	0.4565	0.2870	63	0.3445
4	2.2130	0.2915	60	0.3810	0.2815	62	0.3330
5	2.4775	0.3310	64	0.4750	0.3470	59	0.3500
6	2.4930	0.3225	63	0.4175	0.2820	56	0.3595
7	2.5085	0.3215	60	0.3835	0.3155	71	0.3400
8	2.4830	0.3260	55	0.3990	0.5030	90	0.3860
9	2.5105	0.3370	54	0.3490	0.5940	90	0.3195
Average	**2.4573**	**0.3258**	**60.3**	**0.4093**	**0.3532**	**61.1**	**0.3471**

Table B.2.23 – Test #23, T250_B516_2

	Post-Fracture Measurements						
		Front Side, inches			Back Side, inches		
Meas. Num.	**Root Notch, inches**	**Throat, inches**	**Angle, degrees**	**Tension Leg, inches**	**Throat, inches**	**Angle, degrees**	**Tension Leg, inches**
1	2.4785	0.3415	57	0.4115	0.4045	80	0.4530
2	2.4840	0.3120	58	0.4205	0.3440	68	0.3940
3	2.4890	0.3430	59	0.4300	0.5050	80	0.3875
4	2.5015	0.3400	59	0.4185	0.5740	90	0.4130
5	2.4910	0.2915	55	0.4600	0.4835	76	0.4090
6	2.5330	0.3305	56	0.4206	0.3060	64	0.3940
7	2.5020	0.3255	56	0.4100	0.2875	64	0.3715
8	2.4825	0.3650	66	0.4625	0.3155	67	0.3645
9	2.4965	0.4350	72	0.4475	0.3545	70	0.3825
Mean	**2.4953**	**0.3427**	**59.8**	**0.4312**	**0.3972**	**73.2**	**0.3966**

Table B.2.24 – Test #24, T250_B516_3

	Post-Fracture Measurements						
		Front Side, inches			Back Side, inches		
Meas. Num.	**Root Notch, inches**	**Throat, inches**	**Angle, degrees**	**Tension Leg, inches**	**Throat, inches**	**Angle, degrees**	**Tension Leg, inches**
1	2.4675	0.3175	49	0.4380	0.2720	65	0.3935
2	2.5850	0.2840	52	0.3200	0.2775	62	0.3910
3	2.5350	0.3220	50	0.3285	0.3250	69	0.3745
4	2.5345	0.2865	55	0.2960	0.3730	73	0.3795
5	2.6055	0.2610	55	0.2575	0.3165	67	0.3945
6	2.5285	0.2705	10	0.3730	0.3145	61	0.3800
7	2.5220	0.2845	19	0.3850	0.2905	63	0.3535
8	2.5290	0.2850	55	0.3615	0.3080	64	0.3735
9	2.5235	0.3695	67	0.3885	0.3315	62	
Average	**2.5367**	**0.2978**	**45.8**	**0.3498**	**0.3121**	**65.1**	**0.3800**

Table B.2.25 – Test #25, B125_A516_55_1

	Post-Fracture Measurements						
		Front Side, inches			Back Side, inches		
Meas. Num.	**Root Notch, inches**	**Throat, inches**	**Angle, degrees**	**Tension Leg, inches**	**Throat, inches**	**Angle, degrees**	**Tension Leg, inches**
1 - X	1.3040	0.3130	29	0.3650	0.2915	59	0.2655
2	1.2675	0.2975	36	0.3355	0.2870	58	0.3245
3	1.3110	0.2545	31	0.3430	0.2485	57	0.3260
4	1.2665	0.2875	34	0.3515	0.2640	51	0.2705
5	1.2805	0.2835	29	0.3690	0.2570	48	0.3035
6	1.2715	0.2745	35	0.3220	0.2670	44	0.3380
7	1.2050	0.2735	38	0.3100	0.2600	45	0.3295
8	1.2840	0.2505	39	0.3255	0.2760	42	0.3600
Mean	**1.2704**	**0.2789**	**33.9**	**0.3393**	**0.2664**	**50.5**	**0.3150**

Table B.2.26 – Test #26, B125_A516_55_2

	Post-Fracture Measurements						
		Front Side, inches			Back Side, inches		
Meas. Num.	**Root Notch, inches**	**Throat, inches**	**Angle, degrees**	**Tension Leg, inches**	**Throat, inches**	**Angle, degrees**	**Tension Leg, inches**
1 - X	1.2860	0.2780	36	0.3110	0.2740	36	0.3340
2	1.2655	0.2675	39	0.3675	0.2760	35	0.3520
3	1.2565	0.2735	41	0.3555	0.2765	44	0.3465
4	1.2625	0.2600	37	0.3320	0.2930	45	0.3575
5	1.2415	0.2400	33	0.3385	0.2640	49	0.3405
6	1.2735	0.2235	35	0.3120	0.2805	44	0.3455
7	1.2460	0.2335	39	0.3030	0.2880	44	0.3735
8	1.2785	0.2675	36	0.3255	0.2795	45	0.4130
Mean	**1.2607**	**0.2526**	**37.2**	**0.3327**	**0.2793**	**43.1**	**0.3552**

Table B.2.27 – Test #27, B125_A516_55_3

	Post-Fracture Measurements						
		Front Side, inches			Back Side, inches		
Meas. Num.	**Root Notch, inches**	**Throat, inches**	**Angle, degrees**	**Tension Leg, inches**	**Throat, inches**	**Angle, degrees**	**Tension Leg, inches**
1 - X	1.3120	0.2735	35	0.3345	0.3175	39	0.3115
2	1.2670	0.2835	63	0.3225	0.3325	67	0.3945
3	1.2675	0.2775	54	0.3310	0.2815	44	0.3560
4	1.2720	0.2640	54	0.3200	0.2390	44	0.3435
5	1.2600	0.2395	51	0.3070	0.2815	46	0.3365
6	1.2830	0.2230	46	0.3200	0.2835	50	0.3405
7	1.2825	0.2160	43	0.3065	0.2695	39	0.3510
8	1.2660	0.2470	40	0.3240	0.2750	38	0.3515
Mean	**1.2741**	**0.2518**	**50.0**	**0.3193**	**0.2831**	**47.1**	**0.3509**

Table B.2.28 – Test #28, B125_A12_55_1

	Post-Fracture Measurements						
		Front Side, inches			Back Side, inches		
Meas. Num.	**Root Notch, inches**	**Throat, inches**	**Angle, degrees**	**Tension Leg, inches**	**Throat, inches**	**Angle, degrees**	**Tension Leg, inches**
1 - X	1.2340	0.4405	65	0.4695	0.4090	54	0.4900
2	1.1955	0.4270	62	0.5085	0.3860	49	0.4720
3	1.2190	0.3945	68	0.4860	0.3890	35	0.4480
4	1.2185	0.4530	71 & 61	0.5155	0.4050	34	0.4900
5	1.2030	0.4130	70	0.4690	0.3795	34	0.4890
6	1.2265	0.4830	75	0.4930	0.4425	38	0.5105
7	1.2410	0.3910	68	0.4610	0.4395	37	0.5565
8	1.2710	0.4485	66	0.4730	0.4980	29	0.5830
Mean	**1.2217**	**0.4291**	**68.2**	**0.4866**	**0.4127**	**38.3**	**0.4996**

Table B.2.29 – Test #29, B125_A12_55_2

	Post-Fracture Measurements						
		Front Side, inches			Back Side, inches		
Meas. Num.	**Root Notch, inches**	**Throat, inches**	**Angle, degrees**	**Tension Leg, inches**	**Throat, inches**	**Angle, degrees**	**Tension Leg, inches**
1 - X	1.2490	0.4735	62	0.5205	0.4280	71	0.5410
2	1.1425	0.4665	75 & 47	0.5335	0.4600	74 & 56	0.5530
3	1.2250	0.4790	80 & 36	0.5285	0.4650	68 & 43	0.4425
4	1.1675	0.4855	83 & 32	0.5575	0.4070	67 & 37	0.5185
5	1.1985	0.4980	86 & 41	0.4725	0.3980	44	0.5455
6	1.1975	0.4660	80 & 40	0.5080	0.4110	60 & 36	0.5005
7	1.1900	0.4660	71 & 61	0.5020	0.3990	64 & 36	0.5100
8	1.1840	0.4370	67	0.4965	0.4170	56 & 36	0.5165
Mean	**1.1905**	**0.4741**	**64.5**	**0.5159**	**0.4232**	**47.4**	**0.5138**

Table B.2.30 – Test #30, B125_A12_55_3

	Post-Fracture Measurements						
		Front Side, inches			Back Side, inches		
Meas. Num.	**Root Notch, inches**	**Throat, inches**	**Angle, degrees**	**Tension Leg, inches**	**Throat, inches**	**Angle, degrees**	**Tension Leg, inches**
1 - X	1.2165	0.4710	64	0.5275	0.4490	51 & 31	0.5075
2	1.2005	0.4400	70 & 46	0.5425	0.4225	36	0.4785
3	1.2150	0.4350	73 & 45	0.5445	0.4170	35	0.4795
4	1.2335	0.4580	77 & 45	0.5315	0.4180	30	0.4815
5	1.2020	0.4440	73 & 47	0.4865	0.3950	38	0.5100
6	1.1735	0.4630	76 & 44	0.5350	0.4745	73 & 47	0.5275
7	1.1885	0.3955	75 & 36	0.4995	0.4710	65	0.5530
8	1.2015	0.4160	64	0.4860	0.4925	68	0.5335
Mean	**1.2030**	**0.4398**	**64.0**	**0.5212**	**0.4377**	**44.2**	**0.5069**

Table B.2.31 – Test #31, B175_A516_3_1

	Post-Fracture Measurements						
		Front Side, inches			Back Side, inches		
Meas. Num.	**Root Notch, inches**	**Throat, inches**	**Angle, degrees**	**Tension Leg, inches**	**Throat, inches**	**Angle, degrees**	**Tension Leg, inches**
1 - X	1.7715	0.2290	61 & 0	0.2885	0.2620	61	0.2500
2	1.7825	0.2525	63 & 0	0.2535	0.2945	56	0.2765
3	1.7360	0.2400	73 & 0	0.3130	0.3075	41	0.3240
4	1.7395	0.2490	52 & 0	0.3140	0.2515	44	0.3035
5	1.7265	0.2640	61 & 30	0.2930	0.2570	47	0.2530
6	1.7390	0.2915	72 & 44	0.3155	0.2480	65	0.2445
7	1.7640	0.2855	56	0.2795	0.2610	72	0.2965
8	1.7835	0.2390	62	0.2770	0.2405	71	0.2860
Mean	**1.7516**	**0.2600**	**56.8**	**0.2933**	**0.2676**	**55.6**	**0.2811**

Table B.2.32 – Test #32, B175_A516_3_2

	Post-Fracture Measurements						
		Front Side, inches			Back Side, inches		
Meas. Num.	**Root Notch, inches**	**Throat, inches**	**Angle, degrees**	**Tension Leg, inches**	**Throat, inches**	**Angle, degrees**	**Tension Leg, inches**
1 - X	1.7540	0.2940	34 & 0	0.3285	0.2605	42	0.2585
2	1.7680	0.2740	52 & 0	0.3260	0.2550	66 & 0	0.2815
3	1.7880	0.2575	71 & 0	0.3010	0.2500	66	0.2480
4	1.7460	0.3120	49 & 41	0.3145	0.2355	49	0.3020
5	1.7390	0.3035	41	0.3235	0.2475	47	0.2750
6	1.7370	0.3130	39	0.3155	0.2515	41	0.2985
7	1.7205	0.2605	36	0.3215	0.2325	44	0.2580
8	1.7645	0.2990	42	0.2620	0.2300	51	0.2415
Mean	**1.7509**	**0.2880**	**39.1**	**0.3143**	**0.2453**	**49.0**	**0.2738**

Table B.2.33 – Test #33, B175_A516_3_3

	Post-Fracture Measurements						
		Front Side, inches			Back Side, inches		
Meas. Num.	**Root Notch, inches**	**Throat, inches**	**Angle, degrees**	**Tension Leg, inches**	**Throat, inches**	**Angle, degrees**	**Tension Leg, inches**
1 - X	1.7435	0.3110	60	0.2640	0.2560	63 & 0	0.3185
2	1.7435	0.2865	72	0.2885	0.2295	68 & 0	0.3050
3	1.6885	0.3010	73	0.3310	0.2605	69 & 0	0.3615
4	1.7385	0.2620	65	0.2950	0.3675	61 & 0	0.3215
5	1.7400	0.2380	57	0.3060	0.2985	59 & 35	0.3030
6	1.7540	0.2310	51	0.2805	0.3075	68 & 46	0.3185
7	1.7665	0.2100	46	0.2530	0.2785	51	0.2740
8	1.7510	0.2250	59	0.2650	0.2595	58	0.2580
Mean	**1.7396**	**0.2564**	**60.5**	**0.2889**	**0.2863**	**51.9**	**0.3107**

Table B.2.34 – Test #34, B175_A12_3_1

	Post-Fracture Measurements						
		Front Side, inches			Back Side, inches		
Meas. Num.	**Root Notch, inches**	**Throat, inches**	**Angle, degrees**	**Tension Leg, inches**	**Throat, inches**	**Angle, degrees**	**Tension Leg, inches**
1 - X	1.7140	0.3265	57 & 0	0.4250	0.4415	65 & 41	0.5845
2	1.6770	0.3655	28	0.4150	0.4405	69	0.5100
3	1.7585	0.3705	64 & 36	0.5215	0.4265	68 & 62	0.4980
4	1.6885	0.4295	69 & 1	0.5065	0.4250	73	0.4625
5	1.6760	0.4175	70 & 2	0.5070	0.4445	70 & 30	0.5140
6	1.6995	0.4335	72 & 0	0.4825	0.4485	81 & 34	0.5045
7	1.6775	0.4235	69 & 0	0.5025	0.4155	82 & 0	0.5585
8	1.6885	0.4260	54	0.4515	0.4680	58 & 31	0.5305
Mean	**1.6968**	**0.4029**	**31.3**	**0.4828**	**0.4361**	**71.0**	**0.5141**

Table B.2.35 – Test #35, B175_A512_3_2

	Post-Fracture Measurements						
		Front Side, inches			Back Side, inches		
Meas. Num.	**Root Notch, inches**	**Throat, inches**	**Angle, degrees**	**Tension Leg, inches**	**Throat, inches**	**Angle, degrees**	**Tension Leg, inches**
1 - X	1.6825	0.4835	70	0.5210	0.4780	57 & 0	0.5410
2	1.6380	0.5580	76	0.4990	0.4725	58 & 11	0.5720
3	1.6795	0.4530	63	0.4930	0.5035	52 & 11	0.5945
4	1.6535	0.5020	69	0.4755	0.4535	63 & 30	0.5835
5	1.6775	0.4185	66	0.4750	0.5040	66	0.5720
6	1.7025	0.4130	66	0.5050	0.5000	69 & 56	0.5010
7	1.6715	0.4380	67	0.4935	0.4770	69	0.5155
8	1.6680	0.3770	64	0.4485	0.4870	68	0.5535
Mean	**1.6710**	**0.4596**	**67.7**	**0.4895**	**0.4848**	**67.6**	**0.5553**

Table B.2.36 – Test #36, B175_A512_3_3

	Post-Fracture Measurements						
		Front Side, inches			Back Side, inches		
Meas. Num.	**Root Notch, inches**	**Throat, inches**	**Angle, degrees**	**Tension Leg, inches**	**Throat, inches**	**Angle, degrees**	**Tension Leg, inches**
1 - X	1.8485	0.4305	74	0.4835	0.4555	16	0.5060
2	1.8025	0.4585	76	0.4405	0.4390	76 & 15	0.5470
3	1.7280	0.4095	70	0.4525	0.5130	86 & 26	0.5290
4	1.7075	0.4520	71	0.4320	0.5125	76 & 39	0.5595
5	1.6945	0.4130	67	0.4860	0.5010	70 & 49	0.5414
6	1.6960	0.5030	78 & 68	0.4890	0.4900	75 & 45	0.5760
7	1.6825	0.4140	68	0.4920	0.4695	63	0.5695
8	1.6870	0.4045	66	0.4905	0.4560	65	0.5595
Mean	**1.7247**	**0.4386**	**70.4**	**0.4680**	**0.4835**	**60.2**	**0.5511**

Table B.2.37 – Test #37, B175_A516_55_1

	Post-Fracture Measurements						
		Front Side, inches			Back Side, inches		
Meas. Num.	**Root Notch, inches**	**Throat, inches**	**Angle, degrees**	**Tension Leg, inches**	**Throat, inches**	**Angle, degrees**	**Tension Leg, inches**
1 - X	1.7195	0.3790	10	0.3935	0.2530	0	0.2380
2	1.7780	0.3190	37	0.3890	0.2390	58	0.3330
3	1.7380	0.3080	44	0.3925	0.2505	61	0.3195
4	1.7605	0.2985	38	0.3090	0.2930	46	0.3105
5	1.7645	0.3035	39	0.3410	0.2250	45	0.3235
6	1.6955	0.3070	41	0.3450	0.2740	41	0.3080
7	1.7370	0.2400	44	0.3300	0.2740	40	0.3360
8	1.7535	0.2630	41	0.3895	0.2465	38	0.3410
9	1.7035	0.2935	52	0.3650	0.2455	39	0.3305
Mean	**1.7428**	**0.2963**	**39.5**	**0.3591**	**0.2565**	**43.9**	**0.3200**

Table B.2.38 – Test #38, B175_A516_55_2

	Post-Fracture Measurements						
		Front Side, inches			Back Side, inches		
Meas. Num.	**Root Notch, inches**	**Throat, inches**	**Angle, degrees**	**Tension Leg, inches**	**Throat, inches**	**Angle, degrees**	**Tension Leg, inches**
1 - X	1.7000	0.2715	45	0.3400	0.3135	35	0.3890
2	1.7260	0.2460	42	0.3535	0.2770	35	0.3520
3	1.7350	0.2285	46	0.3270	0.2630	35	0.3500
4	1.7555	0.2425	44	0.3425	0.2590	41	0.3285
5	1.7110	0.2490	42	0.3545	0.2755	39	0.3720
6	1.7240	0.2480	41	0.3730	0.2705	35	0.3680
7	1.7575	0.2265	39	0.3715	0.2480	40	0.3445
8	1.7110	0.2680	35	0.3905	0.2414	39	0.3440
9	1.7725	0.2485	44	0.3485	0.2815	47	0.3340
Mean	**1.7320**	**0.2458**	**41.6**	**0.3573**	**0.2660**	**38.1**	**0.3524**

Table B.2.39 – Test #39, B175_A516_55_3

	Post-Fracture Measurements						
		Front Side, inches			Back Side, inches		
Meas. Num.	**Root Notch, inches**	**Throat, inches**	**Angle, degrees**	**Tension Leg, inches**	**Throat, inches**	**Angle, degrees**	**Tension Leg, inches**
1 - X	1.7535	0.2340	25	0.3595	0.3180	36 & 2	0.3585
2	1.7595	0.2425	36	0.2835	0.2945	45 & 9	0.3485
3	1.7420	0.2485	38	0.3055	0.3130	36	0.3465
4	1.7275	0.2405	44	0.3290	0.2615	37	0.3280
5	1.7530	0.2370	41	0.2665	0.2760	38	0.3180
6	1.7210	0.2495	35	0.3110	0.2505	41	0.3345
7	1.7010	0.2225	41	0.3350	0.2595	39	0.3420
8	1.7053	0.2445	46	0.2935	0.2465	44	0.3245
9	1.7270	0.2605	44	0.3585	0.2620	47	0.3370
Mean	**1.7311**	**0.2414**	**39.5**	**0.3096**	**0.2737**	**40.0**	**0.3360**

Table B.2.40 – Test #40, B175_A12_55_1

	Post-Fracture Measurements						
		Front Side, inches			Back Side, inches		
Meas. Num.	**Root Notch, inches**	**Throat, inches**	**Angle, degrees**	**Tension Leg, inches**	**Throat, inches**	**Angle, degrees**	**Tension Leg, inches**
1 - X	1.7165	0.4790	12	0.5440	0.4415	67	0.4765
2	1.7175	0.4390	20	0.5315	0.4695	68	0.4725
3	1.7830	0.4185	36 & 5	0.4765	0.3765	70 & 42	0.4265
4	1.6950	0.3980	52 & 24	0.5275	0.4150	71 & 39	0.4490
5	1.7020	0.4285	63 & 28	0.5720	0.4055	74 & 44	0.4965
6	1.6620	0.4485	71 & 36	0.5165	0.4315	71 & 56	0.5020
7	1.6615	0.4675	61	0.5670	0.4235	58	0.4910
8	1.6950	0.5100	63	0.4955	0.4305	64	0.5045
Mean	**1.7038**	**0.4410**	**40.1**	**0.5303**	**0.4222**	**63.3**	**0.4751**

Table B.2.41 – Test #41, B175_A12_55_2

	Post-Fracture Measurements						
		Front Side, inches			Back Side, inches		
Meas. Num.	**Root Notch, inches**	**Throat, inches**	**Angle, degrees**	**Tension Leg, inches**	**Throat, inches**	**Angle, degrees**	**Tension Leg, inches**
1 - X	1.7230	0.4780	56	0.5315	0.4750	69	0.4965
2	1.7160	0.4530	60	0.5315	0.4460	64	0.5615
3	1.7145	0.3890	79 & 40	0.5395	0.4465	76 & 18	0.5470
4	1.6765	0.4435	76 & 36	0.5360	0.4350	76 & 29	0.5295
5	1.6690	0.4485	80 & 58	0.5335	0.4115	71 & 28	0.5120
6	1.7045	0.4560	68	0.5295	0.3825	68 & 49	0.4690
7	1.7095	0.4100	66	0.5240	0.4155	59	0.4960
8	1.6810	0.4470	66	0.5500	0.3695	56	0.4930
Mean	**1.6988**	**0.4370**	**64.2**	**0.5334**	**0.4228**	**61.6**	**0.5161**

Table B.2.42 – Test #42, B175_A12_55_3

	Post-Fracture Measurements						
		Front Side, inches			Back Side, inches		
Meas. Num.	**Root Notch, inches**	**Throat, inches**	**Angle, degrees**	**Tension Leg, inches**	**Throat, inches**	**Angle, degrees**	**Tension Leg, inches**
1 - X	1.7160	0.4380	62	0.5420	0.4515	34	0.5135
2	1.7390	0.4465	81 & 42	0.5455	0.3945	28	0.4820
3	1.6790	0.4305	79 & 38	0.5300	0.3875	50 & 0	0.4855
4	1.6935	0.4385	76 & 43	0.5390	0.4610	71 & 29	0.5345
5	1.7190	0.4290	76 & 64	0.5380	0.4510	78 & 37	0.4825
6	1.7140	0.4155	72 & 65	0.4885	0.4765	74 & 52	0.5250
7	1.8545	0.4325	83 & 64	0.4670	0.4630	75	0.4530
8	1.8275	0.4735	74	0.4595	0.5045	74 & 66	0.5115
Mean	**1.7380**	**0.4350**	**68.0**	**0.5158**	**0.4438**	**49.3**	**0.4961**

Table B.2.43 – Test #43, B175_A516_85_1

	Post-Fracture Measurements						
		Front Side, inches			Back Side, inches		
Meas. Num.	**Root Notch, inches**	**Throat, inches**	**Angle, degrees**	**Tension Leg, inches**	**Throat, inches**	**Angle, degrees**	**Tension Leg, inches**
1 - X	1.7520	0.3120	25	0.3235	0.2930	49	0.2740
2	1.7825	0.2895	34	0.3420	0.2760	54	0.3035
3	1.7495	0.2440	34	0.2865	0.2815	49	0.3200
4	1.7600	0.2725	36	0.3270	0.2355	44	0.2805
5	1.7485	0.2335	35	0.3110	0.2675	43	0.3250
6	1.7590	0.2470	39	0.3010	0.2570	45	0.2990
7	1.7565	0.2480	38	0.3385	0.2490	45	0.2890
8	1.6910	0.2105	54 & 0	0.2955	0.3110	40	0.4295
Mean	**1.7546**	**0.2564**	**34.6**	**0.3166**	**0.2662**	**46.4**	**0.3089**

Table B.2.44 – Test #44, B175_A516_85_2

	Post-Fracture Measurements						
		Front Side, inches			Back Side, inches		
Meas. Num.	**Root Notch, inches**	**Throat, inches**	**Angle, degrees**	**Tension Leg, inches**	**Throat, inches**	**Angle, degrees**	**Tension Leg, inches**
1 - X	1.7730	0.2500	32	0.3280	0.2975	35	0.3210
2	1.7725	0.2325	38	0.3130	0.2735	37	0.3630
3	1.7280	0.2670	36	0.3515	0.2530	45	0.3290
4	1.7465	0.2645	30	0.3325	0.2605	43	0.3170
5	1.7360	0.2615	41	0.3200	0.2530	44	0.3305
6	1.7075	0.2945	33	0.3040	0.2535	42	0.3165
7	1.8550	0.2445	37	0.3470	0.2370	59	0.2620
8	1.7750	0.2645	30	0.3380	0.3060	45	0.3905
Mean	**1.7596**	**0.2603**	**35.2**	**0.3286**	**0.2609**	**44.4**	**0.3242**

Table B.2.45 – Test #45, B175_A516_85_3

	Post-Fracture Measurements						
		Front Side, inches			Back Side, inches		
Meas. Num.	**Root Notch, inches**	**Throat, inches**	**Angle, degrees**	**Tension Leg, inches**	**Throat, inches**	**Angle, degrees**	**Tension Leg, inches**
1 - X	1.7905	0.2645	30	0.2875	0.2815	36 & 16	0.3400
2	1.7105	0.2735	40	0.3450	0.2850	42 & 2	0.3590
3	1.7610	0.2520	40	0.3020	0.2685	45	0.3350
4	1.7210	0.2285	40	0.3240	0.2910	44	0.3275
5	1.7080	0.2400	43	0.3415	0.2775	41	0.3500
6	1.7540	0.2525	40	0.3175	0.2760	43	0.3490
7	1.7685	0.2285	40	0.2935	0.2560	31	0.3590
8	1.7610	0.2520	55	0.2955	0.2650	44 & 0	0.3665
Mean	**1.7420**	**0.2474**	**40.8**	**0.3169**	**0.2754**	**40.8**	**0.3474**

Table B.2.46 – Test #46, B175_A12_85_1

	Post-Fracture Measurements						
		Front Side, inches			Back Side, inches		
Meas. Num.	**Root Notch, inches**	**Throat, inches**	**Angle, degrees**	**Tension Leg, inches**	**Throat, inches**	**Angle, degrees**	**Tension Leg, inches**
1 - X	1.7015	0.4315	64	0.5870	0.4970	68 & 54	0.5865
2	1.6990	0.3700	72 & 52	0.5925	0.4910	81 & 31	0.5475
3	1.6750	0.4985	74	0.5590	0.4600	63	0.5735
4	1.6965	0.4750	74	0.5705	0.4960	66	0.5605
5	1.7025	0.4375	71	0.5390	0.5465	71	0.5355
6	1.6950	0.5885	91 & 71	0.5330	0.4430	64	0.5250
7	1.6835	0.5650	82	0.5915	0.4565	55	0.5850
8	1.7030	0.5635	91 & 73	0.5500	0.4680	67 & 59	0.5575
Mean	**1.6932**	**0.4901**	**73.8**	**0.5648**	**0.4822**	**63.8**	**0.5567**

Table B.2.47 – Test #47, B175_A12_85_2

	Post-Fracture Measurements						
		Front Side, inches			Back Side, inches		
Meas. Num.	**Root Notch, inches**	**Throat, inches**	**Angle, degrees**	**Tension Leg, inches**	**Throat, inches**	**Angle, degrees**	**Tension Leg, inches**
1 - X	1.7200	0.4720	65	0.5425	0.4445	19	0.5155
2	1.7565	0.4575	78	0.4150	0.4345	20	0.5690
3	1.7480	0.4705	76	0.4645	0.4010	40	0.5315
4	1.7065	0.4315	81 & 64	0.4925	0.4025	88 & 33	0.5655
5	1.7220	0.4335	89 & 43	0.5045	0.4990	79 & 49	0.5430
6	1.7140	0.4945	89 & 80	0.4845	0.4650	76 & 61	0.5460
7	1.7025	0.5150	90	0.4955	0.4560	62	0.5805
8	1.6940	0.5165	89 & 81	0.5195	0.4570	61	0.5600
Mean	**1.7227**	**0.4705**	**79.3**	**0.4829**	**0.4440**	**40.6**	**0.5536**

Table B.2.48 – Test #48, B175_A12_85_3

	Post-Fracture Measurements						
		Front Side, inches			Back Side, inches		
Meas. Num.	**Root Notch, inches**	**Throat, inches**	**Angle, degrees**	**Tension Leg, inches**	**Throat, inches**	**Angle, degrees**	**Tension Leg, inches**
1 - X	1.7020	0.4805	67	0.5045	0.4415		0.5770
2	1.7125	0.4320	72 & 37	0.5260	0.4030		0.5220
3	1.7095	0.3945	56 & 46	0.5610	0.4300		0.5455
4	1.7130	0.3570	46 & 33	0.5355	0.4360		0.5035
5	1.7045	0.4340	71	0.4910	0.5185		0.5535
6	1.7540	0.4005	49	0.4570	0.4945		0.5085
7	1.7750	0.3925	47 & 35	0.5415	0.4620		0.4445
8	1.7630	0.5035	64	0.5185	0.4450		0.5085
Mean	**1.7286**	**0.4130**	**60.7**	**0.5178**	**0.4556**		**0.5166**

Table B.2.49 – Test #49, B250_A516_55_1

	Post-Fracture Measurements						
		Front Side, inches			Back Side, inches		
Meas. Num.	**Root Notch, inches**	**Throat, inches**	**Angle, degrees**	**Tension Leg, inches**	**Throat, inches**	**Angle, degrees**	**Tension Leg, inches**
1 - X	2.6345	0.2985	45 & 39	0.3325	0.2260	42 & 12	0.2620
2	2.5890	0.2310	37	0.3290	0.2020	39	0.2705
3	2.5820	0.2600	44 & 33	0.3545	0.2205	44	0.2805
4	2.5940	0.1780	37	0.2975	0.2290	46	0.2875
5	2.5925	0.2535	44	0.3600	0.2345	51	0.2915
6	2.5565	0.2235	34	0.3585	0.2355	53	0.2935
7	2.5305	0.2400	34	0.3535	0.2365	44	0.2790
8	2.5285	0.2600	37	0.3280	0.2315	49	0.3040
9	2.5660	0.2125	47	0.3235	0.2575	51	0.3130
Mean	**2.5712**	**0.2374**	**38.3**	**0.3388**	**0.2287**	**47.1**	**0.2867**

Table B.2.50 – Test #50, B250_A516_55_2

	Post-Fracture Measurements						
		Front Side, inches			Back Side, inches		
Meas. Num.	**Root Notch, inches**	**Throat, inches**	**Angle, degrees**	**Tension Leg, inches**	**Throat, inches**	**Angle, degrees**	**Tension Leg, inches**
1 - X	2.4650	0.2905	45	0.3450	0.2795	50	0.3095
2	2.4975	0.2520	29	0.3075	0.2720	37	0.3305
3	2.5675	0.2600	36	0.3420	0.2390	43	0.2970
4	2.5655	0.2415	54	0.2750	0.2240	46	0.2760
5	2.5995	0.2060	52	0.3100	0.2430	42	0.2965
6	2.5605	0.2520	50	0.2930	0.2250	44	0.2865
7	2.5295	0.2275	47	0.3425	0.2045	44	0.3010
8	2.5650	0.2215	50	0.3165	0.2235	35	0.3030
9	2.5675	0.2405	49	0.3235	0.2270	38	0.3100
Mean	**2.5507**	**0.2404**	**45.6**	**0.3148**	**0.2353**	**41.8**	**0.2999**

Table B.2.51 – Test #51, B250_A516_55_2

	Post-Fracture Measurements						
		Front Side, inches			Back Side, inches		
Meas. Num.	**Root Notch, inches**	**Throat, inches**	**Angle, degrees**	**Tension Leg, inches**	**Throat, inches**	**Angle, degrees**	**Tension Leg, inches**
1 - X	2.5775	0.2540	35	0.3060	0.2400	49 % 0	0.3185
2	2.4845	0.3090	34	0.3495	0.2370	58 & 0	0.3120
3	2.5270	0.2525	32	0.3165	0.2620	34	0.3255
4	2.5400	0.2695	44	0.3155	0.2720	51	0.3290
5	2.5330	0.2740	45	0.3260	0.2715	54	0.3255
6	2.5305	0.2655	46	0.2815	0.2715	45	0.3295
7	2.5470	0.2690	49	0.3035	0.2195	42	0.3150
8	2.5480	0.2555	46	0.3315	0.2280	48	0.2905
9	2.6035	0.1945	42	0.2580	0.2410	50	0.3050
Mean	**2.5367**	**0.2656**	**41.9**	**0.3137**	**0.2504**	**46.1**	**0.3174**

Table B.2.52 – Test #52, B250_A12_55_1

	Post-Fracture Measurements						
		Front Side, inches			Back Side, inches		
Meas. Num.	**Root Notch, inches**	**Throat, inches**	**Angle, degrees**	**Tension Leg, inches**	**Throat, inches**	**Angle, degrees**	**Tension Leg, inches**
1 - X	2.5130	0.4325	68	0.4685	0.3565	64	0.4900
2	2.4845	0.4345	66	0.4990	0.3590	58	0.4855
3	2.4640	0.5100	76 & 63	0.5075	0.3925	65	0.4775
4	2.4575	0.3910	84 & 42	0.5335	0.4365	66	0.4945
5	2.4370	0.4095	71 & 37	0.5285	0.4215	63	0.4835
6	2.4510	0.4455	69 & 61	0.5420	0.4425	70	0.5355
7	2.4420	0.4350	71 & 49	0.5265	0.4990	74	0.5765
8	2.4630	0.4620	74	0.5270	0.4830	75	0.5305
Mean	**2.4600**	**0.4388**	**66.6**	**0.5197**	**0.4245**	**66.4**	**0.5090**

Table B.2.53 – Test #53, B250_A12_55_2

	Post-Fracture Measurements						
		Front Side, inches			Back Side, inches		
Meas. Num.	**Root Notch, inches**	**Throat, inches**	**Angle, degrees**	**Tension Leg, inches**	**Throat, inches**	**Angle, degrees**	**Tension Leg, inches**
1 - X	2.4455	0.4360	59	0.5205	0.5055	75	0.4850
2	2.4335	0.4520	74	0.5030	0.4580	74	0.5990
3	2.4315	0.4930	75	0.5240	0.4695	76	0.5160
4	2.4575	0.4600	70	0.4505	0.4780	78 & 67	0.4745
5	2.4470	0.4425	64	0.4800	0.4440	69 & 65	0.4815
6	2.4280	0.3975	59	0.4825	0.4035	59	0.4630
7	2.4440	0.3960	53	0.5475	0.4070	57	0.4885
8	2.4835	0.4150	59	0.5205	0.4370	60	0.5635
Mean	**2.4433**	**0.4383**	**65.0**	**0.5007**	**0.4468**	**66.6**	**0.5063**

Table B.2.54 – Test #54, B250_A12_55_3

	Post-Fracture Measurements						
		Front Side, inches			Back Side, inches		
Meas. Num.	**Root Notch, inches**	**Throat, inches**	**Angle, degrees**	**Tension Leg, inches**	**Throat, inches**	**Angle, degrees**	**Tension Leg, inches**
1 - X	2.4450	0.4370	63 & 39	0.4560	0.4860	72	0.5630
2	2.4220	0.4085	75 & 8	0.4515	0.4660	71	0.4815
3	2.4330	0.4440	75 & 24	0.4935	0.4900	79	0.5455
4	2.3845	0.3665	69 & 31	0.4905	0.4990	77	0.5300
5	2.4200	0.4910	71 & 51	0.4795	0.4905	73	0.4950
6	2.4370	0.4730	66	0.5175	0.4355	70	0.5305
7	2.4090	0.4200	64	0.5250	0.4770	78 & 64	0.5420
8	2.3845	0.4635	74	0.5295	0.4750	72	0.5170
Mean	**2.4172**	**0.4359**	**66.1**	**0.4929**	**0.4769**	**73.8**	**0.5232**

Table B.2.55 – Test #55, B125_B516_55_1

	Post-Fracture Measurements						
		Front Side, inches			Back Side, inches		
Meas. Num.	**Root Notch, inches**	**Throat, inches**	**Angle, degrees**	**Tension Leg, inches**	**Throat, inches**	**Angle, degrees**	**Tension Leg, inches**
1 - X	1.3055	0.2890	46	0.3340	0.3320	71	0.3465
2	1.2465	0.2895	67	0.3155	0.3770	75	0.3885
3	1.2610	0.3605	69	0.3685	0.4185	83	0.4065
4	1.2355	0.3390	76	0.3160	0.3360	84	0.3760
5	1.2535	0.2925	77	0.3190	0.3885	84	0.3185
6	1.2980	0.3665	76	0.3520	0.3300	82	0.3240
7	1.3620	0.3080	72	0.3005	0.2435	66	0.2480
8	1.1055	0.2665	66	0.3895	0.4080	0	0.4555
Mean	**1.2673**	**0.3200**	**70.7**	**0.3327**	**0.3516**	**73.6**	**0.3508**

Table B.2.56 – Test #56, B125_B516_55_2

	Post-Fracture Measurements						
		Front Side, inches			Back Side, inches		
Meas. Num.	**Root Notch, inches**	**Throat, inches**	**Angle, degrees**	**Tension Leg, inches**	**Throat, inches**	**Angle, degrees**	**Tension Leg, inches**
1 - X	1.3070	0.3680	9	0.3060	0.3365	77	0.3825
2	1.2640	0.3065	18	0.2665	0.3250	74	0.3400
3	1.2585	0.2445	25	0.3040	0.3095	55	0.3915
4	1.2115	0.4010	29	0.3860	0.3405	74	0.3775
5	1.2675	0.3415	35	0.3175	0.3660	76	0.3510
6	1.2620	0.3630	31	0.3150	0.3730	82	0.3615
7	1.2180	0.3470	60	0.3370	0.3405	75	0.4060
8	1.2305	0.3675	55	0.3165	0.3480	82	0.3900
Mean	**1.2496**	**0.3381**	**32.9**	**0.3198**	**0.3424**	**73.5**	**0.3731**

Table B.2.57 – Test #57, B125_B516_55_3

	Post-Fracture Measurements						
		Front Side, inches			Back Side, inches		
Meas. Num.	**Root Notch, inches**	**Throat, inches**	**Angle, degrees**	**Tension Leg, inches**	**Throat, inches**	**Angle, degrees**	**Tension Leg, inches**
1 - X	n/a	0.3780	78	0.2790	0.4485	64	0.5550
2	1.1305	0.3675	79	0.3360	0.4555	61	0.5860
3	1.1100	0.3945	92	0.3035	0.4795	78	0.6035
4	1.1185	0.4205	86	0.2925	0.3945	78	0.5510
5	1.1175	0.4075	85	0.3270	0.5580	63	0.5390
6	1.1115	0.3425	83	0.3205	0.5350	56	0.5630
7	1.1360	0.2670	69	0.3045	0.3670	58	0.4960
8	1.1165	0.3480	72	0.3270	0.3775	64	0.4825
Mean	**1.1201**	**0.3661**	**81.4**	**0.3126**	**0.4584**	**65.5**	**0.5517**

Table B.2.58 – Test #58, B125_B12_55_1

	Post-Fracture Measurements						
		Front Side, inches			Back Side, inches		
Meas. Num.	**Root Notch, inches**	**Throat, inches**	**Angle, degrees**	**Tension Leg, inches**	**Throat, inches**	**Angle, degrees**	**Tension Leg, inches**
1 - X	1.2610	0.5140	71	0.4625	0.3925	76	0.5113
2	1.2420	0.5535	79	0.4880	0.3840	84	0.5335
3	1.2510	0.5780	81	0.4945	0.4750	83	0.5275
4	1.2650	0.5795	79	0.5010	0.4620	80	0.4905
5	1.2705	0.5015	79	0.5145	0.4750	78	0.5100
6	1.2460	0.4075	78	0.5495	0.5490	85	0.5020
7	1.2810	0.4035	70	0.5025	0.5720	62	0.4980
8	1.2575	0.4165	68	0.5200	0.4775	51	0.5085
Mean	**1.2593**	**0.4991**	**76.6**	**0.5062**	**0.4798**	**76.8**	**0.5102**

Table B.2.59 – Test #59, B125_B12_55_2

	Post-Fracture Measurements						
		Front Side, inches			Back Side, inches		
Meas. Num.	**Root Notch, inches**	**Throat, inches**	**Angle, degrees**	**Tension Leg, inches**	**Throat, inches**	**Angle, degrees**	**Tension Leg, inches**
1 - X	1.2830	0.4855	74	0.4475	0.5100	80	0.4555
2	1.2340	0.5040	72	0.4925	0.5875	79	0.4545
3	1.2800	0.4710	77	0.4795	0.5980	83	0.5275
4	1.2195	0.4880	67	0.4625	0.5195	73	0.5460
5	1.1630	0.4835	68	0.4535	0.5870	82	0.4655
6	1.2490	0.4285	71	0.4575	0.4995	76	0.4845
7	1.2345	0.4320	61	0.4585	0.5900	91	0.5015
8	1.2180	0.4365	71	0.4165	0.4300	66	0.4870
Mean	**1.2326**	**0.4670**	**69.7**	**0.4629**	**0.5519**	**79.7**	**0.4934**

Table B.2.60 – Test #60, B125_B12_55_3

	Post-Fracture Measurements						
		Front Side, inches			Back Side, inches		
Meas. Num.	**Root Notch, inches**	**Throat, inches**	**Angle, degrees**	**Tension Leg, inches**	**Throat, inches**	**Angle, degrees**	**Tension Leg, inches**
1 - X	1.2805	0.4170	65	0.5380	0.4505	67	0.5510
2	1.2505	0.5175	79	0.5600	0.3805	59	0.5835
3	1.2010	0.6260	82	0.5905	0.3755	61	0.5895
4	1.1575	0.5265	76	0.5750	0.4110	62	0.5495
5	1.2135	0.3995	61	0.5430	0.4280	40	0.5465
6	1.1990	0.4240	60	0.4700	0.4055	45	0.5705
7	1.1850	0.3640	57	0.5030	0.4885	61	0.5570
8	1.1810	0.4210	59	0.5535	0.4730	62	0.5610
Mean	**1.2048**	**0.4691**	**68.3**	**0.5409**	**0.4207**	**55.9**	**0.5648**

Table B.2.61 – Test #61, B175_B516_3_1

	Post-Fracture Measurements						
		Front Side, inches			Back Side, inches		
Meas. Num.	**Root Notch, inches**	**Throat, inches**	**Angle, degrees**	**Tension Leg, inches**	**Throat, inches**	**Angle, degrees**	**Tension Leg, inches**
1 - X	1.7600	0.4145	71	0.4115	0.4610	71	0.4415
2	1.7745	0.4075	76	0.3545	0.5110	69	0.4360
3	1.6900	0.2750	69	0.3805	0.4355	64	0.4080
4	1.7385	0.2975	56	0.3195	0.3355	1	0.3985
5	1.7450	0.2710	68	0.2905	0.3965	0	0.4020
6	1.7325	0.3130	65	0.3070	0.3960	0	0.3790
7	1.7645	0.3015	64	0.3080	0.4285	0	0.2450
8	1.7565	0.2505	51	0.2810	0.2075	0	0.2950
Mean	**1.7430**	**0.3136**	**65.7**	**0.3291**	**0.4068**	**24.0**	**0.3769**

Table B.2.62 – Test #62, B175_B516_3_2

	Post-Fracture Measurements						
		Front Side, inches			Back Side, inches		
Meas. Num.	**Root Notch, inches**	**Throat, inches**	**Angle, degrees**	**Tension Leg, inches**	**Throat, inches**	**Angle, degrees**	**Tension Leg, inches**
1 - X	1.8020	0.4030	66	0.2835	0.3940	67	0.2475
2	1.7700	0.3900	70	0.3285	0.4085	70	0.2535
3	1.7985	0.3945	69	0.2930	0.3725	69	0.3165
4	1.8015	0.3855	73	0.3155	0.3160	71	0.3175
5	1.7870	0.3350	68	0.2800	0.3840	68	0.2640
6	1.7660	0.3390	68	0.3615	0.2995	66	0.3550
7	1.7920	0.3235	64	0.3690	0.2555	55	0.3015
8	1.8055	0.3200	66	0.3690	0.1955	55	0.2705
Mean	**1.7881**	**0.3613**	**68.3**	**0.3248**	**0.3338**	**65.8**	**0.2960**

Table B.2.63 – Test #63, B175_B516_3_3

	Post-Fracture Measurements						
		Front Side, inches			Back Side, inches		
Meas. Num.	**Root Notch, inches**	**Throat, inches**	**Angle, degrees**	**Tension Leg, inches**	**Throat, inches**	**Angle, degrees**	**Tension Leg, inches**
1 - X	1.7540	0.4190	83	0.3485	0.3875	85	0.3905
2	1.7985	0.4310	82	0.3070	0.3085	83	0.3560
3	1.7535	0.4305	86	0.3495	0.3305	78	0.3735
4	1.7865	0.3695	72	0.2815	0.2755	74	0.3860
5	1.7930	0.3610	69	0.3445	0.2580	63	0.2935
6	1.7860	0.3605	72	0.3165	0.2780	61	0.2925
7	1.7435	0.5495	88	0.3500	0.2775	61	0.3060
8	1.7265	0.4640	89	0.3245	0.2695	46	0.2285
Mean	**1.7723**	**0.4201**	**79.1**	**0.3263**	**0.2931**	**69.4**	**0.3314**

Table B.2.64 – Test #64, B175_B12_3_1

	Post-Fracture Measurements						
		Front Side, inches			Back Side, inches		
Meas. Num.	**Root Notch, inches**	**Throat, inches**	**Angle, degrees**	**Tension Leg, inches**	**Throat, inches**	**Angle, degrees**	**Tension Leg, inches**
1 - X	1.8130	0.4795	70	0.5195	0.5105	66	0.5110
2	1.7640	0.5135	75	0.5230	0.5165	77	0.5285
3	1.7540	0.5315	84	0.5300	0.4230	65	0.5525
4	1.7305	0.5265	83	0.5720	0.4050	64	0.4960
5	1.6560	0.5600	80	0.5500	0.4155	67	0.4885
6	1.7410	0.5320	74	0.5700	0.5100	71	0.5225
7	1.7655	0.4100	65	0.5025	0.4425	71	0.4370
8	1.8830	0.4580	73	0.5260	0.4745	78	0.4020
Mean	**1.7493**	**0.5068**	**76.2**	**0.5389**	**0.4571**	**69.5**	**0.4982**

Table B.2.65 – Test #65, B175_B12_3_2

	Post-Fracture Measurements						
		Front Side, inches			Back Side, inches		
Meas. Num.	**Root Notch, inches**	**Throat, inches**	**Angle, degrees**	**Tension Leg, inches**	**Throat, inches**	**Angle, degrees**	**Tension Leg, inches**
1 - X	1.7650	0.4125	60	0.5515	0.4400	67	0.4940
2	1.7630	0.5885	80	0.5510	0.4850	76	0.5130
3	1.7425	0.5835	79	0.5035	0.5470	79	0.4805
4	1.7635	0.4795	73	0.5105	0.5845	81	0.5025
5	1.7445	0.4645	78	0.4880	0.5045	77	0.5100
6	1.7195	0.4520	71	0.4560	0.5665	81	0.5270
7	1.7325	0.4685	70	0.4935	0.4030	61	0.5095
8	1.7305	0.4675	71	0.5155	0.4050	60	0.5140
Mean	**1.7447**	**0.4978**	**74.0**	**0.5046**	**0.5035**	**74.3**	**0.5067**

Table B.2.66 – Test #66, B175_B12_3_3

	Post-Fracture Measurements						
		Front Side, inches			Back Side, inches		
Meas. Num.	**Root Notch, inches**	**Throat, inches**	**Angle, degrees**	**Tension Leg, inches**	**Throat, inches**	**Angle, degrees**	**Tension Leg, inches**
1 - X	1.8095	0.5310	74	0.5000	0.4400	57	0.5050
2	1.7580	0.5285	74	0.4905	0.4370	79	0.5175
3	1.7935	0.5245	81	0.4895	0.5340	84	0.5420
4	1.7545	0.5105	77	0.4805	0.5740	83	0.5065
5	1.7540	0.4665	79	0.5145	0.5595	87	0.5045
6	1.7320	0.4740	79	0.5575	0.5900	81	0.4960
7	1.7295	0.4290	68	0.5055	0.5155	69	0.4415
8	1.7575	0.4305	66	0.5265	0.3705	60	0.4395
Mean	**1.7573**	**0.4878**	**75.5**	**0.5072**	**0.5188**	**77.8**	**0.4977**

Table B.2.67 – Test #67, B175_B516_55_1

	Post-Fracture Measurements						
		Front Side, inches			Back Side, inches		
Meas. Num.	**Root Notch, inches**	**Throat, inches**	**Angle, degrees**	**Tension Leg, inches**	**Throat, inches**	**Angle, degrees**	**Tension Leg, inches**
1 - X	1.7580	0.2385	37	0.4290	0.3585	79	0.2880
2	1.7835	0.3425	38	0.4010	0.3715	71	0.3075
3	1.7670	0.3465	34	0.4010	0.3080	71	0.2990
4	1.7965	0.3320	23	0.4140	0.3430	76	0.3210
5	1.7590	0.3525	44	0.3965	0.3250	71	0.3345
6	1.7250	0.2945	49	0.3990	0.3425	70	0.3095
7	1.7580	0.3350	66	0.3825	0.2845	69	0.3100
8	1.7555	0.3655	68	0.3890	0.2890	61	0.3110
9	1.7670	0.3660	59	0.4270	0.2465	54	0.3340
Mean	**1.7634**	**0.3343**	**46.2**	**0.4010**	**0.3210**	**69.5**	**0.3130**

Table B.2.68 – Test #68, B175_B516_55_2

	Post-Fracture Measurements						
		Front Side, inches			Back Side, inches		
Meas. Num.	**Root Notch, inches**	**Throat, inches**	**Angle, degrees**	**Tension Leg, inches**	**Throat, inches**	**Angle, degrees**	**Tension Leg, inches**
1 - X	1.8165	0.3645	78	0.3915	0.2975	71	0.2715
2	1.8145	0.3080	69 & 26	0.4315	0.3275	71	0.2670
3	1.7995	0.3620	68 & 25	0.4335	0.3280	66	0.2555
4	1.7925	0.3270	35	0.3765	0.2650	57	0.2300
5	1.8030	0.2680	64	0.3730	0.2230	49	0.2270
6	1.7990	0.3140	60	0.3795	0.2105	30	0.2135
7	1.7845	0.3105	65 & 30	0.4075	0.2775	48	n/a
8	1.8150	0.3100	58	0.3325	0.3340	49	0.2590
9	1.8365	0.3055	65	0.3670	0.1870	54	0.2260
Mean	**1.8040**	**0.3165**	**56.2**	**0.3893**	**0.2765**	**53.9**	**0.2428**

Table B.2.69 – Test #69, B175_B516_55_3

	Post-Fracture Measurements						
		Front Side, inches			Back Side, inches		
Meas. Num.	**Root Notch, inches**	**Throat, inches**	**Angle, degrees**	**Tension Leg, inches**	**Throat, inches**	**Angle, degrees**	**Tension Leg, inches**
1 - X	1.7415	0.3920	77	0.3450	0.3545	72	0.3095
2	1.7685	0.3765	78	0.3875	0.3305	74	0.2925
3	1.7305	0.4045	84	0.3655	0.3620	74	0.3385
4	1.7345	0.3680	79	0.3270	0.3215	75	0.2870
5	1.7730	0.3285	75	0.3205	0.2800	69	0.2270
6	1.7625	0.3685	73	0.3290	0.2805	66	0.2455
7	1.7485	0.3475	70	0.3285	0.2765	70	0.2785
8	1.7635	0.2795	66	0.2850	0.2715	63	0.2675
Mean	**1.7529**	**0.3619**	**75.9**	**0.3395**	**0.3091**	**70.9**	**0.2795**

Table B.2.70 – Test #70, B175_B12_55_1

	Post-Fracture Measurements						
		Front Side, inches			Back Side, inches		
Meas. Num.	**Root Notch, inches**	**Throat, inches**	**Angle, degrees**	**Tension Leg, inches**	**Throat, inches**	**Angle, degrees**	**Tension Leg, inches**
1 - X	1.7250	0.4435	44 & 14	0.4830	0.5110	79	0.4935
2	1.7010	0.4880	31 & 8	0.5440	0.5290	80	0.5200
3	1.7605	0.4740	34 & 0	0.5210	0.5100	77	0.5165
4	1.7190	0.4780	20	0.5550	0.4510	74	0.5255
5	1.7315	0.5150	26	0.4740	0.4815	70	0.5355
6	1.7455	0.4675	61	0.4985	0.3795	61	0.5200
7	1.7145	0.4795	64	0.5500	0.3955	63	0.5255
8	1.7195	0.4715	74	0.4555	0.3880	60	0.5465
Mean	**1.7279**	**0.4804**	**46.7**	**0.5169**	**0.4567**	**70.7**	**0.5234**

Table B.2.71 – Test #71, B175_B12_55_2

	Post-Fracture Measurements						
		Front Side, inches			Back Side, inches		
Meas. Num.	**Root Notch, inches**	**Throat, inches**	**Angle, degrees**	**Tension Leg, inches**	**Throat, inches**	**Angle, degrees**	**Tension Leg, inches**
1 - X	1.8250	0.5170	69	0.4480	0.4425	66	0.5420
2	1.8215	0.5200	77	0.4465	0.3870	63	0.5565
3	1.7740	0.5735	76	0.5015	0.3865	60	0.5425
4	1.7655	0.5520	78	0.4980	0.3800	61	0.5025
5	1.7490	0.4755	74	0.5400	0.4125	65	0.4850
6	1.7120	0.5095	74	0.5660	0.3470	73 & 43	0.4460
7	1.7165	0.4235	66	0.5505	0.4290	64	0.4690
8	1.7280	0.4245	66	0.5535	0.4370	74 & 55	0.5040
Mean	**1.7589**	**0.5042**	**73.3**	**0.5150**	**0.3965**	**63.0**	**0.5031**

Table B.2.72 – Test #72, B175_B12_55_3

	Post-Fracture Measurements						
		Front Side, inches			Back Side, inches		
Meas. Num.	**Root Notch, inches**	**Throat, inches**	**Angle, degrees**	**Tension Leg, inches**	**Throat, inches**	**Angle, degrees**	**Tension Leg, inches**
1 - X	1.7880	0.4100	47	0.4895	0.4210	62	0.5715
2	1.7695	0.4325	61 & 22	0.4870	0.5305	75	0.5770
3	1.7665	0.4130	28	0.4675	0.5140	76	0.5615
4	1.7425	0.4245	39	0.4905	0.5250	75	0.5005
5	1.7810	0.4455	69 & 33	0.4800	0.4990	80	0.5010
6	1.7545	0.4130	41	0.5165	0.4150	64	0.5195
7	1.7595	0.3995	65	0.4905	0.3350	79 & 39	0.4995
8	1.7815	0.4030	69	0.5200	0.3945	79 & 26	0.5010
Mean	**1.7651**	**0.4195**	**45.1**	**0.4907**	**0.4620**	**72.5**	**0.5277**

Table B.2.73 – Test #73, B175_B516_85_1

	Post-Fracture Measurements						
		Front Side, inches			Back Side, inches		
Meas. Num.	**Root Notch, inches**	**Throat, inches**	**Angle, degrees**	**Tension Leg, inches**	**Throat, inches**	**Angle, degrees**	**Tension Leg, inches**
1 - X	1.7195	0.3925	78	0.3875	0.3875	76	0.4755
2	1.7400	0.4665	84	0.3410	0.3785	79	0.4235
3	1.7565	0.4140	84	0.3695	0.4075	82	0.4890
4	1.7395	0.3365	79	0.3395	0.3725	79	0.4245
5	1.7495	0.3355	80	0.2995	0.3745	79	0.4115
6	1.7400	0.4175	84	0.3750	0.3830	82	0.4325
7	1.7280	0.3665	82	0.3335	0.3305	76	0.4460
8	1.7255	0.3225	79	0.2960	0.3545	76	0.4195
Mean	**1.7398**	**0.3854**	**81.7**	**0.3428**	**0.3740**	**79.1**	**0.4390**

Table B.2.74 – Test #74, B175_B516_85_2

	Post-Fracture Measurements						
		Front Side, inches			Back Side, inches		
Meas. Num.	**Root Notch, inches**	**Throat, inches**	**Angle, degrees**	**Tension Leg, inches**	**Throat, inches**	**Angle, degrees**	**Tension Leg, inches**
1 - X	1.7500	0.4425	82	0.4400	0.3575	89	0.4415
2	1.7575	0.4685	88	0.3900	0.4375	84	0.4150
3	1.7180	0.4360	85	0.4195	0.4390	83	0.4260
4	1.7365	0.4240	79	0.3815	0.3845	84	0.4060
5	1.7500	0.3850	86	0.3975	0.3615	84	0.3730
6	1.7680	0.3805	75	0.4030	0.3800	89	0.4695
7	1.7740	0.3535	67	0.2835	0.4195	89 & 84	0.4315
8	1.6650	0.4080	78	0.2815	0.3935	92 & 67	0.5170
Mean	**1.7453**	**0.4101**	**80.0**	**0.3769**	**0.4001**	**85.3**	**0.4276**

Table B.2.75 – Test #75, B175_B516_85_3

	Post-Fracture Measurements						
		Front Side, inches			Back Side, inches		
Meas. Num.	**Root Notch, inches**	**Throat, inches**	**Angle, degrees**	**Tension Leg, inches**	**Throat, inches**	**Angle, degrees**	**Tension Leg, inches**
1 - X	1.6910	0.3700	76	0.3435	0.3990	75	0.4575
2	1.7315	0.3650	79	0.3110	0.4090	82	0.4180
3	1.7150	0.3135	68	0.3020	0.3775	71	0.4065
4	1.7520	0.3395	76	0.3030	0.3565	78	0.4435
5	1.7505	0.2815	67	0.2670	0.3530	84	0.4405
6	1.7510	0.3105	72	0.2435	0.2785	85	0.4770
7	1.7585	0.2850	66	0.2470	0.3220	84	0.4290
8	1.7475	0.2715	68	0.2750	0.4015	85	0.5200
Mean	**1.7401**	**0.3164**	**71.4**	**0.2827**	**0.3558**	**80.6**	**0.4424**

Table B.2.76 – Test #76, B175_B12_85_1

	Post-Fracture Measurements						
		Front Side, inches			Back Side, inches		
Meas. Num.	**Root Notch, inches**	**Throat, inches**	**Angle, degrees**	**Tension Leg, inches**	**Throat, inches**	**Angle, degrees**	**Tension Leg, inches**
1 - X	1.8105	0.4540	67	0.5205	0.5250	75	0.5150
2	1.7935	0.4295	75	0.4600	0.5140	88	0.5025
3	1.7155	0.4805	74	0.4845	0.5735	81	0.5435
4	1.7115	0.6375	85	0.5030	0.5740	80	0.5380
5	1.7375	0.4300	65	0.4620	0.5750	81	0.5190
6	1.7400	0.3795	71	0.4370	0.4475	75	0.5515
7	1.7260	0.4095	67	0.4280	0.4355	68	0.5265
8	1.7175	0.4510	69	0.4450	0.4495	62	0.5865
Mean	**1.7407**	**0.4600**	**72.2**	**0.4650**	**0.5158**	**77.5**	**0.5327**

Table B.2.77 – Test #77, B175_B12_85_2

	Post-Fracture Measurements						
		Front Side, inches			Back Side, inches		
Meas. Num.	**Root Notch, inches**	**Throat, inches**	**Angle, degrees**	**Tension Leg, inches**	**Throat, inches**	**Angle, degrees**	**Tension Leg, inches**
1 - X	1.7380	0.5090	76	0.5480	0.5440	75	0.6210
2	1.7640	0.5195	78	0.4940	0.5770	83	0.5265
3	n/a	0.5470	82	0.5110	0.6380	84	0.5345
4	1.7150	0.5630	83	0.5230	0.4350	68	0.5160
5	1.7245	0.6205	84	0.5170	0.4550	72	0.5340
6	1.6930	0.5295	86	0.5255	0.6640	84	0.5295
7	1.7350	0.5890	86	0.4920	0.4490	70	0.5025
8	1.7185	0.5535	81	0.5515	0.4395	64	0.4995
Mean	**1.7265**	**0.5576**	**82.6**	**0.5153**	**0.5308**	**75.9**	**0.5284**

Table B.2.78 – Test #78, B175_B12_85_3

	Post-Fracture Measurements						
		Front Side, inches			Back Side, inches		
Meas. Num.	**Root Notch, inches**	**Throat, inches**	**Angle, degrees**	**Tension Leg, inches**	**Throat, inches**	**Angle, degrees**	**Tension Leg, inches**
1 - X	1.7190	0.5185	89	0.5695	0.5200	72	0.5035
2	1.7455	0.5950	84	0.5610	0.4885	78	0.4845
3	1.7650	0.5720	88	0.5185	0.4690	71	0.5210
4	1.7730	0.5760	83	0.5105	0.5555	73	0.4970
5	1.7515	0.5670	80	0.5565	0.5730	80	0.4580
6	1.7520	0.3930	65	0.5140	0.5425	70	0.4950
7	1.7640	0.3960	67	0.4605	0.4675	68	0.5545
8	1.8330	0.3810	75	0.3880	0.4715	68	0.4885
Mean	**1.7607**	**0.5082**	**78.4**	**0.5150**	**0.5135**	**72.9**	**0.5010**

Table B.2.79 – Test #79, B250_B516_55_1

	Post-Fracture Measurements						
		Front Side, inches			Back Side, inches		
Meas. Num.	**Root Notch, inches**	**Throat, inches**	**Angle, degrees**	**Tension Leg, inches**	**Throat, inches**	**Angle, degrees**	**Tension Leg, inches**
1 - X	2.4670	0.4725	84	0.4055	0.3395	66	0.3435
2	2.4095	0.4425	85	0.3925	0.3435	68	0.3155
3	2.4425	0.4245	87	0.3575	0.3330	65	0.3345
4	2.4865	0.4170	90 & 76	0.3610	0.3230	60	0.3695
5	2.4665	0.4795	90	0.3955	0.3280	61	0.3450
6	2.4020	0.4290	91	0.4250	0.2885	62	0.3825
7	2.4630	0.4455	91 & 77	0.3955	0.2965	59	0.3155
8	2.3870	0.4425	92	0.3910	0.3315	60	0.3510
9	2.4610	0.3385	72	0.3900	0.2645	58	0.3465
Mean	**2.4397**	**0.4362**	**87.8**	**0.3893**	**0.3185**	**62.1**	**0.3448**

Table B.2.80 – Test #80, B250_B516_55_2

	Post-Fracture Measurements						
		Front Side, inches			Back Side, inches		
Meas. Num.	**Root Notch, inches**	**Throat, inches**	**Angle, degrees**	**Tension Leg, inches**	**Throat, inches**	**Angle, degrees**	**Tension Leg, inches**
1 – X	2.4480	0.4075	81	0.4150	0.3835	73	0.3185
2	2.4715	0.4460	86	0.4280	0.3715	77	0.3375
3	2.5100	0.4360	87	0.3760	0.3270	72	0.3750
4	2.4910	0.4595	86	0.4105	0.3220	64	0.3470
5	2.4500	0.4590	81	0.4240	0.3270	64	0.3615
6	2.4320	0.4395	74	0.3870	0.2970	64	0.3515
7	2.4845	0.3295	69	0.3685	0.3585	66	0.3350
8	2.5040	0.4805	95	0.4235	0.2875	52	0.3475
9	2.4630	0.4370	89	0.4785	0.3175	66	0.3280
Mean	**2.4751**	**0.4342**	**82.8**	**0.4074**	**0.3298**	**66.0**	**0.3477**

Table B.2.81 – Test #81, B250_B516_55_3

	Post-Fracture Measurements						
		Front Side, inches			Back Side, inches		
Meas. Num.	**Root Notch, inches**	**Throat, inches**	**Angle, degrees**	**Tension Leg, inches**	**Throat, inches**	**Angle, degrees**	**Tension Leg, inches**
1 – X	2.5215	0.3470	34	0.4295	0.2730	20	0.3415
2	2.5020	0.3320	33	0.4230	0.3135	33	0.3755
3	2.5115	0.3830	77	0.4170	0.2780	51	0.3415
4	2.5285	0.3630	71	0.4110	0.3270	57	0.3015
5	2.5045	0.3415	73	0.3820	0.3405	60	0.3045
6	2.4735	0.3075	67	0.4060	0.3200	57	0.3740
7	2.5265	0.3325	63	0.3985	0.3225	61	0.3175
8	2.5580	0.2655	61	0.3635	0.2935	54	0.3485
Mean	**2.5118**	**0.3386**	**61.9**	**0.4050**	**0.3127**	**51.1**	**0.3369**

Table B.2.82 – Test #82, B250_B12_55_1

	Post-Fracture Measurements						
		Front Side, inches			Back Side, inches		
Meas. Num.	**Root Notch, inches**	**Throat, inches**	**Angle, degrees**	**Tension Leg, inches**	**Throat, inches**	**Angle, degrees**	**Tension Leg, inches**
1 - X	2.4450	0.5900	68	0.5215	0.6215	72	0.6610
2	2.4160	0.5285	66	0.5375	0.6260	74	0.6705
3	2.4175	0.4585	67	0.5315	0.5225	74	0.6620
4	2.3850	0.4410	69	0.5435	0.4900	59 & 32	0.6135
5	2.3775	0.5770	74	0.5405	0.5005	71 & 25	0.6665
6	2.3830	0.4715	54	0.4990	0.4595	65	0.6740
7	2.4775	0.4845	73	0.4915	0.4995	65	0.6880
8	2.4320	0.5135	69	0.5480	0.5105	69	0.6590
Mean	**2.4131**	**0.5008**	**67.3**	**0.5253**	**0.5225**	**69.6**	**0.6621**

Table B.2.83 – Test #83, B250_B12_55_2

	Post-Fracture Measurements						
		Front Side, inches			Back Side, inches		
Meas. Num.	**Root Notch, inches**	**Throat, inches**	**Angle, degrees**	**Tension Leg, inches**	**Throat, inches**	**Angle, degrees**	**Tension Leg, inches**
1 - X	2.4565	0.6225	79	0.5765	0.6300	74	0.5900
2	n/a	0.6570	81	0.5700	0.6285	73	0.6180
3	2.4155	0.6010	81	0.5735	0.5900	73	0.6110
4	2.4165	0.5650	75	0.5645	0.5525	76	0.5890
5	2.4040	0.5450	79 & 25	0.5185	0.6085	74	0.6205
6	2.4215	0.4270	73 & 44	0.5590	0.6225	80 & 63	0.5940
7	2.3925	0.5385	74	0.5390	0.5185	69	0.6165
8	2.4080	0.5770	75	0.5430	0.4955	76 & 50	0.5965
Mean	**2.4128**	**0.5611**	**77.7**	**0.5548**	**0.5838**	**73.1**	**0.6063**

Table B.2.84 – Test #84, B250_B12_55_3

	Post-Fracture Measurements						
		Front Side, inches			Back Side, inches		
Meas. Num.	**Root Notch, inches**	**Throat, inches**	**Angle, degrees**	**Tension Leg, inches**	**Throat, inches**	**Angle, degrees**	**Tension Leg, inches**
1 - X	2.4000	0.6005	71	0.5850	0.5315	71	0.6270
2	2.4305	0.5930	81	0.5500	0.5585	72	0.6460
3	2.4370	0.5480	77	0.5425	0.5230	72	0.5555
4	2.4485	0.5405	70	0.5445	0.5460	75	0.5995
5	2.4380	0.5560	74	0.5425	0.5945	76	0.5940
6	2.4280	0.4545	73 & 36	0.5325	0.5700	74	0.5755
7	2.4650	0.4670	70	0.5235	0.5690	71	0.6135
8	2.3600	0.4630	60	0.5405	0.5395	63	0.6695
Mean	**2.4335**	**0.5272**	**73.3**	**0.5422**	**0.5571**	**72.5**	**0.6037**

B.3 WELD PROFILES

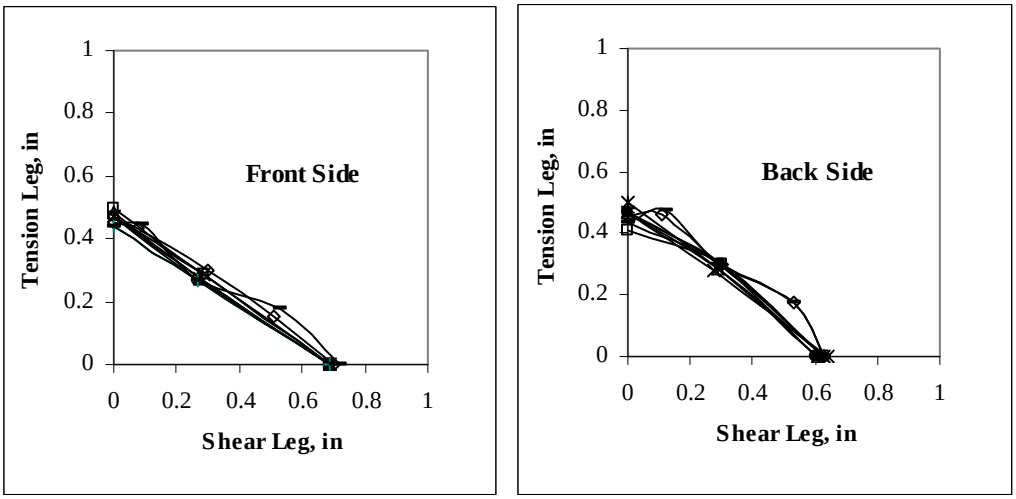

Figure B.3.1 – Test #1, T125_A12_1

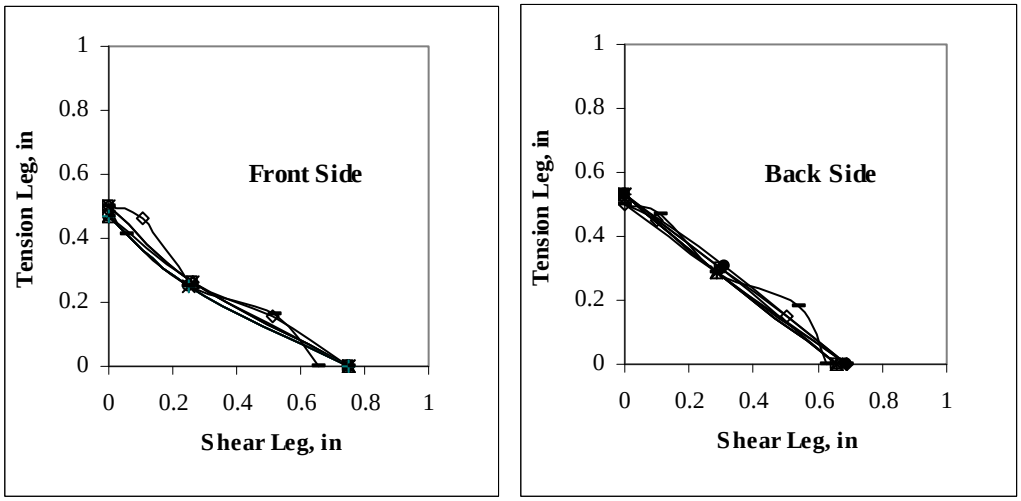

Figure B.3.2 – Test #2, T125_A12_2

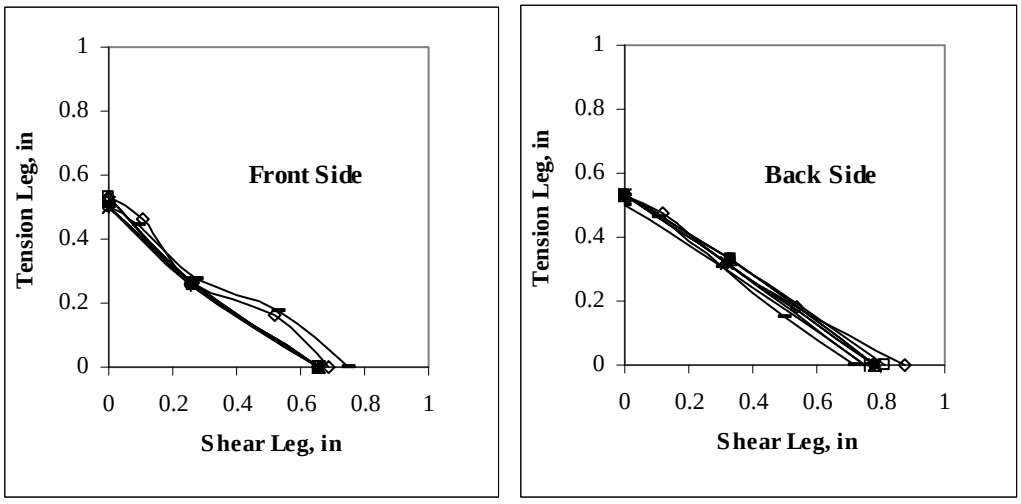

Figure B.3.3 – Test #3, T125_A12_3

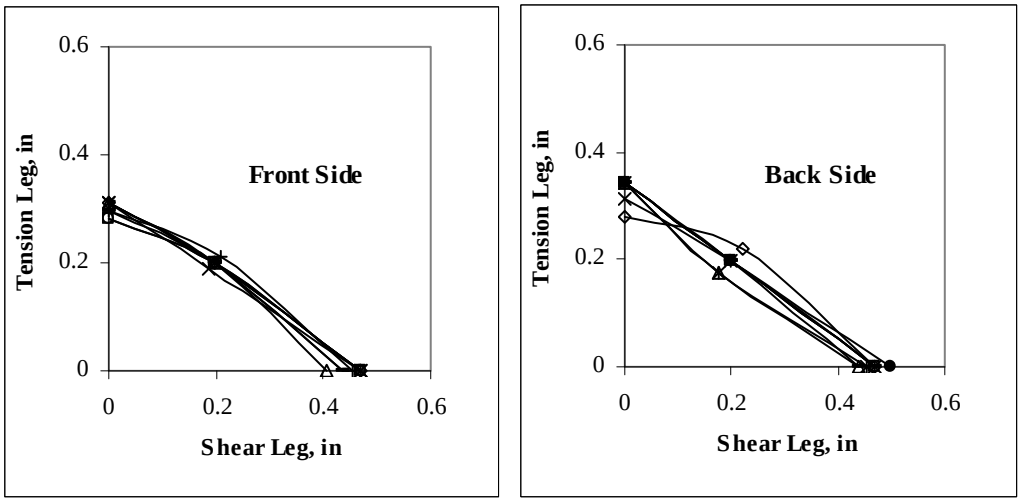

Figure B.3.4 – Test #4, T125_A516_1

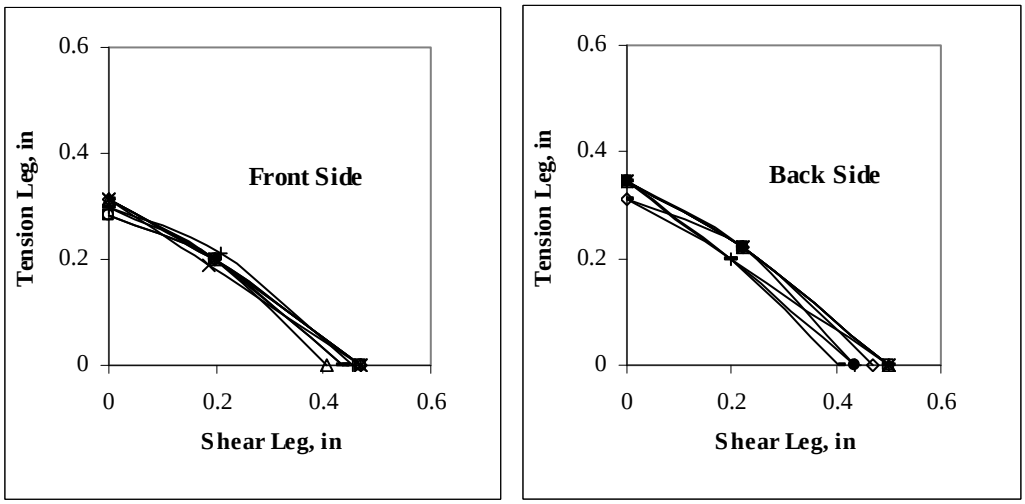

Figure B.3.5 – Test #5, T125_A516_2

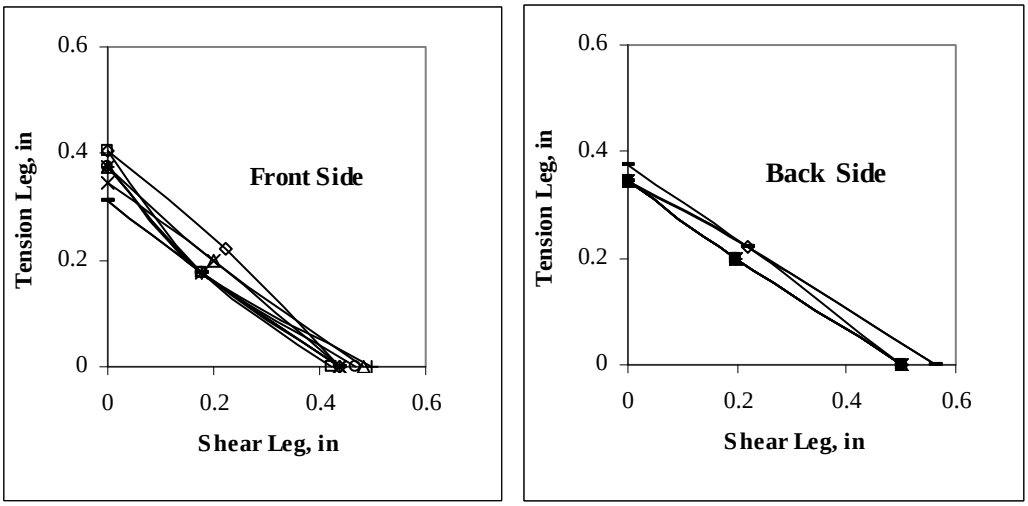

Figure B.3.6 – Test #6, T125_A516_3

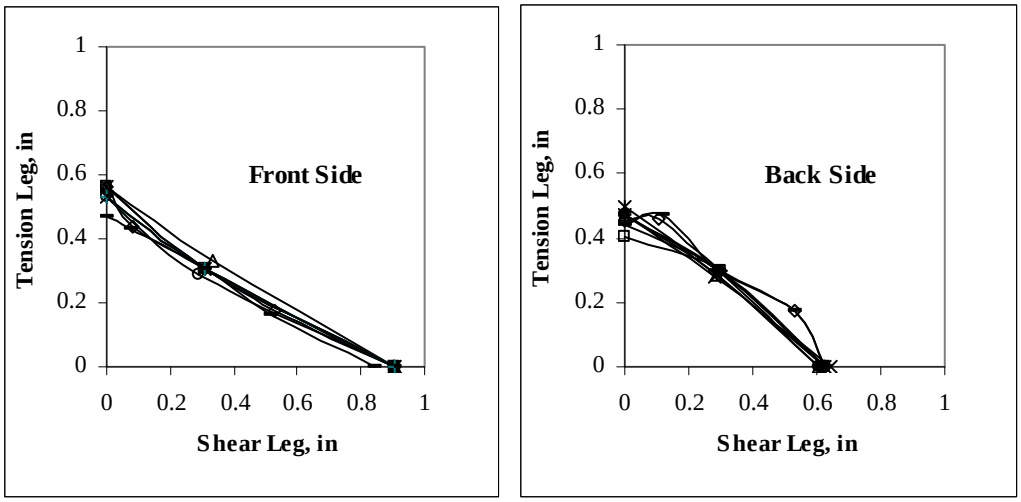

Figure B.3.7 – Test #7, T250_A12_1

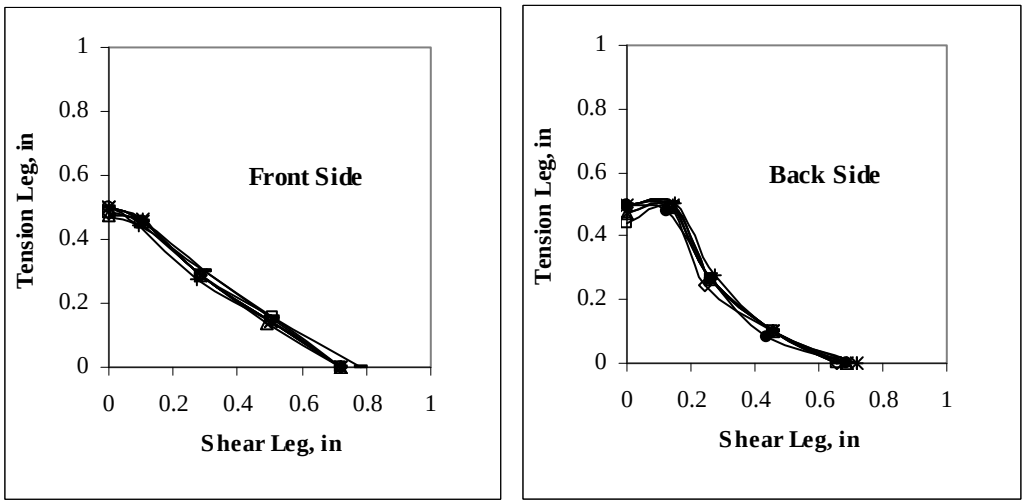

Figure B.3.8 – Test #8, T250_A12_2

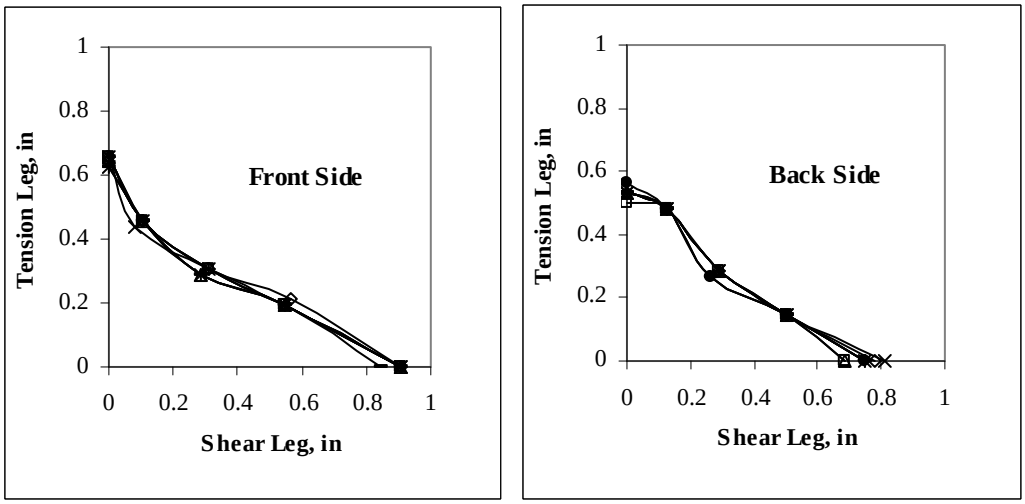

Figure B.3.9 – Test #9, T250_A12_3

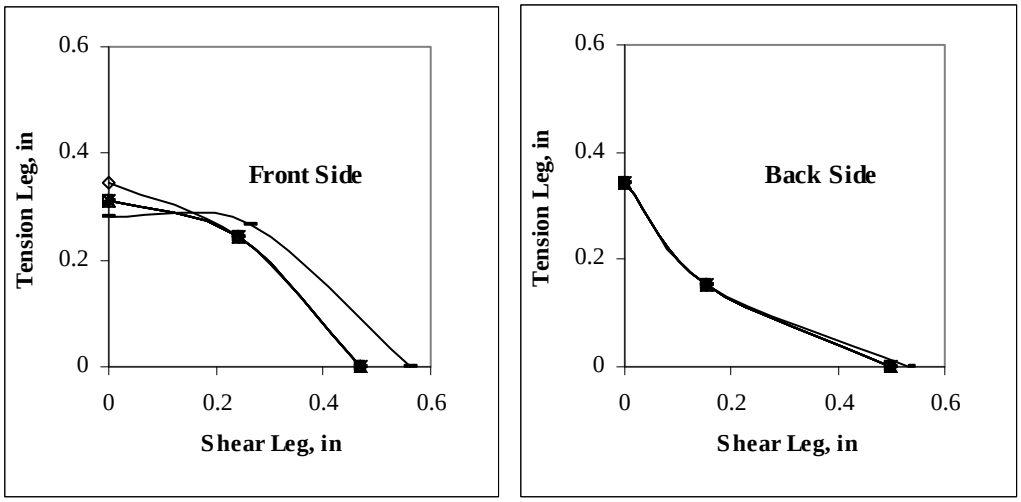

Figure B.3.10 – Test #10, T250_A516_1

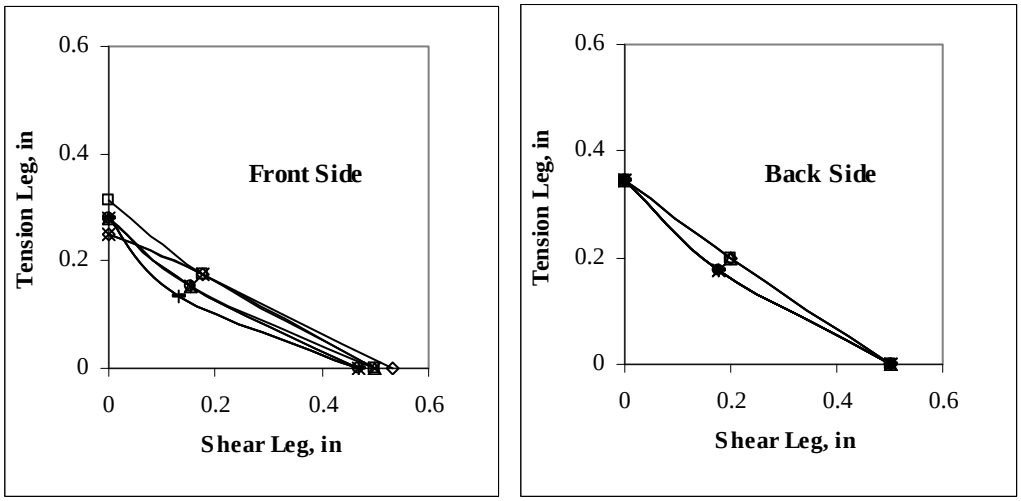

Figure B.3.11 – Test #11, T250_A516_2

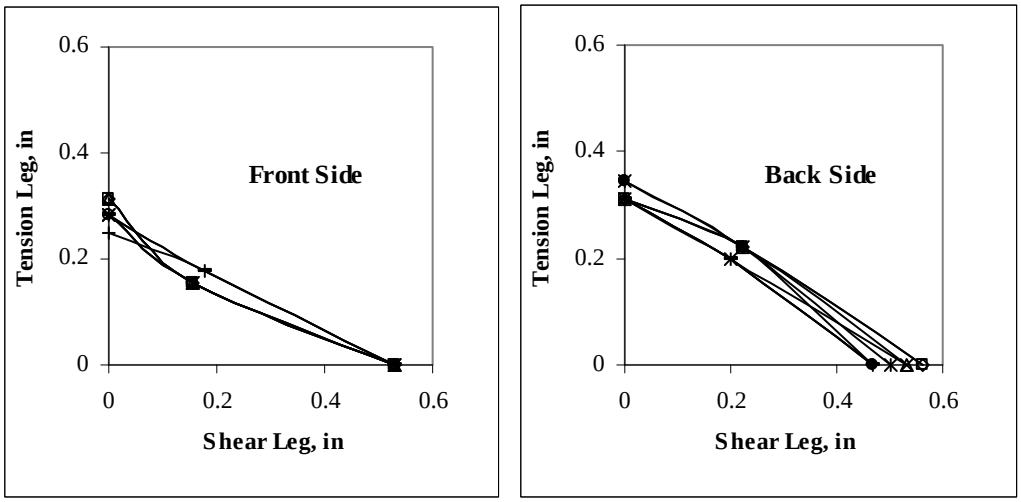

Figure B.3.12 – Test #12, T250_A516_3

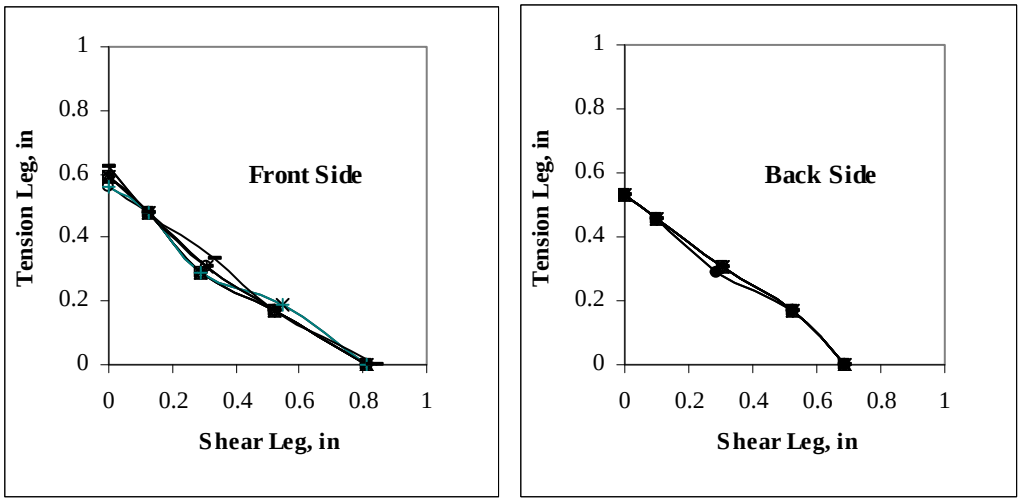

Figure B.3.13 – Test #13, T125_B12_1

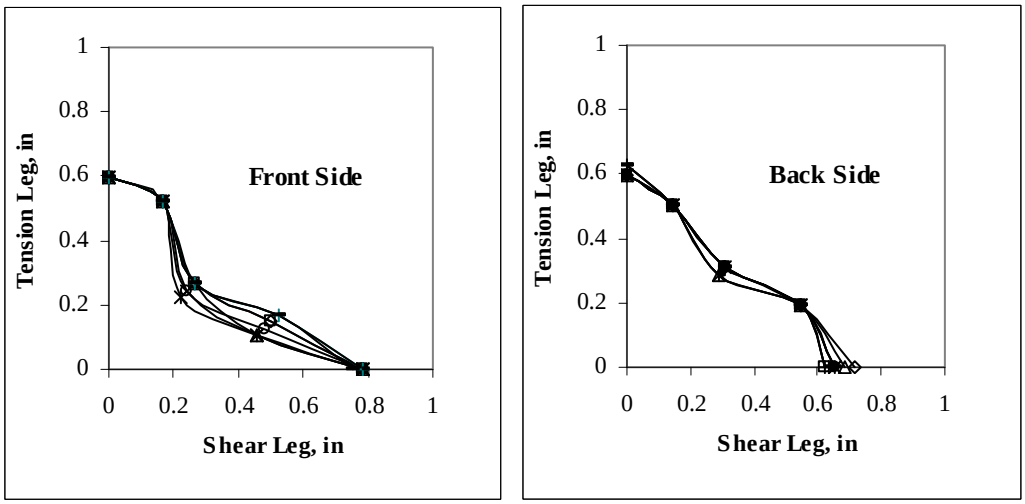

Figure B.3.14 – Test #14, T125_B12_2

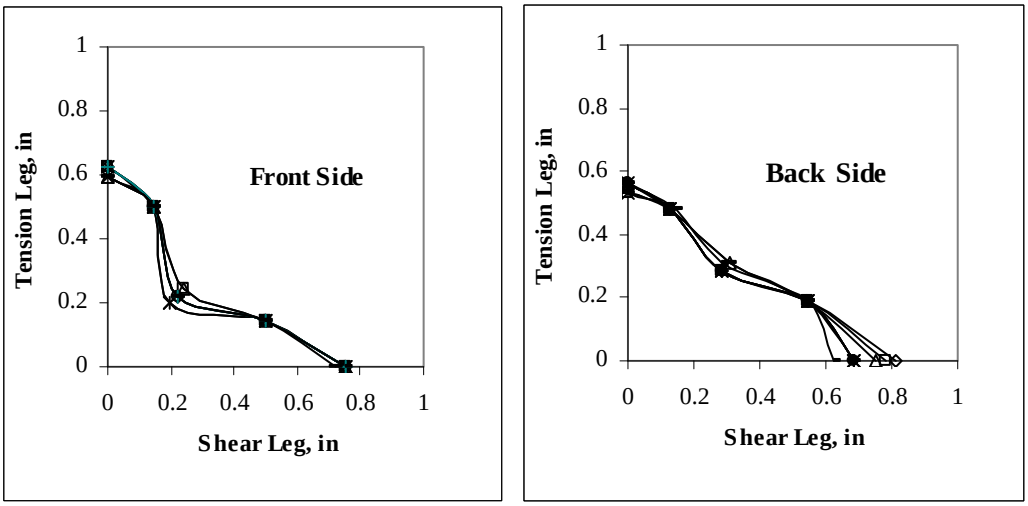

Figure B.3.15 – Test #15, T125_B12_3

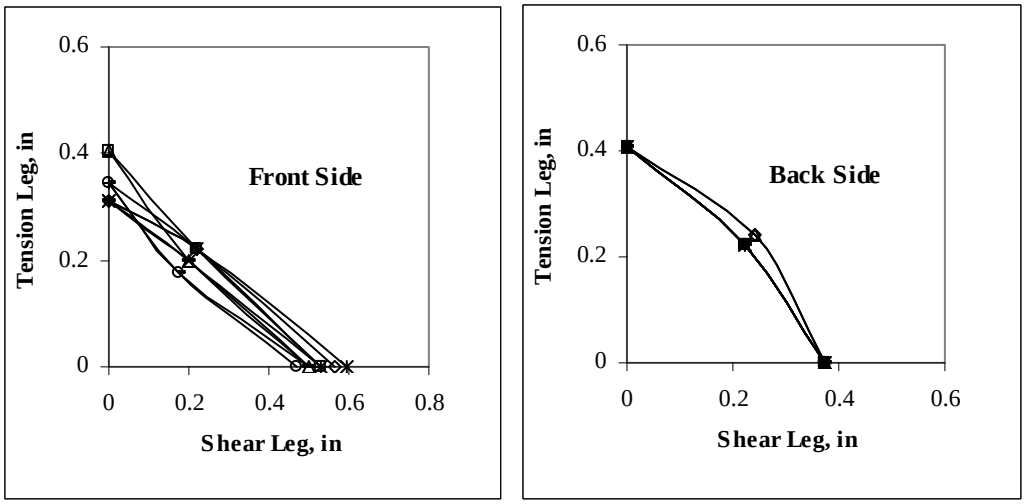

Figure B.3.16 – Test #16, T125_B516_1

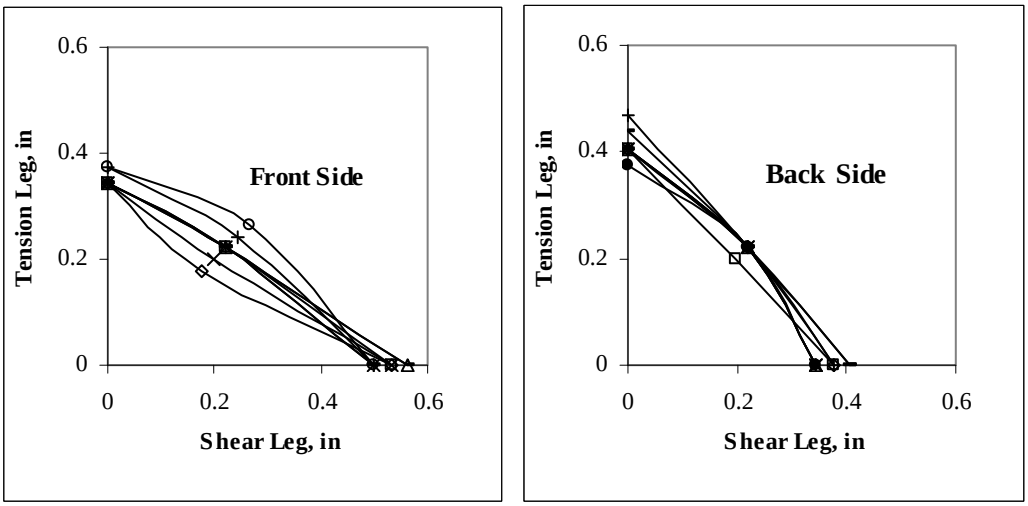

Figure B.3.17 – Test #17, T125_B516_2

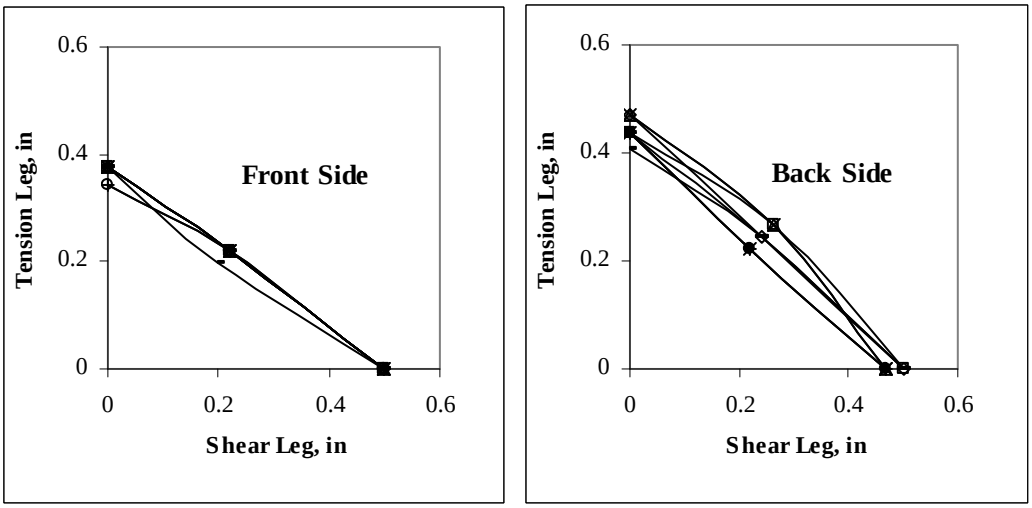

Figure B.3.18 – Test #18, T125_B516_3

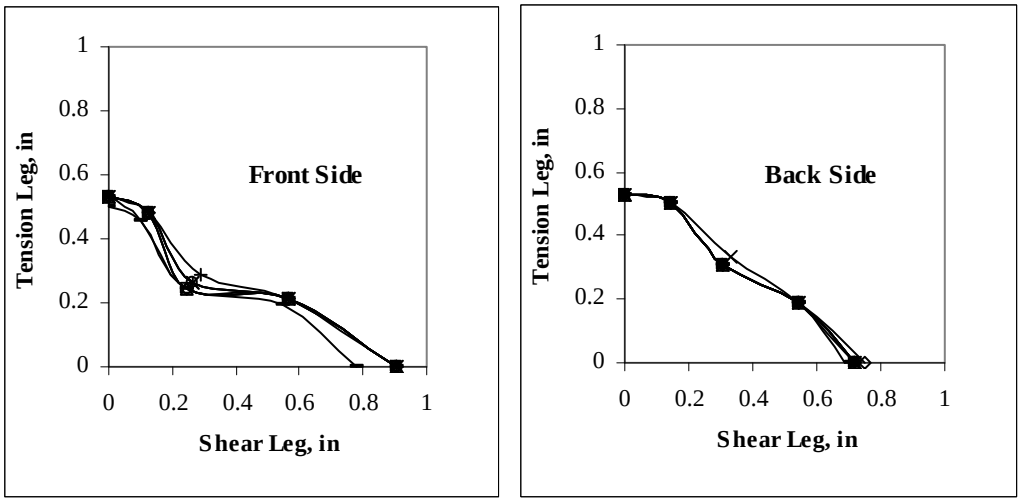

Figure B.3.19 – Test #19, T250_B12_1

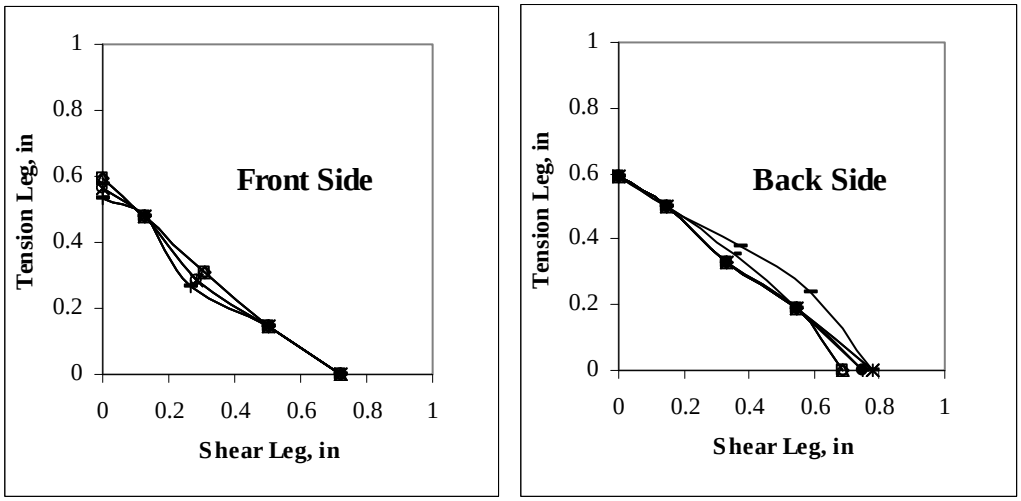

Figure B.3.20 – Test #20, T250_B12_2

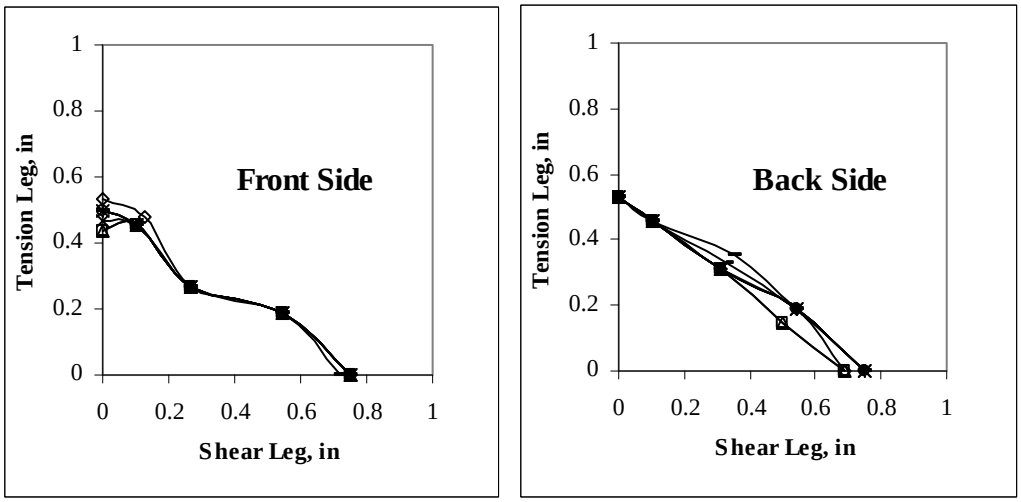

Figure B.3.21 – Test #21, T250_B12_3

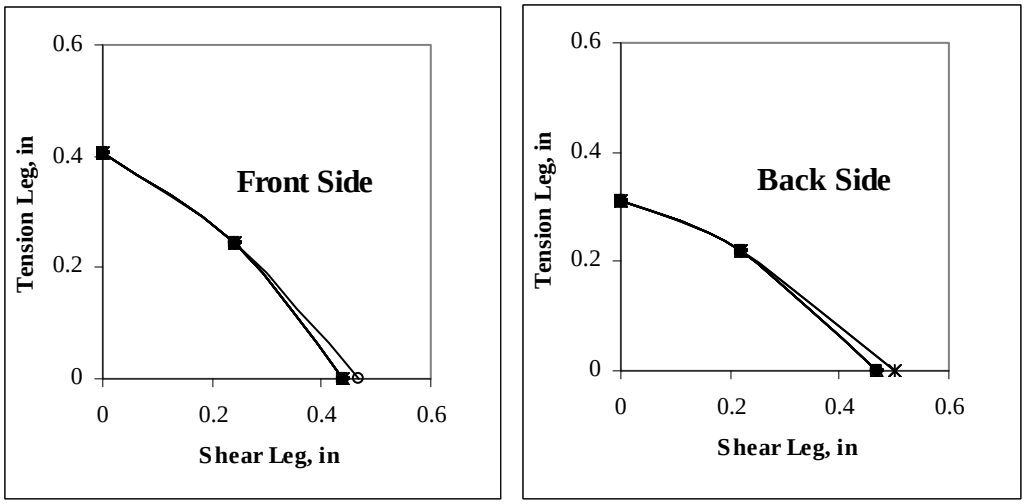

Figure B.3.22 – Test #22, T250_B516_1

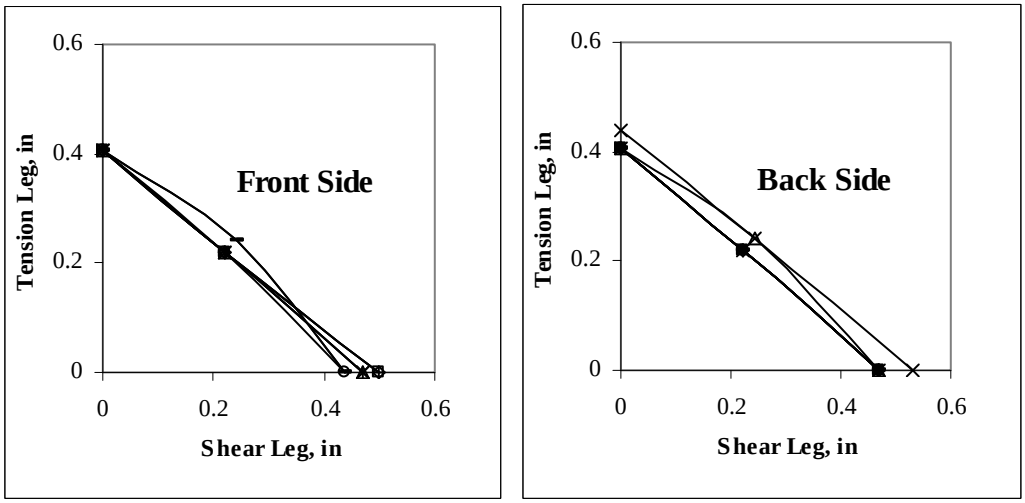

Figure B.3.23 – Test #23, T250_B516_2

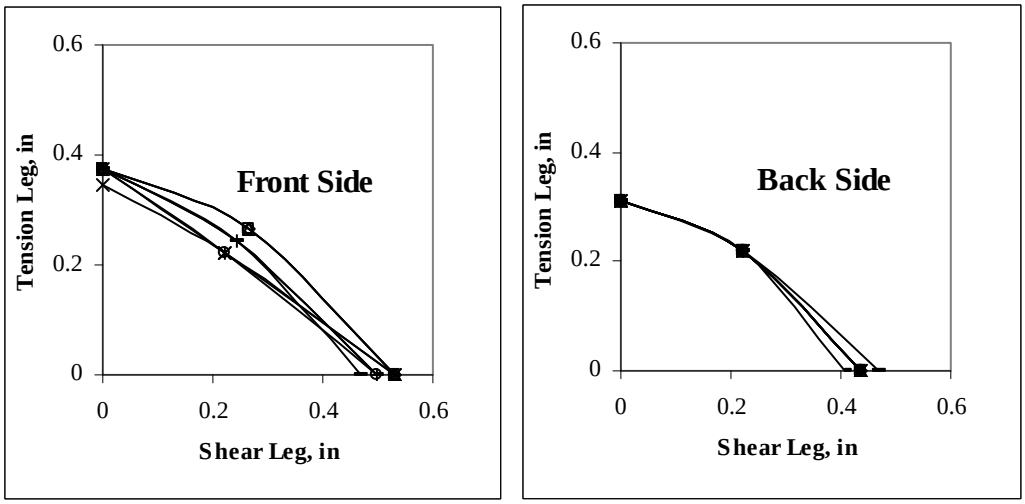

Figure B.3.24 – Test #24, T250_B516_3

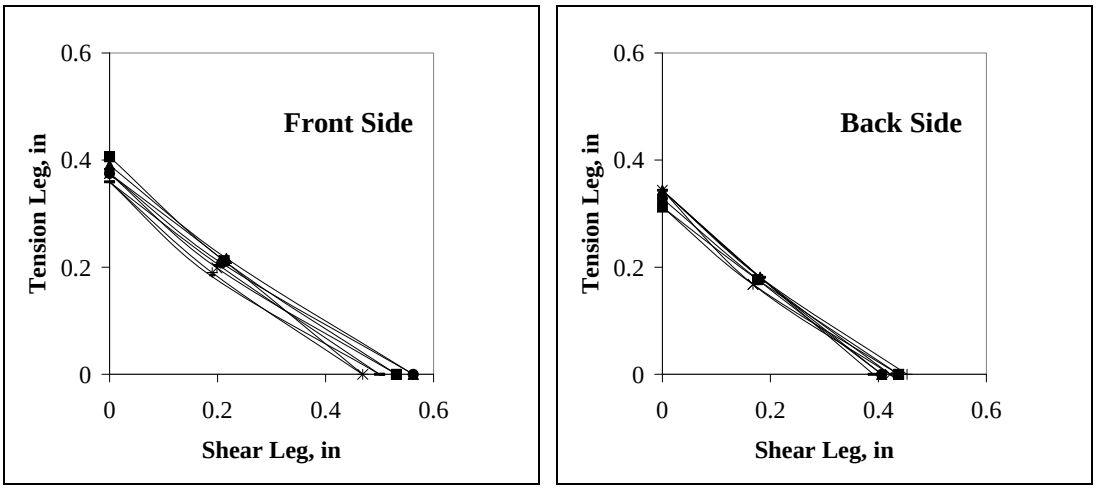

Figure B.3.25 – Test #25, B125_A516_55_1

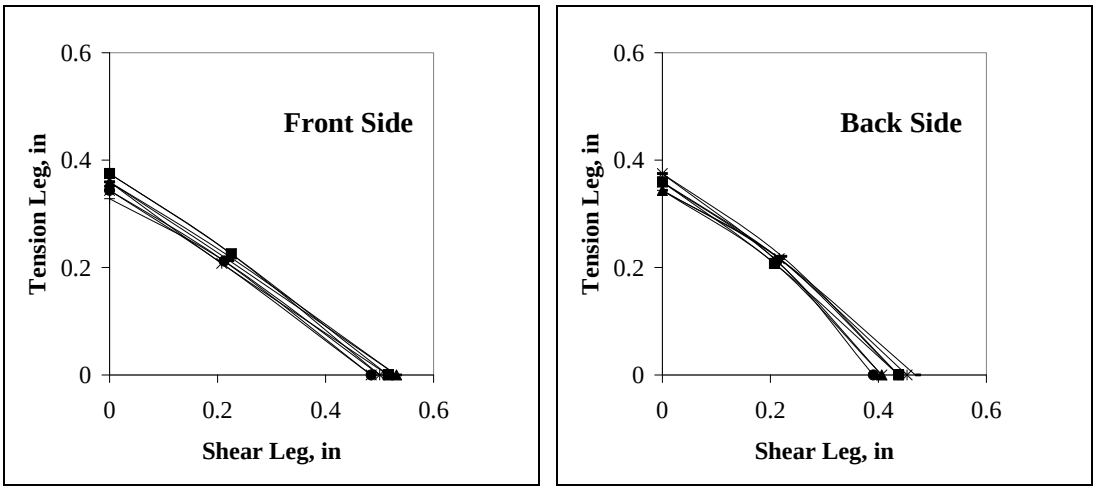

Figure B.3.26 – Test #26, B125_A516_55_2

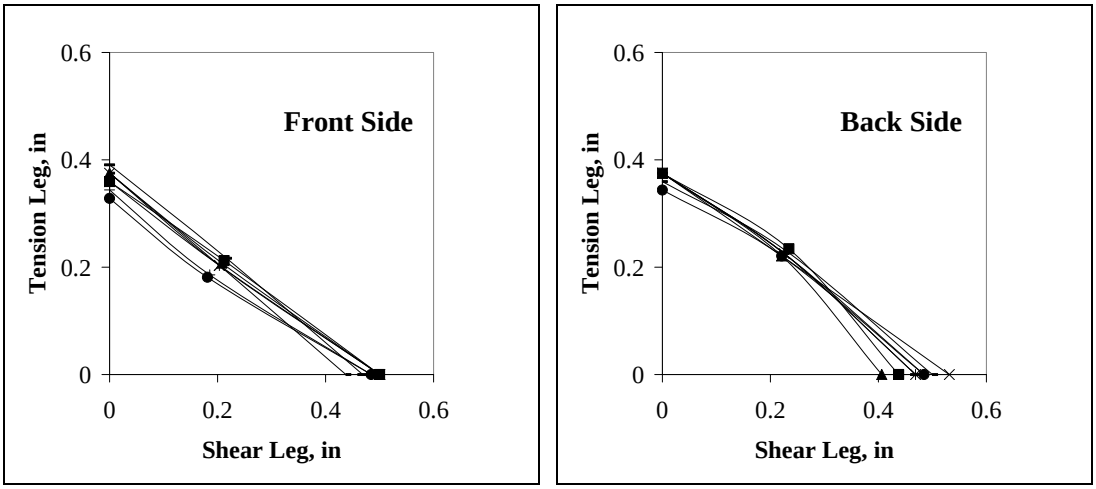

Figure B.3.27 – Test #27, B125_A516_55_3

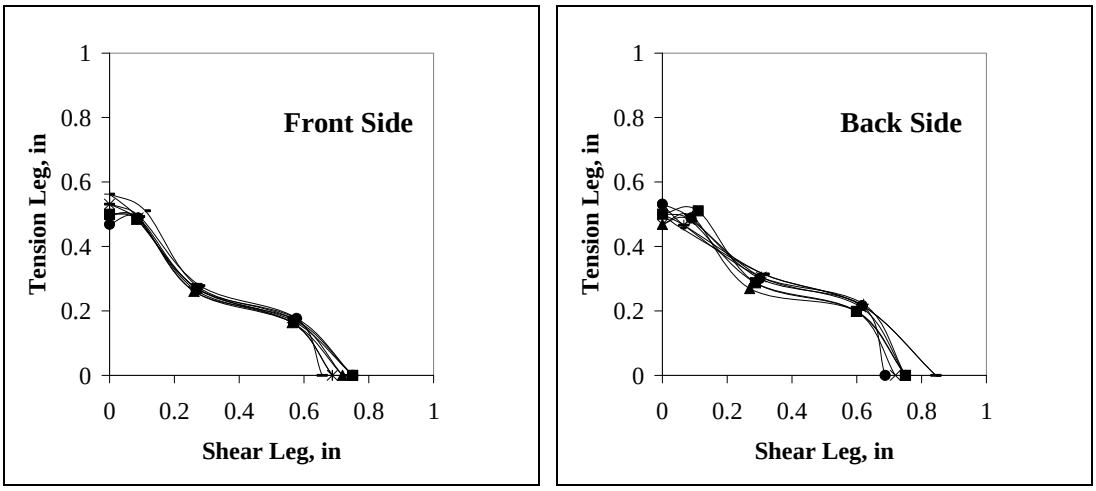

Figure B.3.28 – Test #28, B125_A12_55_1

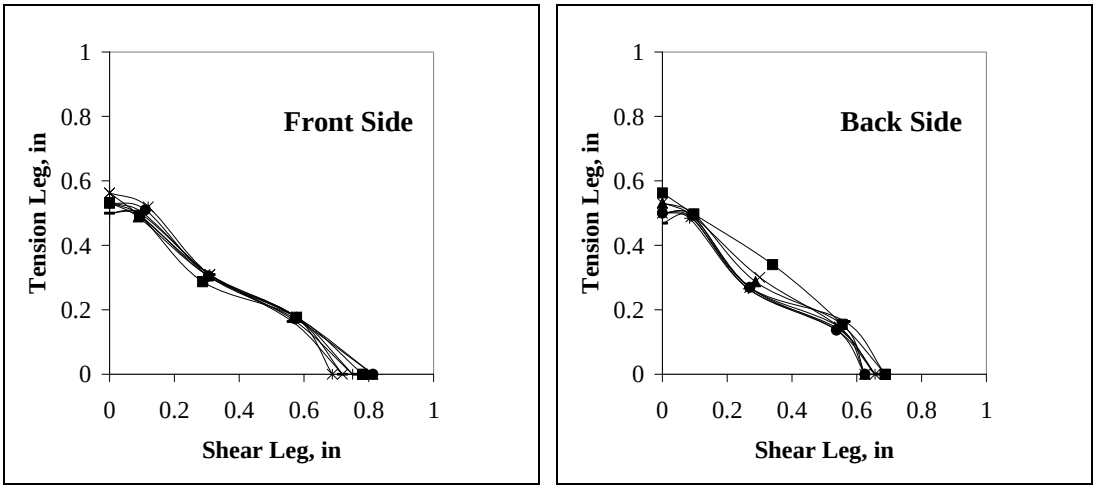

Figure B.3.29 – Test #29, B125_A12_55_2

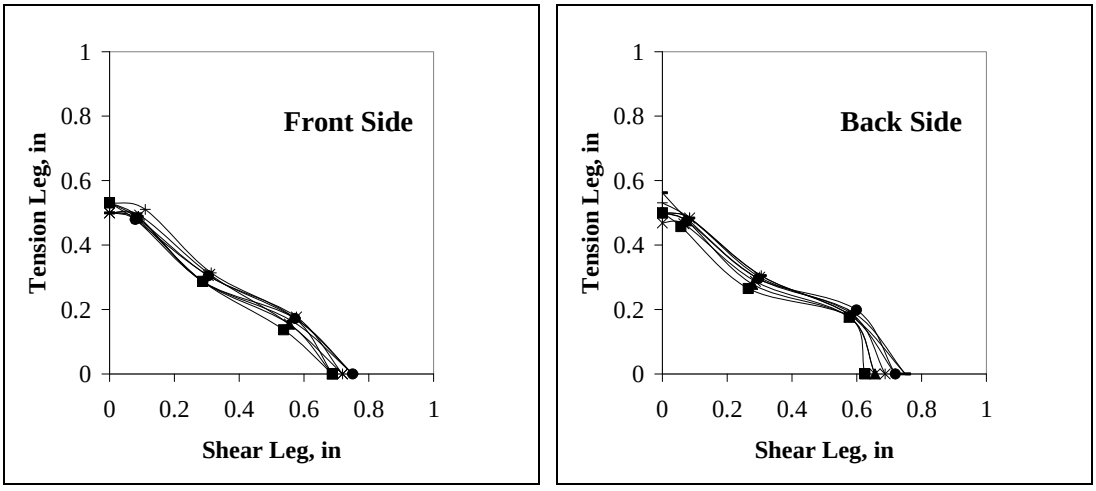

Figure B.3.30 – Test #30, B125_A12_55_3

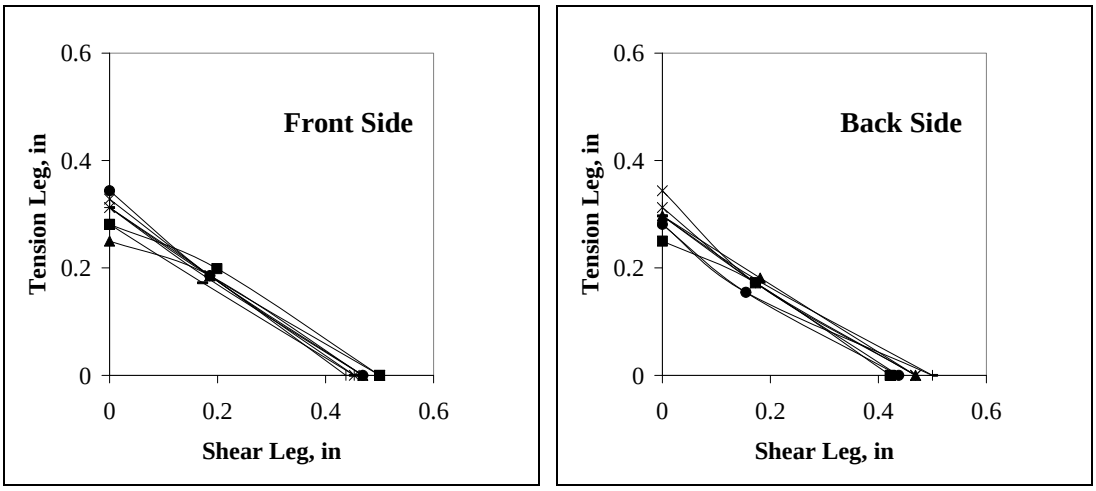

Figure B.3.31 – Test #31, B175_A516_3_1

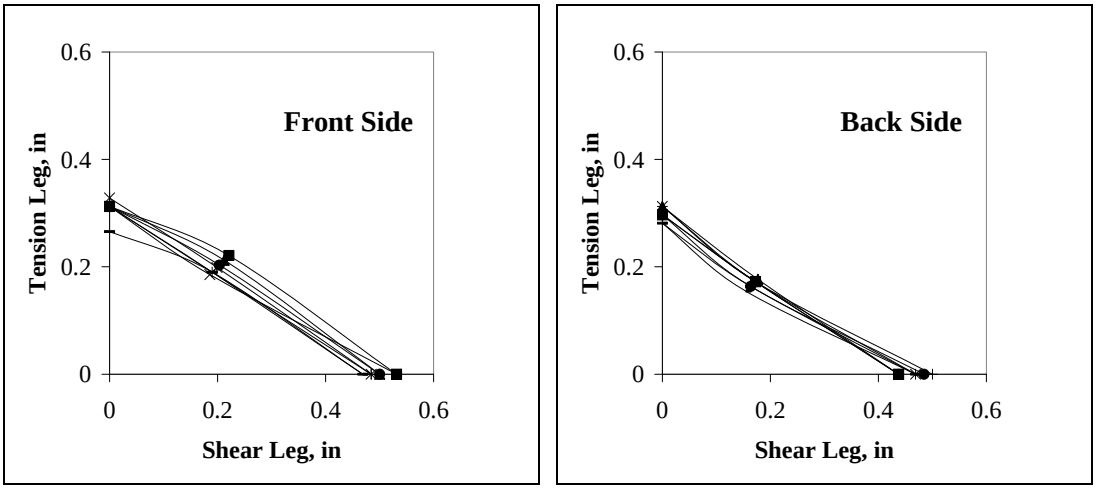

Figure B.3.32 – Test #32, B175_A516_3_2

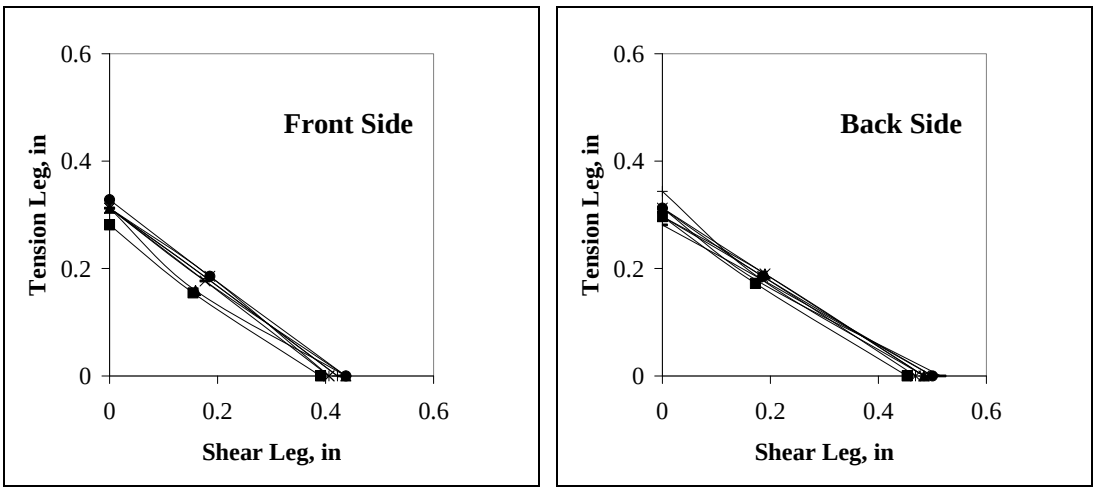

Figure B.3.33 – Test #33, B175_A516_3_3

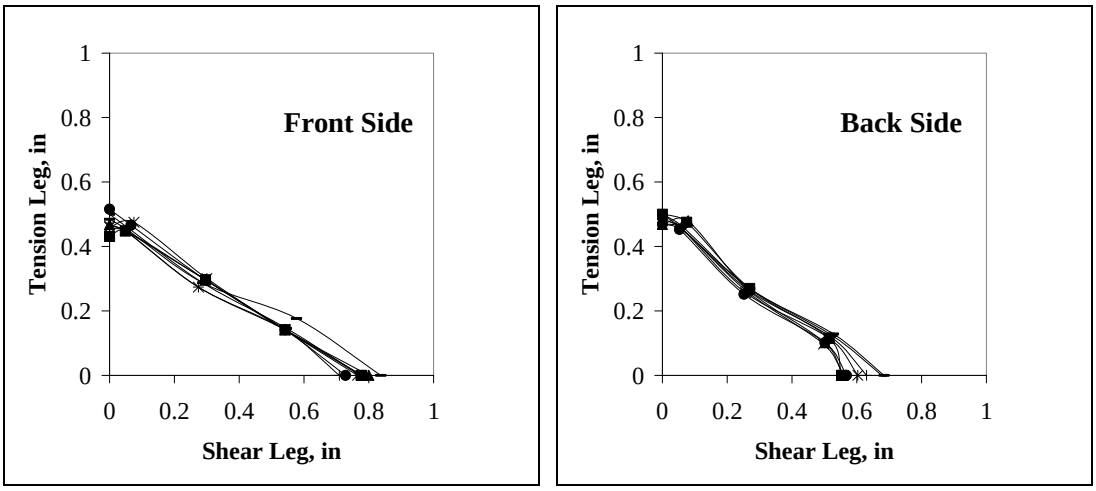

Figure B.3.34 – Test #34, B175_A12_3_1

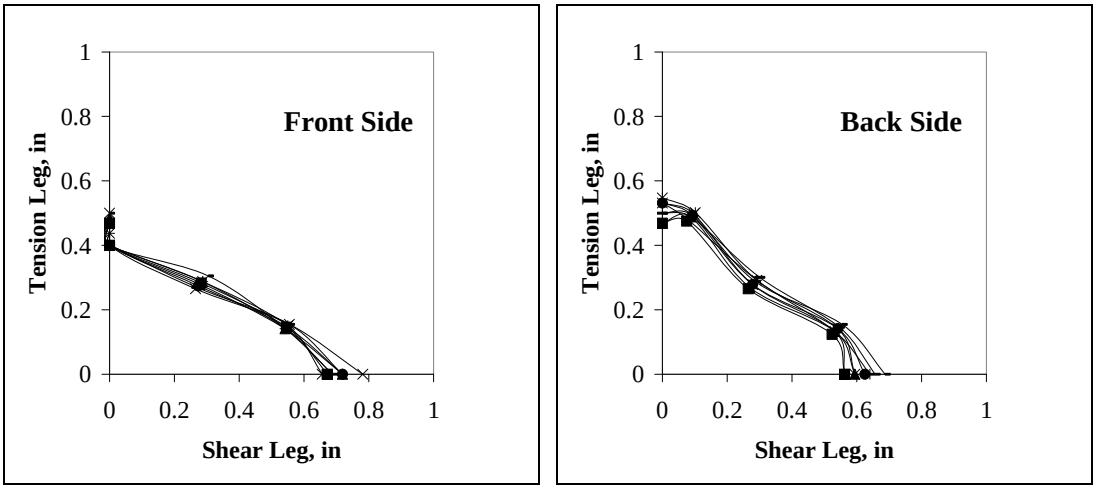

Figure B.3.35 – Test #35, B175_A12_3_2

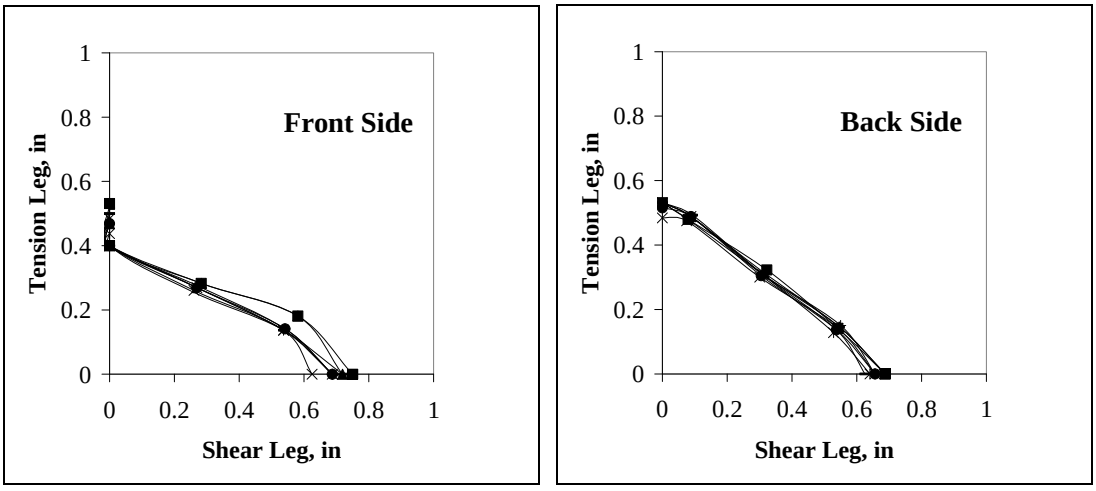

Figure B.3.36 – Test #36, B175_A12_3_3

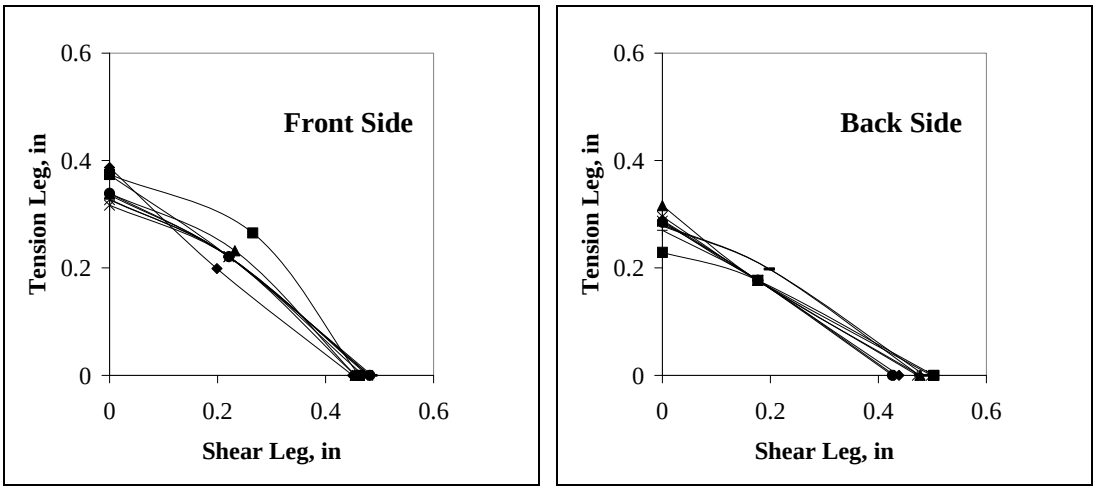

Figure B.3.37 – Test #37, B175_A516_55_1

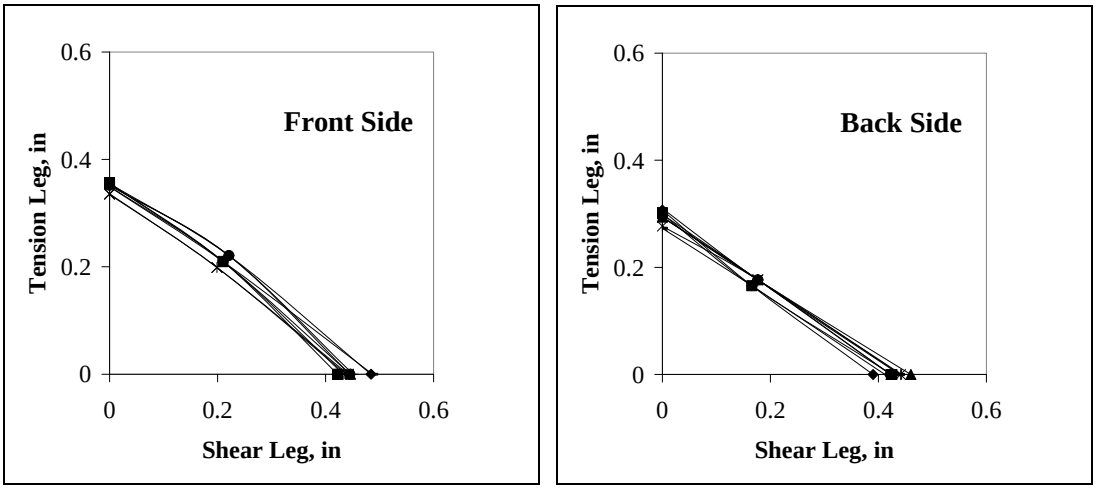

Figure B.3.38 – Test #38, B175_A516_55_2

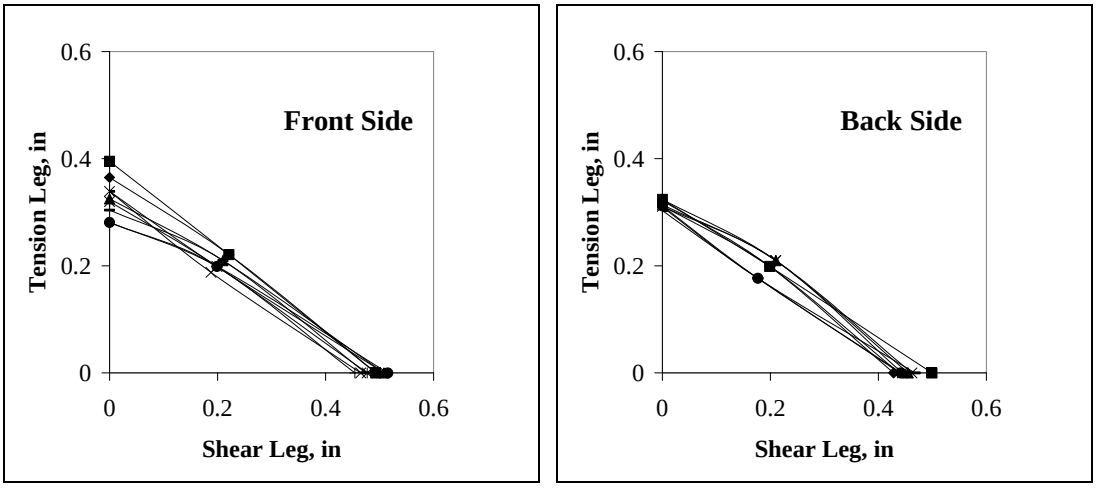

Figure B.3.39 – Test #39, B175_A516_55_3

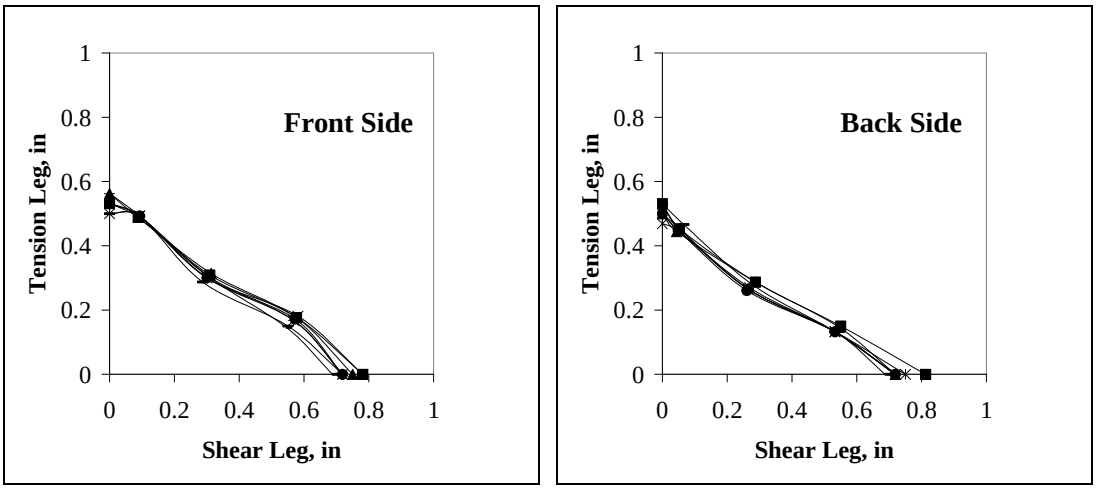

Figure B.3.40 – Test #40, B175_A12_55_1

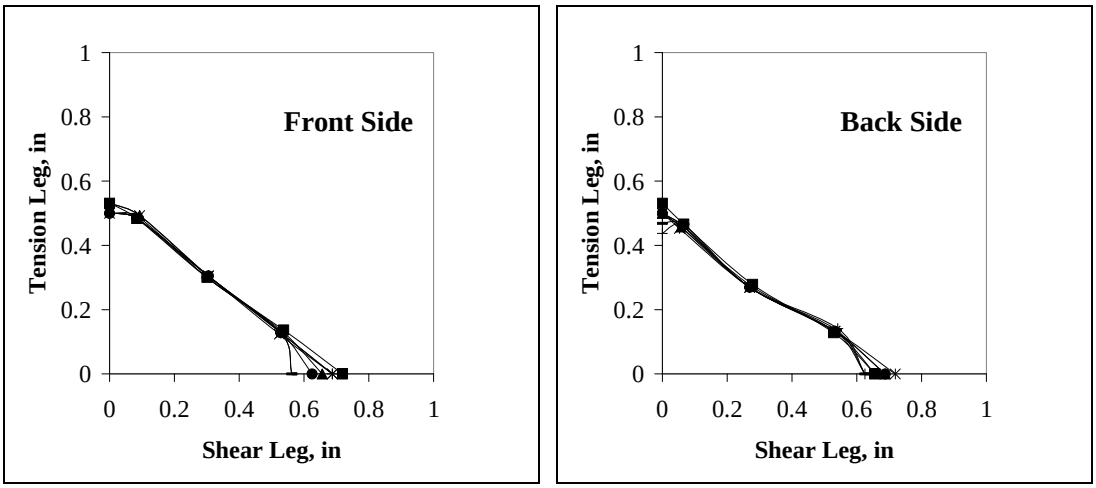

Figure B.3.41 – Test #41, B175_A12_55_2

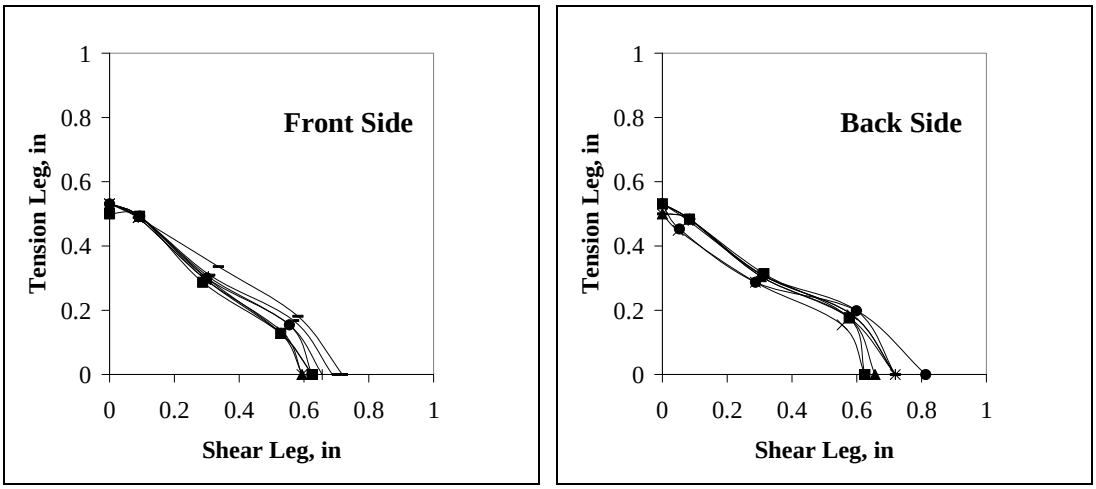

Figure B.3.42 – Test #42, B175_A12_55_3

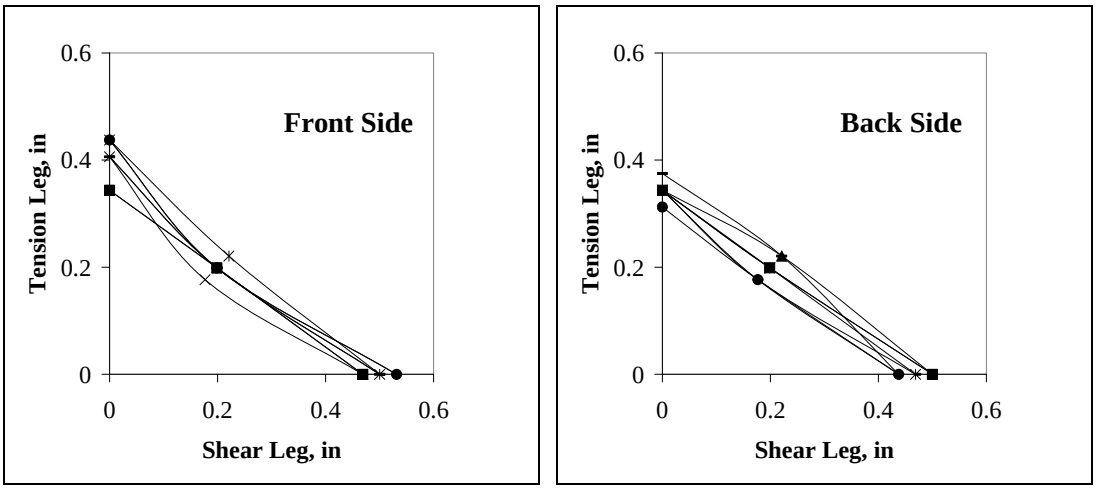

Figure B.3.43 – Test #43, B175_A516_85_1

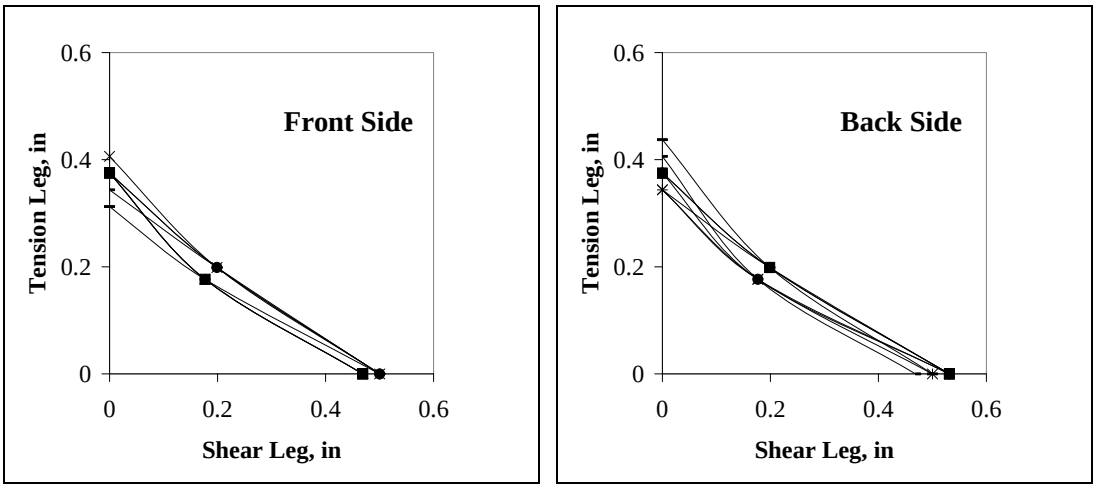

Figure B.3.44 – Test #44, B175_A516_85_2

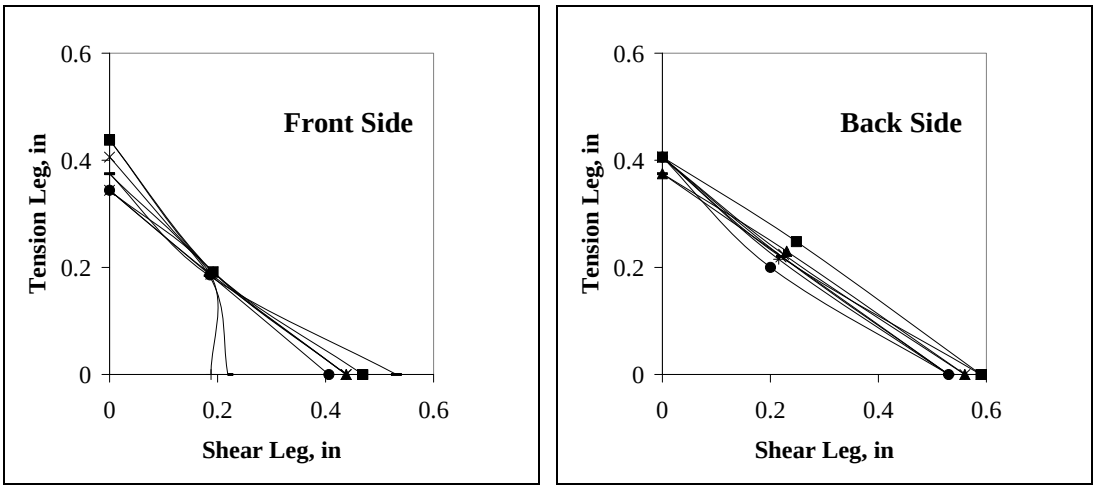

Figure B.3.45 – Test #45, B175_A516_85_3

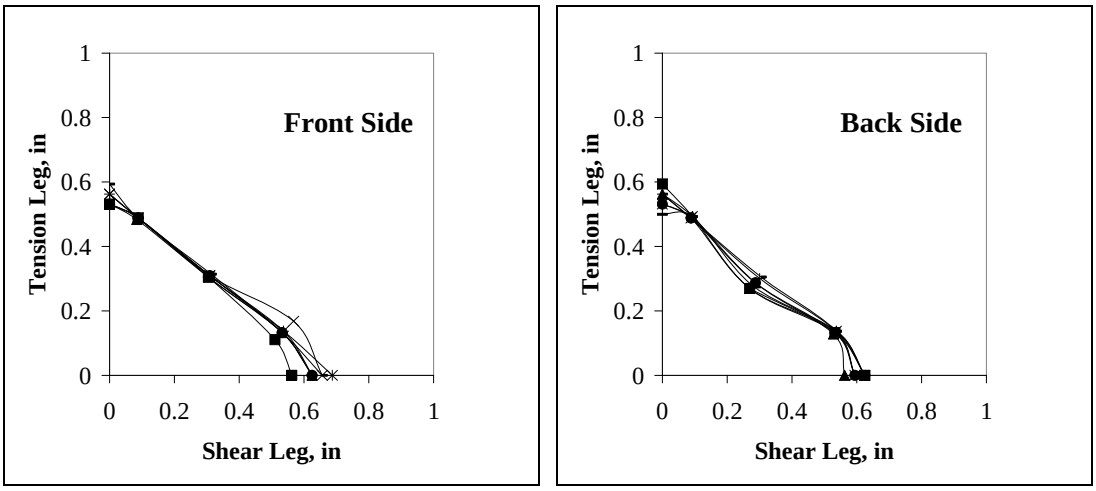

Figure B.3.46 – Test #46, B175_A12_85_1

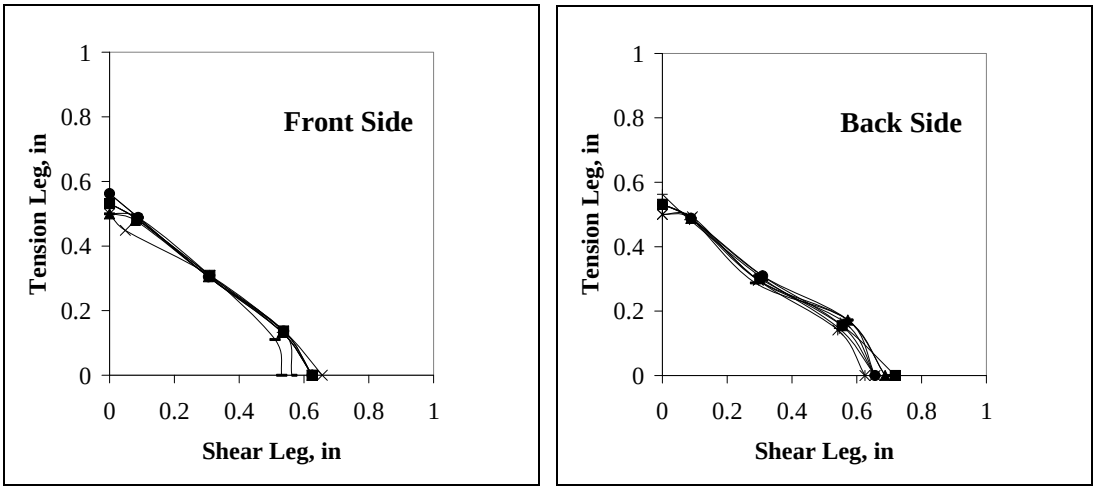

Figure B.3.47 – Test #47, B175_A12_85_2

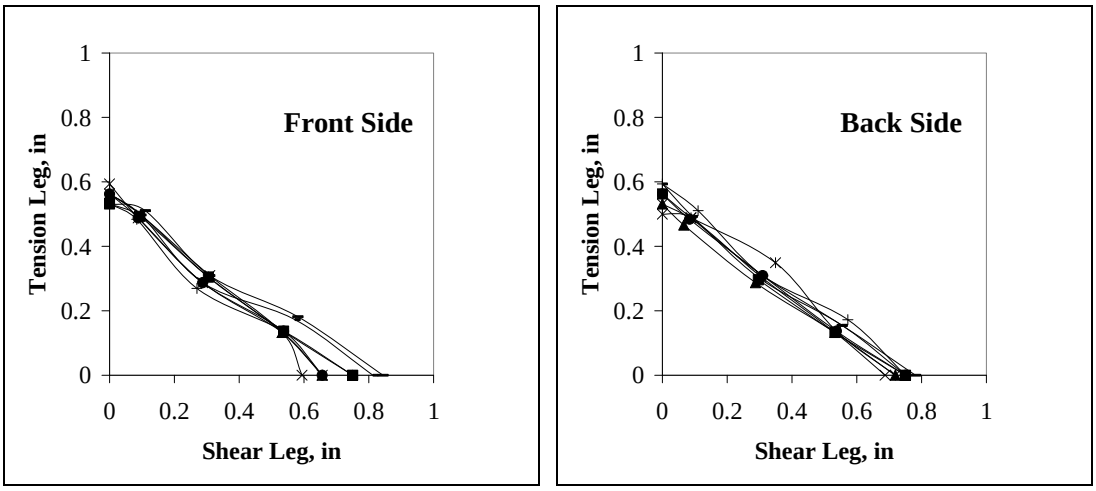

Figure B.3.48– Test #48, B175_A12_85_3

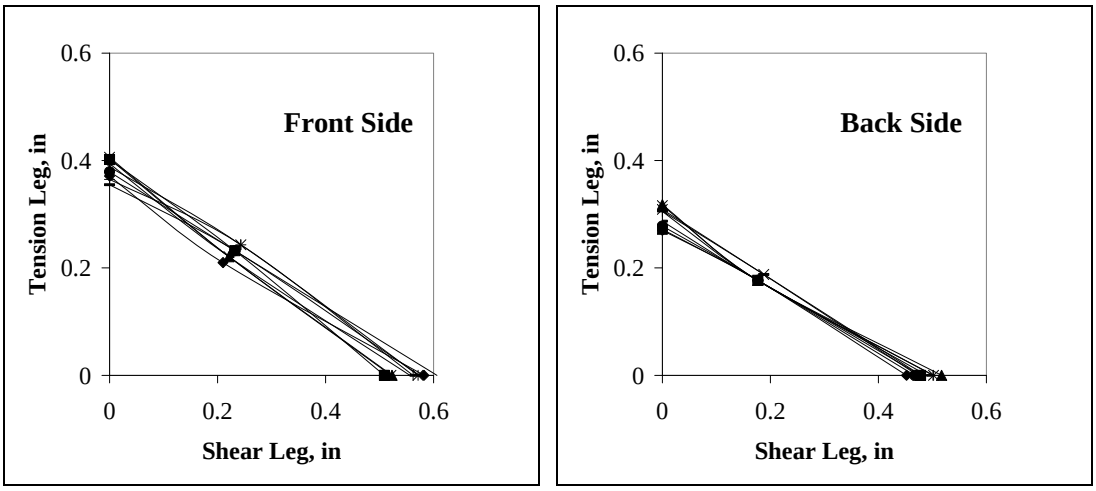

Figure B.3.49 – Test #49, B250_A516_55_1

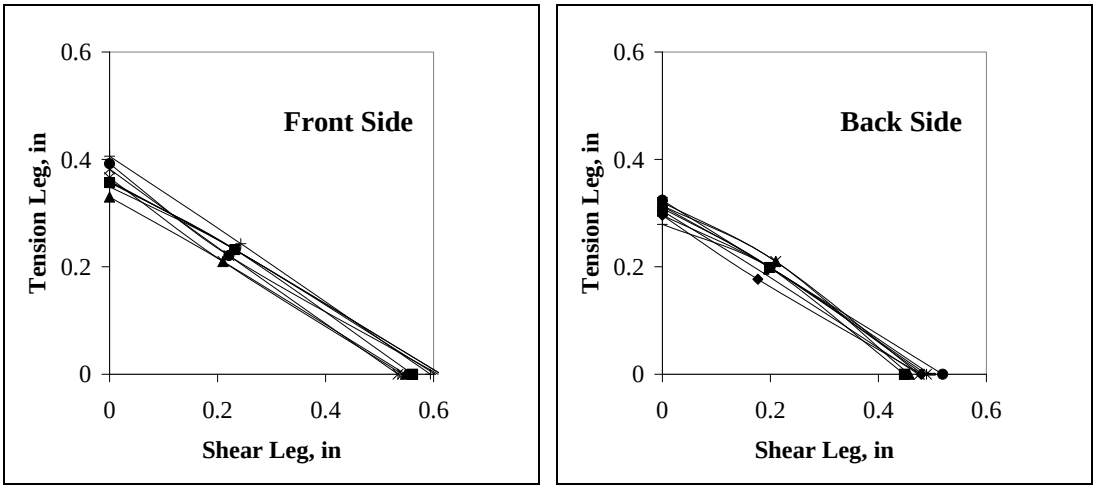

Figure B.3.50 – Test #50, B250_A516_55_2

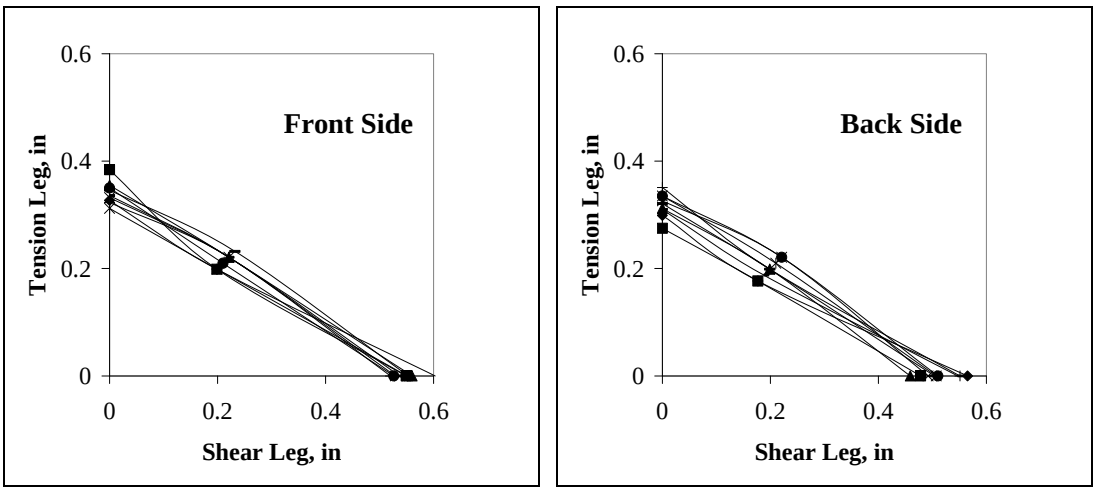

Figure B.3.51 – Test #51, B250_A516_55_3

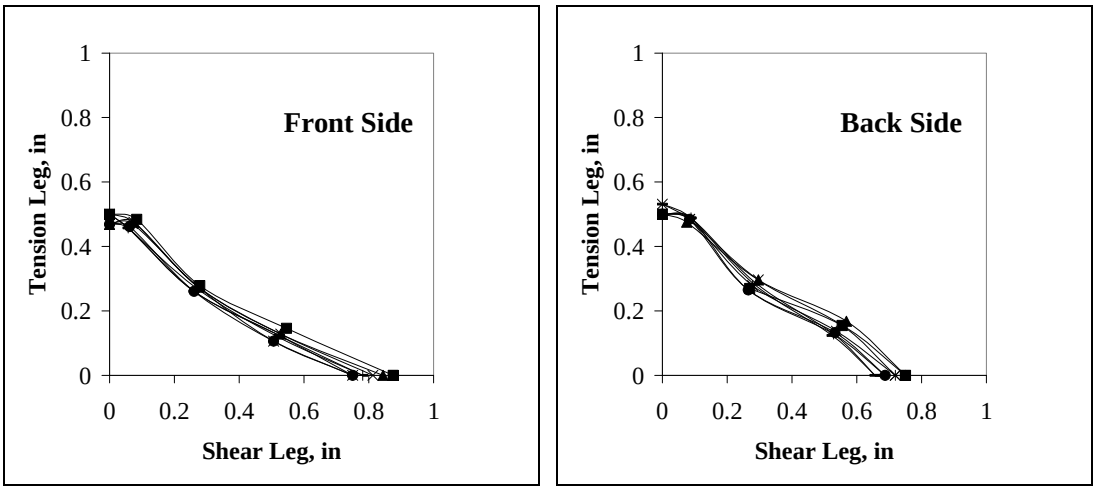

Figure B.3.52 – Test #52, B250_A12_55_1

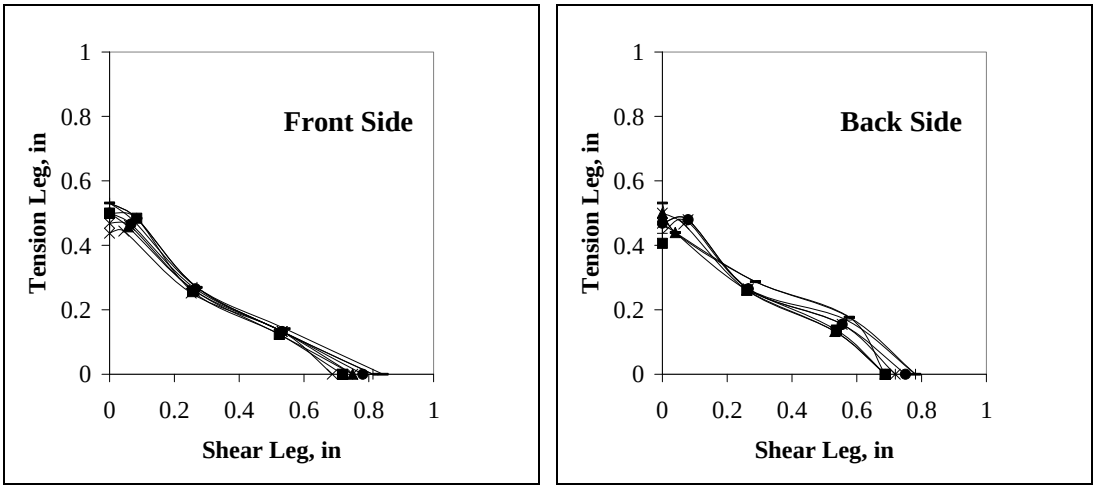

Figure B.3.53 – Test #53, B250_A12_55_2

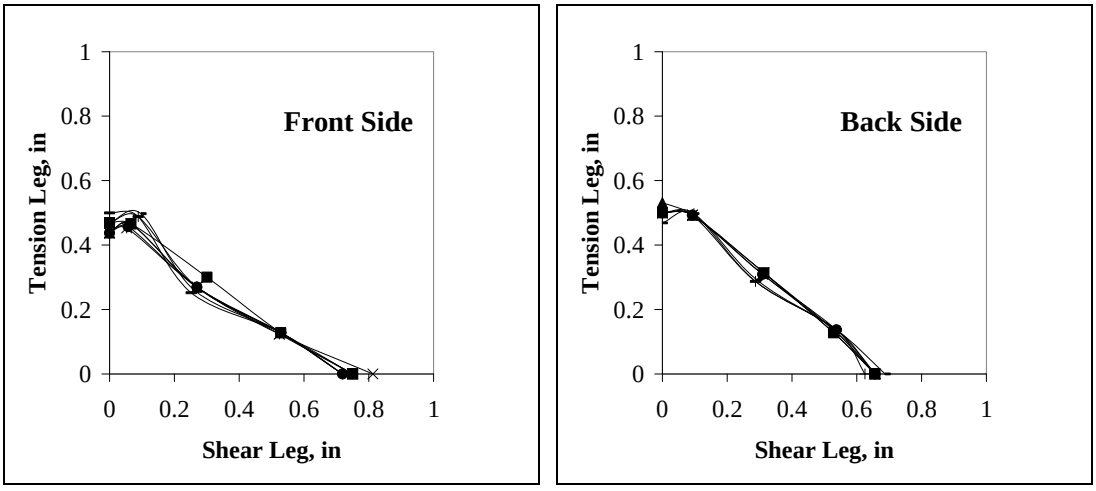

Figure B.3.54 – Test #54, B250_A12_55_3

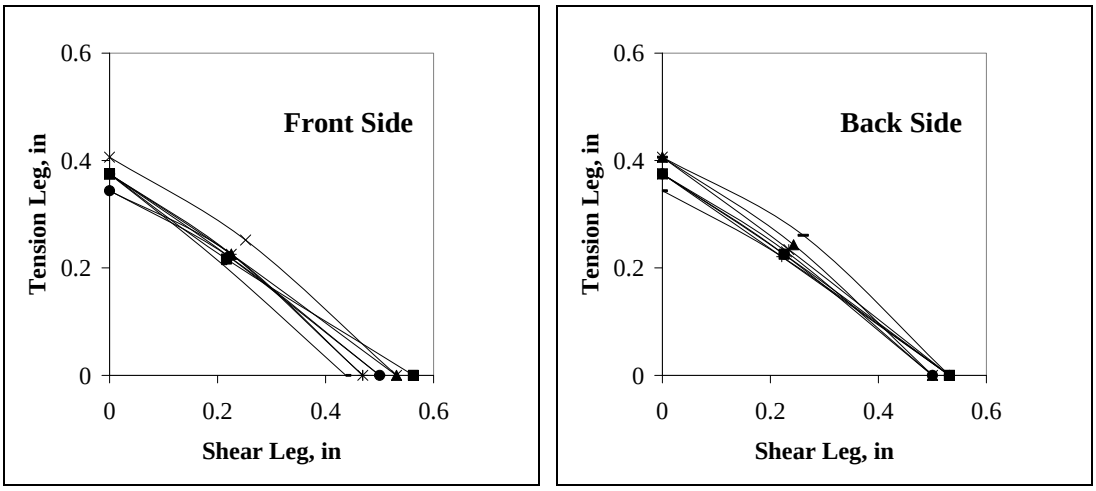

Figure B.3.55 – Test #55, B125_B516_55_1

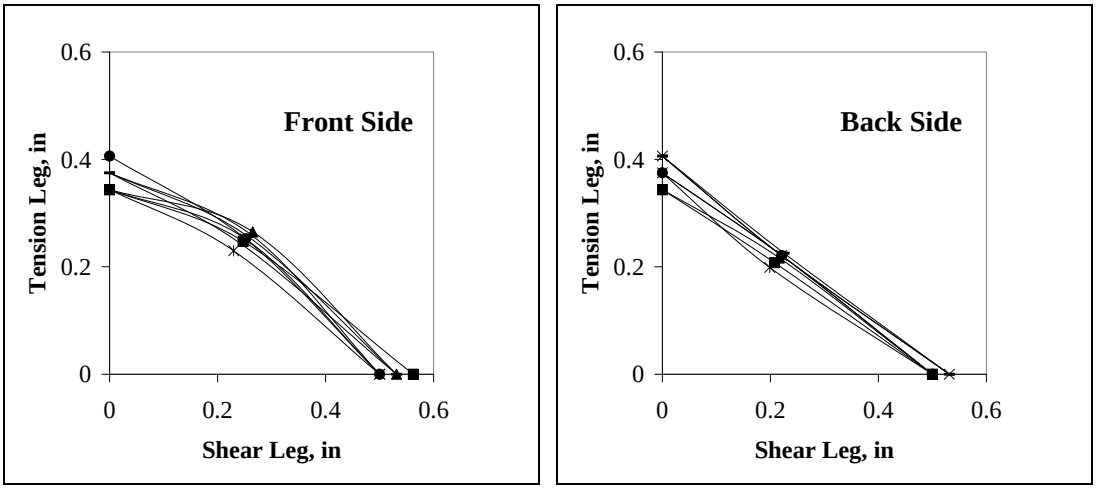

Figure B.3.56 – Test #56, B125_B516_55_2

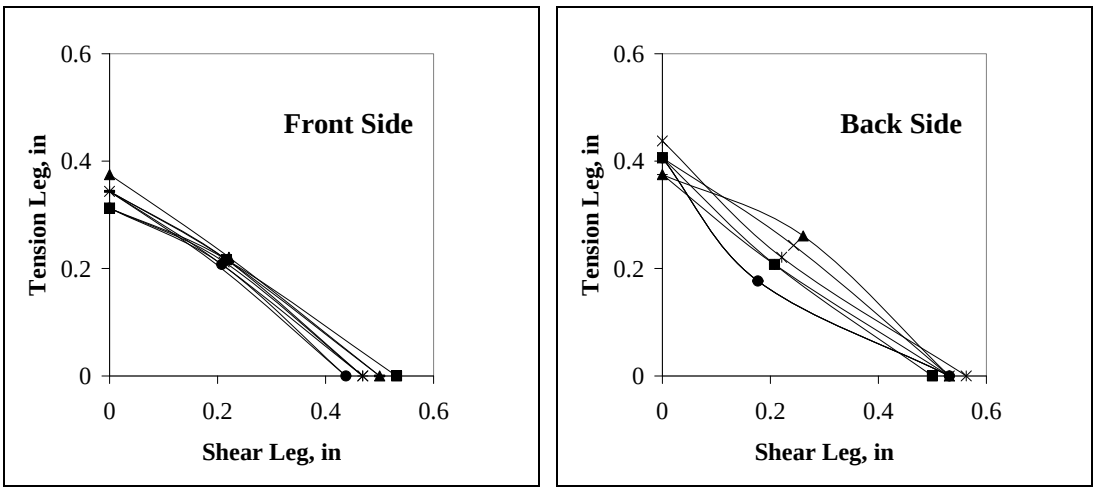

Figure B.3.57 – Test #57, B125_B516_55_3

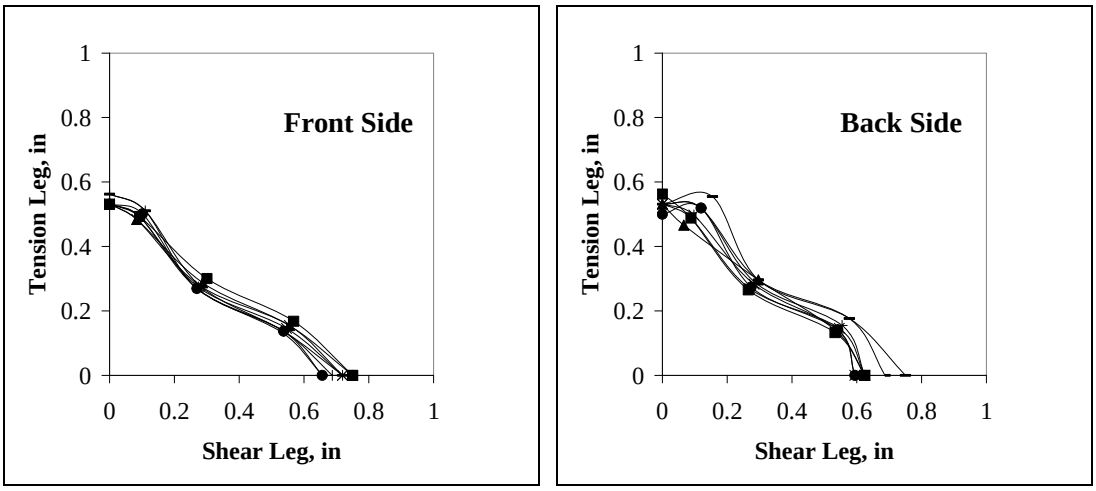

Figure B.3.58 – Test #58, B125_B55_55_1

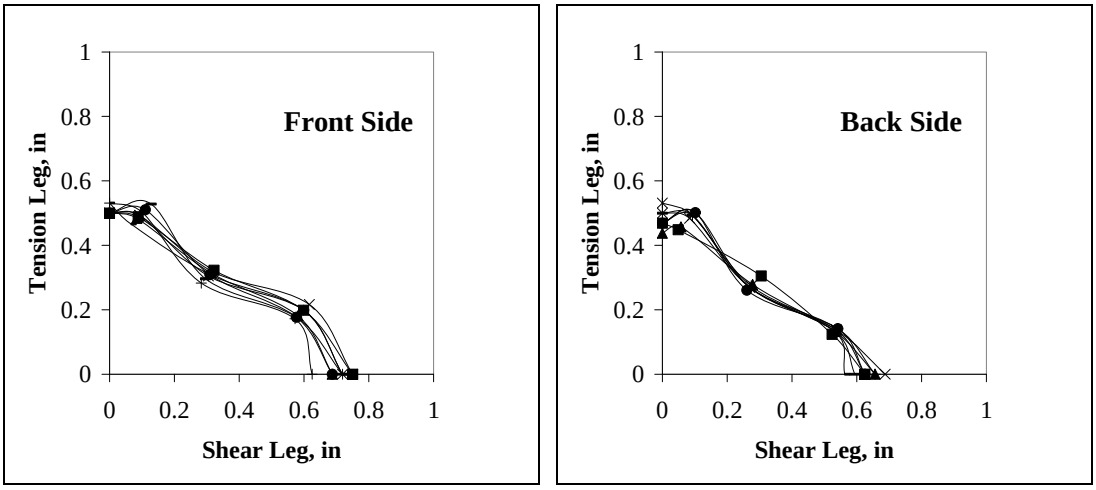

Figure B.3.59 – Test #59, B125_B12_55_2

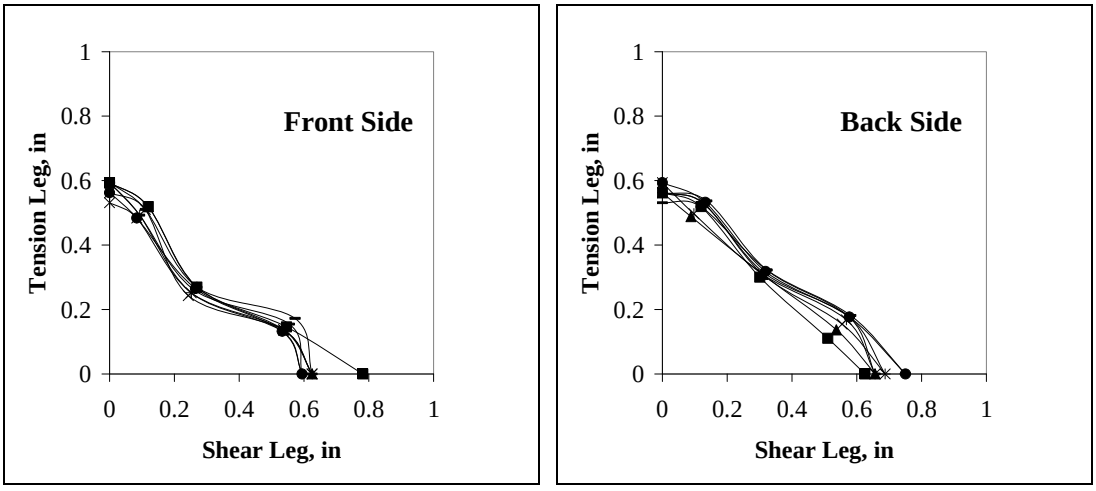

Figure B.3.60 – Test #60, B125_B12_55_3

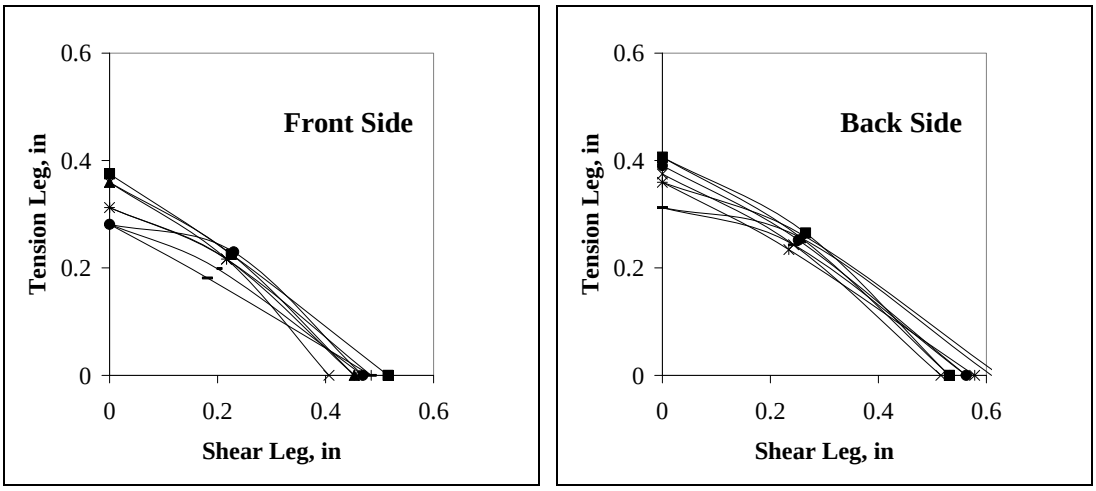

Figure B.3.61 – Test #61, B175_B516_3_1

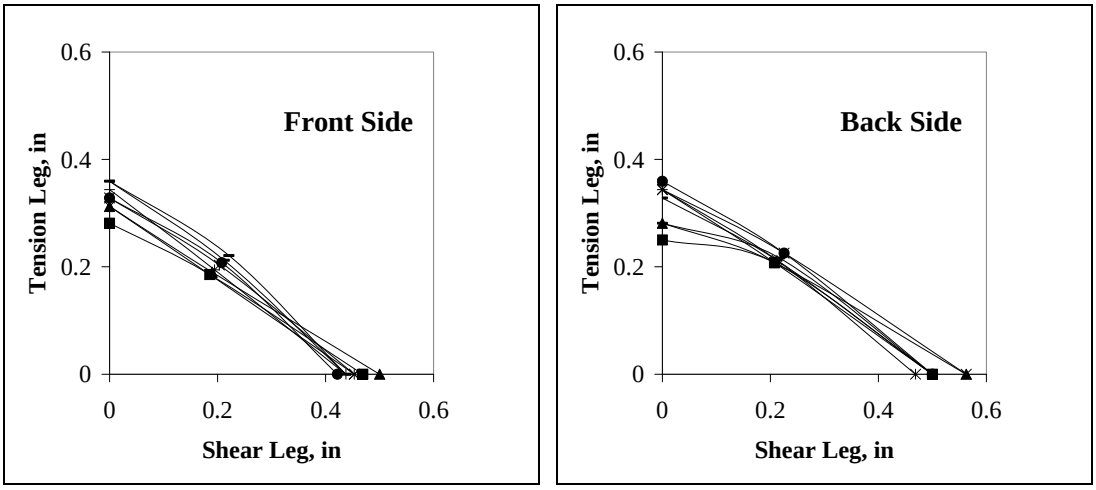

Figure B.3.62 – Test #62, B175_B516_3_2

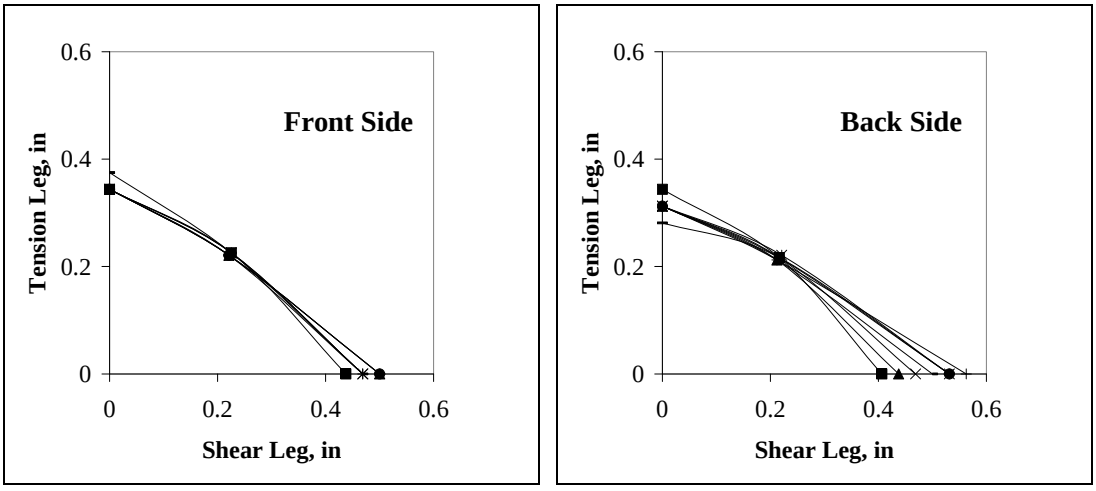

Figure B.3.63 – Test #63, B175_B516_3_3

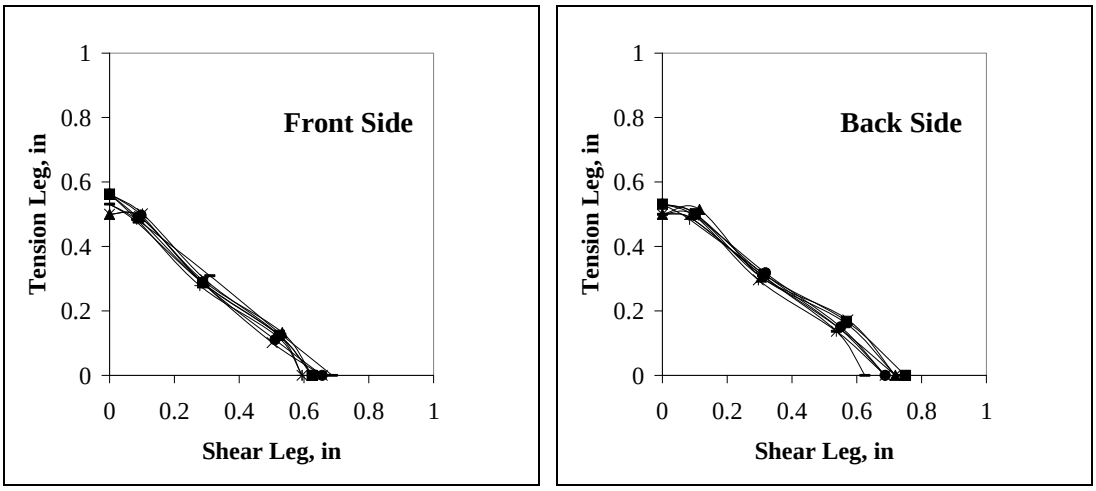

Figure B.3.64 – Test #64, B175_B12_3_1

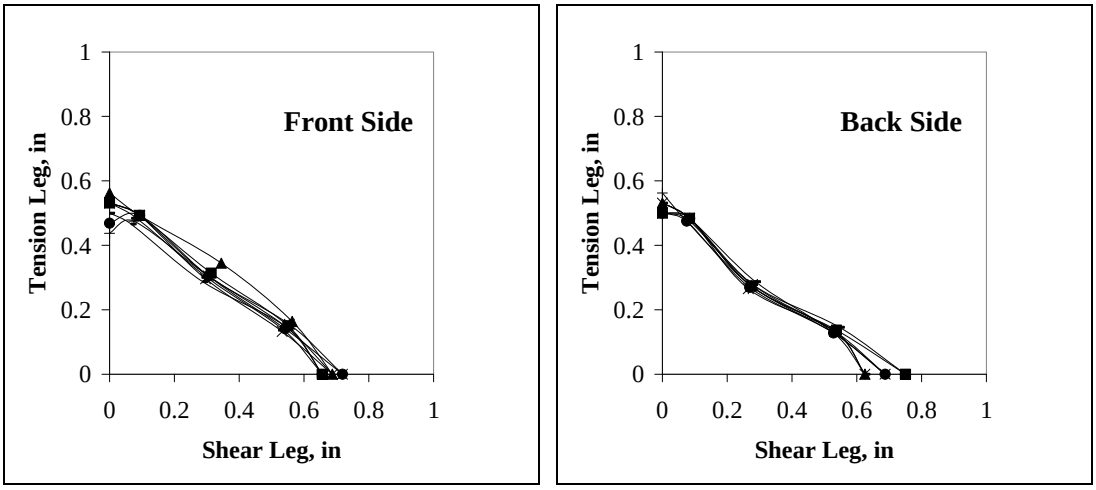

Figure B.3.65 – Test #65, B175_B12_3_2

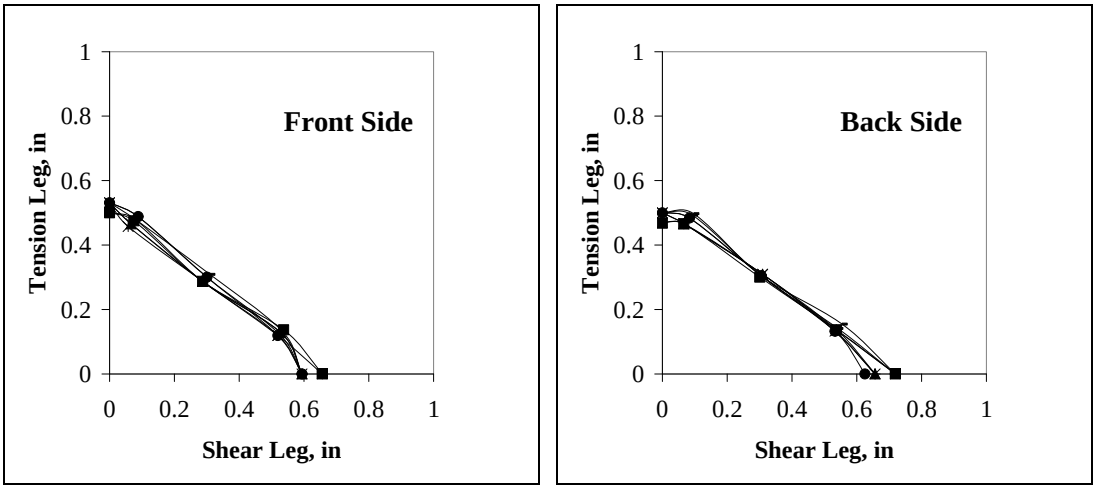

Figure B.3.66 – Test #66, B175_B12_3_3

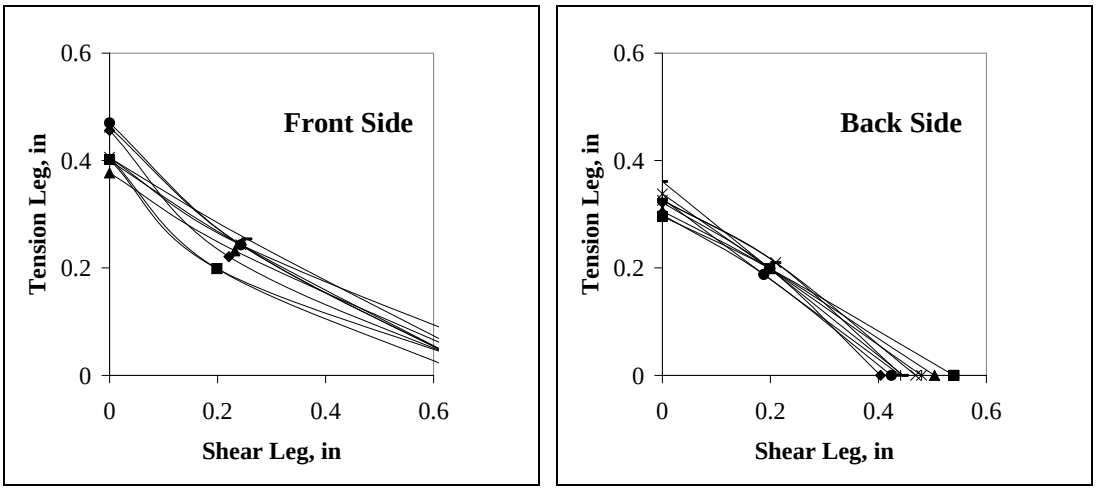

Figure B.3.67 – Test #67, B175_B516_55_1

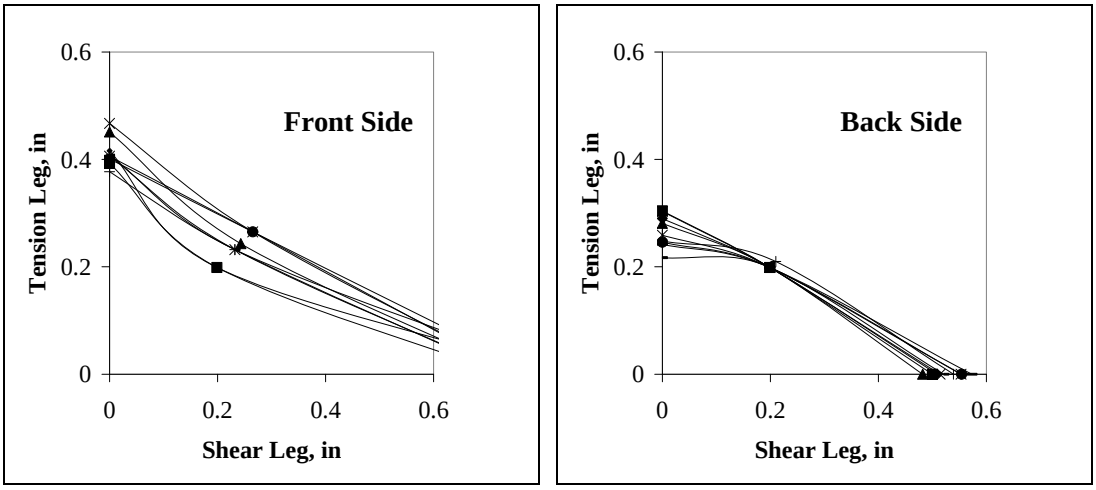

Figure B.3.68 – Test #68, B175_B516_55_2

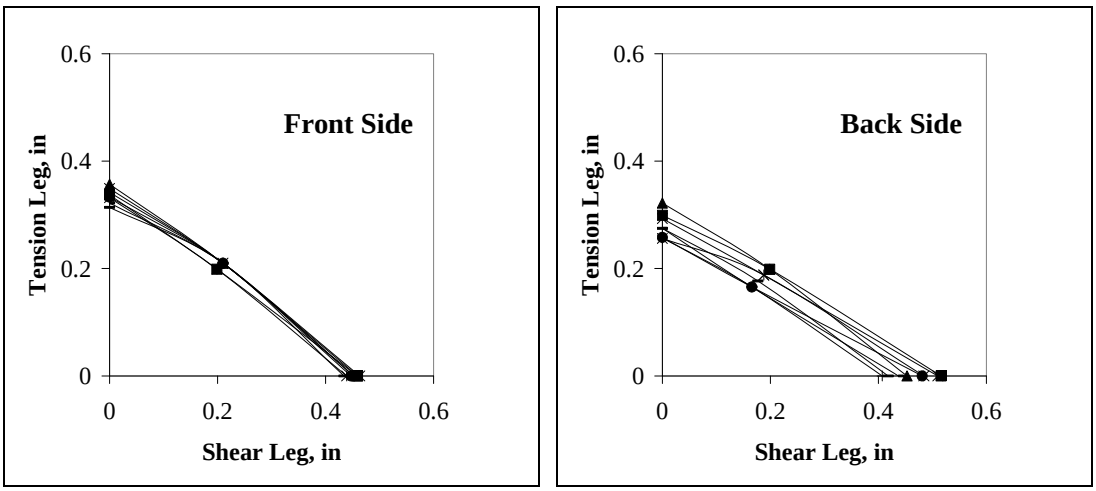

Figure B.3.69 – Test #69, B175_B516_55_3

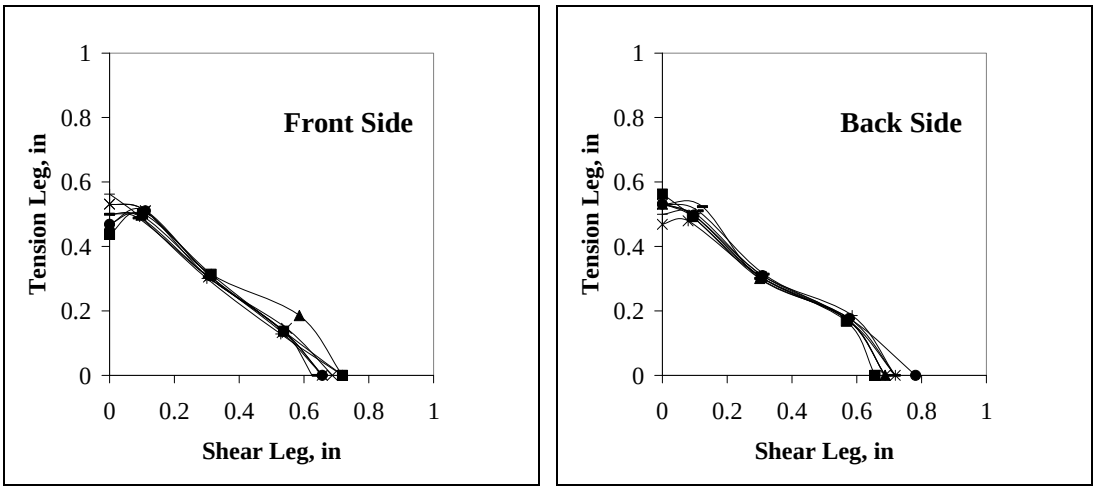

Figure B.3.70 – Test #70, B175_B12_55_1

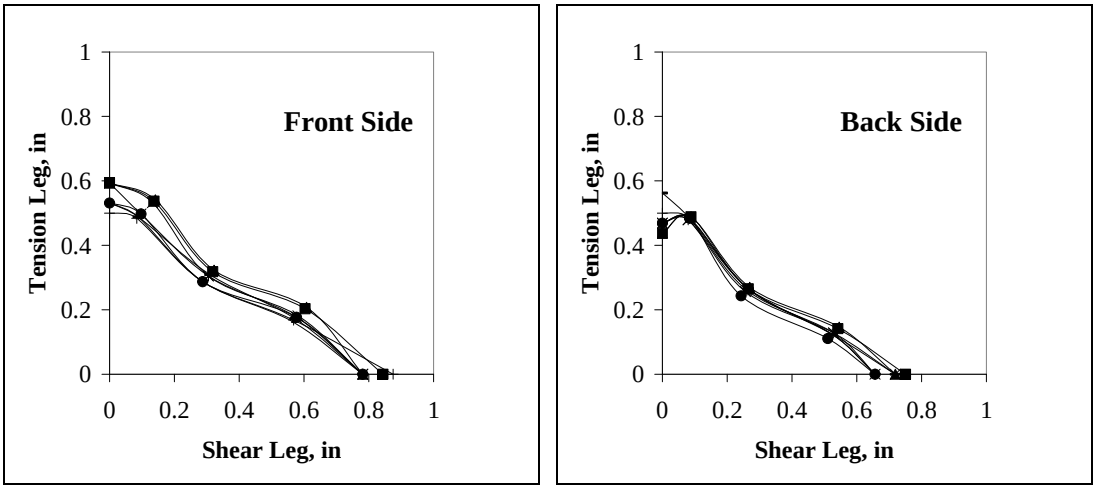

Figure B.3.71 – Test #71, B175_B12_55_2

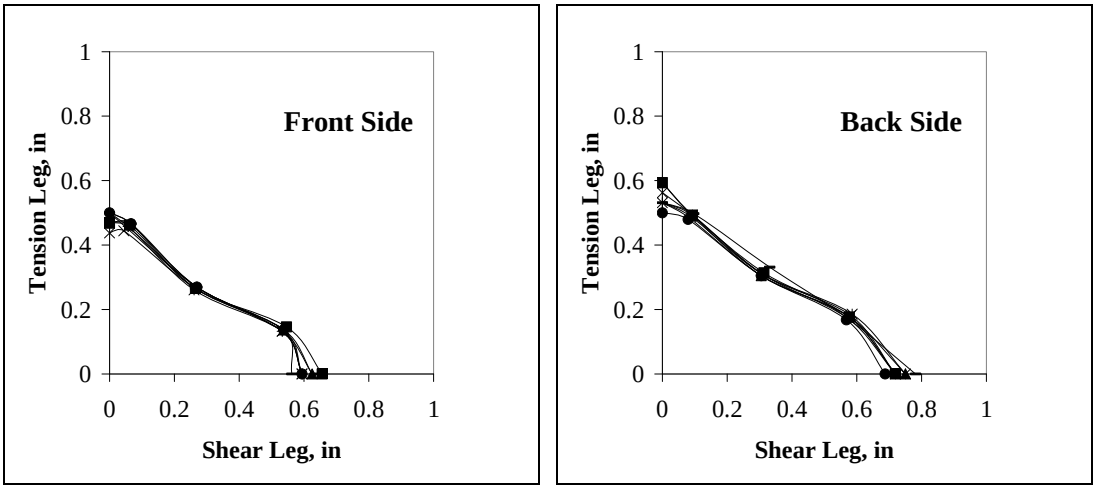

Figure B.3.72 – Test #72, B175_B12_55_3

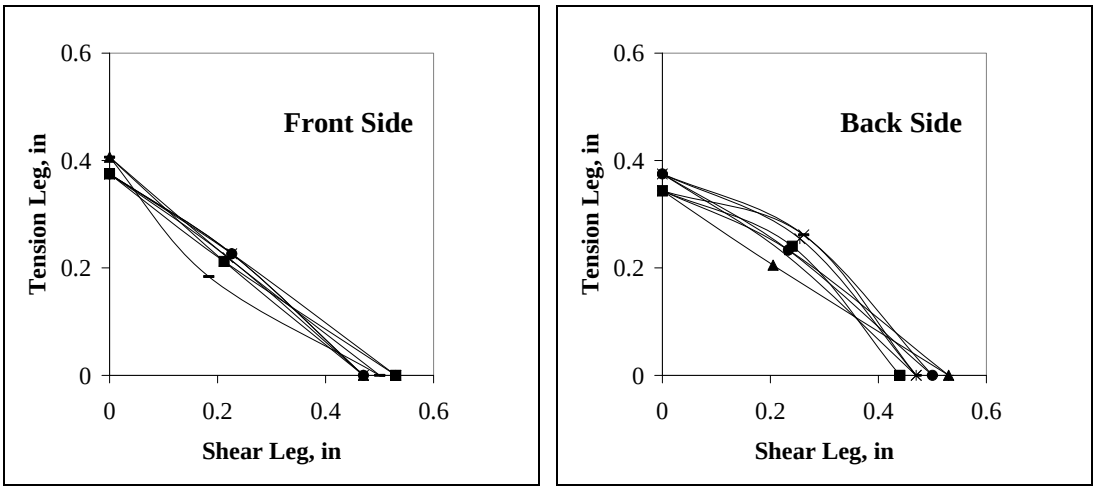

Figure B.3.73 – Test #73, B175_B516_85_1

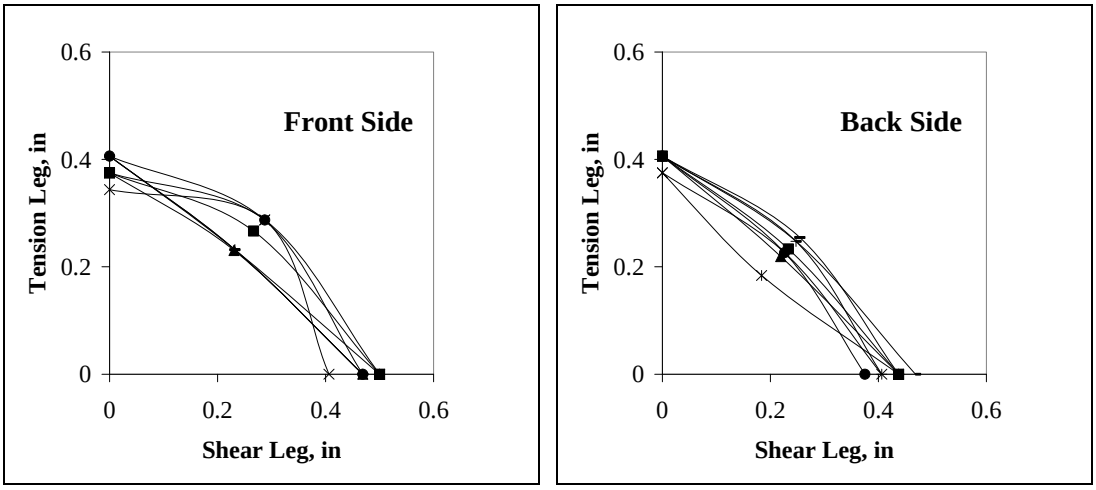

Figure B.3.74 – Test #74, B175_B516_85_2

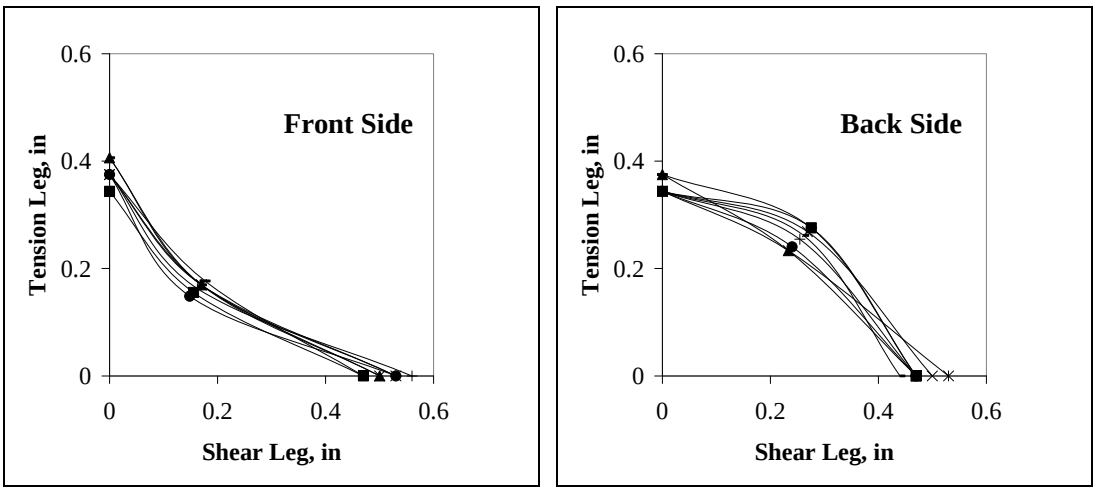

Figure B.3.75 – Test #75, B175_B516_85_3

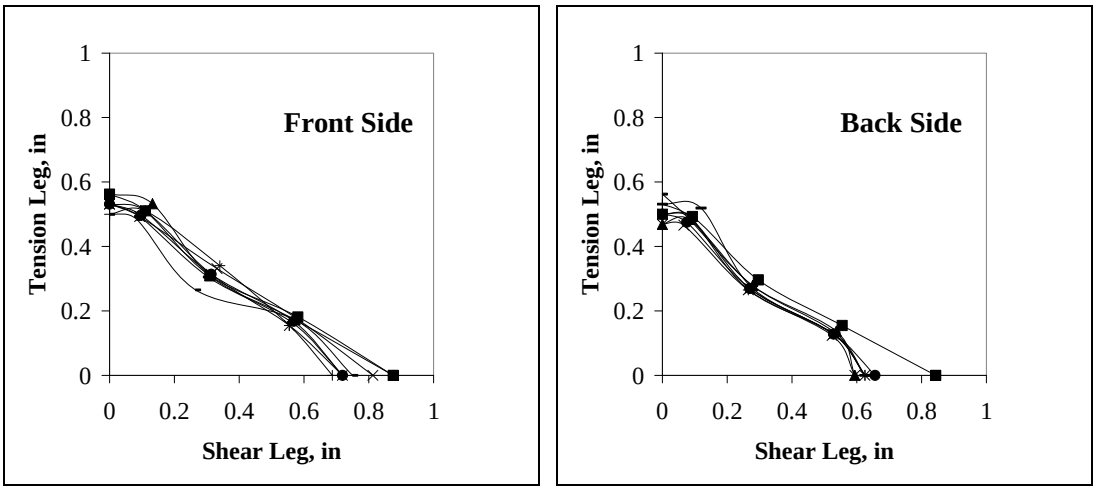

Figure B.3.76 – Test #76, B175_B12_85_1

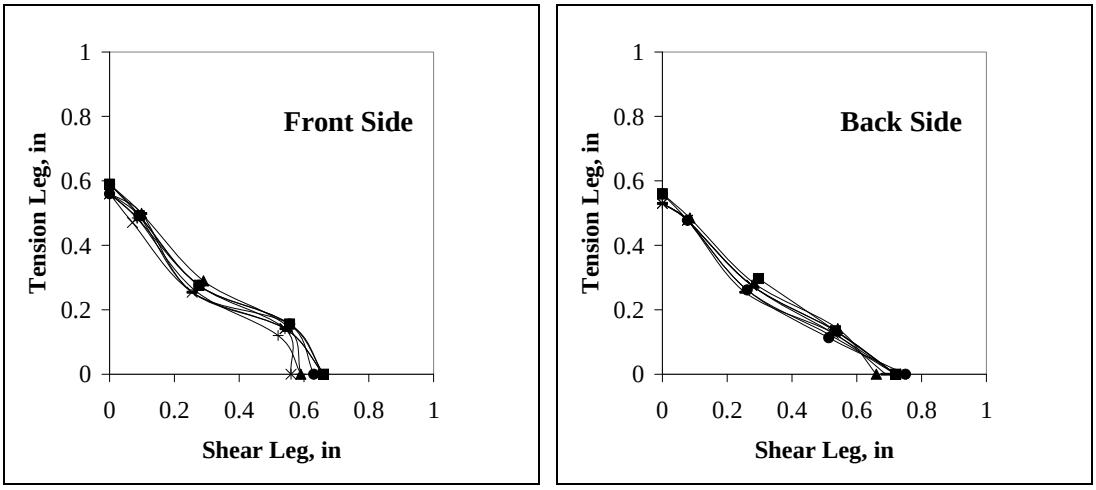

Figure B.3.77 – Test #77, B175_B12_85_2

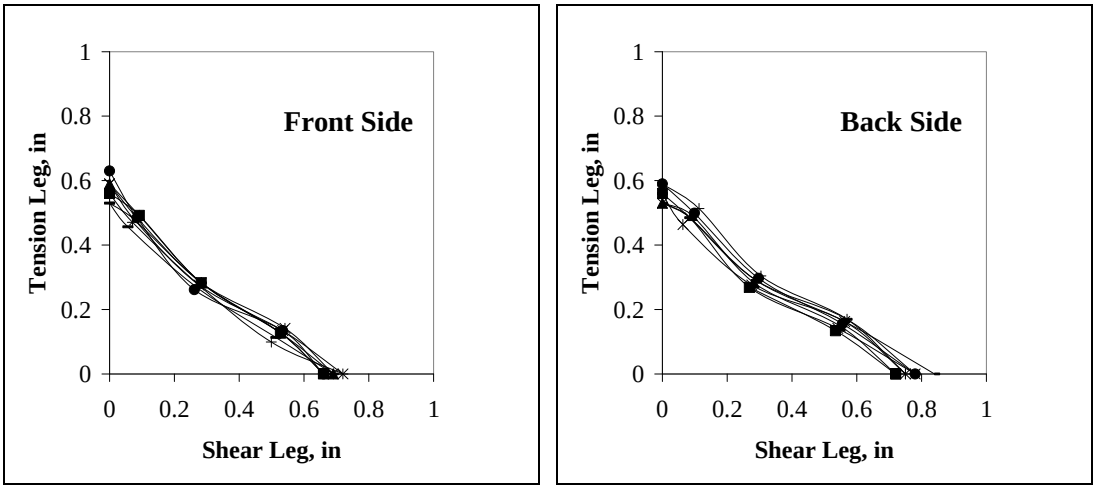

Figure B.3.78 – Test #78, B175_B12_85_3

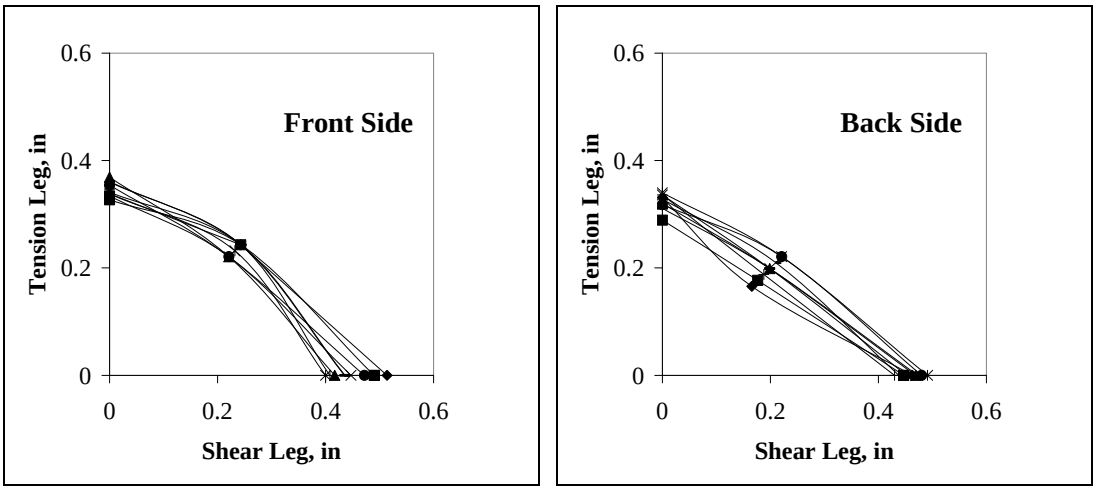

Figure B.3.79 – Test #79, B250_B516_55_1

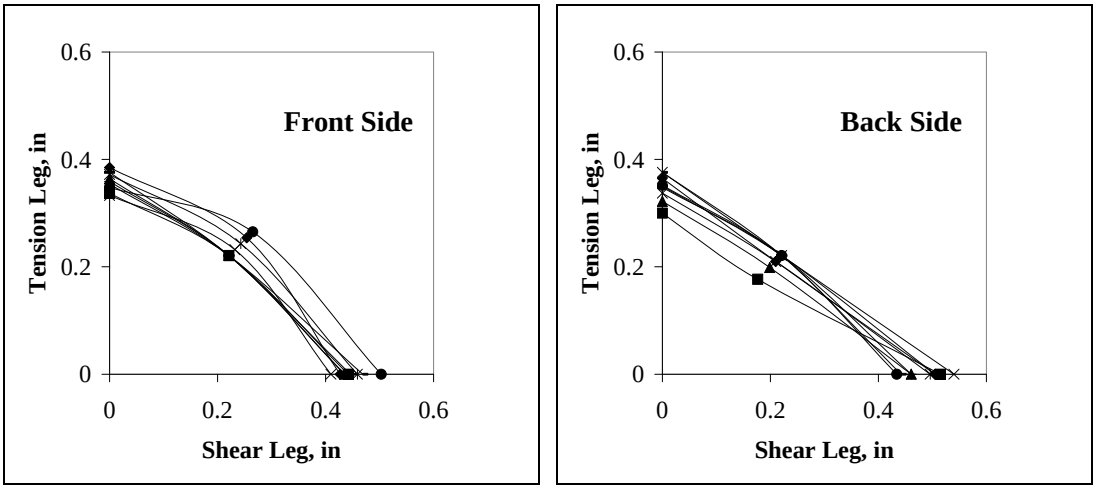

Figure B.3.80 – Test #80, B250_B516_55_2

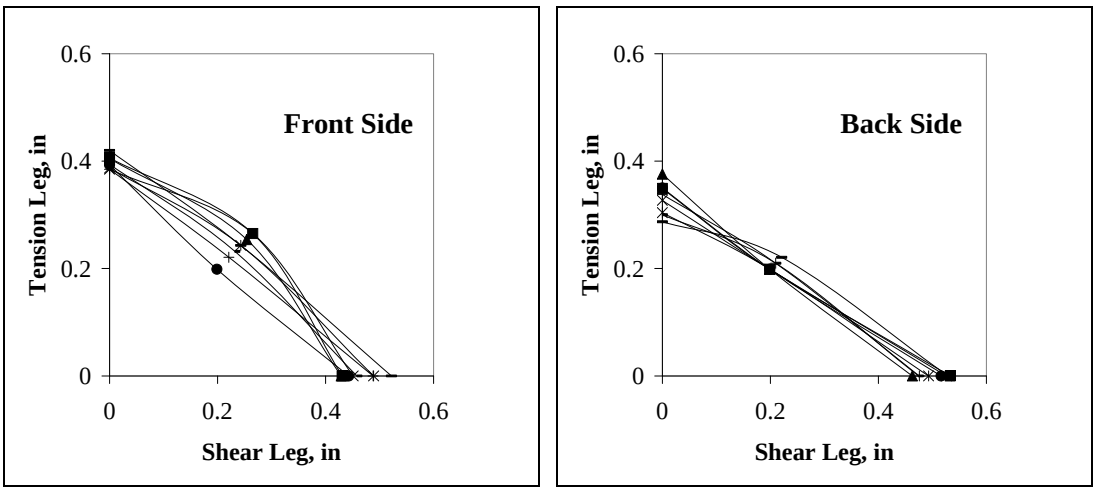

Figure B.3.81 – Test #81, B250_B516_55_3

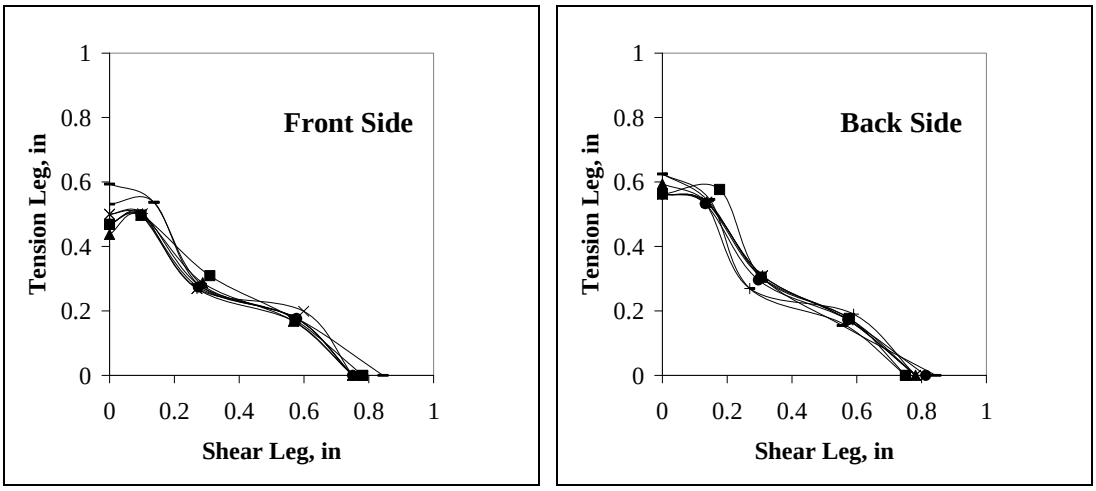

Figure B.3.82 – Test #82, B250_B12_55_1

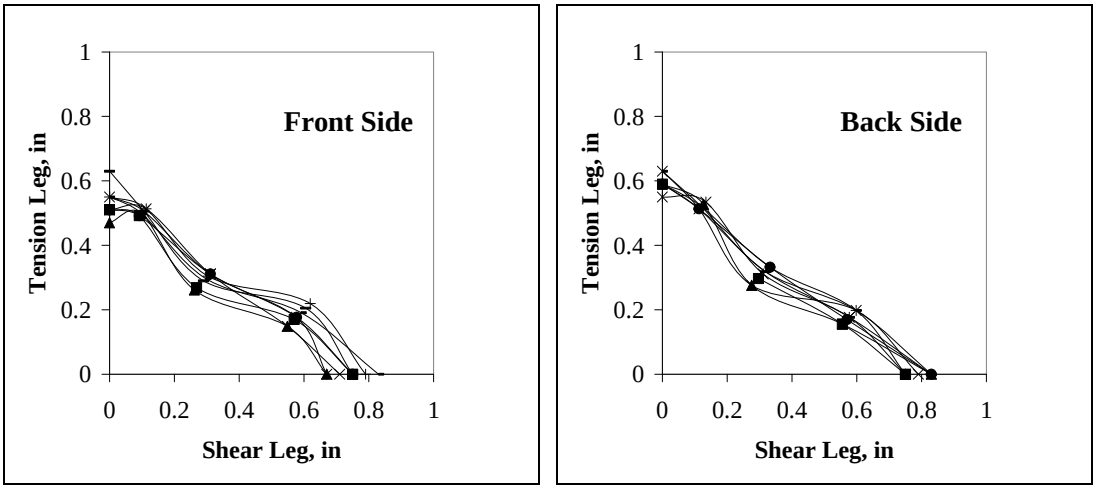

Figure B.3.83 – Test #83, B250_B12_55_2

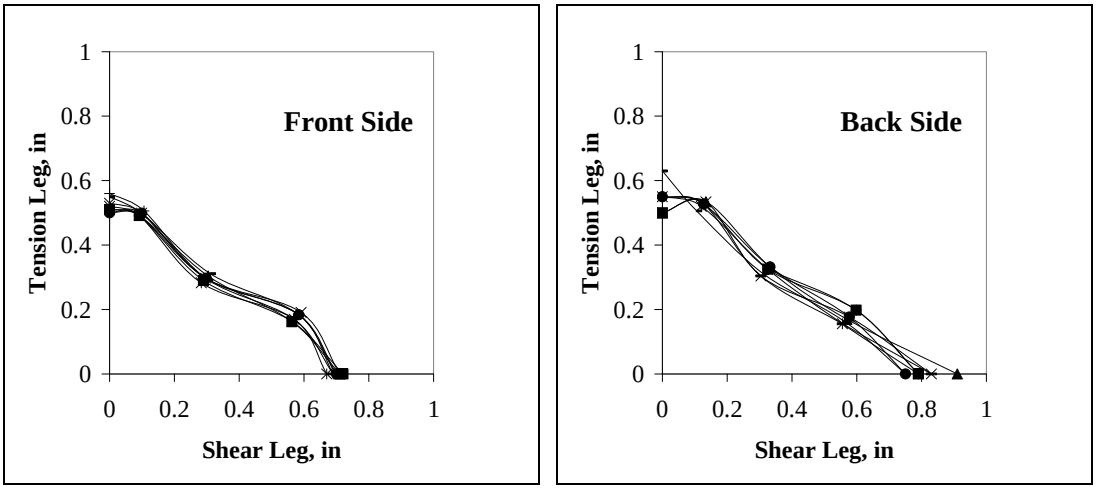

Figure B.3.84 – Test #84, B250_B12_55_3

B.4 MEASURED LENGTHS OF NOMINAL FOUR INCH WELD

Test Number	Specimen	Weld Length, inches		Test Number	Specimen	Weld Length, inches	
		Front Side	Back Side			Front Side	Back Side
1	T125_A12_1	4.010	4.039	43	B175_A516_85_1	3.870	3.890
2	T125_A12_2	3.901	3.908	44	B175_A516_85_2	3.806	3.819
3	T125_A12_3	3.939	3.940	45	B175_A516_85_3	3.919	3.900
4	T125_A516_1	3.948	3.943	46	B175_A12_85_1	4.056	4.070
5	T125_A516_2	4.060	4.065	47	B175_A12_85_2	4.070	4.062
6	T125_A516_3	4.150	4.155	48	B175_A12_85_3	4.011	4.062
7	T250_A12_1	3.860	3.855	49	B250_A516_55_1	4.081	4.162
8	T250_A12_2	4.080	4.067	50	B250_A516_55_2	3.977	3.985
9	T250_A12_3	3.900	4.014	51	B250_A516_55_3	4.111	4.116
10	T250_A516_1	4.128	4.132	52	B250_A12_55_1	3.947	4.004
11	T250_A516_2	4.033	4.037	53	B250_A12_55_2	4.138	4.174
12	T250_A516_3	3.923	3.976	54	B250_A12_55_3	4.118	4.101
13	T125_B12_1	3.886	3.934	55	B125_B516_55_1	3.779	n/a
14	T125_B12_2	3.922	3.929	56	B125_B516_55_2	3.848	3.828
15	T125_B12_3	3.973	3.979	57	B125_B516_55_3	3.750	3.760
16	T125_B516_1	3.910	3.915	58	B125_B12_55_1	4.027	3.973
17	T125_B516_2	4.065	4.065	59	B125_B12_55_2	3.943	3.950
18	T125_B516_3	4.030	4.035	60	B125_B12_55_3	4.104	4.101
19	T250_B12_1	4.074	4.075	61	B175_B516_3_1	3.977	4.013
20	T250_B12_2	3.926	3.945	62	B175_B516_3_2	4.132	4.096
21	T250_B12_3	3.877	3.875	63	B175_B516_3_3	4.081	4.061
22	T250_B516_1	4.018	4.137	64	B175_B12_3_1	4.072	4.085
23	T250_B516_2	3.942	3.949	65	B175_B12_3_2	4.036	4.045
24	T250_B516_3	3.871	3.873	66	B175_B12_3_3	4.056	4.083
25	B125_A516_55_1	3.877	3.875	67	B175_B516_55_1	3.993	4.058
26	B125_A516_55_2	3.906	3.914	68	B175_B516_55_2	4.015	4.040
27	B125_A516_55_3	3.818	3.925	69	B175_B516_55_3	4.034	4.051
28	B125_A12_55_1	3.814	3.999	70	B175_B12_55_1	4.002	4.026
29	B125_A12_55_2	3.960	3.912	71	B175_B12_55_2	3.914	3.816
30	B125_A12_55_3	3.970	4.000	72	B175_B12_55_3	3.947	3.816
31	B175_A516_3_1	3.930	3.959	73	B175_B516_85_1	4.070	4.090
32	B175_A516_3_2	3.982	3.985	74	B175_B516_85_2	3.977	3.977
33	B175_A516_3_3	4.077	4.067	75	B175_B516_85_3	3.960	3.990
34	B175_A12_3_1	3.868	3.872	76	B175_B12_85_1	4.076	4.073
35	B175_A12_3_2	4.001	3.998	77	B175_B12_85_2	4.000	3.990
36	B175_A12_3_3	3.816	3.910	78	B175_B12_85_3	3.790	3.830
37	B175_A516_55_1	4.067	4.058	79	B250_B516_55_1	3.940	4.096
38	B175_A516_55_2	4.050	4.055	80	B250_B516_55_2	3.965	3.985
39	B175_A516_55_3	3.927	3.977	81	B250_B516_55_3	3.965	3.883
40	B175_A12_55_1	4.085	4.079	82	B250_B12_55_1	4.004	3.995
41	B175_A12_55_2	3.797	3.825	83	B250_B12_55_2	3.900	3.950
42	B175_A12_55_3	3.919	3.885	84	B250_B12_55_3	3.850	3.920

B.5 POSITIONING OF STRAIN GAGES

Test Number	Specimen	Test Side	Distance from Loading Edge, inches			Distance from Center Plate Edge, inches		
			"Compression" Gage	"Center" Gage	"Tension" Gage	"Compression" Gage	"Center" Gage	"Tension" Gage
57	B125_B516_55_3	Front	0.81	1.88	3.06	0.91	0.81	0.75
60	B125_B12_55_3	Front	0.73	1.88	3.32	1.09	1.03	1.09
63	B175_B516_3_3	Back	0.69	1.97	3.41	0.97	1.03	1.06
66	B175_B12_3_3	Back	0.81	2.06	3.34	1.06	1.13	1.00
69	B175_B516_55_3	Back	0.75	1.97	3.25	0.88	0.97	0.94
72	B175_B12_55_3	Front	0.88	2.06	3.25	1.13	1.03	1.03
76	B175_B12_85_1	Front	0.72	2.00	3.38	1.03	1.00	1.06
81	B250_B516_55_3	Back	0.72	2.00	3.25	0.97	0.94	0.97
82	B250_B12_55_1	Back	0.65	1.90	3.24	1.28	1.25	1.19

Appendix C

Ancillary Test Data

C.1 ALL-WELD TENSION COUPON TESTS

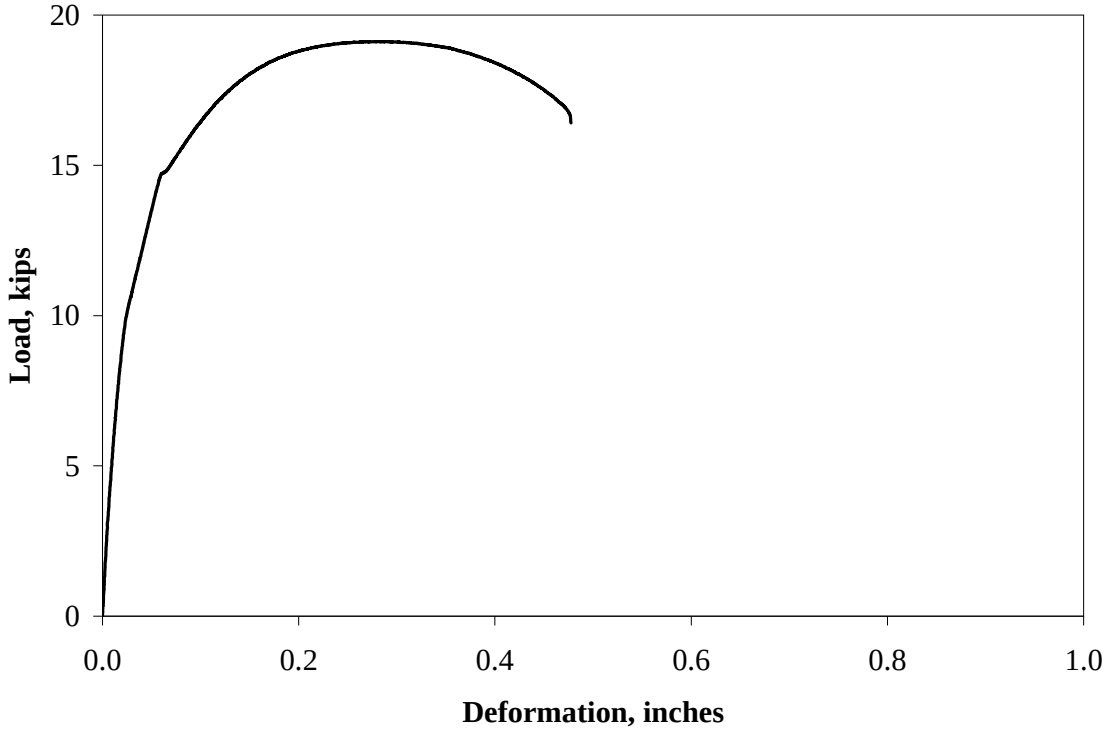

Figure C.1.1 – Load-Deformation Curve for Electrode E70T-7, Test 1

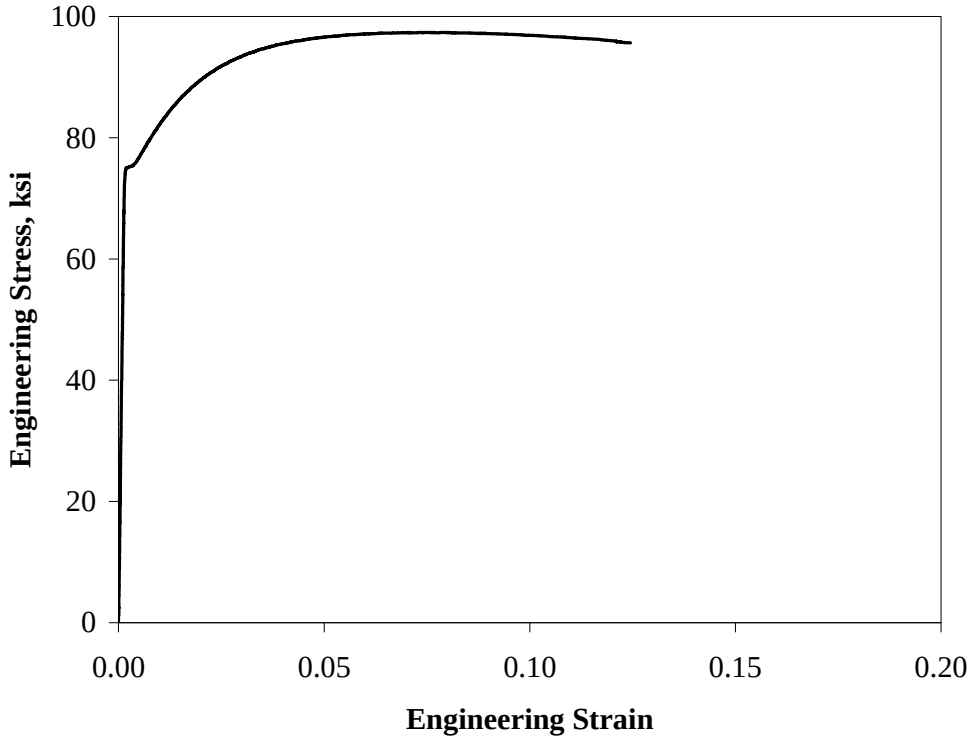

Figure C.1.2 – Stress-Strain Curve for Electrode E70T-7, Test 1

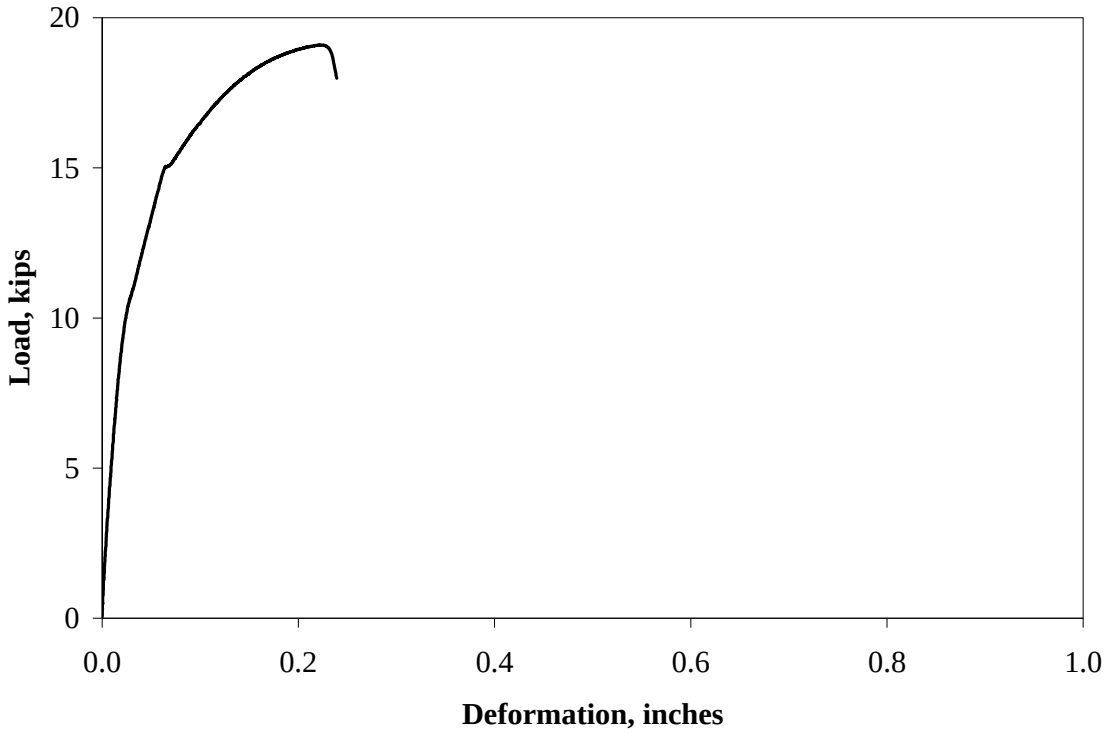

Figure C.1.3 – Load-Deformation Curve for Electrode E70T-7, Test 2

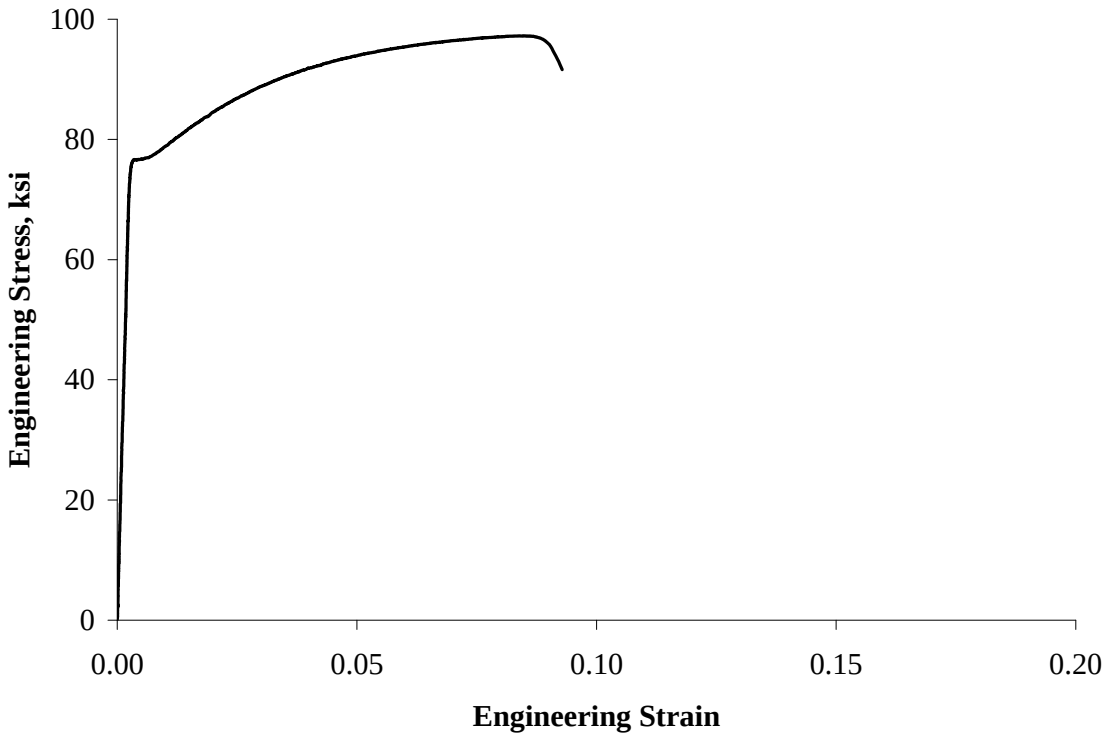

Figure C.1.4 – Stress-Strain Curve for Electrode E70T-7, Test 2

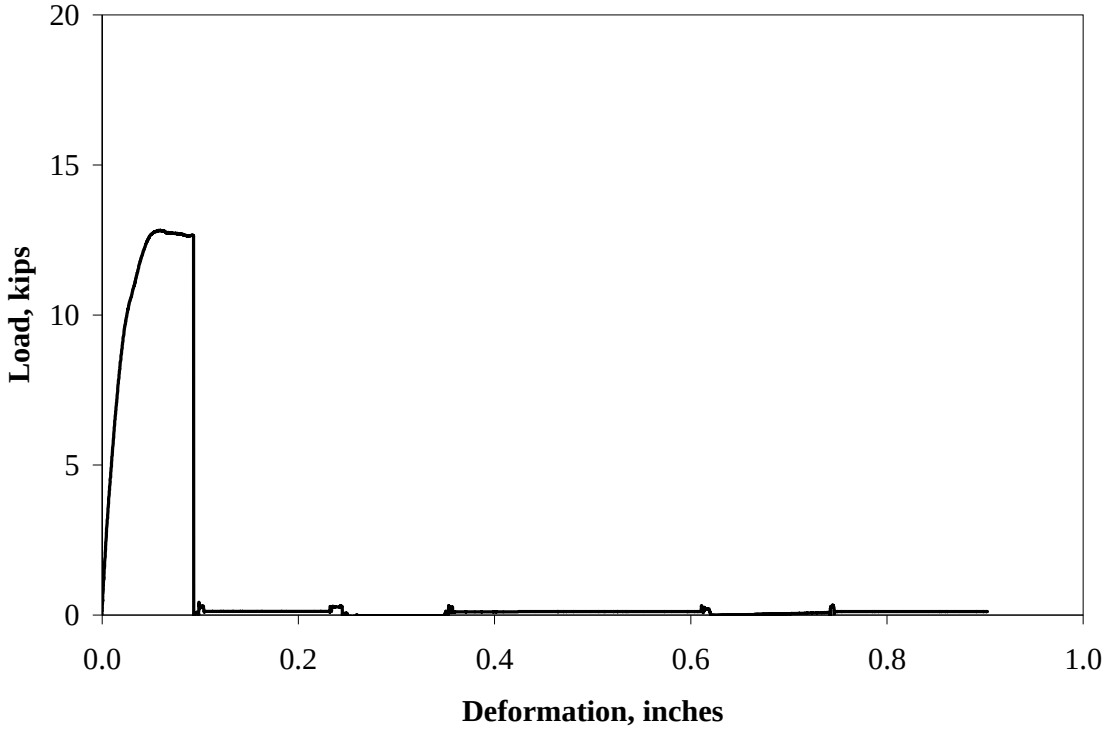

Figure C.1.5 – Load-Deformation Curve for Electrode E70T7-K2, Test 1

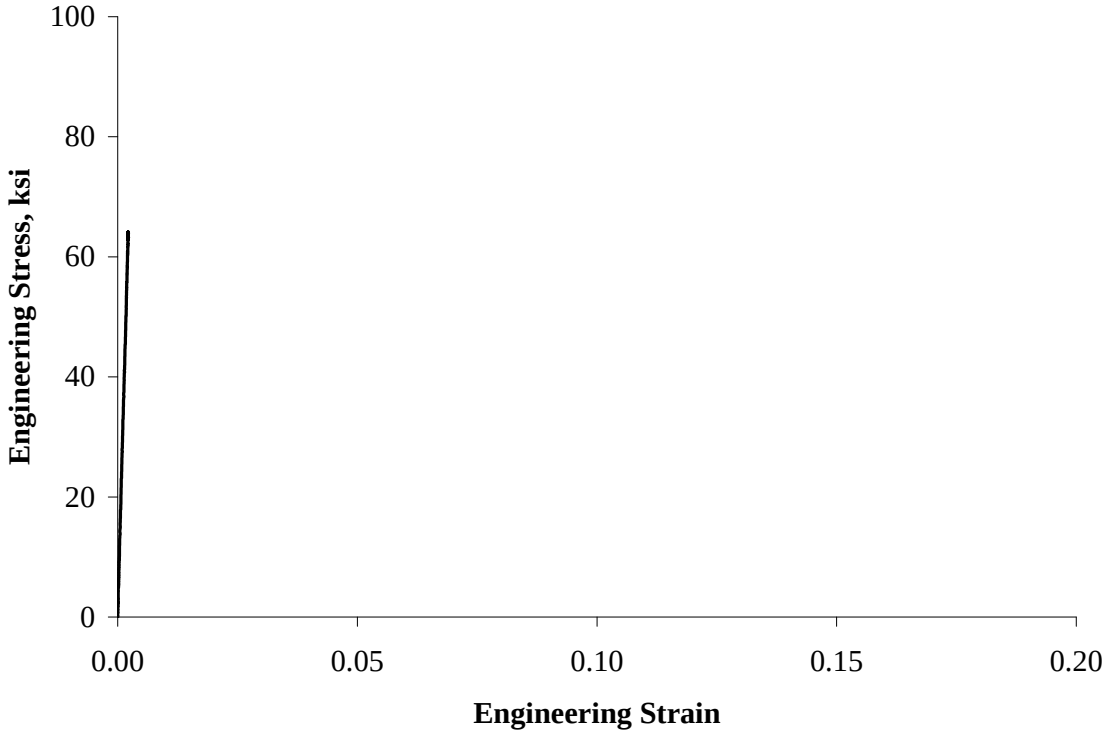

Figure C.1.6 – Stress-Strain Curve for Electrode E70T7-K2, Test 1

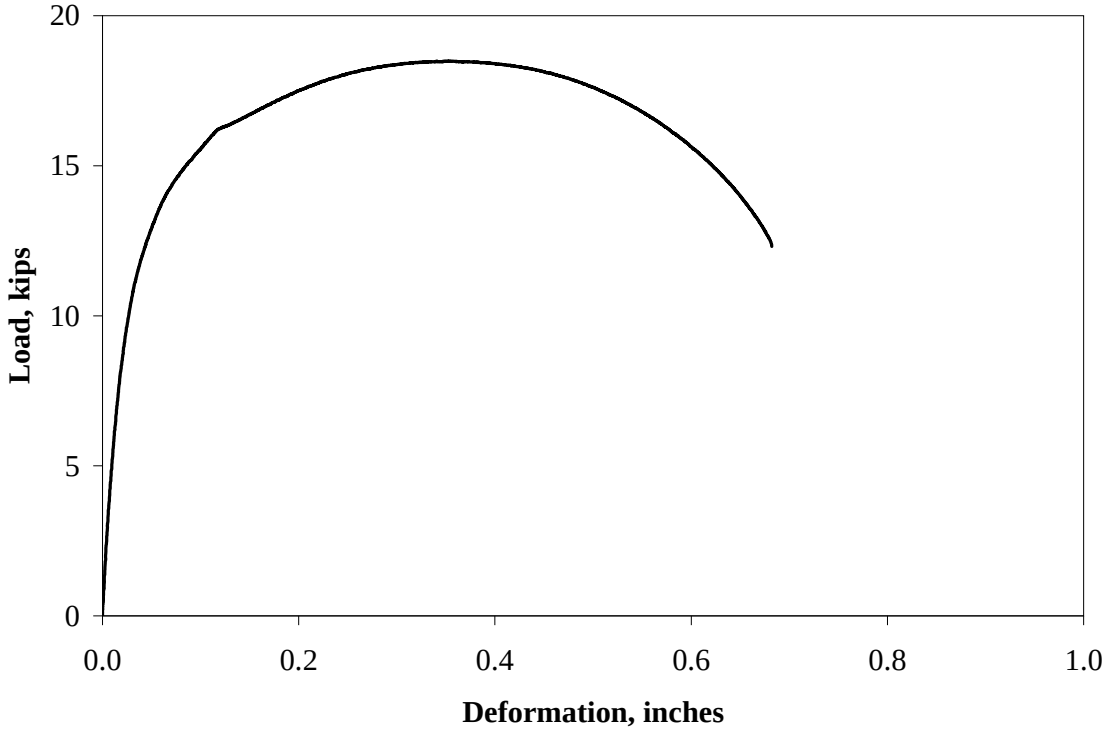

Figure C.1.7 – Load-Deformation Curve for Electrode E70T7-K2, Test 2

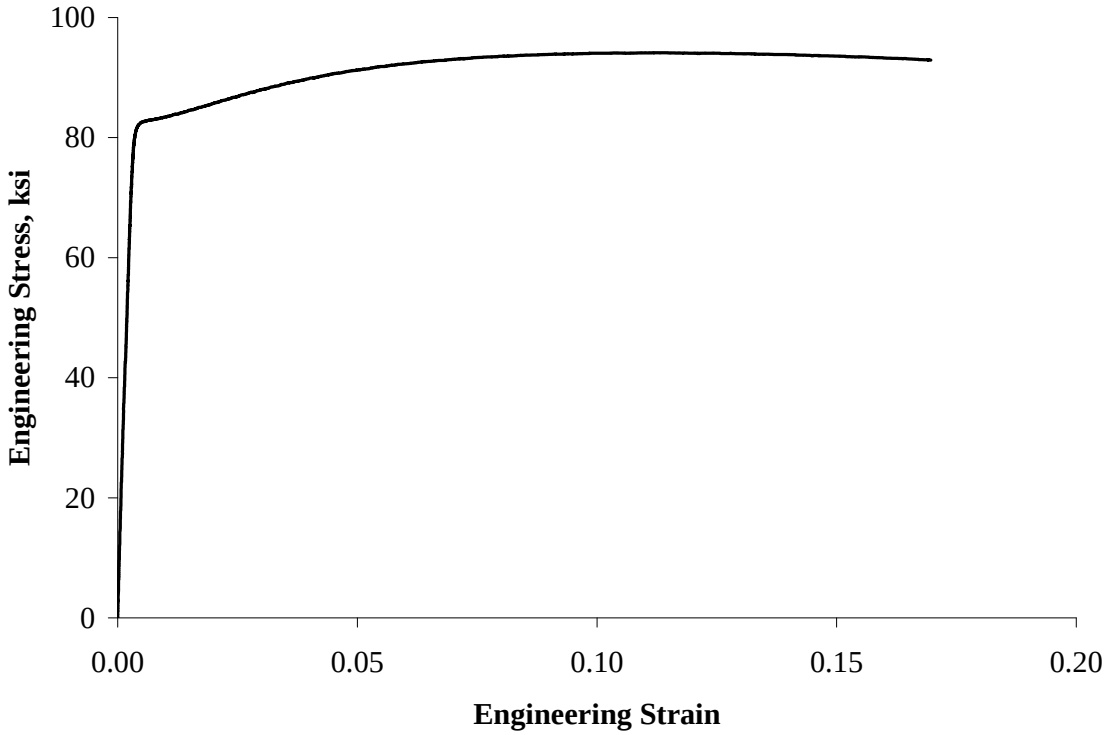

Figure C.1.8 – Stress-Strain Curve for Electrode E70T7-K2, Test 2

C.2 BASE METAL TENSION COUPON TESTS

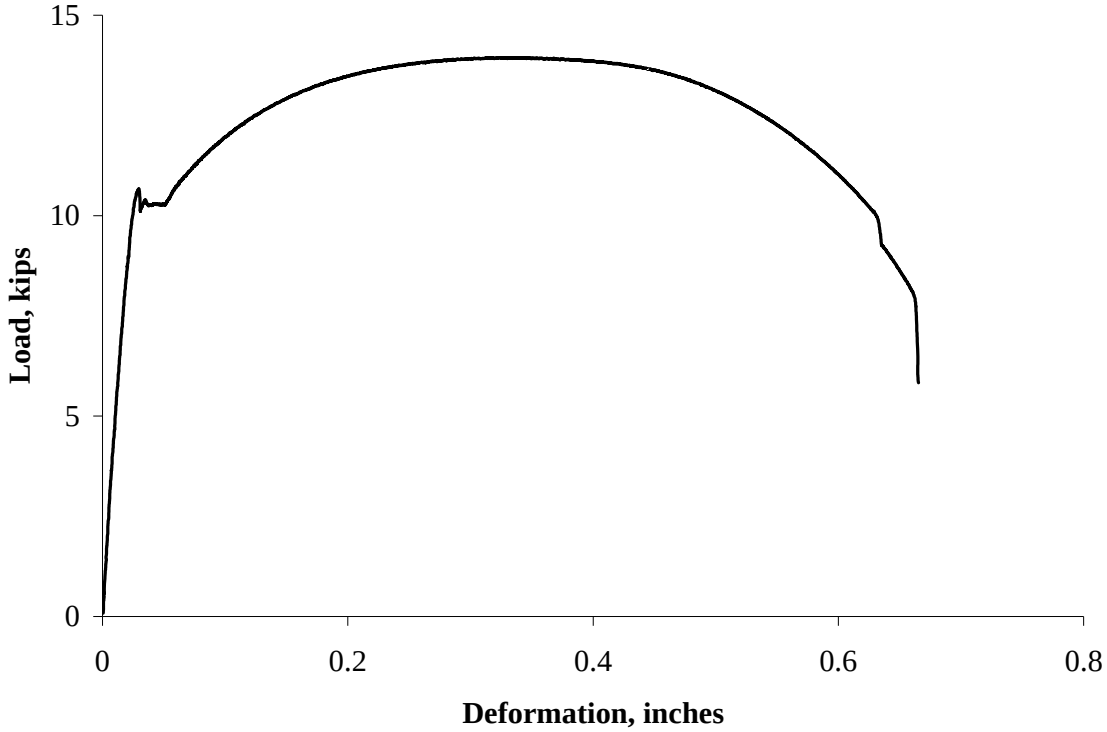

Figure C.2.1 – Load-Deformation Curve for Base Metal A572, Test 1

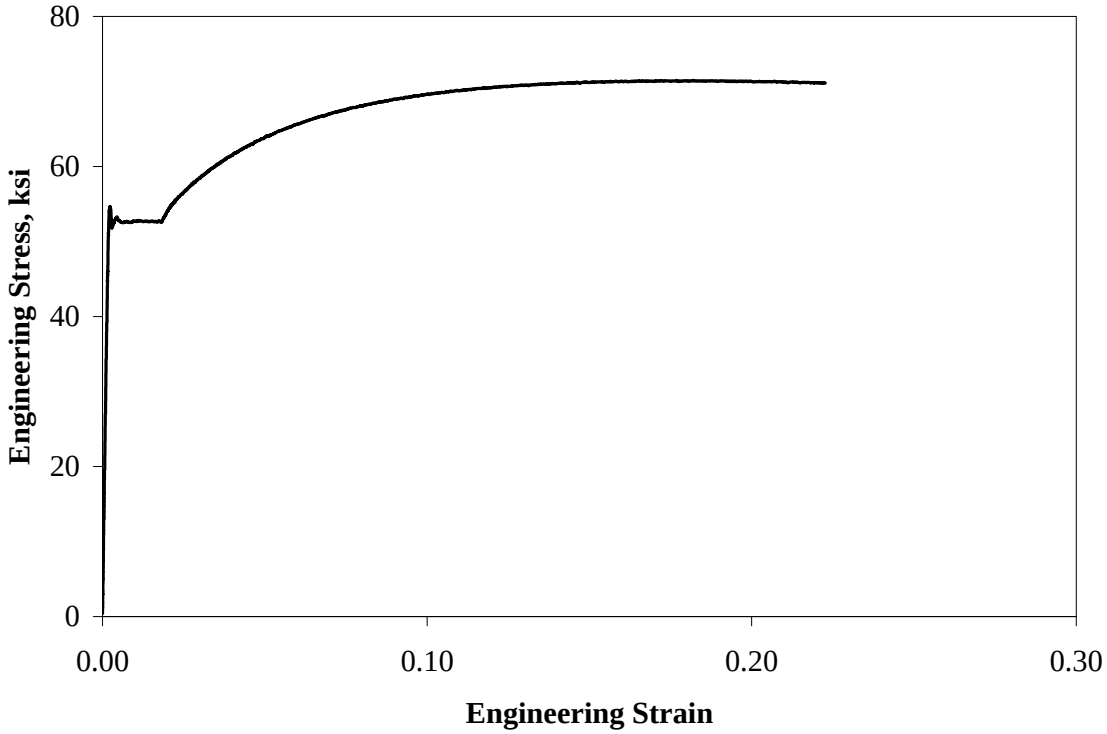

Figure C.2.2 – Stress-Strain Curve for Base Metal A572, Test 1

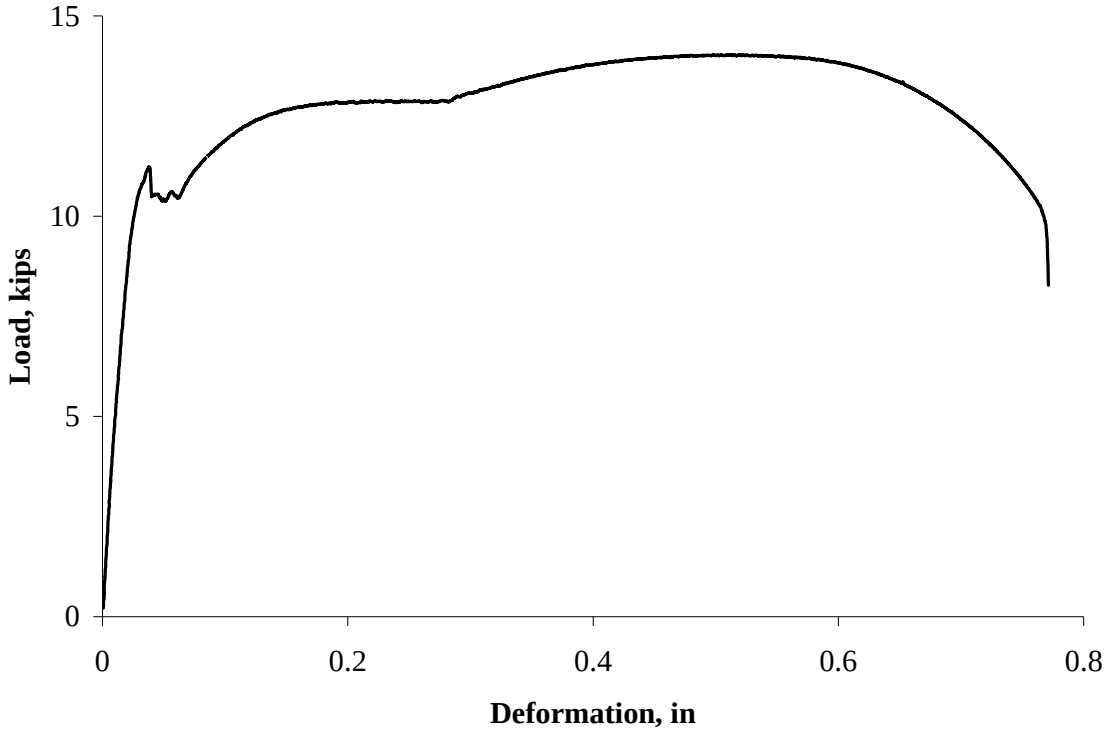

Figure C.2.3 – Load-Deformation Curve for Base Metal A572, Test 2

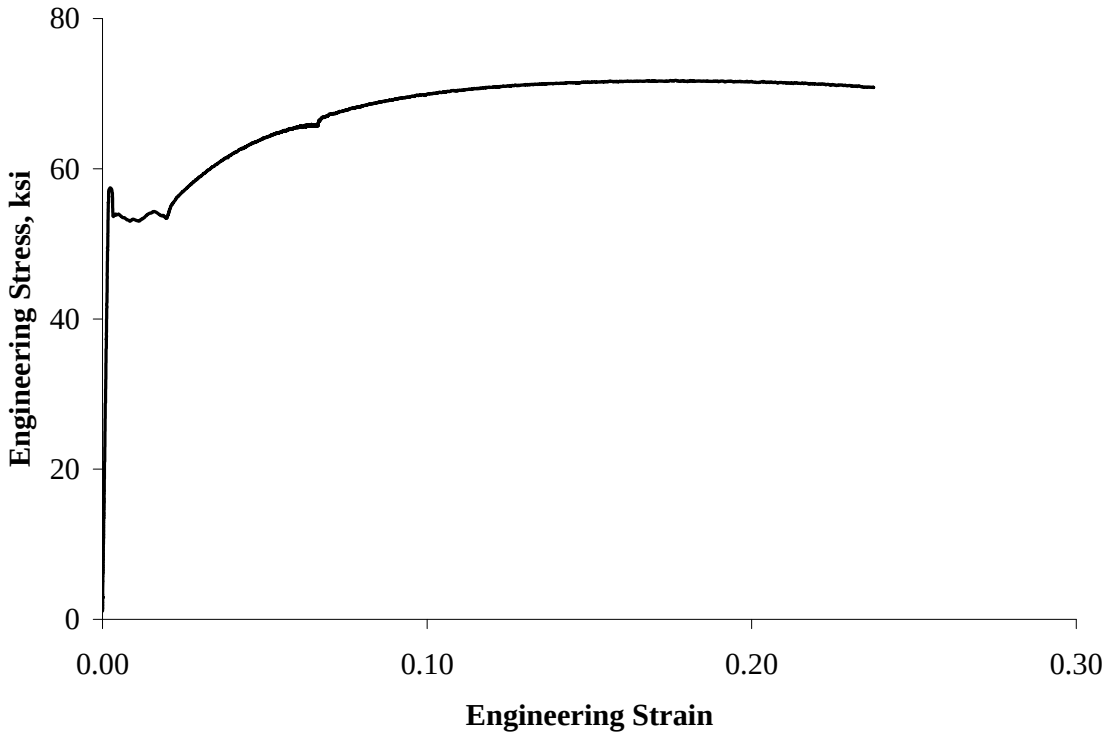

Figure C.2.4 – Stress-Strain Curve for Base Metal A572, Test 2

C.3 CHARPY V-NOTCH IMPACT

Table C.3.1 – Data from Charpy V-Notch Impact Tests

(ASTM A 370-06; 10x10x55 mm size)

Weld Classification	Temperature (°F)	Energy Absorbed (ft-lbs)	
		Test 1	Test 2
E70T-7	-20	5.5	6
	70	19	18
	212	41	41
E70T7-K2	-20	30	23
	70	56	62
	212	88	88

C.4 SPECTROCHEMICAL ANALYSIS

Table C.4.1 – Data from Spectrochemical Analysis (reported as weight percent)

Element	E70T-7	E70T7-K2
Aluminum (Al)	1.74	1.16
Carbon (C)	0.33	0.08
Chromium (Cr)	0.02	0.03
Copper (Cu)	0.02	0.03
Manganese (Mn)	0.37	1.27
Molybdenum (Mo)	0.01	0.02
Nickel (Ni)	0.01	1.68
Phosphorus (P)	0.006	0.009
Silicon (Si)	0.08	0.24
Sulfur (S)	0.005	0.005
Titanium (Ti)	<0.005	<0.005
Vanadium (V)	<0.005	<0.005

Appendix D

Tension Test Load-Deformation Curves

NOTE: Pots A, B, C, and D refer to the following diagram

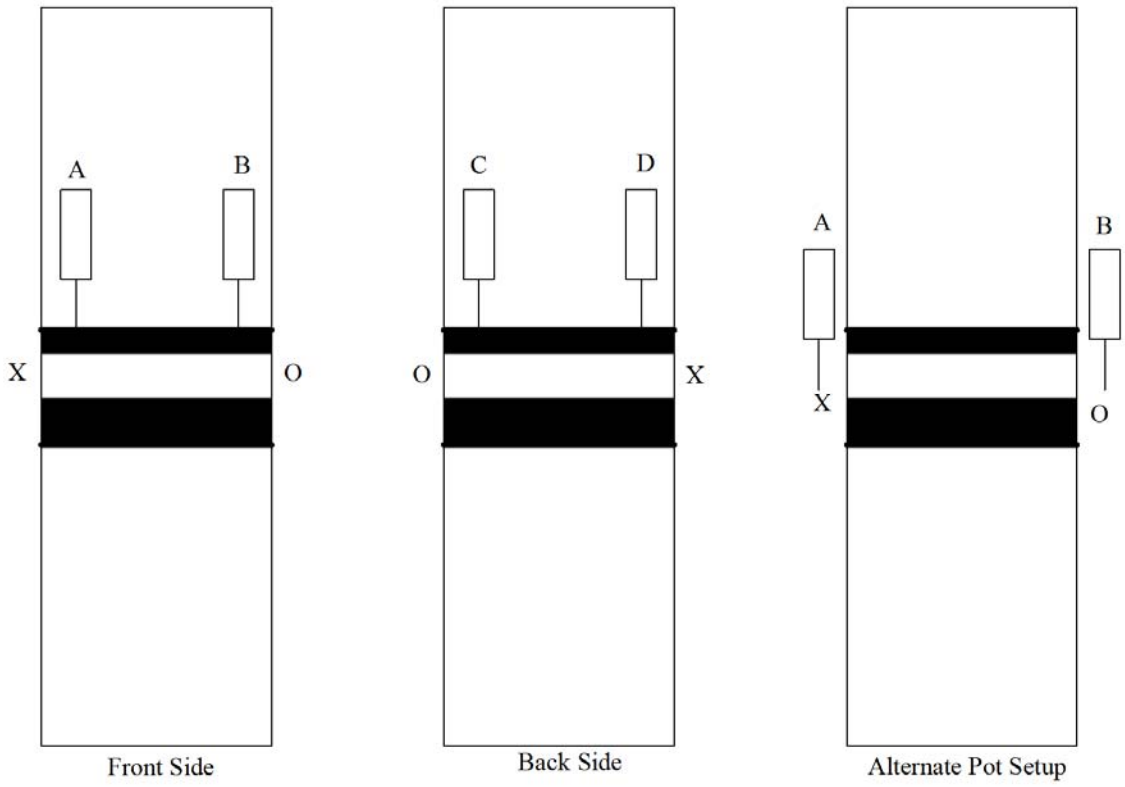

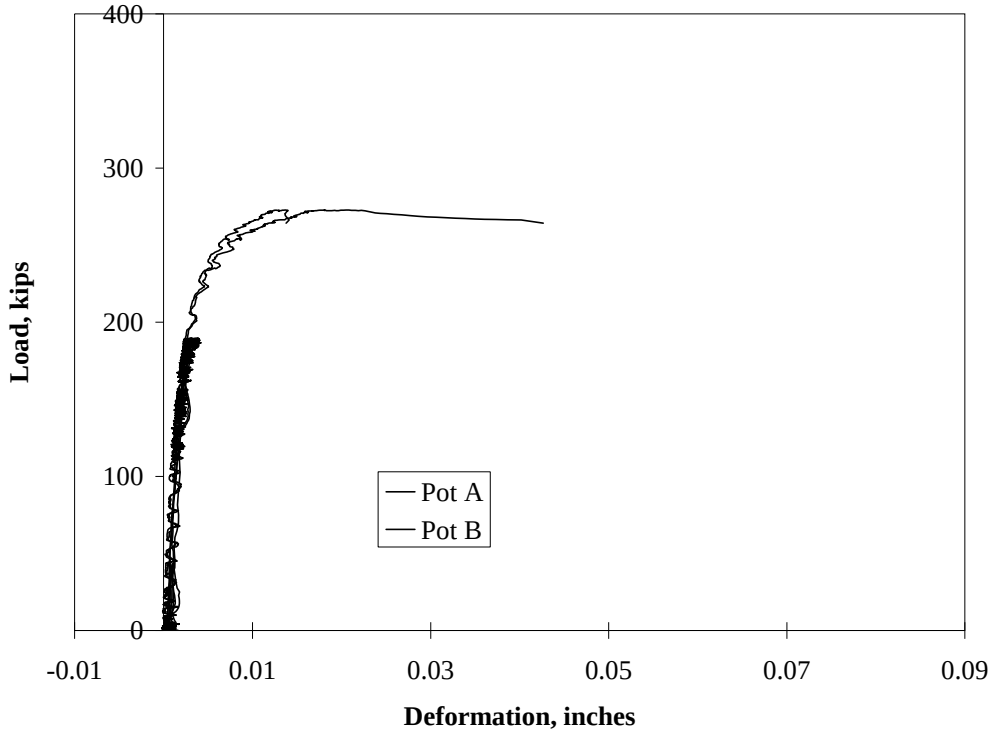

Figure D.1 – Test #1, T125_A12_1[1] (Alternate Setup)

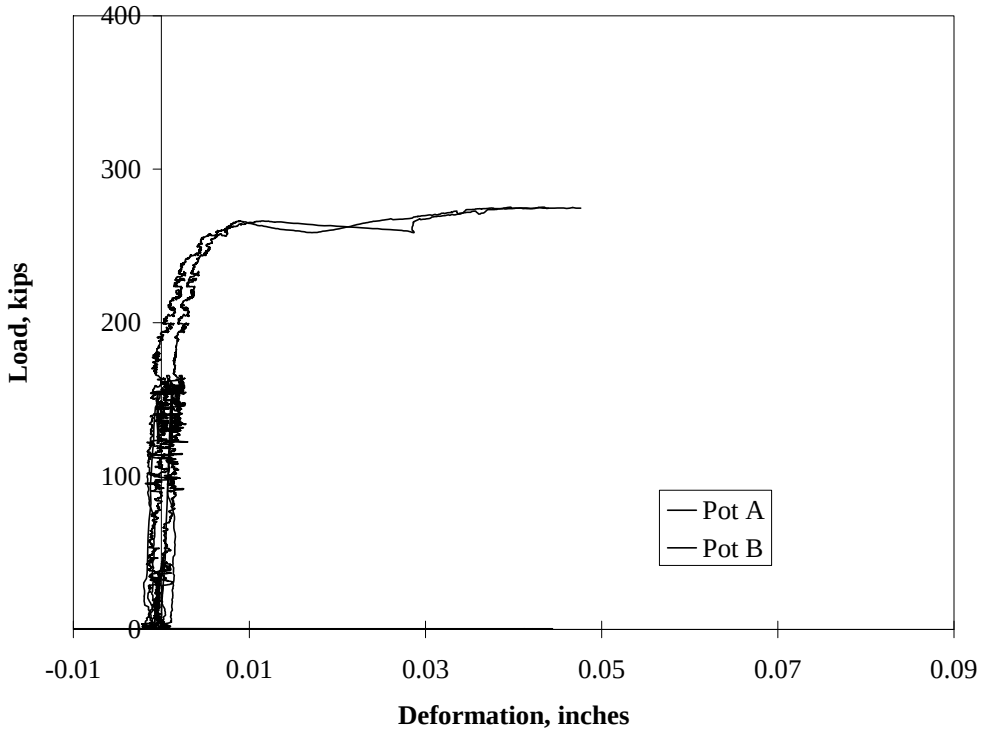

Figure D.2 – Test #2, T125_A12_2 (Alternate Setup)

[1] For specimen nomenclature details, refer to Appendix B, page B-2

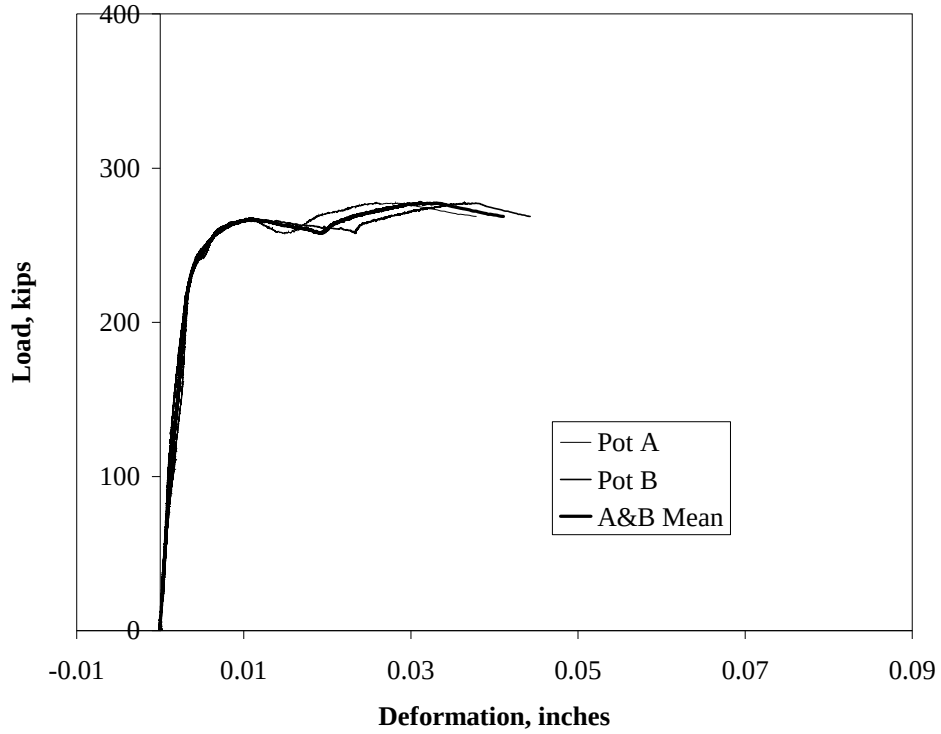

Figure D.3 – Test #3: T125_A12_3, Front Side Weld (1st Fracture)

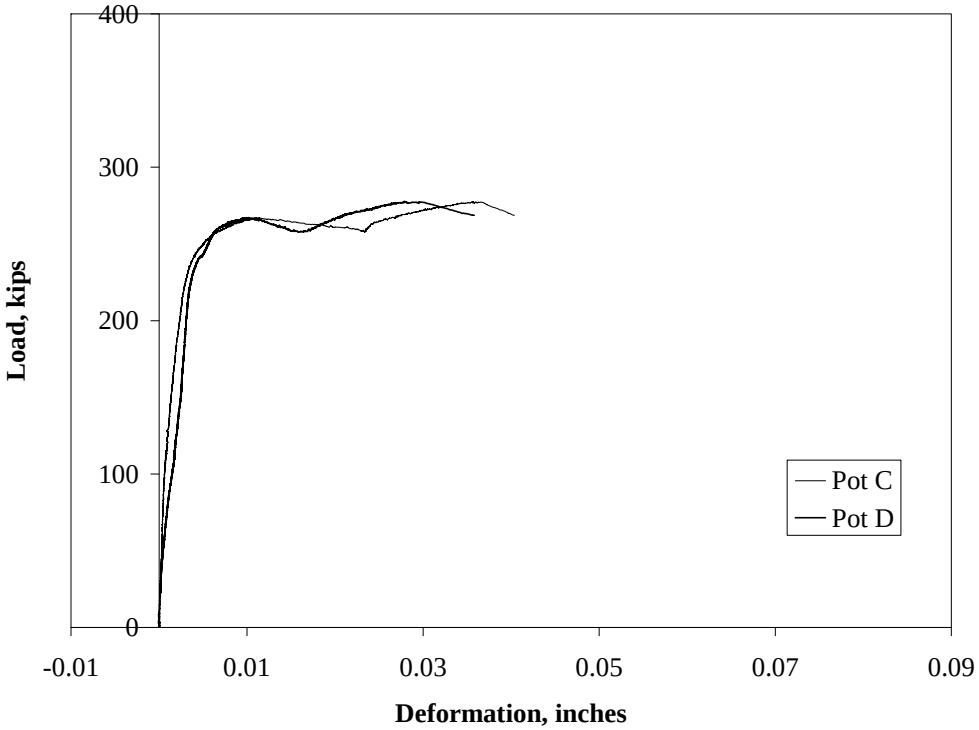

Figure D.4 – Test #3: T125_A12_3, Back Side Weld (2nd Fracture)

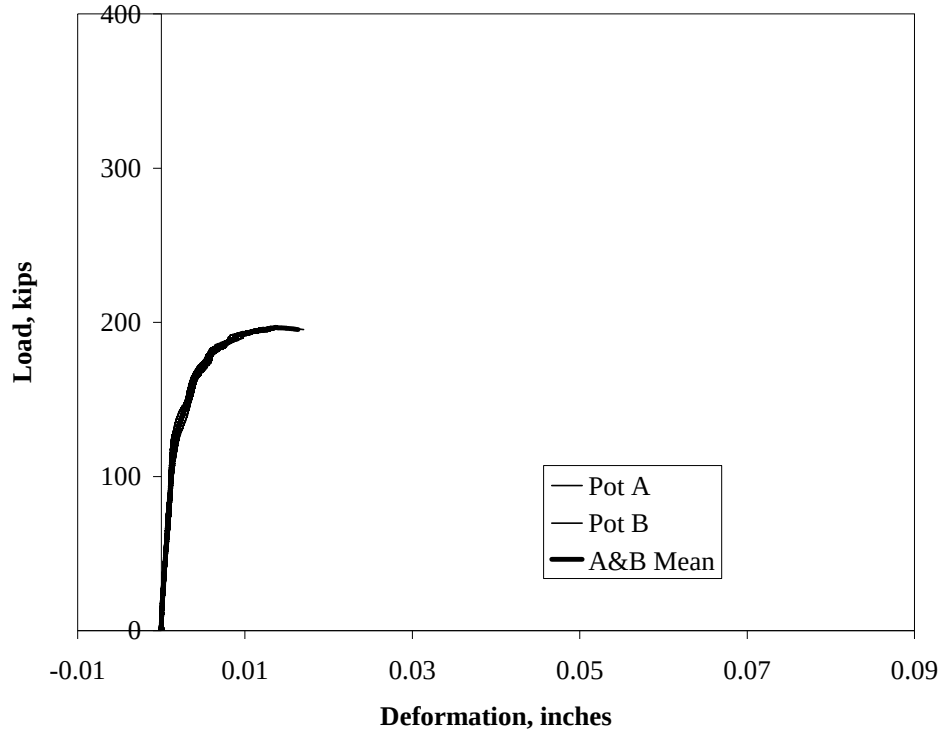

Figure D.5 – Test #4, T125_A516_1, Front Side Weld (1st Fracture)

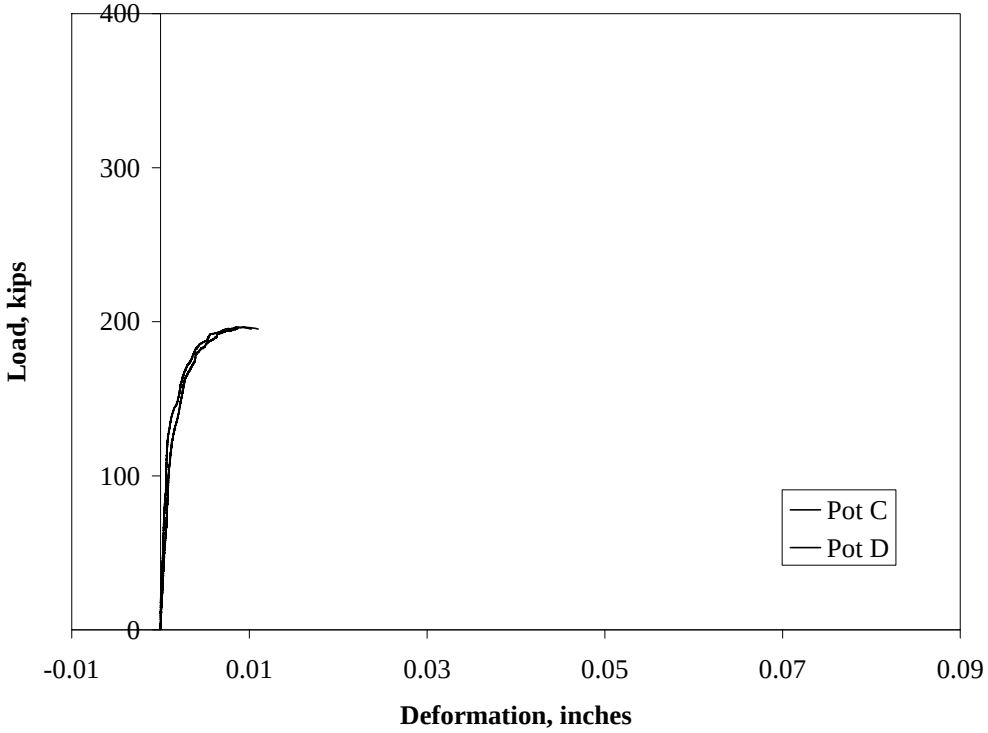

Figure D.6 – Test #4, T125_A516_1, Back Side Weld (2nd Fracture)

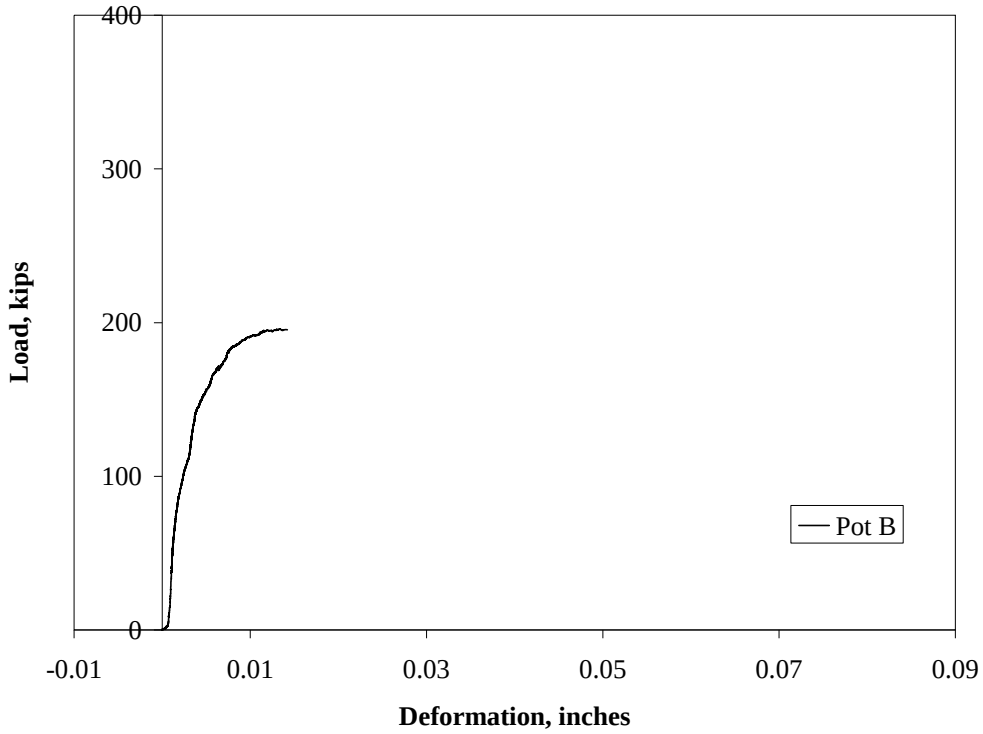

Figure D.7 – Test #5, T125_A516_2, Front Side Weld (2nd Fracture)

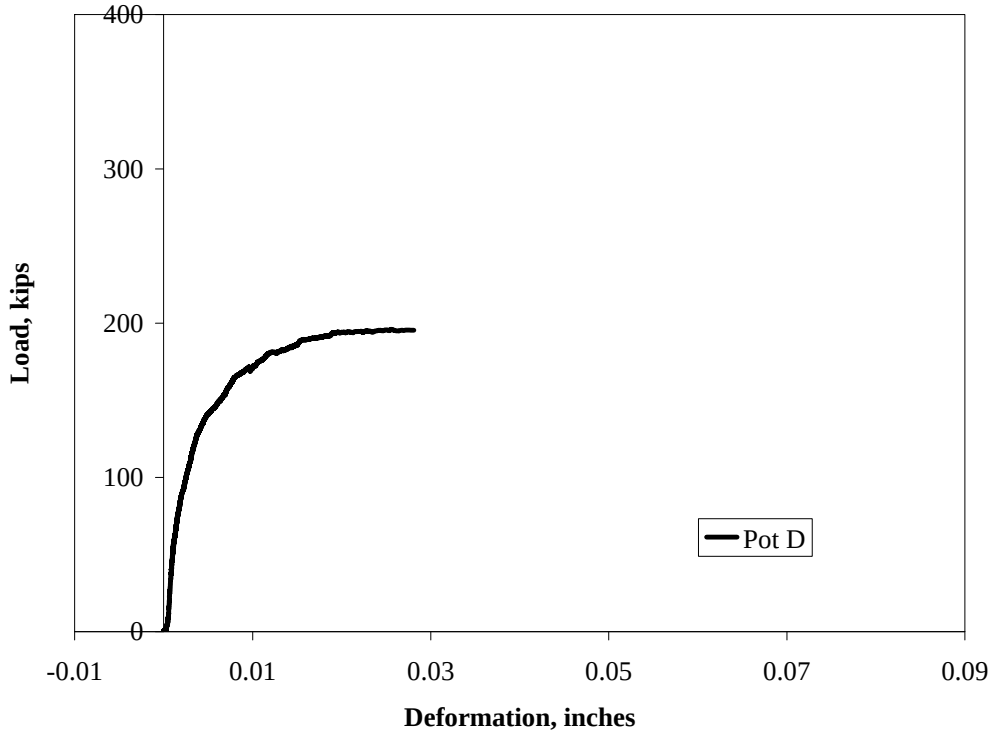

Figure D.8 – Test #5, T125_A516_2, Back Side Weld (1st Fracture)

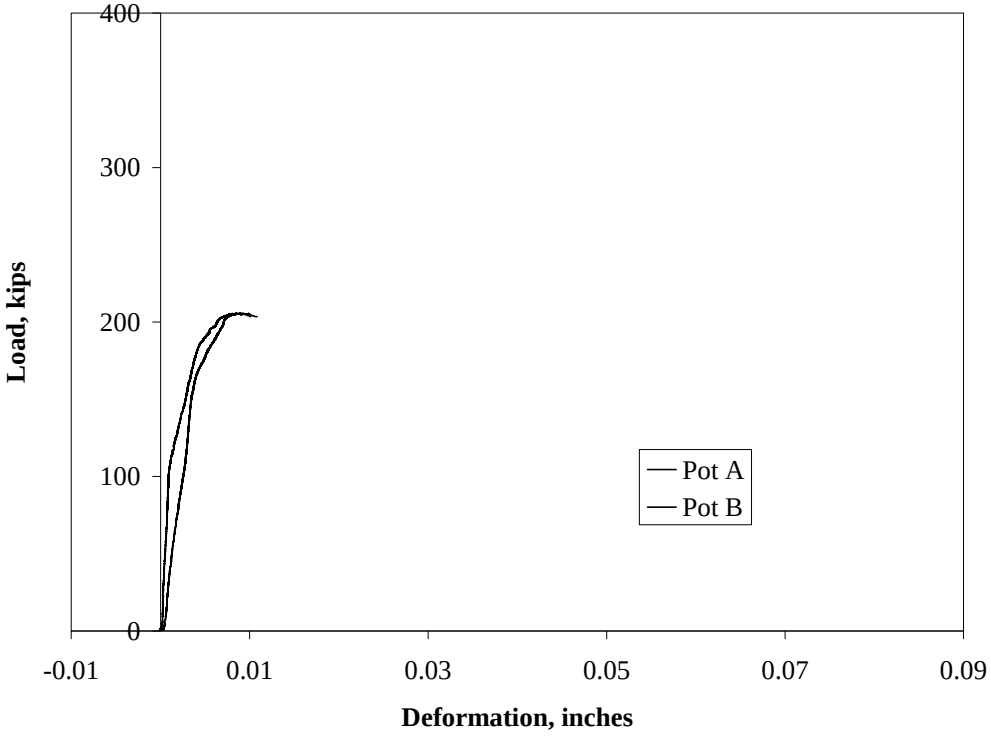

Figure D.9 – Test #6, T125_A516_3, Front Side Weld (2nd Fracture)

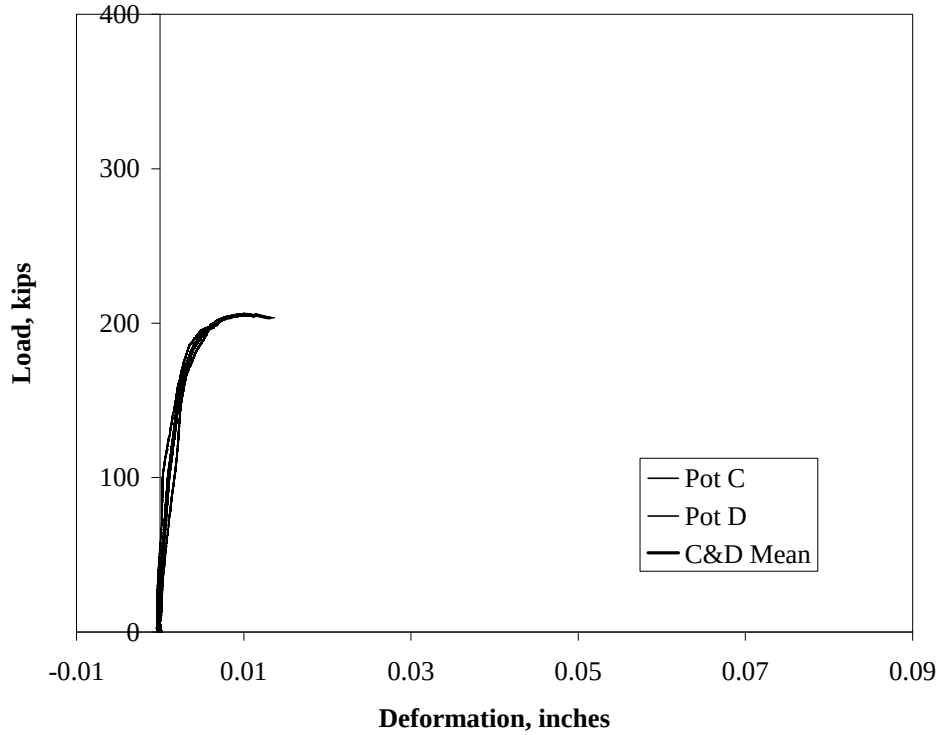

Figure D.9 – Test #6, T125_A516_3, Back Side Weld (1st Fracture)

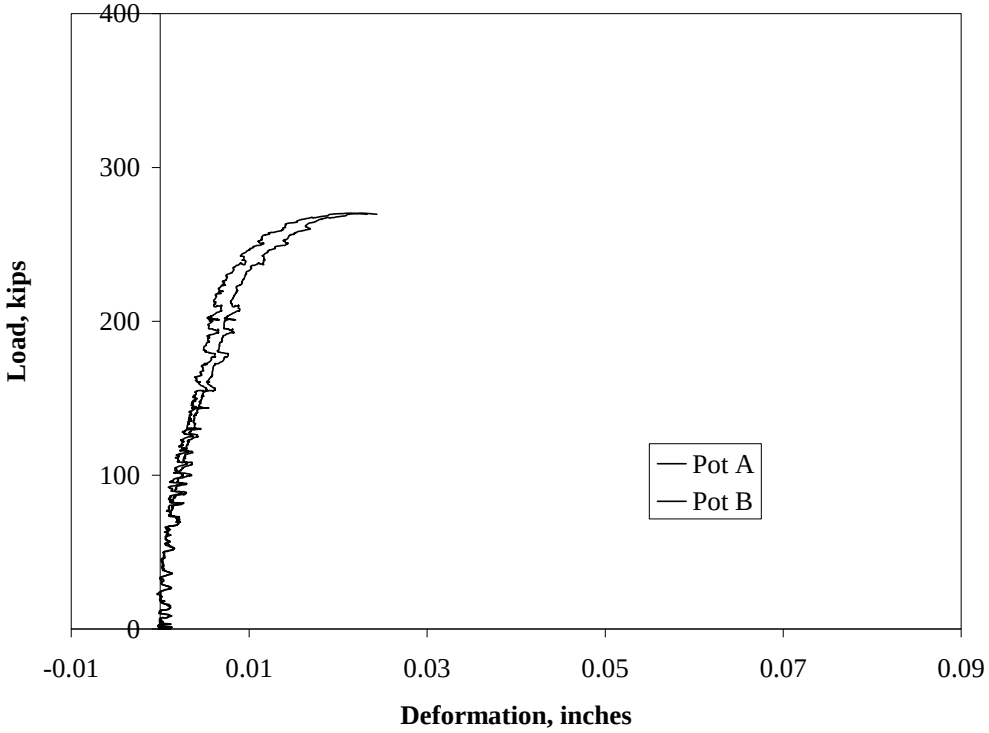

Figure D.10 – Test #7, T250_A12_1 (Alternate Setup)

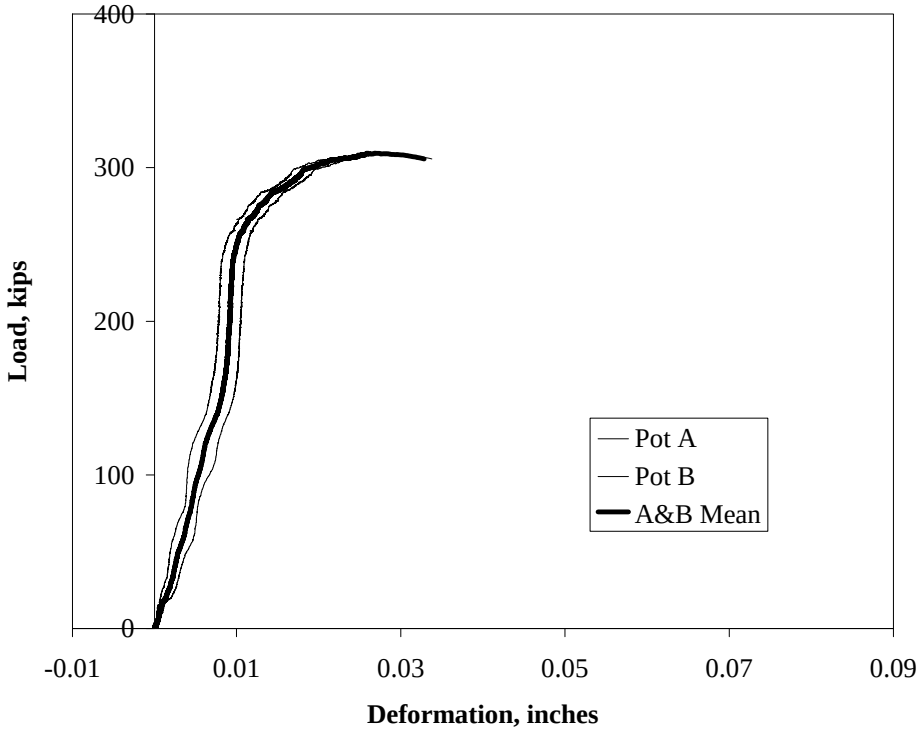

Figure D.11 – Test #8, T250_A12_2, Front Side Weld (1st Fracture)

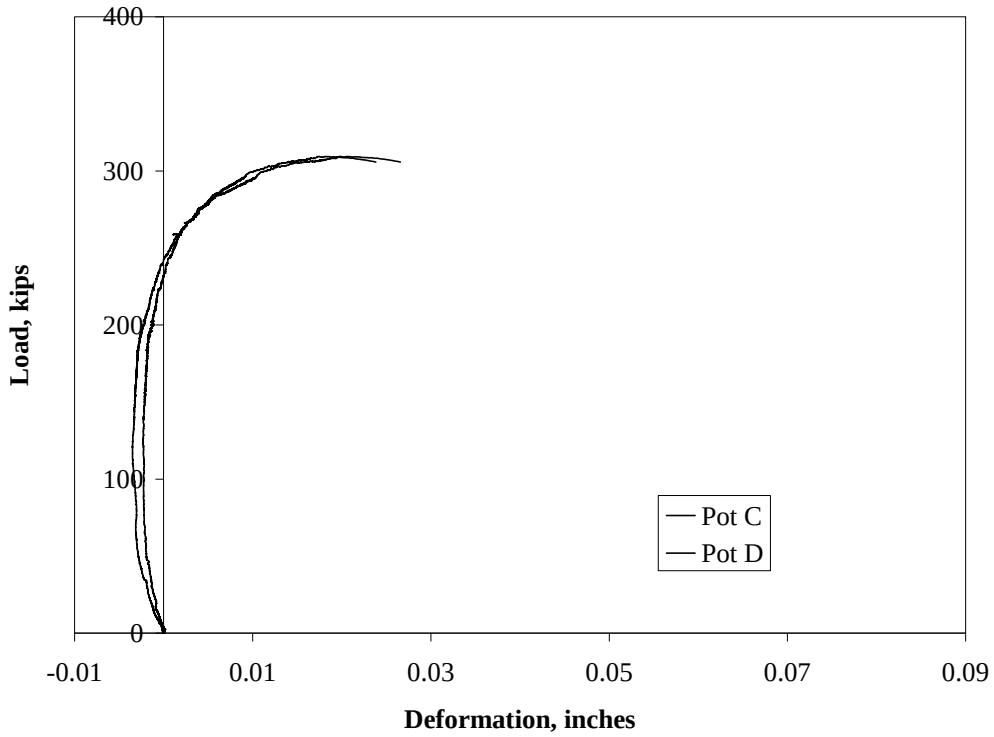

Figure D.12 – Test #8, T250_A12_2, Back Side Weld (2nd Fracture)

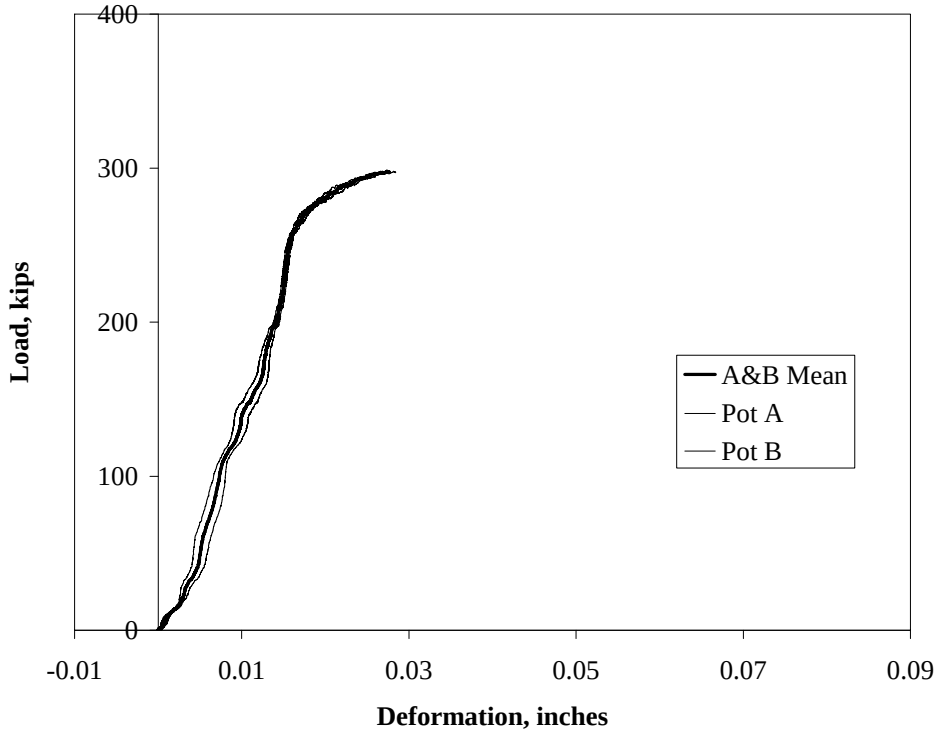

Figure D.13 – Test #9, T250_A12_3, Front Side Weld (1st Fracture)

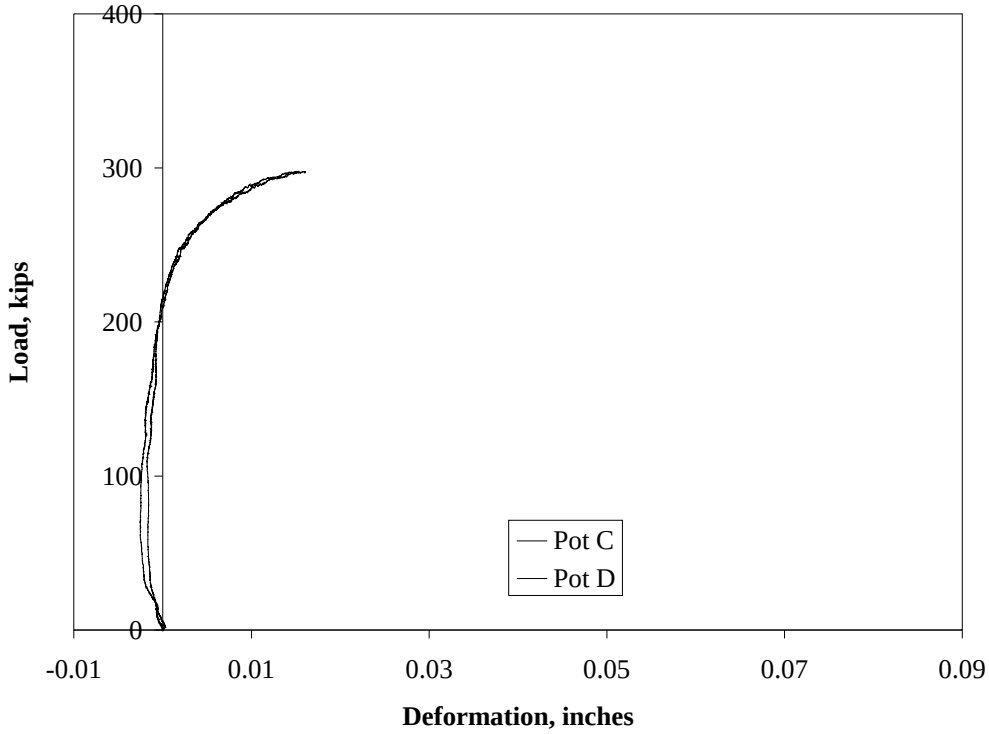

Figure D.14 – Test #9, T250_A12_3, Back Side Weld (2nd Fracture

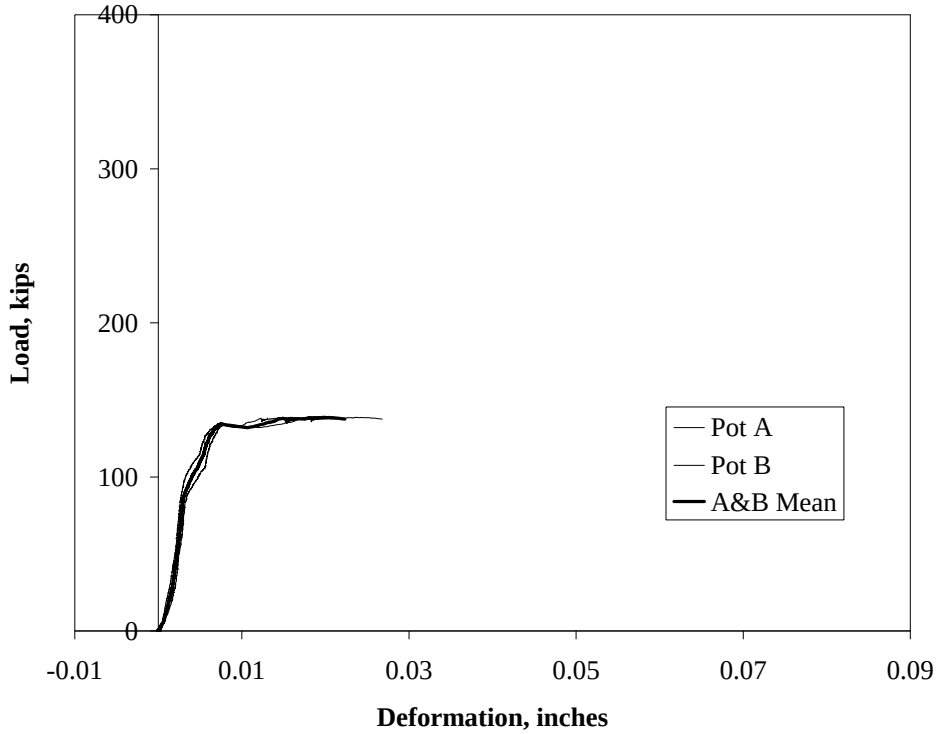

Figure D.15 – Test #10, T250_A516_1, Front Side Weld (1st Fracture)

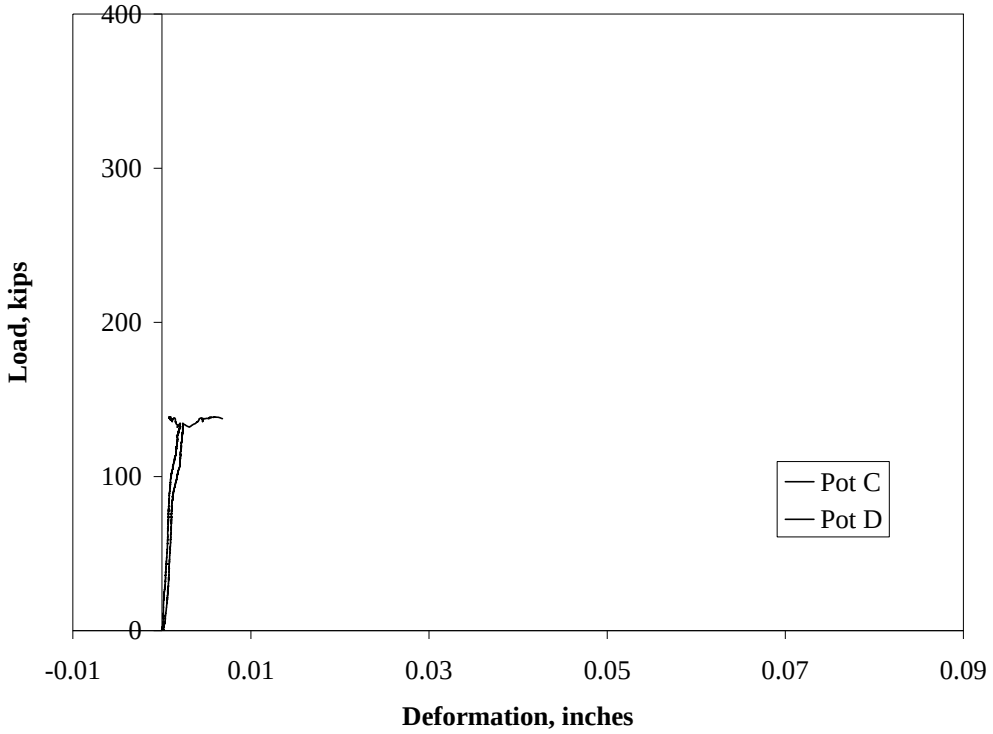

Figure D.16 – Test #10, T250_A516_1, Back Side Weld (2nd Fracture)

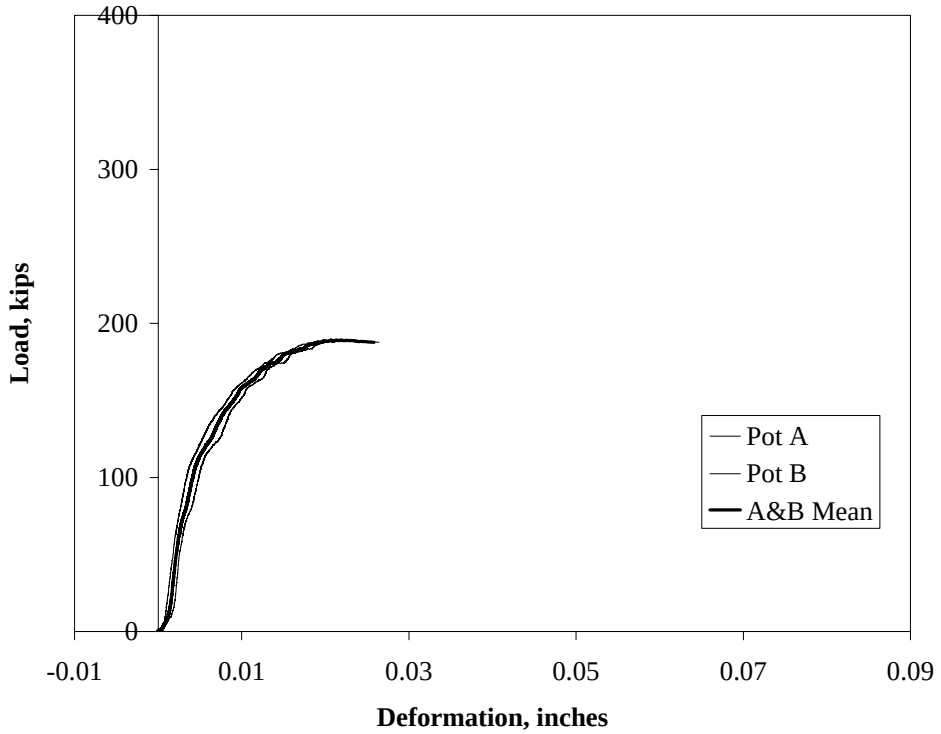

Figure D.17 – Test #11, T250_A516_2, Front Side Weld (1st Fracture)

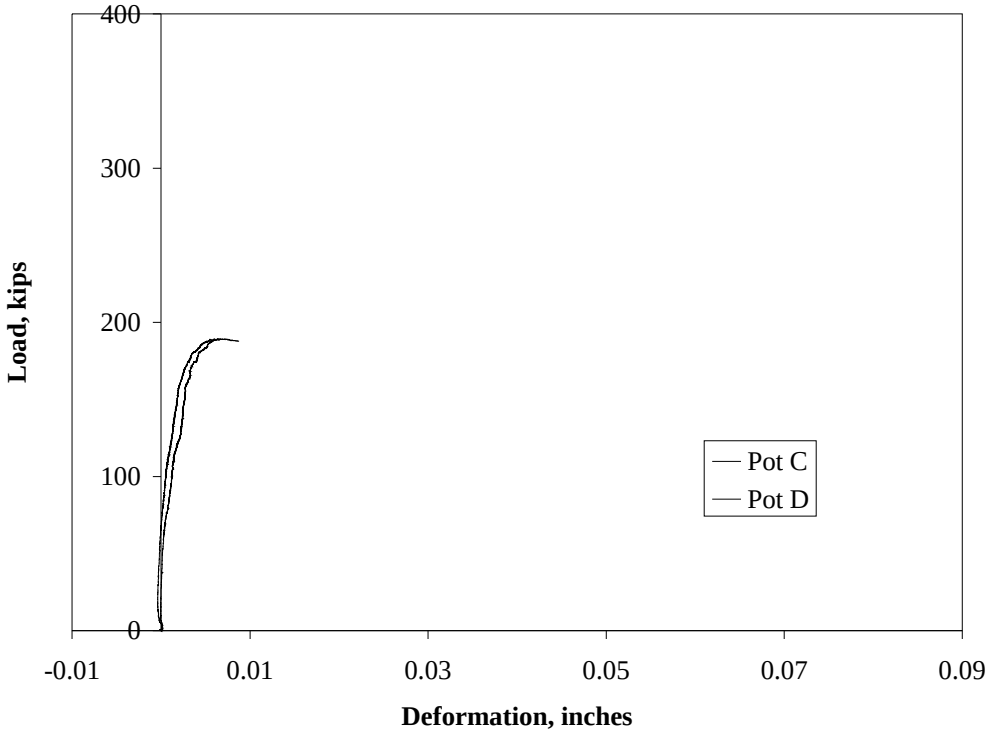

Figure D.18 – Test #11, T250_A516_2, Back Side Weld (2nd Fracture)

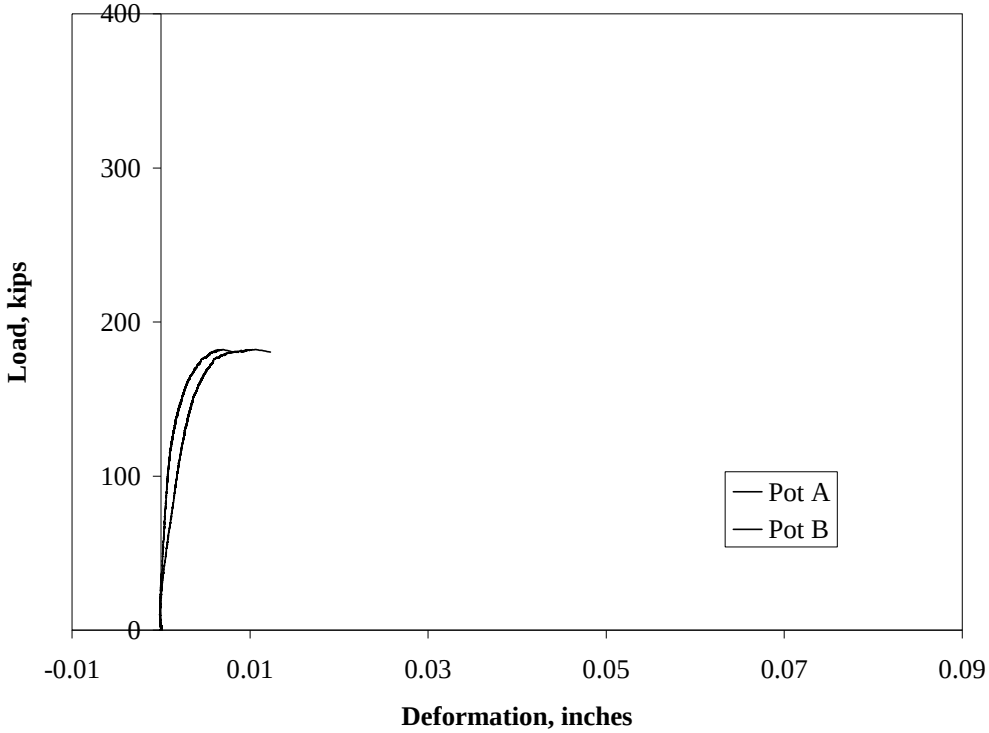

Figure D.19 – Test #12, T250_A516_3, Front Side Weld (2nd Fracture)

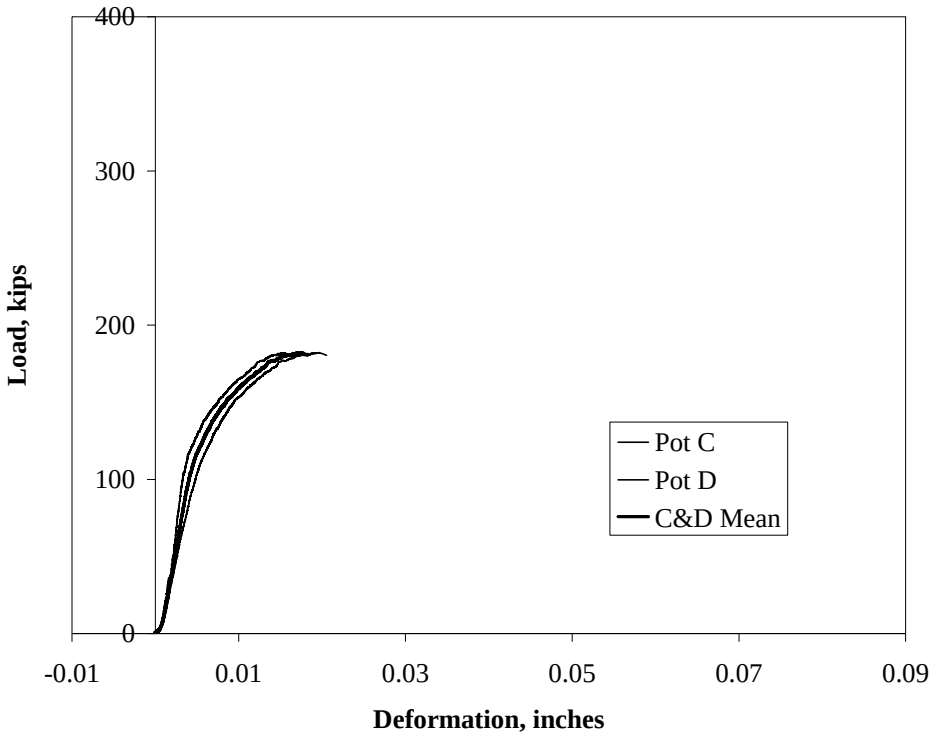

Figure D.20 – Test #12, T250_A516_3, Back Side Weld (1st Fracture)

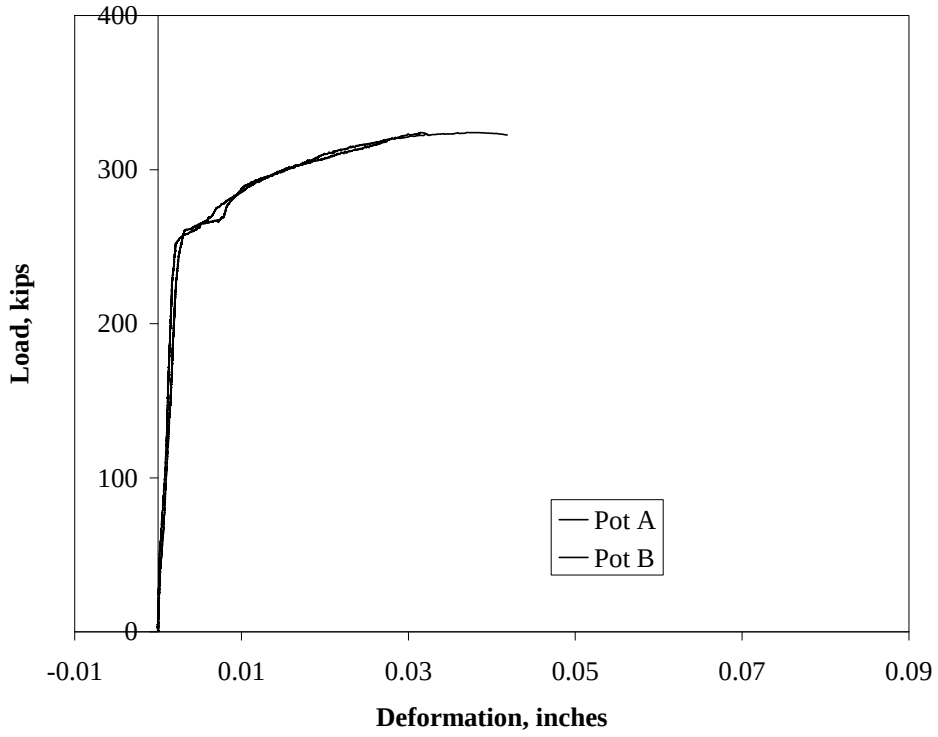

Figure D.21 – Test #13, T125_B12_1, Front Side Weld (2nd Fracture)

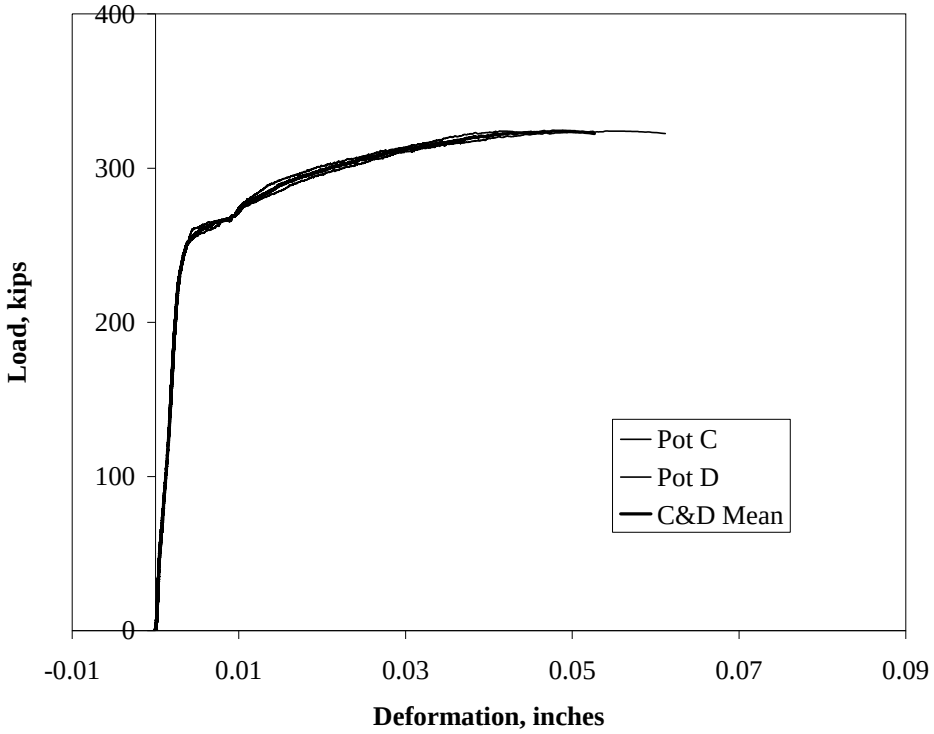

Figure D.22 – Test #13, T125_B12_1, Back Side Weld (1st Fracture)

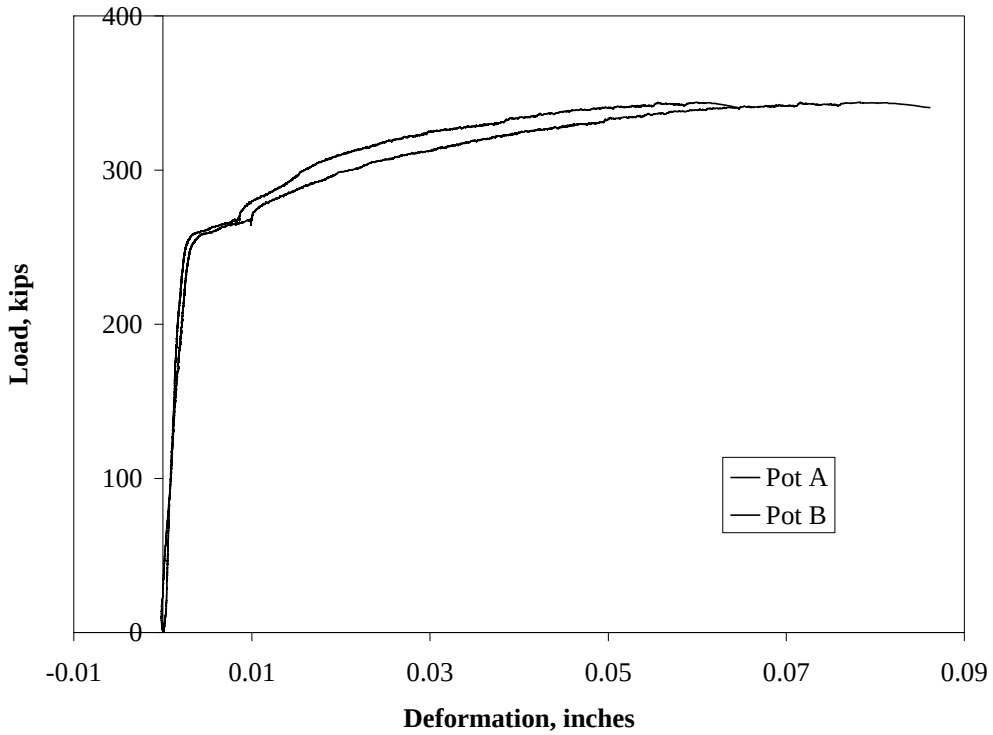

Figure D.23 – Test #14, T125_B12_2, Front Side Weld (2nd Fracture)

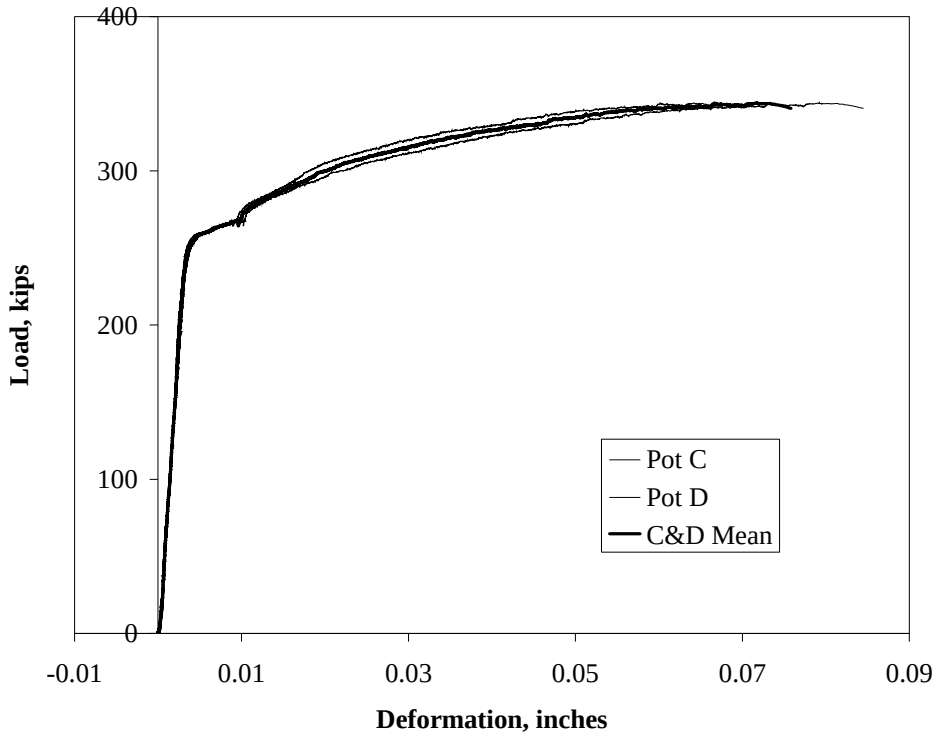

Figure D.24 – Test #14, T125_B12_2, Back Side Weld (1st Fracture)

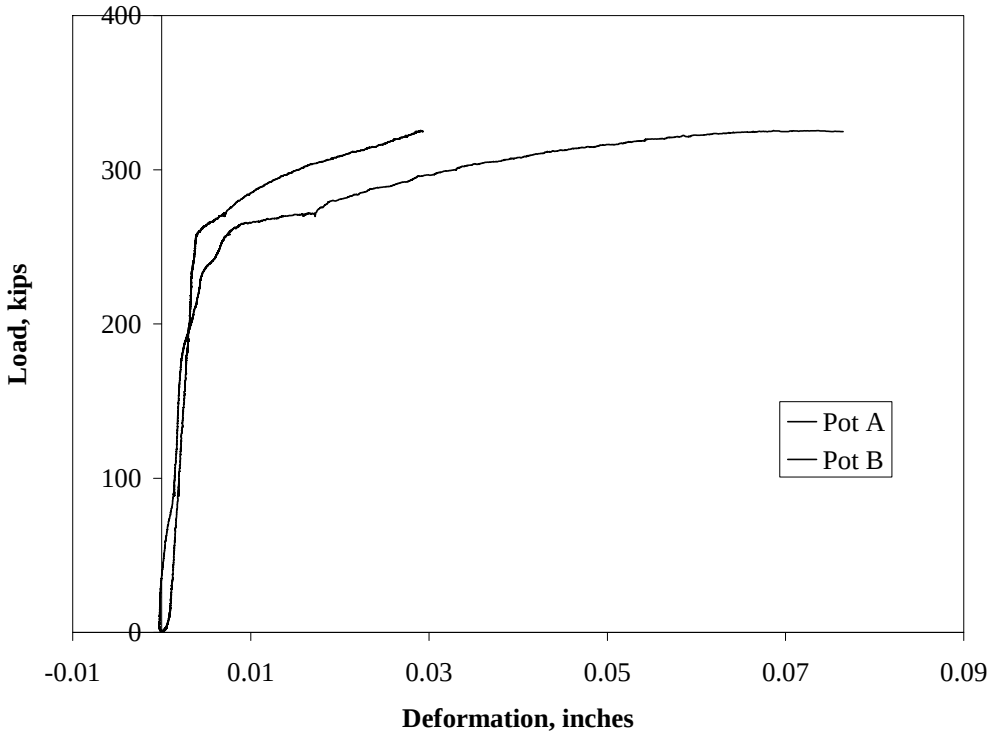

Figure D.25 – Test #15, T125_B12_3, Front Side Weld (2nd Fracture)

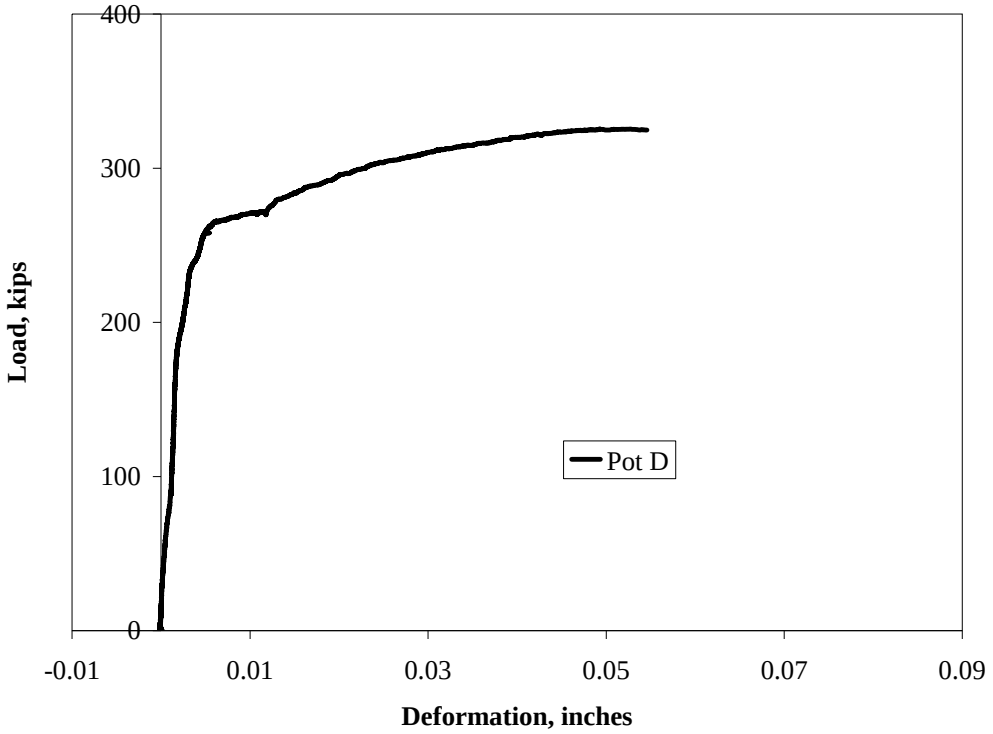

Figure D.26 – Test #15, T125_B12_3, Back Side Weld (1st Fracture)

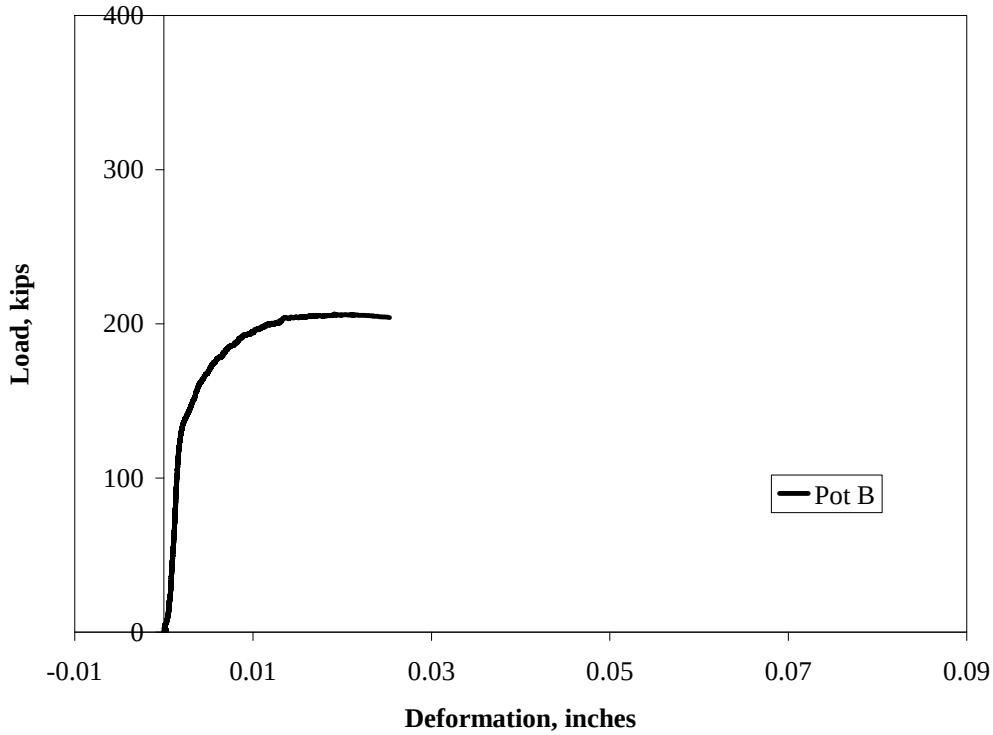

Figure D.27 – Test #16, T125_B516_1, Front Side Weld (1st Fracture)

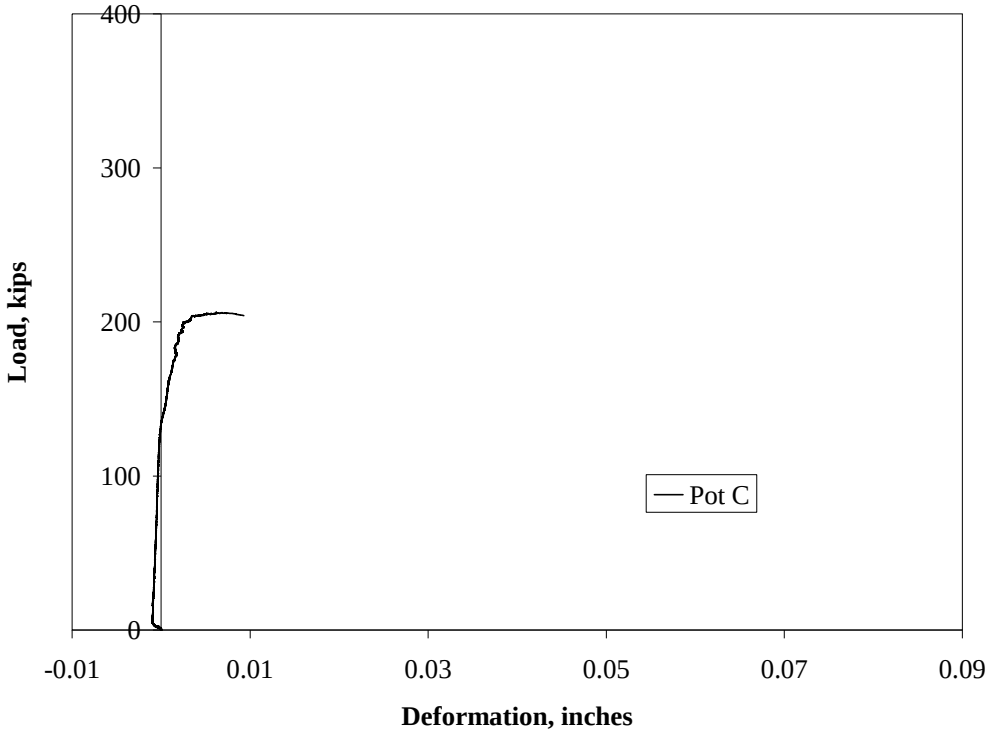

Figure D.28 – Test #16, T125_B516_1, Back Side Weld (2nd Fracture)

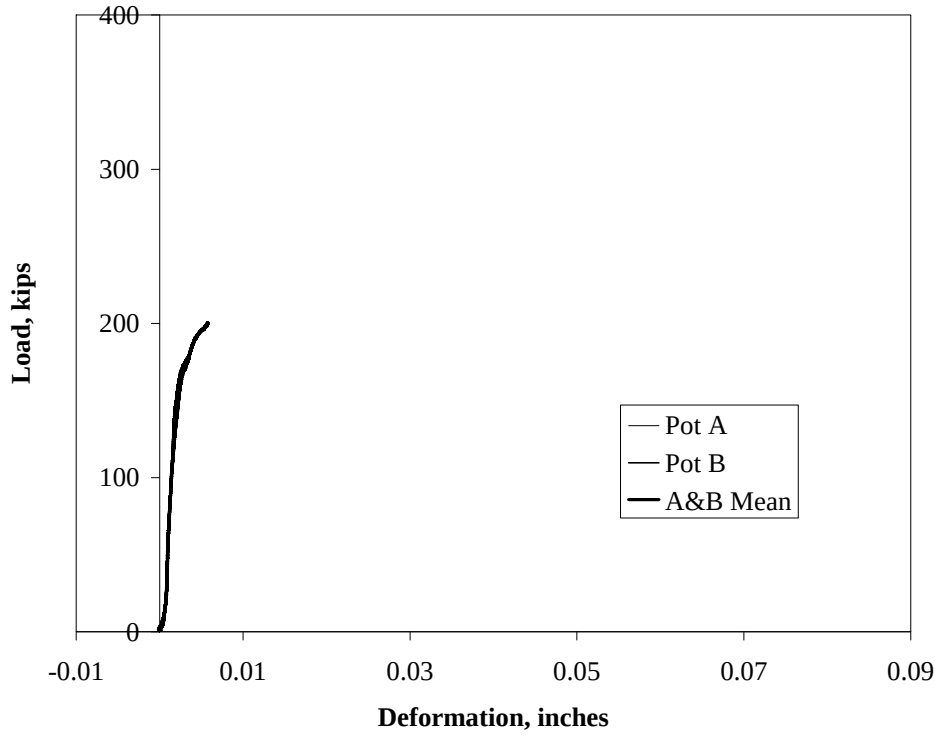

Figure D.29 – Test #17, T125_B516_2, Front Side Weld (1st Fracture)

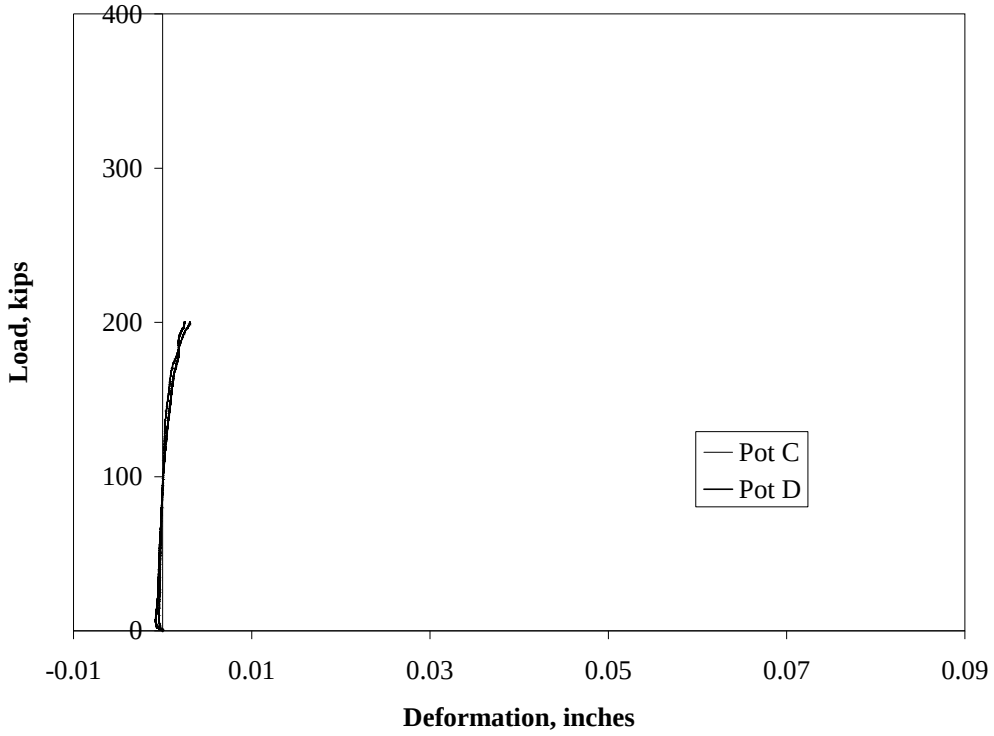

Figure D.30 – Test #17, T125_B516_2, Back Side Weld (2nd Fracture)

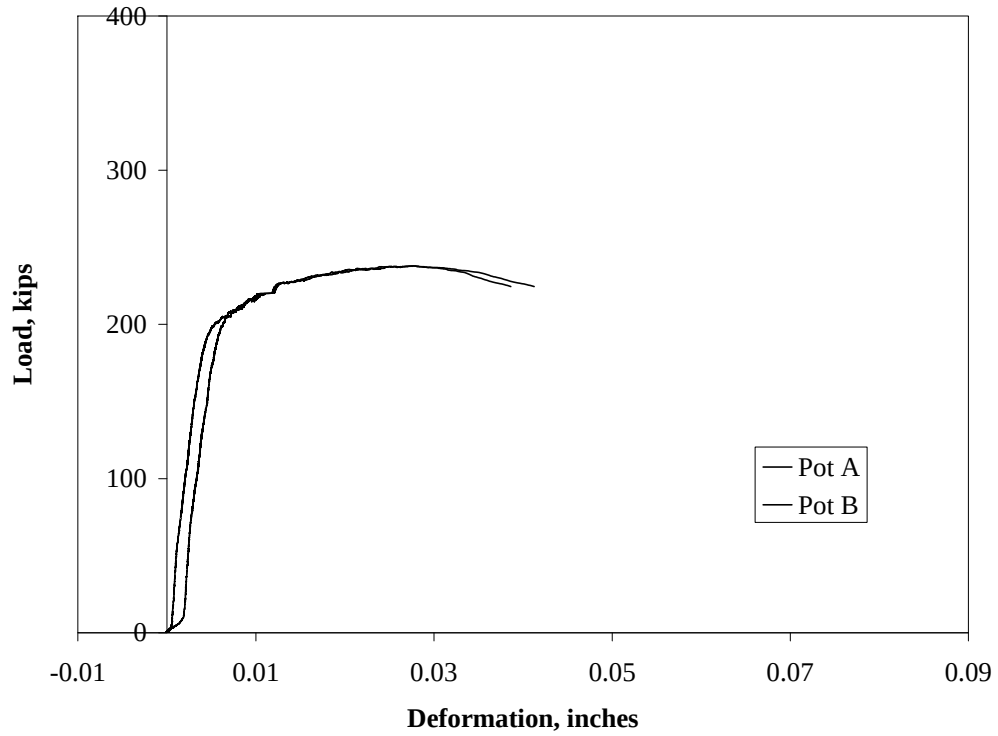

Figure D.31 – Test #18, T125_B516_3, Front Side Weld (2nd Fracture)

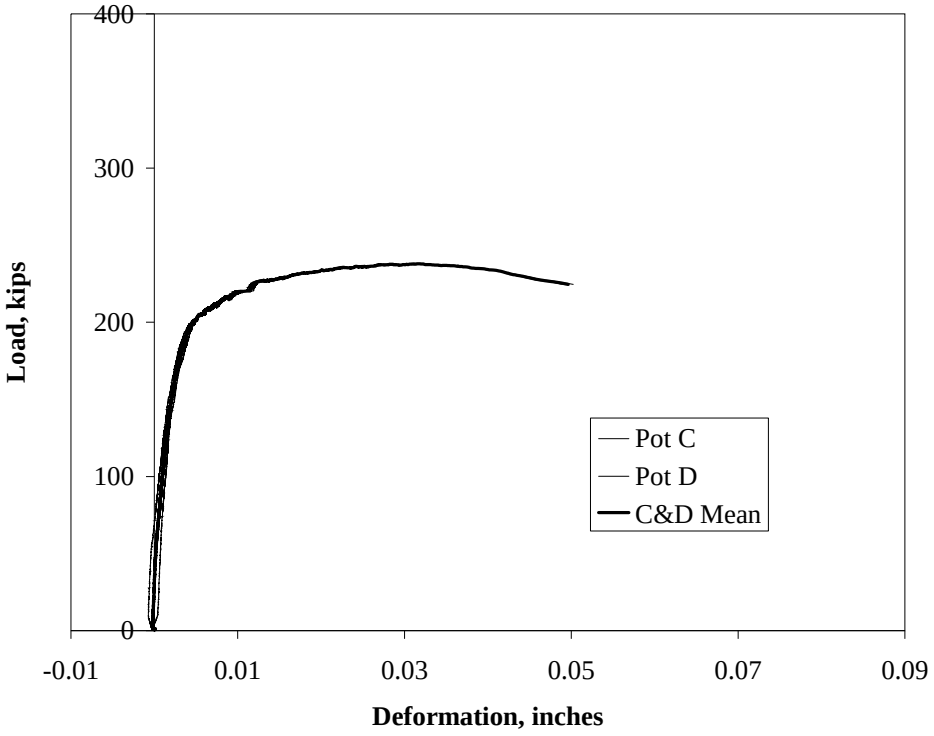

Figure D.32 – Test #18, T125_B516_3, Back Side Weld (1st Fracture)

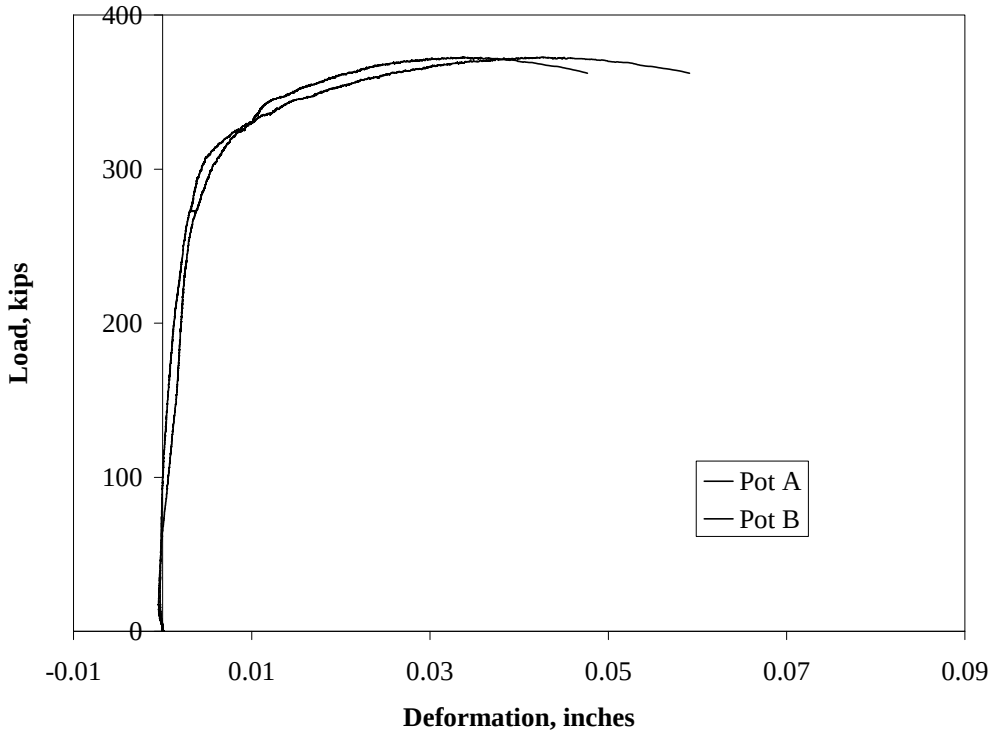

Figure D.33 – Test #19, T250_B12_1, Front Side Weld (2nd Fracture)

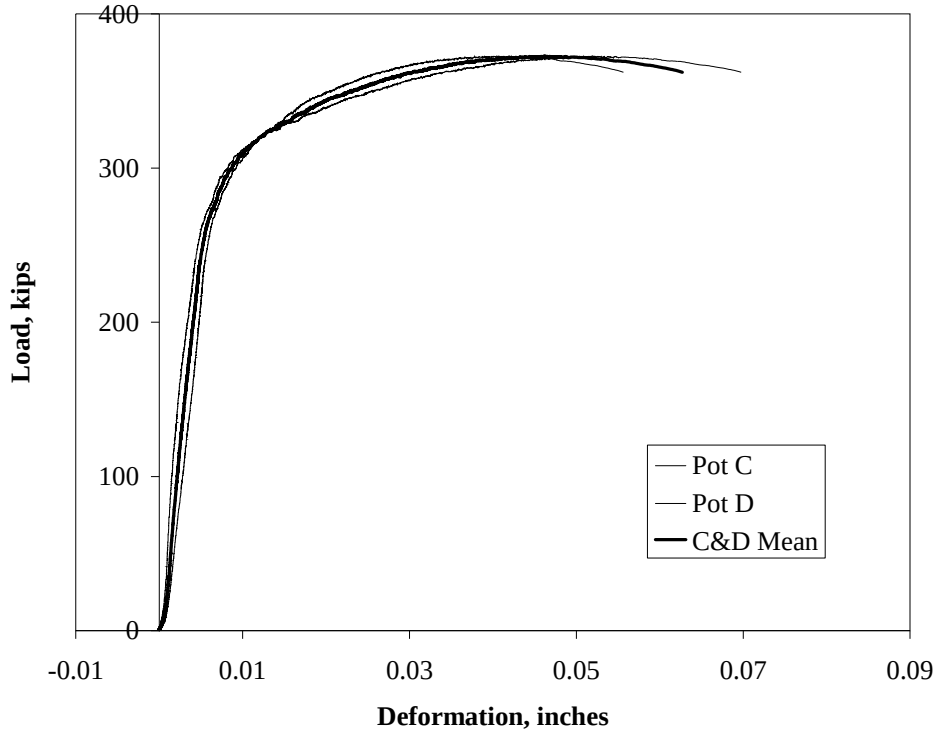

Figure D.34 – Test #19, T250_B12_1, Back Side Weld (1st Fracture)

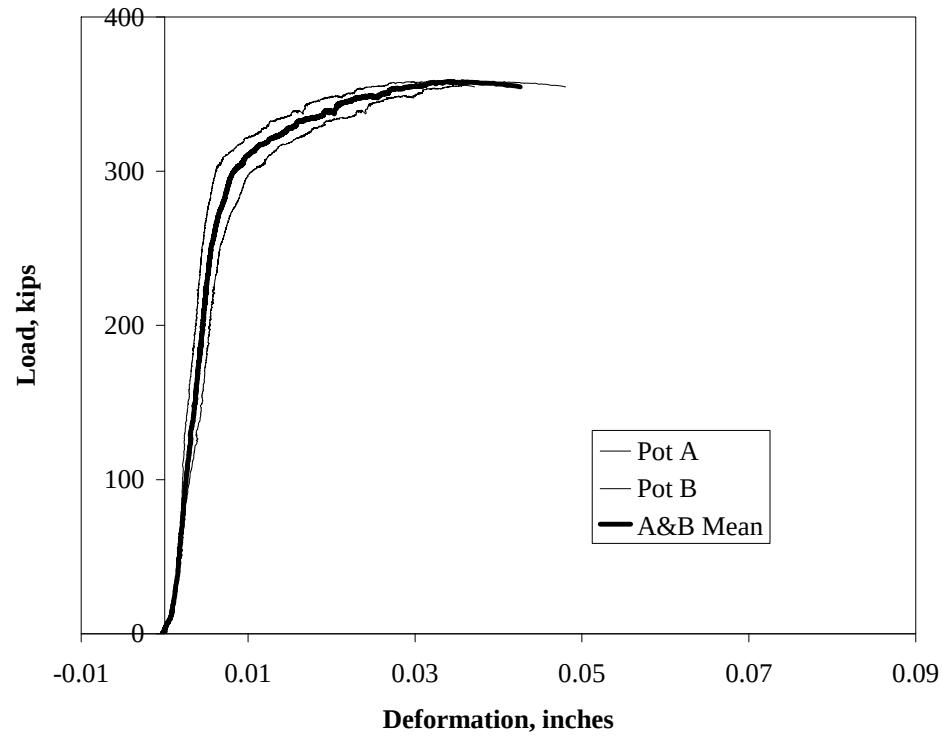

Figure D.35 – Test #20, T250_B12_2, Front Side Weld (1st Fracture)

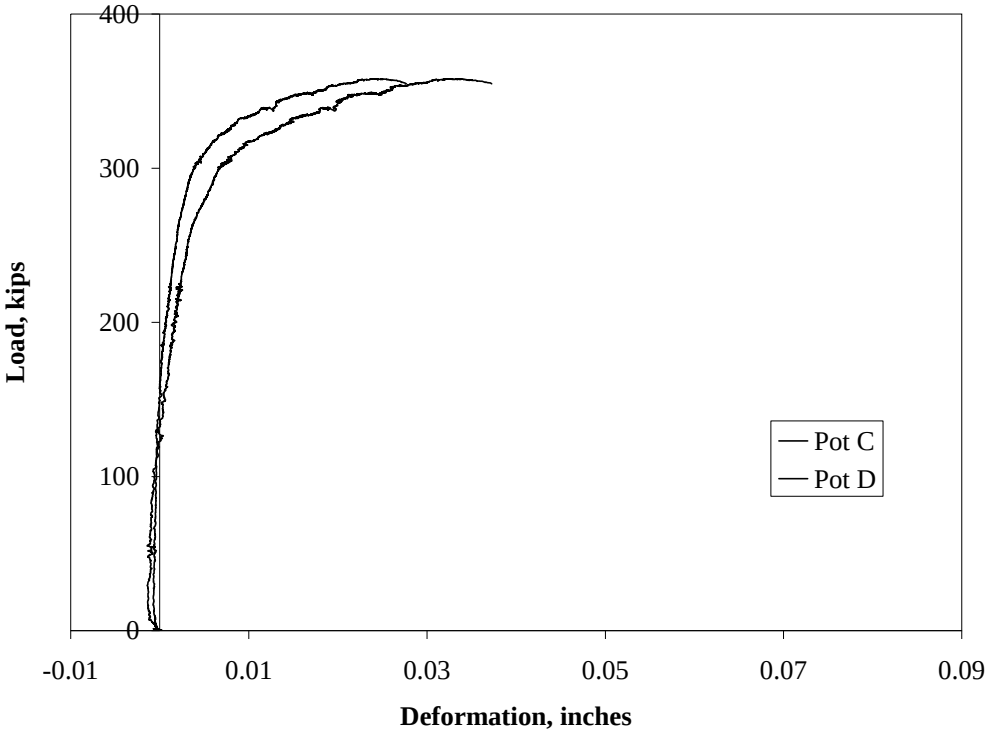

Figure D.36 – Test #20, T250_B12_2, Back Side Weld (2nd Fracture)

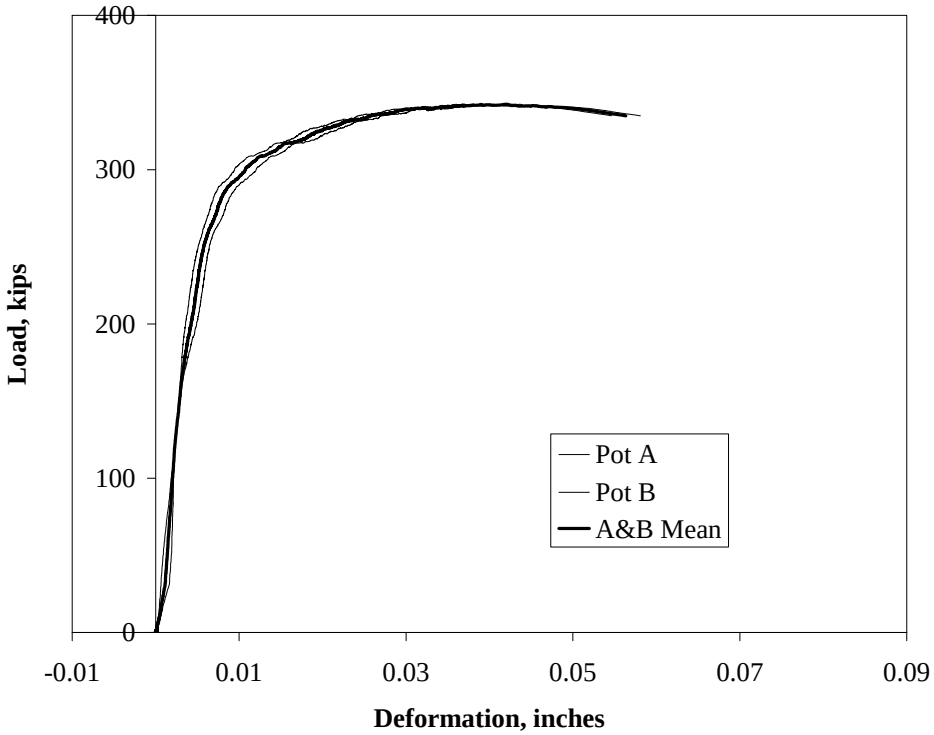

Figure D.37 – Test #21, T250_B12_3, Front Side Weld (1st Fracture)

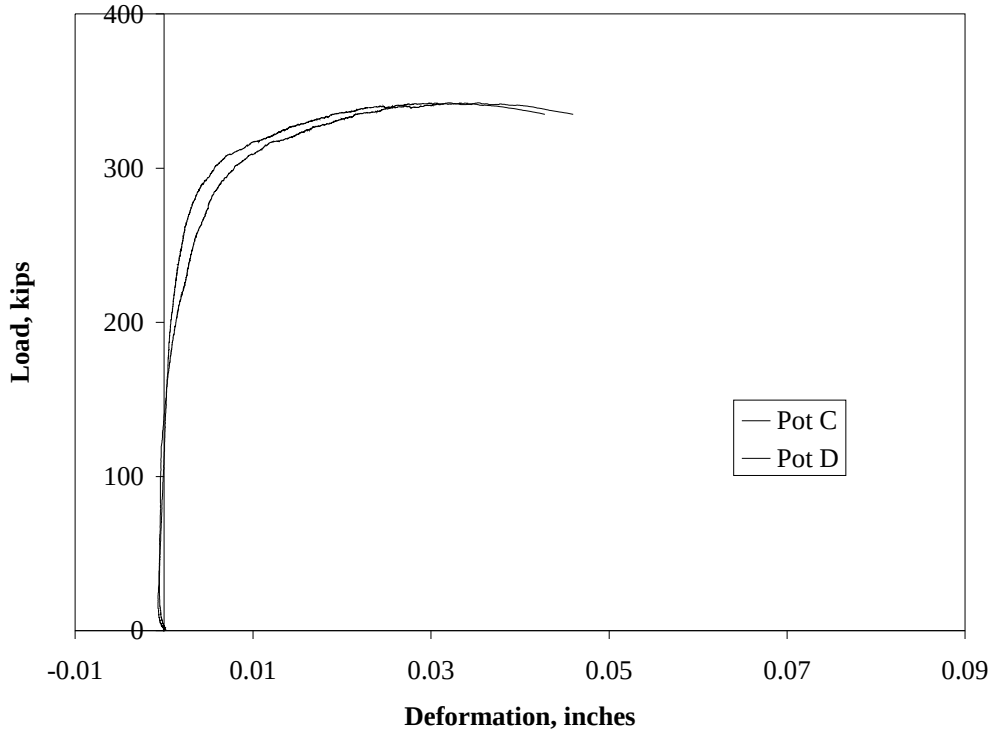

Figure D.38 – Test #21, T250_B12_3, Back Side Weld (2nd Fracture)

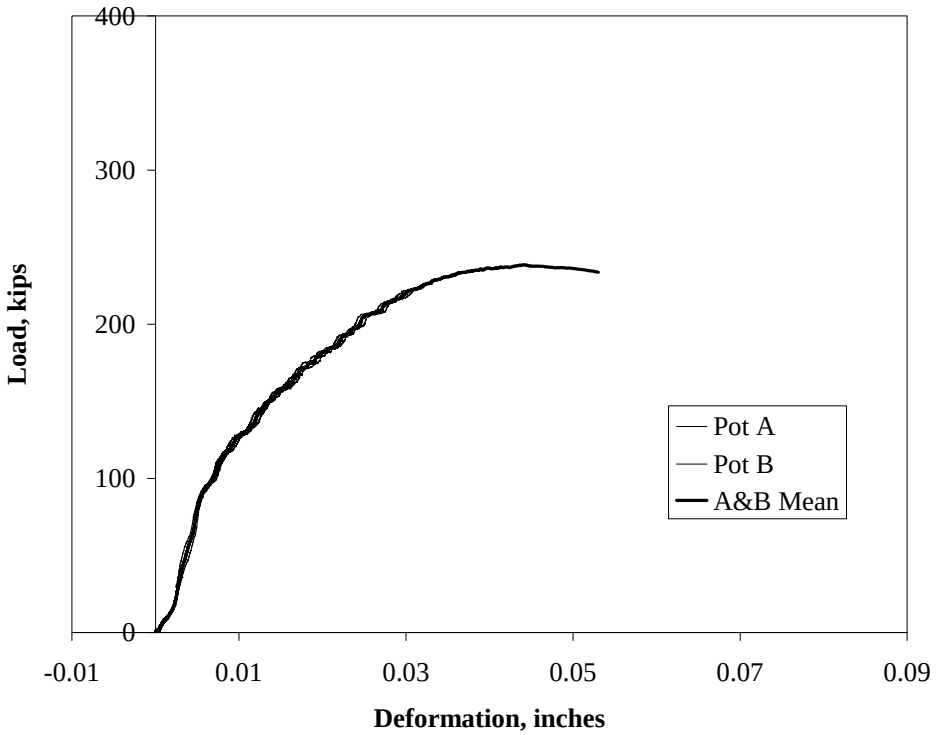

Figure D.39 – Test #22, T250_B516_1, Front Side Weld (1st Fracture)

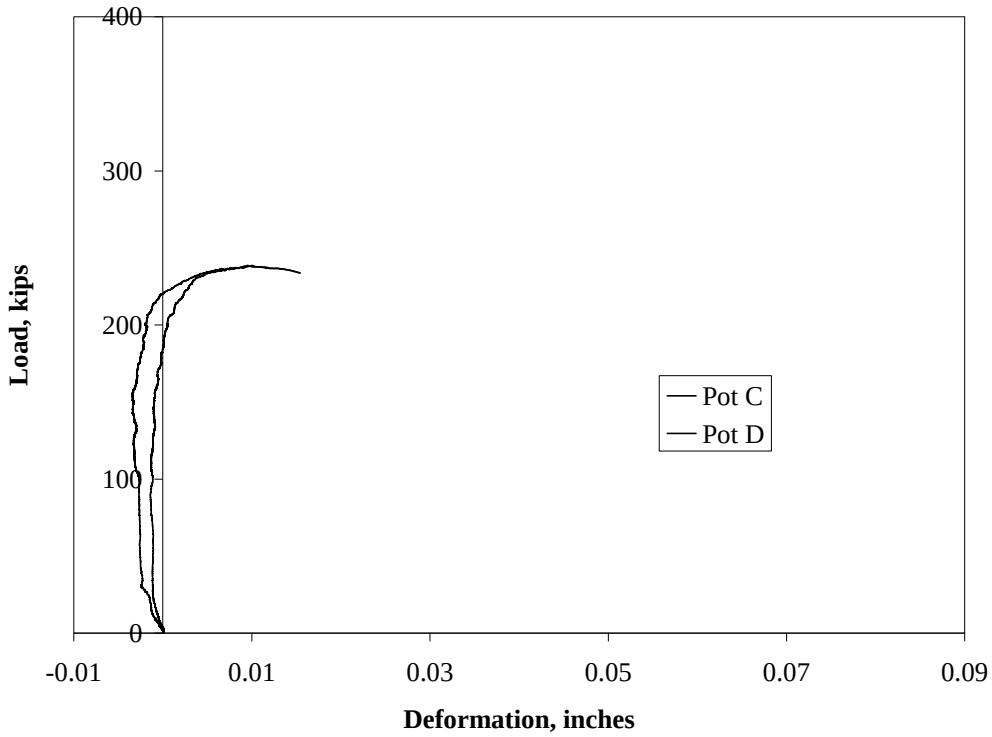

Figure D.40 – Test #22, T250_B516_1, Back Side Weld (2nd Fracture)

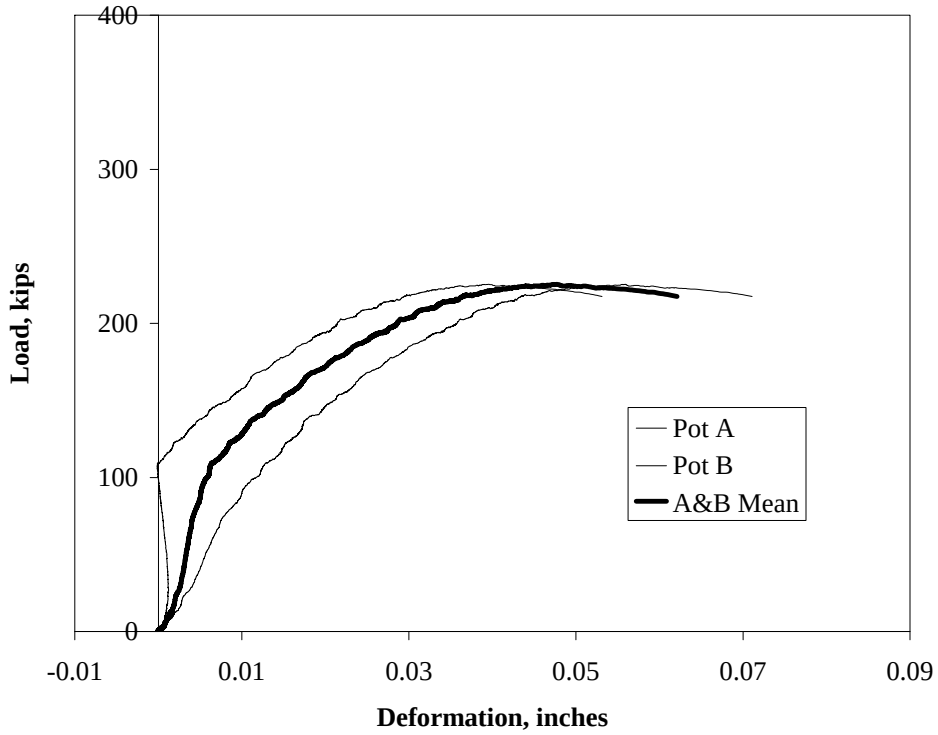

Figure D.41 – Test #23, T250_B516_2, Front Side Weld (1st Fracture)

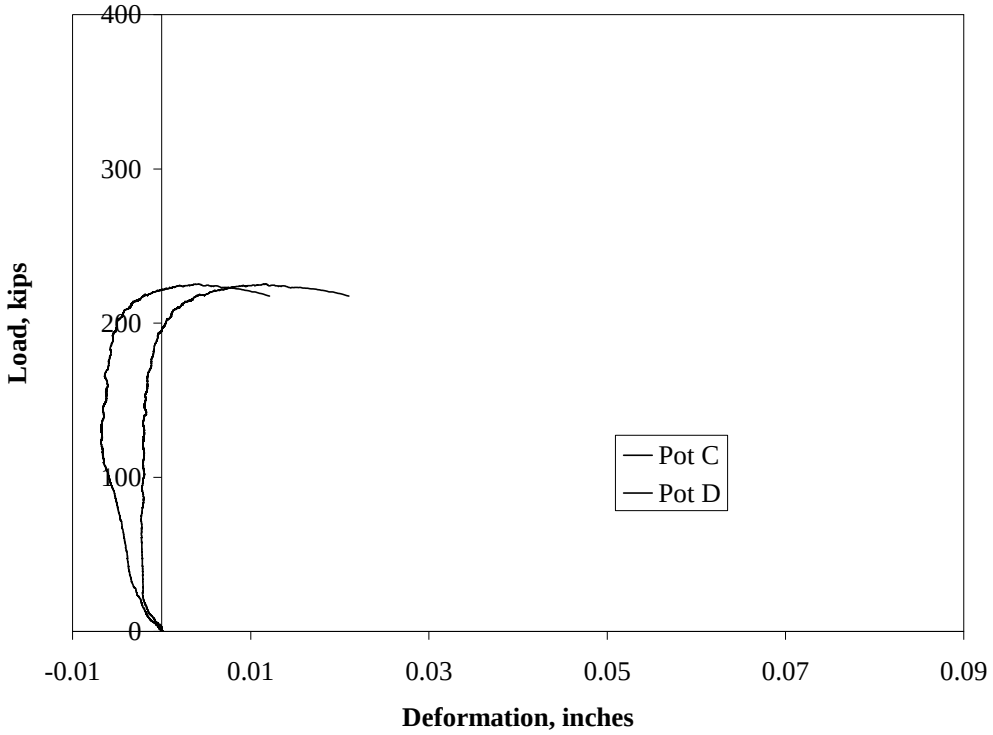

Figure D.42 – Test #23, T250_B516_2, Back Side Weld (2nd Fracture)

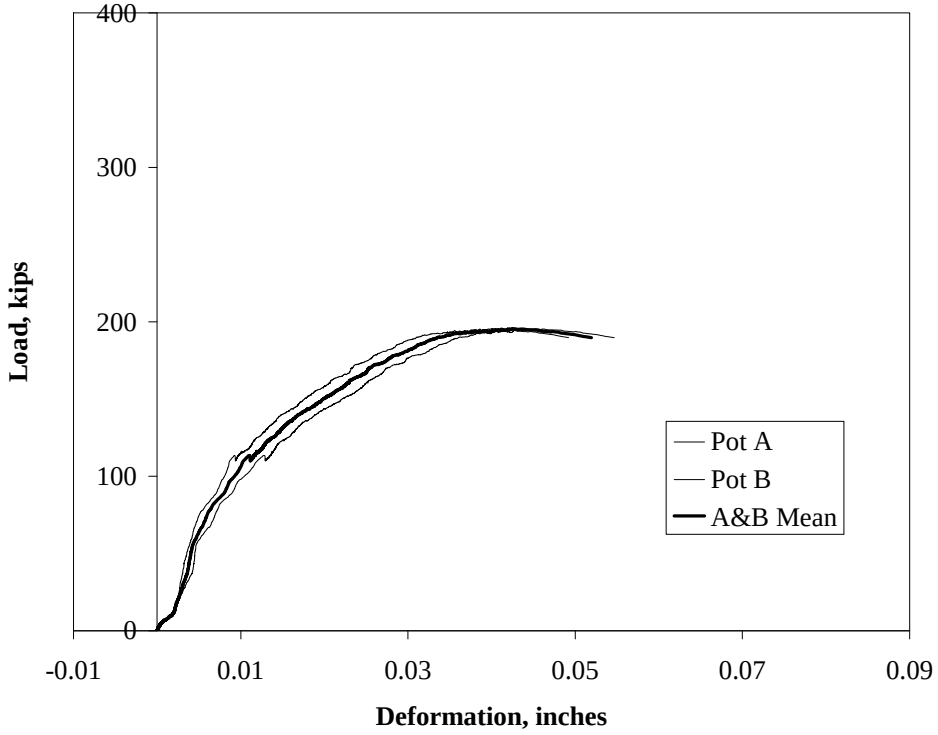

Figure D.43 – Test #24, T250_B516_3, Front Side Weld (1st Fracture)

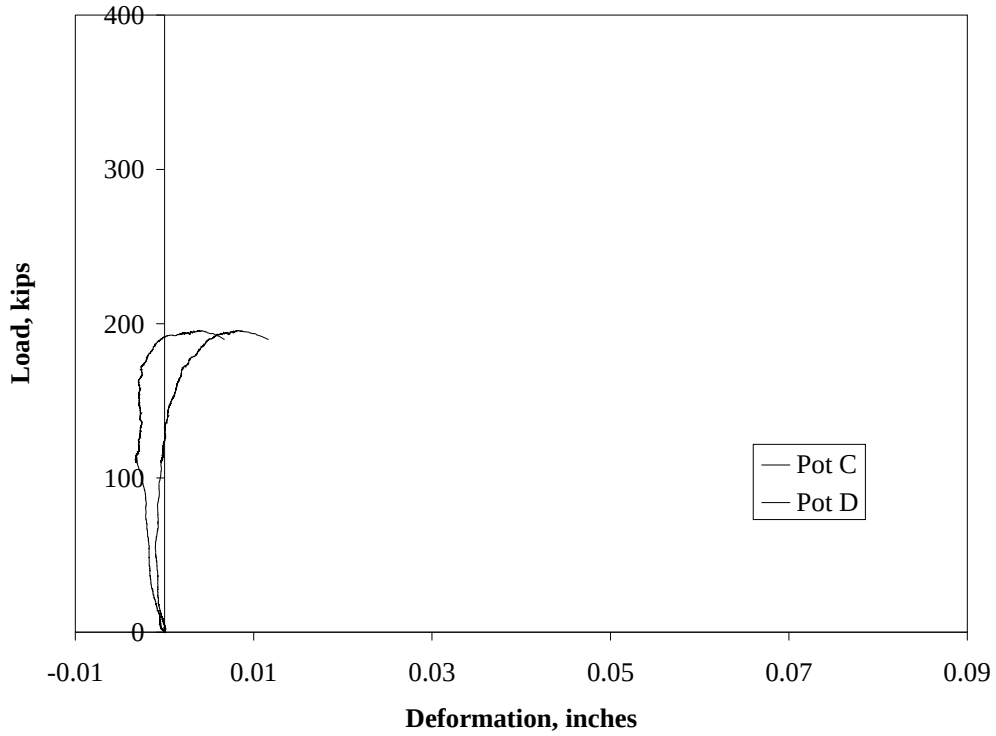

Figure D.44 – Test #24, T250_B516_3, Back Side Weld (2nd Fracture)

Appendix E

Bend Test Experimental Response Results[1]

[1] Refer to Chapter 4 for figure details

E.1 DEFORMATION RESPONSE

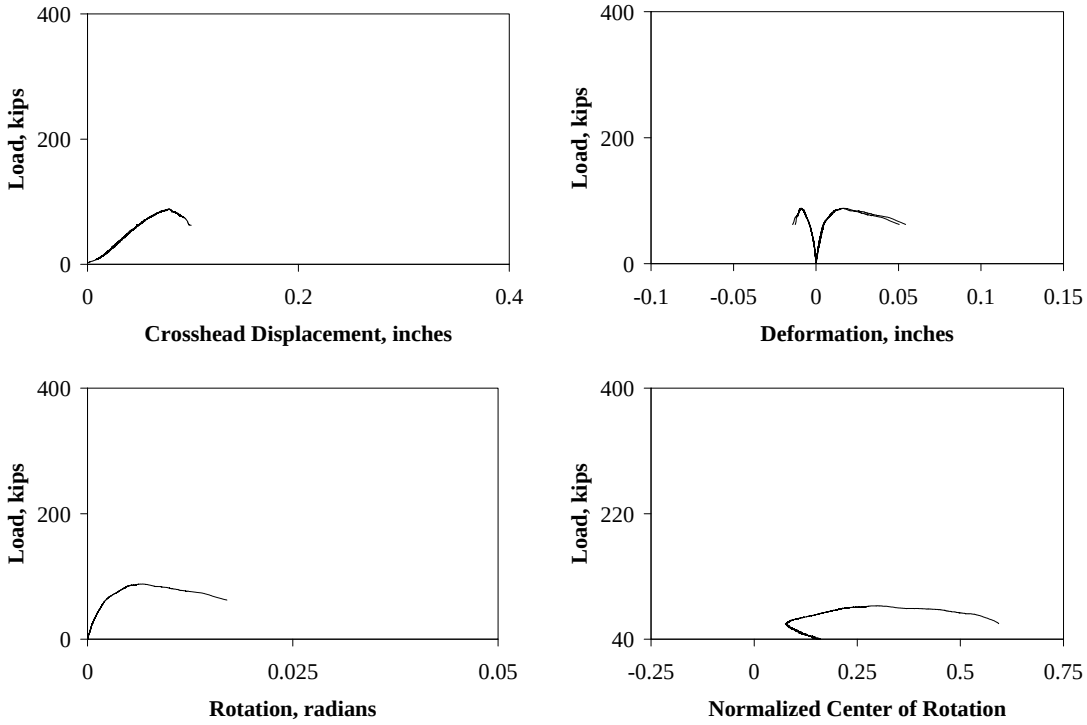

Figure E.1.1 – Test #25, B125_A516_55_1[2]

[2] For specimen nomenclature details, refer to Appendix B, page B-2

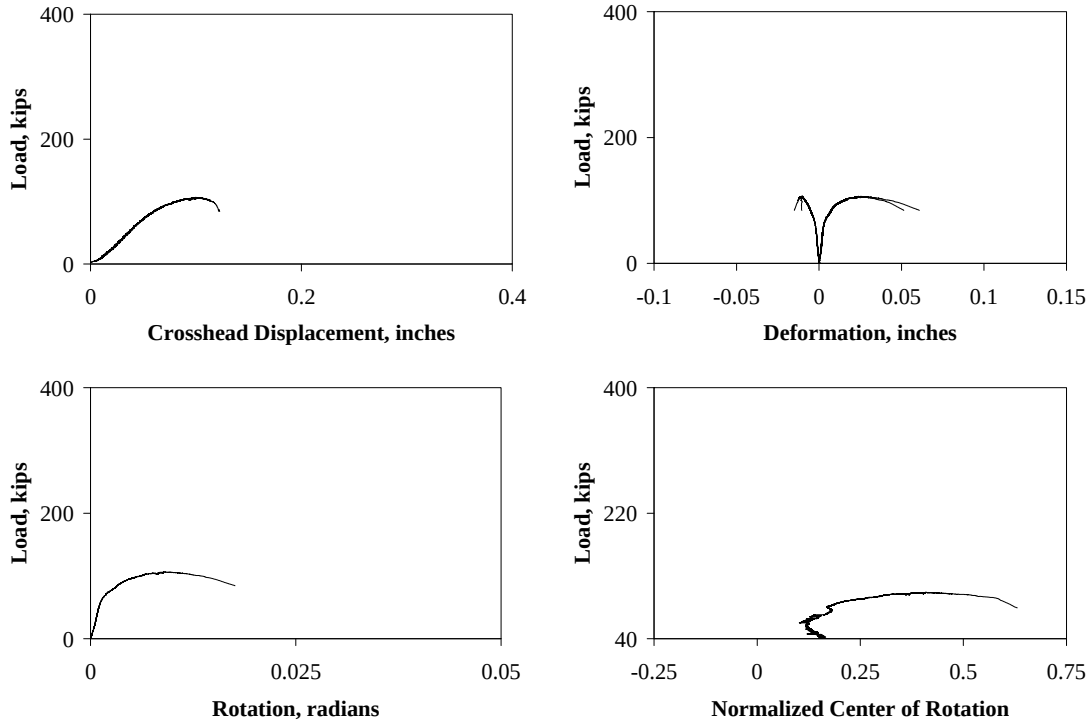

Figure E.1.2 – Test #26, B125_A516_55_2

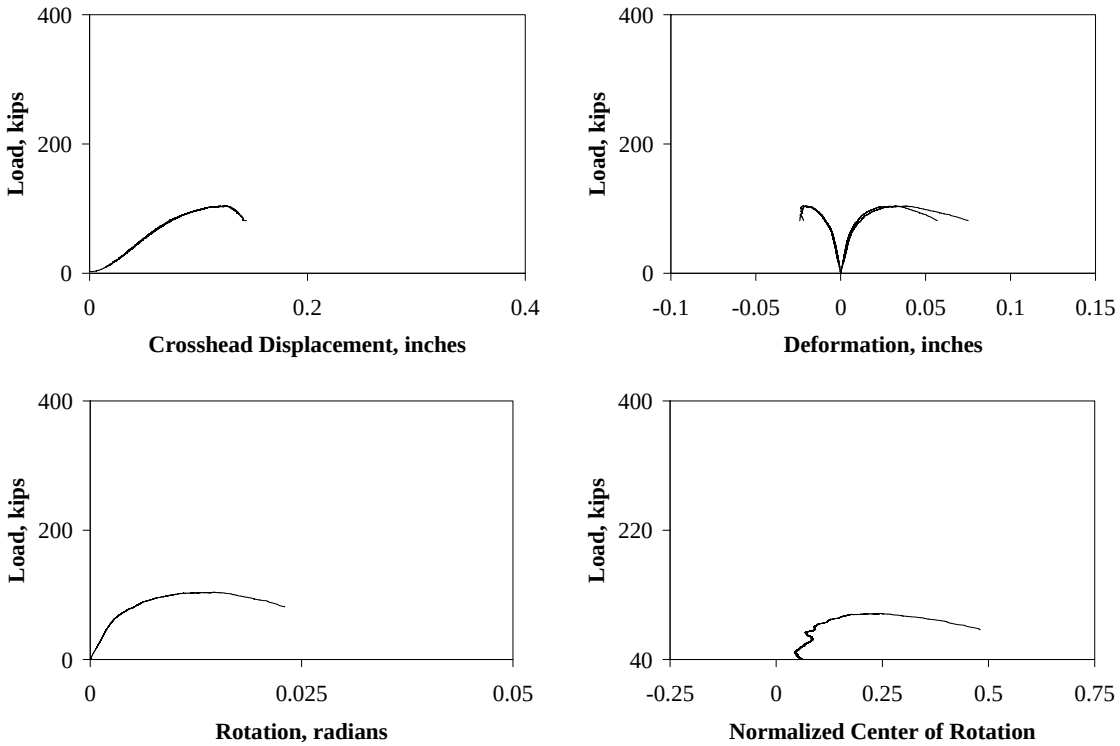

Figure E.1.3 – Test #27, B125_A516_55_3

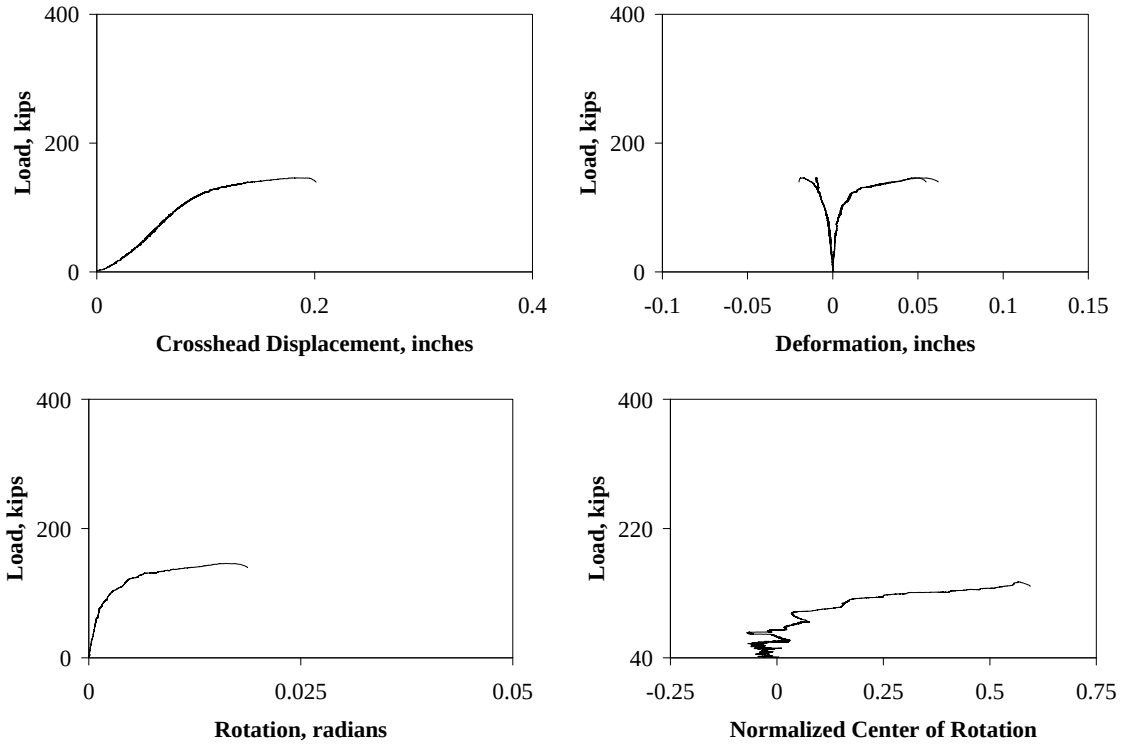

Figure E.1.4 – Test #28, B125_A12_55_1

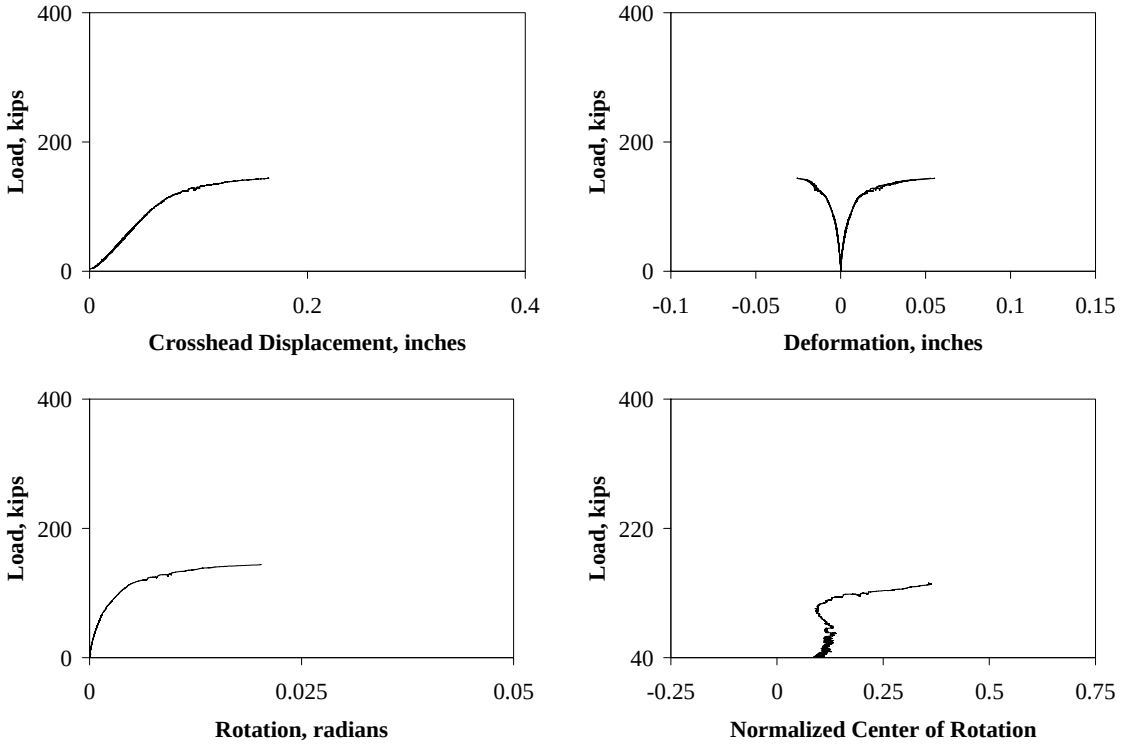

Figure E.1.5 – Test #29, B125_A12_55_2

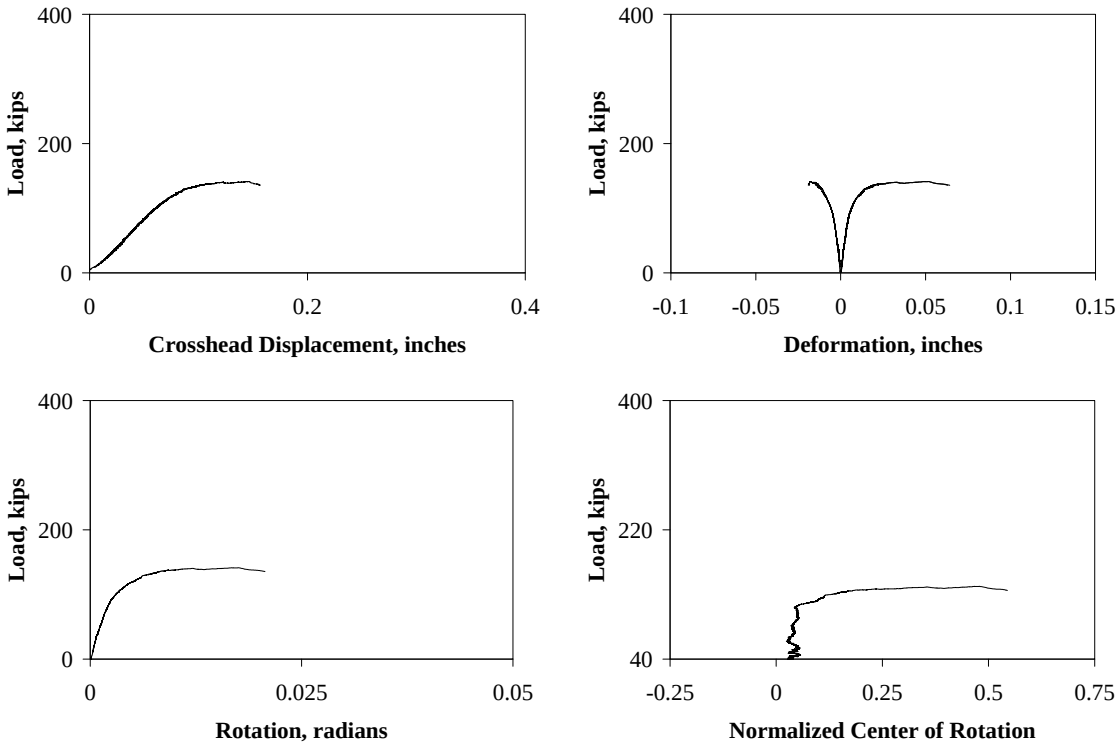

Figure E.1.6 – Test #30, B125_A12_55_3

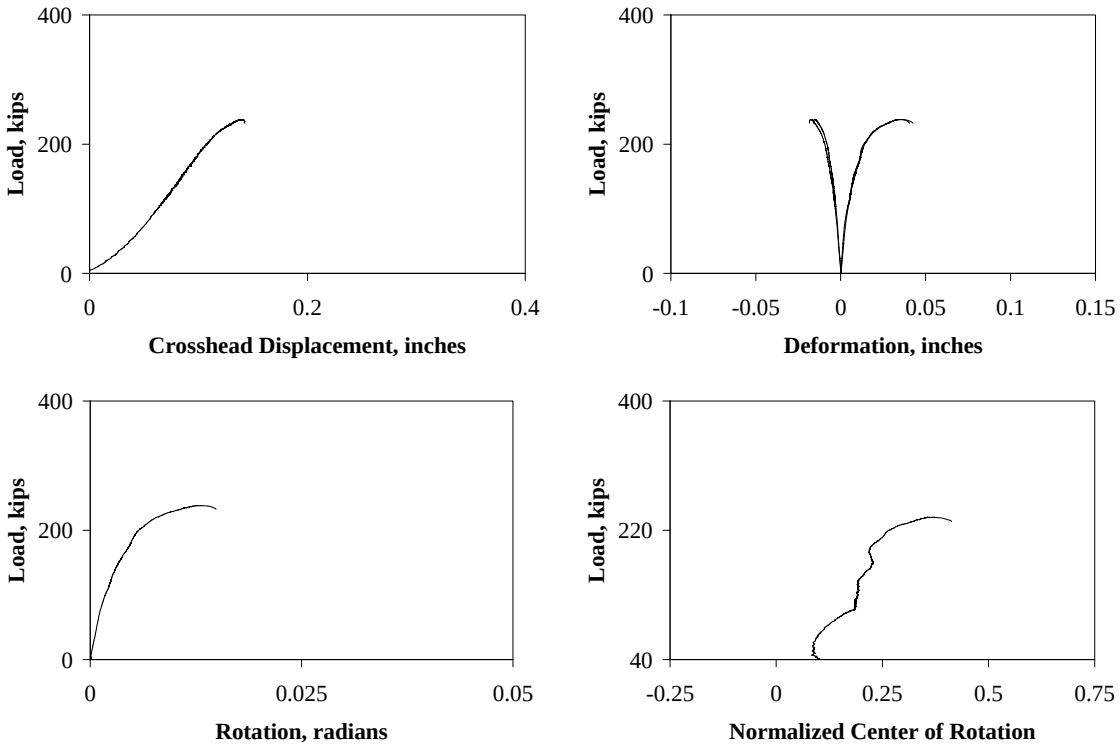

Figure E.1.7 – Test #31, B175_A516_3_1

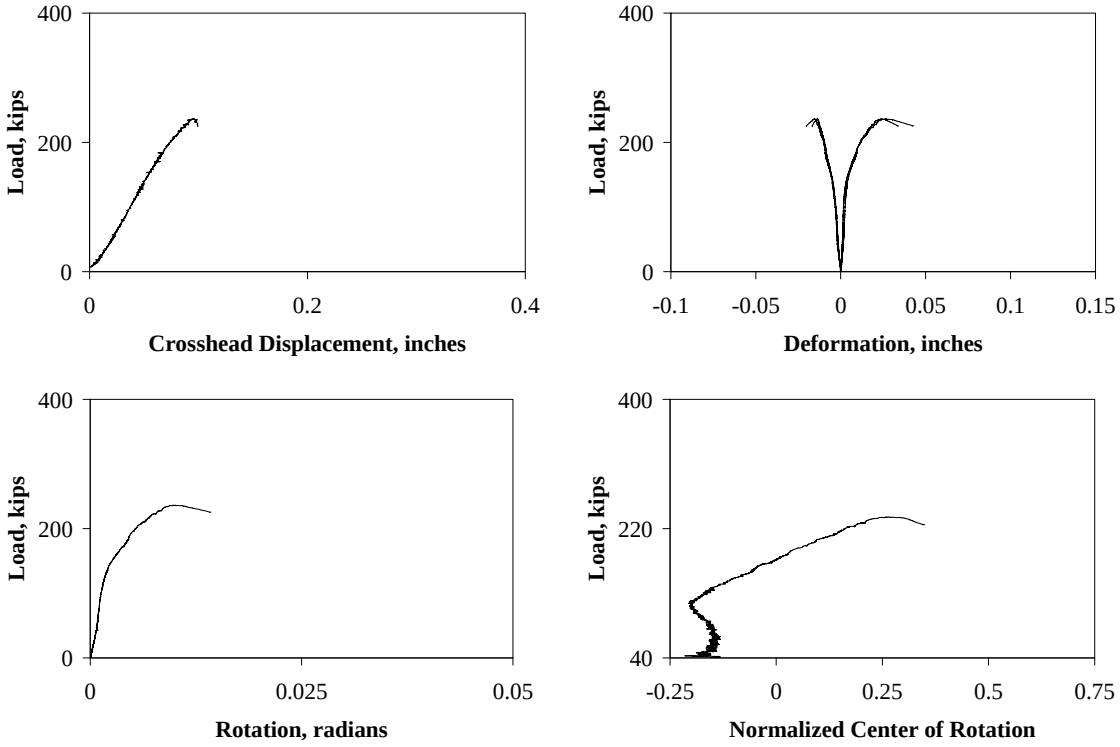

Figure E.1.8 – Test #32, B175_A516_3_2

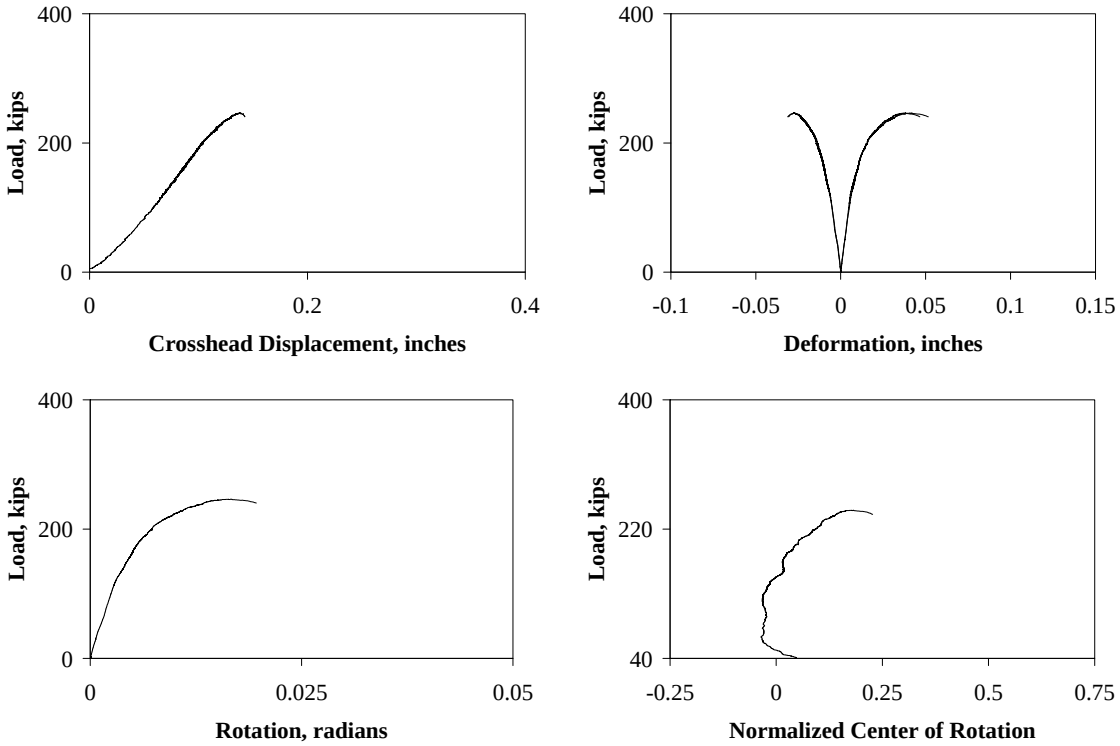

Figure E.1.9 – Test #33, B175_A516_3_3

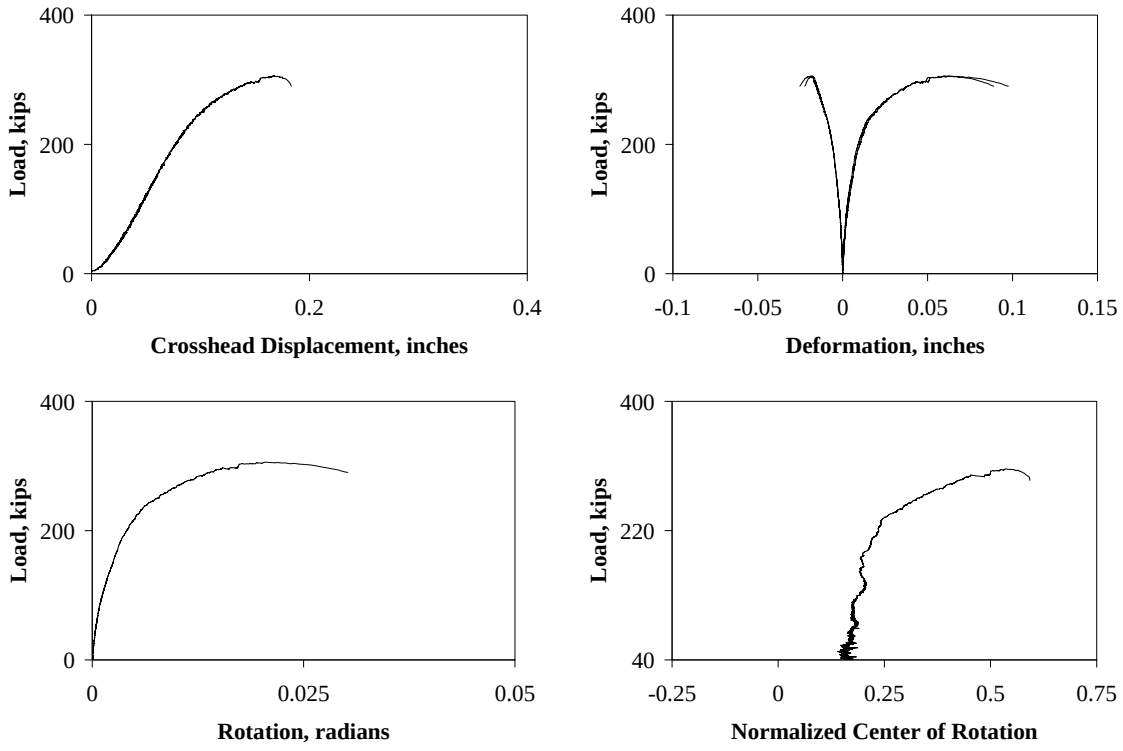

Figure E.1.10 – Test #34, B175_A12_3_1

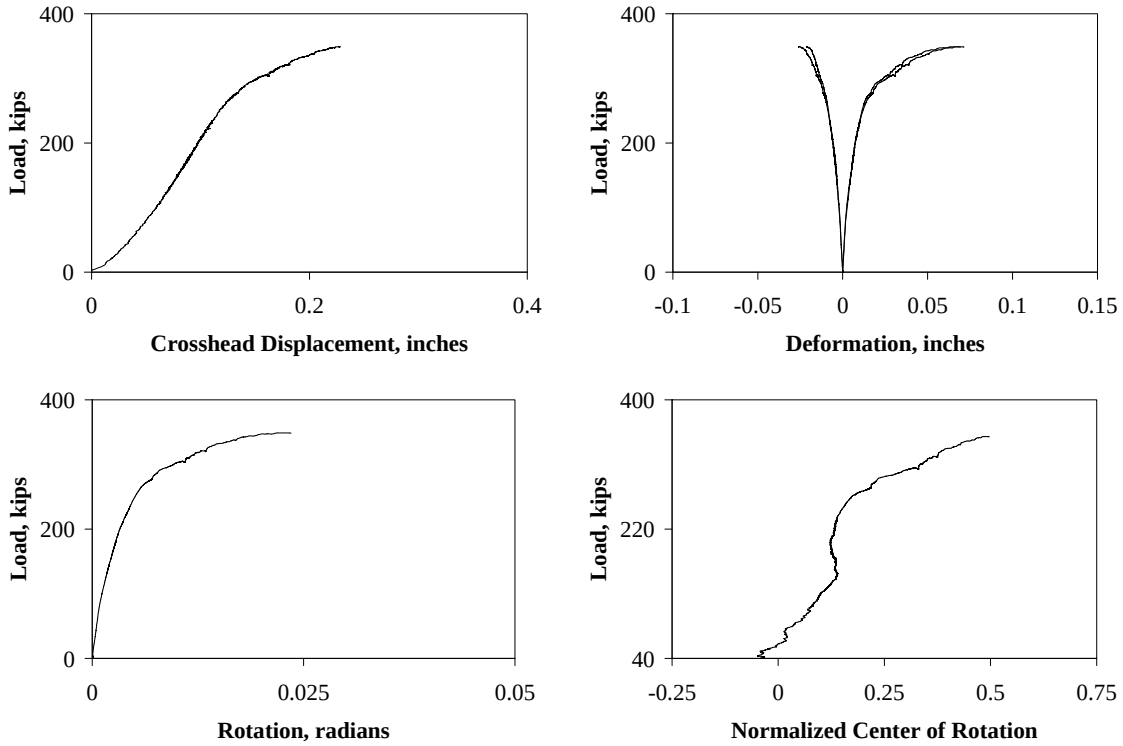

Figure E.1.11 – Test #35, B175_A12_3_2

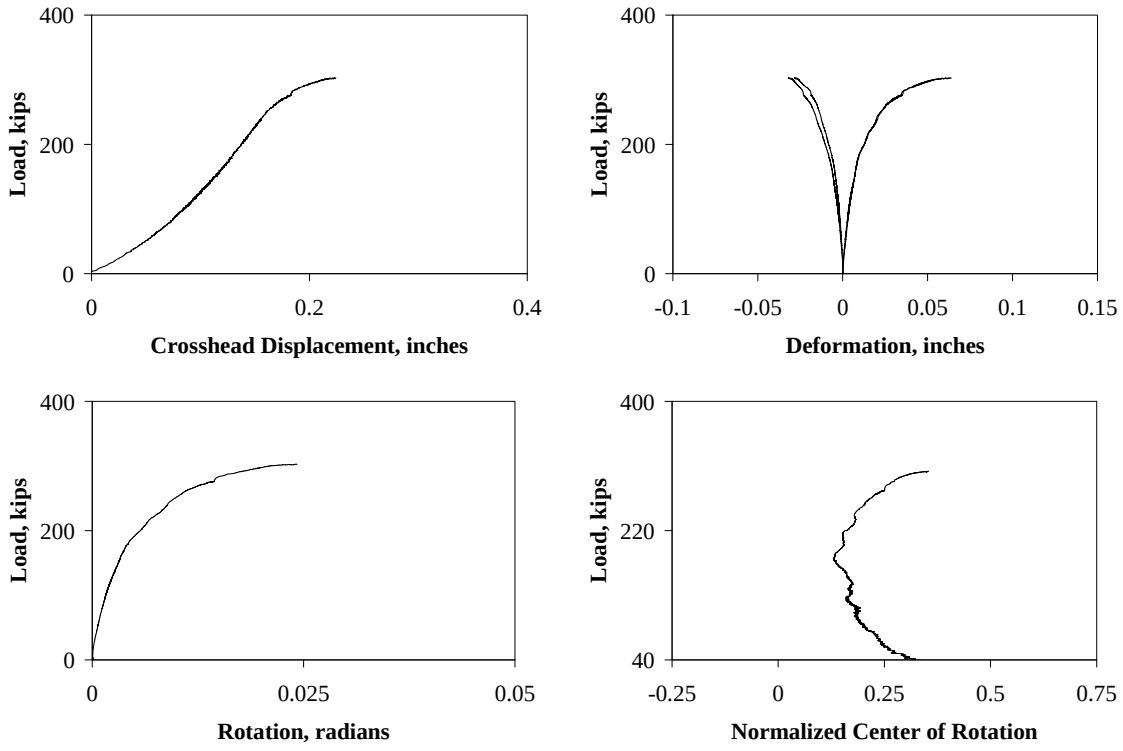

Figure E.1.12 – Test #36, B175_A12_3_3

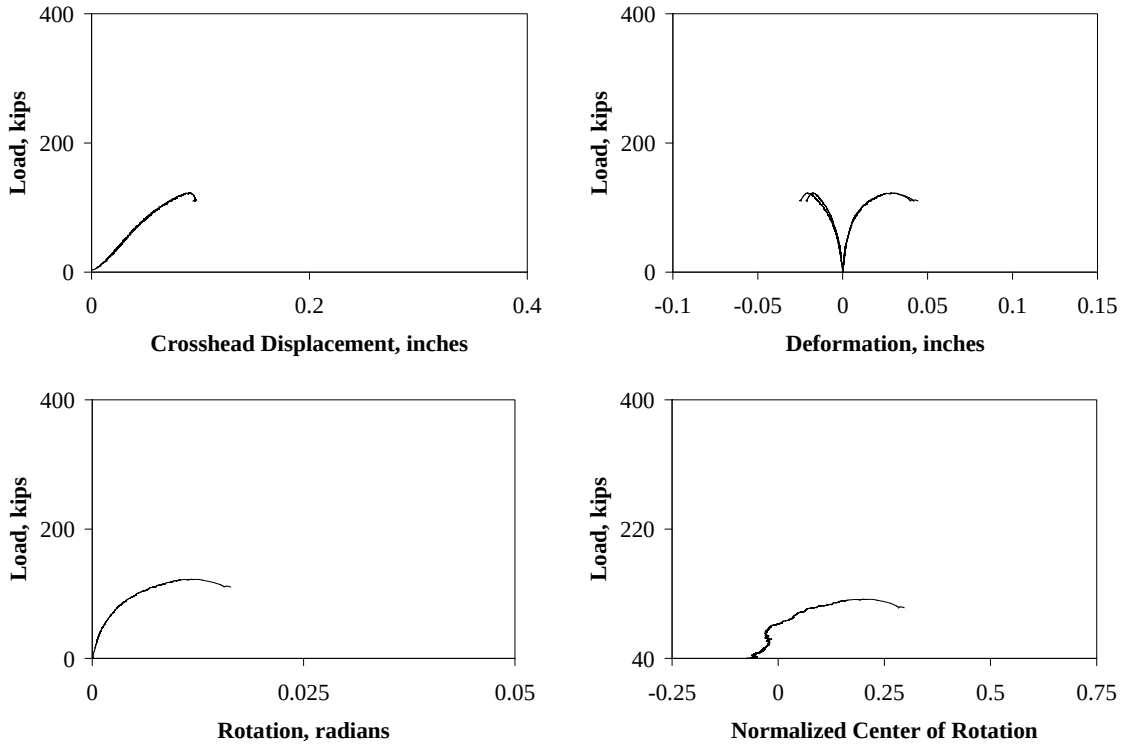

Figure E.1.13 – Test #37, B175_A516_55_1

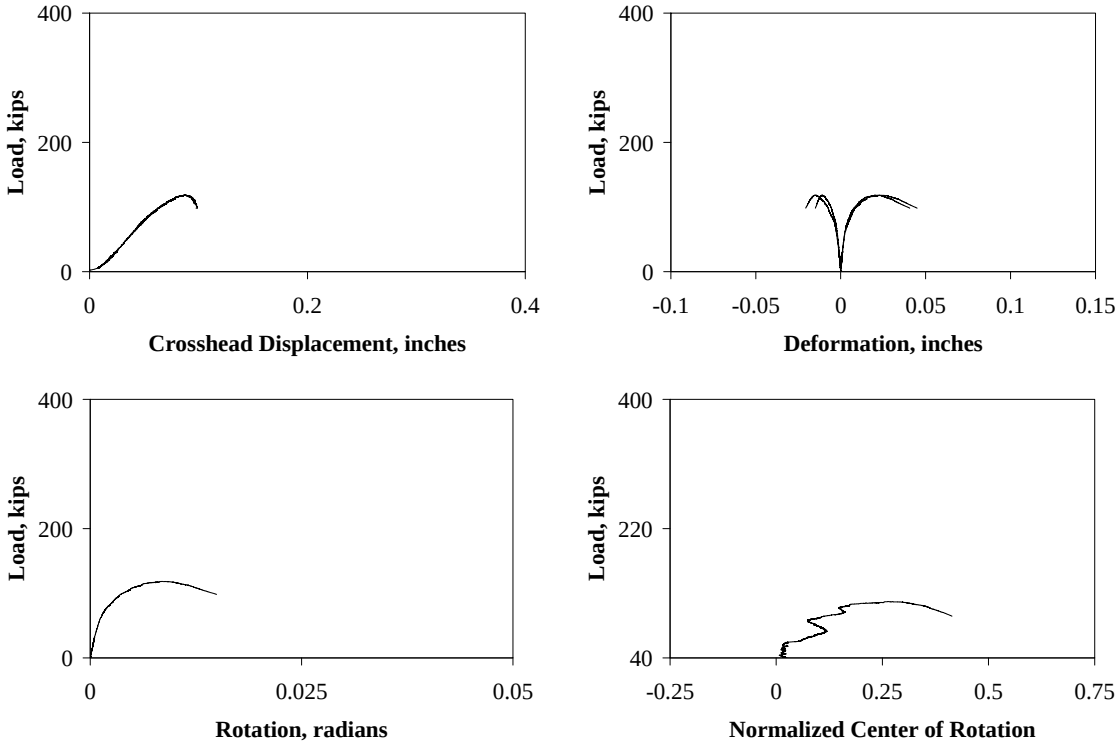

Figure E.1.14 – Test #38, B175_A516_55_2

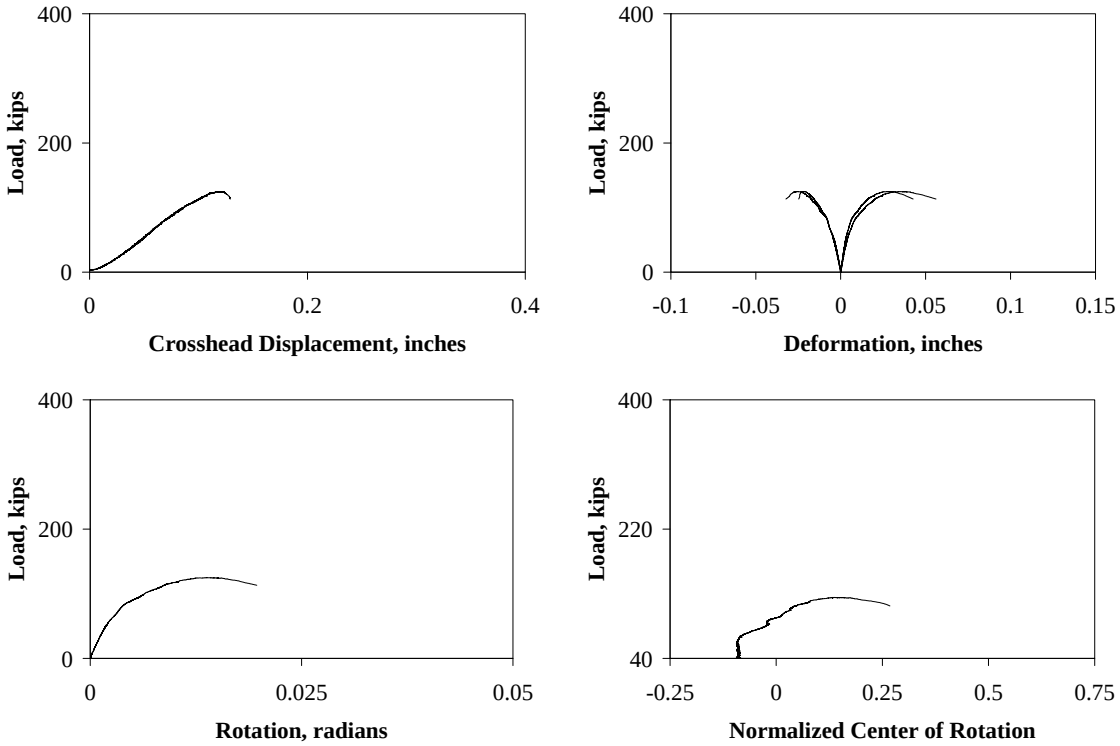

Figure E.1.15 – Test #39, B175_A516_55_3

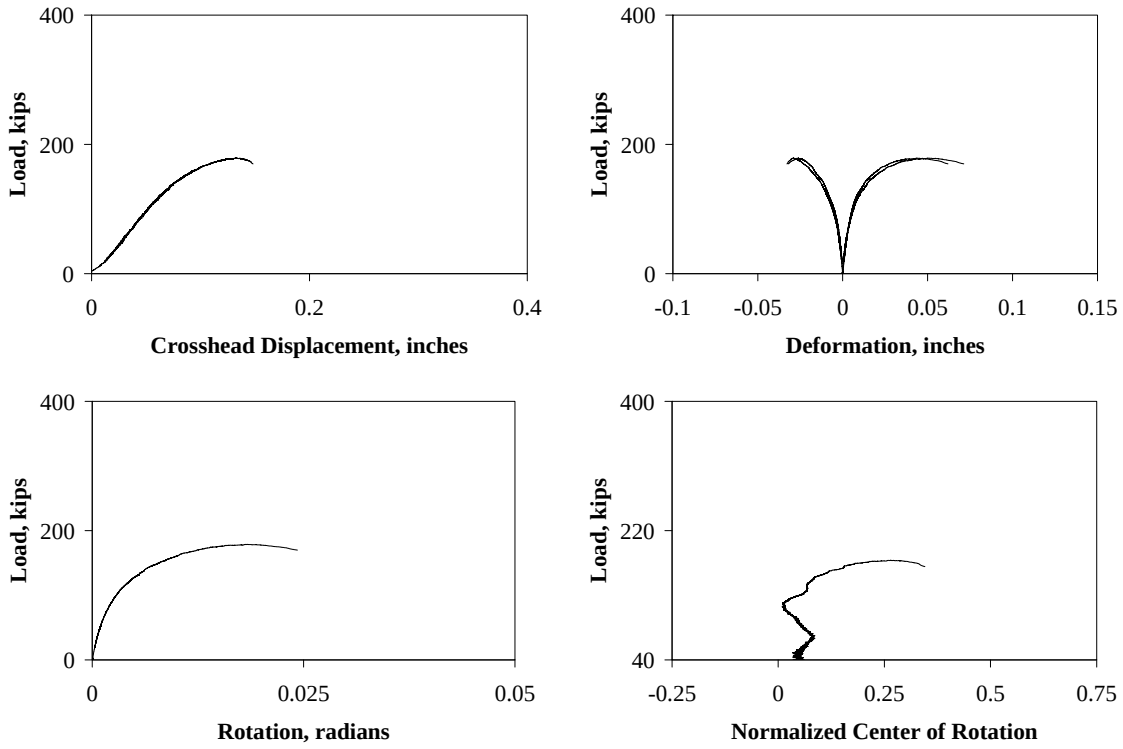

Figure E.1.16 – Test #40, B175_A12_55_1

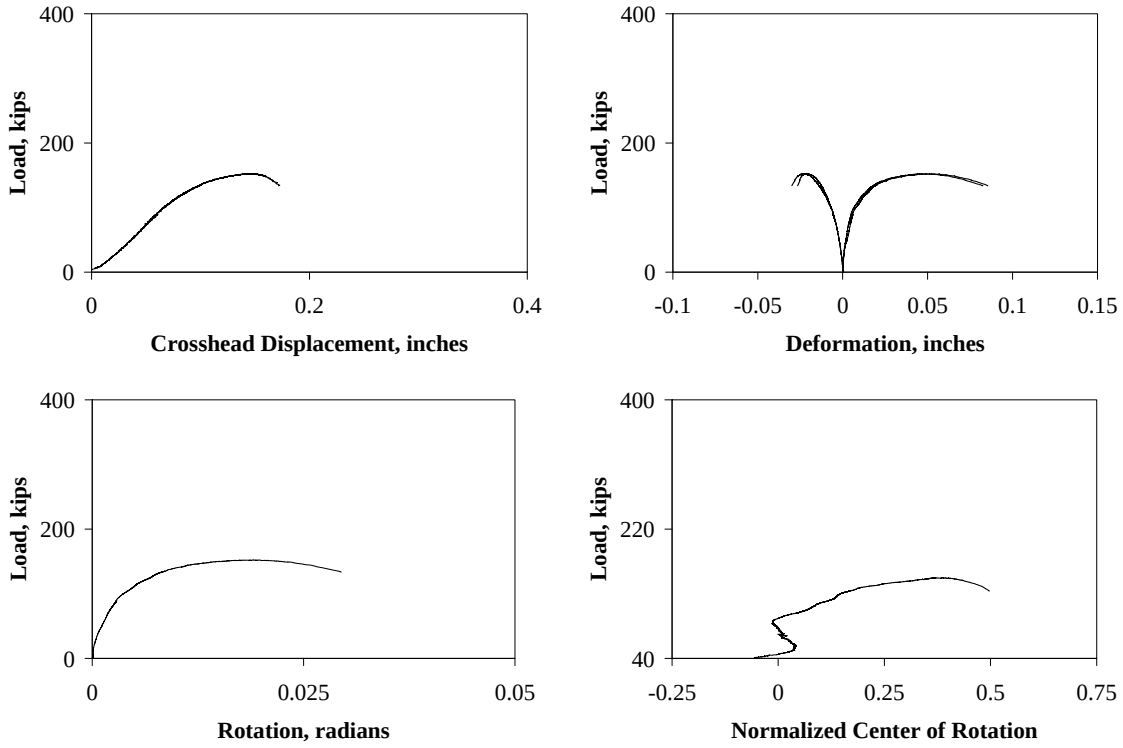

Figure E.1.17 – Test #41, B175_A12_55_2

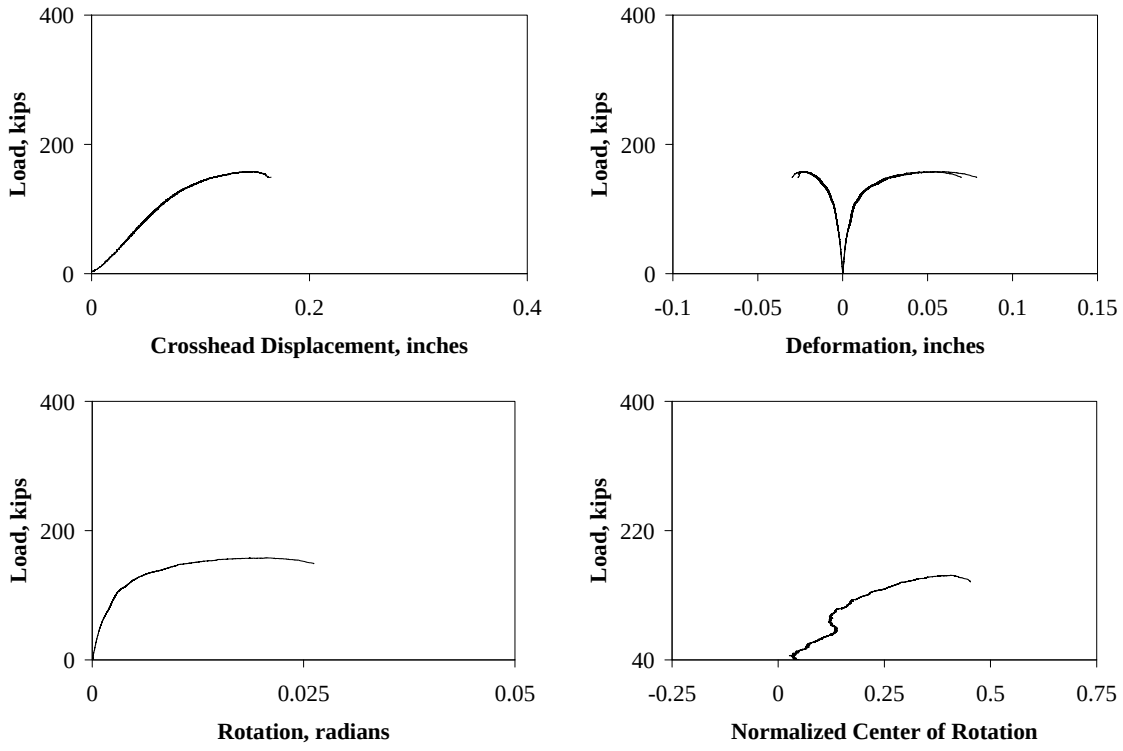

Figure E.1.18 – Test #42, B175_A12_55_3

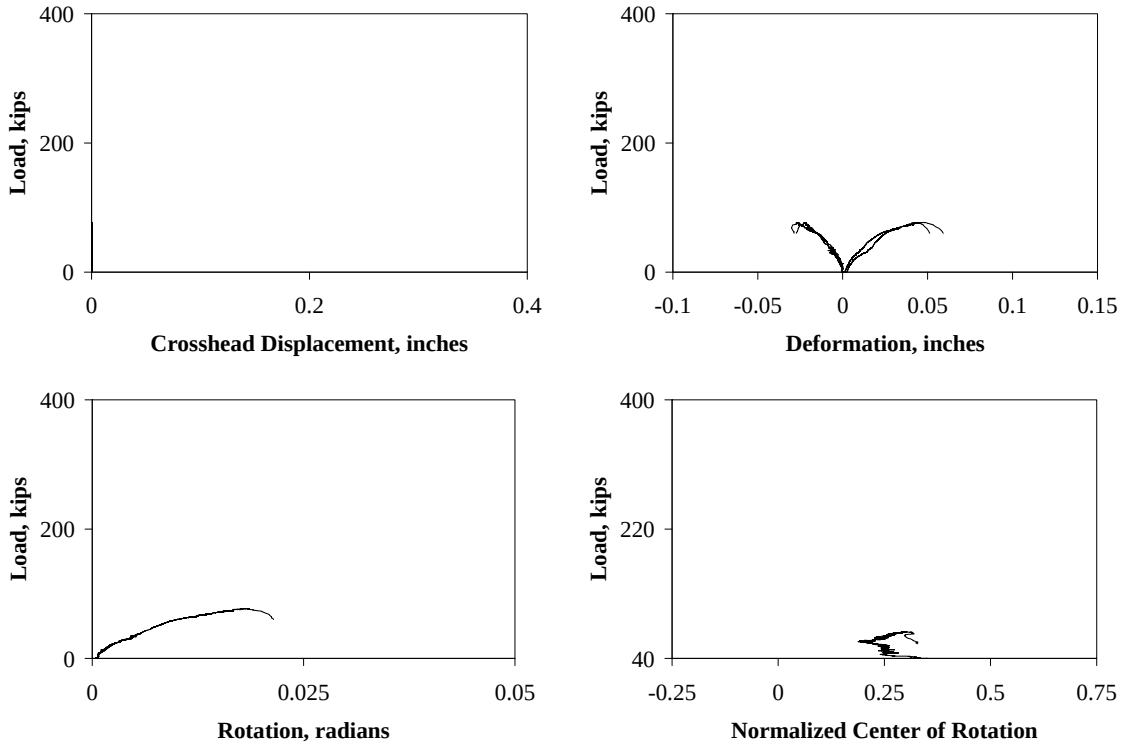

Figure E.1.19 – Test #43, B175_A516_85_1

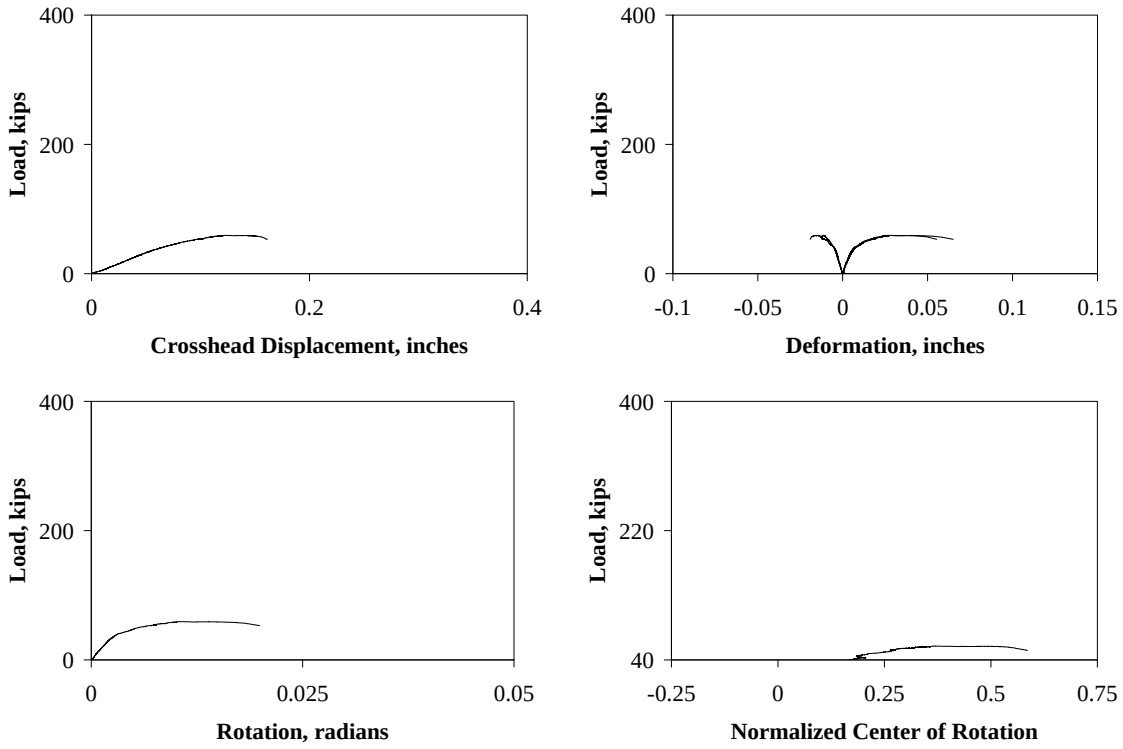

Figure E.1.20 – Test #44, B175_A516_85_2

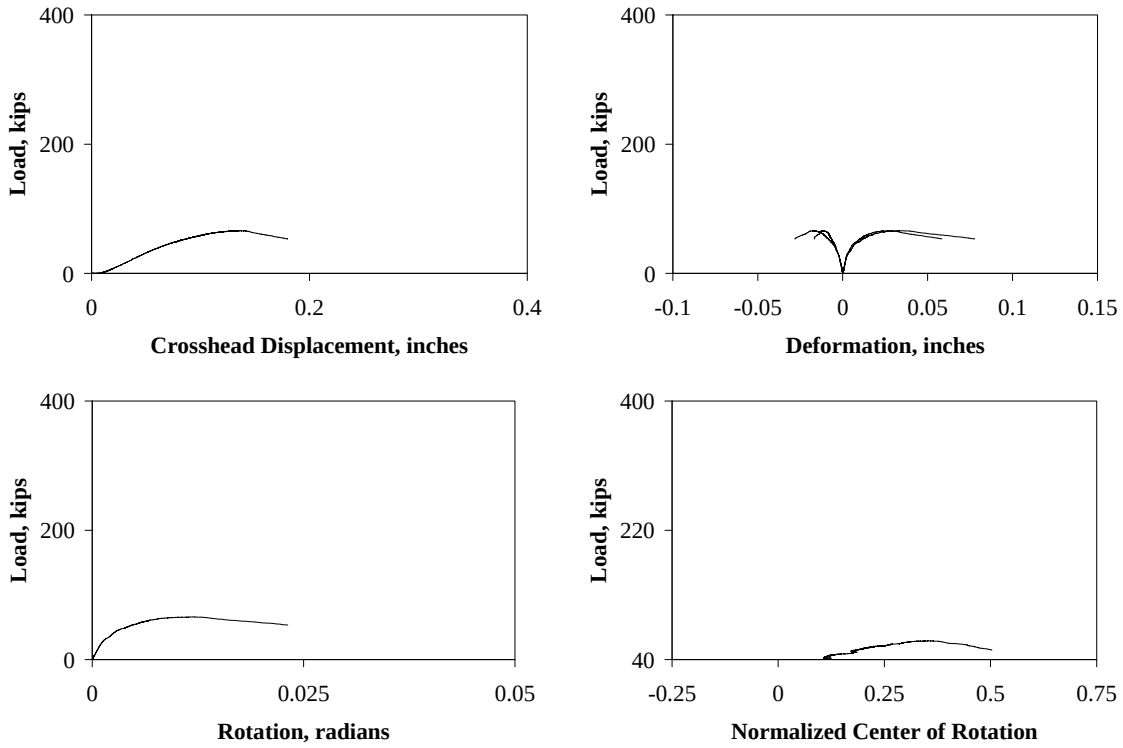

Figure E.1.21 – Test #45, B175_A516_85_3

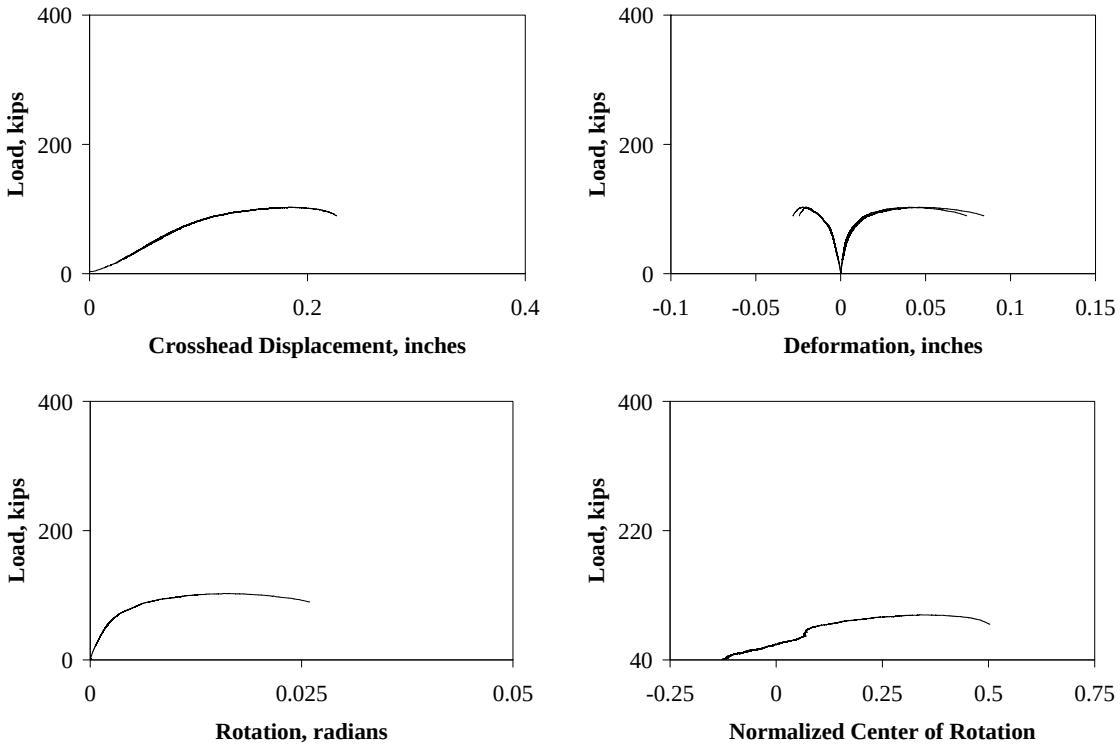

Figure E.1.22 – Test #46, B175_A12_85_1

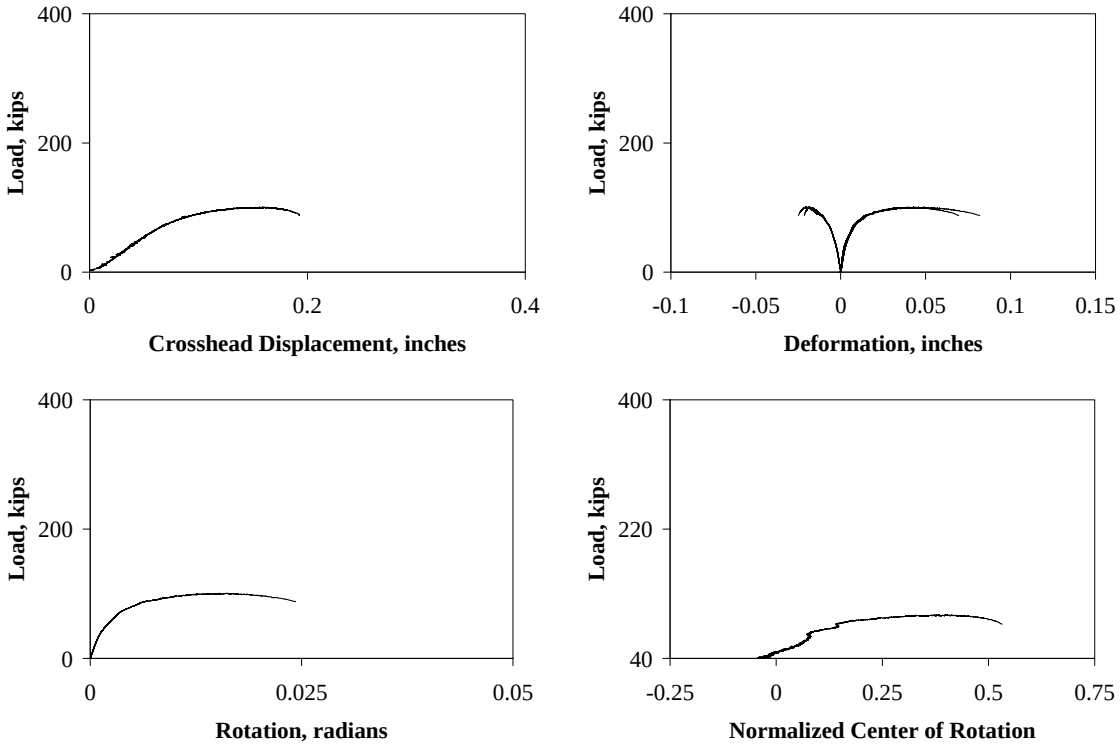

Figure E.1.23 – Test #47, B175_A12_85_2

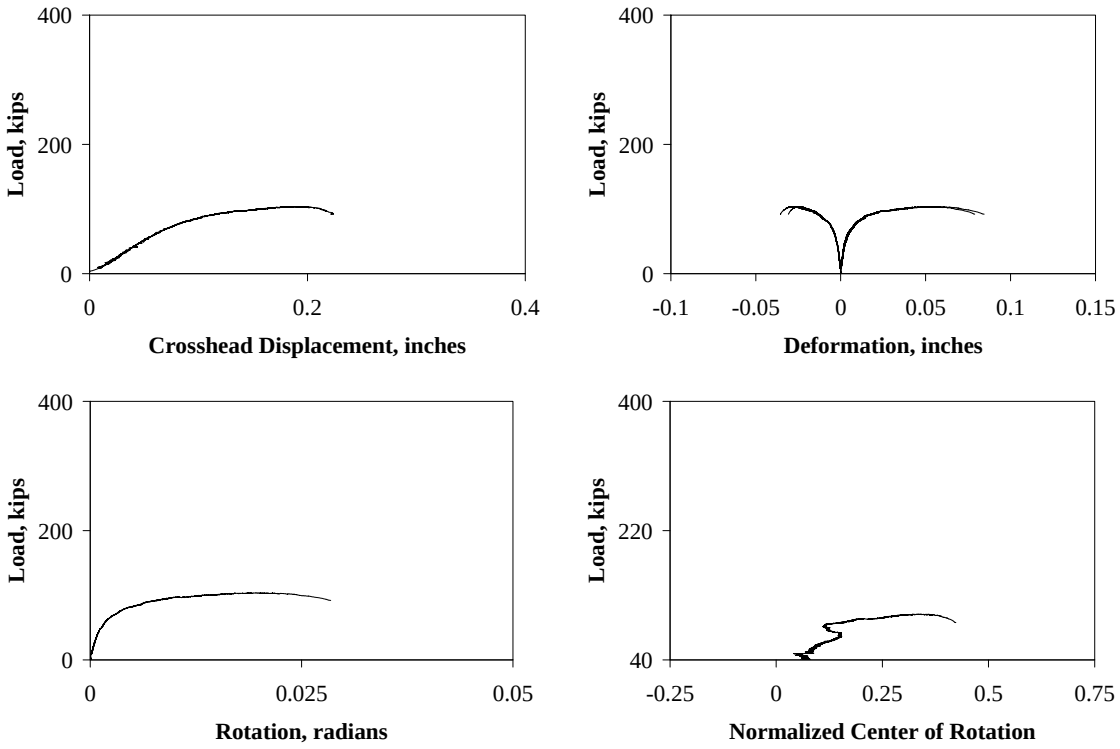

Figure E.1.24 – Test #48, B175_A12_85_3

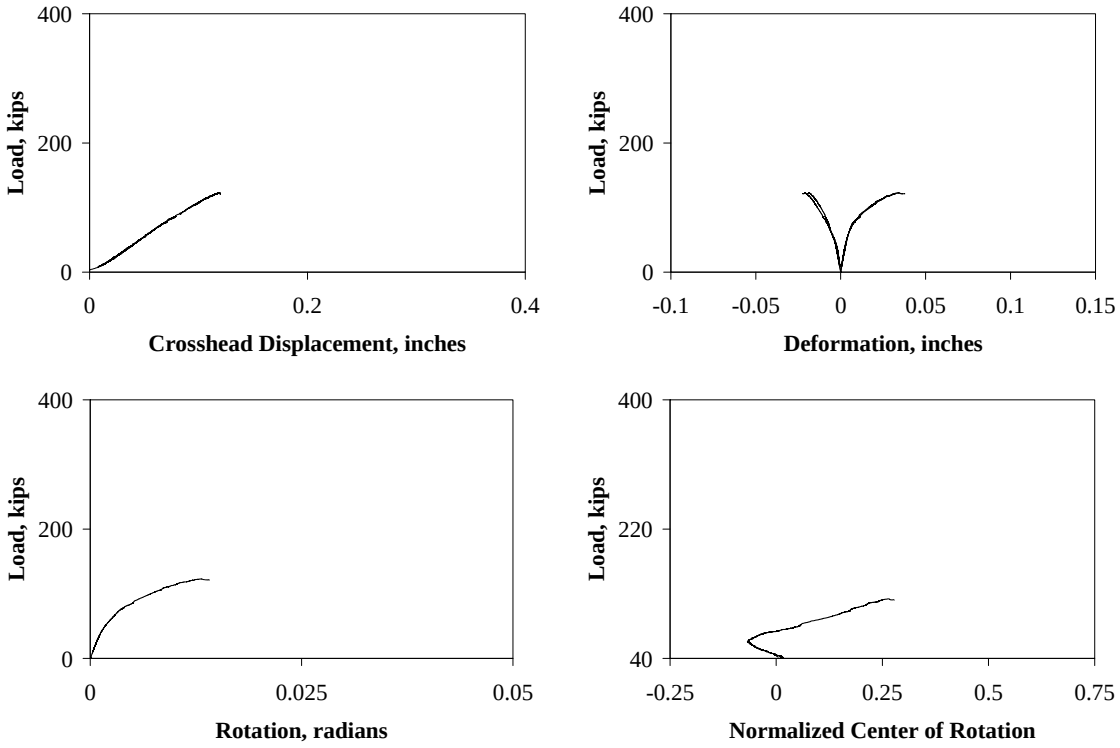

Figure E.1.25 – Test #49, B250_A516_55_1

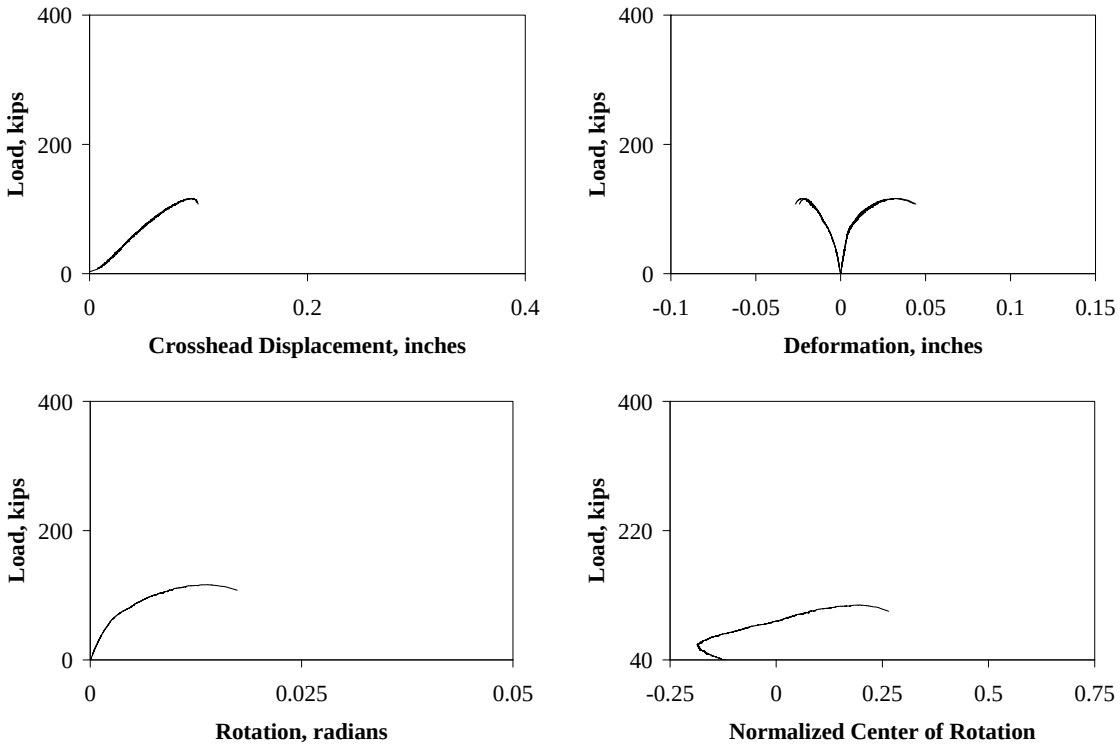

Figure E.1.26 – Test #50, B250_A516_55_2

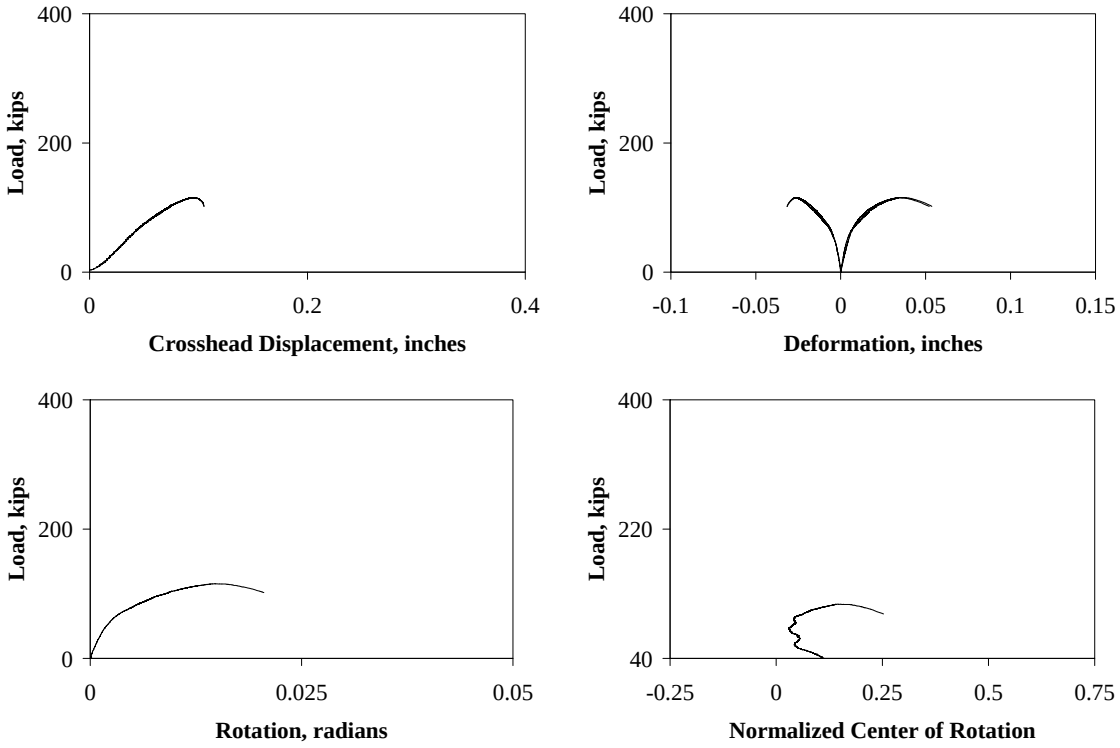

Figure E.1.27 – Test #51, B250_A516_55_3

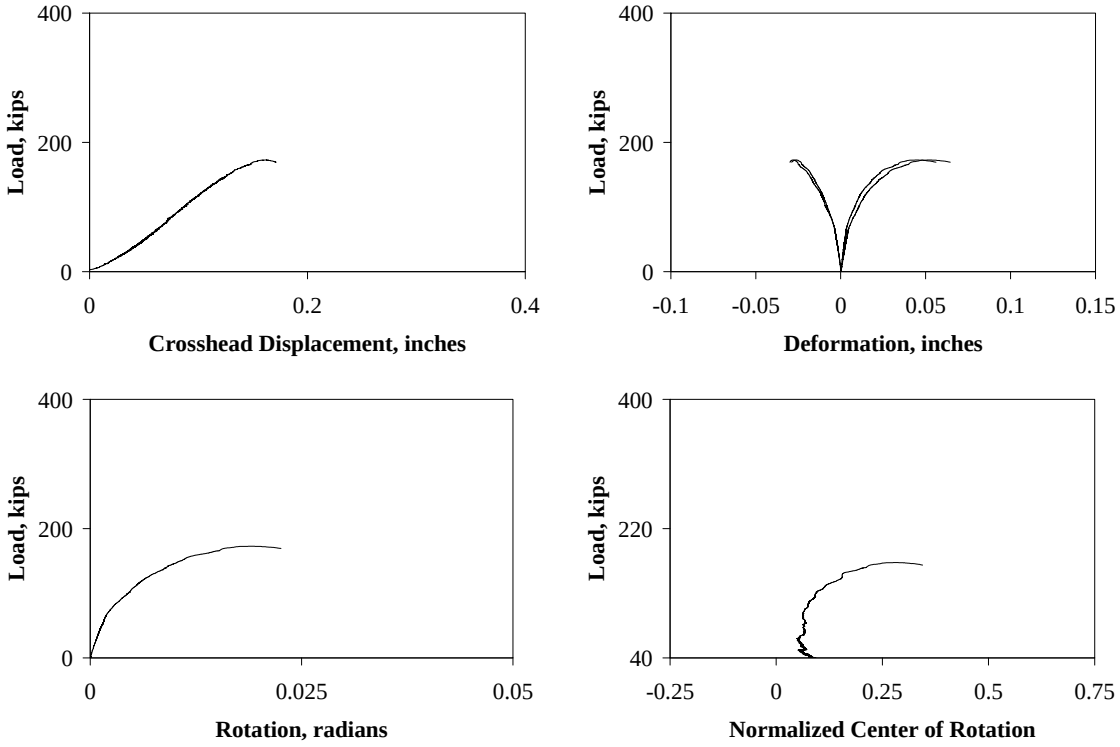

Figure E.1.28 – Test #52, B250_A12_55_1

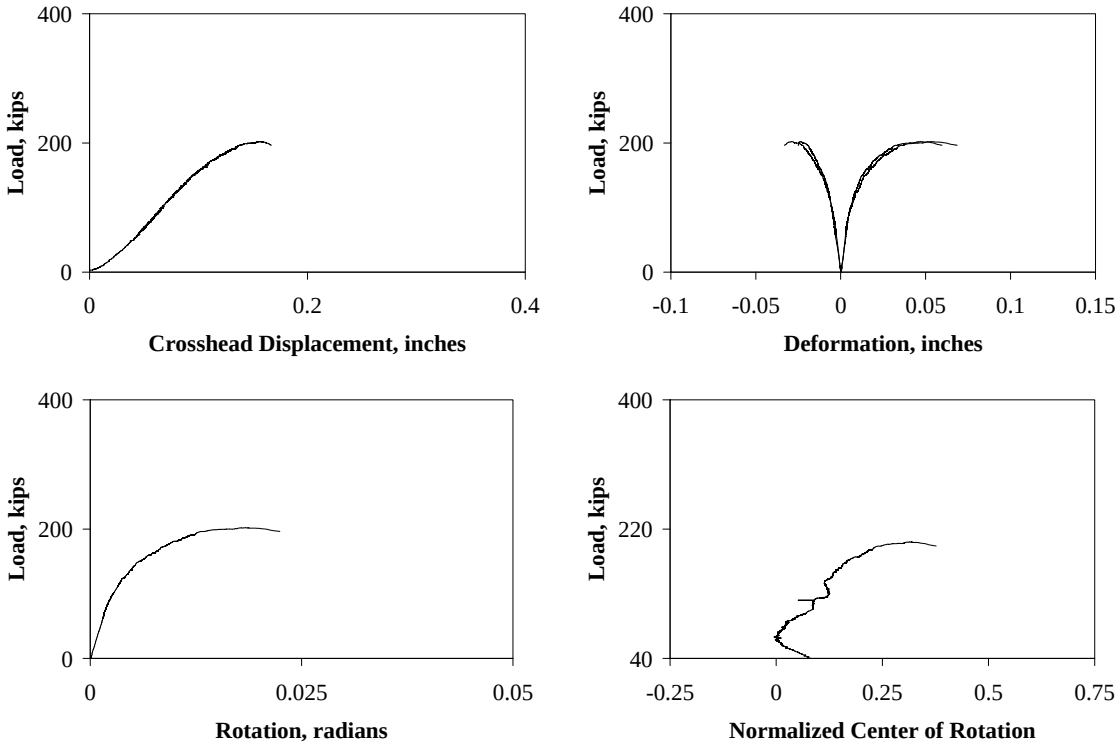

Figure E.1.29 – Test #53, B250_A12_55_2

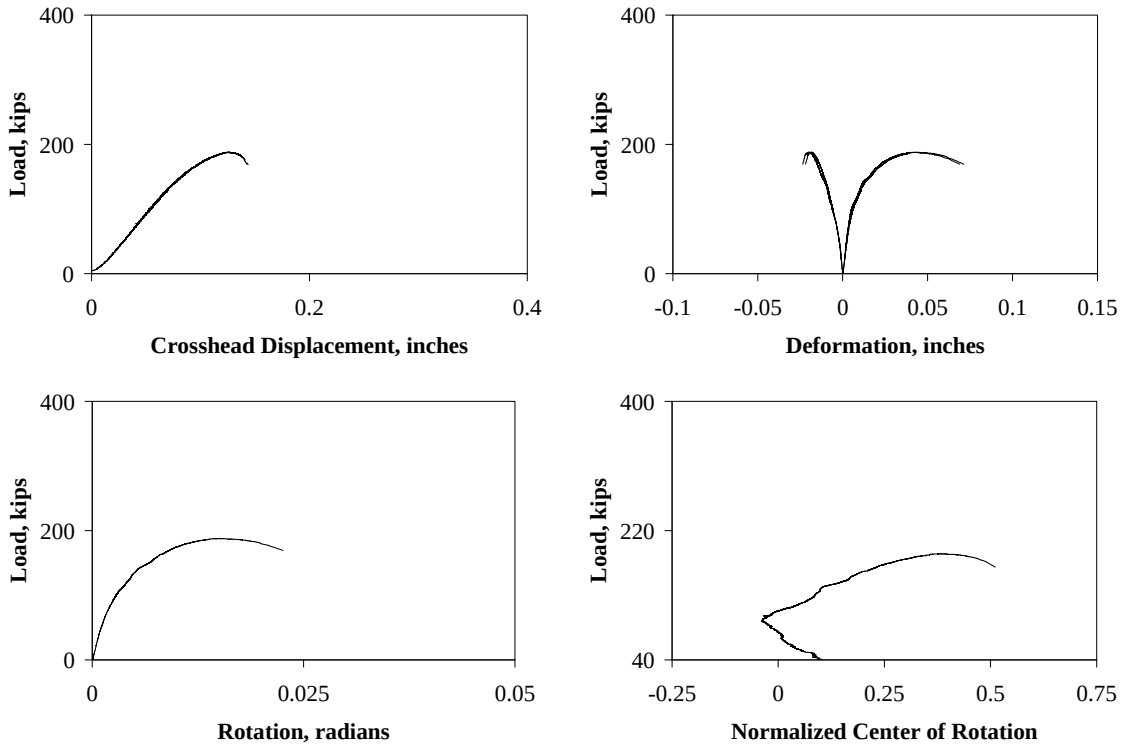

Figure E.1.30 – Test #54, B250_A12_55_3

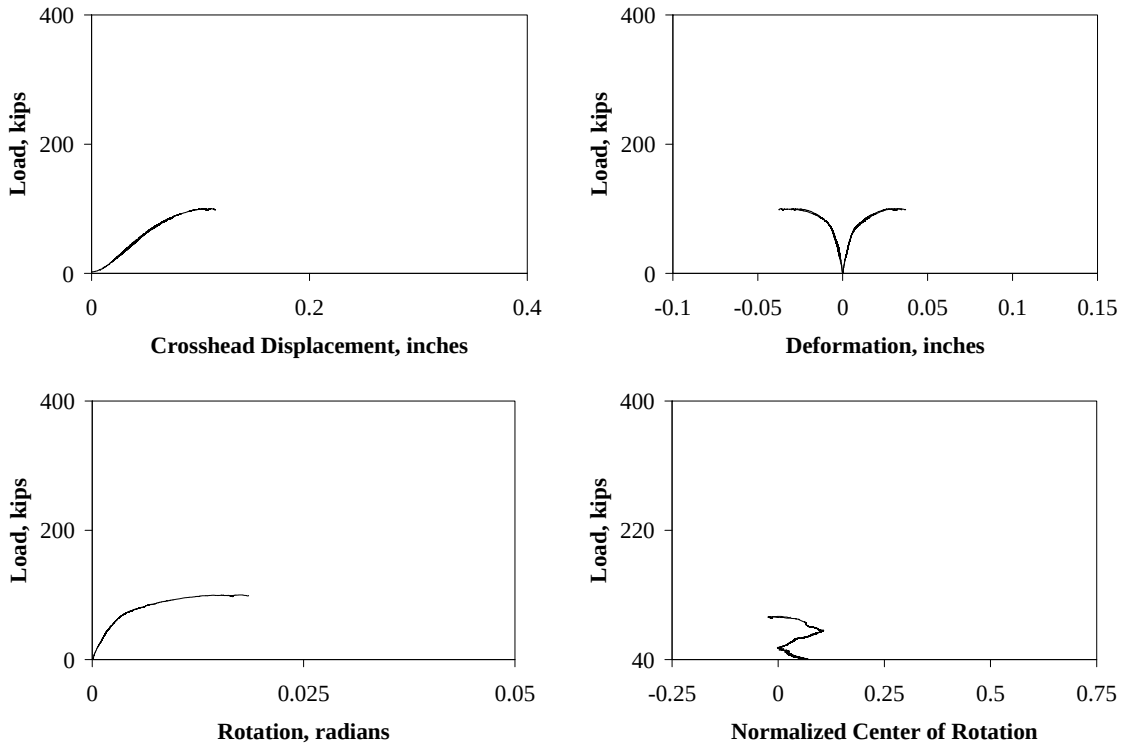

Figure E.1.31 – Test #55, B125_B516_55_1

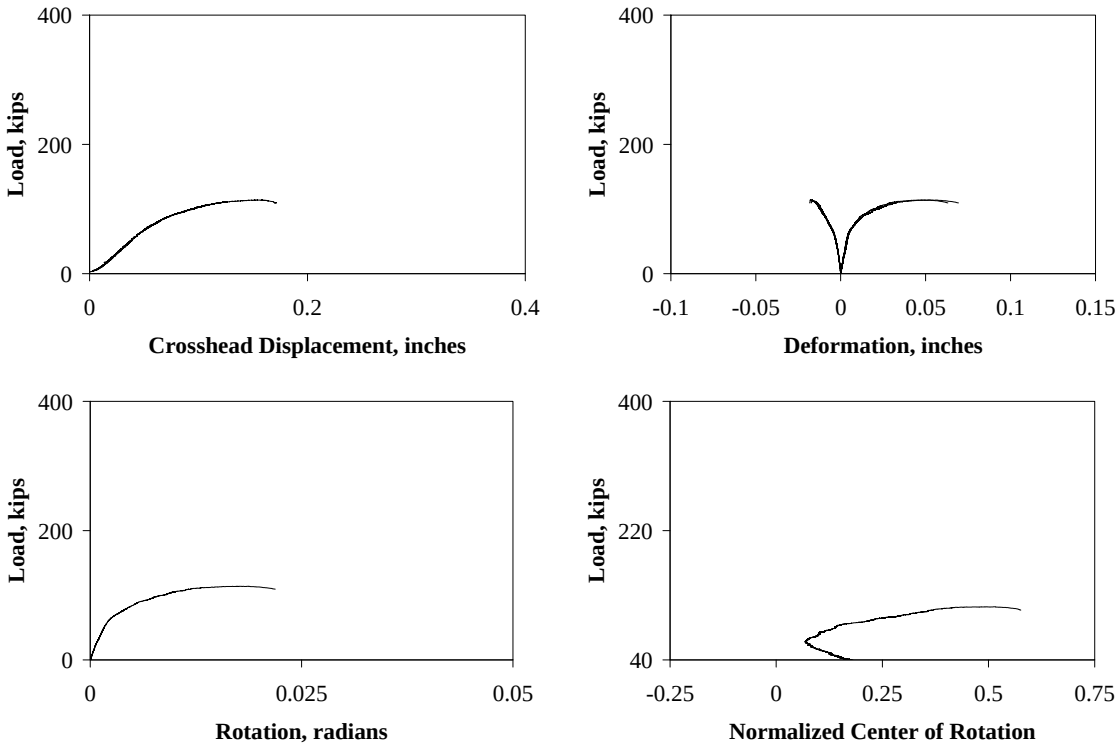

Figure E.1.32 – Test #56, B125_B516_55_2

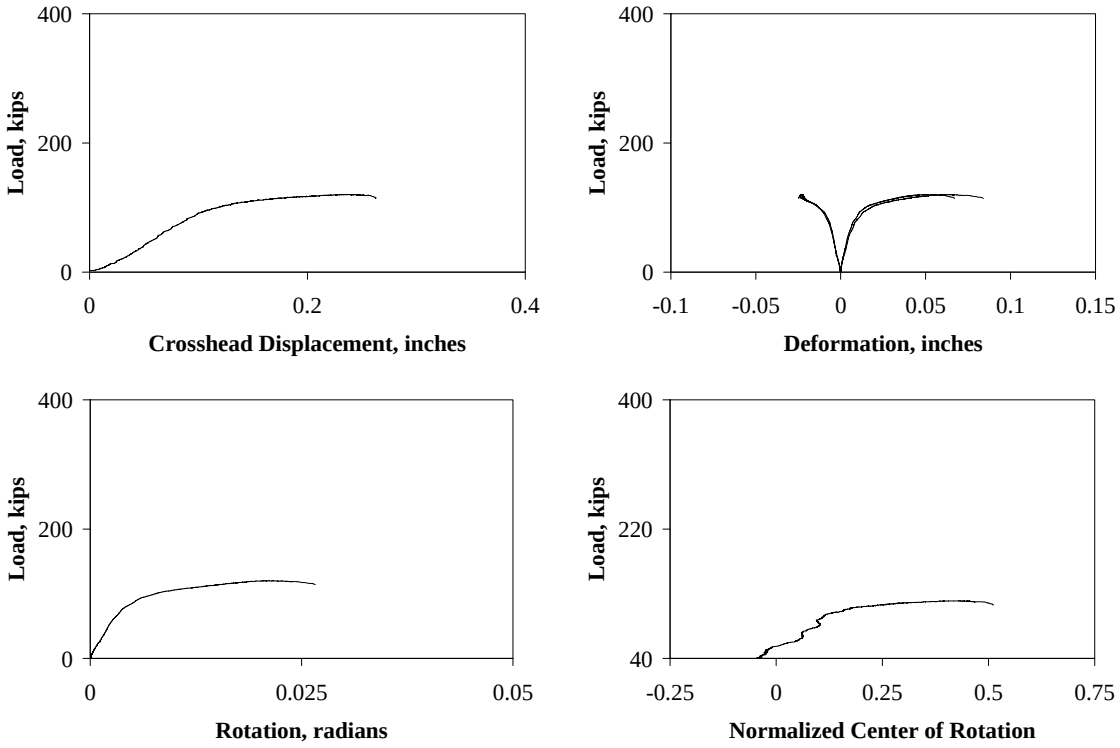

Figure E.1.33 – Test #57, B125_B516_55_3

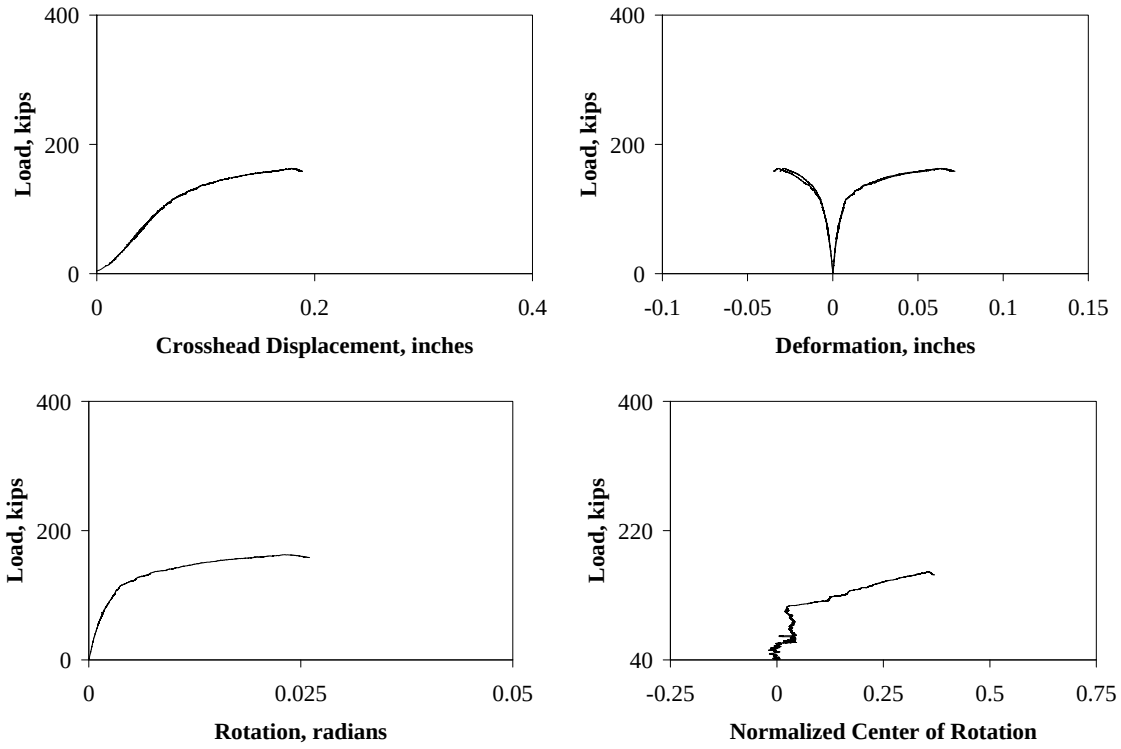

Figure E.1.34 – Test #58, B125_B12_55_1

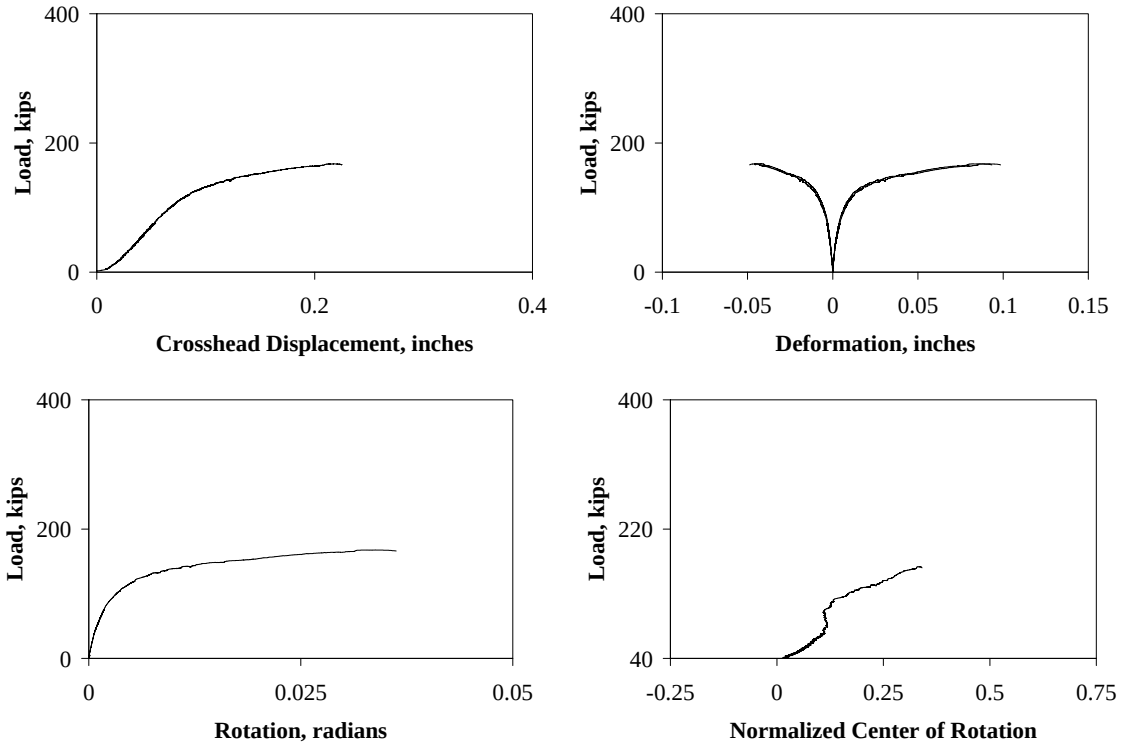

Figure E.1.35 – Test #59, B125_B12_55_2

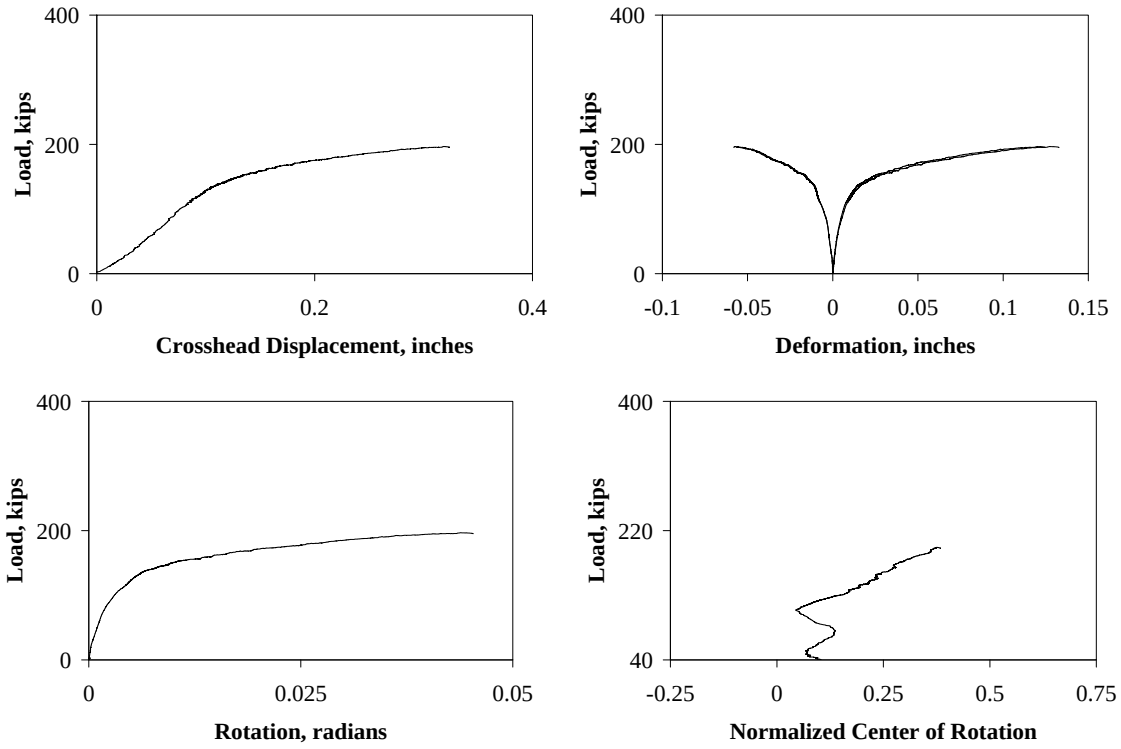

Figure E.1.36 – Test #60, B125_B12_55_3

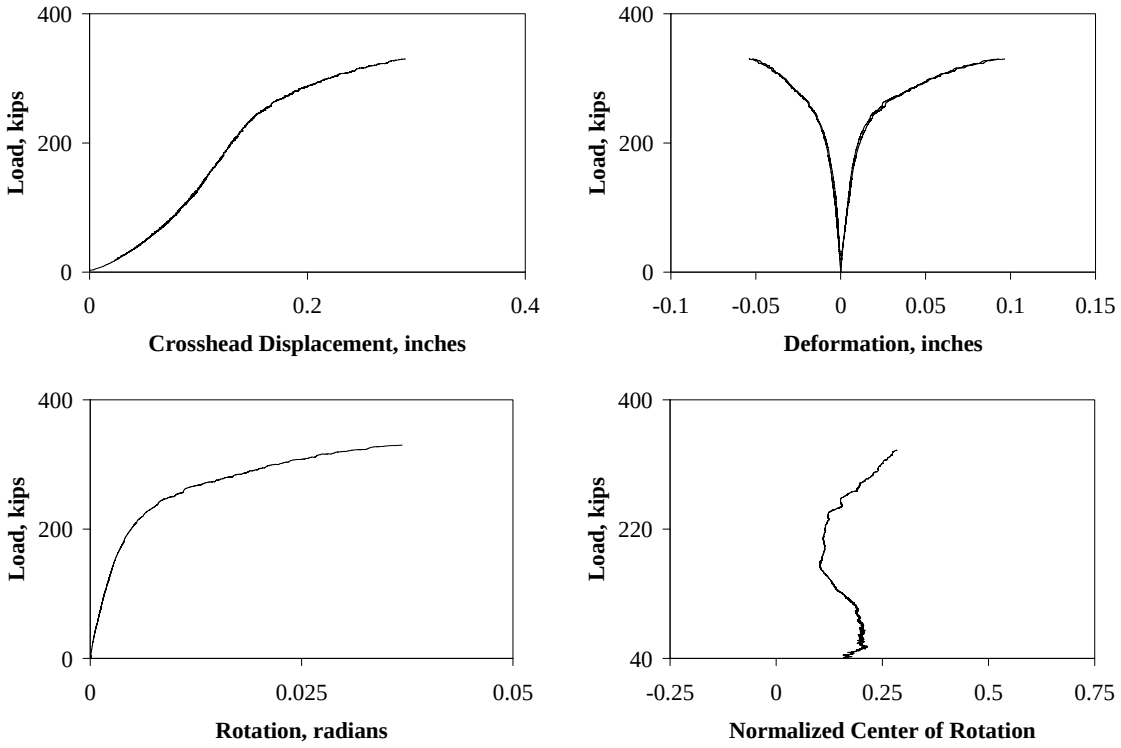

Figure E.1.37 – Test #61, B175_B516_3_1

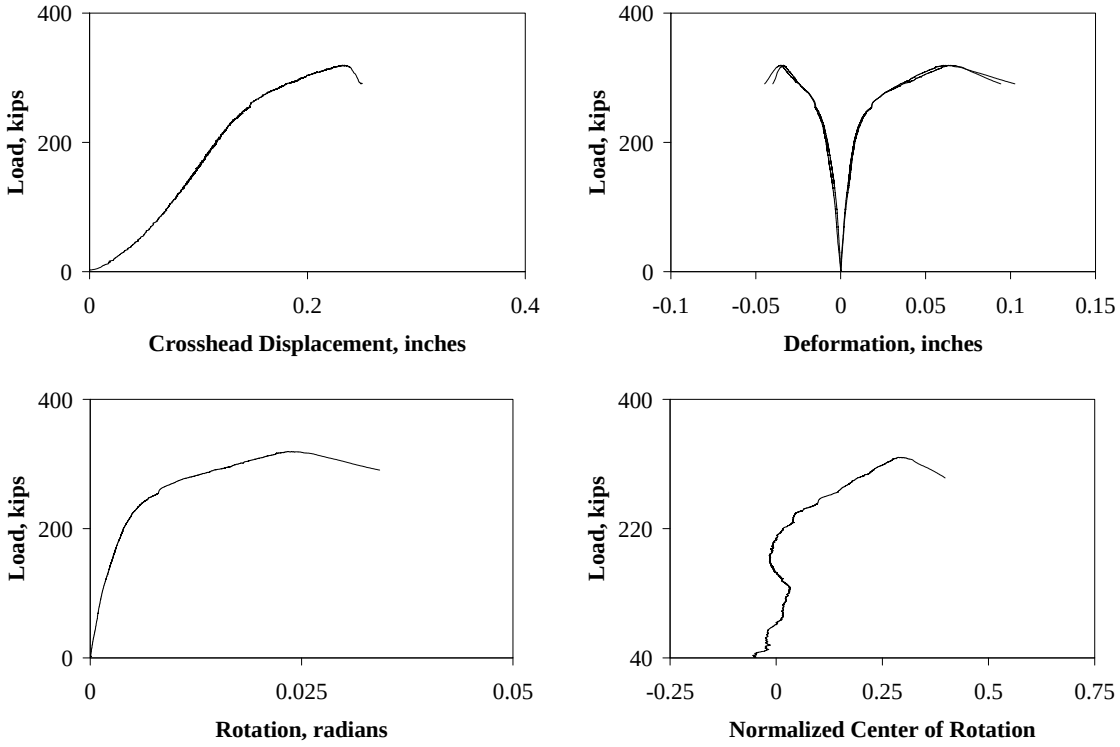

Figure E.1.38 – Test #62, B175_B516_3_2

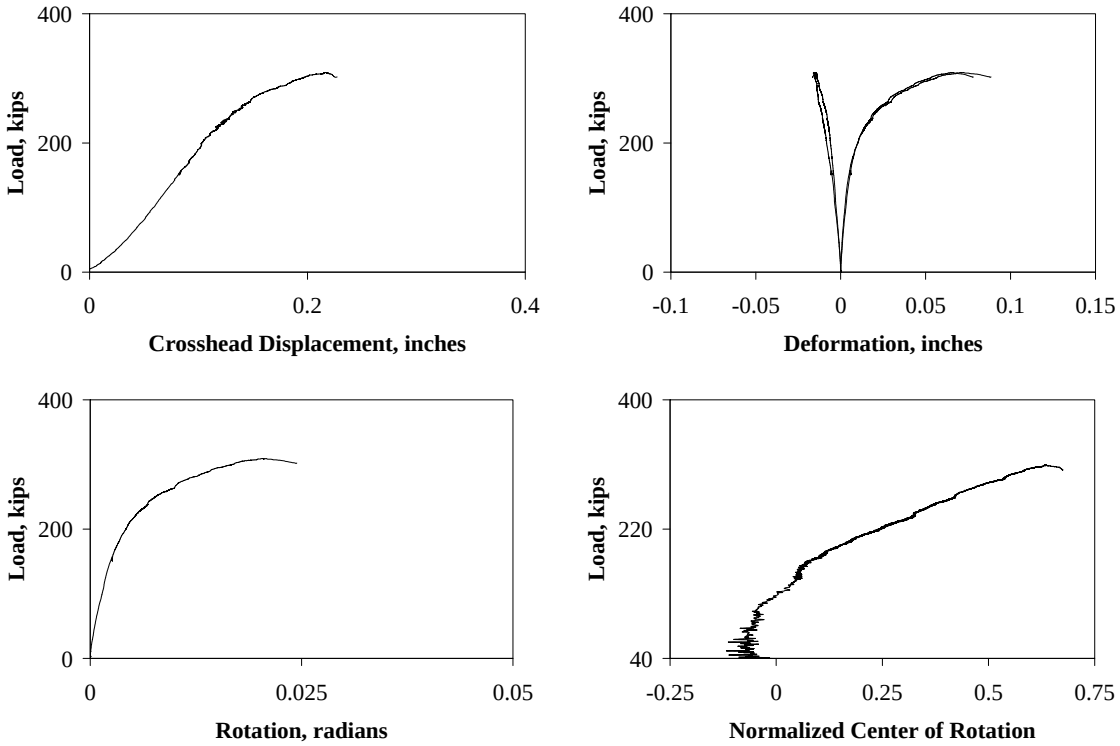

Figure E.1.39 – Test #63, B175_B516_3_3

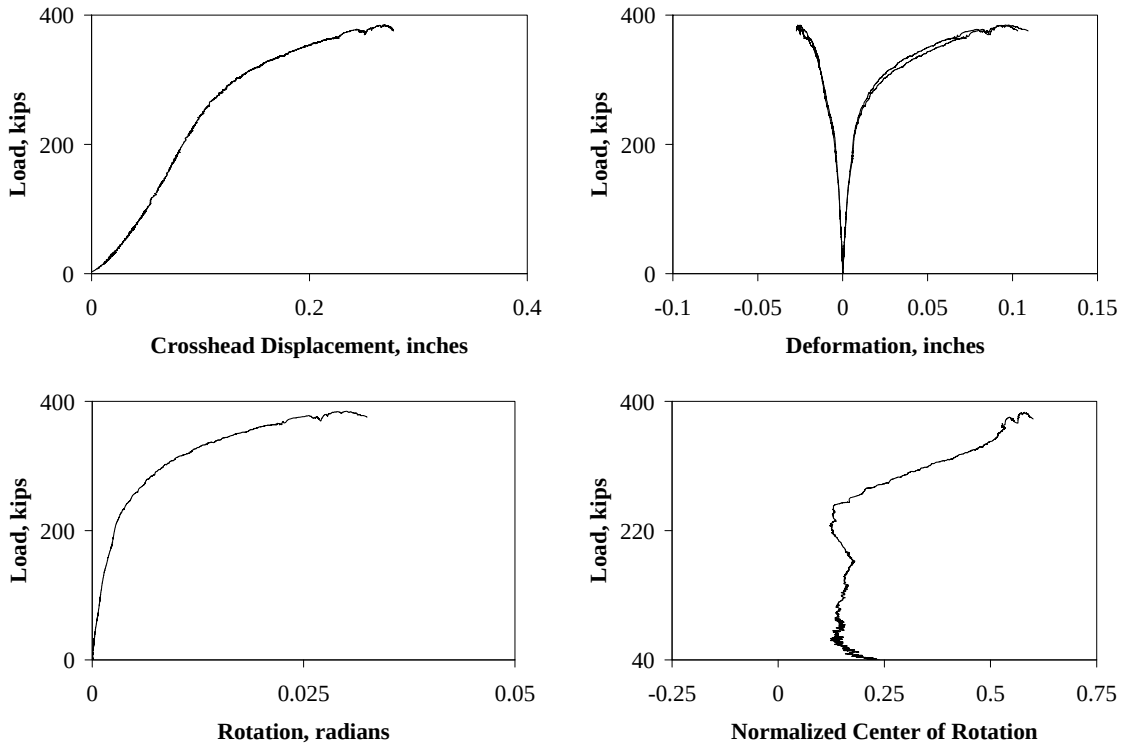

Figure E.1.40 – Test #64, B175_B12_3_1

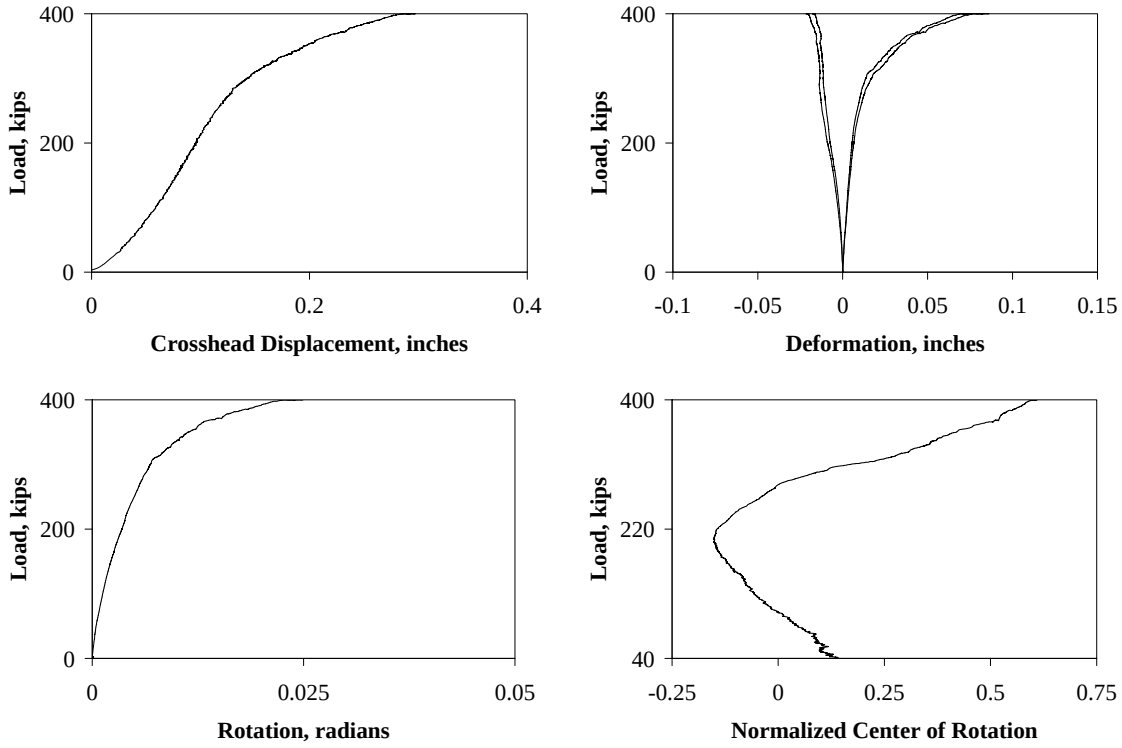

Figure E.1.41 – Test #65, B175_B12_3_2

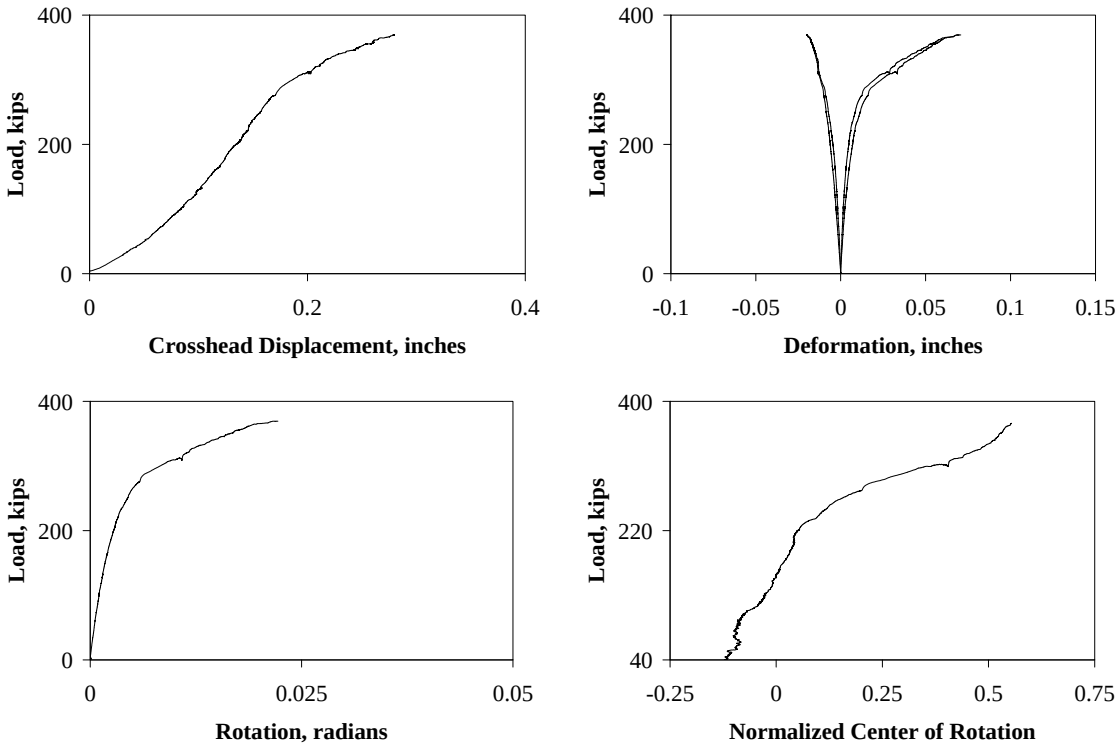

Figure E.1.42 – Test #66, B175_B12_3_3

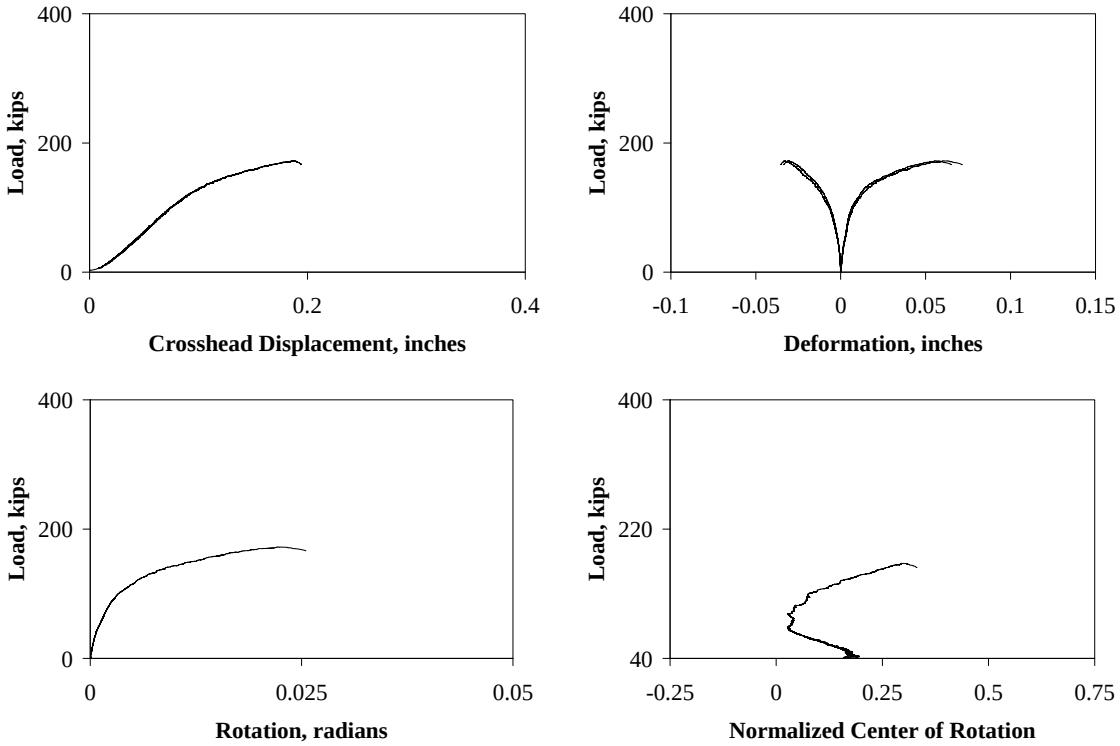

Figure E.1.43 – Test #67, B175_B516_55_1

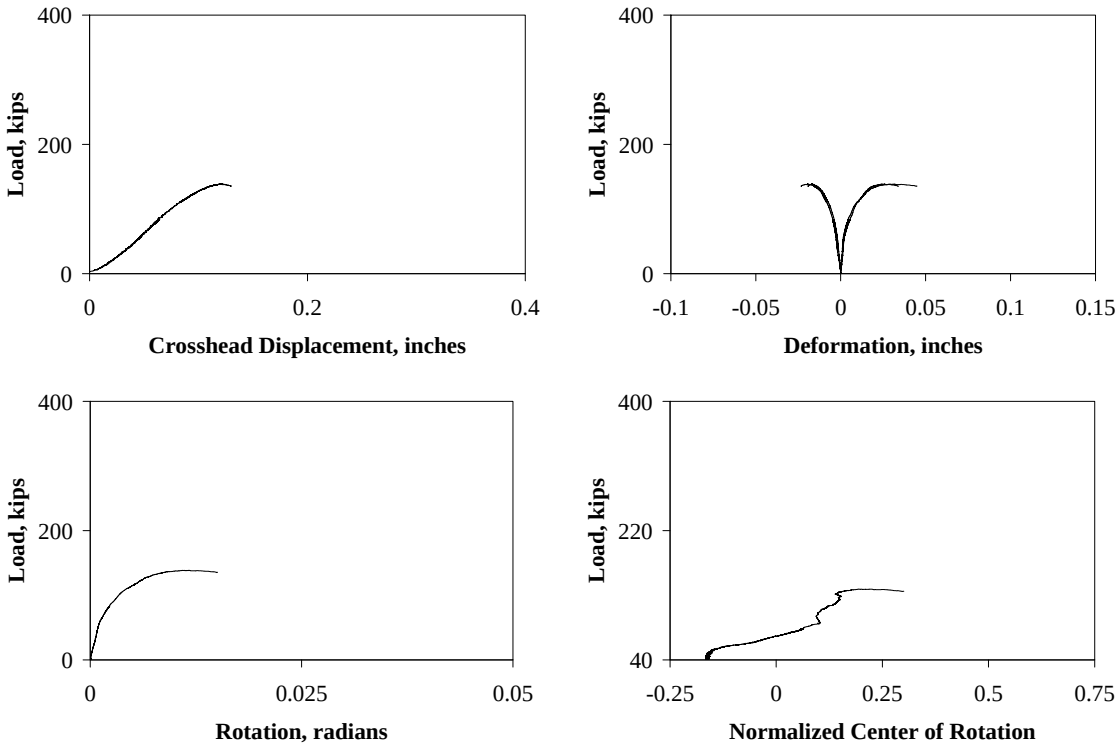

Figure E.1.44 – Test #68, B175_B516_55_2

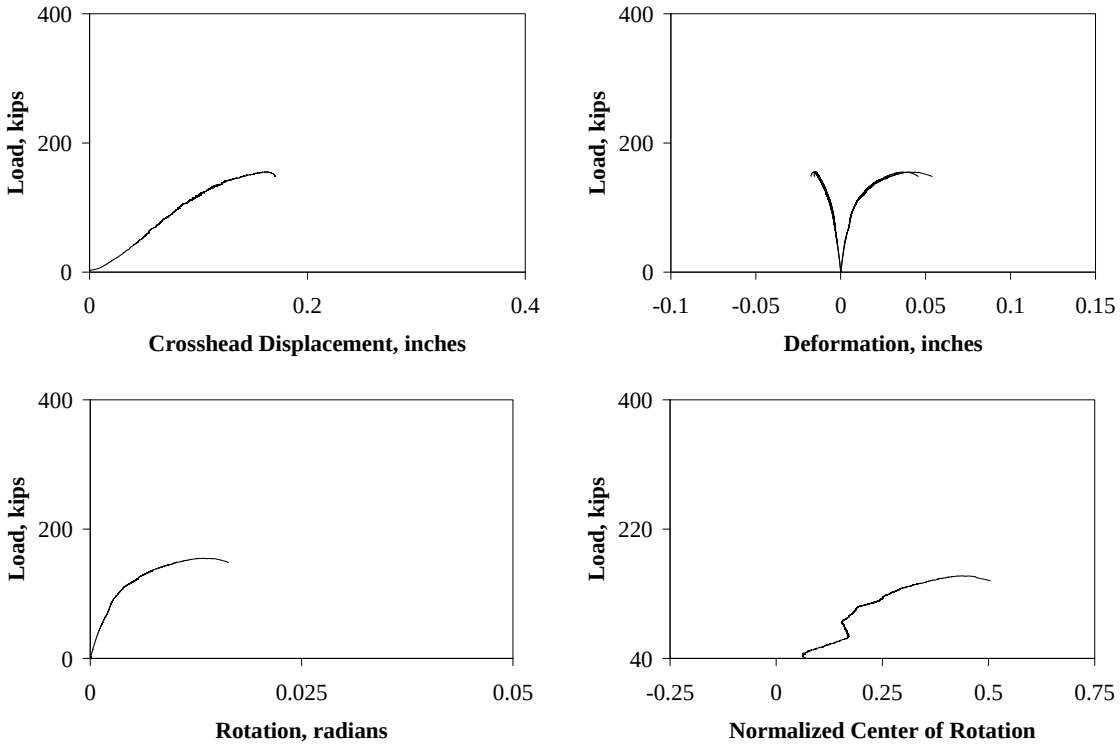

Figure E.1.45 – Test #69, B175_B516_55_3

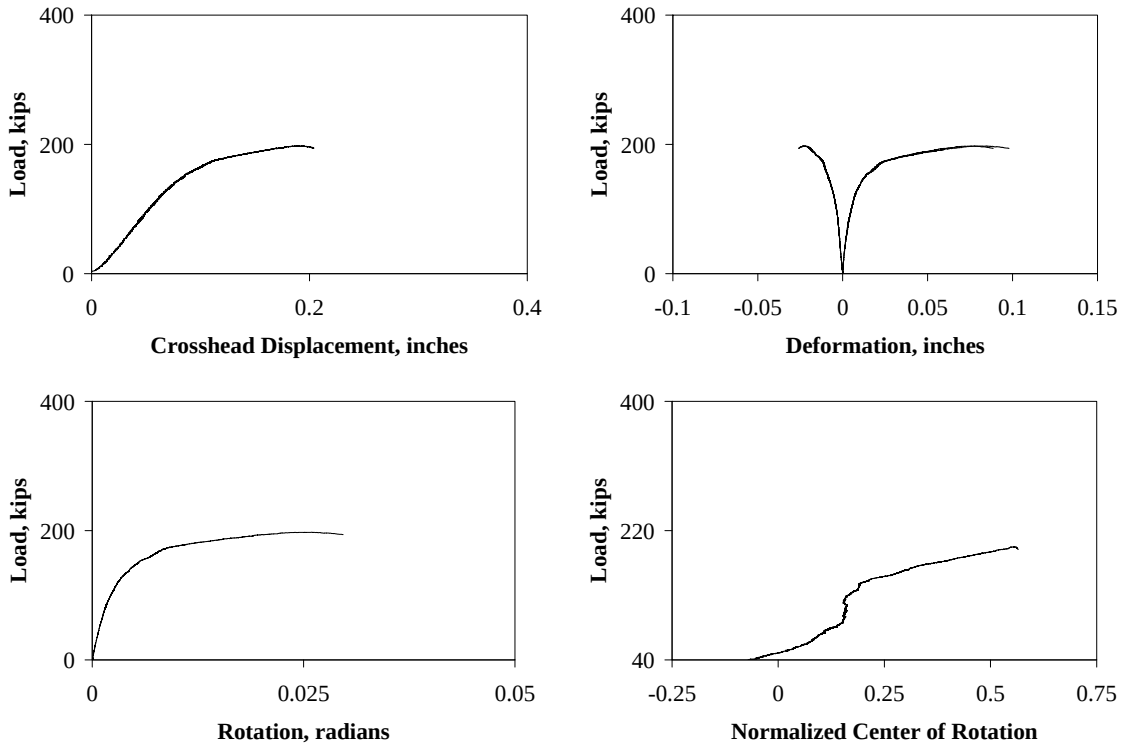

Figure E.1.46 – Test #70, B175_B12_55_1

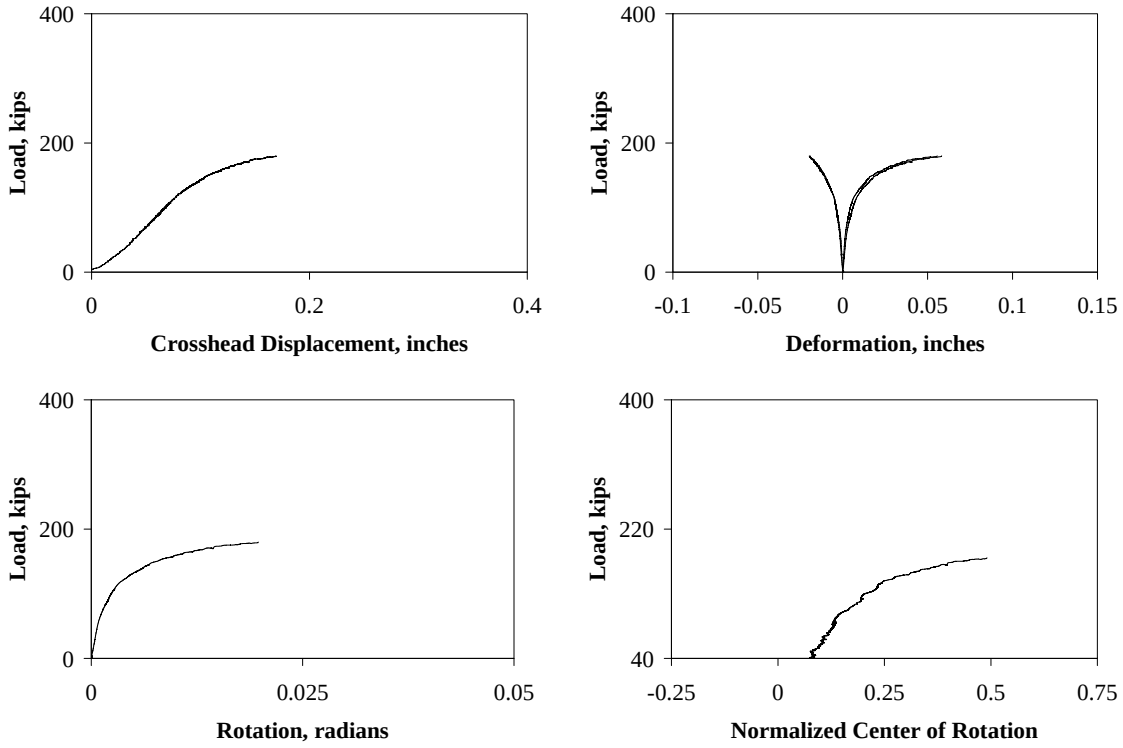

Figure E.1.47 – Test #71, B175_B12_55_2

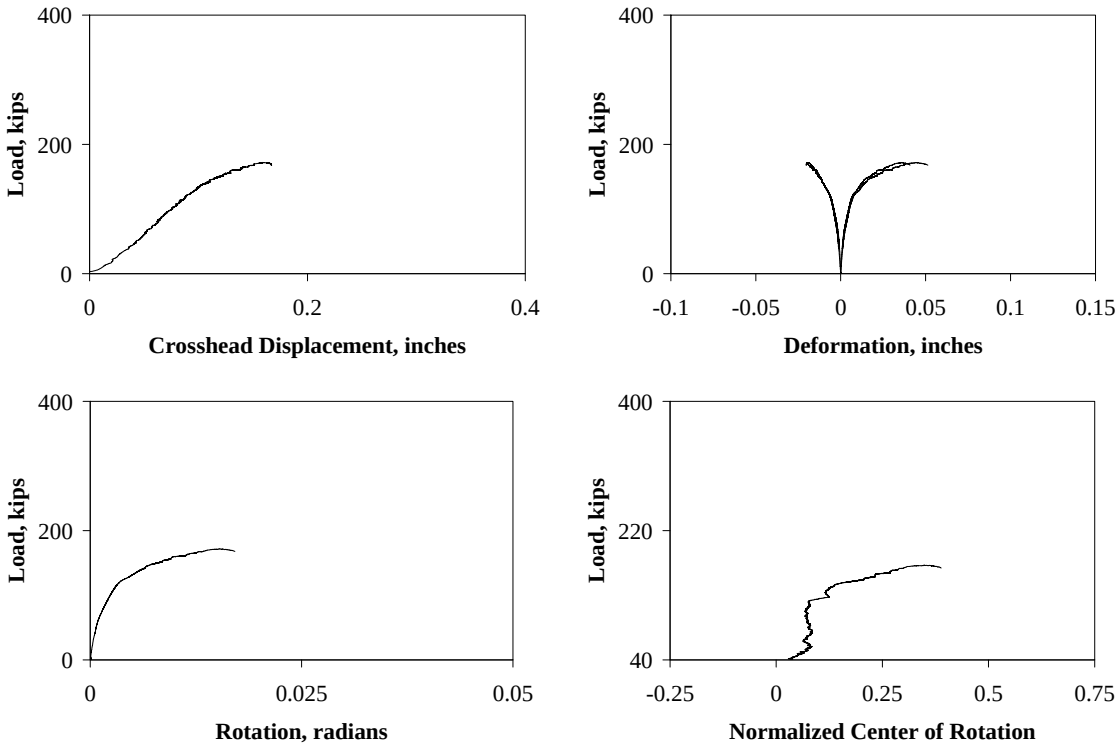

Figure E.1.48 – Test #72, B175_B12_55_3

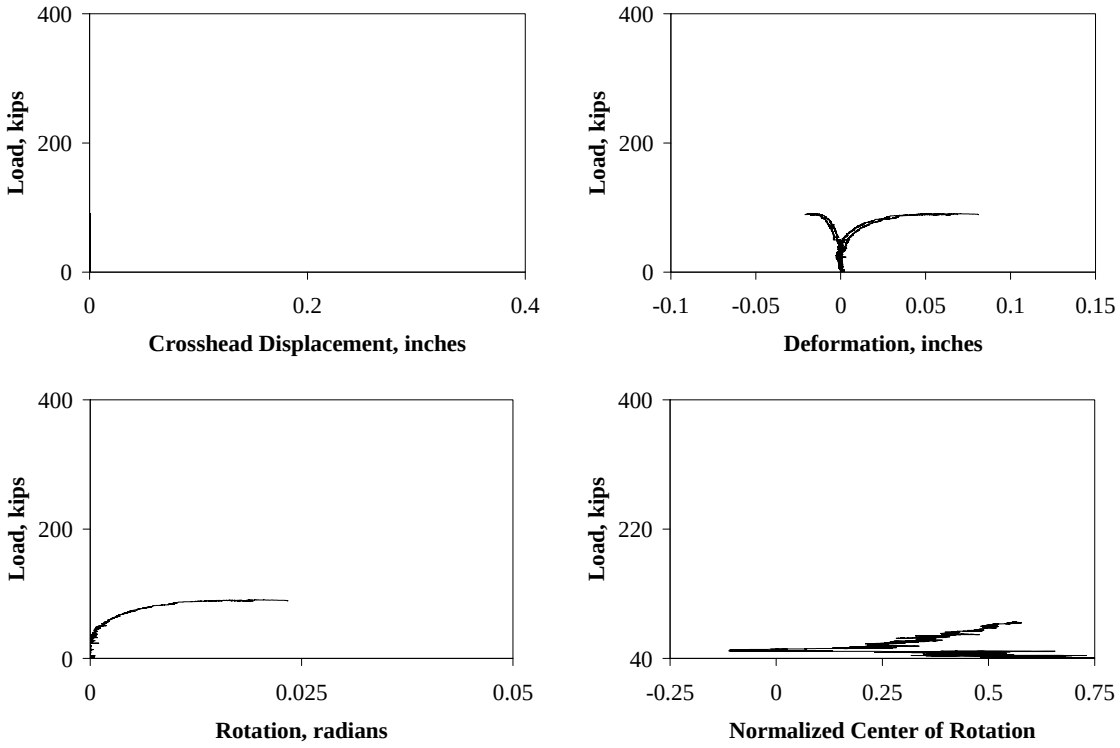

Figure E.1.49 – Test #73, B175_B516_85_1

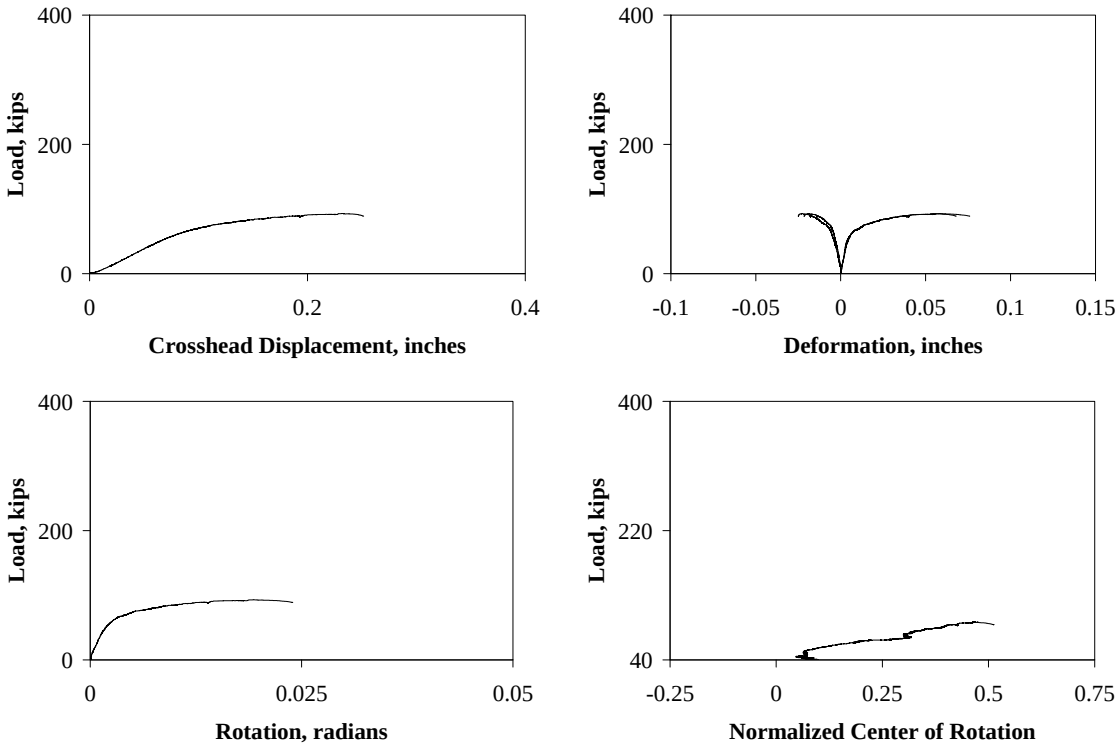

Figure E.1.50 – Test #74, B175_B516_85_2

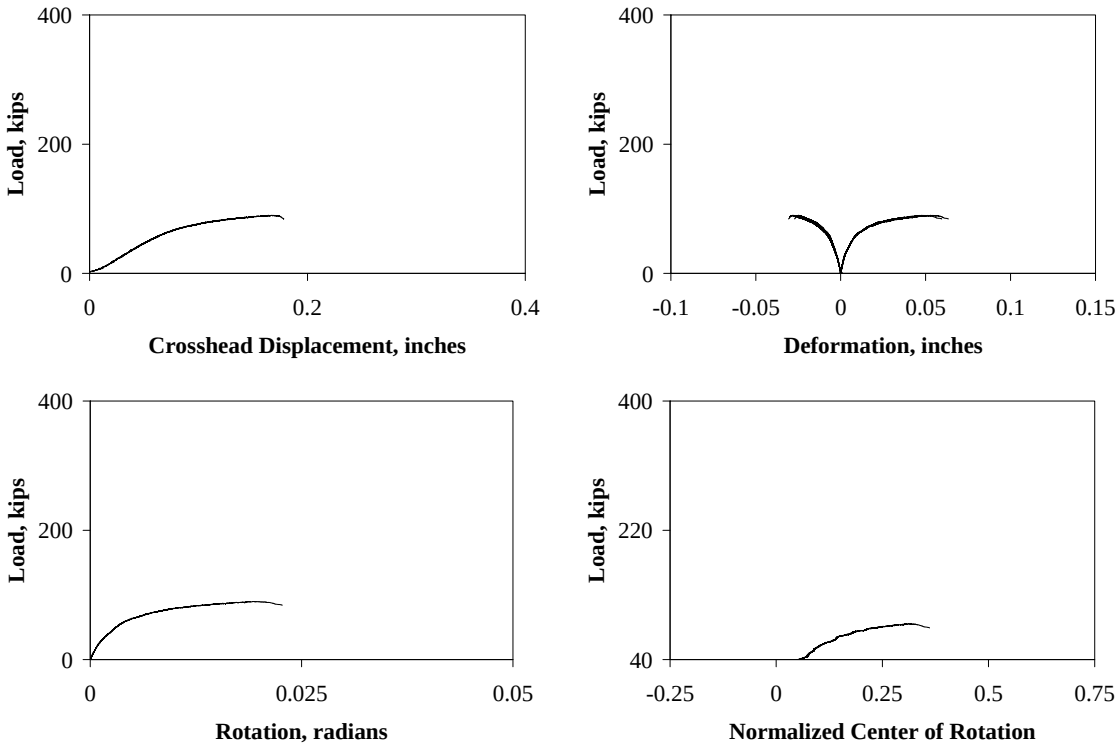

Figure E.1.51 – Test #75, B175_B516_85_3

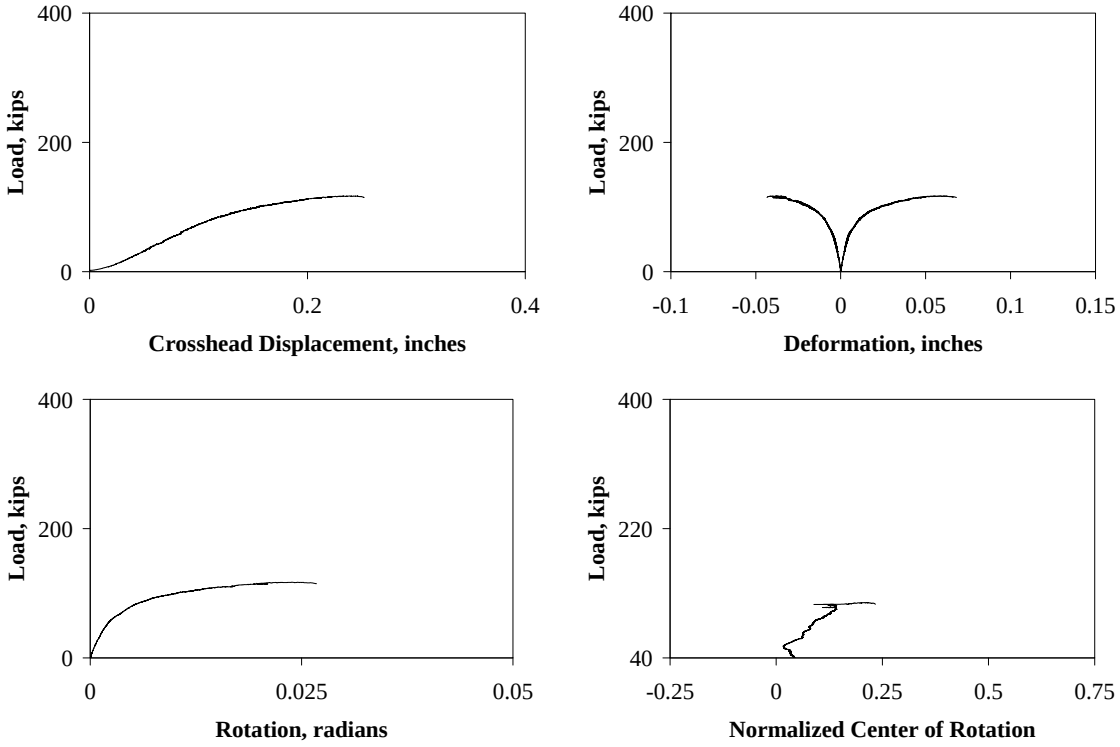

Figure E.1.52 – Test #76, B175_B12_85_1

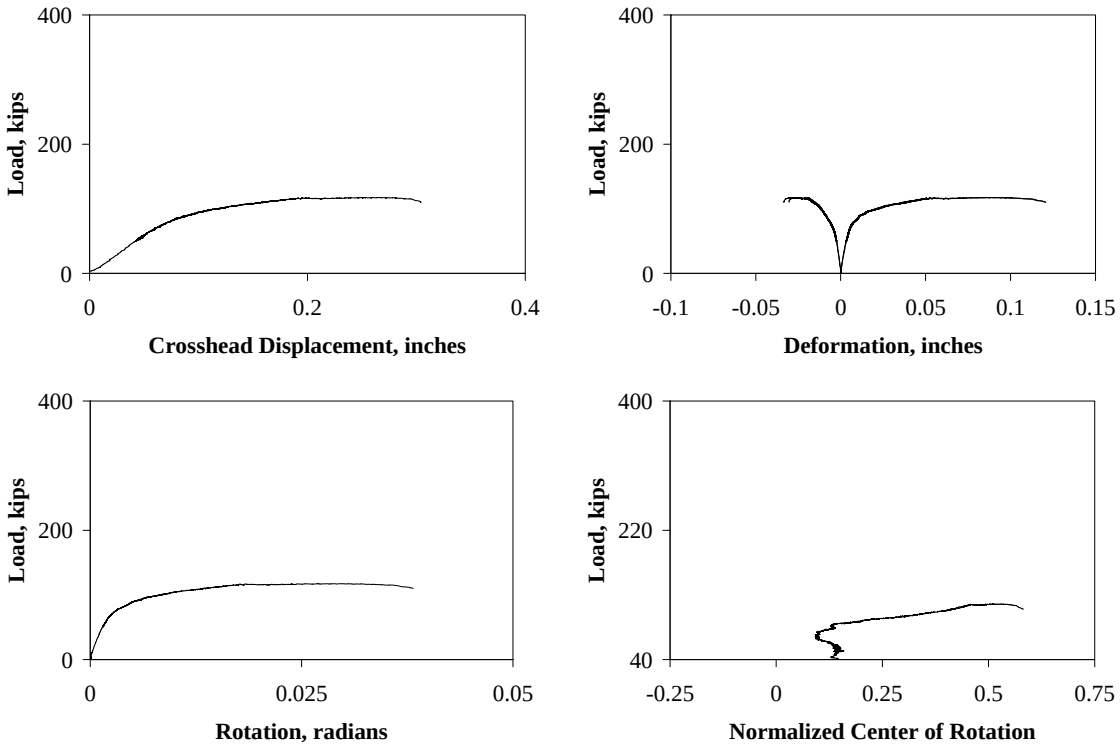

Figure E.1.53 – Test #77, B175_B12_85_2

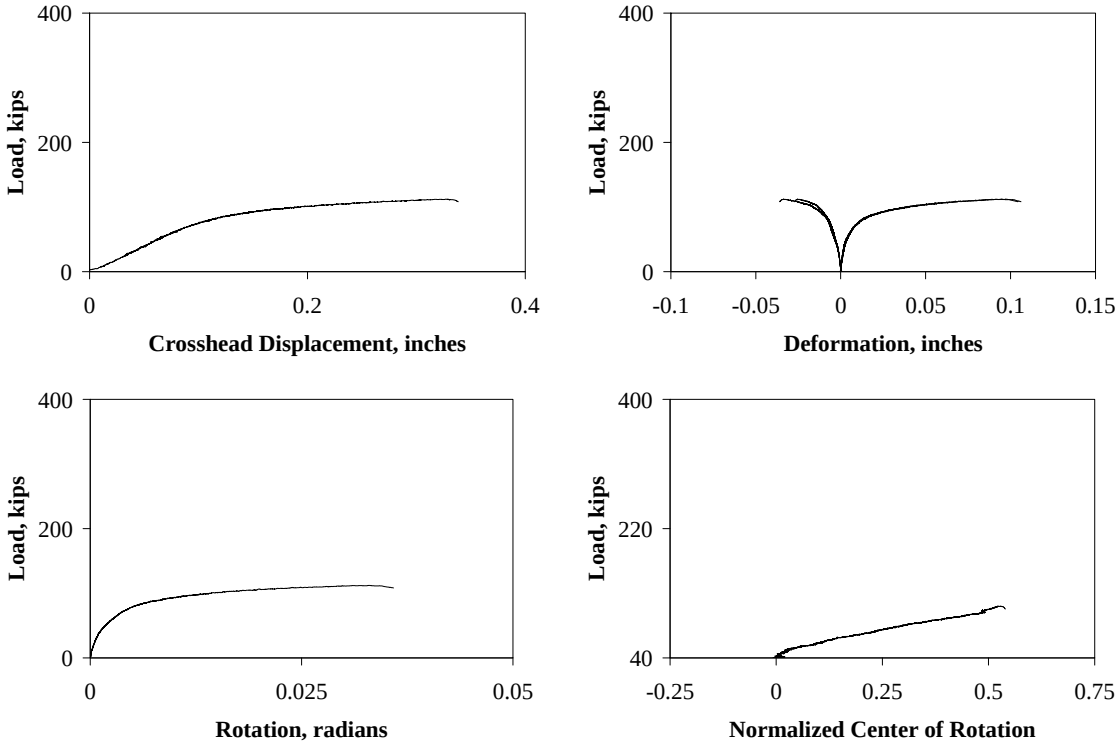

Figure E.1.54 – Test #78, B175_B12_85_3

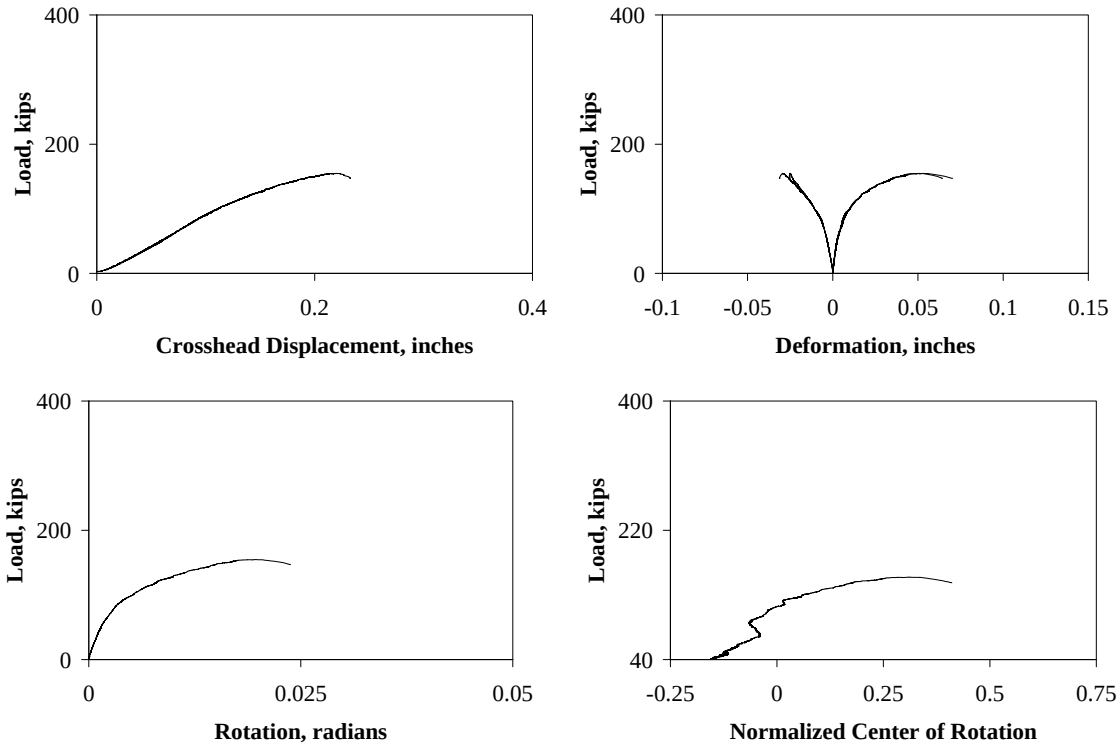

Figure E.1.55 – Test #79, B250_B516_55_1

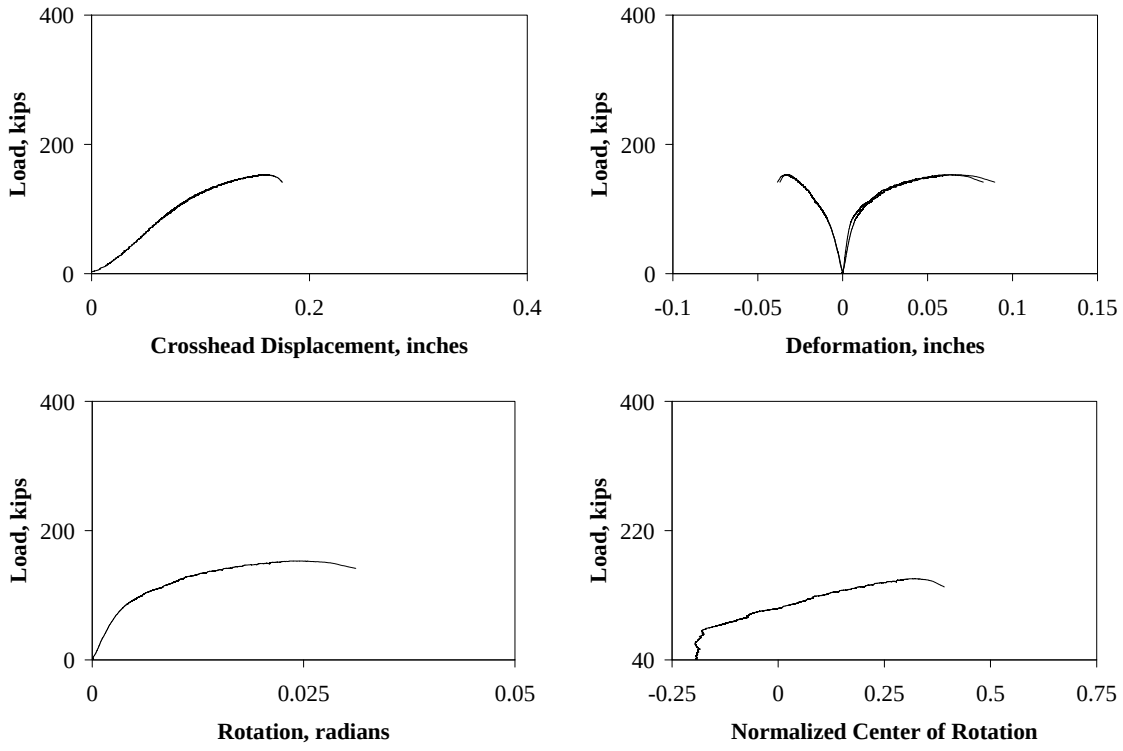

Figure E.1.56 – Test #80, B250_B516_55_2

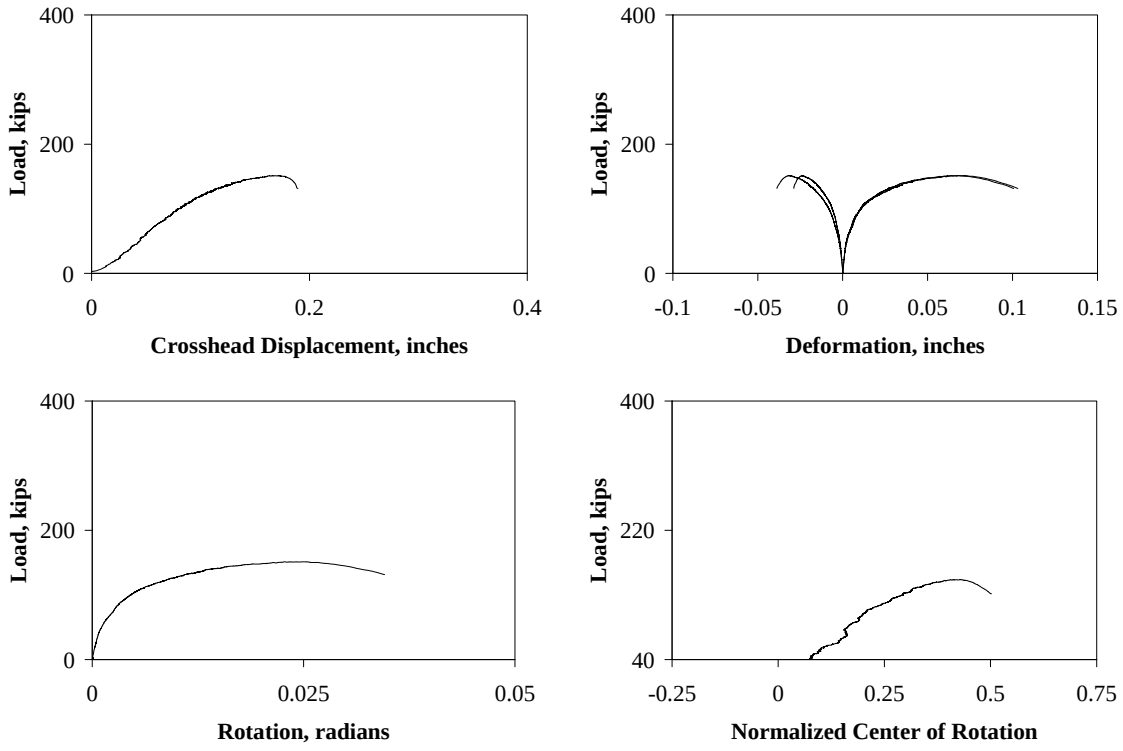

Figure E.1.57 – Test #81, B250_B516_55_3

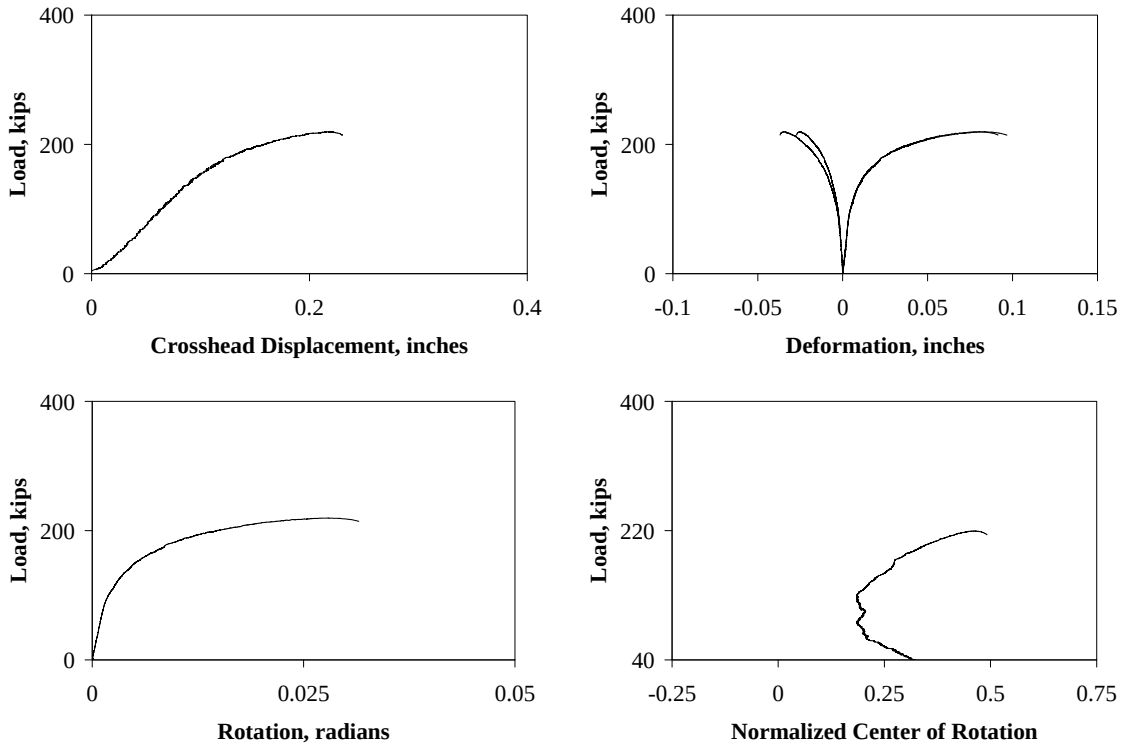

Figure E.1.58 – Test #82, B250_B12_55_1

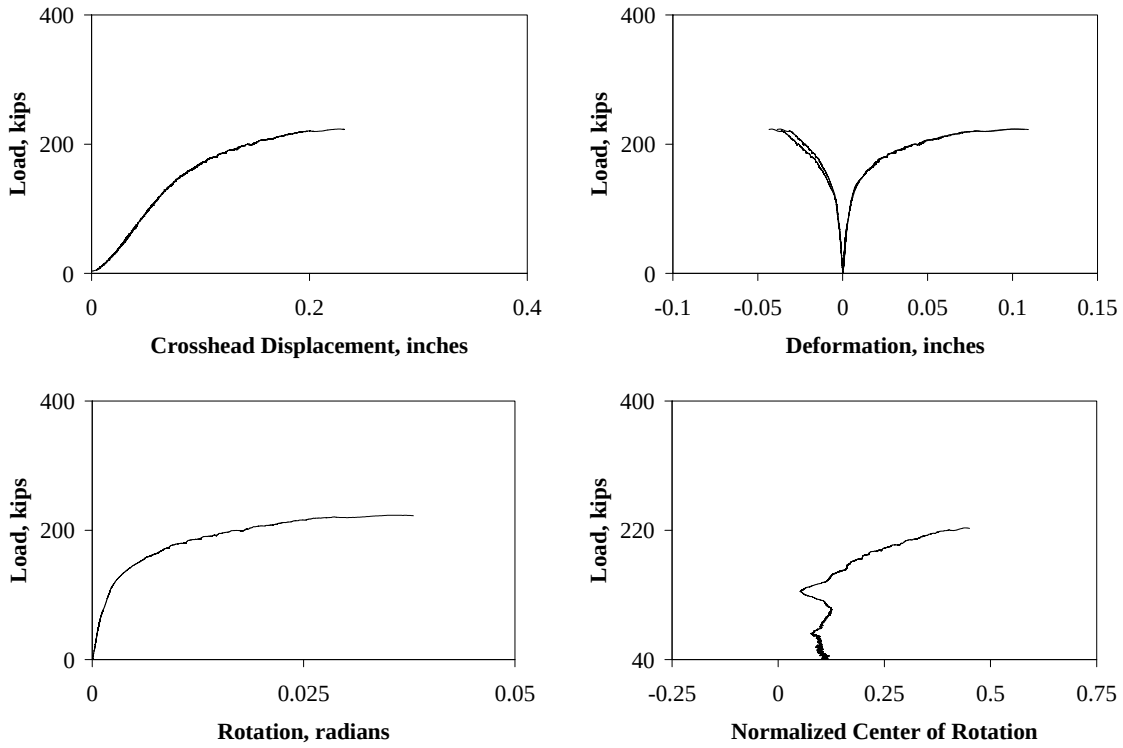

Figure E.1.59 – Test #83, B250_B12_55_2

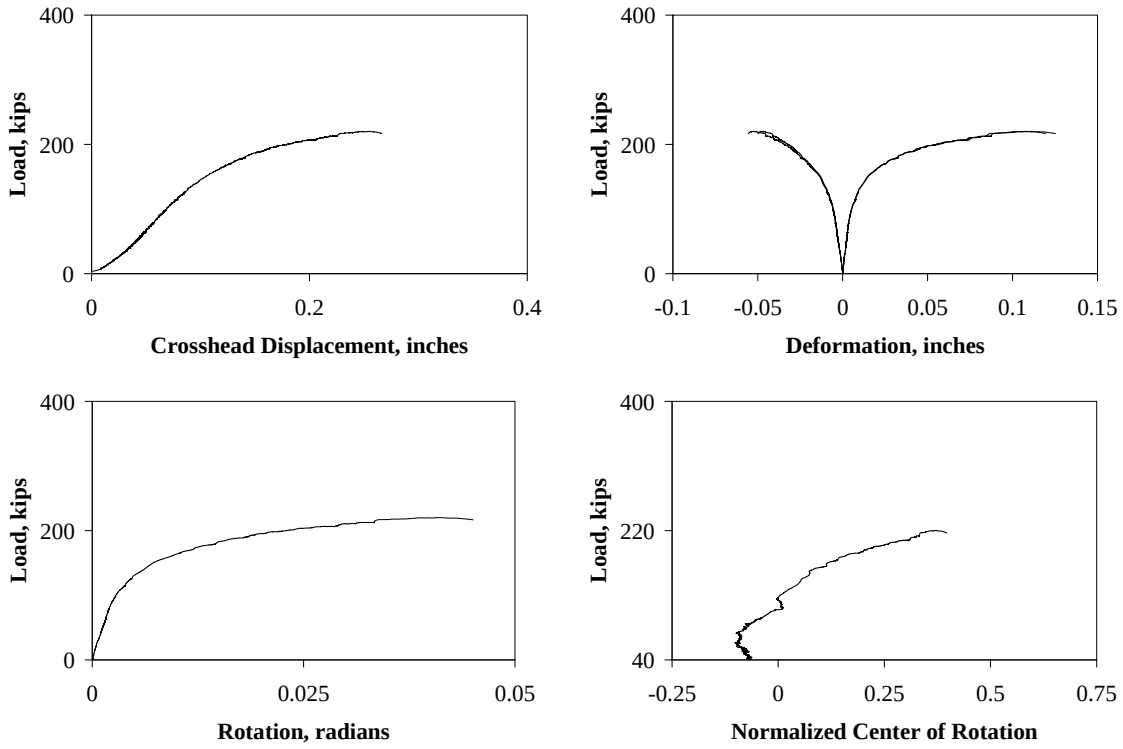

Figure E.1.60 – Test #84, B250_B12_55_3

E.2 Strain Response

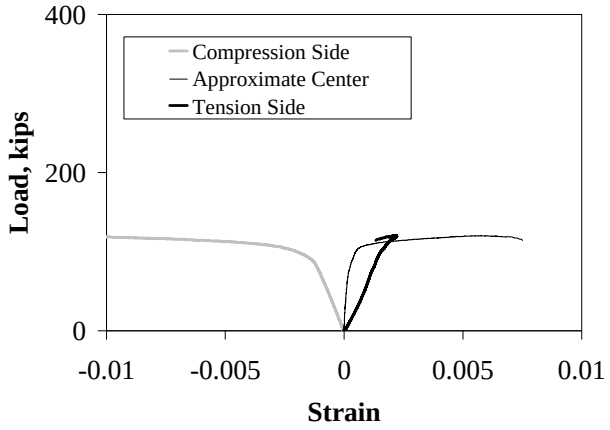

Figure E.2.1 – Test #57, B125_B516_55_3

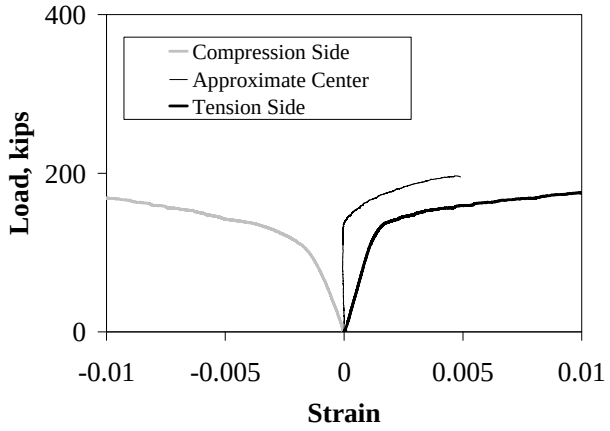

Figure E.2.2 – Test #60, B125_B12_55_3

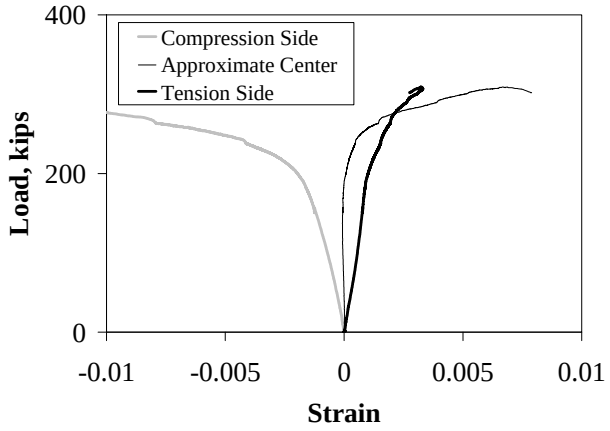

Figure E.2.3 – Test #63, B175_B516_3_3

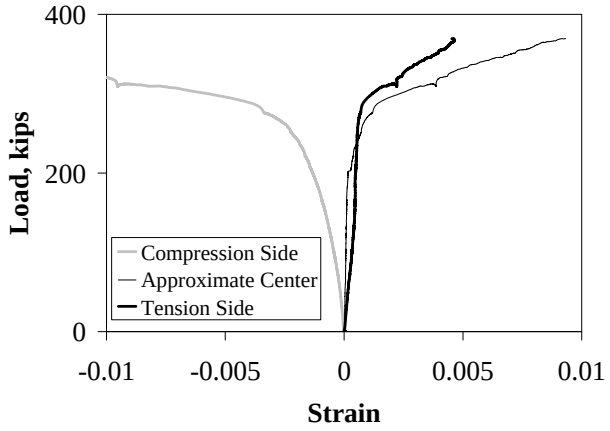

Figure E.2.4 – Test #66, B175_B12_3_3

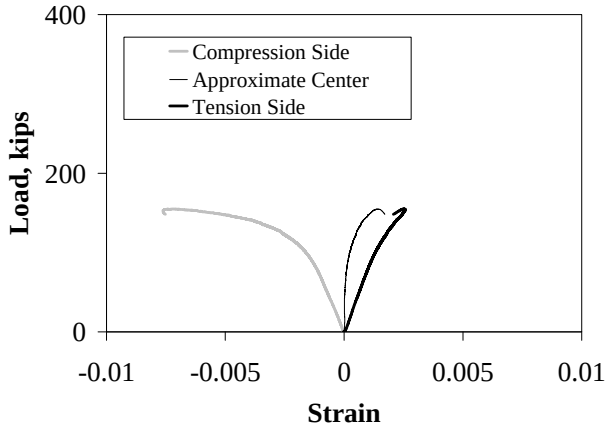

Figure E.2.5 – Test #69, B175_B516_55_3

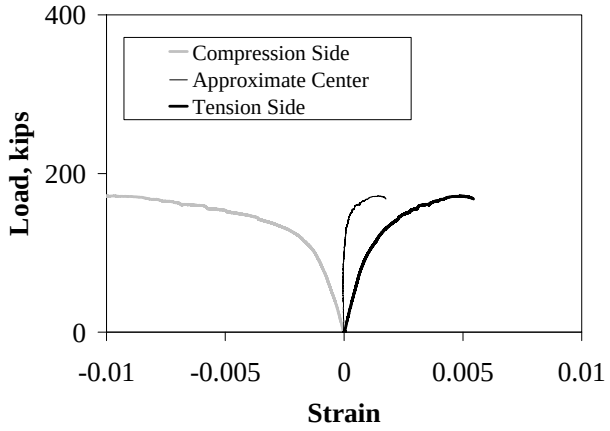

Figure E.2.6 – Test #72, B175_B12_55_3

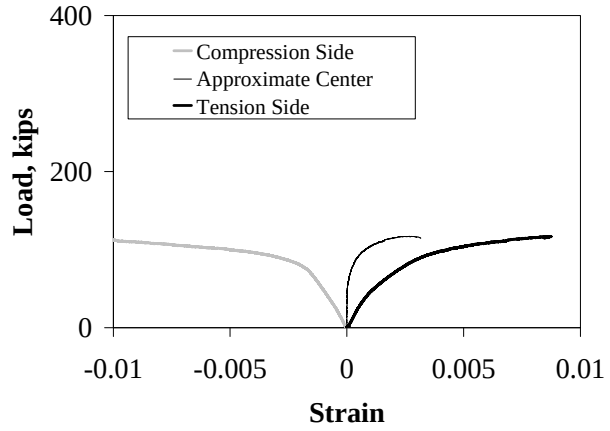

Figure E.2.7 – Test #76, B175_B12_85_1

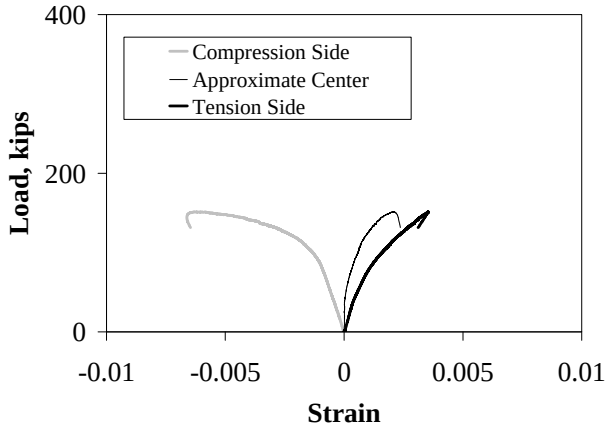

Figure E.2.8 – Test #81, B250_B516_55_3

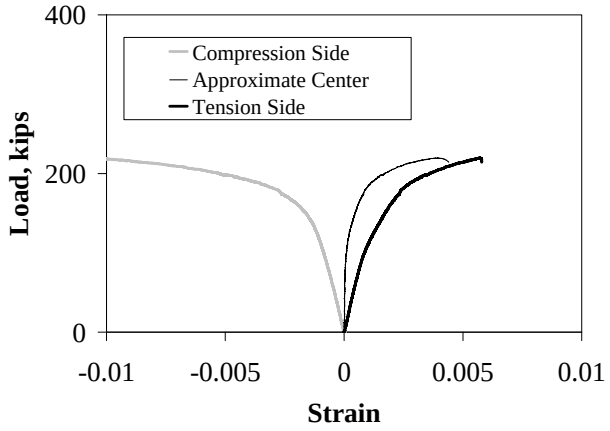

Figure E.2.9– Test #82, B250_B12_55_1

Appendix F

Instantaneous Center of Rotation Approach

Dawe and Kulak developed an iterative procedure for welded joints loaded out-of-plane by modeling the plate bearing in the compression zone using a triangular stress block, combined with the instantaneous center of rotation approach in the tension zone. The instantaneous center of rotation approach requires that the weld on the tension side of the joint be modeled by discrete weld segments. To obtain a solution, initial values for r_o and y_o (see Figure F.1) are assumed, which establishes the location of the instantaneous center. Each weld element has it own resisting force oriented in a direction perpendicular to the radial distance to the instantaneous center. The force in each weld segment has vertical and horizontal components $(R_i)_v$ and $(R_i)_h$. In the compression zone the normal force H_b represents the resultant of the triangular stress block and the vertical force V_b represents the strength of the weld in the compression zone loaded at an angle $\theta = 0°$.

$$V_b = \frac{y_o}{(L - y_o)} \sum_1^n (R_i)_v \qquad [F.1]$$

The resultant force of the triangular stress distribution as shown in Figure F.1 acts two-thirds y_o below the neutral axis and is expressed as:

$$H_b = \frac{y_o \sigma_y t}{2} \qquad [F.2]$$

where σ_y is the maximum stress in the compression zone, taken as the yield strength of the plate material, and *t* is the plate thickness. The sum of the moments created by all the forces about the instantaneous center is equal to

$$P(e + r_o) - \sum_1^n (R_i r_i) - r_o V_b - \left(\frac{2}{3}\right) y_o H_b = 0 \qquad [F.3]$$

Similarly, the sum of the vertical forces on the connection is equal to:

$$\sum_1^n (R_i)_v + V_b - P = 0 \qquad [F.4]$$

Substituting *P* from Equation F.3 into Equation F.4, gives:

$$\sum_1^n (R_i)_v + V_b = \left[\frac{\sum_1^n (R_i r_i) + r_o V_b + \left(\frac{2}{3}\right) y_o H_b}{e + r_o} \right] \qquad [F.5]$$

The sum of the horizontal forces gives:

$$H_b - \sum_{1}^{n} (R_i)_h = 0 \qquad \text{[F.6]}$$

Once the values r_o and y_o satisfy Equation F.5, it can be used to evaluate the terms in Equation F.6. If both equations are satisfied, the ultimate load has been determined and it can be computed by using Equation F.4. If the pair of values does not satisfied in Equation F.6, then the procedure is need to repeat by choosing another values of r_o and y_o.

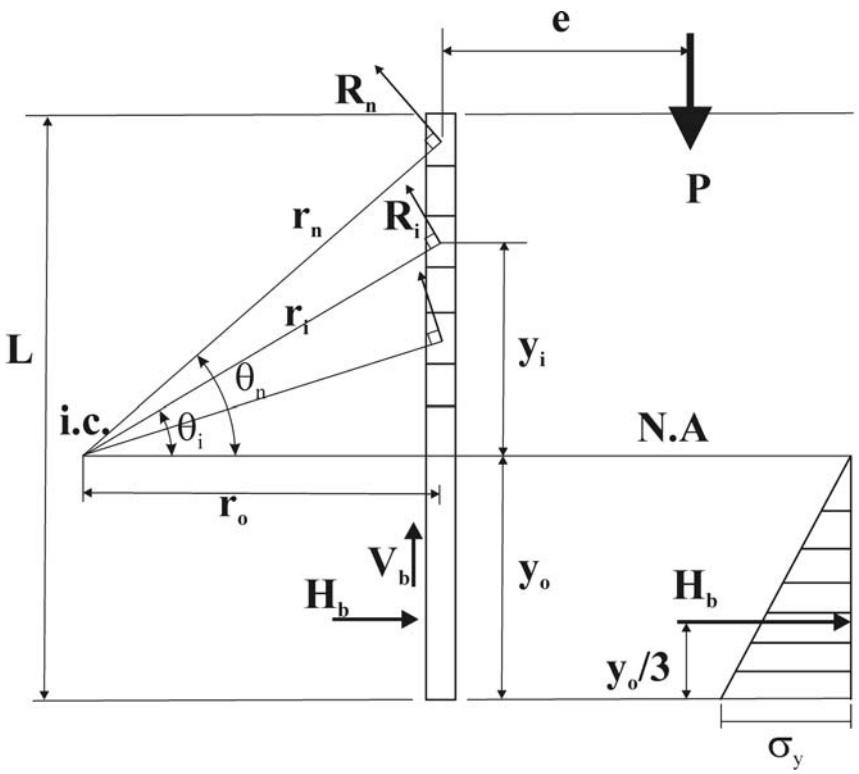

Figure F.1 – Force distribution in weld loaded in shear and bending

Sample Calculations

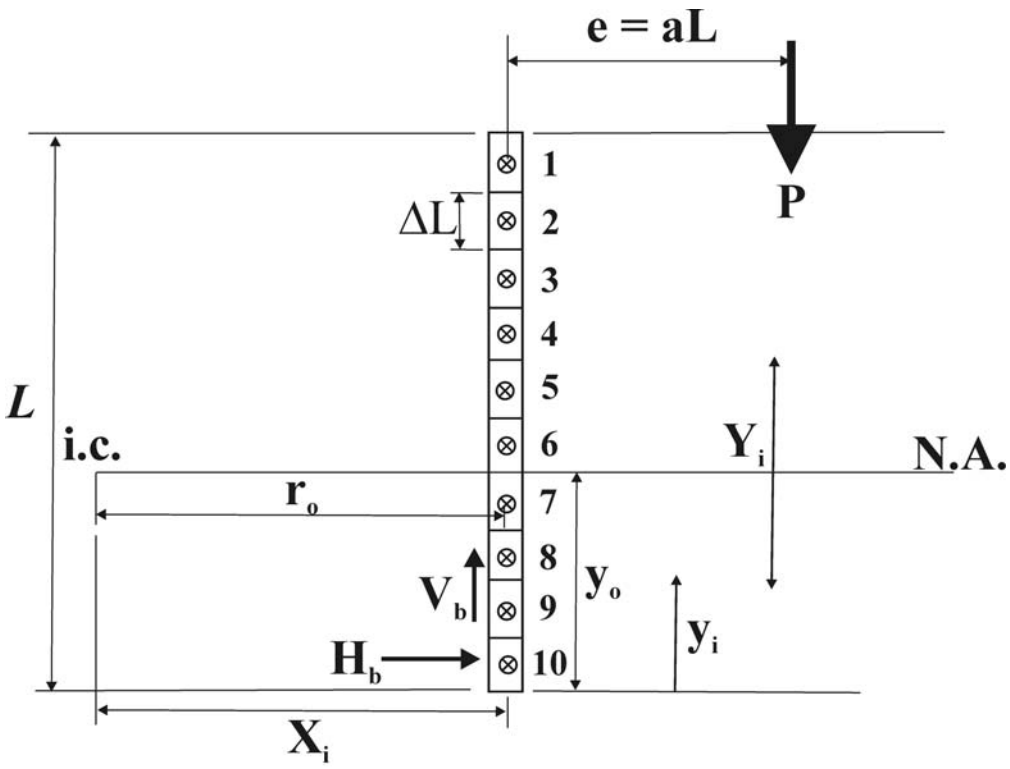

Figure F.2 – Data for sample calculation

Given,

L = 4 in., D (weld size) = 0.4 in., e = 8.5 in., t = 1.76 in, F_{exx} = 97.3 ksi

Assume:

ΔL = 0.4 in.

r_o = 0.110 in.

y_o = 2.235 in.

Solution

Calculation of geometry

In order to perform the calculation, the weld is divided into 10 elements. Together with the configuration presented in Figure F.2 and the assumed position of the instantaneous center, the coordinates of each element of the weld group according to $X_i = x_i + r_o$ and $Y_i = y_i - y_o$ can be computed. The detailed calculations for the geometry of the weld group are presented in Table F.1. It is noted that, when $Y_i = y_i - y_o$ becomes negative, the weld

segment is below the neutral axis. Therefore, the load is transferred through the bearing plate with a triangular stress block.

Table F.1 Summary of example calculations

Elements	x_i	y_i	$X_i = x_i + r_o$	$Y_i = y_i - y_o$	$r_i = \sqrt{X_i^2 + Y_i^2}$	$\lvert\tan\theta_i\rvert$	θ_i
	(in)	(in)	(in)	(in)	(in)		
1	0	3.8	0.110	1.565	1.569	14.181	85.97
2	0	3.4	0.110	1.165	1.170	10.557	84.59
3	0	3.0	0.110	0.765	0.773	6.933	81.79
4	0	2.6	0.110	0.365	0.382	3.309	73.19
5	0	2.2	0.110	-0.035	0.116		
6	0	1.8	0.110	-0.435	0.449		
7	0	1.4	0.110	-0.835	0.842		
8	0	1.0	0.110	-1.235	1.240		
9	0	0.6	0.110	-1.635	1.638		
10	0	0.2	0.110	-2.035	2.038		

Elements	Δ_{max}	Δ_i	μ_i	λ_i	R_{ulti}	R_i	$(R_i)_v$	$(R_i)_h$	$R_i r_i$
	(in)	(in)			(kips)	(kips)	(kips)	(kips)	(kips in)
1	0.027	0.0208	199.8	1.403	15.7	16.0	1.1	15.9	25.0
2		0.0155	196.7	1.375	15.7	15.2	1.4	15.2	17.8
3		0.0102	190.6	1.320	15.7	13.3	1.9	13.2	10.3
4		0.0051	172.7	1.164	15.6	8.6	2.5	8.3	3.3
5									
6									
7									
8									
9									
10									
						$\sum =$	**7.0**	**52.5**	**56.4**

Calculation of resisting force

Since the deformation of each weld element is assumed to be directly proportional to its distance from the instantaneous center, the deformation of the i^{th} weld element is

$$\Delta_i = \frac{r_i}{r_n}\Delta_{max} \qquad [F.7]$$

Once the angle θ_i is obtained for all elements, the values of Δ_{max} and Δ_i are computed using Equations 2.2 and F.7, respectively. The resisting force for each weld segment (R_i) is calculated using the Equations 2.1, and 2.3 to 2.5, with the adjustments of the weld dimensions (the equations proposed by Butler and Kulak (1971) are based on a weld size

of 0.25 in.) and E60 electrode. The force in weld segment *i*, R_i, has vertical and horizontal force components given by

$$\left(R_i\right)_v = \frac{r_o}{r_i} \times R_i \qquad [F.8]$$

$$\left(R_i\right)_h = \frac{y_i}{r_i} \times R_i \qquad [F.9]$$

The sum of the vertical and horizontal components in each element is also presented in the last row of the table. Hence, V_b and H_b can be obtained by Equations F.1 and F.2. In this example only half of the plate thickness and one single weld are considered. Therefore, H_b should be calculated based on half of the plate thickness instead of the full plate thickness (0.88 in. instead of 1.76 in.). For a joint with two fillet welds, the load is simply twice the load presented in this example.

Lastly, Equations F.5 and F.6 are checked. For the selected position of the instantaneous center, Equation F.6 indicates an unbalanced horizontal force 0.00216, which is considered to be negligibly small. Therefore, the assumed values of r_o and y_o represent a valid solution. The ultimate load (*P*) of the single fillet weld is obtained using Equations F.4 and F.5. It is found to be 15.8 kips. The total ultimate capacity for a joint with two fillet welds and a plate twice as thick as the one used for the calculations would be 31.6 kips.

Dawe and Kulak developed a FORTRAN program to predict the ultimate capacity of eccentrically loaded fillet welded joints. The program generates successive approximations for the location of the neutral axis, y_o, along the weld length and the distance between the weld axis and the instantaneous center, r_o, by using the Regula Falsi iterative technique. Pairs of y_o and r_o are successively generated until the connection is in equilibrium. However, the program as written by Dawe and Kulak has a number of restrictions about the size and number of individual weld segments. In order to remove the restrictions on the number and size of weld segments and to facilitate the experimentation of the method of instantaneous center of rotation with various loads versus deformation models for the weld and stress distributions in the compression zone, a computer generated spreadsheet was developed for all the iterative procedures described above.

Appendix G

Predicted Welded Joint Capacity for All Existing Models

The predicted welded joint capacities of tested specimens from Dawe and Kulak (1972), Beaulieu and Picard (1985) and UC Davis using the existing models are presented in this section. Eight existing models, described in Chapters 5 and 6, are used for the predictions. Measured and predicted test results are presented in Tables G1 to G16.

The test results presented by Dawe and Kulak are analyzed and presented in Tables G1 to G3 using Models 1 to 6, Cases 1 to 7 in Model 7 and Model 8. It should be noted Cases 6 and 7 in Model 7 are used together to cover all test specimens as Case 6 is applicable for thick plates (failure in weld) and Case 7 is applicable for thin plates (failure in plate). Model 8, presented in Table G3, separates the test specimens based on the eccentricity ratio (a) for $a < 0.4$ and $a \geq 0.4$. The specimens tested by Dawe and Kulak are subjected to higher eccentricity ratios of $a \geq 0.4$.

The measured ultimate load and test-to-predicted ratios for the specimens tested by Beaulieu and Picard are presented in Tables G4 to G9. As mentioned in Chapter 5, the measured weld tensile strength (F_{EXX}) was not reported by the researchers. Therefore, F_{EXX} was assumed to be either 80.1 ksi or 67.2 ksi. The analysis using F_{EXX} of 80.1 ksi are presented in Tables G4 to G6. The analysis is then repeated using F_{EXX} of 67.2 ksi and the results are shown in Tables G7 to G9. Only 17 specimens that failed by weld are considered for predictions using Models 1 to 6 because these models are only valid for weld failure. The test specimens that failed by plate failure are not considered for these models. Since the first six models were developed based on the method of instantaneous centre of rotation, they are applicable for any load eccentricity ratio. On the other hand, for all cases in Model 7 the specimens that were subjected to low eccentricity ratios are ignored because these models are only applicable to test specimens for which failure was governed by bending rather than shear (only 11 test specimens subjected to high eccentricity ratios are analyzed). Model 8 is applicable for the weld failure under any load eccentricity. Therefore a total of 17 specimens from the test program of Beaulieu and Picard are considered in the comparison. The test specimens that failed by plate failure, either strength or stability, are not considered with Model 8.

In Tables G10 to G12, the analyzed results for UC Davis specimens using the existing models are presented. Total of 60 test specimens subjected to weld failure are examined using each model. Model 8 in Table G12 contains two equations for high and low eccentricity ratios. In this set of test data, all specimens are loaded under higher eccentricity; therefore, only one equation is used.

Lastly, the proposed new model is used to analyze all the test data and the results are presented in Tables G13 to G16. In Table G13, the prediction models are compared to the eight specimens presented by Dawe and Kulak. The specimens are classified according to their failure modes; weld failure and plate failure. Under weld failure, the specimens are further classified according to the eccentricity ratio using *a/Q*. For $a/Q \leq 0.59$ the eccentricity is small and shear failure of the weld is the predominant failure mode and for $a/Q > 0.59$ the eccentricity is considered to be large and failure is governed by bending. The proposed new model, model 9, considers both thick plate and thin plate behavior. In this case the capacity was calculated based on weld failure (small or large eccentricity) or on plate failure and the smaller predicted capacity is taken as the joint capacity.

The results of the analysis of the Beaulieu and Picard test data are presented in Tables G14 and G15 for F_{EXX} = 80.1 ksi and F_{EXX} = 67.2 ksi, respectively. As opposed to the previous model, all 22 specimens, including those that failed by plate tearing, are analyzed. Since the weld metal strength F_{EXX} affects the value of Q, it directly affects the classification according to a/Q, i.e. small or large eccentricity. Table G14, based on F_{EXX} of 80.1 ksi, shows that four specimens should have failed by plate tearing as opposed to five specimens that actually failed by plate tearing. This discrepancy can be explained by the fact that the weld metal strength, F_{EXX}, had to be assumed, which may have affected the selection of prediction equation, leading to the prediction of the incorrect failure mode in one case. It is noted that although a small number test specimens failed in the plate rather than in the weld, thus making validation of the proposed thin plate failure model difficult, none of the specimens that failed by weld failure in the experimental program were predicted to fail by plate rupture. Since there is a discrepancy between the predicted and actual failure for one of the five specimens that failed by plate rupture (indicated in Table G14 by asterisks), the test-to-predicted ratio for this failure mode is based on the predicted capacity based on plate failure rather than the minimum predicted failure load. It should be noted that the level of confidence in the results of a reliability analysis based on only five test specimens yields a low level of confidence. The specimens indicated by asterisks in Table G14 (specimens that failed in the plate) were not included in the calculations of the mean and coefficient of variation for the weld failure model. The same procedure was used for the data presented in Table G15 for F_{EXX} = 67.2 ksi. The total of 60 test specimens data collected at UC Davis are analyzed using the proposed new model and illustrated in Table G16. The predicted failure modes for all specimens agree with the observed actual failure mode, namely, weld failure.

The professional factor and coefficient of variation for each model are summarized in Table 6.1 of Chapter 6. The predicted capacity was calculated using Equation 2.6 for models involving the Lesik and Kennedy load-deformation relationship (Models 3 to 8 and 9) and based on "measured" ultimate shear strength. As mentioned in Chapter 6, the measured weld shear strength (τ_u) was not reported by the researchers. Therefore, a ratio of shear strength to tensile strength of 0.78, obtained from test results on joints with longitudinal welds only provided by Deng *et al.* (2003) and calculated based on the fracture surface area, was used to estimate the actual shear strength of the weld and substituted in Equation 2.6 to calculate the predicted capacity.

Table G1 – Predicted capacity for test results from University of Alberta (Dawe and Kulak, 1972) (Models 1 to 6)

Specimen number	Measured ultimate load, (kip)	Model 1	Model 2	Model 3	Model 4	Model 5	Model 6
		Test/predicted	Test/predicted	Test/predicted	Test/predicted	Test/predicted	Test/predicted
A-1	62.5	1.004	0.791	1.079	0.903	1.065	0.865
A-2	39	0.917	0.720	0.977	0.814	0.957	0.782
A-3	23.1	0.746	0.585	0.792	0.660	0.775	0.634
A-4	19.5	0.790	0.621	0.839	0.700	0.827	0.678
A-5	23.6	0.932	0.695	0.954	0.771	0.797	0.653
A-6	32.6	0.847	0.693	0.928	0.791	1.012	0.828
A-7	59.7	0.752	0.608	0.821	0.696	0.866	0.706
A-8	49.6	0.820	0.653	0.882	0.741	0.898	0.734
Mean		0.851	0.671	0.909	0.760	0.900	0.735
Coefficient of variation, V		0.109	0.101	0.104	0.103	0.116	0.114

Table G2 – Predicted capacity for test results from University of Alberta (Dawe and Kulak, 1972) (Model 7, Cases 1 to 7)

Specimen number	Measured ultimate load, (kip)	Case 1	Case 2	Case 3	Case 4	Case 5	Case 6 / Case 7
		Test/predicted	Test/predicted	Test/predicted	Test/predicted	Test/predicted	Test/predicted
A-1	62.5	0.972	0.787	0.947	0.787	0.773	1.133[1]
A-2	39	0.889	0.720	0.866	0.720	0.707	1.037[1]
A-3	23.1	0.724	0.586	0.705	0.586	0.575	0.844[1]
A-4	19.5	0.768	0.622	0.750	0.622	0.611	0.896[1]
A-5	23.6	0.885	0.695	0.818	0.695	0.685	0.781[2]
A-6	32.6	0.837	0.693	0.849	0.693	0.679	0.993[1]
A-7	59.7	0.738	0.606	0.738	0.606	0.594	0.870[1]
A-8	49.6	0.801	0.653	0.791	0.653	0.641	0.939[1]
Mean		0.827	0.627	0.808	0.670	0.658	0.937
Coefficient of variation, V		0.104	0.108	0.098	0.099	0.100	0.122

(1) Predicated capacity is based on Case 6
(2) Predicated capacity is based on Case 7

Table G3 – Predicted capacity for test results from University of Alberta (Dawe and Kulak, 1972) (Model 8)

Specimen number	Measured ultimate load, (kip)	Model 8	
		$a < 0.4$	$a \geq 0.4$
		Test/predicted	Test/predicted
A-1	62.5	—	1.428
A-2	39	—	1.306
A-3	23.1	—	1.063
A-4	19.5	—	1.128
A-5	23.6	—	1.280
A-6	32.6	—	1.243
A-7	59.7	—	1.091
A-8	49.6	—	1.180
Mean		—	1.215
Coefficient of variation, V		—	0.101

Table G4 - Predicted capacity for test results from Université Laval (Beaulieu and Picard,1985) using F_{EXX} = 80.1 ksi (Models 1 to 6)

Specimen number	Measured ultimate load (kips)	Model 1	Model 2	Model 3	Model 4	Model 5	Model 6
		Test/predicted	Test/predicted	Test/predicted	Test/predicted	Test/predicted	Test/predicted
A-12-375-1	61.9	1.205	0.837	1.142	0.856	0.561	0.459
A-6-125-1	157.9	1.139	0.831	1.161	0.936	0.916	0.715
A-6-125-2	141.7	1.027	0.752	1.051	0.850	0.841	0.656
A-6-375-1	50.9	1.127	0.820	1.126	0.891	0.826	0.675
A-6-75-2	245.9	1.081	0.809	1.177	1.019	1.066	0.781
B-10-125-1	266.2	1.014	0.830	1.153	1.009	1.197	0.935
B-10-125-2	249.5	0.944	0.760	1.056	0.914	1.066	0.834
B-10-375-1	61.3	0.670	0.515	0.703	0.579	0.649	0.530
B-10-375-2	109.1	1.191	0.915	1.248	1.027	1.145	0.935
B-10-75-1	381.5	0.874	0.726	1.057	0.979	1.089	0.799
B-10-75-2	358.7	0.812	0.689	0.993	0.924	1.028	0.754
B-8-125-1	235.7	0.888	0.716	1.007	0.876	1.032	0.806
B-8-125-2	286.6	1.086	0.878	1.232	1.076	1.272	0.994
B-8-375-1	93.5	1.017	0.780	1.065	0.876	0.974	0.796
B-8-375-2	96.1	1.033	0.796	1.086	0.895	1.008	0.823
B-8-75-1	334.6	0.880	0.804	1.177	1.130	1.288	0.945
B-8-75-2	313.4	0.871	0.790	1.158	1.116	1.276	0.936
Mean		0.992	0.779	1.094	0.938	1.014	0.787
Coefficient of variation, V		0.146	0.114	0.114	0.137	0.204	0.187

Table G5 - Predicted capacity for test results from Université Laval (Beaulieu and Picard, 1985) using F_{EXX} = 80.1 ksi (Model 7, Cases 1 to 7)

Specimen number	Measured ultimate load (kips)	Case 1	Case 2	Case 3	Case 4	Case 5	Case 6 / Case 7
		Test/predicted	Test/predicted	Test/predicted	Test/predicted	Test/predicted	Test/predicted
A-12-375-1	61.9	1.096	0.736	0.823	0.803	0.798	1.250(2)
A-6-125-1	157.9	1.058	0.755	0.879	0.811	0.802	1.475(2)
A-6-125-2	141.7	0.956	0.684	0.798	0.734	0.725	1.323(2)
A-6-375-1	50.9	1.054	0.756	0.883	0.811	0.801	1.036(2)
B-10-125-2	249.5	0.901	0.715	0.860	0.725	0.713	1.046(1)
B-10-375-1	61.3	0.644	0.507	0.607	0.515	0.506	0.550(2)
B-10-375-2	109.1	1.144	0.901	1.077	0.914	0.899	0.979(2)
B-8-125-1	235.7	0.849	0.677	0.817	0.687	0.674	0.989(1)
B-8-125-2	286.6	1.039	0.830	1.002	0.841	0.826	1.212(1)
B-8-375-1	93.5	0.977	0.769	0.918	0.780	0.767	0.839(2)
B-8-375-2	96.1	0.994	0.785	0.939	0.796	0.783	0.845(2)
Mean		0.974	0.738	0.873	0.765	0.754	1.049
Coefficient of variation, V		0.142	0.135	0.139	0.135	0.135	0.246

(1) Predicated capacity is based on Case 6

(2) Predicated capacity is based on Case 7

Table G6 - Predicted capacity for test results from Université Laval (Beaulieu and Picard, 1985) using F_{EXX} = 80.1 ksi (Model 8)

Specimen number	Measured ultimate load (kips)	Model 8	
		$a < 0.4$	$a \geq 0.4$
		Test/predicted	Test/predicted
A-12-375-1	61.9	—	1.532
A-6-125-1	157.9	—	1.513
A-6-125-2	141.7	—	1.368
A-6-375-1	50.9	—	1.509
B-10-125-1	266.2	—	1.427
B-10-125-2	249.5	—	1.320
B-10-375-1	61.3	—	0.940
B-10-375-2	109.1	—	1.670
B-8-125-1	235.7	—	1.247
B-8-125-2	286.6	—	1.526
B-8-375-1	93.5	—	1.425
B-8-375-2	96.1	—	1.452
A-6-75-2	245.9	1.266	—
B-10-75-1	381.5	1.185	—
B-10-75-2	358.7	1.112	—
B-8-75-1	334.6	1.298	—
B-8-75-2	313.4	1.270	—
Mean		1.226	1.411
Coefficient of variation, V		0.062	0.131

Table G7 - Predicted capacity for test results from Université Laval (Beaulieu and Picard, 1985) using F_{EXX} = 67.2 ksi (Models 1 to 6)

Specimen number	Measured ultimate load (kips)	Model 1	Model 2	Model 3	Model 4	Model 5	Model 6
		Test/predicted	Test/predicted	Test/predicted	Test/predicted	Test/predicted	Test/predicted
A-12-375-1	61.9	1.244	0.875	1.195	0.910	0.669	0.547
A-6-125-1	157.9	1.195	0.891	1.255	1.037	1.092	0.853
A-6-125-2	141.7	1.078	0.808	1.138	0.944	1.002	0.782
A-6-375-1	50.9	1.182	0.876	1.205	0.971	0.985	0.805
A-6-75-2	245.9	1.143	0.896	1.305	1.175	1.271	0.931
B-10-125-1	266.2	1.092	0.923	1.292	1.158	1.426	1.114
B-10-125-2	249.5	1.013	0.841	1.177	1.044	1.271	0.994
B-10-375-1	61.3	0.712	0.566	0.765	0.642	0.773	0.632
B-10-375-2	109.1	1.266	1.005	1.359	1.140	1.365	1.115
B-10-75-1	381.5	0.947	0.831	1.213	1.148	1.297	0.953
B-10-75-2	358.7	0.882	0.781	1.142	1.084	1.225	0.898
B-8-125-1	235.7	0.955	0.803	1.124	1.004	1.231	0.961
B-8-125-2	286.6	1.169	0.985	1.379	1.234	1.517	1.184
B-8-375-1	93.5	1.081	0.856	1.159	0.971	1.161	0.948
B-8-375-2	96.1	1.099	0.875	1.183	0.994	1.201	0.981
B-8-75-1	334.6	1.002	0.938	1.375	1.336	1.536	1.126
B-8-75-2	313.4	0.981	0.924	1.355	1.319	1.521	1.115
Mean		1.061	0.863	1.213	1.065	1.208	0.938
Coefficient of variation, V		0.133	0.114	0.120	0.157	0.204	0.187

Table G8 - Predicted capacity for test results from Université Laval (Beaulieu and Picard, 1985) using F_{EXX} = 67.2 ksi (Model 7, Cases 1 to 7)

Specimen number	Measured ultimate load (kips)	Case 1	Case 2	Case 3	Case 4	Case 5	Case 6 / Case 7
		Test/predicted	Test/predicted	Test/predicted	Test/predicted	Test/predicted	Test/predicted
A-12-375-1	61.9	1.139	0.779	0.883	0.846	0.839	1.250(2)
A-6-125-1	157.9	1.121	0.818	0.965	0.874	0.862	1.475(2)
A-6-125-2	141.7	1.013	0.741	0.876	0.791	0.780	1.323(2)
A-6-375-1	50.9	1.118	0.820	0.972	0.875	0.863	1.036(2)
B-10-125-2	249.5	0.974	0.788	0.960	0.798	0.783	1.147(1)
B-10-375-1	61.3	0.694	0.558	0.676	0.565	0.554	0.813(1)
B-10-375-2	109.1	1.233	0.990	1.200	1.003	0.985	1.444(1)
B-8-125-1	235.7	0.920	0.748	0.914	0.757	0.742	1.087(1)
B-8-125-2	286.6	1.126	0.917	1.121	0.928	0.909	1.331(1)
B-8-375-1	93.5	1.052	0.844	1.022	0.855	0.840	1.231(1)
B-8-375-2	96.1	1.072	0.863	1.047	0.874	0.857	1.257(1)
Mean		1.042	0.806	0.967	0.833	0.819	1.218
Coefficient of variation, V		0.138	0.137	0.143	0.134	0.134	0.156

(1) Predicated capacity is based on Case 6

(2) Predicated capacity is based on Case 7

Table G9 - Predicted welded joint capacity on test results from Université Laval, Beaulieu and Picard (1985) using FEXX = 67.2 ksi (Model 8)

Specimen number	Measured ultimate load (kips)	Model 8	
		$a < 0.4$	$a \geq 0.4$
		Test/predicted	Test/predicted
A-12-375-1	61.9	—	1.603
A-6-125-1	157.9	—	1.615
A-6-125-2	141.7	—	1.461
A-6-375-1	50.9	—	1.614
B-10-125-1	266.2	—	1.561
B-10-125-2	249.5	—	1.439
B-10-375-1	61.3	—	1.022
B-10-375-2	109.1	—	1.816
B-8-125-1	235.7	—	1.362
B-8-125-2	286.6	—	1.668
B-8-375-1	93.5	—	1.548
B-8-375-2	96.1	—	1.580
A-6-75-2	245.9	1.447	—
B-10-75-1	381.5	1.353	—
B-10-75-2	358.7	1.271	—
B-8-75-1	334.6	1.488	—
B-8-75-2	313.4	1.457	—
Mean		1.403	1.524
Coefficient of variation, V		0.064	0.129

Table G10 - Predicted capacity for test results from University of California, Davis (Models 1 to 6)

Specimen number	Measured ultimate load (kips)	Model 1	Model 2	Model 3	Model 4	Model 5	Model 6
		Test/predicted	Test/predicted	Test/predicted	Test/predicted	Test/predicted	Test/predicted
B_125_A12_55_1	73.4	1.779	1.279	1.754	1.370	1.190	0.971
B_125_A12_55_2	72.2	1.702	1.226	1.681	1.316	1.154	0.942
B_125_A12_55_3	71.1	1.656	1.192	1.636	1.279	1.119	0.913
B_125_A516_55_1	44.4	1.218	0.916	1.257	1.022	1.082	0.883
B_125_A516_55_2	53.7	1.451	1.091	1.498	1.218	1.291	1.054
B_125_A516_55_3	52.5	1.432	1.071	1.473	1.194	1.248	1.019
B_175_A12_3_1	153.4	1.654	1.253	1.734	1.426	1.547	1.244
B_175_A12_3_2	175.0	1.764	1.335	1.850	1.521	1.647	1.323
B_175_A12_3_3	152.1	1.629	1.226	1.699	1.391	1.487	1.197
B_175_A12_55_1	90.0	1.539	1.148	1.580	1.278	1.327	1.082
B_175_A12_55_2	76.6	1.527	1.151	1.579	1.286	1.372	1.120
B_175_A12_55_3	79.6	1.510	1.128	1.552	1.257	1.313	1.072
B_175_A12_85_1	51.9	1.407	1.048	1.439	1.164	1.206	0.987
B_175_A12_85_2	51.3	1.394	1.043	1.430	1.159	1.209	0.990
B_175_A12_85_3	53.0	1.432	1.059	1.455	1.169	1.172	0.959
B_175_A516_3_1	120.0	1.461	1.204	1.645	1.422	1.794	1.442
B_175_A516_3_2	119.0	1.411	1.160	1.586	1.369	1.714	1.377
B_175_A516_3_3	123.9	1.414	1.165	1.596	1.379	1.734	1.392
B_175_A516_55_1	61.7	1.277	1.038	1.398	1.188	1.493	1.218
B_175_A516_55_2	59.7	1.246	1.013	1.365	1.160	1.457	1.188
B_175_A516_55_3	63.0	1.371	1.112	1.498	1.272	1.593	1.300
B_175_A516_85_1	39.0	1.306	1.033	1.394	1.166	1.391	1.139
B_175_A516_85_2	30.1	1.038	0.819	1.106	0.924	1.101	0.901
B_175_A516_85_3	33.4	1.101	0.872	1.178	0.986	1.178	0.965
B_250_A12_55_1	86.9	1.256	1.002	1.356	1.141	1.385	1.130
B_250_A12_55_2	101.6	1.353	1.082	1.464	1.233	1.503	1.226
B_250_A12_55_3	94.5	1.361	1.051	1.420	1.201	1.480	1.207
B_250_A516_55_1	62.0	0.985	0.836	1.115	0.973	1.325	1.081
B_250_A516_55_2	58.7	1.000	0.849	1.131	0.987	1.349	1.101
B_250_A516_55_3	58.3	0.932	0.795	1.058	0.926	1.274	1.039
B_125_B12_55_1	82.0	1.889	1.360	1.865	1.459	1.275	1.040

Table G10 – Cont'd

Specimen number	Measured ultimate load (kips)	Model 1	Model 2	Model 3	Model 4	Model 5	Model 6
		Test/predicted	Test/predicted	Test/predicted	Test/predicted	Test/predicted	Test/predicted
B_125_B12_55_2	84.5	2.001	1.449	1.988	1.565	1.414	1.154
B_125_B12_55_3	98.8	2.147	1.541	2.113	1.648	1.415	1.154
B_125_B516_55_1	50.5	1.418	1.056	1.453	1.174	1.214	0.991
B_125_B516_55_2	57.4	1.563	1.165	1.602	1.296	1.343	1.096
B_125_B516_55_3	60.8	1.739	1.300	1.785	1.445	1.500	1.225
B_175_B12_3_1	193.2	1.841	1.382	1.922	1.569	1.668	1.339
B_175_B12_3_2	200.0	1.937	1.463	2.021	1.654	1.766	1.418
B_175_B12_3_3	185.4	1.785	1.350	1.873	1.539	1.665	1.336
B_175_B12_55_1	99.3	1.771	1.325	1.822	1.478	1.549	1.263
B_175_B12_55_2	90.0	1.721	1.283	1.762	1.424	1.464	1.195
B_175_B12_55_3	86.6	1.667	1.252	1.718	1.396	1.471	1.201
B_175_B12_85_1	59.3	1.591	1.187	1.628	1.317	1.363	1.115
B_175_B12_85_2	59.9	1.639	1.222	1.677	1.356	1.401	1.146
B_175_B12_85_3	57.1	1.717	1.269	1.742	1.398	1.398	1.144
B_175_B516_3_1	165.2	1.861	1.501	2.059	1.760	2.142	1.721
B_175_B516_3_2	160.4	1.743	1.423	1.950	1.679	2.078	1.667
B_175_B516_3_3	155.3	1.711	1.394	1.911	1.642	2.025	1.625
B_175_B516_55_1	86.7	1.711	1.343	1.825	1.520	1.770	1.444
B_175_B516_55_2	69.8	1.410	1.115	1.513	1.266	1.490	1.215
B_175_B516_55_3	78.0	1.643	1.341	1.805	1.537	1.944	1.586
B_175_B516_85_1	45.9	1.369	1.086	1.465	1.227	1.475	1.207
B_175_B516_85_2	46.8	1.493	1.182	1.595	1.335	1.597	1.307
B_175_B516_85_3	46.0	1.463	1.158	1.564	1.309	1.567	1.282
B_250_B12_55_1	110.5	1.540	1.215	1.648	1.378	1.631	1.330
B_250_B12_55_2	112.0	1.597	1.253	1.702	1.418	1.661	1.355
B_250_B12_55_3	110.7	1.639	1.294	1.754	1.467	1.745	1.424
B_250_B516_55_1	77.9	1.333	1.142	1.516	1.332	1.857	1.515
B_250_B516_55_2	77.0	1.314	1.120	1.491	1.303	1.793	1.463
B_250_B516_55_3	76.4	1.325	1.126	1.500	1.307	1.784	1.456
Mean		1.520	1.175	1.603	1.326	1.493	1.215
Coefficient of variation, V		0.167	0.144	0.150	0.142	0.167	0.162

Table G11 - Predicted capacity for test results from University of California, Davis (Model 7, Cases 1 to 7)

Specimen number	Measured ultimate load (kips)	Case 1	Case 2	Case 3	Case 4	Case 5	Case 6 / Case 7
		Test/predicted	Test/predicted	Test/predicted	Test/predicted	Test/predicted	Test/predicted
B_125_A12_55_1	73.4	1.651	1.353	1.536	1.256	1.249	1.781[2]
B_125_A12_55_2	72.2	1.581	1.297	1.475	1.205	1.191	1.604[2]
B_125_A12_55_3	71.1	1.538	1.261	1.434	1.171	1.159	1.597[2]
B_125_A516_55_1	44.4	1.160	0.976	1.142	0.916	0.902	1.048[2]
B_125_A516_55_2	53.7	1.382	1.162	1.361	1.091	1.074	1.255[2]
B_125_A516_55_3	52.5	1.360	1.142	1.334	1.071	1.055	1.279[2]
B_175_A12_3_1	153.4	1.573	1.325	1.553	1.244	1.225	1.630[2]
B_175_A12_3_2	175.0	1.677	1.412	1.654	1.325	1.305	1.760[2]
B_175_A12_3_3	152.1	1.546	1.299	1.518	1.218	1.200	1.656[2]
B_175_A12_55_1	90.0	1.460	1.224	1.427	1.147	1.130	1.354[2]
B_175_A12_55_2	76.6	1.455	1.226	1.437	1.151	1.133	1.316[2]
B_175_A12_55_3	79.6	1.434	1.204	1.405	1.128	1.112	1.305[2]
B_175_A12_85_1	51.9	1.335	1.120	1.307	1.050	1.034	1.179[2]
B_175_A12_85_2	51.3	1.325	1.113	1.301	1.044	1.029	1.157[2]
B_175_A12_85_3	53.0	1.353	1.130	1.312	1.057	1.043	1.233[2]
B_175_A516_3_1	120.0	1.431	1.243	1.506	1.181	1.157	1.694[1]
B_175_A516_3_2	119.0	1.380	1.198	1.449	1.138	1.115	1.632[1]
B_175_A516_3_3	123.9	1.383	1.201	1.454	1.141	1.118	1.637[1]
B_175_A516_55_1	61.7	1.256	1.089	1.318	1.035	1.014	1.484[1]
B_175_A516_55_2	59.7	1.226	1.063	1.286	1.010	0.989	1.449[1]
B_175_A516_55_3	63.0	1.348	1.168	1.412	1.109	1.087	1.592[1]
B_175_A516_85_1	39.0	1.272	1.092	1.307	1.033	1.014	1.487[1]
B_175_A516_85_2	30.1	1.010	0.867	1.037	0.820	0.805	1.180[1]
B_175_A516_85_3	33.4	1.073	0.922	1.104	0.873	0.857	1.256[1]
B_250_A12_55_1	86.9	1.226	1.056	1.268	1.000	0.981	1.438[1]
B_250_A12_55_2	101.6	1.321	1.139	1.369	1.079	1.059	1.552[1]
B_250_A12_55_3	94.5	1.279	1.105	1.332	1.048	1.028	1.506[1]
B_250_A516_55_1	62.0	0.982	0.868	1.071	0.831	0.811	1.185[1]
B_250_A516_55_2	58.7	0.998	0.883	1.089	0.845	0.825	1.204[1]
B_250_A516_55_3	58.3	0.931	0.825	1.020	0.790	0.771	1.126[1]
B_125_B12_55_1	82.0	1.754	1.438	1.634	1.335	1.321	1.786[2]
B_125_B12_55_2	84.5	1.865	1.535	1.753	1.428	1.411	1.886[2]

Table G11 – Cont'd

Specimen number	Measured ultimate load (kips)	Case 1	Case 2	Case 3	Case 4	Case 5	Case 6 / Case 7
		Test/predicted	Test/predicted	Test/predicted	Test/predicted	Test/predicted	Test/predicted
B_125_B12_55_3	98.8	1.990	1.629	1.846	1.511	1.495	2.078(2)
B_125_B516_55_1	50.5	1.345	1.127	1.314	1.056	1.041	1.238(2)
B_125_B516_55_2	57.4	1.483	1.243	1.449	1.165	1.148	1.359(2)
B_125_B516_55_3	60.8	1.650	1.385	1.615	1.298	1.279	1.512(2)
B_175_B12_3_1	193.2	1.744	1.464	1.708	1.372	1.352	1.881(2)
B_175_B12_3_2	200.0	1.836	1.542	1.801	1.446	1.425	1.966(2)
B_175_B12_3_3	185.4	1.696	1.428	1.672	1.340	1.320	1.806(2)
B_175_B12_55_1	99.3	1.682	1.413	1.651	1.325	1.305	1.553(2)
B_175_B12_55_2	90.0	1.631	1.366	1.592	1.280	1.262	1.473(2)
B_175_B12_55_3	86.6	1.586	1.333	1.559	1.251	1.232	1.396(2)
B_175_B12_85_1	59.3	1.510	1.267	1.479	1.188	1.170	1.328(2)
B_175_B12_85_2	59.9	1.556	1.305	1.522	1.223	1.206	1.368(2)
B_175_B12_85_3	57.1	1.622	1.354	1.571	1.267	1.249	1.473(2)
B_175_B516_3_1	165.2	1.809	1.559	1.874	1.477	1.449	2.124(1)
B_175_B516_3_2	160.4	1.699	1.470	1.774	1.395	1.368	2.003(1)
B_175_B516_3_3	155.3	1.668	1.442	1.739	1.368	1.341	1.965(1)
B_175_B516_55_1	86.7	1.658	1.419	1.691	1.340	1.317	1.932(1)
B_175_B516_55_2	69.8	1.371	1.177	1.407	1.113	1.093	1.602(1)
B_175_B516_55_3	78.0	1.618	1.406	1.704	1.337	1.309	1.917(1)
B_175_B516_85_1	45.9	1.335	1.148	1.376	1.087	1.066	1.563(1)
B_175_B516_85_2	46.8	1.454	1.249	1.496	1.182	1.160	1.701(1)
B_175_B516_85_3	46.0	1.425	1.225	1.467	1.159	1.137	1.668(1)
B_250_B12_55_1	110.5	1.496	1.282	1.532	1.212	1.191	1.746(1)
B_250_B12_55_2	112.0	1.548	1.324	1.579	1.251	1.229	1.803(1)
B_250_B12_55_3	110.7	1.593	1.367	1.634	1.292	1.269	1.861(1)
B_250_B516_55_1	77.9	1.332	1.183	1.466	1.134	1.107	1.615(1)
B_250_B516_55_2	77.0	1.314	1.164	1.437	1.114	1.088	1.588(1)
B_250_B516_55_3	76.4	1.325	1.171	1.444	1.121	1.094	1.598(1)
Mean		1.459	1.240	1.467	1.168	1.148	1.556
Coefficient of variation, V		0.155	0.144	0.135	0.140	0.142	0.169

(1) Predicated capacity is based on Case 6

(2) Predicated capacity is based on Case 7

Table G12 - Predicted capacity for test results from University of California, Davis (2008) (Model 8)

Specimen number	Measured ultimate load (kips)	Model 8	
		a < 0.4	a ≥ 0.4
		Test/predicted	Test/predicted
B_125_A12_55_1	73.4	—	2.410
B_125_A12_55_2	72.2	—	2.240
B_125_A12_55_3	71.1	—	2.201
B_125_A516_55_1	44.4	—	1.682
B_125_A516_55_2	53.7	—	2.007
B_125_A516_55_3	52.5	—	1.999
B_125_B12_55_1	82.0	—	2.483
B_125_B12_55_2	84.5	—	2.667
B_125_B12_55_3	98.8	—	2.831
B_125_B516_55_1	50.5	—	1.945
B_125_B516_55_2	57.4	—	2.140
B_125_B516_55_3	60.8	—	2.394
B_175_A12_3_1	153.4	—	2.285
B_175_A12_3_2	175.0	—	2.433
B_175_A12_3_3	152.1	—	2.269
B_175_A12_55_1	90.0	—	2.111
B_175_A12_55_2	76.6	—	2.121
B_175_A12_55_3	79.6	—	2.068
B_175_A12_85_1	51.9	—	1.936
B_175_A12_85_2	51.3	—	1.919
B_175_A12_85_3	53.0	—	1.966
B_175_A516_3_1	120.0	—	2.130
B_175_A516_3_2	119.0	—	2.046
B_175_A516_3_3	123.9	—	2.048
B_175_A516_55_1	61.7	—	1.858
B_175_A516_55_2	59.7	—	1.817
B_175_A516_55_3	63.0	—	2.007
B_175_A516_85_1	39.0	—	1.876
B_175_A516_85_2	30.1	—	1.488
B_175_A516_85_3	33.4	—	1.576

Table G12 – Cont'd

Specimen number	Measured ultimate load (kips)	Model 8	
		a < 0.4	a ≥ 0.4
		Test/predicted	Test/predicted
B_175_B12_3_1	193.2	—	2.529
B_175_B12_3_2	200.0	—	2.663
B_175_B12_3_3	185.4	—	2.470
B_175_B12_55_1	99.3	—	2.445
B_175_B12_55_2	90.0	—	2.331
B_175_B12_55_3	86.6	—	2.261
B_175_B12_85_1	59.3	—	2.186
B_175_B12_85_2	59.9	—	2.250
B_175_B12_85_3	57.1	—	2.352
B_175_B516_3_1	165.2	—	2.681
B_175_B516_3_2	160.4	—	2.502
B_175_B516_3_3	155.3	—	2.460
B_175_B516_55_1	86.7	—	2.452
B_175_B516_55_2	69.8	—	2.022
B_175_B516_55_3	78.0	—	2.405
B_175_B516_85_1	45.9	—	1.970
B_175_B516_85_2	46.8	—	2.141
B_175_B516_85_3	46.0	—	2.106
B_250_A12_55_1	86.9	—	1.821
B_250_A12_55_2	101.6	—	1.957
B_250_A12_55_3	94.5	—	1.887
B_250_A516_55_1	62.0	—	1.489
B_250_A516_55_2	58.7	—	1.500
B_250_A516_55_3	58.3	—	1.401
B_250_B12_55_1	110.5	—	2.196
B_250_B12_55_2	112.0	—	2.286
B_250_B12_55_3	110.7	—	2.363
B_250_B516_55_1	77.9	—	2.046
B_250_B516_55_2	77.0	—	1.979
B_250_B516_55_3	76.4	—	1.968
Mean		—	2.134
Coefficient of variation, V		—	0.147

Table G13 – Predicted capacity for test results from University of Alberta, Dawe and Kulak (1972) (Model 9)

Specimen number	Measured ultimate load, (kip)	a/Q	Q	Weld Failure Test/predicted		Plate Failure Test/predicted	Predicated Failure Mode	Actual Failure Mode
				a/Q ≤ 0.59	a/Q > 0.59			
A-1	62.5	0.47	2.20	0.758	—	0.566	Weld Failure	Weld Failure
A-2	39	0.69	2.20	—	0.784	0.482	Weld Failure	Weld Failure
A-3	23.1	0.92	2.20	—	0.638	0.381	Weld Failure	Weld Failure
A-4	19.5	1.14	2.24	—	0.678	0.395	Weld Failure	Weld Failure
A-5	23.6	1.23	1.65	—	0.750	0.522	Weld Failure	Weld Failure
A-6	32.6	0.73	2.76	—	0.761	0.397	Weld Failure	Weld Failure
A-7	59.7	0.50	2.55	0.575	—	0.385	Weld Failure	Weld Failure
A-8	49.6	0.71	2.38	-	0.713	0.414	Weld Failure	Weld Failure
Mean				0.667	0.721	—		
Coefficient of variation, V				0.194	0.076	—		

Table G14 - Predicted capacity on test results from Université Laval (Beaulieu and Picard, 1985) using FEXX = 80.1 ksi (Model 9)

Specimen number	Measured ultimate load, (kip)	a/Q	Q	Weld Failure Test/predicted		Plate Failure Test/predicted	Predicated Failure Mode	Actual Failure Mode
				a/Q ≤ 0.59	a/Q > 0.59			
A-12-125-1	164.8	0.69	0.73	—	(0.750)	0.914*	Plate Failure	Plate Failure
A-12-375-1	61.9	2.00	0.75	—	0.843	0.733	Weld Failure	Weld Failure
A-12-375-2	68.4	1.99	0.75	—	(0.933)	0.810*	Weld Failure	Plate Failure
A-12-75-1	240.9	0.37	0.80	(0.800)	—	1.088*	Plate Failure	Plate Failure
A-12-75-2	254.4	0.38	0.78	(0.813)	—	1.134*	Plate Failure	Plate Failure
A-6-125-1	157.9	0.39	1.27	0.908	—	0.865	Weld Failure	Weld Failure
A-6-125-2	141.7	0.38	1.30	0.825	—	0.775	Weld Failure	Weld Failure
A-6-375-1	50.9	1.13	1.33	—	0.868	0.608	Weld Failure	Weld Failure
A-6-75-1	267.7	0.30	0.99	(1.019)	—	1.190*	Plate Failure	Plate Failure
A-6-75-2	245.9	0.23	1.28	1.148	—	1.096	Weld Failure	Weld Failure
B-10-125-1	266.2	0.22	2.24	0.994	—	0.705	Weld Failure	Weld Failure
B-10-125-2	249.5	0.24	2.09	0.897	—	0.670	Weld Failure	Weld Failure
B-10-375-1	61.3	0.77	1.96	—	0.559	0.354	Weld Failure	Weld Failure
B-10-375-2	109.1	0.77	1.95	—	0.992	0.630	Weld Failure	Weld Failure
B-10-75-1	381.5	0.16	1.86	1.095	—	0.840	Weld Failure	Weld Failure
B-10-75-2	358.7	0.16	1.90	1.033	—	0.778	Weld Failure	Weld Failure
B-8-125-1	235.7	0.23	2.18	0.863	—	0.623	Weld Failure	Weld Failure
B-8-125-2	286.6	0.23	2.21	1.059	—	0.758	Weld Failure	Weld Failure
B-8-375-1	93.5	0.78	1.93	—	0.846	0.540	Weld Failure	Weld Failure
B-8-375-2	96.1	0.75	1.99	—	0.864	0.544	Weld Failure	Weld Failure
B-8-75-1	334.6	0.12	2.55	1.244	—	0.726	Weld Failure	Weld Failure
B-8-75-2	313.4	0.11	2.69	1.224	—	0.681	Weld Failure	Weld Failure
Mean				1.026	0.829	1.027		
Coefficient of variation, V				0.140	0.173	0.155		

Table G15 - Predicted capacity for test results from Université Laval (Beaulieu and Picard, 1985) using FEXX = 67.2 ksi (Model 9)

Specimen number	Measured ultimate load, (kip)	a/Q	Q	Weld Failure Test/predicted		Plate Failure Test/predicted	Predicated Failure Mode	Actual Failure Mode
				a/Q ≤ 0.59	a/Q > 0.59			
A-12-125-1	164.8	0.58	0.87	(0.792)	—	0.914*	Plate Failure	Plate Failure
A-12-375-1	61.9	1.67	0.89	—	0.893	0.733	Weld Failure	Weld Failure
A-12-375-2	68.4	1.67	0.90	—	(0.989)	0.810*	Weld Failure	Plate Failure
A-12-75-1	240.9	0.31	0.96	(0.910)	—	1.088*	Plate Failure	Plate Failure
A-12-75-2	254.4	0.32	0.93	(0.924)	—	1.134*	Plate Failure	Plate Failure
A-6-125-1	157.9	0.33	1.52	1.015	—	0.865	Weld Failure	Weld Failure
A-6-125-2	141.7	0.32	1.55	0.924	—	0.775	Weld Failure	Weld Failure
A-6-375-1	50.9	0.95	1.59	—	0.942	0.608	Weld Failure	Weld Failure
A-6-75-1	267.7	0.25	1.18	(1.169)	—	1.190*	Plate Failure	Plate Failure
A-6-75-2	245.9	0.20	1.52	1.326	—	1.096	Weld Failure	Weld Failure
B-10-125-1	266.2	0.19	2.67	1.138	—	0.705	Weld Failure	Weld Failure
B-10-125-2	249.5	0.20	2.49	1.024	—	0.670	Weld Failure	Weld Failure
B-10-375-1	61.3	0.64	2.34	—	0.617	0.354	Weld Failure	Weld Failure
B-10-375-2	109.1	0.65	2.32	—	1.095	0.630	Weld Failure	Weld Failure
B-10-75-1	381.5	0.14	2.22	1.273	—	0.840	Weld Failure	Weld Failure
B-10-75-2	358.7	0.13	2.27	1.202	—	0.778	Weld Failure	Weld Failure
B-8-125-1	235.7	0.19	2.60	0.988	—	0.623	Weld Failure	Weld Failure
B-8-125-2	286.6	0.19	2.64	1.212	—	0.758	Weld Failure	Weld Failure
B-8-375-1	93.5	0.65	2.31	—	0.934	0.540	Weld Failure	Weld Failure
B-8-375-2	96.1	0.63	2.37	—	0.955	0.544	Weld Failure	Weld Failure
B-8-75-1	334.6	0.10	3.04	1.454	—	0.726	Weld Failure	Weld Failure
B-8-75-2	313.4	0.09	3.21	1.431	—	0.681	Weld Failure	Weld Failure
Mean				1.181	0.906	1.027		
Coefficient of variation, V				0.153	0.174	0.155		

Table G16 - Predicted capacity for test results from University of California, Davis (Model 9)

Specimen number	Measured ultimate load, (kip)	a/Q	Q	Weld Failure Test/predicted		Plate Failure Test/predicted	Predicated Failure Mode	Actual Failure Mode
				a/Q ≤ 0.59	a/Q > 0.59			
B_125_A12_55_1	73.4	1.20	1.17	—	1.339	1.271	Weld Failure	Weld Failure
B_125_A12_55_2	72.2	1.17	1.20	—	1.285	1.210	Weld Failure	Weld Failure
B_125_A12_55_3	71.1	1.16	1.19	—	1.249	1.183	Weld Failure	Weld Failure
B_125_A516_55_1	44.4	0.82	1.73	—	0.989	0.782	Weld Failure	Weld Failure
B_125_A516_55_2	53.7	0.81	1.73	—	1.179	0.934	Weld Failure	Weld Failure
B_125_A516_55_3	52.5	0.85	1.68	—	1.157	0.930	Weld Failure	Weld Failure
B_175_A12_3_1	153.4	0.44	1.76	1.259	—	1.214	Weld Failure	Weld Failure
B_175_A12_3_2	175.0	0.43	1.75	1.348	—	1.314	Weld Failure	Weld Failure
B_175_A12_3_3	152.1	0.46	1.70	1.237	—	1.210	Weld Failure	Weld Failure
B_175_A12_55_1	90.0	0.82	1.65	—	1.238	1.012	Weld Failure	Weld Failure
B_175_A12_55_2	76.6	0.82	1.75	—	1.244	0.975	Weld Failure	Weld Failure
B_175_A12_55_3	79.6	0.84	1.67	—	1.218	0.982	Weld Failure	Weld Failure
B_175_A12_85_1	51.9	1.26	1.66	—	1.133	0.878	Weld Failure	Weld Failure
B_175_A12_85_2	51.3	1.24	1.69	—	1.128	0.866	Weld Failure	Weld Failure
B_175_A12_85_3	53.0	1.35	1.56	—	1.139	0.909	Weld Failure	Weld Failure
B_175_A516_3_1	120.0	0.28	2.67	1.195	—	0.929	Weld Failure	Weld Failure
B_175_A516_3_2	119.0	0.29	2.64	1.156	—	0.905	Weld Failure	Weld Failure
B_175_A516_3_3	123.9	0.28	2.66	1.172	—	0.910	Weld Failure	Weld Failure
B_175_A516_55_1	61.7	0.52	2.63	0.992	—	0.714	Weld Failure	Weld Failure
B_175_A516_55_2	59.7	0.52	2.63	0.970	—	0.697	Weld Failure	Weld Failure
B_175_A516_55_3	63.0	0.54	2.60	1.094	—	0.767	Weld Failure	Weld Failure
B_175_A516_85_1	39.0	0.95	2.30	—	1.128	0.730	Weld Failure	Weld Failure
B_175_A516_85_2	30.1	0.98	2.28	—	0.894	0.582	Weld Failure	Weld Failure
B_175_A516_85_3	33.4	0.94	2.31	—	0.953	0.613	Weld Failure	Weld Failure
B_250_A12_55_1	86.9	0.58	2.39	1.064	—	0.727	Weld Failure	Weld Failure
B_250_A12_55_2	101.6	0.55	2.41	1.093	—	0.785	Weld Failure	Weld Failure
B_250_A12_55_3	94.5	0.54	2.49	1.042	—	0.748	Weld Failure	Weld Failure
B_250_A516_55_1	62.0	0.39	3.43	0.685	—	0.487	Weld Failure	Weld Failure
B_250_A516_55_2	58.7	0.40	3.43	0.696	—	0.493	Weld Failure	Weld Failure
B_250_A516_55_3	58.3	0.38	3.51	0.647	—	0.457	Weld Failure	Weld Failure

Table G16 – Cont'd

Specimen number	Measured ultimate load, (kip)	a/Q	Q	Weld Failure Test/predicted		Plate Failure Test/predicted	Predicated Failure Mode	Actual Failure Mode
				a/Q ≤ 0.59	a/Q > 0.59			
B_125_B12_55_1	82.0	1.16	1.19	—	1.424	1.350	Weld Failure	Weld Failure
B_125_B12_55_2	84.5	1.10	1.26	—	1.526	1.405	Weld Failure	Weld Failure
B_125_B12_55_3	98.8	1.17	1.15	—	1.610	1.551	Weld Failure	Weld Failure
B_125_B516_55_1	50.5	0.89	1.64	—	1.138	0.924	Weld Failure	Weld Failure
B_125_B516_55_2	57.4	0.87	1.64	—	1.256	1.019	Weld Failure	Weld Failure
B_125_B516_55_3	60.8	0.88	1.66	—	1.401	1.126	Weld Failure	Weld Failure
B_175_B12_3_1	193.2	0.44	1.67	1.404	—	1.399	Weld Failure	Weld Failure
B_175_B12_3_2	200.0	0.44	1.68	1.477	—	1.463	Weld Failure	Weld Failure
B_175_B12_3_3	185.4	0.42	1.74	1.368	—	1.339	Weld Failure	Weld Failure
B_175_B12_55_1	99.3	0.81	1.69	—	1.431	1.153	Weld Failure	Weld Failure
B_175_B12_55_2	90.0	0.87	1.63	—	1.381	1.125	Weld Failure	Weld Failure
B_175_B12_55_3	86.6	0.83	1.71	—	1.351	1.074	Weld Failure	Weld Failure
B_175_B12_85_1	59.3	1.25	1.66	—	1.282	0.992	Weld Failure	Weld Failure
B_175_B12_85_2	59.9	1.29	1.65	—	1.320	1.024	Weld Failure	Weld Failure
B_175_B12_85_3	57.1	1.44	1.55	—	1.363	1.089	Weld Failure	Weld Failure
B_175_B516_3_1	165.2	0.31	2.41	1.496	—	1.236	Weld Failure	Weld Failure
B_175_B516_3_2	160.4	0.29	2.54	1.437	—	1.147	Weld Failure	Weld Failure
B_175_B516_3_3	155.3	0.29	2.52	1.402	—	1.126	Weld Failure	Weld Failure
B_175_B516_55_1	86.7	0.63	2.17	—	1.459	1.020	Weld Failure	Weld Failure
B_175_B516_55_2	69.8	0.60	2.27	—	1.213	0.823	Weld Failure	Weld Failure
B_175_B516_55_3	78.0	0.51	2.69	1.263	—	0.909	Weld Failure	Weld Failure
B_175_B516_85_1	45.9	0.89	2.34	—	1.186	0.763	Weld Failure	Weld Failure
B_175_B516_85_2	46.8	0.93	2.31	—	1.291	0.835	Weld Failure	Weld Failure
B_175_B516_85_3	46.0	0.92	2.31	—	1.265	0.817	Weld Failure	Weld Failure
B_250_B12_55_1	110.5	0.61	2.25	—	1.322	0.912	Weld Failure	Weld Failure
B_250_B12_55_2	112.0	0.64	2.18	—	1.363	0.953	Weld Failure	Weld Failure
B_250_B12_55_3	110.7	0.62	2.27	—	1.410	0.964	Weld Failure	Weld Failure
B_250_B516_55_1	77.9	0.37	3.66	0.914	—	0.637	Weld Failure	Weld Failure
B_250_B516_55_2	77.0	0.40	3.49	0.914	—	0.644	Weld Failure	Weld Failure
B_250_B516_55_3	76.4	0.41	3.41	0.930	—	0.657	Weld Failure	Weld Failure
Mean				1.130	1.265	—		
Coefficient of variation, V				0.219	0.121	—		

Appendix H

Simplified Strength Prediction Model

H.1 INTRODUCTION

The proposed simplified model (Model 9) is represented by three equations to cover the full range of load eccentricity and relative plate strength to weld strength in welded joints under combined shear and out-of-plane bending. The joint configuration under consideration consists of a single plate bracket welded using two fillet welds oriented parallel to the line of action of the applied force. Four different possible failure conditions are identified as followed:

Weld failure:

- Under large load eccentricity, the flexural capacity of the weld governs the capacity of the joint. The flexural resistance is developed through tension in part of the weld length and bearing between the welded plates in the compression zone of the welded joint. The shear resistance of the weld located in the compression zone of the joint is sufficient to resist the applied shear force.
- Under small load eccentricity, the capacity of the joint is governed by the shear capacity of the weld. A smaller portion of the joint is required to develop the required moment resistance.

Plate failure:

- Plate failure primarily in flexure when the load eccentricity is large.
- Plate failure primarily in shear when the load eccentricity is small.

The following sections present closed form calculation procedures to determine the capacity of welded joints with combined shear and out-of-plane bending. Both weld failure and plate failure are considered.

H.2 THICK PLATE BEHAVIOR (WELD FAILURE)

When thick plate behavior prevails the strength of the joint is governed either by flexure or shear resistance of the weld, depending on the magnitude of the load eccentricity. The load eccentricity is commonly expressed as the product of the eccentricity ratio (a) and the weld length. For a larger eccentricity ratio, the flexural capacity of the welded joint is critical and when the value of a is small, the shear force becomes dominant. The simplified model used to calculate the flexural capacity of a welded joint with combined shear and out-of-plane bending is illustrated in Figure H.1. On the tension side of the joint the tensile stresses are carried by the two fillet welds whereas the compressive

stresses on the compression side of the joint are carried by bearing of the two plates. Since the weld on the compression side of the joint does not contribute to the flexural resistance of the joint, it carries the shear force applied on the joint.

Based on the above discussion, the value of *a* that marks the change of joint behavior from flexure critical to shear critical can be determined by equating the maximum moment capacity of the welded joint to the shear capacity of the weld in the compression zone of the joint.

As shown in Figure H.1, when flexural behavior dominates, the load carrying capacity of the joint, P_m, can be determined from:

$$P_m = \frac{0.637 F_y t L}{a(Q + 1.273)} \qquad [H.1]$$

The depth of the compression zone, y_o, can be determined from equilibrium of the compression and tension forces as follows:

$$y_o = \frac{1.273 L}{Q + 1.273} \qquad [H.2]$$

The shear capacity of the fillet welds in the flexural compression zone can be obtained from:

$$P_v = 2(0.60)(0.707) D\, F_{EXX}\, y_o \qquad [H.3]$$

Substituting Equation H.2 into Equation H.3 and equating the resulting equation to Equation H.1, we obtain:

$$\frac{0.637\, F_y\, t\, L}{a\,(Q + 1.273)} = 2(0.60)(0.707)\, D\, F_{EXX}\, \frac{1.273 L}{Q + 1.273} \qquad [H.4]$$

The critical value of *a* follows as:

$$a = 0.59 Q \qquad [H.5]$$

Therefore, the flexural capacity of a welded joint under combined shear and out-of-plane bending is critical when $a/Q > 0.59$ and shear dominates when $a/Q < 0.59$.

H.2.1 Joint Capacity when $a/Q > 0.59$

When failure is governed by flexural behavior, the stress distribution presented in Figure 1 can be adopted for estimating the strength of a welded joint. Except for a few minor differences, the proposed model is similar to that proposed by Beaulieu and Picard (1985). Rectangular stress blocks are assumed in both tension and compression zones. The stress in the tension zone reaches the value predicted by Lesik and Kennedy (1990)

for a weld loaded at 90° to its axis. The stress in the compression zone is equal to the yield strength of the connected plates. In contrast to the earlier model of Beaulieu and Picard, this model uses the throat area rather than the weld leg area to calculate the distributed force on the tension side of the joint. For the stress distribution proposed, the compression force (C) and the tension force (T) are equal to:

$$C = F_y\ t\ y_o \qquad [H.6]$$

$$T = 2(0.60)(1.5)(0.707)\ D\ F_{EXX}\ (L - y_o) \qquad [H.7]$$

All the terms in these equations are as defined previously.

Substituting equation H.1 into H.7 and equating equations H.6 and H.7, we obtain:

$$P_m = \frac{0.637\ F_y\ t\ L}{a\ (Q + 1.273)} \qquad [H.8]$$

H.2.2 Joint Capacity when *a*/*Q* < 0.59

An equilibrium model suitable for estimating the joint capacity when the load eccentricity is small (the moment can be resisted without mobilizing the full depth of the joint) is illustrated in Figure H.2. Once again, rectangular stress blocks are used to represent the stress distributions in the tension and compression zones. However, because the eccentricity is small, the rectangular stress blocks do not develop over the full joint depth. As for the model used for $a/Q > 0.59$, it is assumed that the tensile resistance is provided by the weld and the compressive resistance is provided by bearing of the plates. The shear resistance is provided by the entire weld length with the exclusion of the tension zone and it is denoted as $y + y_o$ in Figure H.2. The depth of the joint required to resist the applied shear force can be determined from equilibrium consideration.

$$C = F_y\ t\ (L - l^* - y) \qquad [H.9]$$

$$T = 2(0.60)(1.5)(0.707)\ D\ F_{EXX}\ \ (L - y_o - y) \qquad [H.10]$$

where,

$$l^* = (L - y_o - y) \qquad [H.11]$$

By equilibrium and solve for y_o,

$$yo = \frac{1.273(L - y)}{Q + 1.273} \qquad [H.12]$$

The moment resistance can be obtained either from the normal stress distribution shown in Figure H.2 or as the shear resistance of the weld over the length $y + y_o$ times the load eccentricity, *aL*. The resulting expressions for moment resistance are as follows:

$$M_1 = F_y\ t\ y_o \left(\frac{L+y}{2} \right) \qquad [H.13]$$

$$M_2 = 2(0.60)(0.707)DF_{EXX}\,(y + y_o)aL \qquad [H.14]$$

By equating Equations H.13 and H.14 and substituting the value of y_o we obtain:

$$F_y t\left[\frac{1.273(L-y)}{Q+1.273} \right]\left(\frac{L+y}{2} \right) = 2(0.60)(0.707)DF_{EXX} \left\{ y + \left[\frac{1.273(L-y)}{Q+1.273} \right] \right\} aL \qquad [H.15]$$

From equation H.15 one can obtain the following expression for y:

$$y = \frac{0.6667L(\sqrt{a^2Q - 3.819a + 2.25Q} - a\sqrt{Q})}{\sqrt{Q}} \qquad [H.16]$$

Therefore, the portion of the joint capable of providing shear resistance ($y + y_o$) is given as:

$$y + y_o = \frac{1.273L}{Q+1.273} - \left(\frac{0.6667L(\sqrt{a^2Q - 3.819a + 2.25Q} - a\sqrt{Q})}{\sqrt{Q}} \right)\left(\frac{1.273}{Q+1.273} - 1 \right) \qquad \ldots [H.17]$$

By rearranging Equation [H.14], the predicted weld capacity for *a/Q* < 0.59 is:

$$\mathrm{P_r} = 2(0.60)(0.707)DF_{EXX}\,(y + y_o) \qquad [H.18]$$

Considering the complexity of Equation H.17, which is required to solve Equation H.18, a simpler approach is desirable. In order to provide a simpler expression for the weld strength in the range of *a/Q* between 0.0 and 0.59, Beaulieu and Picard suggested either a linear interpolation or a quadratic interpolation. A linear interpolation would result in:

$$P_r = P_{ro}\left(1 - 1.69\left(a/Q\right)\right) + 1.69\left(a/Q\right)P_{r59} \qquad [H.19]$$

where P_{ro} is the shear strength for a joint with no eccentricity given as:

$$P_{ro} = 2(0.60)(0.707)DF_{EXX}\,L \qquad [H.20]$$

and P_{r59} is obtained from Equation H.8 for *a/Q* = 0.59. Figure H.3 shows a comparison between the simplified Equation H.19 and Equation H.18 for values of *Q* varying from

0.615 to 4.0. The linear expression is a good representation of the more complex expression for small values of *Q*, but tends to over-estimate the capacities predicted by Equation H.18 for high values of *Q*. Since Equation H.18 tends to be conservative, the higher capacity predicted by the simpler linear equation is not expected to create a problem.

H.3 THIN PLATE CONNECTIONS (PLATE FAILURE)

The model proposed to predict the capacity of the plate under combined bending and shear is based on a lower bound model presented by Chen and Han (1988). It assumes an elastic-plastic stress distribution as shown in Figure 4 where the extreme fibers reached their yield strength while the middle portion reaches normal stresses below the yield level. The shear capacity is provided by the elastic portion of the cross-section. This simple lower bound model results in the following interaction equation:

$$\frac{M}{M_p} = 1 - \frac{3}{4}\left(\frac{P}{V_p}\right)^2 \qquad \text{[H.21]}$$

where,

$$M = PaL \qquad \text{[H.22]}$$

$$M_p = \frac{1}{4}tL^2F_u \qquad \text{[H.23]}$$

$$V_p = \frac{1}{2}tLF_u \qquad \text{[H.24]}$$

Solving Equation H.21 for P, and substituting Equations H.23 and H.24 yields the following expression for P_r:

$$P_r = \frac{2V_p(\sqrt{a^2L^2V_P{}^2 + 3M_p{}^2} - aLV_p)}{3M_p} \qquad \text{[H.25]}$$

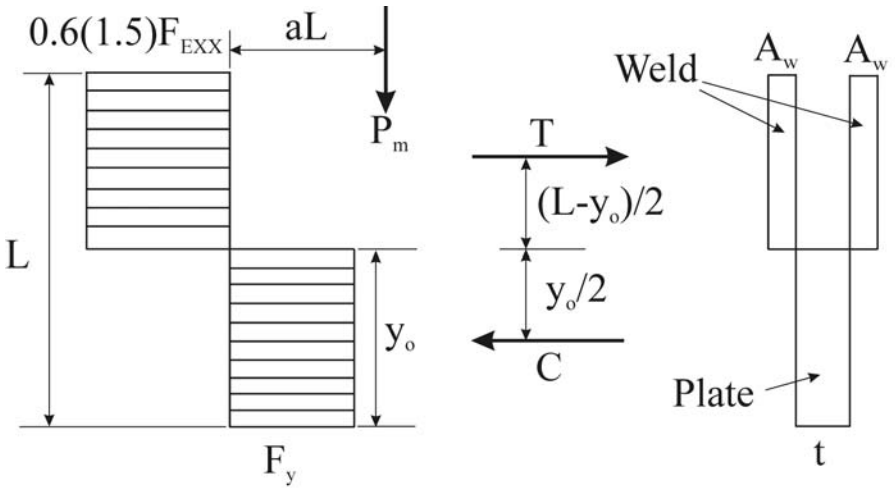

Figure H.1 – Proposed Flexure Model for Large Eccentricity

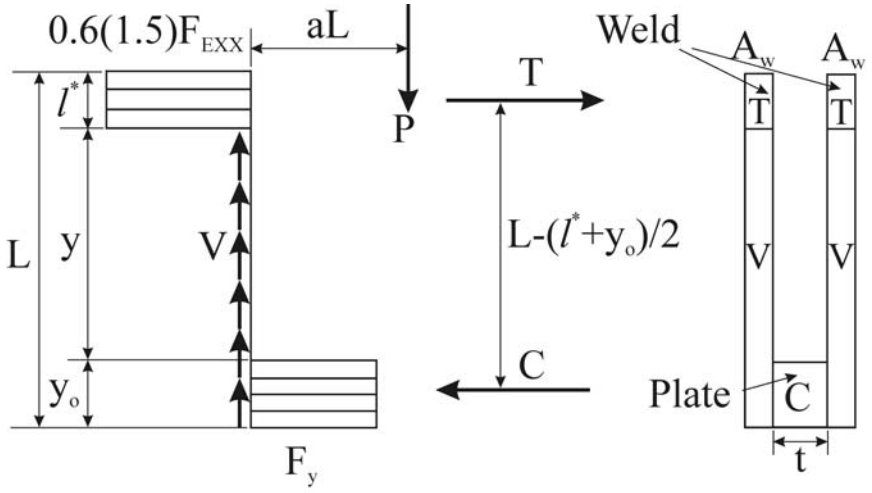

Figure H.2 – Flexure Model for Small Load Eccentricity

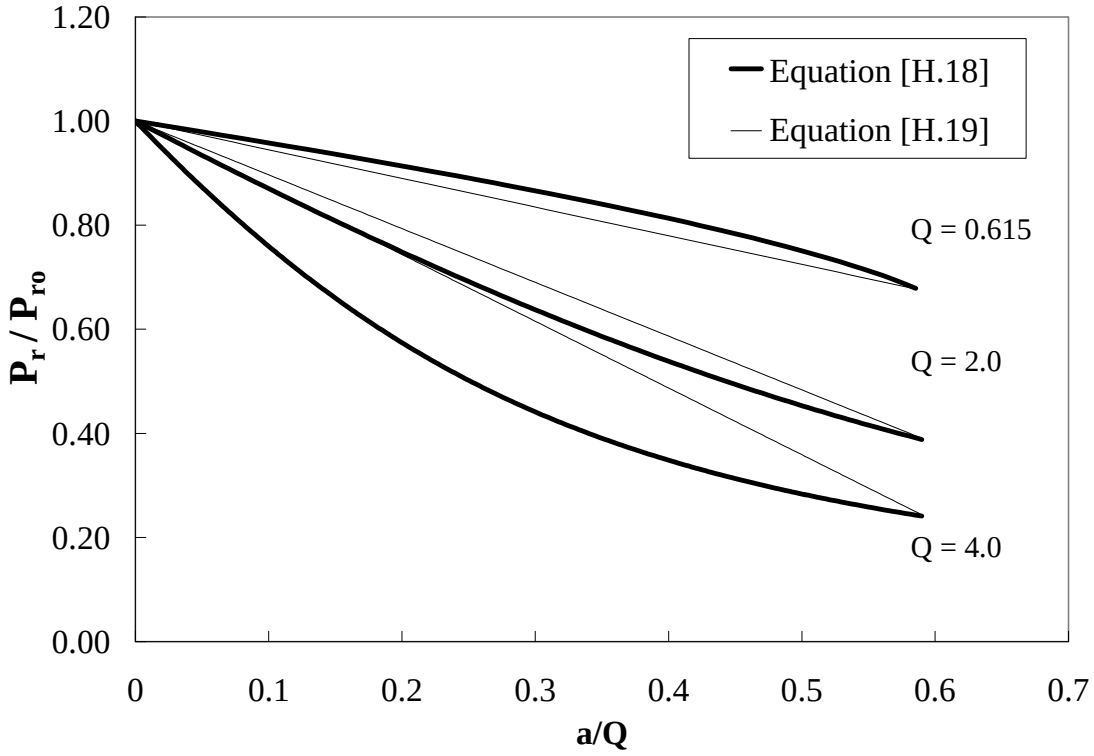

Figure H.3 – Comparison Between Equations [H.18] and [H.19]

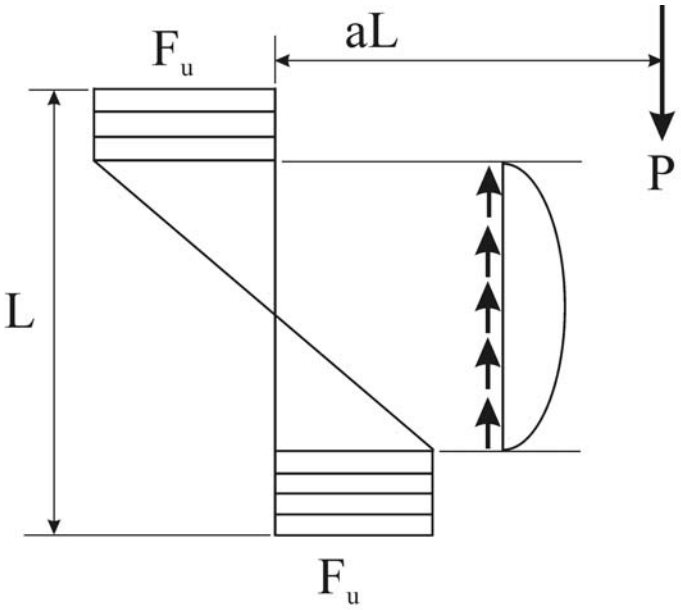

Figure H.4 – Combined Flexure and Shear Model

Appendix I

Proposed Design Tables

The coefficients C' listed in Tables I.1 to I.6 are based on an electrode tensile strength F_{EXX} = 70 ksi, a base metal yield strength F_y = 44 ksi, a base metal tensile strength, F_u = 65.3 ksi, and a resistance factor, $\phi = 0.75$. To determine the capacity P of the eccentrically loaded weld group, multiply the appropriate coefficient C' for the desired weld size by the length of the weld in inches.

$$P = C'L \qquad [I.1]$$

To determine the required weld length, divide the factored load, P, by the appropriate coefficient for a specific weld size.

$$L = P/C' \qquad [I.2]$$

The shaded cells in the design tables are the cases where thin plate behavior governs (plate failure), whereas, all other are the thick plate connections (weld failure). Details about the models used for deriving the values presented in the design tables are presented in Appendix H.

Table I.1- Coefficients C' for plate thickness 5/16 to 7/16 in.

Plate Thickness, t		5/16 in.		3/8 in.			7/16 in.			
Weld Size, D (in)		3/16	1/4	3/16	1/4	5/16	3/16	1/4	5/16	3/8
	0.0	8.35	8.83	8.35	10.60	10.60	8.35	11.14	12.36	12.36
	0.1	7.74	7.87	7.79	9.44	9.44	7.83	10.34	11.02	11.02
	0.2	7.02	7.02	7.23	8.43	8.43	7.31	9.54	9.83	9.83
	0.3	6.29	6.29	6.67	7.54	7.54	6.80	8.74	8.80	8.80
	0.4	5.65	5.65	6.11	6.78	6.78	6.28	7.91	7.91	7.91
	0.5	5.10	5.10	5.55	6.12	6.12	5.76	7.14	7.14	7.14
	0.6	4.62	4.62	4.98	5.55	5.55	5.24	6.35	6.47	6.47
	0.7	4.02	4.22	4.42	5.05	5.06	4.72	5.50	5.90	5.90
	0.8	3.52	3.86	3.87	4.42	4.64	4.20	4.81	5.30	5.41
	0.9	3.13	3.52	3.44	3.93	4.27	3.71	4.28	4.71	4.98
a	1.0	2.81	3.17	3.10	3.53	3.86	3.34	3.85	4.24	4.55
	1.2	2.34	2.64	2.58	2.95	3.22	2.78	3.21	3.54	3.79
	1.4	2.01	2.26	2.21	2.52	2.76	2.39	2.75	3.03	3.25
	1.6	1.76	1.98	1.94	2.21	2.41	2.09	2.41	2.65	2.84
	1.8	1.56	1.76	1.72	1.96	2.14	1.86	2.14	2.36	2.53
	2.0	1.41	1.58	1.55	1.77	1.93	1.67	1.93	2.12	2.28
	2.2	1.28	1.44	1.41	1.61	1.75	1.52	1.75	1.93	2.07
	2.4	1.17	1.32	1.29	1.47	1.61	1.39	1.60	1.77	1.90
	2.6	1.08	1.22	1.19	1.36	1.48	1.28	1.48	1.63	1.75
	2.8	1.00	1.13	1.11	1.26	1.38	1.19	1.38	1.52	1.63
	3.0	0.94	1.06	1.03	1.18	1.29	1.11	1.28	1.41	1.52

Table I.2- Coefficients C' for plate thickness 5/8 in.

Plate Thickness, t		5/8 in.					
Weld Size, D (in)		1/4	5/16	3/8	7/16	1/2	9/16
a	0.0	11.14	13.92	16.70	17.66	17.66	17.66
	0.1	10.47	12.98	15.48	15.74	15.74	15.74
	0.2	9.80	12.05	14.05	14.05	14.05	14.05
	0.3	9.14	11.11	12.57	12.57	12.57	12.57
	0.4	8.47	10.18	11.30	11.30	11.30	11.30
	0.5	7.81	9.24	10.20	10.20	10.20	10.20
	0.6	7.14	8.31	9.25	9.25	9.25	9.25
	0.7	6.47	7.37	8.04	8.43	8.43	8.43
	0.8	5.81	6.45	7.03	7.51	7.73	7.73
	0.9	5.14	5.74	6.25	6.68	7.04	7.12
	1.0	4.60	5.16	5.63	6.01	6.34	6.58
	1.2	3.83	4.30	4.69	5.01	5.28	5.51
	1.4	3.28	3.69	4.02	4.29	4.53	4.73
	1.6	2.87	3.23	3.52	3.76	3.96	4.13
	1.8	2.55	2.87	3.13	3.34	3.52	3.68
	2.0	2.30	2.58	2.81	3.01	3.17	3.31
	2.2	2.09	2.35	2.56	2.73	2.88	3.01
	2.4	1.91	2.15	2.34	2.50	2.64	2.76
	2.6	1.77	1.99	2.16	2.31	2.44	2.54
	2.8	1.64	1.84	2.01	2.15	2.26	2.36
	3.0	1.53	1.72	1.88	2.00	2.11	2.21

Table I.3- Coefficients C' for plate thickness 3/4 in.

Plate Thickness, t		3/4 in.							
Weld Size, D (in)		1/4	5/16	3/8	7/16	1/2	9/16	5/8	11/16
a	0.0	11.14	13.92	16.70	19.49	21.19	21.19	21.19	21.19
	0.1	10.54	13.07	15.58	18.08	18.88	18.88	18.88	18.88
	0.2	9.94	12.22	14.46	16.67	16.85	16.85	16.85	16.85
	0.3	9.34	11.37	13.34	15.09	15.09	15.09	15.09	15.09
	0.4	8.74	10.51	12.21	13.55	13.55	13.55	13.55	13.55
	0.5	8.14	9.66	11.09	12.23	12.23	12.23	12.23	12.23
	0.6	7.54	8.81	9.97	11.03	11.10	11.10	11.10	11.10
	0.7	6.94	7.96	8.85	9.52	10.10	10.12	10.12	10.12
	0.8	6.34	7.11	7.74	8.33	8.84	9.27	9.27	9.27
	0.9	5.74	6.26	6.88	7.41	7.85	8.24	8.54	8.54
	1.0	5.14	5.64	6.20	6.67	7.07	7.42	7.72	7.90
	1.2	4.14	4.70	5.16	5.55	5.89	6.18	6.43	6.66
	1.4	3.55	4.03	4.43	4.76	5.05	5.30	5.52	5.71
	1.6	3.11	3.52	3.87	4.17	4.42	4.64	4.83	4.99
	1.8	2.76	3.13	3.44	3.70	3.93	4.12	4.29	4.44
	2.0	2.48	2.82	3.10	3.33	3.53	3.71	3.86	3.99
	2.2	2.26	2.56	2.82	3.03	3.21	3.37	3.51	3.63
	2.4	2.07	2.35	2.58	2.78	2.95	3.09	3.22	3.33
	2.6	1.91	2.17	2.38	2.56	2.72	2.85	2.97	3.07
	2.8	1.77	2.01	2.21	2.38	2.52	2.65	2.76	2.85
	3.0	1.66	1.88	2.07	2.22	2.36	2.47	2.57	2.66

Table I.4- Coefficients C' for plate thickness 1 in.

Plate Thickness, t		1 in.								
Weld Size, D (in)		5/16	3/8	7/16	1/2	9/16	5/8	11/16	3/4	13/16
	0.0	13.92	16.70	19.49	22.27	25.05	27.84	28.25	28.25	28.25
	0.1	13.20	15.74	18.26	20.77	23.27	25.18	25.18	25.18	25.18
	0.2	12.48	14.78	17.04	19.28	21.49	22.47	22.47	22.47	22.47
	0.3	11.75	13.81	15.82	17.78	19.71	20.11	20.11	20.11	20.11
	0.4	11.03	12.85	14.59	16.28	17.93	18.07	18.07	18.07	18.07
	0.5	10.31	11.88	13.37	14.79	16.15	16.31	16.31	16.31	16.31
	0.6	9.59	10.92	12.15	13.29	14.37	14.80	14.80	14.80	14.80
	0.7	8.87	9.96	10.93	11.80	12.49	13.09	13.49	13.49	13.49
	0.8	8.15	8.99	9.70	10.33	10.93	11.46	11.93	12.36	12.36
	0.9	7.43	8.03	8.57	9.18	9.71	10.18	10.61	10.99	11.33
a	1.0	6.71	7.09	7.72	8.26	8.74	9.17	9.55	9.89	10.20
	1.2	5.31	5.91	6.43	6.88	7.28	7.64	7.96	8.24	8.50
	1.4	4.55	5.07	5.51	5.90	6.24	6.55	6.82	7.06	7.28
	1.6	3.98	4.43	4.82	5.16	5.46	5.73	5.97	6.18	6.37
	1.8	3.54	3.94	4.29	4.59	4.86	5.09	5.30	5.49	5.67
	2.0	3.19	3.55	3.86	4.13	4.37	4.58	4.77	4.94	5.10
	2.2	2.90	3.22	3.51	3.75	3.97	4.17	4.34	4.49	4.64
	2.4	2.65	2.96	3.21	3.44	3.64	3.82	3.98	4.12	4.25
	2.6	2.45	2.73	2.97	3.18	3.36	3.53	3.67	3.80	3.92
	2.8	2.28	2.53	2.76	2.95	3.12	3.27	3.41	3.53	3.64
	3.0	2.12	2.36	2.57	2.75	2.91	3.06	3.18	3.30	3.40

Table I.5- Coefficients C' for plate thickness 1 1/2 in.

Plate Thickness, t		1 1/2 in.								
Weld Size, D (in)		7/16	1/2	9/16	5/8	11/16	3/4	13/16	7/8	15/16
	0.0	19.49	22.27	25.05	27.84	30.62	33.41	36.19	38.97	41.76
	0.1	18.52	21.07	23.61	26.14	28.65	31.16	33.66	36.16	37.77
	0.2	17.55	19.87	22.16	24.43	26.68	28.92	31.13	33.34	33.71
	0.3	16.58	18.67	20.72	22.73	24.71	26.67	28.61	30.17	30.17
	0.4	15.62	17.47	19.27	21.03	22.75	24.43	26.08	27.11	27.11
	0.5	14.65	16.27	17.83	19.33	20.78	22.18	23.55	24.47	24.47
	0.6	13.68	15.07	16.38	17.62	18.81	19.94	21.02	22.07	22.20
	0.7	12.71	13.87	14.94	15.92	16.84	17.69	18.40	19.05	19.64
	0.8	11.74	12.67	13.49	14.22	14.82	15.49	16.10	16.66	17.19
	0.9	10.78	11.47	12.05	12.53	13.18	13.77	14.31	14.81	15.28
a	1.0	9.81	10.27	10.64	11.28	11.86	12.39	12.88	13.33	13.75
	1.2	7.87	8.28	8.87	9.40	9.88	10.33	10.73	11.11	11.46
	1.4	6.54	7.10	7.60	8.05	8.47	8.85	9.20	9.52	9.82
	1.6	5.72	6.21	6.65	7.05	7.41	7.74	8.05	8.33	8.59
	1.8	5.09	5.52	5.91	6.26	6.59	6.88	7.16	7.41	7.64
	2.0	4.58	4.97	5.32	5.64	5.93	6.20	6.44	6.67	6.87
	2.2	4.16	4.52	4.84	5.13	5.39	5.63	5.85	6.06	6.25
	2.4	3.82	4.14	4.43	4.70	4.94	5.16	5.37	5.55	5.73
	2.6	3.52	3.82	4.09	4.34	4.56	4.77	4.95	5.13	5.29
	2.8	3.27	3.55	3.80	4.03	4.24	4.43	4.60	4.76	4.91
	3.0	3.05	3.31	3.55	3.76	3.95	4.13	4.29	4.44	4.58

Table I.6 – Coefficients C' for plate thickness 2 in.

Plate Thickness, t		2 in.								
Weld Size, D (in)		7/16	1/2	9/16	5/8	11/16	3/4	13/16	7/8	15/16
	0.0	19.49	22.27	25.05	27.84	30.62	33.41	36.19	38.97	41.76
	0.1	18.69	21.27	23.84	26.40	28.94	31.48	34.01	36.53	39.04
	0.2	17.89	20.27	22.62	24.95	27.26	29.55	31.82	34.08	36.32
	0.3	17.08	19.27	21.41	23.51	25.58	27.62	29.64	31.63	33.61
	0.4	16.28	18.26	20.19	22.07	23.90	25.70	27.46	29.19	30.89
	0.5	15.48	17.26	18.97	20.62	22.22	23.77	25.28	26.74	28.18
	0.6	14.68	16.26	17.76	19.18	20.54	21.84	23.09	24.30	25.46
	0.7	13.88	15.26	16.54	17.74	18.86	19.92	20.91	21.85	22.74
	0.8	13.08	14.26	15.33	16.30	17.18	17.99	18.73	19.40	19.99
	0.9	12.28	13.26	14.11	14.85	15.50	16.06	16.54	17.15	17.77
a	1.0	11.48	12.26	12.89	13.41	13.82	14.19	14.83	15.43	15.99
	1.2	9.88	10.25	10.46	10.62	11.24	11.82	12.36	12.86	13.33
	1.4	8.28	8.25	8.53	9.10	9.64	10.13	10.59	11.02	11.42
	1.6	6.68	6.91	7.46	7.96	8.43	8.87	9.27	9.64	10.00
	1.8	5.61	6.14	6.63	7.08	7.50	7.88	8.24	8.57	8.89
	2.0	5.05	5.53	5.97	6.37	6.75	7.09	7.42	7.72	8.00
	2.2	4.59	5.03	5.43	5.79	6.13	6.45	6.74	7.01	7.27
	2.4	4.21	4.61	4.97	5.31	5.62	5.91	6.18	6.43	6.66
	2.6	3.89	4.25	4.59	4.90	5.19	5.46	5.70	5.94	6.15
	2.8	3.61	3.95	4.26	4.55	4.82	5.07	5.30	5.51	5.71
	3.0	3.37	3.69	3.98	4.25	4.50	4.73	4.94	5.14	5.33

Table I.7 – Coefficients C' for plate thickness 2 1/2 in.

Plate Thickness, t		2 1/2 in.								
Weld Size, D (in)		7/16	1/2	9/16	5/8	11/16	3/4	13/16	7/8	15/16
	0.0	19.49	22.27	25.05	27.84	30.62	33.41	36.19	38.97	41.76
	0.1	18.80	21.41	24.00	26.59	29.16	31.72	34.27	36.81	39.35
	0.2	18.12	20.55	22.96	25.33	27.69	30.03	32.35	34.65	36.94
	0.3	17.44	19.69	21.91	24.08	26.23	28.34	30.43	32.49	34.53
	0.4	16.76	18.83	20.86	22.83	24.76	26.65	28.51	30.33	32.12
	0.5	16.07	17.97	19.81	21.58	23.30	24.96	26.59	28.17	29.71
	0.6	15.39	17.11	18.76	20.33	21.83	23.28	24.67	26.01	27.30
	0.7	14.71	16.25	17.71	19.08	20.37	21.59	22.75	23.85	24.89
	0.8	14.02	15.40	16.66	17.82	18.90	19.90	20.82	21.68	22.49
	0.9	13.34	14.54	15.61	16.57	17.44	18.21	18.90	19.52	20.08
a	1.0	12.66	13.68	14.56	15.32	15.97	16.52	16.98	17.36	17.73
	1.2	11.29	11.96	12.46	12.82	13.04	13.15	13.59	14.20	14.78
	1.4	9.93	10.24	10.36	10.31	10.50	11.10	11.65	12.17	12.67
	1.6	8.56	8.52	8.26	8.64	9.19	9.71	10.20	10.65	11.08
	1.8	7.20	6.80	7.15	7.68	8.17	8.63	9.06	9.47	9.85
	2.0	5.83	5.93	6.44	6.91	7.35	7.77	8.16	8.52	8.87
	2.2	4.90	5.39	5.85	6.28	6.68	7.06	7.41	7.75	8.06
	2.4	4.49	4.94	5.37	5.76	6.13	6.47	6.80	7.10	7.39
	2.6	4.14	4.56	4.95	5.32	5.66	5.97	6.27	6.55	6.82
	2.8	3.85	4.24	4.60	4.94	5.25	5.55	5.83	6.09	6.33
	3.0	3.59	3.95	4.29	4.61	4.90	5.18	5.44	5.68	5.91